DOT/FAA/TC-15/23

Federal Aviation Administration
William J. Hughes Technical Center
Aviation Research Division
Atlantic City International Airport
New Jersey 08405

Development of a Titanium Alloy Ti-6Al-4V Material Model Used in LS-DYNA

May 2016

Final Report

U.S. Department of Transportation
Federal Aviation Administration

NOTICE

Technical Report Documentation Page

1. Report No.	2. Government Accession No.	3. Recipient's Catalog No.
DOT/FAA/TC-15/23		

4. Title and Subtitle	5. Report Date
Development of a Titanium Alloy Ti-6Al-4V Material Model Used in LS-DYNA	May 2016
	6. Performing Organization Code

7. Author(s)	8. Performing Organization Report No.
Sean Haight[1], Leyu Wang[2], Paul Du Bois[1], Kelly Carney[3], Cing-Dao Kan[1]	

9. Performing Organization Name and Address	10. Work Unit No. (TRAIS)
[1] George Mason University Center for Collision Safety and Analysis 45085 University Drive Ashburn, VA 20147 [2] The George Washington University FHWA/NHTSA National Crash Analysis Center 20101 Academic Way Ashburn, VA 20147 [3] NASA Glenn Research Center 21000 Brookpark Road Cleveland, OH 44135	11. Contract or Grant No. 13-G-020

12. Sponsoring Agency Name and Address	13. Type of Report and Period Covered
U.S. Department of Transportation Federal Aviation Administration Air Traffic Organization Operations Planning Office of Aviation Research and Development Washington, DC 20591	Final Report
	14. Sponsoring Agency Code

15. Sponsoring Agency Name and Address

The Federal Aviation Administration William J. Hughes Technical Center Aviation Research Division Technical Monitor was William Emmerling.

16. Abstract

George Mason University, Ohio State University, NASA John H. Glenn Research Center, and the Federal Aviation Administration (FAA) Aircraft Catastrophic Failure Prevention Program are working together to support the FAA initiative on certification by analysis. In this effort, the team has developed material data and analytical modeling that allow for a tabulation of actual material data into LS-DYNA using the *MAT_224 material model for Titanium-6Al-4V. The tabulation includes data from many tests, including tension, compression, impact, shear, and biaxial stress states. It also includes temperature and strain rate effects. This report documents the incorporation of the material test data into the material model input deck for *MAT 224. This requires a process of test data reduction, stability checks, and smoothness checks to ensure the model input can reliably produce repeatable results. Desired curves are smooth and convex in the plastic region of the stress-strain curve. This report on Titanium-6Al-4V covers a 1/2-inch rolled plate manufactured to Aeronautic Material Standard 4911 in the annealed condition. It documents the processes for developing the material model and failure surface from the test data and the 1/2-inch material model. Data are included in appendix D for a 1/4-inch thick plate.

17. Key Words	18. Distribution Statement
Material model development, Titanium alloy, Ti	This document is available to the U.S. public through the National Technical Information Service (NTIS), Springfield, Virginia 22161. This document is also available from the Federal Aviation Administration William J. Hughes Technical Center at actlibrary.tc.faa.gov.

19. Security Classif. (of this report)	20. Security Classif. (of this page)	21. No. of Pages	22. Price
Unclassified	Unclassified	353	

TABLE OF CONTENTS

LIST OF FIGURES

LIST OF TABLES

LIST OF ACRONYMS

*MAT_024	A piecewise linear plasticity material model in LS-DYNA
*MAT_224	An elasto-viscoplastic material model in LS-DYNA with arbitrary stress-strain input curve(s) and strain rate dependency which can be user-defined
DIC	Digital image correlation
FAA	Federal Aviation Administration
OSU	Ohio State University
SI	International System of Units, or metric units

EXECUTIVE SUMMARY

George Mason University, Ohio State University, NASA John H. Glenn Research Center, and the Federal Aviation Administration (FAA) Aircraft Catastrophic Failure Prevention Program are working together to support the FAA initiative on certification by analysis. In this effort, the team has developed material data and analytical modeling that allow for a tabulation of actual material data into LS-DYNA using the *MAT_224 material model. The tabulation includes data from many tests, including tension, compression, impact, shear, and biaxial stress states. It also includes temperature and strain-rate effects.

This report documents the incorporation of the material test data into the material model input deck for *MAT_224. This requires a process of test data reduction, stability checks, and smoothness checks to ensure the model input can reliably produce repeatable results. Desired curves are smooth and convex in the plastic region of the stress-strain curves.

This report on Ti-6Al-4V covers a 1/2-inch rolled plate manufactured to Aeronautic Material Standard-4911 in the annealed condition. It documents the processes for developing the material model and failure surface from the test data and the 1/2-inch material model. As part of this effort, data are also included for a 1/4-inch-thick plate; however, a material model was not developed for this plate thickness. Because of the anisotropic properties of the 1/4-inch-plate material, torsion tests did not produce useable results; in addition, a 3-D failure surface could not be created because of the thinness of the plate. Therefore, the data for the 1/4-inch plate are included in appendix D for informational purposes.

1. INTRODUCTION

Titanium alloy Ti6-Al4-V is an important engineering material widely used in aerospace applications. However, current constitutive models fall short in predicting the plastic and failure behavior of this material under medium and low strain rates. One reason for this may be the high dependency of the properties of titanium sheet on the manufacturing process and, therefore, on the thickness of the sheet. Therefore, this research effort involves the development and validation of a set of material constants using the tabulated input method of material model *MAT_224 in LS-DYNA, with consideration given to strain rate and temperature, specifically for a rolled 1/2-inch Ti-6Al-4V sheet. *MAT_224 is an elastic-plastic material with arbitrary stress versus strain curves and arbitrary strain-rate dependency, all of which can be defined by the user. Thermomechanical and comprehensive plastic failure criteria can also be defined for the material [1].

The chemical composition and microstructure of this material are summarized by the NASA John H. Glenn Research Center [2] in appendix B. The deformation portion of the material model produced in this effort is based on the results of uniaxial tensile testing conducted by Ohio State University (OSU) [3–5] under plane stress conditions at varying strain rates and temperatures. Material model failure is based on the results of tests conducted by OSU under many differing states of stress and test geometries. Material model development and validation procedures are included in this report as a reference for similar study. Material directional anisotropy; tension compression anisotropy; plane stress and plane strain comparison; and temperature effects are evaluated by comparing the simulation results with the test results provided by OSU [3–5].

The resulting LS-DYNA material model is presented in appendix F. In addition to the Ti-6Al-4V input parameters being available in the units presented in this report (mm, ms, kg, kN), the parameters are also available in International System of Units (SI) units (mm, s, t, N) and English units (inch, s, lbf·s^2, psi).

2. METHODOLOGY

Many factors contribute to the variations of Ti-6Al-4V measured material properties, such as the manufacturing and post-manufacturing processes; test specimen orientation in regard to plate grain direction; etc. To minimize some of these discrepancies, the material studied here is a Ti-6Al-4V 1/2-inch plate manufactured by a single company, as listed in appendix C.

The 1/2-inch rolled plate metal Ti-6Al-4V material is modeled using *MAT_224 in LS-DYNA. This is an isotropic elasto-thermo-visco-plastic constitutive relationship that states that stress is dependent on strain, strain rate, and temperature:

$$\sigma_{ij} = \sigma_{ij}(\varepsilon_{ij}, \dot{\varepsilon}_{ij}, T) \tag{1}$$

where σ_{ij} is stress, ε_{ij} is strain, $\dot{\varepsilon}_{ij}$ is the strain rate, and T is the temperature. In the elastic region, the Jaumann rate of the stress tensor, $\overset{\nabla}{\sigma}_{ij}$, is obtained as a linear function of elastic strain rates; this is a generalization of hypo-elasticity:

$$\overset{\nabla}{\sigma}_{ij} = \lambda(\dot{\varepsilon}_{kk} - \dot{\varepsilon}^{p}_{kk})\delta_{ij} + 2\mu(\varepsilon_{ij} - \dot{\varepsilon}^{p}_{ij}) \tag{2}$$

where $\dot{\varepsilon}^{p}_{ij}$ are the components of the plastic strain rate tensor and λ and μ are Lamé constants. Young's modulus, E, and Poisson's ratio, ν, may be converted by:

$$E = \frac{\mu(3\lambda + 2\mu)}{\lambda + \mu} \tag{3}$$

$$\nu = \frac{\lambda}{2(\lambda + \mu)} \tag{4}$$

The material response in the plastic region is determined by a von Mises-type yield surface in a six-dimension stress space that can expand/contract because of strain hardening, rate effects, and thermal softening:

$$\sigma_{vm}(\sigma_{ij}) \le \sigma_{y}(\varepsilon^{p}_{ij}, \dot{\varepsilon}^{p}_{ij}, T) = \sigma_{y}(\varepsilon^{p}_{eff}, \dot{\varepsilon}^{p}_{eff}, T) \tag{5}$$

where σ_{vm} is the von Mises stress, ε^{p}_{eff} is the equivalent plastic strain and $\dot{\varepsilon}^{p}_{eff}$ is the equivalent plastic strain rate. As the material is assumed isotropic, the dependency of the yield surface on plastic strain and plastic strain rate can be expressed purely as a function of the second invariant of each tensor. Note that states on the yield surface are plastic, whereas states below the yield surface are elastic. Mathematically, this is expressed as follows:

$$\begin{aligned} &\sigma_{vm}\left(\sigma_{ij}\right) - \sigma_{y}\left(\varepsilon^{p}_{eff}, \dot{\varepsilon}^{p}_{eff}, T\right) \le 0 \\ &\varepsilon^{p}_{eff} \ge 0 \\ &\dot{\varepsilon}^{p}_{eff} \cdot \left(\sigma_{vm}\left(\sigma_{ij}\right) - \sigma_{y}(\varepsilon^{p}_{eff}, \dot{\varepsilon}^{p}_{eff}, T)\right) \end{aligned} \tag{6}$$

The plastic strain rates are determined by associated flow leading to the well-known plastic incompressibility condition typical of metals:

$$\dot{\varepsilon}^{p}_{ij} = \dot{\varepsilon}^{p}_{eff} \frac{\partial \sigma_{vm}}{\partial \sigma_{ij}} \Rightarrow \sum_{k=1}^{3} \dot{\varepsilon}^{p}_{kk} \equiv 0 \tag{7}$$

2.1 STRESS-STRAIN RELATIONSHIP

A realistic stress-strain relationship is critical to accurate material modeling. This report begins by addressing several of the issues that hinder the accuracy of some common material modeling methods. The process by which the titanium alloy Ti-6Al-4V was modeled is then presented.

2.1.1 Common Elastic-Plastic Modeling Revisited

A review of common plastic material modeling procedures demonstrates the limitations and errors that can be introduced into the process. What follows is a detailed review, including typical assumptions, of the typical elastic-plastic material modeling procedure.

The material modeling begins with a standardized tensile test. A dogbone specimen under a constant grip speed is pulled in a test machine (see figure 1). Two measurements are recorded; the force versus time relationship, *F(t)*, is measured with the tensile machine, and the displacement versus time relationship, *D(t)*, is measured by a gauge or an extensometer fixed to the specimen. The force versus displacement curve is then generated by cross-plotting these two curves.

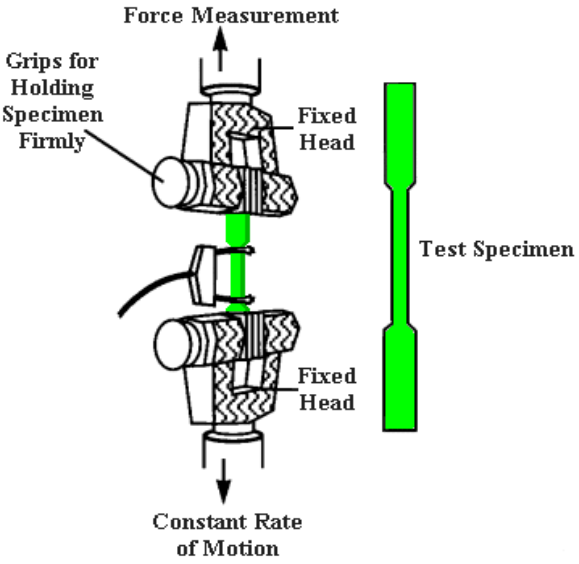

Figure 1. Standard tensile test [6]

After acquiring the force versus displacement curve, simple formulas are used to calculate engineering stress and engineering strain.

$$\sigma_{eng}(t) \equiv \frac{F(t)}{A_0}$$
$$\varepsilon_{eng}(t) \equiv \frac{L(t) - L_0}{L_0} = \frac{D(t)}{L_0} \tag{8}$$

where $\sigma_{eng}(t)$ is the engineering stress versus time relationship, ε_{eng} is the engineering strain, *F(t)* is the force in the axial direction, A_0 is the original cross-sectional area, *L(t)* is the instantaneous gauge length, L_0 is the original gauge length, and *D* is the displacement.

After knowing σ_{eng} and ε_{eng}, engineering stress may be converted into the true stress using the formula in equation 9 (a detailed derivation is provided in appendix A, section A.2):

$$\sigma = \sigma_{eng}(1+\varepsilon_{eng}) \tag{9}$$

Similarly, true strain may be converted by the following (see details in appendix A):

$$\varepsilon = \ln(\varepsilon_{eng}+1) \tag{10}$$

In applying equations 8–10, five assumptions have already been made (see details in appendix A):

- Assumption 1: Stress $\sigma_{ij}(t)$ is uniform over the mid cross-section of the specimen at any time.
- Assumption 2: Cross-sectional area is constant in the area measured by the extensometer.
- Assumption 3: Zero stress exists in the transverse and in the thickness direction.
- Assumption 4: Strain components in the transversal and thickness directions are given as $-k\varepsilon_{11}$, where ε_{11} is longitudinal strain and *k* is close to 0.5.
- Assumption 5: Strain is uniform in the area measured by the extensometer.

Any deviation from these assumptions will introduce errors in the derived stress-strain relationship.

With respect to Young's modulus, the elastic region of the final *MAT_224 Ti-6Al-4V material model will use 110 GPa [7]. However, this value may not match all of the test data exactly. Therefore, when the hardening curves for the various test conditions are developed, a value that matches each specific test is adopted to enable the simulated hardening curve to start at the same point as the test curve. Starting at the same point is required to compare the fit of the hardening curve being developed. When the model is complete, the stress evolution follows the above modulus value up to the proportional limit departure point for the different hardening curves, depending on stress state, rate, and temperature.

Using a test-specific Young's modulus allows for a determination of the yield strength, σ_Y, and strain at yield, ε_Y. Traditionally, the yield stress is determined by loading the specimen just above the yield point and then unloading it completely, such that the remaining plastic strain under zero stress is 0.2%. Because this approach can be both costly and time consuming, many practitioners simply find the slope of the elastic region and shift this line by 0.2% to the right. The intersection between this line and the stress-strain curve is traditionally called the yield point (see figure 2). However, for LS-DYNA, the elastic region corresponds to the linear portion of the

strain-stress curve, and the yield strength, σ_Y, needs to be defined as the end of the linear portion. The elastic part is modeled by giving two elastic material constants: Young's modulus, *E*, and Poisson's ratio, *v*.

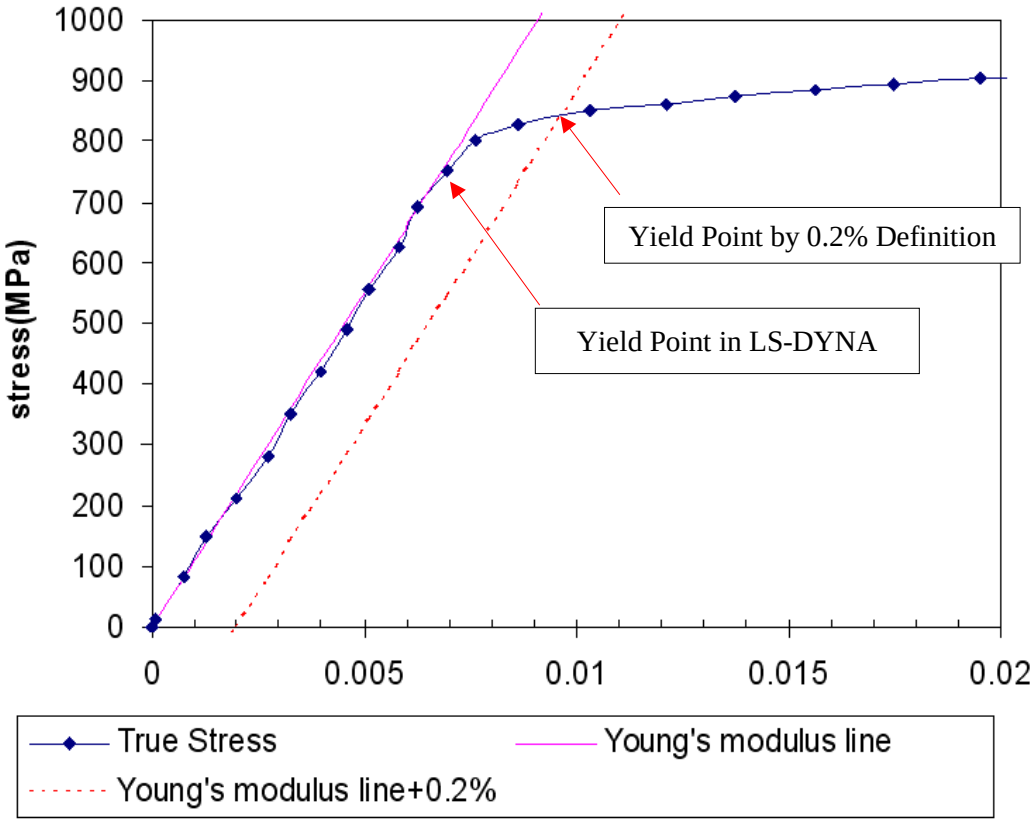

Figure 2. Finding yield stress by shifting elastic region by 0.2%

For modeling the plastic region, the plastic strain, ε_p, is computed as:

$$\varepsilon_p \equiv \varepsilon - \sigma / E \tag{11}$$

After obtaining the plastic strain versus stress relationship curve, input data are prepared for an LS-DYNA piecewise linear plasticity material model (*MAT_024). As shown in figure 3, the stress value of the starting point of this curve has the same value as the stress at the proportional limit. This is critical to maintain a continuous transition between the elastic and plastic regions.

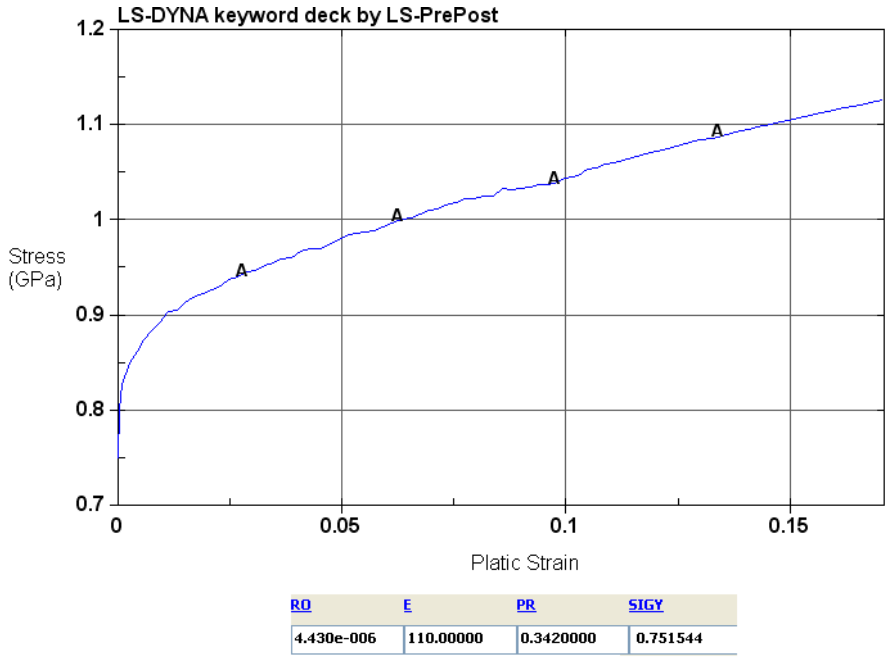

Figure 3. LS-DYNA input deck of a piecewise liner plasticity material model (*MAT_024) of a typical test result

Under the five assumptions discussed in this section, the load curve giving longitudinal stress versus longitudinal plastic strain is identical to the relationship between the effective plastic strain, ε_{eff}^{p}, and yield stress, σ_Y. This relationship will be used to determine the deformation behavior after the elastic region.

Effective plastic strain, ε_{eff}^{p}, is a monotonically increasing scalar value. It is calculated incrementally as a function of $\dot{\varepsilon}_{ij}^{p}$, the plastic component of the rate of deformation tensor. In tensorial notation, this is expressed as:

$$\varepsilon_{eff}^{p} \int_{t=0}^{t1} d\varepsilon_{eff}^{p} = \int_{0}^{t} \sqrt{2/3 \dot{\varepsilon}_{ij}^{p} \cdot \dot{\varepsilon}_{ij}^{p}} dt \tag{12}$$

If plastic deformation occurs at constant volume, then:

$$\dot{\varepsilon}_{ij}^{p} = \dot{\varepsilon}_{1}^{p} \begin{pmatrix} 1 & 0 & 0 \\ 0 & -0.5 & 0 \\ 0 & 0 & -0.5 \end{pmatrix} \Rightarrow \dot{\varepsilon}_{eff}^{p} = \varepsilon_{1}^{p} \tag{13}$$

Additionally,

$$\varepsilon_{eff}^{p} = \int_{t=0}^{t1} d\varepsilon_{eff}^{p} = \int_{0}^{t} \dot{\varepsilon}_{1}^{p} dt = \varepsilon_{1}^{p} \tag{14}$$

The yield surface can be determined by equation 15:

$$\sigma_{vm} \leq \sigma_{y} = f_{h}(\varepsilon_{eff}^{p}) \tag{15}$$

where $f_h(\varepsilon_{eff}^{p})$ is the tabulated input and $f_h(0)$ is the yield stress that denotes the value of f_h when $\varepsilon_{eff}^{p} = 0$ (the starting point of the plastic strain versus stress curve).

The effective stress according to von Mises, σ_{vm}, is defined as follows:

$$\sigma_{vm} = \sqrt{\frac{1}{2}\left[(\sigma_x - \sigma_y)^2 + (\sigma_y - \sigma_z)^2 + (\sigma_z - \sigma_x)^2 + 6\sigma_{xy}{}^2 + 6\sigma_{yz}{}^2 + 6\sigma_{zx}{}^2\right]} \tag{16}$$

It can be observed that it is identical to the longitudinal stress under conditions of uniaxial tension:

$$\sigma_{ij} = \sigma_1 \begin{pmatrix} 1 & 0 & 0 \\ 0 & 0 & 0 \\ 0 & 0 & 0 \end{pmatrix} \Rightarrow \sigma_{vm} = \sigma_1 (\sigma_1 > 0) \tag{17}$$

2.1.2 Violations of Common Assumptions

The common method for modeling elastic-plastic materials presented in the previous section is invalid after the necking point because at least three out of five assumptions are violated.

Assumption 1 is still considered valid because the stress, $\sigma_{ij}(t)$, varies little over the cross-sectional area at any time.

Assumption 4 is still valid because the material remains isotropic and plastically incompressible after onset of the plastic instability.

Assumption 2 is invalid, because the cross-sectional area is much smaller in the localized region after necking and, therefore, not a constant in the region spanned by an extensometer.

Assumption 3 is invalid, because transversal stresses will develop after the onset of necking, and additional stresses in the thickness direction will develop after the onset of local necking. Consequently, after necking, the specimen is no longer in a uniaxial stress condition.

Before necking, under uniaxial stress conditions, the only non-zero stress component is the axial stress, σ_l:

$$\sigma = \begin{pmatrix} \sigma_l & 0 & 0 \\ 0 & 0 & 0 \\ 0 & 0 & 0 \end{pmatrix} \qquad \sigma_{vm} = \sigma_l \tag{18}$$

After necking, a transverse stress, σ_t, appears because the material will resist shrinking in the transverse direction:

$$\sigma = \begin{pmatrix} \sigma_l & 0 & 0 \\ 0 & \sigma_t & 0 \\ 0 & 0 & 0 \end{pmatrix} \qquad \sigma_{vm} \neq \sigma_l \tag{19}$$

As the local neck develops, we see additional stresses in the thickness direction, σ_{tt}:

$$\sigma = \begin{pmatrix} \sigma_l & 0 & 0 \\ 0 & \sigma_t & 0 \\ 0 & 0 & \sigma_{tt} \end{pmatrix} \qquad \sigma_{vm} \neq \sigma_l \tag{20}$$

An accurate measurement of σ_l can be obtained by applying the instantaneous necking cross-sectional area (measured by digital imaging) in the stress calculation. However, it is not possible to measure the transverse stress, σ_t, nor the thickness stress, σ_{tt}. Therefore, σ_{vm} is generally unknown after necking. If the uniaxial stress assumption is still applied (assume $\sigma_{vm} \approx \sigma_t$ after necking) and this false von Mises stress versus effective plastic strain relationship is used to define the behavior of material, then the simulation result will deviate from the real test.

Assumption 5 is invalid because the strain is not uniform within the measuring distance of the extensometer. After the onset of necking, the neck will have a higher strain than the rest of the part. An accurate measurement of strain, the region of necking can be obtained via a digital image correlation (DIC).

2.1.3 Stress-Strain Relationship After Necking

The following method is used to create an accurate material model and simulate the tensile test in LS-DYNA:

1. Estimate several post-necking plastic stress-strain curves as input by extrapolating the curve before necking.

2. Compare the simulation force versus displacement curve with test results and pick the input curve that gives the closest match. Note that the complete specimen geometry must be precisely modeled by measuring the actual specimen rather than using the design values on the blueprint. At this stage in the process, the strain-rate effect is not considered in the simulation.

3. Input a single stress-strain curve associated with a particular strain rate, thereby making the material model strain rate-independent (at this point in the modeling process, the material model will behave the same no matter the loading speed as long as inertia effects are sufficiently small). Because of this strain rate independence, the simulation can be performed with an arbitrary (higher) loading speed instead of the actual loading speed that was used in the test, allowing for a much shorter simulation time.

4. To safely implement the method, run several simulations to determine a good artificial loading speed in the simulation (see figure 4).

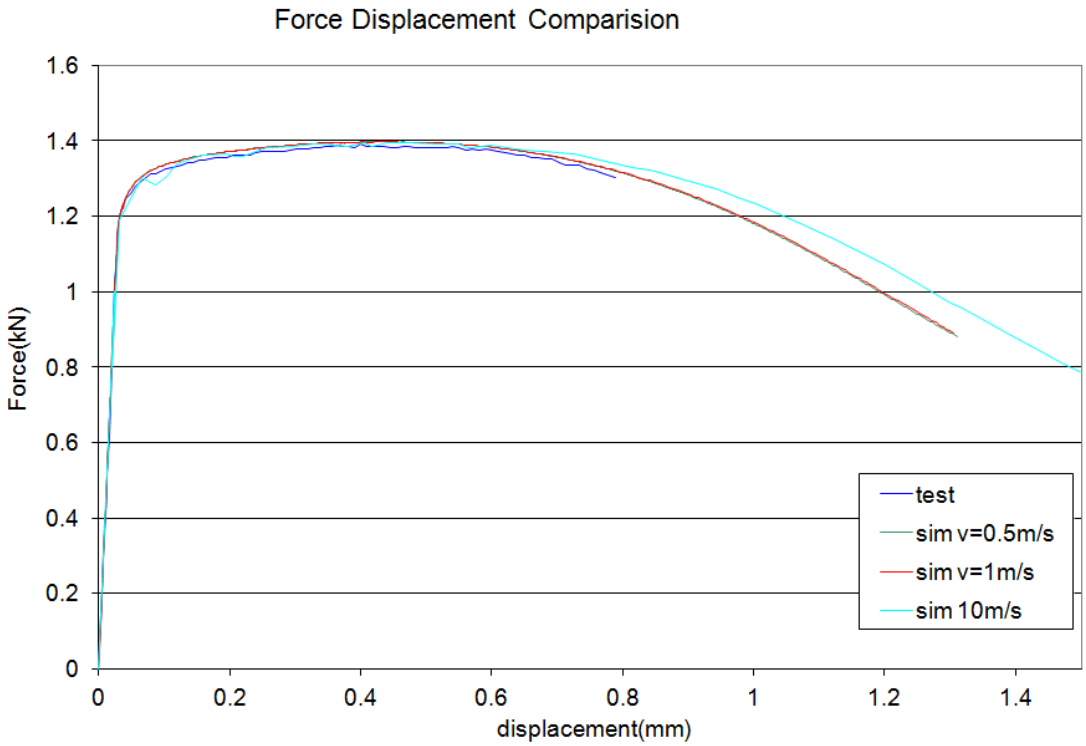

Figure 4. Artificial loading speed determinations of a typical test result

The rate-independent material model will have a dynamic effect if loaded at a very high speed because of the inertia effects. Therefore, start with a high loading speed of 10 m/s and gradually reduce it to the point in which further reduction no longer changes the results. Use that final speed for loading the simulation; in this case, it was 1 m/s.

The necking point is identified by making the assumption that necking occurs at maximum load (see appendix A, section A.3 for more details). The necking point is given by the intersection

between the true-strain versus true-stress curve and its own derivative. So necking occurs where the true stress is equal to the tangent modulus:

$$\begin{cases} \sigma = \sigma(\varepsilon) \\ \sigma = \dfrac{d\sigma}{d\varepsilon} \end{cases} \tag{21}$$

After the necking point is determined, only the part of the strain-stress curve before necking is used for further processing (see figure 5).

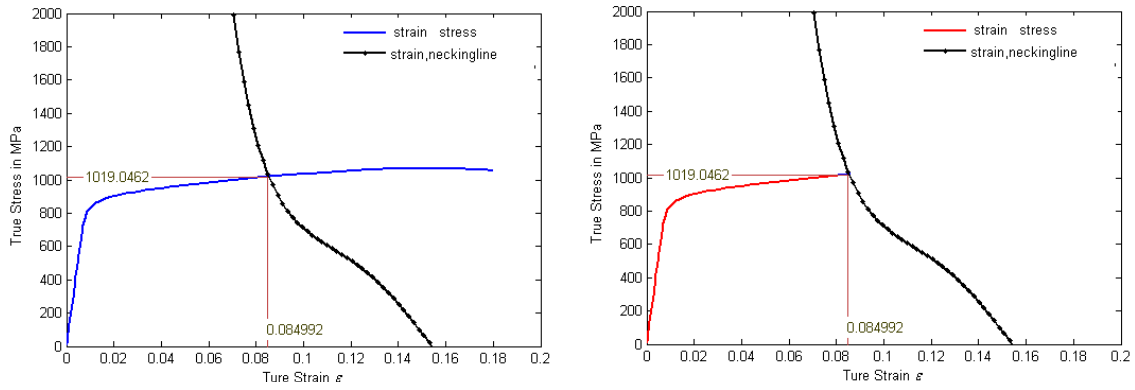

Figure 5. The (a) necking judgment line and stress-strain curve and (b) stress-strain curve after trimming

The hardening curves are extrapolated after necking using the following formula:

$$\sigma = k[\varepsilon_e + \varepsilon_p]^n \tag{22}$$

where k, ε_e, and n are fitting parameters and the exponent n is expected to vary between 0 and 1 because the hardening curve is expected to be monotonically increasing and to have a monotonically decreasing tangent.

At the necking point, this curve should be continuous:

$$A \equiv \sigma|_{\varepsilon=\varepsilon 0}\ ,\ B \equiv \varepsilon|_{\varepsilon=\varepsilon 0} \tag{23}$$

and smooth:

$$A \equiv \sigma|_{\varepsilon=\varepsilon 0}\ ,\ C \equiv \frac{d\sigma}{d\varepsilon}|_{\varepsilon=\varepsilon 0} \tag{24}$$

where A is the stress at necking, $B \equiv \varepsilon_0$ is the plastic strain at necking, and C is the slope (hardening modulus) at necking. Note that there are three variables but only two boundary conditions. Therefore, the extrapolation is not uniquely defined, and one of the three parameters can be freely chosen; because it has a bounded domain, it is typical to choose the exponent, n. Given a specific n value, ε_e and k are determined from the following relationships:

$$k = A\left(\frac{An}{C}\right)^{-n}$$
$$\varepsilon_e = \frac{An}{C} - B \tag{25}$$

After assuming different n values, a cluster of curves can be generated (see figure 6).

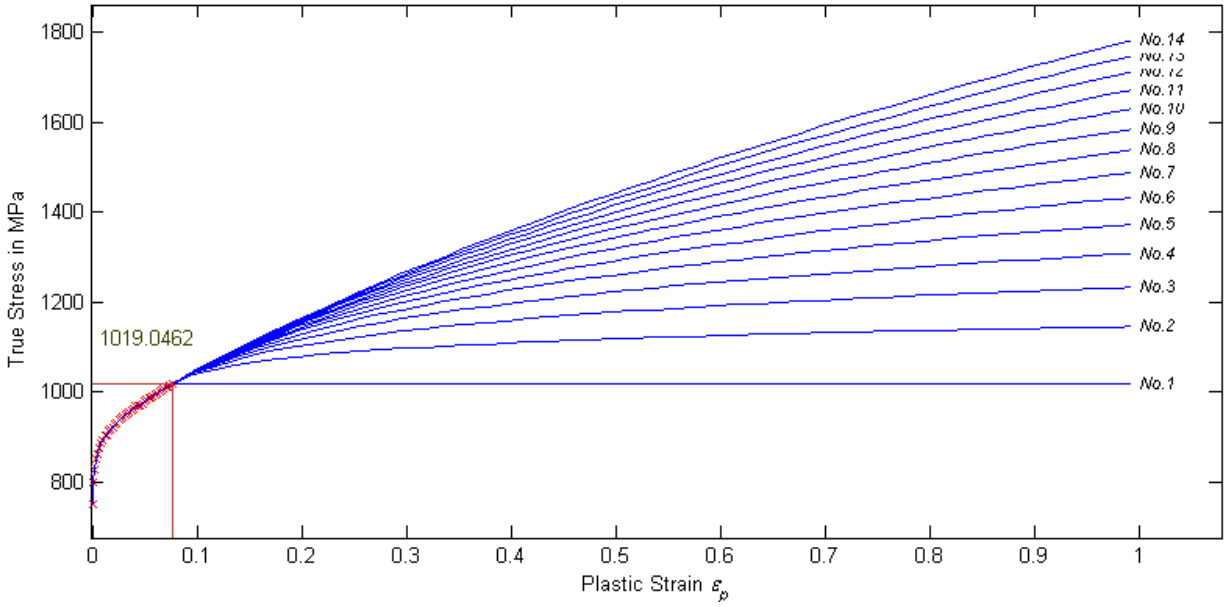

Figure 6. Extrapolated curves after necking point

Several candidate curves were chosen from the generated plastic strain versus stress curves (see figure 6), and these curves were input into the material model to simulate a tensile test (see figure 7). Note that the original plastic strain versus stress curve before trimming at the necking point is added for reference and labeled "direct input," and the von Mises stress contour is shown in figure 8.

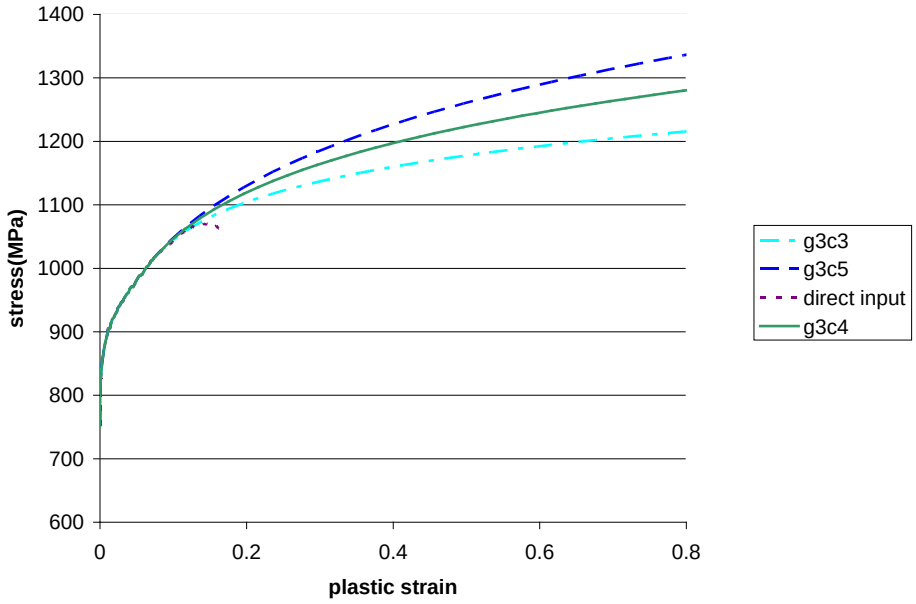

Figure 7. Candidate material plastic strain versus stress curves for tensile test simulation

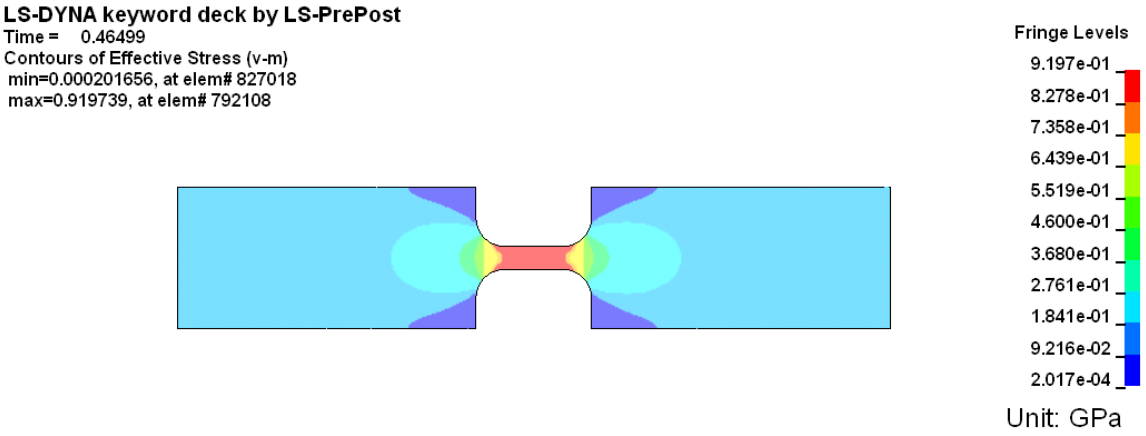

Figure 8. Von Mises stress contour of simulated tensile test

Figure 9 shows the force displacement curves obtained by four simulations overlaid with the real-life tensile test result. The curve named "g3c4" predicts a force displacement curve that is close to the test. Therefore, this curve is a good estimation of plastic strain versus stress relationship. Note that "direct input curve," which would be produced by the approach presented in section 2.1.1, deviates significantly from the test result after the onset of necking.

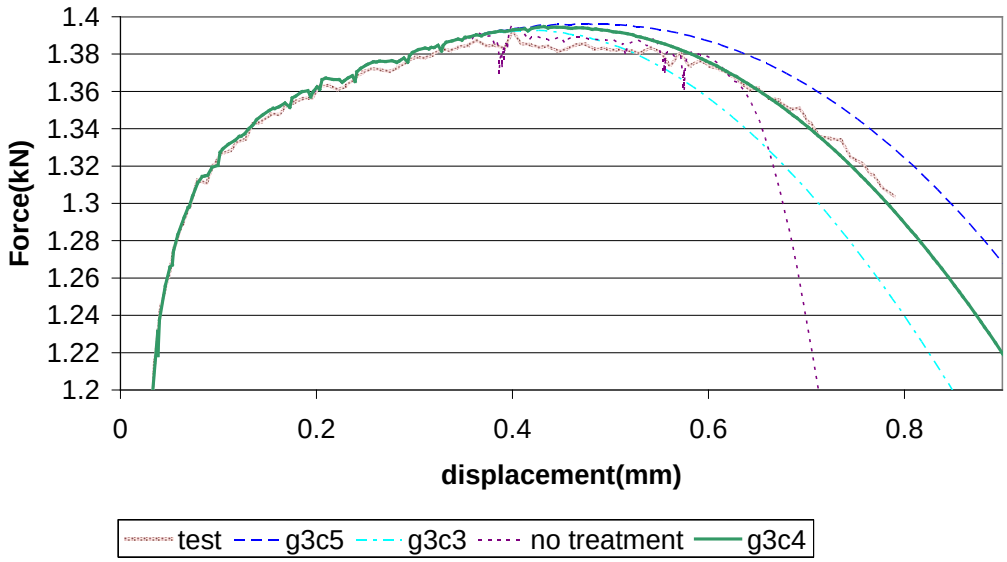

Figure 9. Force displacement result of tensile test simulations with different hardening curve inputs

As a supplementary evaluation, the 1st principal plastic strain contour at failure of the simulation is compared with the longitudinal strain DIC data in the physical test. These two contours must be relatively similar to justify the estimated stress-strain relationship curve (see figure 10).

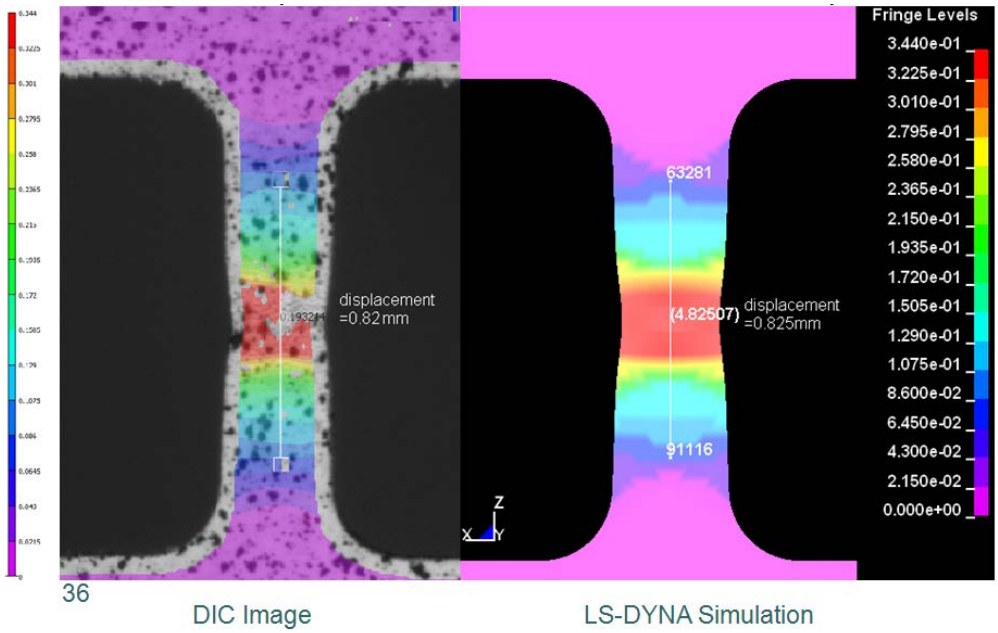

Figure 10. First principal plastic strain contour at failure comparison

The process described in this section takes the raw data and smoothes it to ensure that the analysis will properly converge and execute. It also avoids using the erroneous assumptions described in section 2.1.2. The input data developed in this process matches the actual test data

as closely as possible while removing high-frequency oscillations and negative-slope areas that could cause convergence problems.

2.2 ISOTHERMAL EFFECTS

The method described in section 2.1 is valid for all quasistatic, isothermal, uniaxial tensile tests independent of the temperature at which they were performed. The quasistatic testing must be performed at a low-enough strain rate that the process is isothermal and no thermomechanical coupling occurs during the experiment. The yield curve obtained by the process described in section 2.1 can then be allocated to the specific temperature at which the test was conducted, which is necessary because *MAT_224 requires an isothermal input curve.

In this way, a table of isothermal, temperature-dependent yield curves can be created by individually simulating all high- and low-temperature tensile tests for a given strain rate without considering any thermal coupling in the simulations. That table can then be used (in conjunction with the table of rate-dependent yield curves) as input for simulations of dynamic experiments in which thermal effects and strain-rate effects occur simultaneously and interact with each other, such as in cases in which the strain rate is high enough and the test is concluded quickly enough that there is no time for conductive dissipation of the heat energy created during the material deformation process.

2.3 STRAIN RATE DEPENDENCY

2.3.1 Tabulated Input

Rolled titanium alloy Ti-6Al-4V plate has a strain rate and temperature dependency in the plastic region:

$$\sigma_{ij} = \sigma_{ij}(\varepsilon_{ij,}\dot{\varepsilon}_{ij,}T) \tag{26}$$

Multiple tensile tests were conducted using different strain rates. Each of the different strain rate tests was processed using the method described in section 2.1. The end result is shown in figure 11; each curve represents the plastic strain versus stress relationship corresponding to a particular strain rate.

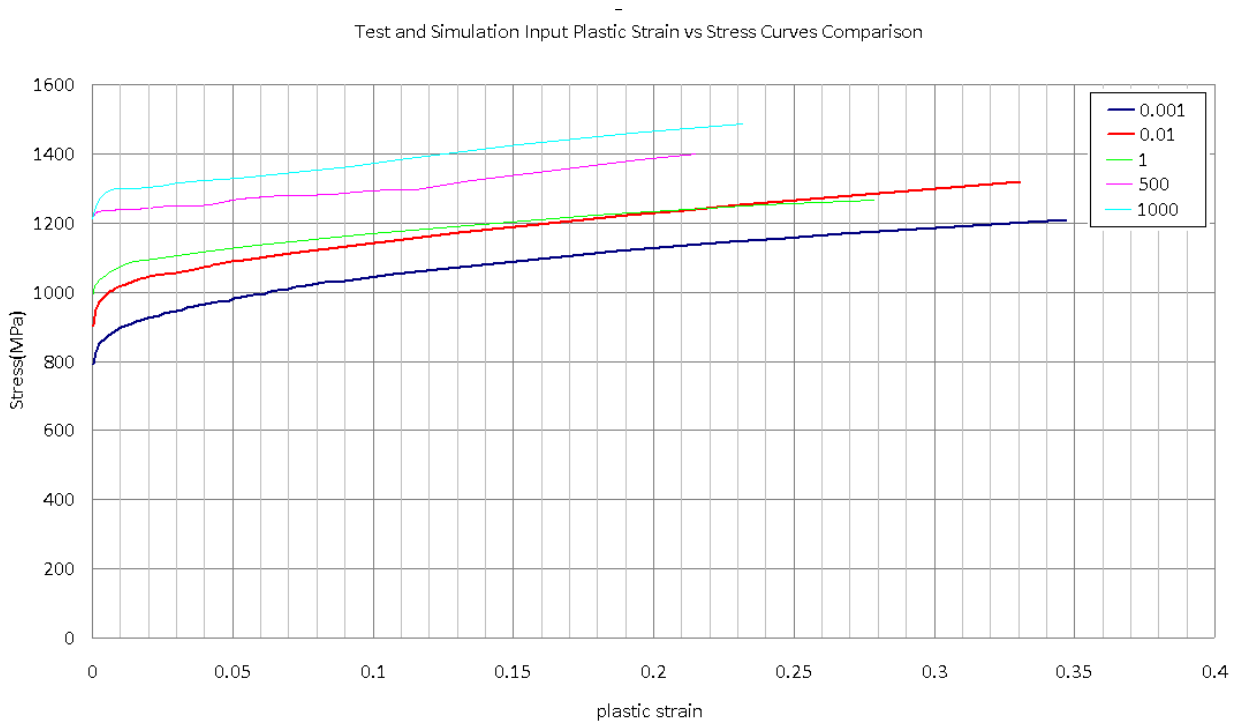

Figure 11. Plastic strain, stress relationship of rolled Ti-6Al-4V sheet under different strain rates

These curves were bundled together as a tabulated input for *MAT_224 [1]. Additional curves representing intermediate and higher strain rates were created through interpolation and extrapolation, as described in section 2.3.3. Intermediate curves are created internally by LS-DYNA through linear interpolation between user input curves. Unlike material models that use curve-fitting to fit an analytical formula to the test data and derive values for material constants, this method reads all of the input curves and precisely generates an internal yield surface numerically.

2.3.2 Strain Rate is Not a Constant

Initially, the strain rate is assumed to be either the nominal strain rate of the test or the grip speed divided by the initial length of the sample covered by the extensometer. However, this assumption is incorrect and there are two influential factors. First, it is simple (see the derivation in appendix A, section A.4) to show that:

$$\frac{d\varepsilon}{dt}(t) = \frac{1}{l(t)}\frac{dl}{dt} \tag{27}$$

Consequently, the strain rate is not constant under constant grip loading speed. Though the strain rate is uniform over the sample until necking occurs, it varies (decreases) with time if the grip speed is constant.

Second, after the onset of necking, all plastic deformation will localize in the necked area, whereas the plastic strain will remain constant outside the neck. Therefore, after necking, the strain rate will increase in the necked area and will no longer be uniform over the sample.

As shown in figure 12, within the gauge length, L_0, the specimen is uniformly deformed before necking. After necking, the deformation is localized. Only a small piece of material at the necking point undergoes further deformation, whereas the material elsewhere remains at constant plastic strain.

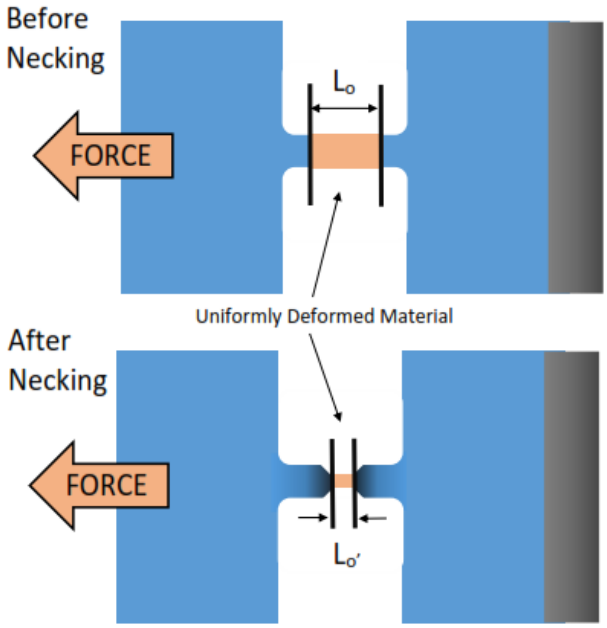

Figure 12. Length of uniformed deformed material is much shorter after necking

Assuming the deformation at the necking point is still uniform over a smaller distance, L_0', then the engineering strain rate before necking is:

$$\dot{\varepsilon}_{eng\_bf\_necking} = \frac{\dot{L}(t)}{L_0} \tag{28}$$

whereas the engineering strain rate after necking is:

$$\dot{\varepsilon}_{eng\_af\_necking} = \frac{\dot{L}(t)}{L_0'} \tag{29}$$

Consequently, the engineering strain rate will increase considerably in the necked area:

$$\begin{aligned} &\because L_0^{'} << L_0 \\ &\therefore \dot{\varepsilon}_{eng\_af\_necking} > \dot{\varepsilon}_{eng\_bf\_necking} \end{aligned} \tag{30}$$

The same tendency is true for the true strain rate, though it is more difficult to show.

Other variations in the testing procedure (e.g., non-constant grip speed, non-fixed boundary conditions, etc.) may also influence the strain rate value and cause the nominal strain rate to deviate from the physical value. Therefore, the measured displacement time history from the test must be input into the numerical model to accurately simulate the strain rates that occurred in each test.

2.3.3 High Strain-Rate Sensitivity

As described in section 2.3.2, the strain rate in a test with localization is not a constant. Localization is especially early and extreme in the higher strain rate Ti-6AL-4V tests. The strain rate in the region of localization may reach values significantly above the nominal strain rate for the specimen. As a result, tension test data must be supplemented with synthetic curves generated using rate sensitivity trends from compression tests. The compression tests reached much higher strain rates than the tension test but, because of friction and boundary conditions, complete stress-strain curves are difficult to derive from compression tests. Therefore, synthetic curves are created using a combination of information from the compression and tension tests. This section describes the process of creating the synthetic curves. These synthetic curves are combined with the stress-strain curves derived directly from the tension tests. Additional trial-and-error iterations may be required before the outcome is a close match between the test and the analysis results.

Though the compression tests are also problematic in their use for defining failure, they yield excellent information on the strain-rate sensitivity of the yield stress and plastic behavior of the material. The compression tests shown in figure 13 were performed by OSU [5]. Looking at the stress at a particular strain (specifically, 5% strain) across all tests categorized by differing strain rates demonstrates the strain-rate sensitivity (see figure 13). As shown in figure 13, there is a wide spread in the stresses from the different test categories at any given strain rate. The strain rate abscissa is plotted on a logarithmic scale.

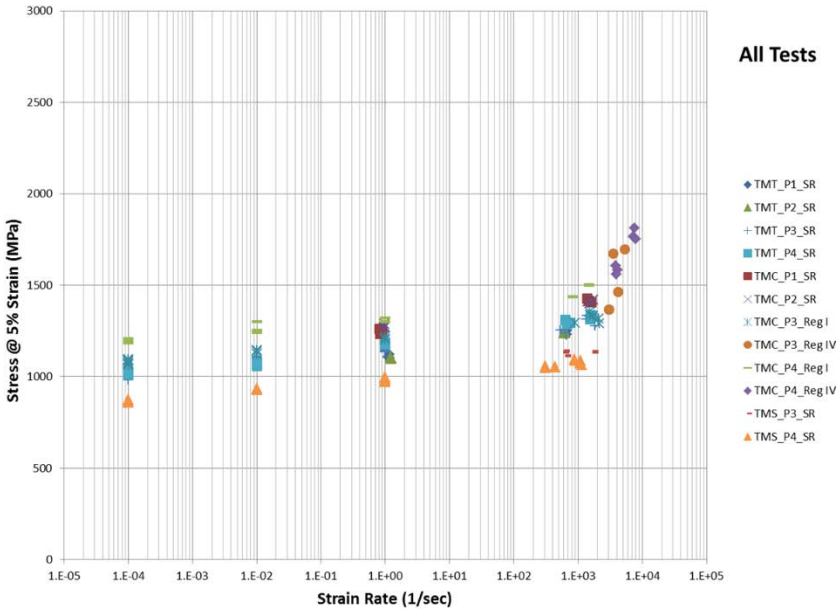

Figure 13. Stress at 5% strain – all tests

The strain-rate sensitivity was assessed using a single category of tests with the greatest range of available test results. These were compression tests, which also have the advantage of having minimal differences in test configuration between tests of varying strain rates. In addition, they maintain a more constant strain rate than the tension tests because of relatively small localization. Figure 14 shows the stress at 5% strain of the compression tests. The strain rate sensitivity is shown to conform to the theory that the yield strength increases as a logarithmic function of strain rate between rates of ~10^{-4} sec^{-1} and ~10^{3} sec^{-1} and at strain rates greater than ~10^{3} sec^{-1}, the stress increases as a linear function of the increase in strain rate due to a change in the physical processes causing the change [8].

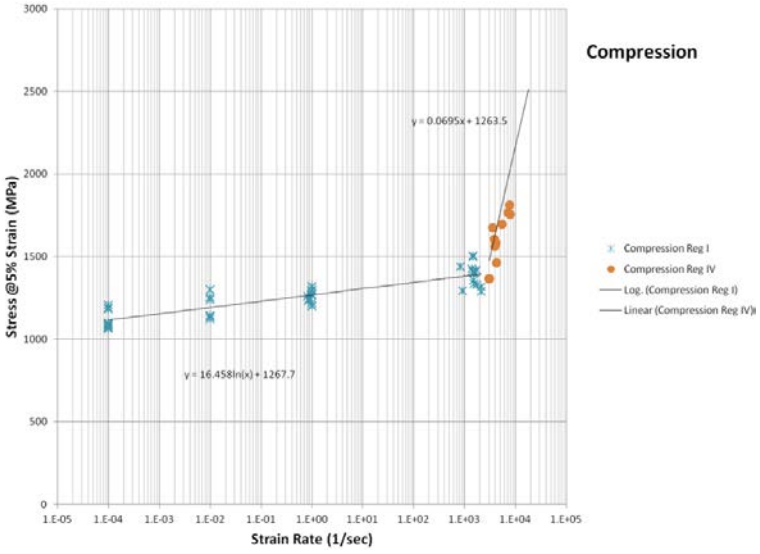

Figure 14. Stress at 5% strain—compression tests

The initial curve fits (y = 16.458 ln (x) +1267.7 for the lower strain rates and y = 0.0695 x + 1263.5 for the higher strain rates) were translated so that their stresses passed through the tension tests on the 1/2-inch plate. These tension tests are the basis of the material model presented in this report. As mentioned previously, in tension tests conducted at the nominal strain rate of 103 sec^{-1}, the strain rates are not constant. In addition, the physical processes causing the strain rate sensitive behavior of the material at these intermediate rates is transitioning and a combination of both the lower and higher rate physics. As a result, the exact stress-strain behavior can neither be obtained by extrapolation nor reading it directly from the tests. The strain-rate sensitivity was established by trial-and-error matching of the tension test data. The obtained sensitivity in the transition region is shown in figure 15.

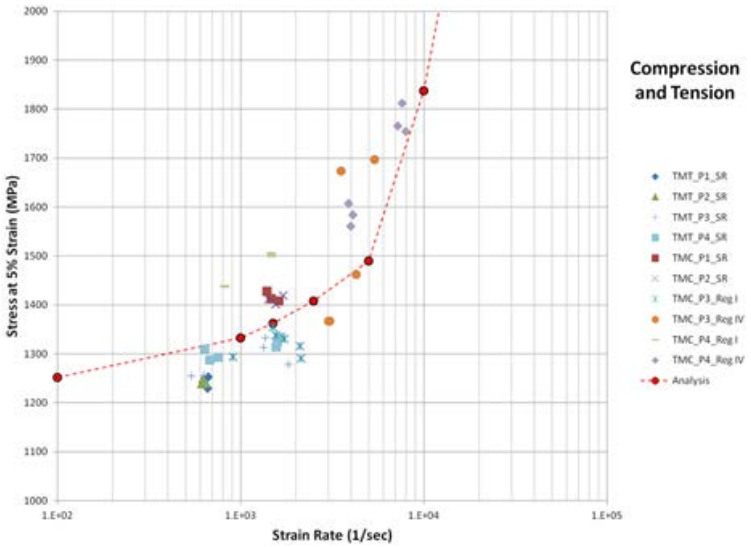

Figure 15. Stress at 5% strain—transition region

As discussed in section 2.2, the stress-strain curves required by *MAT_224 must be isothermal. The tests at the higher strain rates were simultaneously not at a constant strain rate and not isothermal; this is another reason why synthetic stress-strain curves were required. The synthetic stress-strain curve generated for the 10 sec^{-1} rate was used as the basis for all of the higher-rate curves. Each curve's stress was translated so that its value at 5% strain was at the desired value.

2.4 CONVERSION OF PLASTIC WORK INTO HEAT (TAYLOR-QUINNEY EFFECT)

In the higher-rate tests within the localized region of necking, there is not sufficient time for conduction to carry away the heat generated by the plastic deformation, and so the process becomes adiabatic. This adiabatic process causes a significant increase in the temperature in the specimen locally and governs the behavior at larger strains. As a result, the simulation of the tension tests is sensitive to the amount of energy generated by the plastic work, which is converted into thermal energy.

The percentage of plastic work that is converted into thermal energy is defined by the Taylor-Quinney coefficient, typically signified as β. Research by Ravichandran [9] and Rosakis [10] yielded values for the Taylor-Quinney coefficient for α-titanium (see figure 16) [9]. Note

that this value is not constant but is a function of both strain rate and, to a lesser extent, plastic strain. In addition, both Ravichandran and Rosakis also present variable values of βs for Al2024, which are a strong function of plastic strain. The capability to input a variable β in *MAT_224 is currently in development, so a constant β value of 0.8—which best matched the stress-strain test behavior exhibited in the tension tests—was determined through trial-and-error.

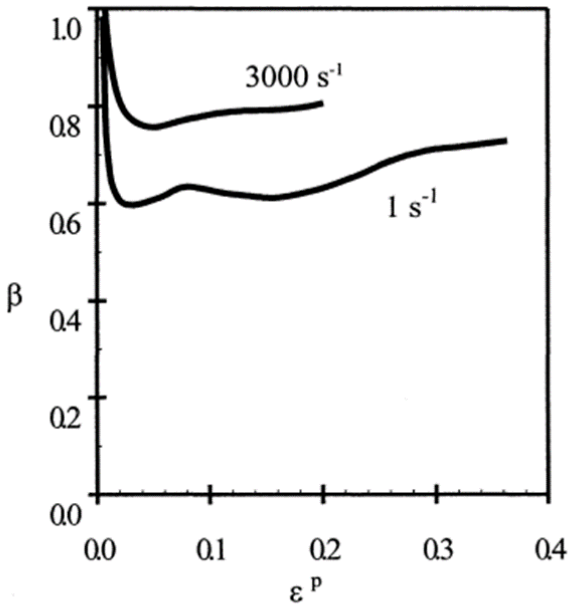

Figure 6. Fraction of plastic work rate converted to heating β vs. engineering plastic strain at two different strain rates for α-titanium.

Figure 16. The Taylor-Quinney coefficient for titanium [9]

With this information, a fully coupled thermal solution using *MAT_224 in LS-DYNA can be performed. This simulates the conduction of thermal energy away from highly strained elements. Without including conduction, temperatures will rise more in the simulations than in tests, leading to non-physical analytical results. This non-physical result will be very small in high-rate, short-duration simulations and can be safely ignored. The inclusion of conduction may be required for accurate analysis in simulations in which both high-rate and low-rate loading occurs simultaneously and significant strains are introduced into elements at a lower rate (i.e., longer duration simulation, such as full engine blade loss) and at high rates.

In the future, once tabularized β input has been included in *MAT_224, a rate-dependent β_{eff} may be defined. This would allow for the avoidance of using the fully coupled thermal solution when it might be otherwise required. The β_{eff} could be reduced at lower rates, therefore balancing out the thermal energy being produced in an element. By reducing this thermal energy, approximately the same amount that would be conducted away in a fully coupled thermal solution, an accurate structural analysis could be performed.

2.5 FLOW CHART OF STRESS-STRAIN RELATIONSHIP MODELING PROCEDURE

This section provides a flow chart (see figure 17) showing where iterations are made to improve the results.

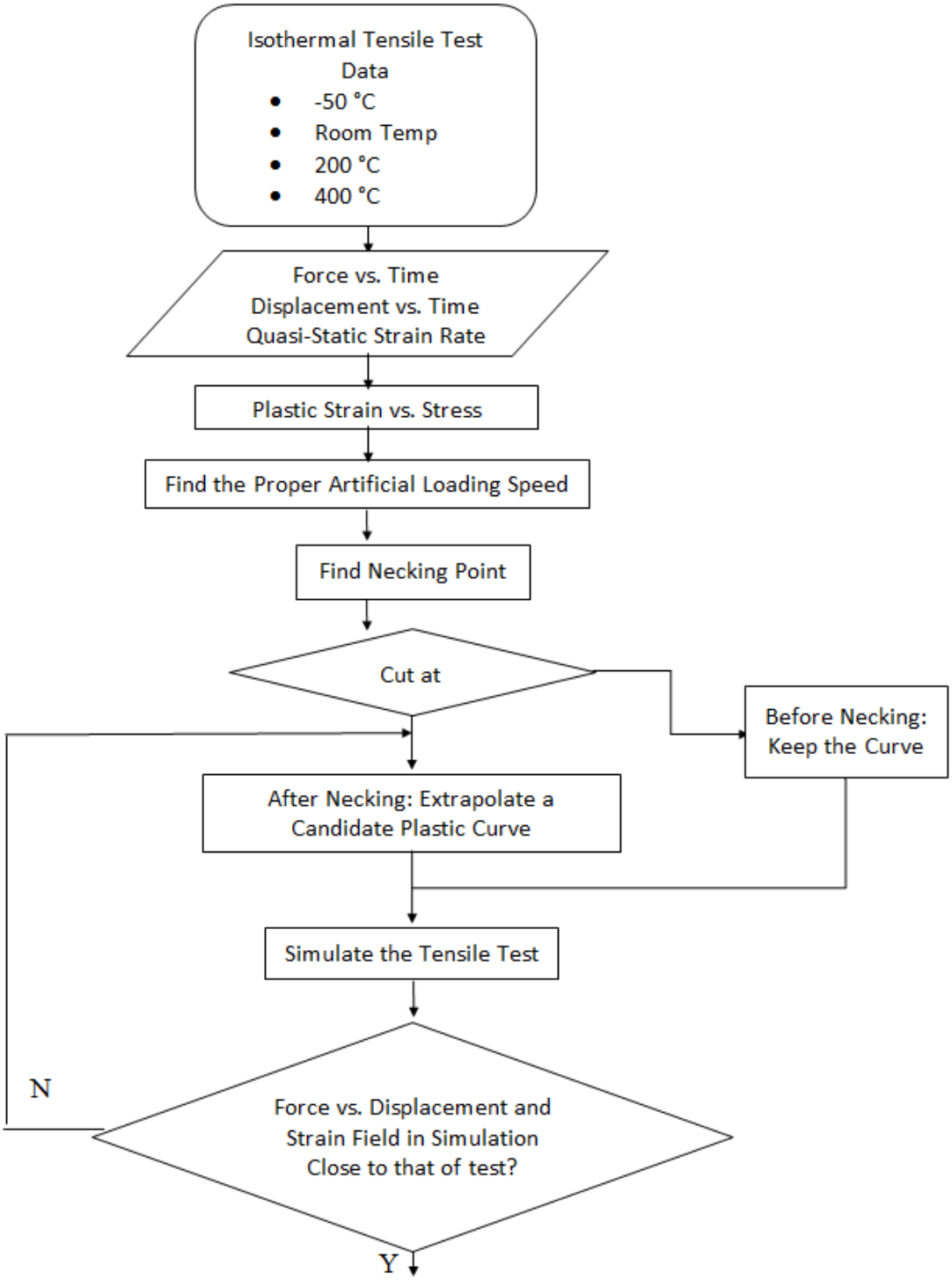

Figure 17. Flow chart of stress-strain relationship modeling procedure

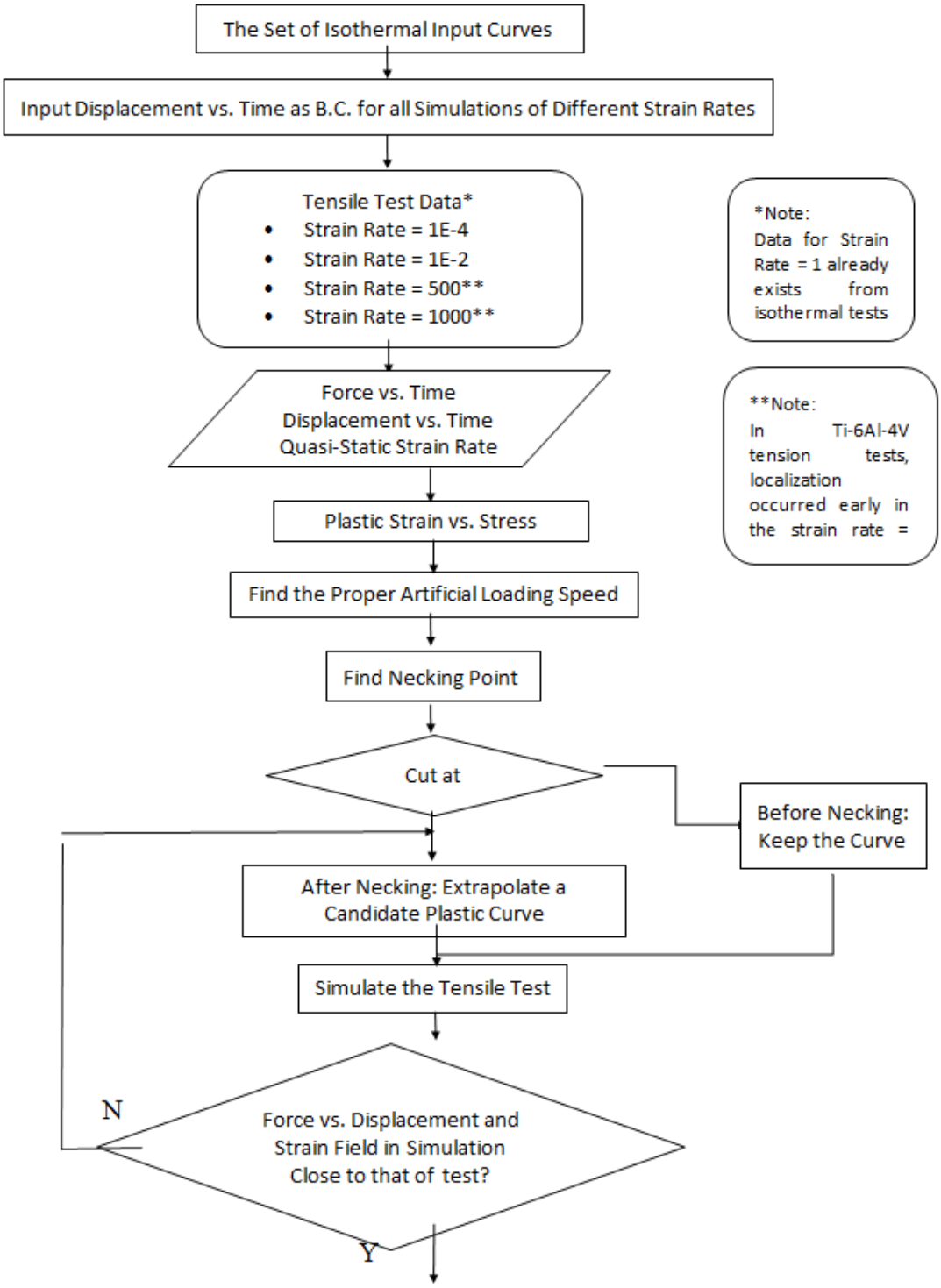

Figure 17. Flow chart of stress-strain relationship modeling procedure (continued)

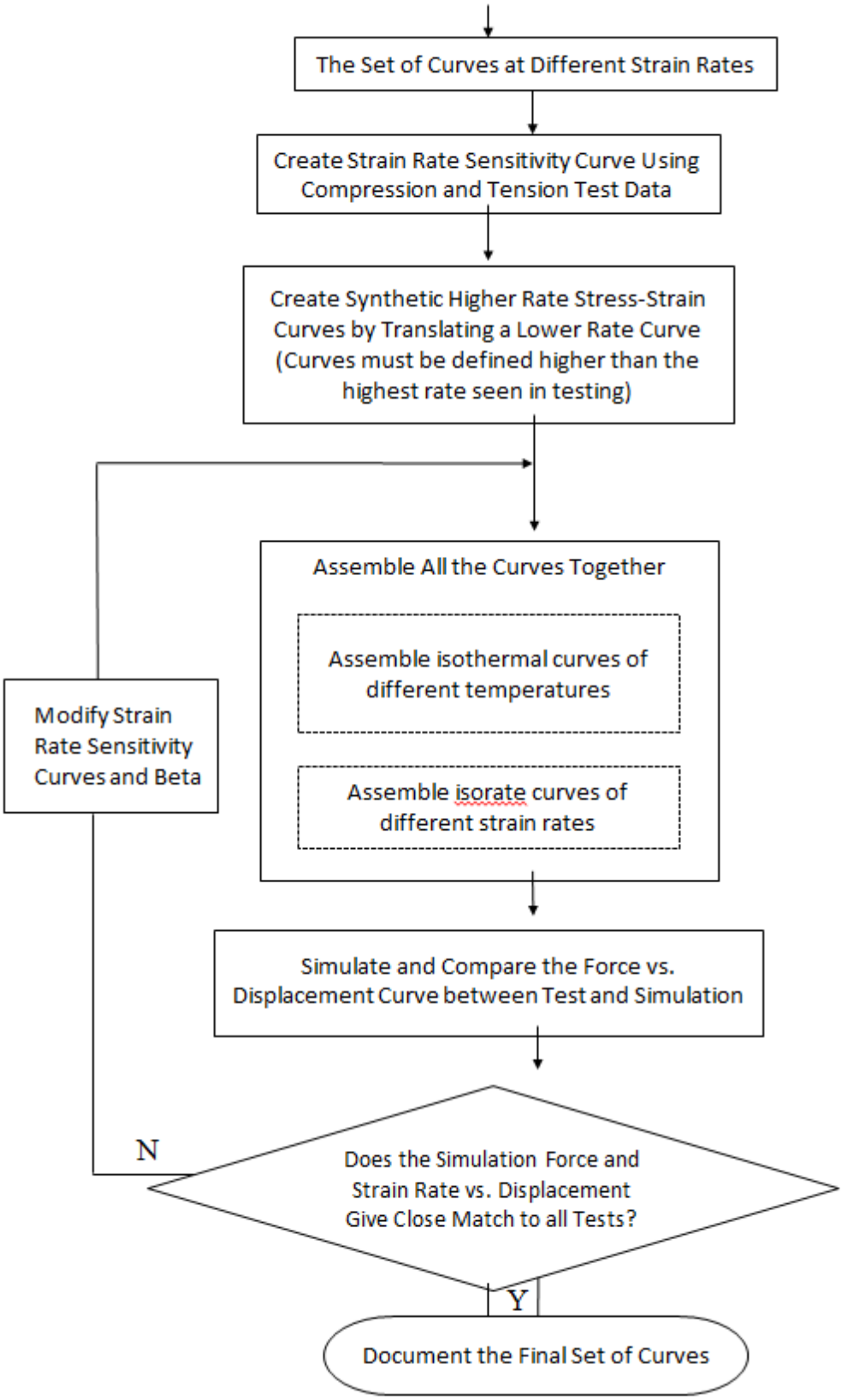

Figure 17. Flow chart of stress-strain relationship modeling procedure (continued)

3. MATERIAL MODEL CREATION BY SIMULATION OF MECHANICAL PROPERTY TESTS

3.1 TEST DATA

The test data include time, force, and displacement information. Every test comes with a computer-aided design image showing the exact specimen dimensions from measurement. A DIC image taken at the time of failure (the last data point of the test data) is also included [4].

The tests in table 1 are provided by and documented in Yatnalkar [3], Hammer [4], and Seidt [5], of OSU.

Table 1. Tests series provided by OSU

Test Series	Test Name	Plate Stock	Specimen type	Specimen Orientation	Strain Rate	Temperature °C
Tension Strain Rate Series	M2-TMT-P4-SG1-O1-SR1-T1-N1	0.5"	Flat Dogbone	Rolled	1.00E-04	RT
	M2-TMT-P4-SG1-O1-SR1-T1-N3	0.5"	Flat Dogbone	Rolled	1.00E-04	RT
	M2-TMT-P4-SG1-O1-SR1-T1-N4	0.5"	Flat Dogbone	Rolled	1.00E-04	RT
	M2-TMT-P4-SG1-O1-SR1-T1-N4	0.5"	Flat Dogbone	Rolled	1.00E-02	RT
	M2-TMT-P4-SG1-O1-5R2-T1-N2	0.5"	Flat Dogbone	Rolled	1.00E-02	RT
	M2-TMT-P4-SG1-O1-5R2-T1-N3	0.5"	Flat Dogbone	Rolled	1.00E-02	RT
	M2-TMT-P4-SG1-O1-5R3-T1-N2	0.5"	Flat Dogbone	Rolled	0.94	RT
	M2-TMT-P4-SG1-O1-5R3-T1-N3	0.5"	Flat Dogbone	Rolled	1.12	RT
	M2-TMT-P4-SG1-O1-5R3-T1-N4	0.5"	Flat Dogbone	Rolled	1.13	RT
	M2-TMT-P4-SG1-O1-5R4-T1-N1	0.5"	Flat Dogbone	Rolled	637.4	RT
	M2-TMT-P4-SG1-O1-5R4-T1-N3	0.5"	Flat Dogbone	Rolled	648	RT
	M2-TMT-P4-SG1-O1-5R4-T1-N6	0.5"	Flat Dogbone	Rolled	676.9	RT
	M2-TMT-P4-SG1-O1-SR5-T1-N3	0.5"	Flat Dogbone	Rolled	1,557	RT
	M2-TMT-P4-SG1-O1-5R5-T1-N4	0.5"	Flat Dogbone	Rolled	1,587	RT
	M2-TMT-P4-SG1-O1-5R5-T1-N5	0.5"	Flat Dogbone	Rolled	1,637	RT
Tension Temperature Series	M2-TMT-P4-SG1-O1-SR3-T2-N2	0.5"	Flat Dogbone	Rolled	1	200
	M2-TMT-P4-SG1-O1-SR3-T2-N3	0.5"	Flat Dogbone	Rolled	1	200
	M2-TMT-P4-SG1-O1-SR3-T2-N4	0.5"	Flat Dogbone	Rolled	1	200
	M2-TMT-P4-SG1-O1-SR3-T3-N2	0.5"	Flat Dogbone	Rolled	1	400
	M2-TMT-P4-SG1-O1-SR3-T3-N4	0.5"	Flat Dogbone	Rolled	1	400
	M2-TMT-P4-SG1-O1-SR3-T3-N5	0.5"	Flat Dogbone	Rolled	1	400
	M2-TMT-P4-SG1-O1-5R3-T4-N1	0.5"	Flat Dogbone	Rolled	1	600
	M2-TMT-P4-SG1-O1-SR3-T4-N2	0.5"	Flat Dogbone	Rolled	1	600
	M2-TMT-P4-SG1-O1-SR3-T4-N3	0.5"	Flat Dogbone	Rolled	1	600
	M2-TMT-P3-SG1-O1-SR3-T5-N2	0.5"	Flat Dogbone	Rolled	1	-50
	M2-TMT-P3-SG1-O1-SR3-T5-N3	0.5"	Flat Dogbone	Rolled	1	-50
	M2-TMT-P3-SG1-O1-SR3-T5-N5	0.5"	Flat Dogbone	Rolled	1	-50
	M2-TMT-P4-SG1-O1-SR3-T5-N2	0.5"	Flat Dogbone	Rolled	1	-50
	M2-TMT-P4-SG1-O1-SR3-T5-N3	0.5"	Flat Dogbone	Rolled	1	-50
	M2-TMT-P4-SG1-O1-SR3-T5-N4	0.5"	Flat Dogbone	Rolled	1	-50

RT = room temperature

3.2 TEMPERATURE EFFECT

Fifteen tests measuring the temperature effect of the material are listed in the Tension Temperature Series section of table 1 and plotted in figure 18. In addition to the room temperature tests, four additional temperature groups were selected: -50°C, 200°C, 400°C, and 600°C.

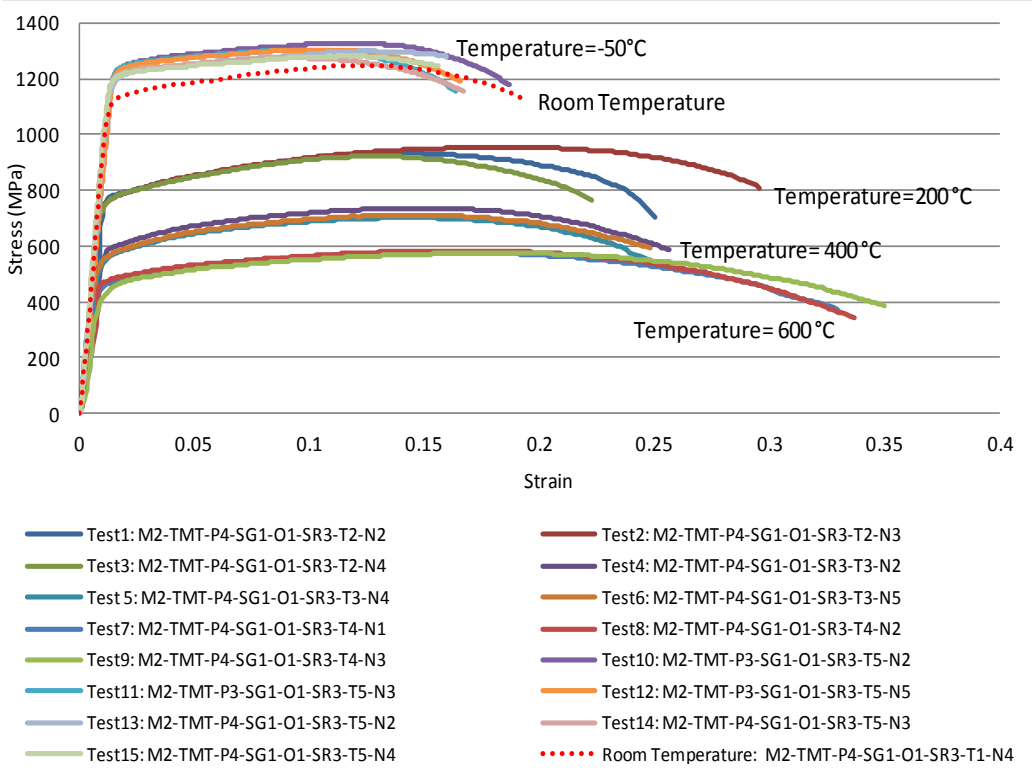

Figure 18. Temperature effect

The temperature effect was studied with input decks for *MAT_224 based on single hardening curves at the test rate of 1 sec^{-1}. All of the thermal tests were conducted at this rate. Use of a single stress-strain curve creates a strain-rate insensitive analysis and allows the displacement to be applied at an artificially high grip speed of 1 m/s.

In these models, the sample dimensions match the corresponding test specimen precisely. The simulation units are kg, mm, ms, kN, and GPa.

3.2.1 Stress-Strain Relationship at Room Temperature

Three tests at room temperature and strain rate 1 sec^{-1} are listed in table 2. An engineering strain versus stress relationship was derived using equation 8, which gives the engineering stress-strain curves in figure 19. Test 6: M2-TMT-P4-SG1-O1-SR2-T1-N3 was selected to represent this group of data and undergo further processing. The selection criteria were based on engineering judgment considering smoothness, representation, and the monotone increasing function requirement of the input curve. Following the procedure introduced in section 2.1.3, the true stress-strain relationship is shown in figure 20.

Table 2. Strain rate dependence series data of strain rate = 1 sec^{-1}

Series	Test Name	Plate Stock	Specimen Geometry	Specimen Orientation	Strain Rate (sec^{-1})	Temp (°C)
Tension Strain Rate Dependence	M2-TMT-P4-SG1-O1-SR3-T1-N2	0.5″	Flat Dogbone	Rolled	1	RT
	M2-TMT-P4-SG1-O1-SR3-T1-N3	0.5″	Flat Dogbone	Rolled	1	RT
	M2-TMT-P4-SG1-O1-SR3-T1-N4	0.5″	Flat Dogbone	Rolled	1	RT

RT = room temperature

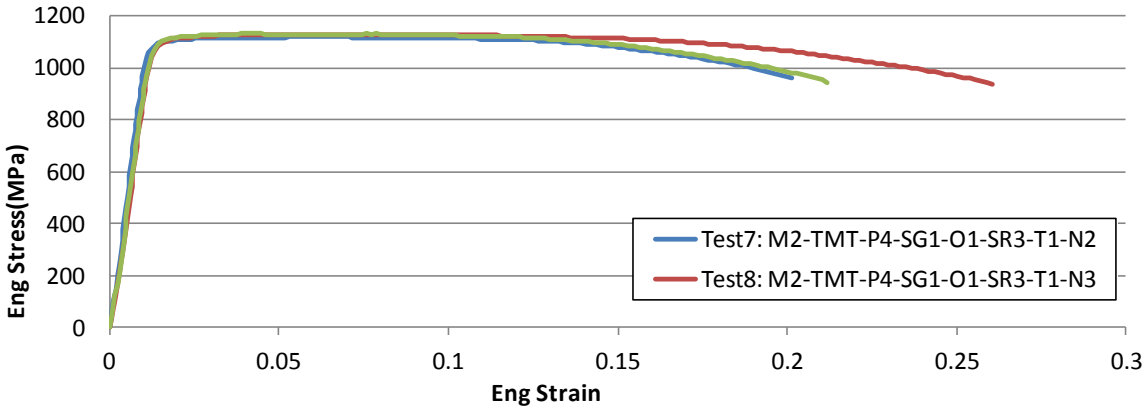

Figure 19. Engineering stress-strain relationship of strain rate = 1 sec^{-1} tests

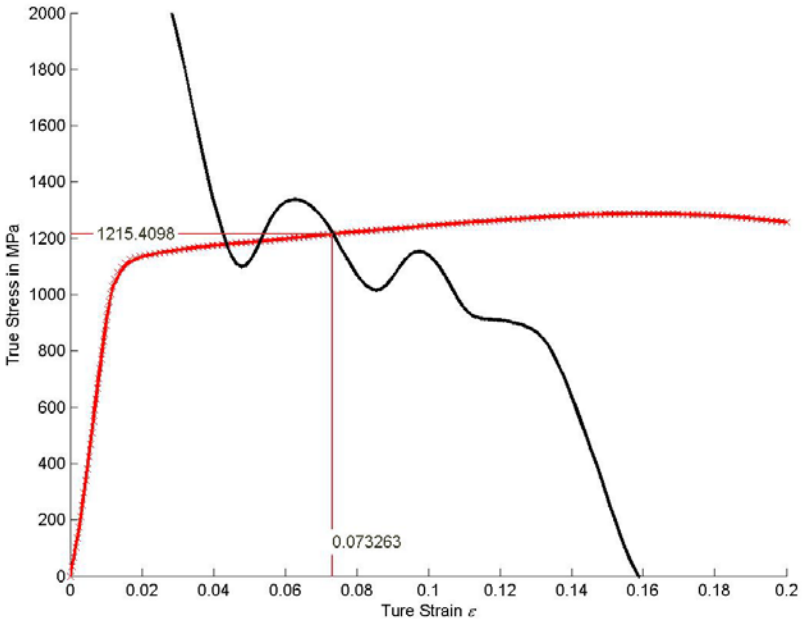

Figure 20. True stress-strain relationship and necking point judgment of strain rate = 1 sec-1 tests (Test: M2-TMT-P4-SG1-O1-SR3-T1-N3)

By applying equation 11 and adopting a Young's modulus of 92.0 GPa (derived directly from the test data, as discussed in section 2.1.1), the plastic strain versus stress relationship was calculated. To determine the necking point, the true strain versus stress curve was twice smoothed by an 18-point moving average and, subsequently, equations 24 and 25 (differentiation stress with respect to strain) were used to obtain the tangent modulus curve. Another 18-point moving average was performed on the tangent modulus curve, and the intersection between these two lines defines the necking point, as shown in figure 20. The true stress and true strain at necking were recorded.

Corresponding plastic strain at necking was evaluated using equation 21, and only the part of the hardening curve before necking was kept. By applying equation 22, the hardening curve was extrapolated beyond necking.

Twenty-eight curves were generated by varying the exponent *n* between ~0.1 and 0.2 (see figure 21). The 28 values of *n* were obtained by non-uniform incremental steps. The remaining two parameters, ε_e and *k*, were calculated using equation 25. Extrapolation was performed using MATLAB. Each of the generated hardening curves was used in an LS-DYNA *MAT_224 input deck simulating the tensile test. An example LS-DYNA input deck can be found in appendix F. In this model, the sample dimensions match the sample of test M2-TMT-P3-SG1-O1-SR1-T1-N1 exactly: width = 2.062mm and thickness = 0.861mm.

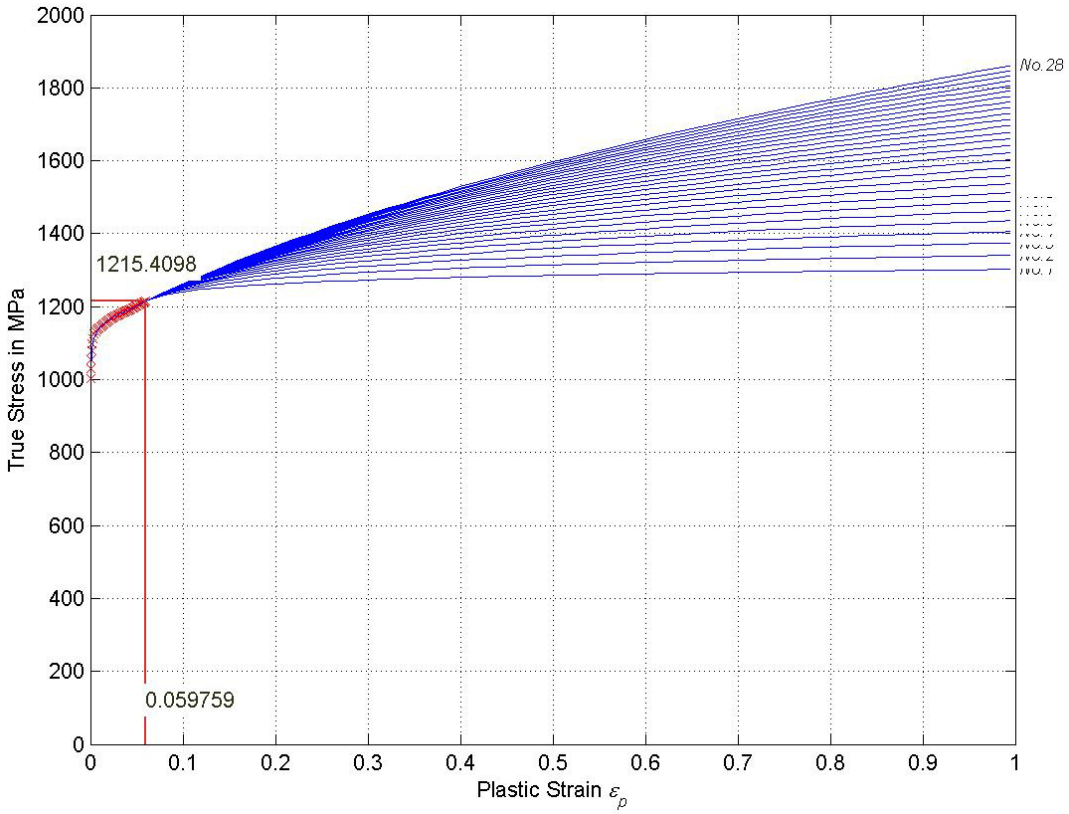

Figure 21. Plastic strain versus stress relationship of strain rate = 1 sec^{-1} (Test 8: M2-TMT-P4-SG1-O1-SR3-T1-N3)

DATABASE_CROSS_SECTION was defined to measure the cross-sectional force. Two nodal points corresponding to the base points of the extensometer are stored in the NODOUT file (see figure 22). The difference in *z* displacement of these two nodal points gives the elongation of the extensometer as predicted in the simulation. The measuring nodes have an initial distance of 4 mm. The cross-section for force measurement is located at the center of the specimen. A cross-plot of this elongation with the cross-sectional force can be directly compared to the force displacement curve from the test.

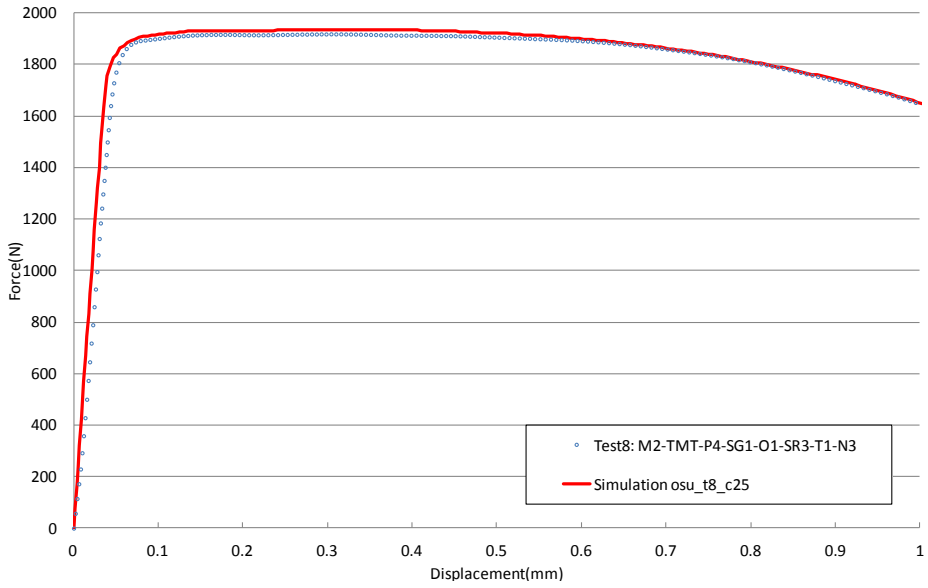

Figure 22. Force displacement result, curve #25 (Test M2-TMT-P4-SG1-O1-SR3-T1-N3)

This simulation was performed repeatedly for all the extrapolated candidate input curves until one matched the force displacement response of the test. The stress-strain curve in figure 23 gives the best match, as demonstrated in figure 22.

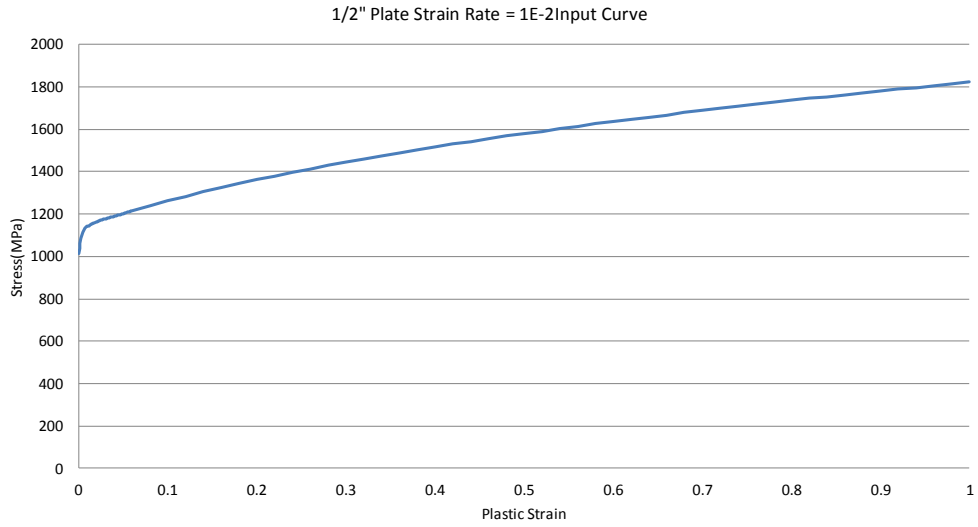

Figure 23. Strain rate = 1 sec^{-1} group hardening curve input result

In figure 24, a simulation contour of the 1st principal strain is compared to the DIC image from the test at the time right before failure; the result yields good agreement.

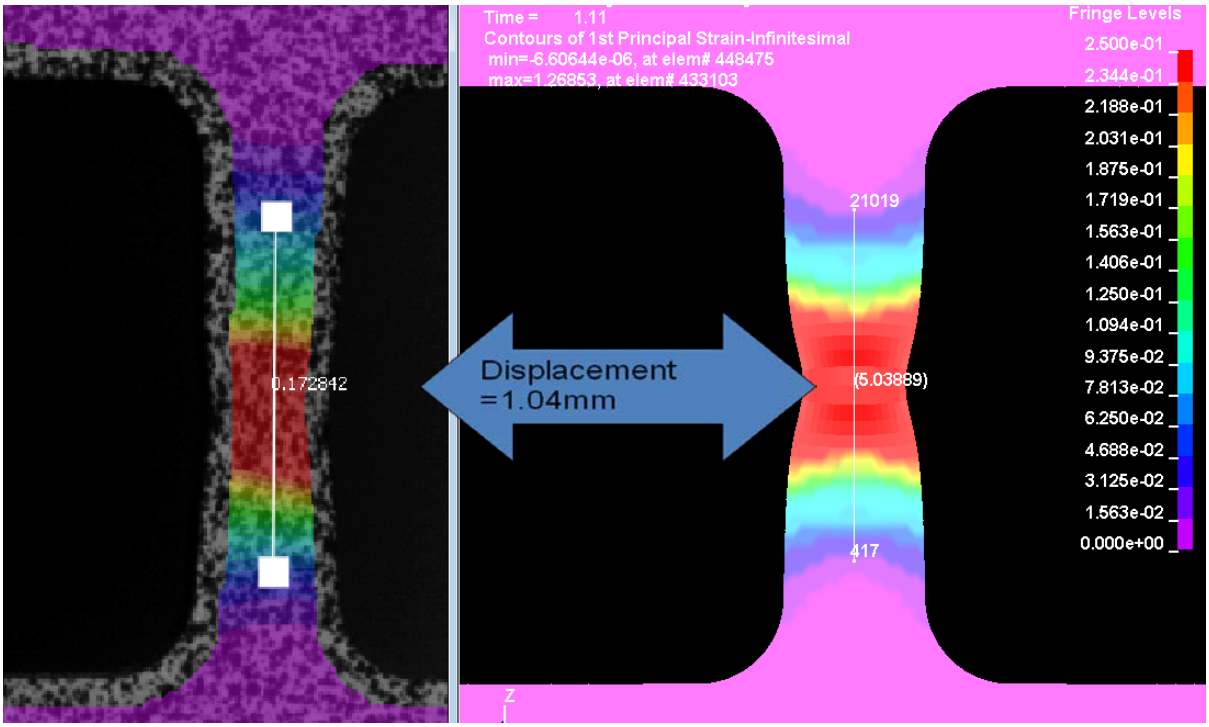

(a) (b)

Figure 24. The (a) plastic strain DIC image immediately before failure and (b) 1st principal strain simulation contour immediately before failure time (Test: M2-TMT-P4-SG1-O1-SR3-T1-N3; Strain Rate = 1 sec^{-1})

3.2.2 Stress-Strain Relationship at Other Temperatures

By applying the same curve extrapolation and selection method used in section 3.2.1, isothermal, temperature-dependent stress-strain curves were generated (see figure 25).

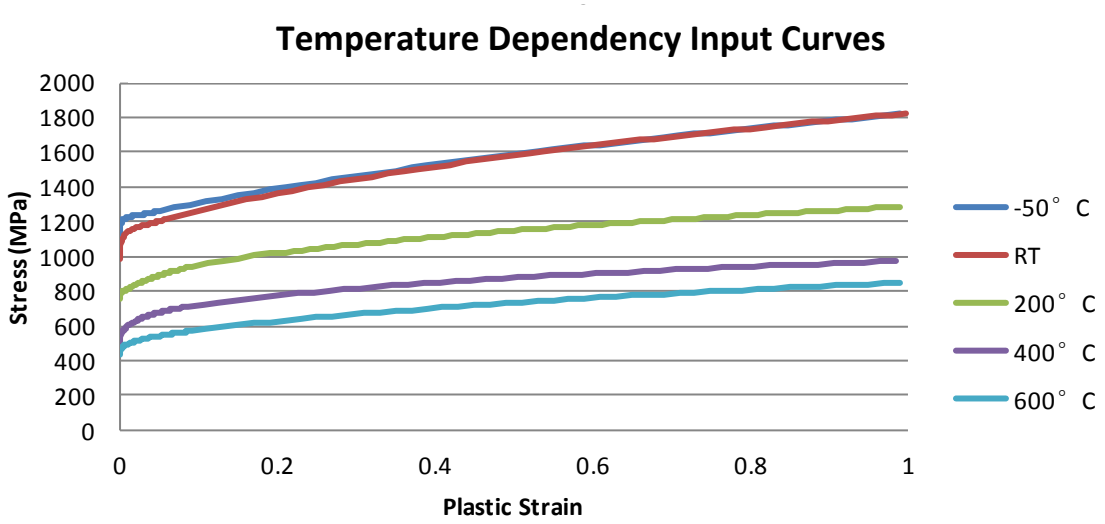

Figure 25. Temperature dependency input curves

The resulting force-displacement comparisons for four individual temperatures (600°C, 400°C, 200°C, and -50°C) are shown in figures 26–29, respectively.

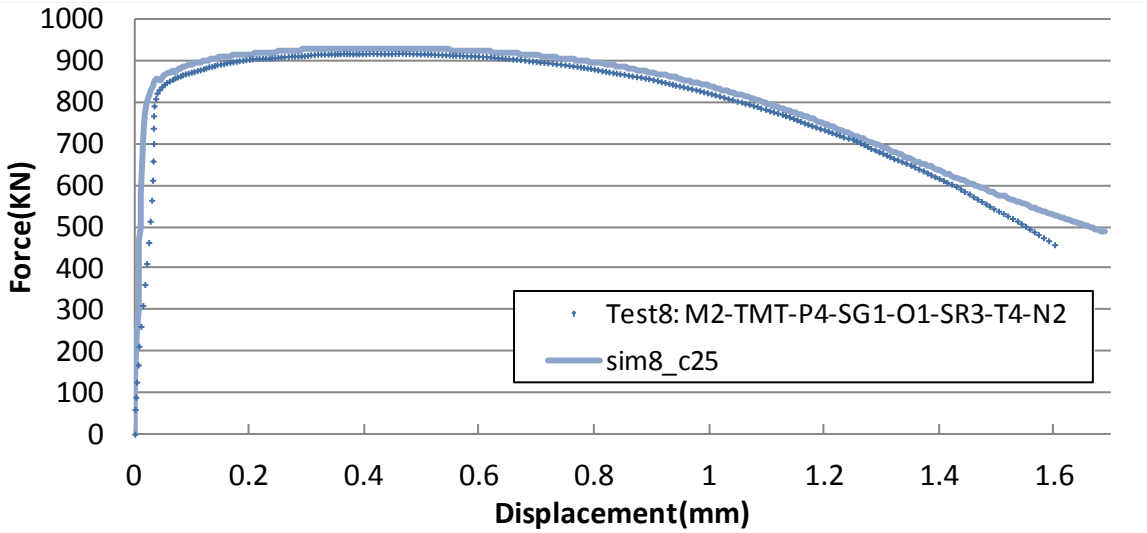

Figure 26. Force displacement curve (Test: M2-TMT-P4-SG1-O1-SR3-T4-N2; strain rate = 1 sec^{-1}; Temperature = 600°C)

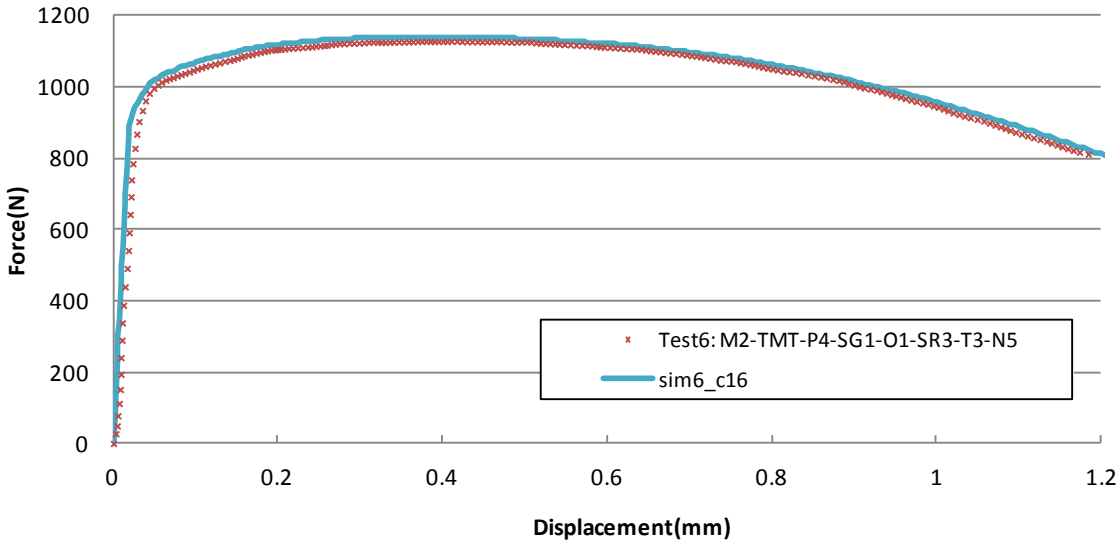

Figure 27. Force displacement curve (Test: M2-TMT-P4-SG1-O1-SR3-T3-N5; strain rate = 1 sec^{-1}; temperature = 400°C)

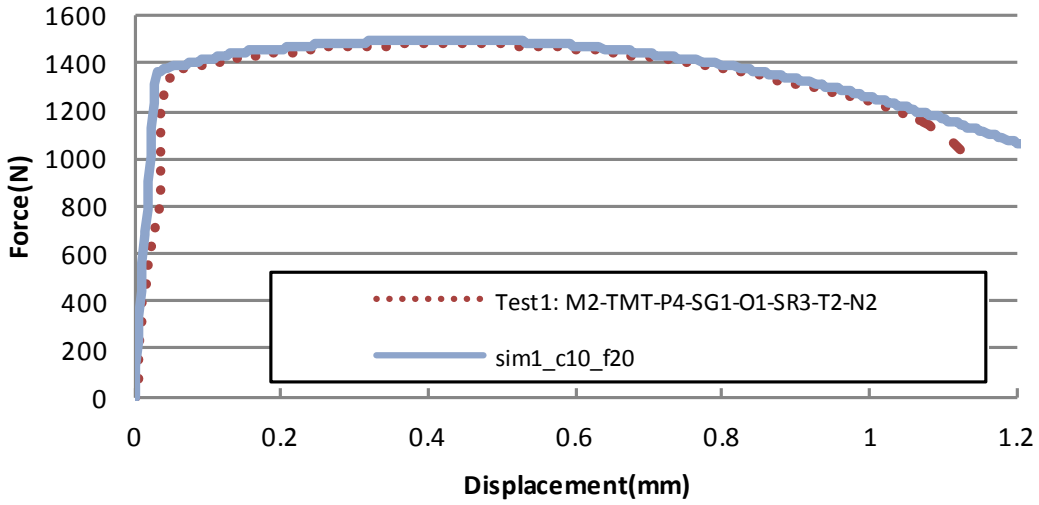

Figure 28. Force displacement curve (Test: M2-TMT-P4-SG1-O1-SR3-T2-N2; strain rate = 1 sec^{-1}; temperature = 200°C)

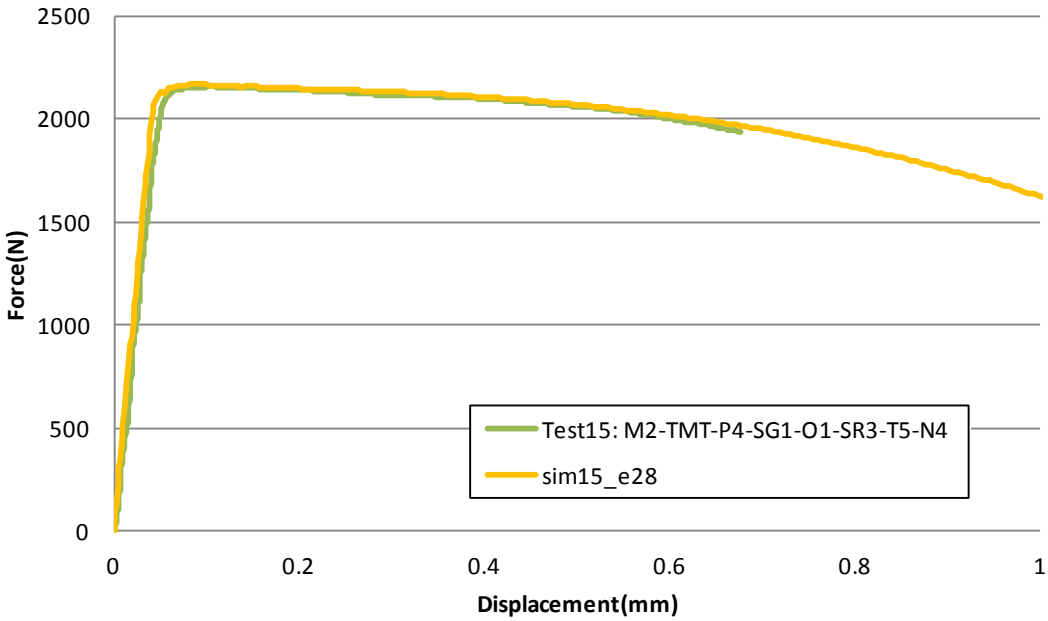

Figure 29. Force displacement curve (Test: M2-TMT-P4-SG1-O1-SR3-T2-N2; strain rate = 1 sec^{-1}; temperature = -50°C)

The 1st principal strain contours of the DIC and the simulation for tests at 600°C, 400°C, and 200°C are shown in figures 30–32, respectively.

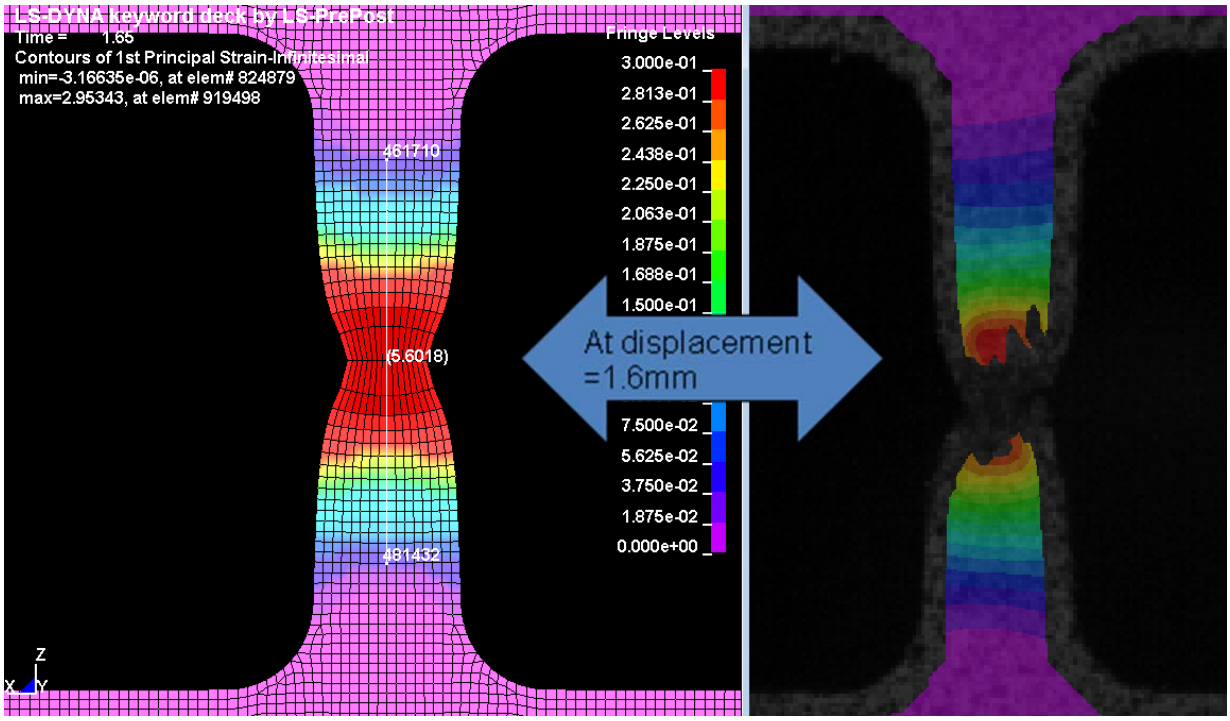

(a) (b)

Figure 30. The (a) simulation contour and (b) DIC image (Test: M2-TMT-P4-SG1-O1-SR3-T4-N2; strain rate = 1 sec^{-1}; temperature = 600°C)

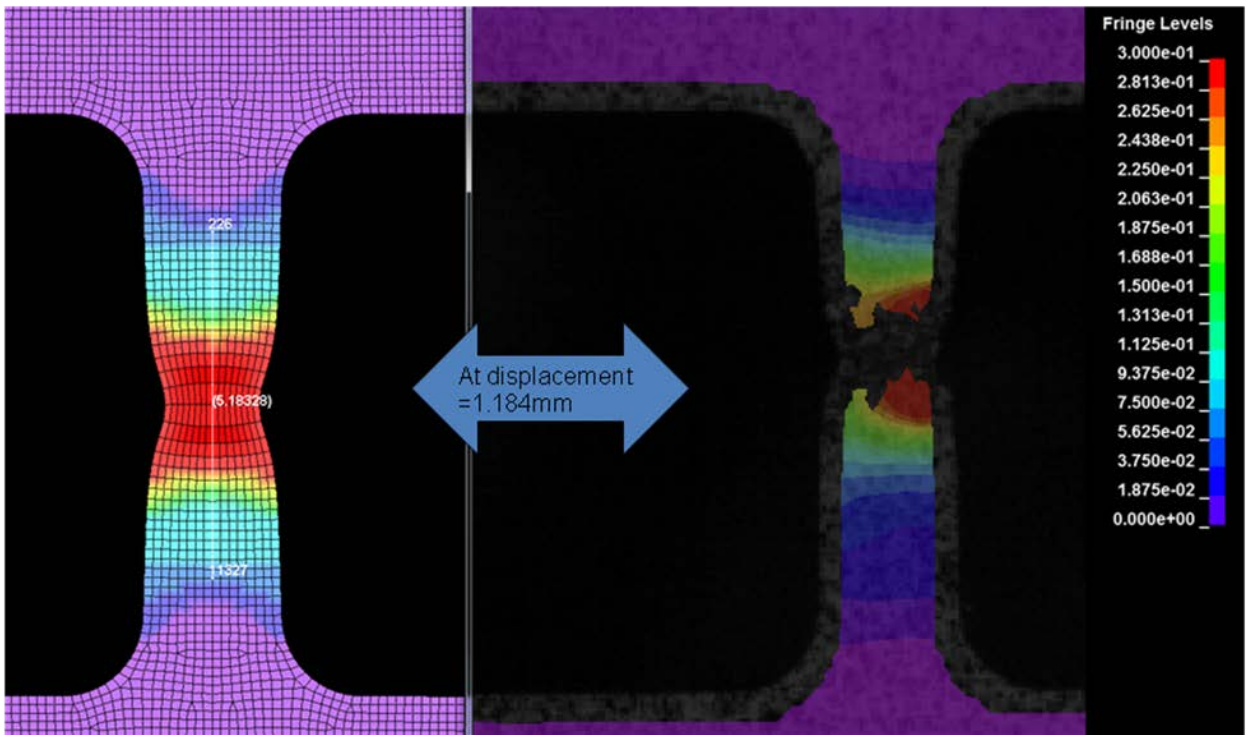

(a) (b)

Figure 31. The (a) simulation contour and (b) DIC image
(Test: M2-TMT-P4-SG1-O1-SR3-T3-N5; strain rate = 1 sec^{-1}; temperature = 400°C)

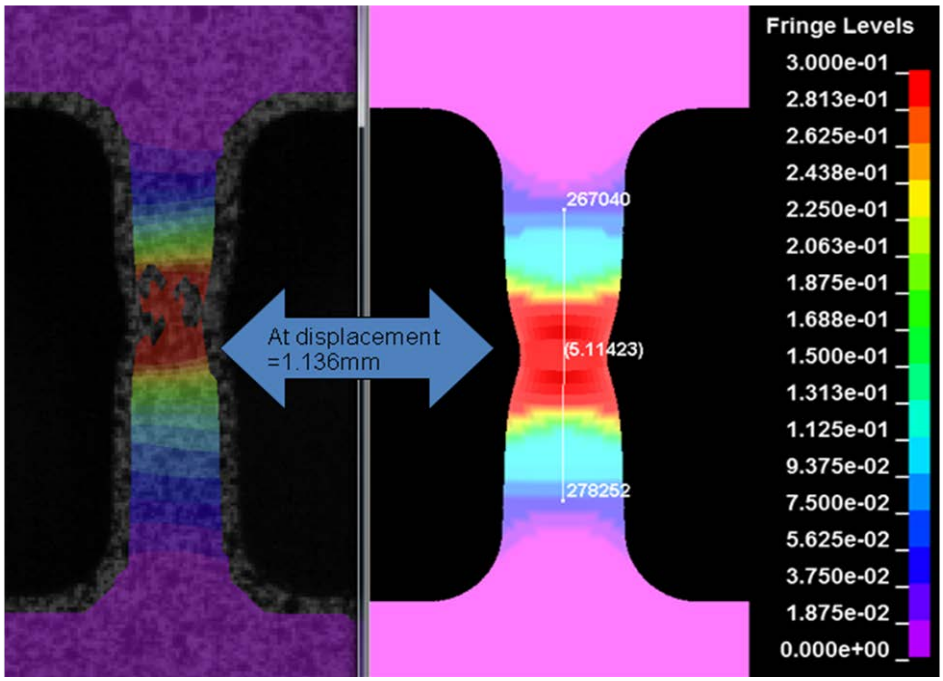

(a) (b)

Figure 32. The (a) simulation contour and (b) DIC image
(Test: M2-TMT-P4-SG1-O1-SR3-T2-N2; strain rate = 1 sec^{-1}; temperature = 200°C)

3.3 STRESS-STRAIN RELATIONSHIP AT SINGLE VARYING STRAIN RATES

A hardening curve was derived for each strain rate from the "Tension Strain Rate Dependence" series of table 3. Flat dogbone specimens were pulled at room temperature on the Instron machine. Displacement and force were measured at a fixed time interval. All simulations in section 3.4 were performed with an arbitrary loading speed of 1 m/s (for the reason given in section 2.1.3).

Table 3. Strain-rate dependence series data of strain rate = 1E-4 sec^{-1}

Series	Test Name	Plate Stock (in)	Specimen Geometry	Specimen Orientation	Strain Rate (sec^{-1})	Temp (°C)
Tension Strain Rate Dependence	M2-TMT-P4-SG1-O1-SR1-T1-N1	0.5″	Flat Dogbone	Rolled	1.0E-04	RT
	M2-TMT-P4-SG1-O1-SR1-T1-N3	0.5″	Flat Dogbone	Rolled	1.1E-04	RT
	M2-TMT-P4-SG1-O1-SR1-T1-N4	0.5″	Flat Dogbone	Rolled	1.0E-04	RT

RT = room temperature

3.3.1 Stress-Strain Relationship of Strain Rate = 1E-4 sec^{-1}

The three quasistatic tests at strain rate 1E-4 sec^{-1} are listed in table 3. Engineering strain versus stress relationship is derived using equation 8 and produces the engineering stress-strain curves shown in figure 33. Test 1: M2-TMT-P4-SG1-O1-SR1-T1-N1 and Test 3: M2-TMT-P4-SG1-O1-SR1-T1-N4 were selected to represent this strain rate and undergo further processing. The selection criterion is based on engineering judgment considering smoothness, representation, and the monotone increasing function requirement of the input curve. The final analytical results need to match these two test results using the same stress-strain input curve.

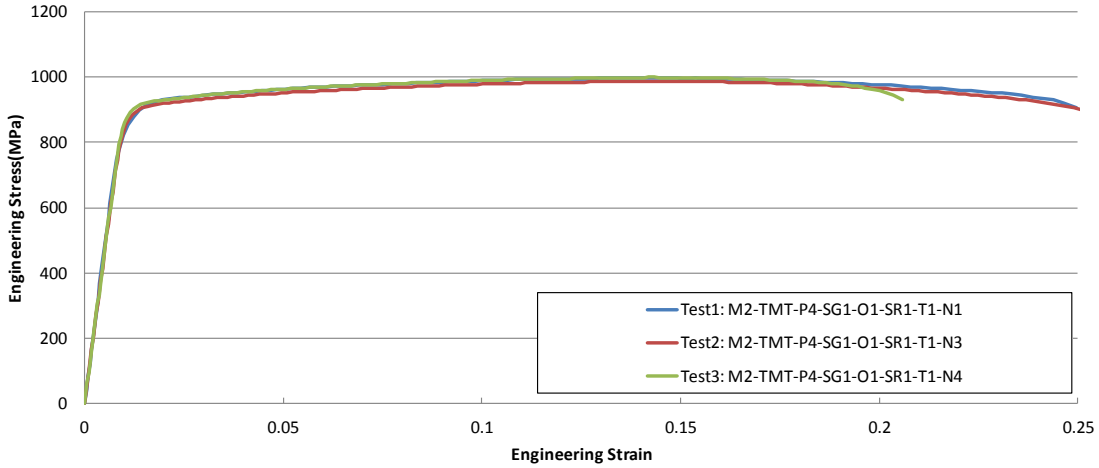

Figure 33. Engineering stress-strain relationship of strain rate = 1E-4 sec^{-1} tests

Matching each test individually is required because each specimen has a unique geometry. The exact geometry from measurement is used in the finite element model. If the exact test geometry is not used in the analysis, significant errors can result. Though the input curve, because it is a function of stress and strain, can be created from an average of all the test results, only a single geometry can be used in the simulation. The force displacement result from the simulations will vary from each other, whereas the stress-strain results will not.

Applying equations 9 and 10, the engineering stress-strain relationship is converted to a true stress-strain relationship (see figure 34).

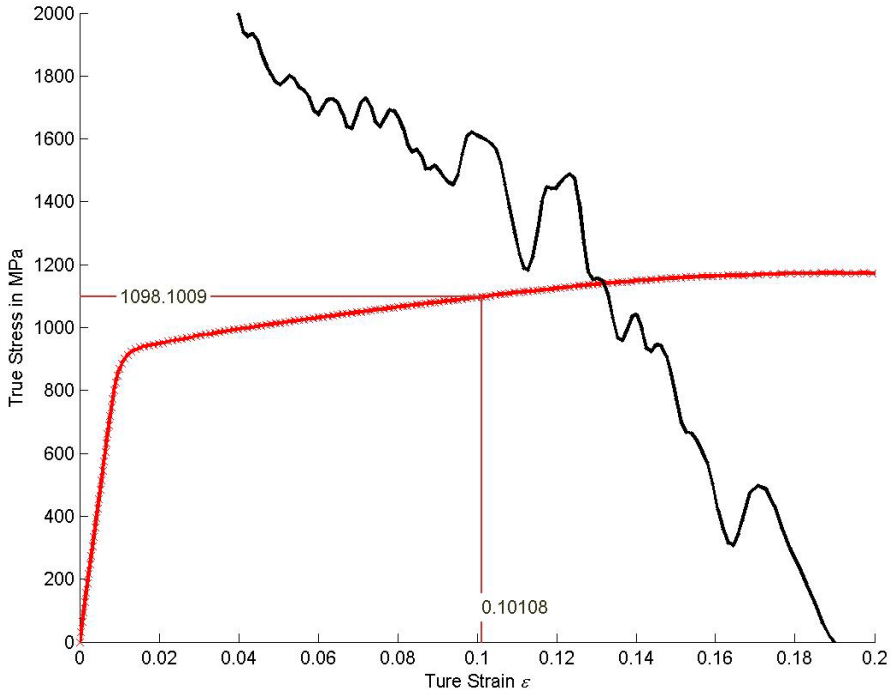

Figure 34. True stress-strain relationship and necking point judgment of strain rate = 1E-4 sec^{-1} tests (Test: M2-TMT-P4-SG1-O1-SR1-T1-N1)

By applying equation 11 and adopting a Young's modulus of 93.5 GPa (derived directly from the test data), the plastic strain versus stress relationship was calculated. To determine the necking point, the true strain versus stress curve was smoothed by a nine-point moving average; subsequently equations 24 and 25 (differentiation stress with respect to strain) were used to obtain the tangent modulus curve. Another nine-point moving average was performed on the tangent modulus curve, and the intersection between these two lines defines the necking point. Using engineering judgment, the plastic strain at necking was determined to be 0.1 sec^{-1} (see figure 34).

The true stress and true strain at necking were determined. The corresponding plastic strain at necking was evaluated using equation 21 and only the part of the hardening curve before necking was kept. By applying equation 22, the hardening curve was extrapolated beyond necking. Twenty-eight curves were generated by varying the exponent, *n*, between ~0.1 and 0.2 (see figure 35). The 28 values of *n* were obtained by non-uniform incremental steps. The remaining

two parameters, ε_e and *k*, were calculated using equation 25. Extrapolation was performed using MATLAB.

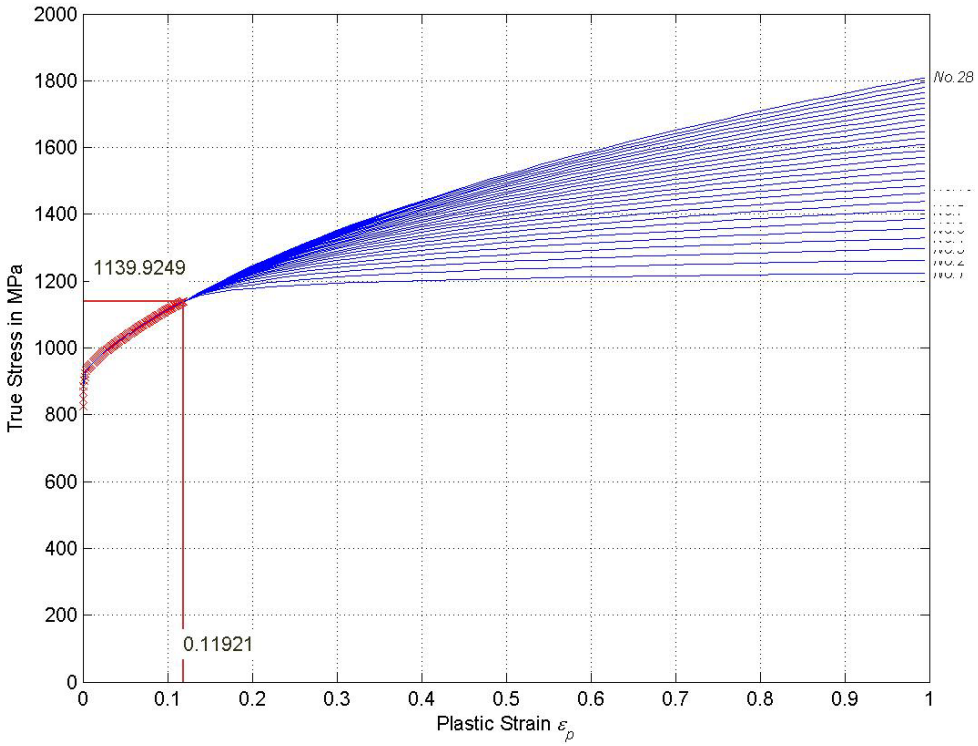

Figure 35. Plastic strain versus stress extrapolation of strain rate = 1E-4 sec^{-1} (Test 1: M2-TMT-P4-SG1-O1-SR1-T1-N1)

Each of the generated hardening curves were then entered into an LS-DYNA *MAT_224 input deck and used to perform a simulation of the tensile test (see appendix F for the LS-DYNA input decks). In this model, the sample dimensions match the sample of Test M2-TMT-P3-SG1-O1-SR1-T1-N1 exactly: width = 2.057mm, thickness = 0.826 mm.

A cross-plot of cross-section elongation with cross-sectional force is compared to the force displacement curve from the test. This simulation is repeated for all the extrapolated candidate input curves until one matches the force displacement response of the test (figure 36). Figure 37 shows the selected curve for the 1E-4 sec^{-1} strain-rate hardening curve. The extrapolation parameters used to create this curve were n = 0.18231, ε_e = 0.054066, and k = 1564.6077.

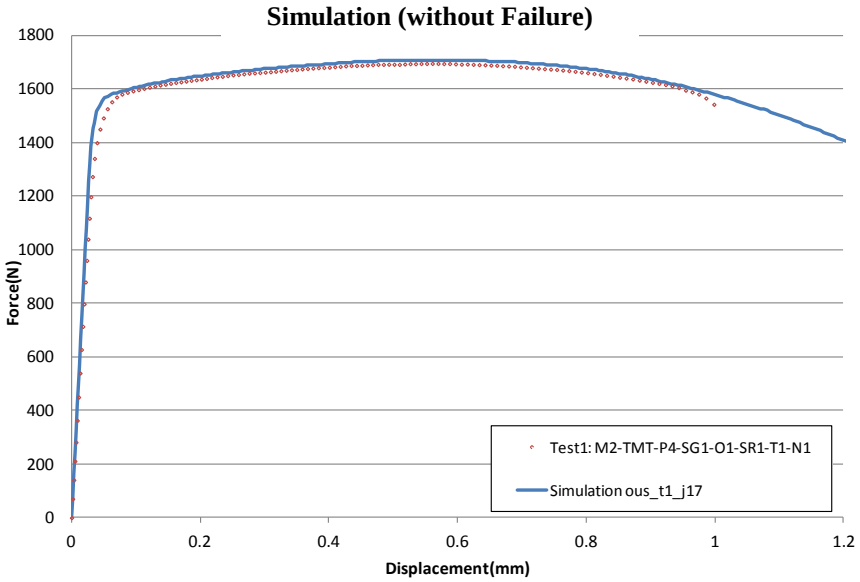

Figure 36. Force displacement result, curve #17 (Test M2-TMT-P3-SG1-O1-SR1-T1-N1)

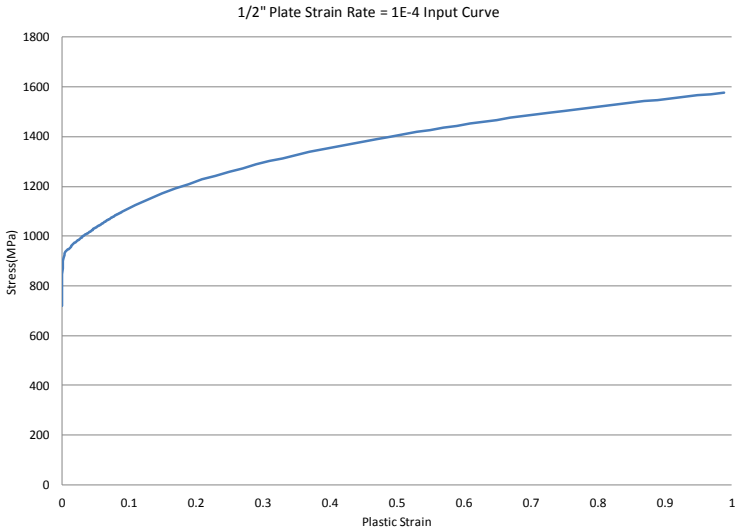

Figure 37. Strain rate = 1E-4 sec^{-1} group hardening curve input result

A simulation contour of the 1st principal strain is compared to the DIC image from the test at the time immediately before failure, with good agreement between the results (see figure 38). For verification purposes, the resulting hardening curve was also used to simulate test M2-TMT-P4-SG1-O1-SR1-T1-N4. This analysis also yields a good match with the tests for both the force displacement curve and the DIC contour (see figures 39 and 40).

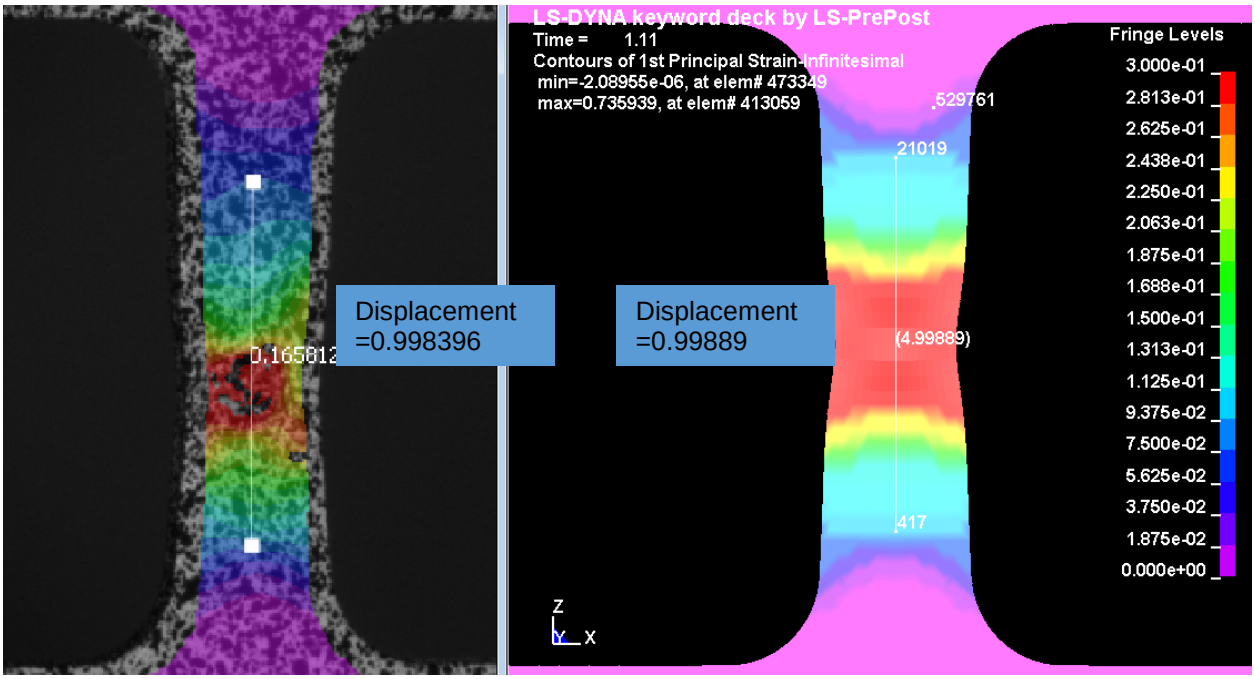

(a) (b)

Figure 38. The (a) plastic strain DIC image immediately before failure and (b) 1st principal strain simulation contour immediately before failure (Test 1: M2-TMT-P4-SG1-O1-SR1-T1-N1; strain rate = 1E-4 sec^{-1})

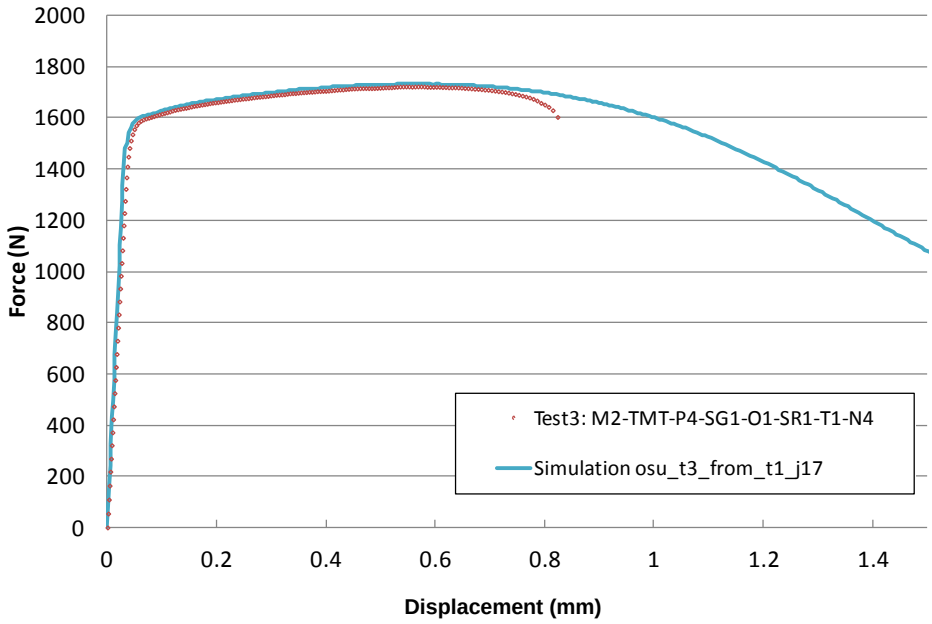

Figure 39. Force displacement result, curve #17 (Test M2-TMT-P4-SG1-O1-SR1-T1-N4)

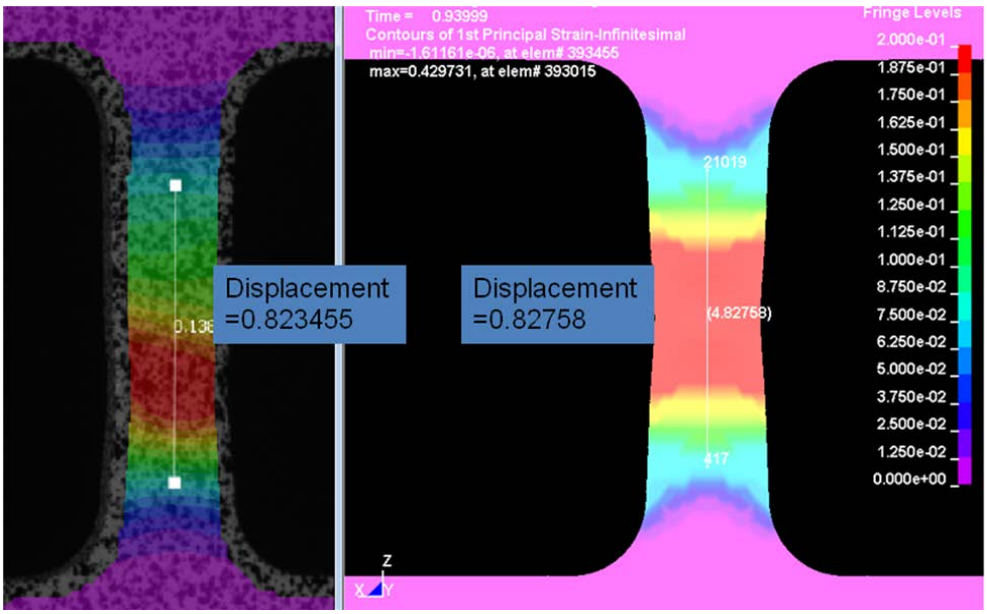

(a) (b)

Figure 40. The (a) plastic strain DIC image immediately before failure and (b) 1st principal strain simulation contour immediately before failure (Test: M2-TMT-P4-SG1-O1-SR1-T1-N3)

3.3.2 Stress-Strain Relationship of Strain Rate = 1E-2 SEC^{-1}

Tests at strain rate 1E-2 sec^{-1} are listed in table 4. The engineering strain versus stress relationship was derived using equation 8 and yields the engineering stress-strain curves shown in figure 41. Test 6: M2-TMT-P4-SG1-O1-SR2-T1-N3 was selected to represent this group of data and undergo further processing. The selection criterion was based on engineering judgment considering smoothness, representation, and the monotone increasing function requirement of the input curve.

Table 4. Strain rate dependence series data of strain rate = 1E-2 sec^{-1}

Series	Test Name	Plate Stock	Specimen Geometry	Specimen Orientation	Strain Rate (sec^{-1})	Temp (°C)
Tension Strain Rate Dependence	M2-TMT-P4-SG1-O1-SR2-T1-N1	0.5″	Flat Dogbone	Rolled	1.0E-02	RT
	M2-TMT-P4-SG1-O1-SR2-T1-N2	0.5″	Flat Dogbone	Rolled	1.1E-02	RT
	M2-TMT-P4-SG1-O1-SR2-T1-N3	0.5″	Flat Dogbone	Rolled	1.0E-02	RT

RT = room temperature

A plot of the engineering stress-strain curve is shown in figure 41. Following the same procedure as in section 3.4.1, the true stress-strain relationship is shown in figure 42. In this case, the Young's modulus used was 92.0 GPa (derived directly from the test data) and the true strain

versus stress curve was smoothed twice by an 18-point moving average; subsequently, equations 24 and 25 were used to obtain the tangent modulus curve. Another 18-point moving average was performed on the tangent modulus curve to determine the necking point.

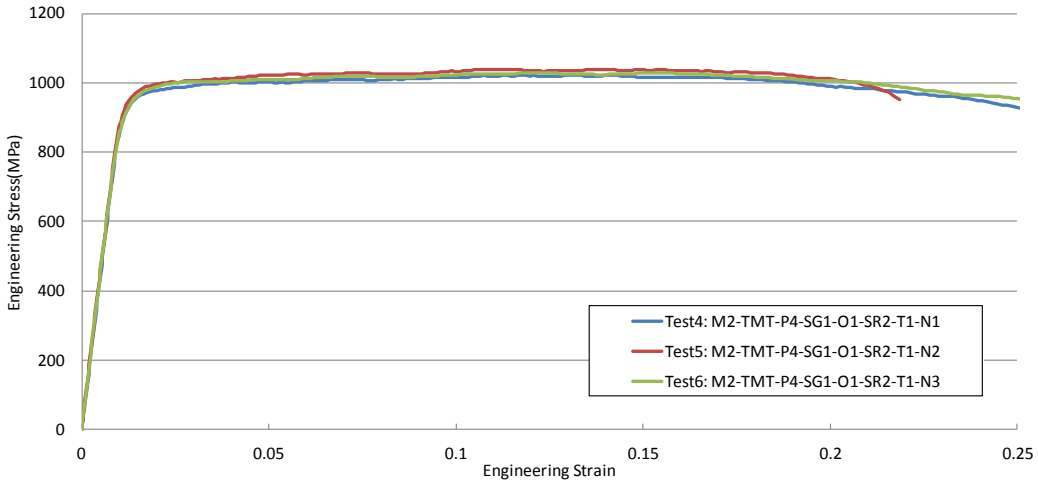

Figure 41. Engineering stress-strain relationship of strain rate = 1E-2 sec^{-1} tests

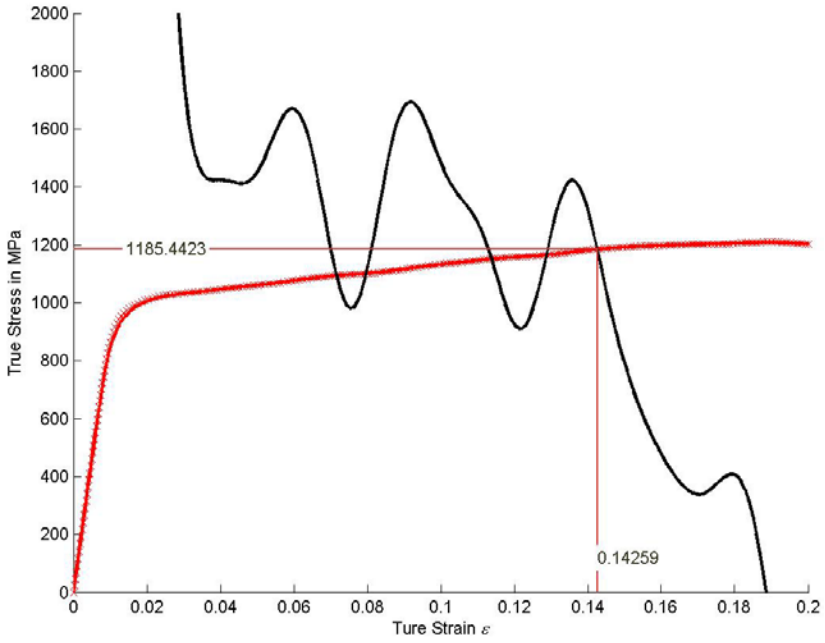

Figure 42. True stress-strain relationship and necking point judgment of strain rate = 1E-2 sec^{-1} tests (Test: M2-TMT-P4-SG1-O1-SR2-T1-N3)

As explained in section 3.4.1, 28 curves were generated by varying the exponent, *n*, between ~0.1 and 0.2 (see figure 43). In this model, the sample dimensions match the sample of test M2-TMT-P3-SG1-O1-SR1-T1-N1 exactly: width = 2.062mm and thickness = 0.861mm.

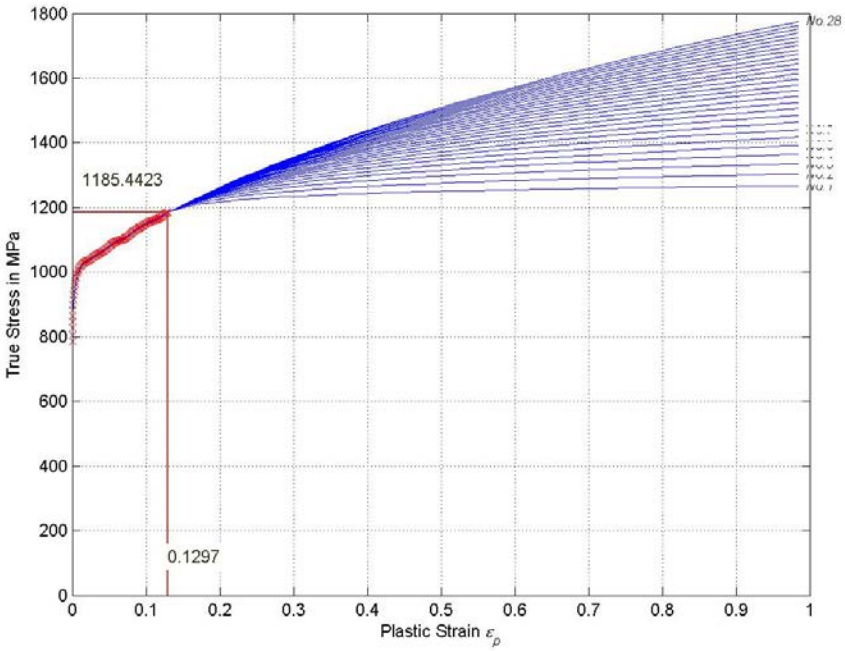

Figure 43. Plastic strain versus stress relationship of strain rate = 1E-2 sec^{-1} (Test 6: M2-TMT-P4-SG1-O1-SR2-T1-N3)

In addition, as explained in section 3.4.1, this simulation is repeated for each of the extrapolated candidate input curves until one matches the force-displacement response of the test (see figure 44). The stress-strain curve created by the extrapolation parameters n = 0.17198, ε_e = 0.040292, and k = 1606.2139 (also shown in figure 45) yields the best match. In figure 46, a simulation contour of 1st principal strain is compared to the DIC image from the test at the time immediately before failure, and the result yields good agreement.

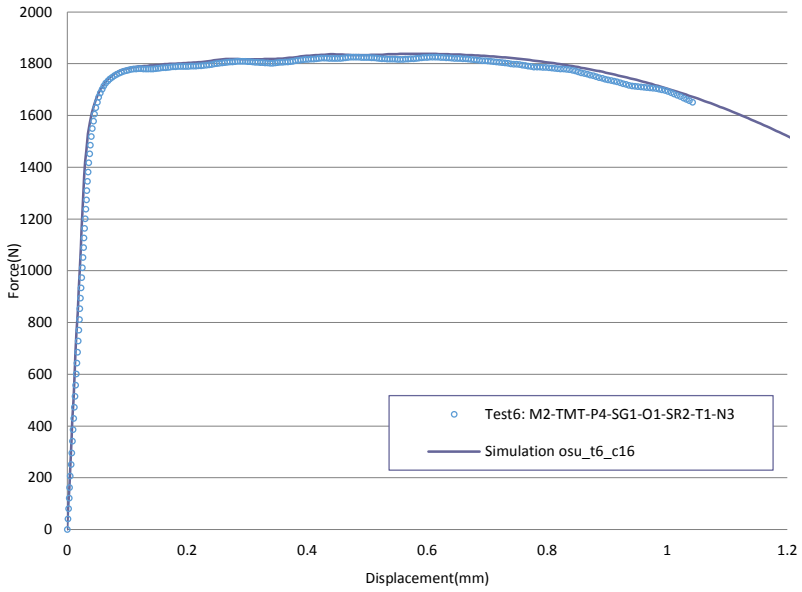

Figure 44. Force displacement result, curve #16 (Test: M2-TMT-P4-SG1-O1-SR2-T1-N3)

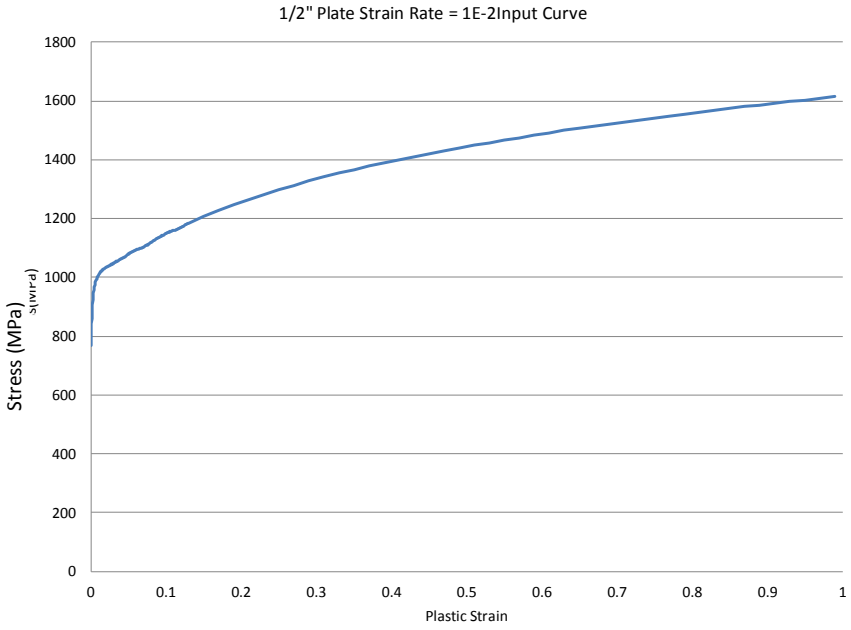

Figure 45. Strain rate = 1E-2 sec^{-1} group hardening curve input result

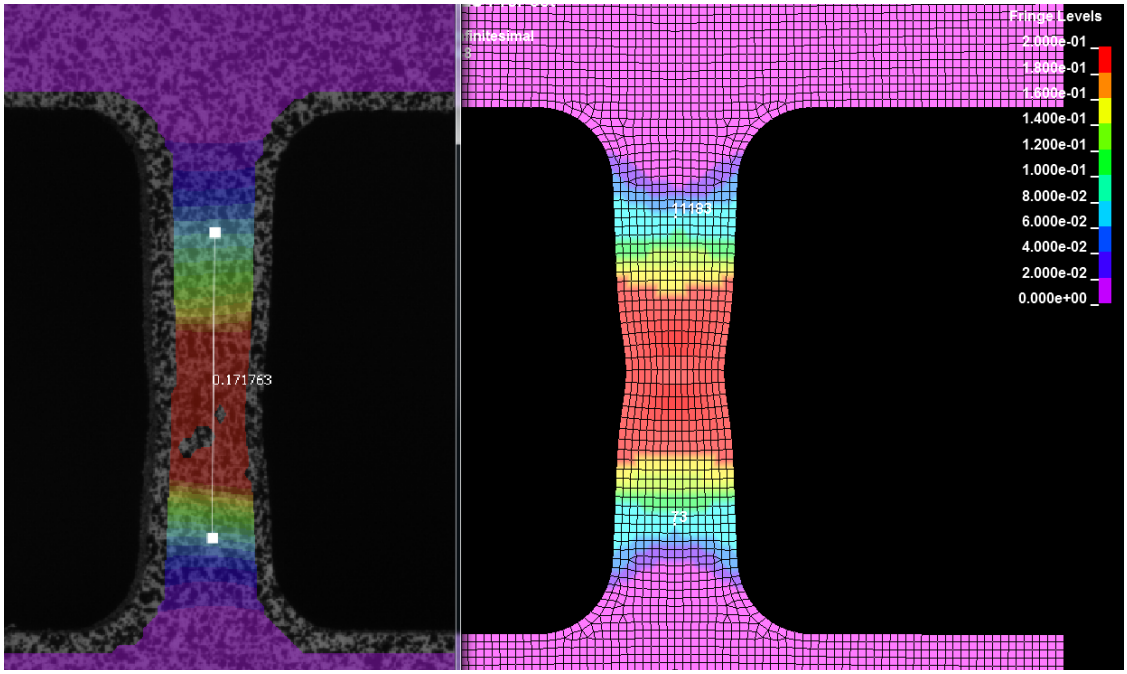

(a) (b)

Figure 46. The (a) plastic strain DIC image immediately before failure and (b) 1st principal strain simulation contour immediately before failure (Test 1: M2-TMT-P4-SG1-O1-SR2-T1-N3; Strain Rate = 1E-2 sec^{-1})

3.4 STRESS-STRAIN TABULATED INPUT OF MULTIPLE STRAIN RATES AND TEMPERATURES

The testing analyzed in the following sections was performed as described in Hammer [5], a method commonly referred to as a split-Hopkinson bar tension test, a Kolsky test, or simply a high strain-rate test. This method differs from the dogbone specimen tension testing described in section 3.3 in that the specimen undergoes impulsive loading rather than being machine-loaded following a prescribed path; therefore, higher strain rates can be achieved.

Appendix E contains an account of a typical, but in this case unsuccessful, method for creating the higher strain-rate curves using each high-rate test one at a time. Though this method was unsuccessful with Ti-6Al-4V at higher strain rates because of its early and extreme localization, it may be successful with other metals at these (and even more elevated) rates.

As explained in section 2.3.3, the process used for creating the higher-rate stress-strain curves required combining information from higher-rate compression tests with lower, constant strain-rate tension tests. A trial-and-error process was performed, wherein both the magnitude of the stresses in the transition and higher strain-rate regions, and the Taylor-Quinney coefficient, β, were varied simultaneously. Each of the tests described in sections 3.4.1 and 3.4.2 were analyzed multiple times until a satisfactory match to all of the test data was achieved. The final stress-strain curves resulting from the trial-and-error process are shown in figure 47. The analytical results shown in sections 3.4.1 and 3.4.2 used these curves as input.

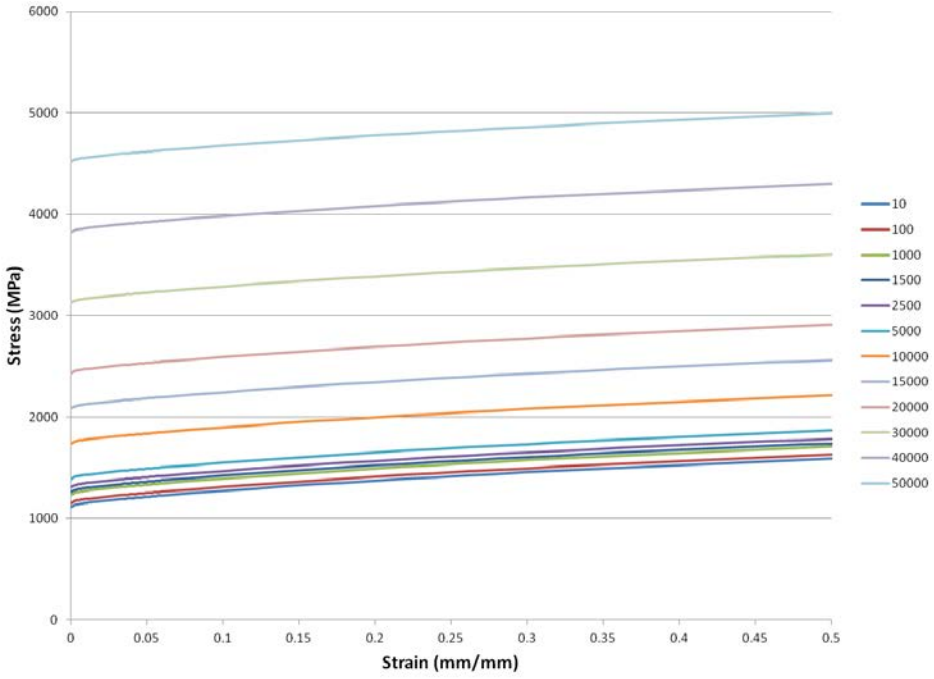

Figure 47. Higher-rate synthetic stress-strain curves

3.4.1 Stress-Strain Relationship of Strain Rate = 650 sec^{-1}

The split-Hopkinson bar tension tests were performed by OSU. In this test, the specimen is glued into adapters that are attached to the bars. During the test, the bars are not fixed.. Figures 48–50 show the overall displacements at each end of the specimen. As a result, the exact conditions that would allow for simulation of the complete experimental setup were not known. Therefore, simulations of these were performed by applying the test displacements taken from the DIC directly to the ends of the specimens.

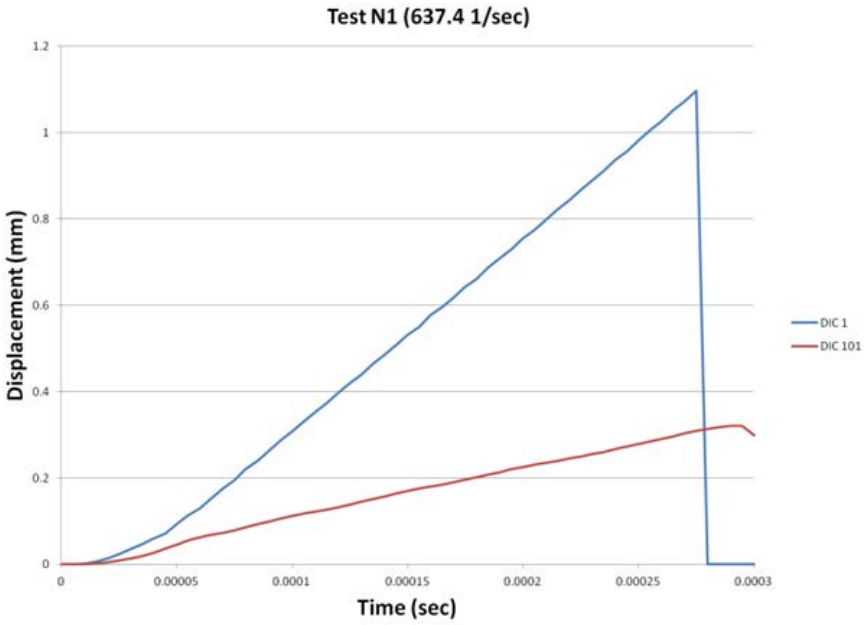

Figure 48. End displacements of test N1 (strain rate = 637.4 sec^{-1})

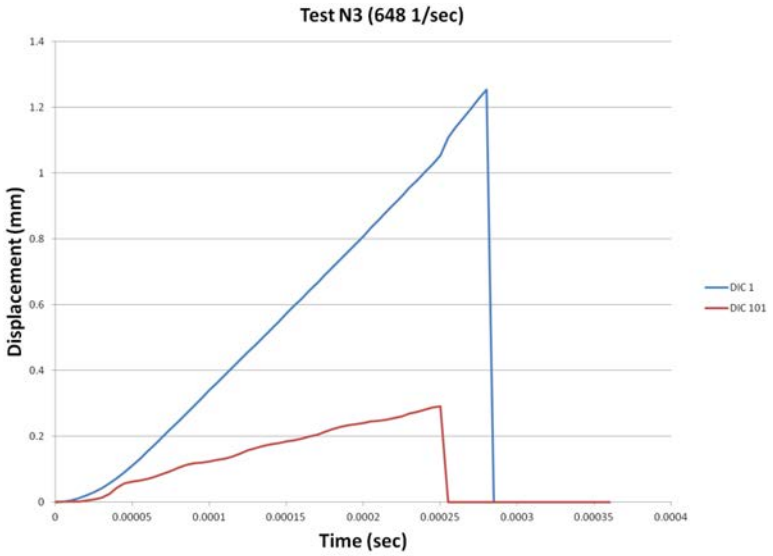

Figure 49. End displacements of test N3 (strain rate = 648 sec^{-1})

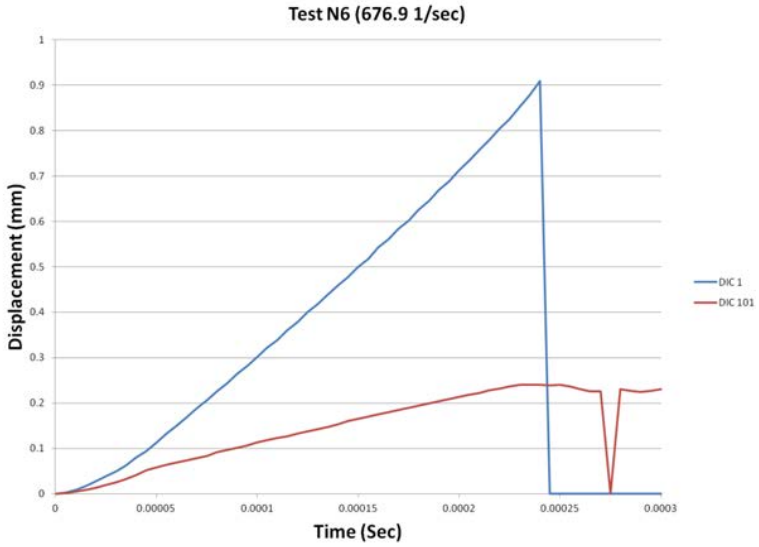

Figure 50. End displacements of test N6 (strain rate = 676.9 sec^{-1})

All three of these tests were analyzed and comparisons made to the physical test results. Figures 51–53 show a comparison of maximum strain, force, and strain contour plots (DIC and LS-DYNA generated) for Test: M2-TMT-P4-SG1-O1-SR4-T1-N1 (referred to as N1). The strain rate for this test, calculated using the overall strain, was 637.4 sec^{-1}. In the region of localization, the strain rate reached approximately 2500 sec^{-1}.

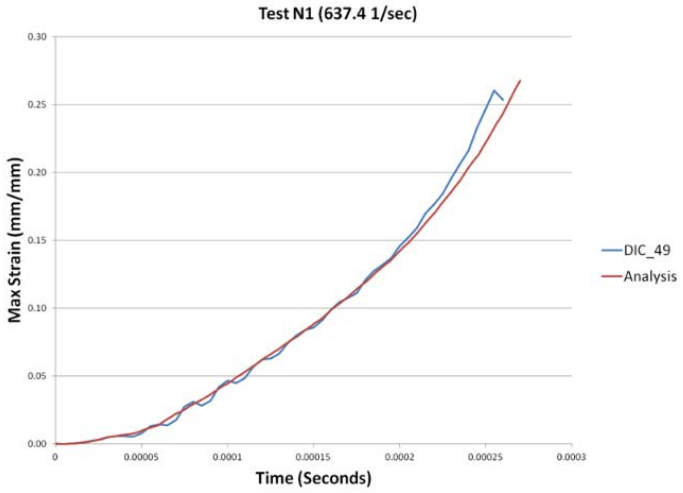

Figure 51. Strain versus time (Test: M2-TMT-P4-SG1-O1-SR4-T1-N1)

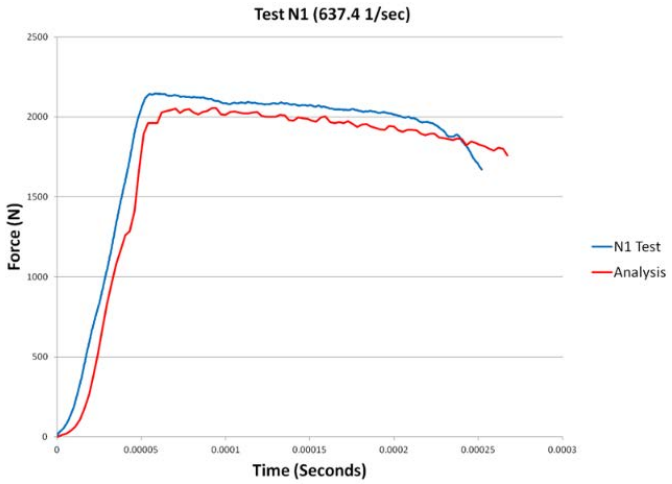

Figure 52. Force versus time (Test: M2-TMT-P4-SG1-O1-SR4-T1-N1)

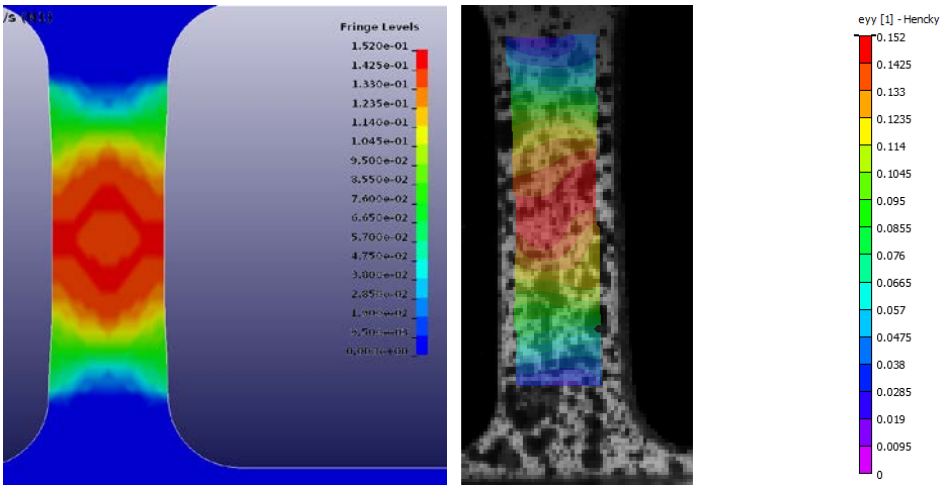

Figure 53. Strain contour at 0.0002 Seconds (Test: M2-TMT-P4-SG1-O1-SR4-T1-N1)

Figure 54 shows a comparison of the stress-strain curve from the analysis of Test N1 with the stress-strain curves of Tests N1, N3, and N6. Figure 54 shows that there is some scatter in the test results. The difference between the analysis of Test N1 and the actual test data is within this test-to-test data scatter.

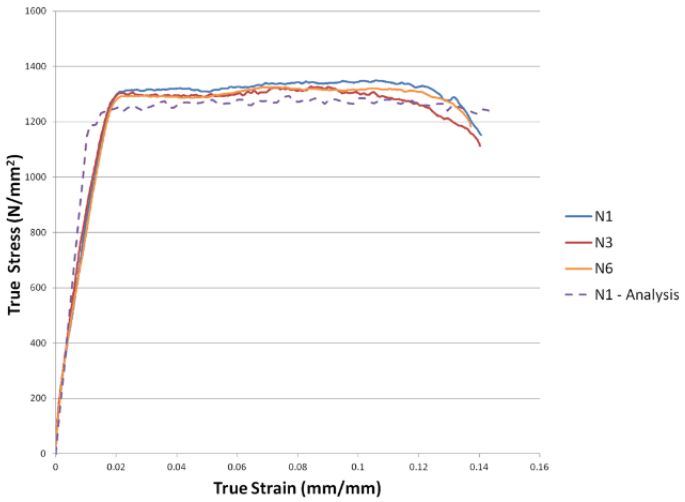

Figure 54. Comparison of three ~650 sec^{-1} tests

Figures 55–57 show a comparison of maximum strain, force, and strain contour plots (DIC and LS-DYNA generated) for Test M2-TMT-P4-SG1-O1-SR4-T1-N3 (referred to as N3). The strain rate for this test, calculated using the overall strain, was 648 sec^{-1}. In the region of localization, the strain rate reached approximately 2500 sec^{-1}. Note that in figure 49, there is a small oscillation in the applied displacement at approximately 0.00005 seconds. This is the cause of the unrealistic response in the elastic region of the force response at the same time of approximately 0.00005 seconds, as shown in figure 56.

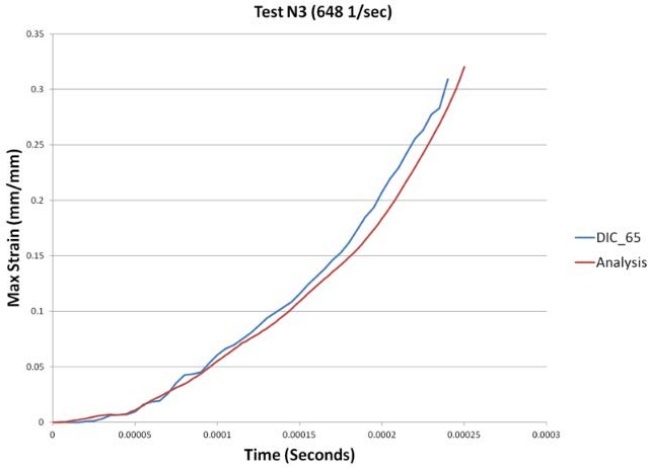

Figure 55. Strain versus time (Test: M2-TMT-P4-SG1-O1-SR4-T1-N3)

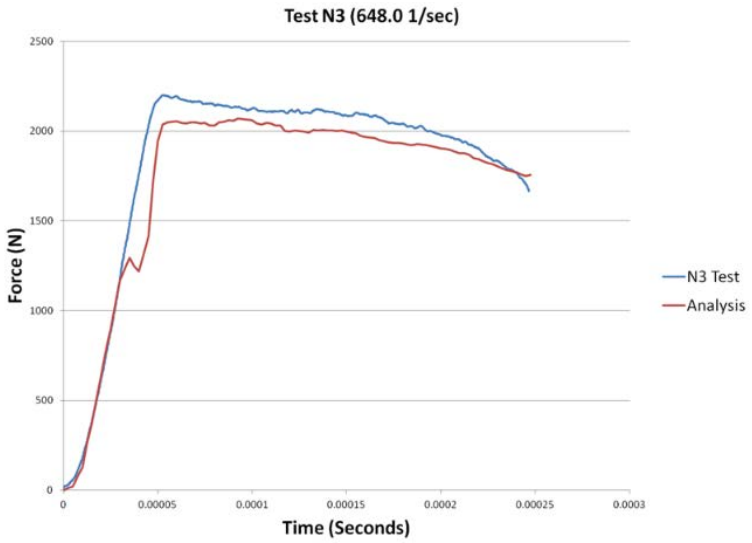

Figure 56. Force versus time (Test: M2-TMT-P4-SG1-O1-SR4-T1-N3)

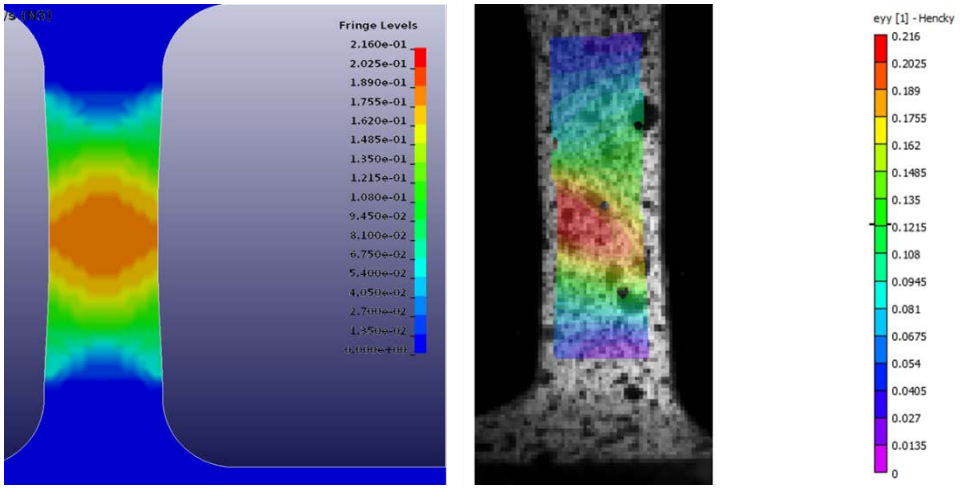

Figure 57. Strain contour at 0.0002 seconds (Test: M2-TMT-P4-SG1-O1-SR4-T1-N3)

Figures 58–60 show a comparison of maximum strain, force, and strain contour plots (DIC and LS-DYNA-generated) for Test M2-TMT-P4-SG1-O1-SR4-T1-N6 (referred to as N6). The strain rate for this test, calculated using the overall strain, was 676.9 sec^{-1}. The test strain shown in figure 58 was recovered at a point in the center of the specimen, and the maximum strain occurred near the edge of the specimen. This is the reason why the test strain is lower than the analysis strain. In the region of localization, the strain rate reached approximately 5000 sec^{-1}.

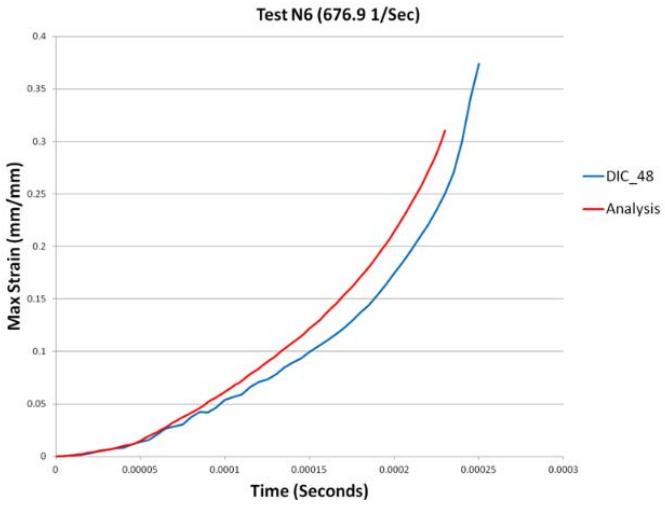

Figure 58. Strain versus time (Test: M2-TMT-P4-SG1-O1-SR4-T1-N6)

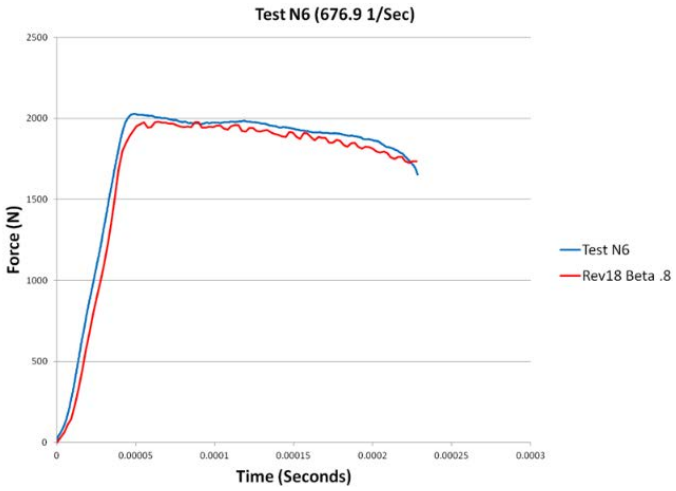

Figure 59. Force versus time (Test: M2-TMT-P4-SG1-O1-SR4-T1-N6)

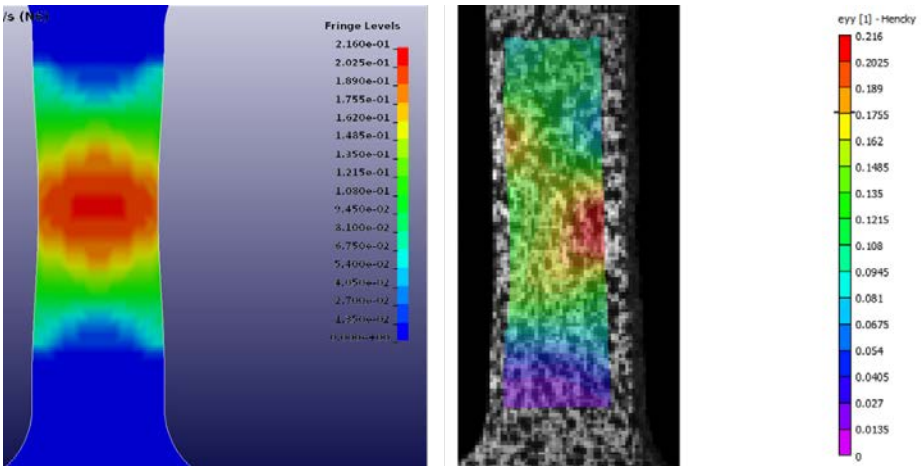

Figure 60. Strain contour at 0.0002 seconds (Test: M2-TMT-P4-SG1-O1-SR4-T1-N6)

3.4.2 Stress-Strain Relationship of Strain Rate = 1600 Sec^{-1}

As in the 650 sec^{-1} tests, neither of the boundary conditions of the split-Hopkinson bar tension tests were fully fixed, as shown in figure 61. As discussed in section 3.5.1, simulations of these tests were performed by applying the test displacements taken from DIC directly to the ends of the specimens.

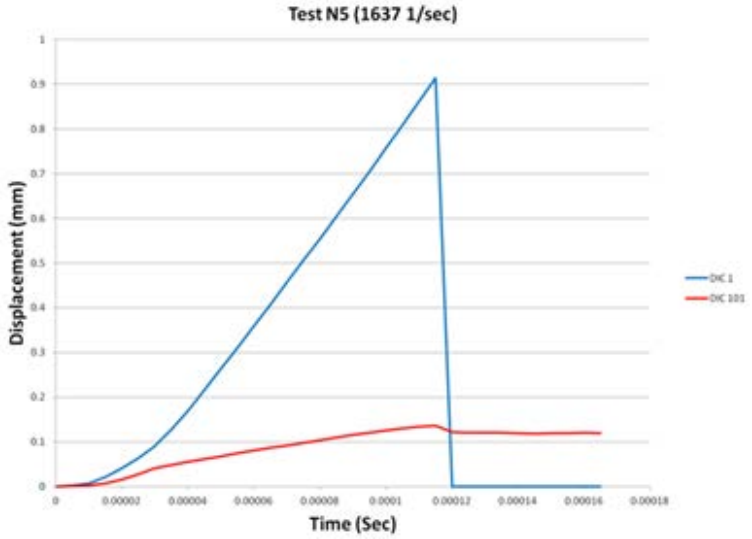

Figure 61. End displacements (Test: M2-TMT-P4-SG1-O1-SR5-T1-N5; strain rate = 637.4 sec^{-1})

Figures 62–64 show a comparison of maximum strain, force, and strain contour plots (DIC and LS-DYNA-generated) for Test M2-TMT-P4-SG1-O1-SR5-T1-N5 (referred to as N5). The strain rate for this test, calculated using the overall strain, was 1637 sec^{-1}. In the region of localization, the strain rate reached approximately 7000 sec^{-1}.

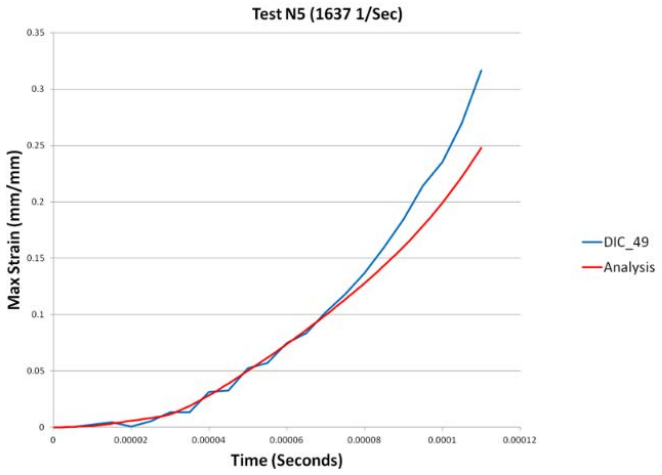

Figure 62. Strain versus time (Test: M2-TMT-P4-SG1-O1-SR5-T1-N5)

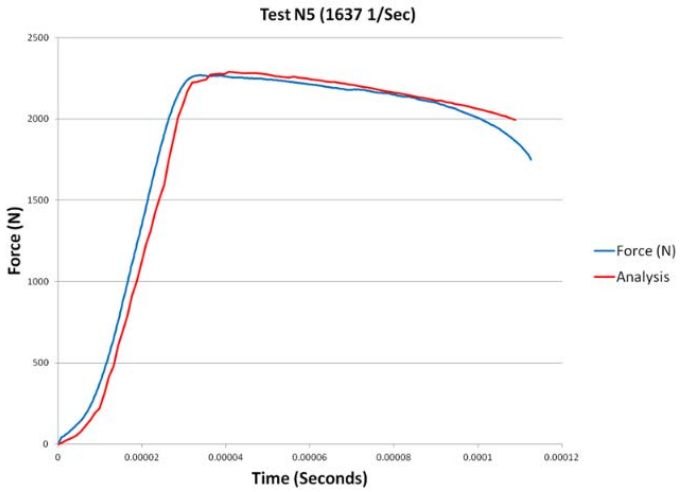

Figure 63. Force versus time (Test: M2-TMT-P4-SG1-O1-SR5-T1-N5)

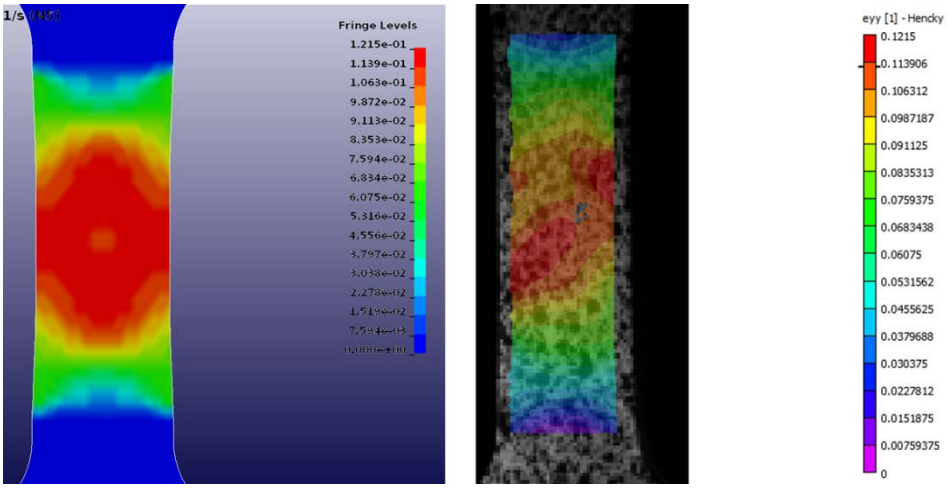

Figure 64. Strain contour at 0.000075 seconds (Test: M2-TMT-P4-SG1-O1-SR5-T1-N5)

4. METHODOLOGY FOR FAILURE MODEL CREATION

This section describes the methodology for generating and implementing a failure surface for the *MAT_TABULATED_JOHNSON_COOK (*MAT_224) material model. The input for the LS-DYNA material model is explained and a method is discussed for generating the tabulated values that represent the failure surface.

4.1 FAILURE SURFACE IMPLEMENTATION IN *MAT_224

The *MAT_224 material model currently has four input parameters that calculate the accumulated damage for a given element. The first parameter is a load curve (or table of curves) that defines the plastic failure strain as a function of triaxiality (and Lode parameter). For shell elements, a single load curve defining failure as a function of triaxiality is sufficient. If the table option is used for this parameter, a failure surface is defined, which is appropriate for solid elements. The second parameter is a load curve that defines the plastic failure strain as a function

of plastic strain rate. The third parameter is a load curve that defines the plastic failure strain as a function of temperature. The last parameter is a load curve (or table of curves) that defines that plastic failure strain as a function of element size and triaxiality.

Triaxiality is defined by the equation:

$$\tau = \frac{p}{\sigma_{vm}} \tag{31}$$

where p is the pressure and σ_{vm} is the von Mises stress.

The Lode parameter is defined by the equation:

$$\theta_L = \frac{27 s_1 s_2 s_3}{2\sigma_{vm}^3} \tag{32}$$

where s_1, s_2, and s_3 are the principal deviatoric stresses and σ_{vm} is the von Mises stress.

Overall, the plastic failure strain is defined by:

$$\varepsilon_{pf} = f(\tau, \theta_L) g(\dot{\varepsilon}_p) h(T) i(l_c) \tag{33}$$

where τ is the triaxiality, θ_L is the Lode parameter, $\dot{\varepsilon}_p$ is the plastic strain rate, and l_c is the element size. When more than one of the failure parameters are used, the net plastic failure strain is the product of the functions defined in equation 33. For reference, the possible range of triaxiality is negative infinity to positive infinity; however, the area of interest for this analysis is negative one to positive one.

The failure criterion for *MAT_224 is based on an accumulated damage parameter. When this damage parameter is greater than or equal to one in an integration point, the solid element is eroded. The damage parameter is defined by:

$$D = \int \frac{\dot{\varepsilon}_p}{\varepsilon_{pf}} dt \tag{34}$$

where $\dot{\varepsilon}_p$ is the plastic strain rate and ε_{pf} is the plastic failure strain.

A description of how each of the variables was parameterized can be found in section 5. To determine the failure surface, many types of specimen geometries were created and tested. Each specimen geometry has a unique triaxiality and Lode parameter that represents a portion of the failure surface. To generate an accurate and complete failure surface, there should be as many specimen geometries as possible. Using the triaxiality, Lode parameter, and failure strain data provided by the specimen testing, a 3-D curve fitting tool can be used to create a full surface.

After a failure surface is generated, the remaining parameter load curves can be created. The same strain rate test series and temperature test series (as described in section 3.1) can be used to determine the next two failure parameters. Finally, by varying the size of the elements in the mesh of a sample analysis, a load curve can be created that accounts for many different sizes of discretization.

4.2 DEVELOPMENT OF FAILURE SURFACE GENERATION TOOL

This section describes the strategy and implementation of a new failure surface generation tool. The overall goal was to develop a code that can be easily implemented for any type of material and any range of specimen types. The source code is written in MathWorks MATLAB and can be edited and executed within the MATLAB software interface.

The fundamental strategy of this tool is to use points that represent triaxiality, Lode parameter, and failure strain of many different types of specimens to develop a full surface. Suppose a material testing program yields 20 different material tests with the average states of stress found in figure 65 (note that, in figure 66, the terms “plane stress” and “plane strain” represent families of specimen designs and only one of each of these families is actually in plane stress or plane strain). Because it is often difficult for experimentalists to engineer specimens that can represent a broad range of triaxiality and Lode parameters, there are sometimes areas of the surface that are not covered by physical tests. For example, there is a large area of the surface (approximately triaxiality -0.2, Lode parameter 0) in which there are no specimens. Because of this, a “grid and control point strategy” was developed.

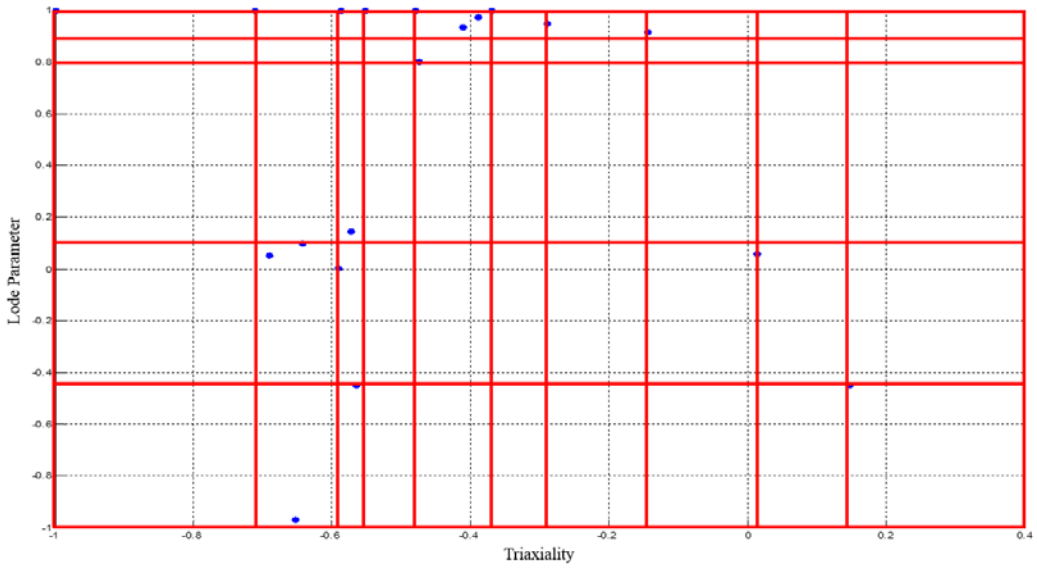

Figure 65. Example stress states of different material tests

An orthogonal grid structure can be overlaid onto the existing plot. These grid lines can be arbitrary but should be based on existing physical testing. If there are many specimens that are closely lumped together, one grid line can represent those points. That is, each point (or group of

points) creates a grid line. Figure 65 shows an example of the grid structure for the data from figure 66.

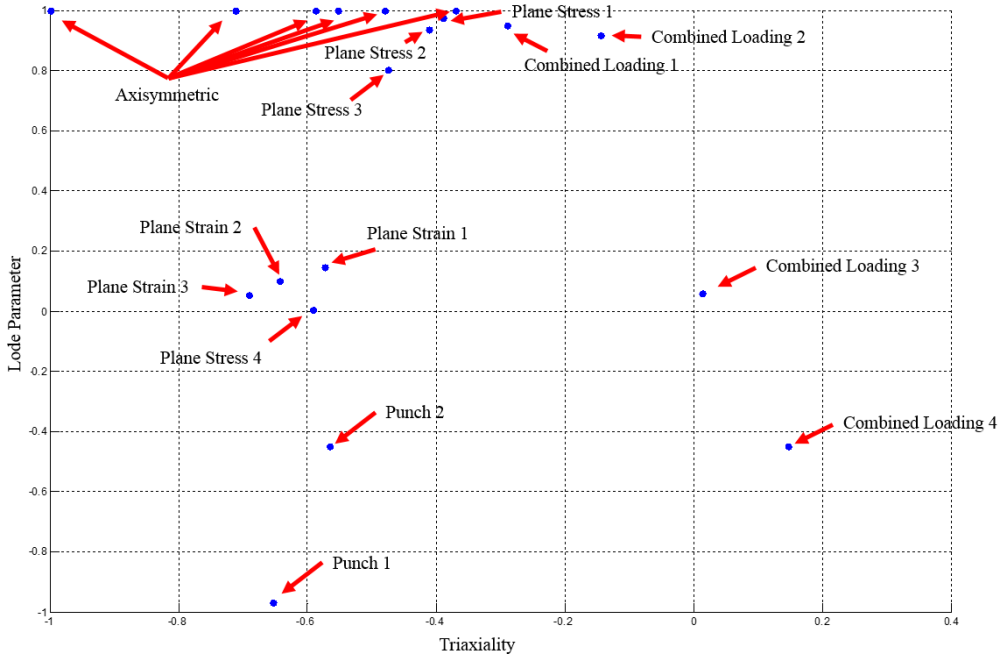

Figure 66. Example grid structure

Using these grid lines, a new set of points can be saved based on the points of grid line intersection. For each grid line intersection, a point on the triaxiality-Lode plane is created. In this example, there are 66 "control points." Three 66-point, one-dimensional vectors can be created using: 1) the triaxiality of the control points, 2) the Lode parameter of the control points, and 3) the failure strain for each of the control points. The failure strain is determined manually by the user of the tool. At control point locations where there is a single physical test, that specimen's failure strain defines the control point failure strain. If there are a group of points that represent one control point, those points are averaged using equal weights. If there is no physical test for a given control point, the nearest point, or the average of many nearby points, is used. Using this method, all three of the 66-point one-dimensional vectors are now complete with values.

After the input vectors are defined, the user can execute the program. MATLAB begins by implementing a subroutine that was developed using the Curve Fitting Toolbox. This subroutine passes the three 66-point one-dimensional vectors and returns a fit surface. The subroutine uses a cubic interpolation routine to generate the 3-D surface. The software then displays two plots of the surface (see figure 67).

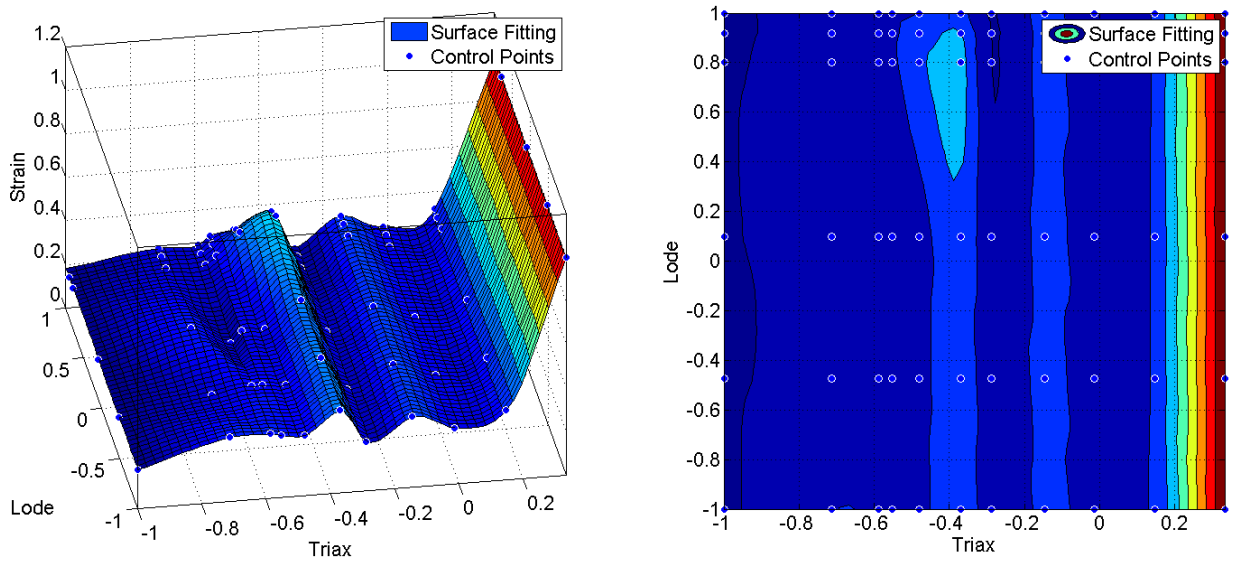

Figure 67. Surface plots generated by the MATLAB subroutine

The next step of the failure surface generation tool is to discretize the 3-D surface into individual points for input into LS-DYNA. The 3-D surface is sampled into 2814 points (134 triaxiality points by 21 Lode angle points). The tool also shows a visual representation of the discretization of the 3-D surface (see figure 68).

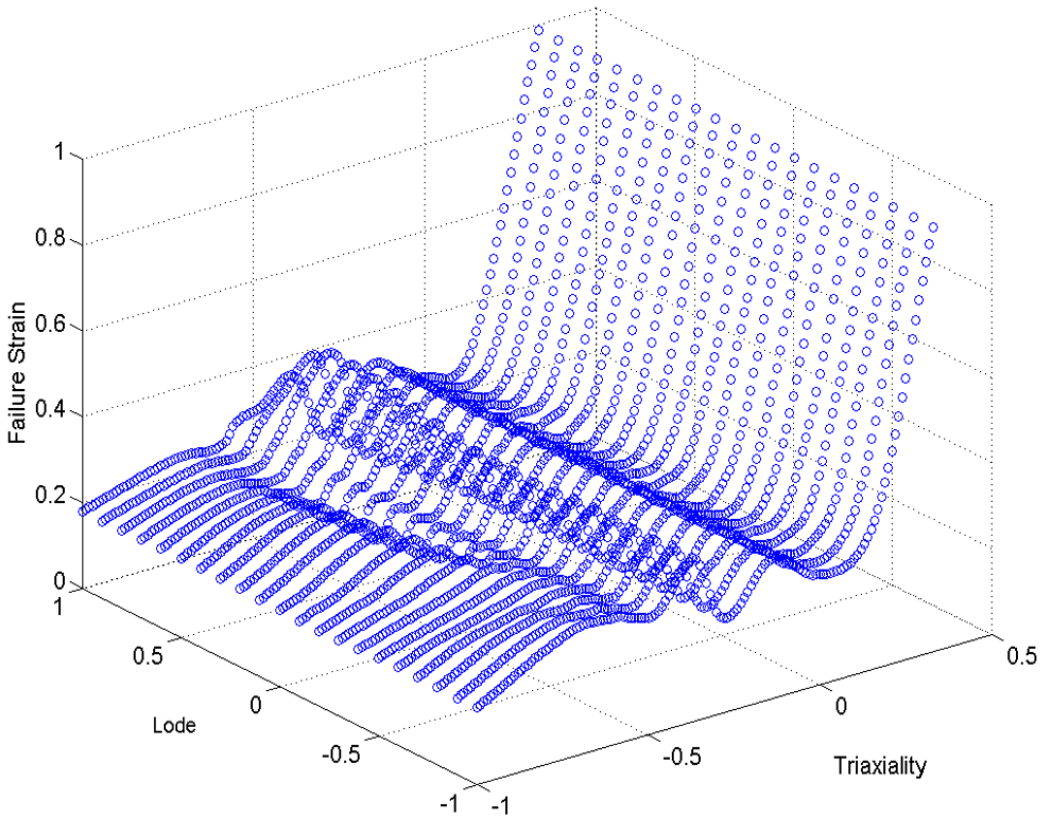

Figure 68. Discretized 3-D surface generated by LS-DYNA

The final step for the failure surface generation tool is to automatically generate a keyword file to use in LS-DYNA. This file includes a *DEFINE_TABLE which has 21 values ranging from -1 to 1 that represent the line for each Lode parameter shown in figure 68. Also included are the 21 *DEFINE_CURVE keywords that represent the failure strain as a function of triaxiality. Each of these curves has 134 points. This keyword file can then be directly included into the simulation model. This is valuable to the analyst because typically there are many iterations of failure surface generations that must be completed to obtain a representative surface for a given material. After each specimen is simulated, the displacement at failure is checked against the experimental test result. If the simulation reaches the failure criteria too late or too early in the simulation (i.e., the failure strain is too high or too low), the control point(s) near that specimen's state of stress can be adjusted and the surface can be immediately regenerated.

4.3 FLOW CHART OF FAILURE SURFACE MODELING PROCEDURE

Figure 69 is a flow chart of the procedure used for modeling the failure surface.

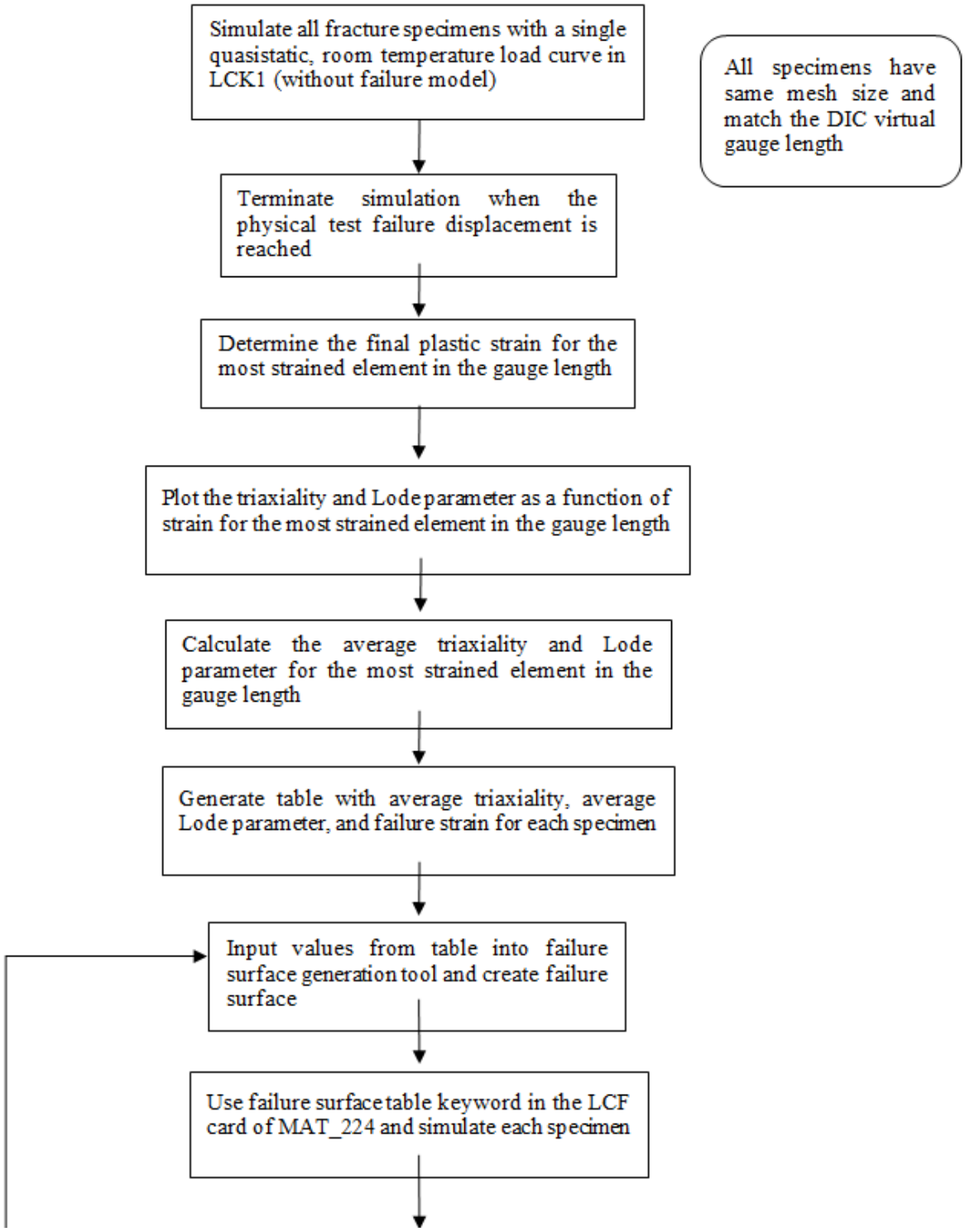

Figure 69. Flow chart of failure surface modeling procedure

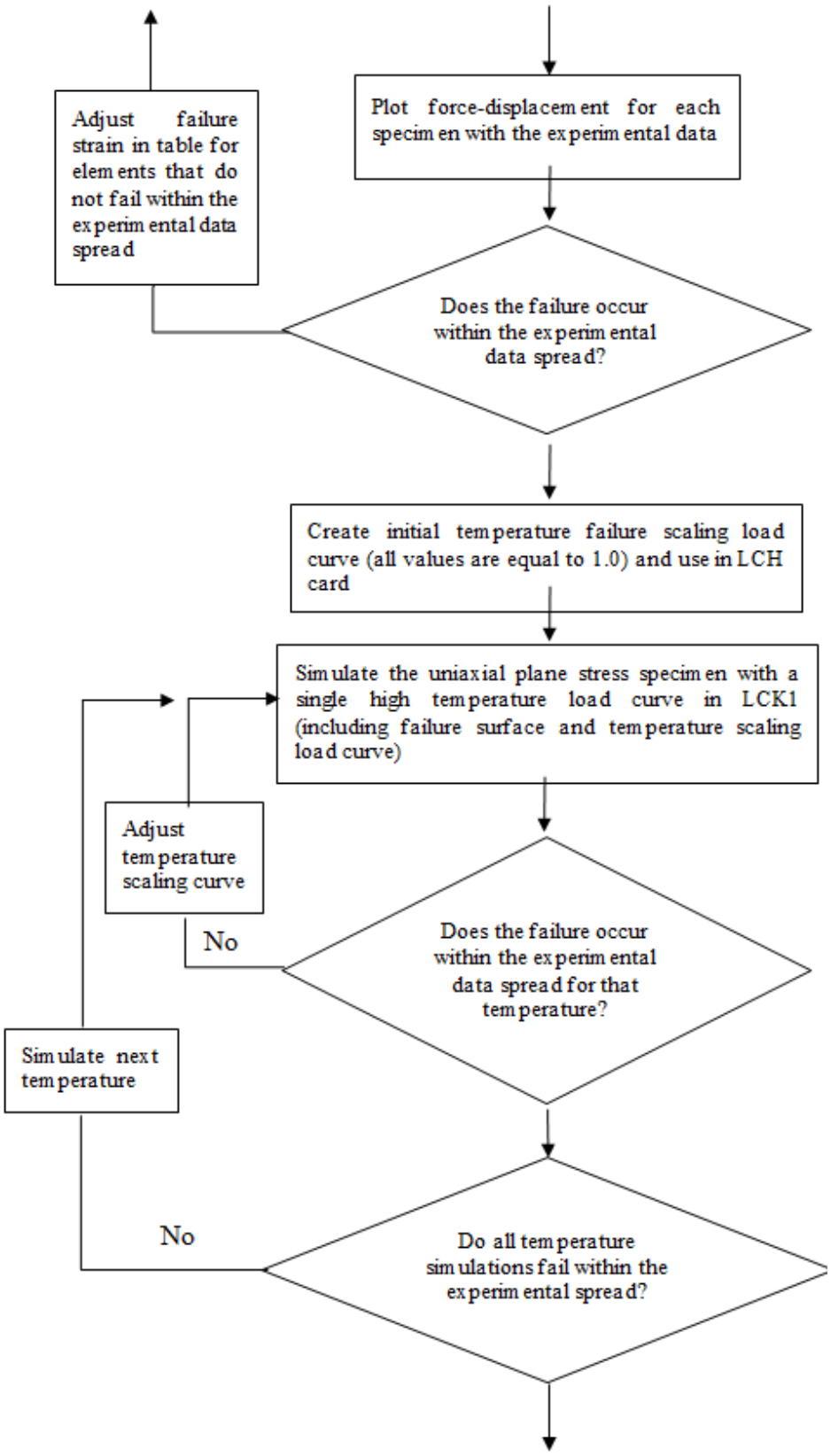

Figure 69. Flow chart of failure surface modeling procedure (continued)

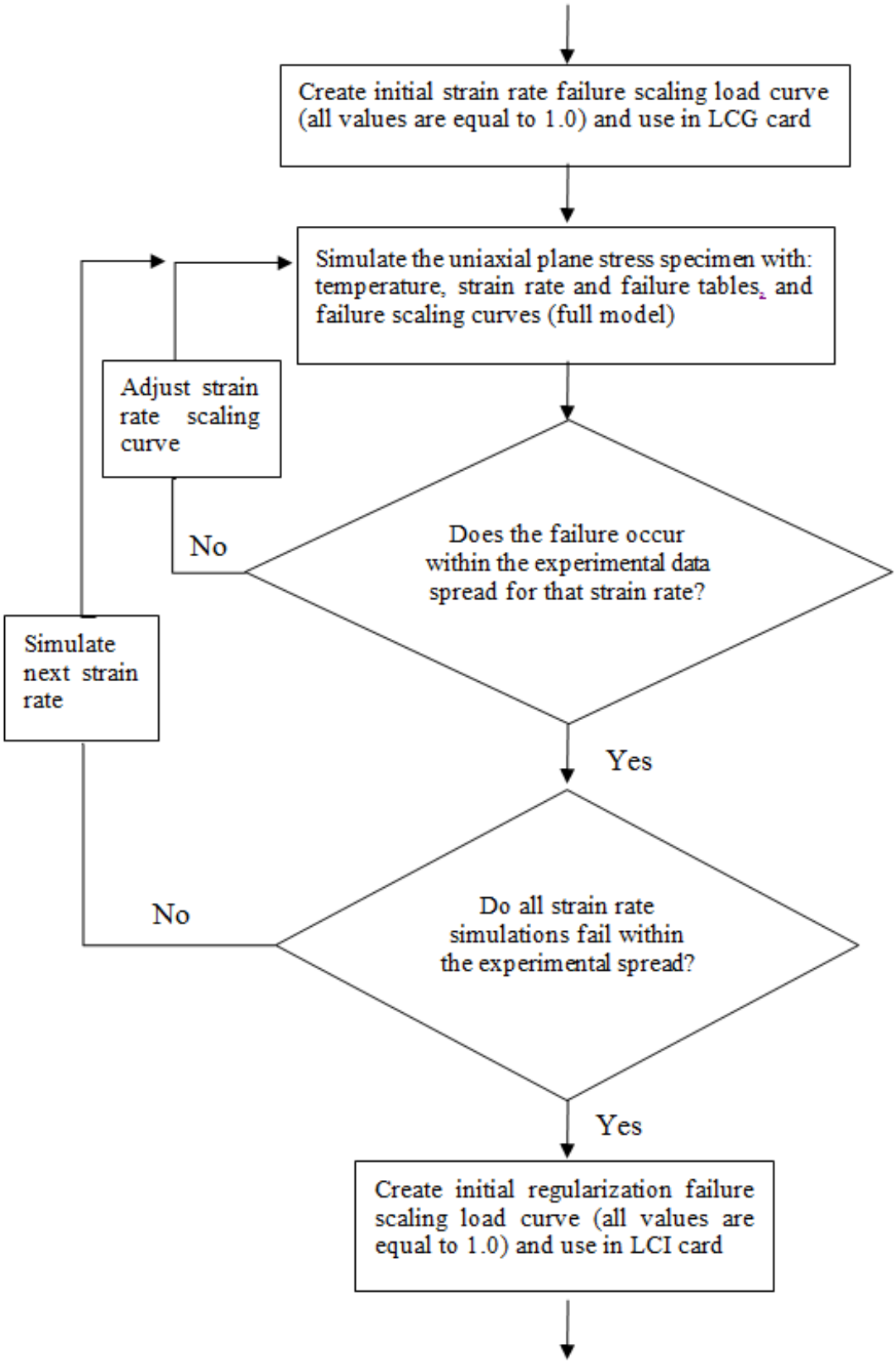

Figure 69. Flow chart of failure surface modeling procedure (continued)

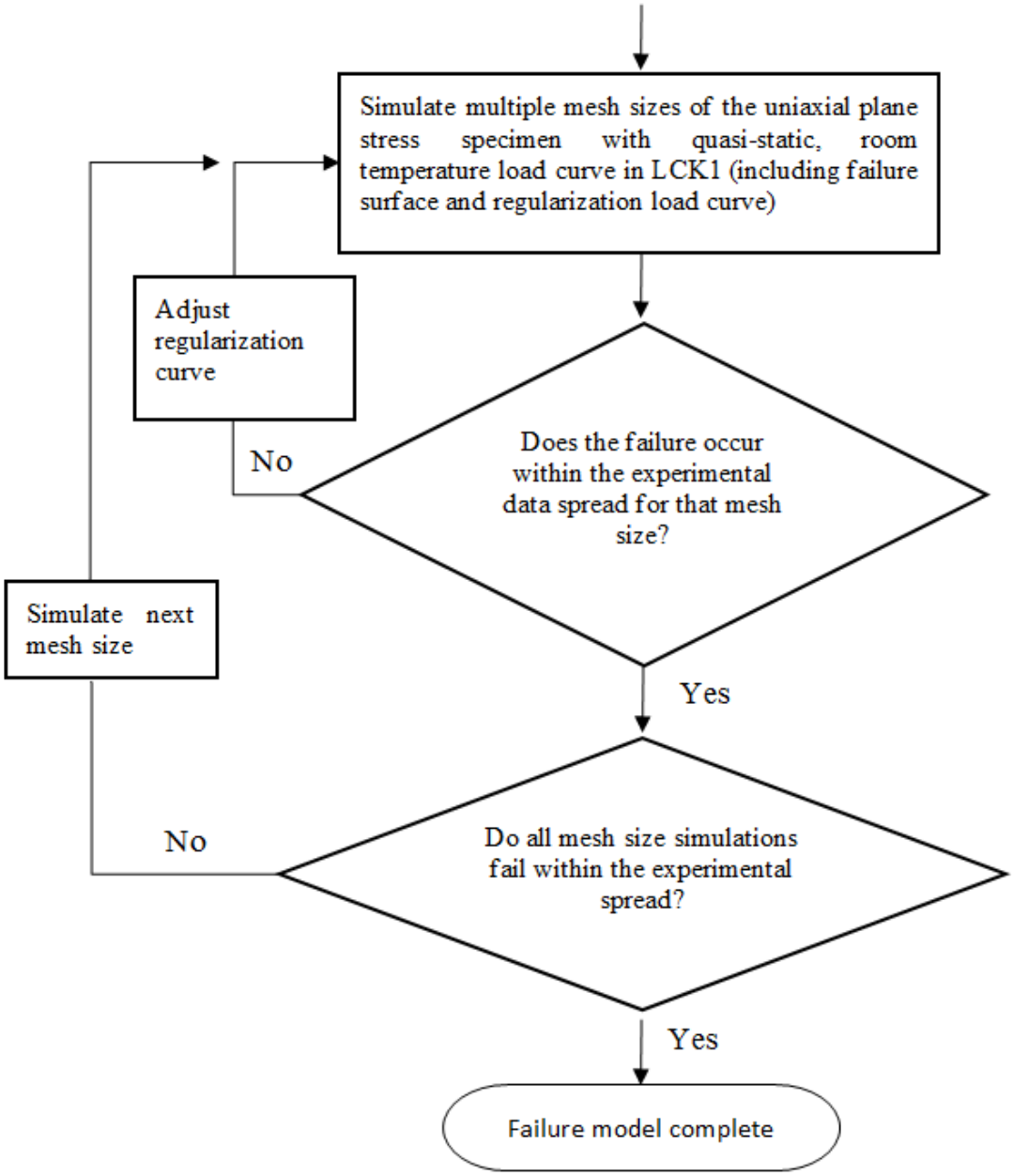

Figure 69. Flow chart of failure surface modeling procedure (continued)

5. FAILURE MODEL CREATION BY SIMULATION OF MECHANICAL PROPERTY TESTS

To generate an effective failure surface, many different tests using different geometries that produce varying states of stress must be completed. These tests must vary in both triaxiality and Lode parameter (see section 4) at the localization point or the point of failure. To create a broad surface that would represent as many states of stress as possible, there should be as many combinations of triaxiality and Lode parameters as possible. If too few specimens are chosen for

analysis, the surface will not be fully represented in some areas. Optimal sampling would result in a uniform coverage of stress space, but is hard to achieve in practice.

The mechanical property tests were performed by OSU, which provided the specimen geometry, force data, displacement data, strain data, and DIC images. Twenty different specimens were used to determine the failure surface model. The 20 specimens and their identifying labels are:

1. SG1: Plane stress specimen (pure tension)
2. SG2: Plane stress specimen
3. SG3: Plane stress specimen
4. SG4: Plane stress specimen
5. SG5: Axisymmetric specimen (pure tension)
6. SG6: Axisymmetric specimen
7. SG7: Axisymmetric specimen
8. SG8: Axisymmetric specimen
9. SG9: Axisymmetric specimen
10. SG10: Axisymmetric specimen
11. SG11: Plane strain specimen
12. SG12: Plane strain specimen
13. SG13: Plane strain specimen
14. LR1: Combined (tension/torsion) specimen
15. LR2: Combined (tension/torsion) specimen
16. LR3: Torsion specimen
17. LR4: Combined (compression/torsion) specimen
18. Punch1: Large diameter punch specimen
19. Punch2: Large diameter punch specimen
20. Compression: Uniaxial (cylindrical) compression specimen

Note that, for this list, the terms “plane stress” and “plane strain” actually represent families of specimen design, and only the first of each of these families actually creates plane stress or plane strain. The other specimens within each family include various notches that create additional variations in the states of stress. Each specimen (and its associated finite element model) will be more thoroughly described in sections 5.1–5.5.

5.1 CREATION OF A FAILURE SURFACE

This section describes the specimen modeling process, simulation of the corresponding tests performed by OSU, and results using the failure surface generation tool. The dimensions shown in the specimen diagrams are nominal and were used for the creation of the specimen finite element model. The actual dimensions may differ slightly from specimen to specimen. The mesh used in each analysis must be adjusted to precisely match the actual test specimen dimensions. All dimensions are in mm, ms, kg, and kN. Unless otherwise noted, all simulations were computed using LS-DYNA version SMP S R6.1.1, revision: 78769.

For each initial simulation, the titanium material was modeled using the *MAT_TABULATED_JOHNSON_COOK (*MAT_224) material model in LS-DYNA. The input parameters for this material card are shown in figure 70.

```
*KEYWORD
*MAT_TABULATED_JOHNSON_COOK_TITLE
Ti-6-4
$#   mid          ro          e          pr        cp        tr        beta     numint
       2  4.4300E-6 110.00000   0.342000     540     293  1.000000  1.000000
$# tabk1       tabkt        lcf        lcg       lch       lci
       1
```

Figure 70. LS-DYNA input deck for *MAT_TABULATED_JOHNSON_COOK titanium model

For the initial simulations, a single curve was given for the effective stress as a function of effective plastic strain (see figure 71). A description of how this curve was generated is given in section 3 and based on the quasistatic, pure tension, room-temperature test conditions.

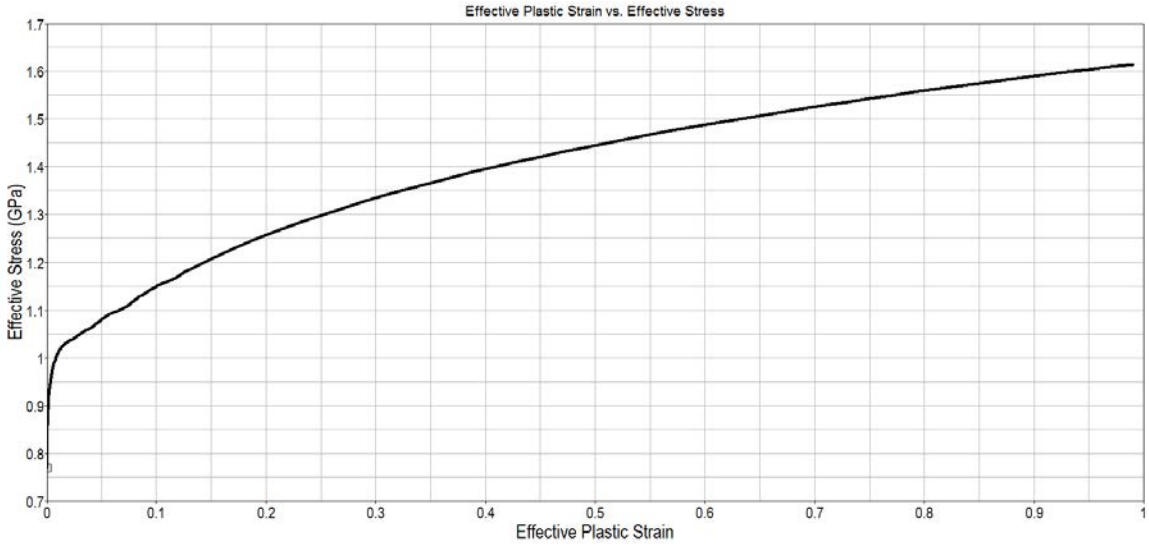

Figure 71. Input curve for initial simulations

Because these simulations use only a single yield curve in the tabk1 position of the material card, the simulation strain rate can be arbitrary, as described in section 2. That is, there is no strain-rate effect applied within the material algorithm in these initial simulations. Therefore, the simulation of the motion and termination time can be arbitrary. To decrease computational time, each specimen was simulated at a much faster speed than in the physical test. Each simulation was checked to ensure that the speed of the motion was slow enough to cause oscillatory or unstable conditions within the material. In addition, simulations were performed at a lower speed to verify that the simulation results remained unaffected.

5.1.1 SG1—Plane Stress Specimen (Pure Tension)

SG1 is a plane stress (pure tension) specimen that was previously used to determine the stress-strain relationships provided earlier in this report. The dimensions of the specimen are shown in figure 72.

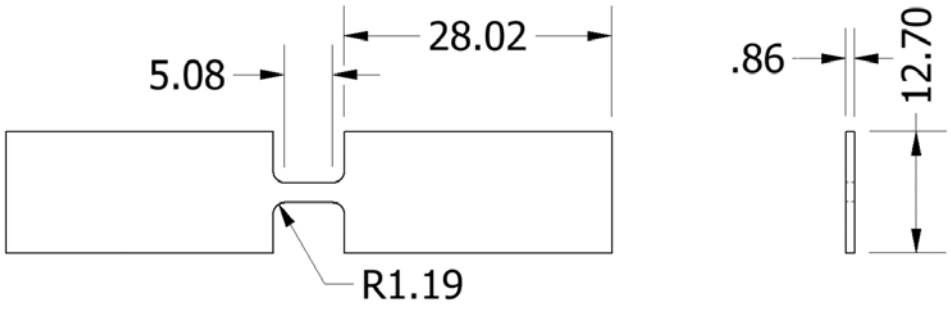

Figure 72. Geometry of specimen SG1

This specimen was then meshed with solid elements so that the average element size was 0.2 mm. The mesh of the SG1 specimen is shown in figure 73. An enlargement of the area containing the 4.00 mm virtual (DIC) extensometer gauge length is also shown in more detail. The mesh for this specimen contains approximately 33,000 solid elements. To model the mechanical grips of the material testing machine, some of the nodes on each end of the specimen were considered rigid elements. Of the 33,000 elements, approximately 24,000 were considered rigid solid elements (shown in gray). Figure 73 shows the proportion of rigid solid elements and elements modeled as titanium (shown in white).

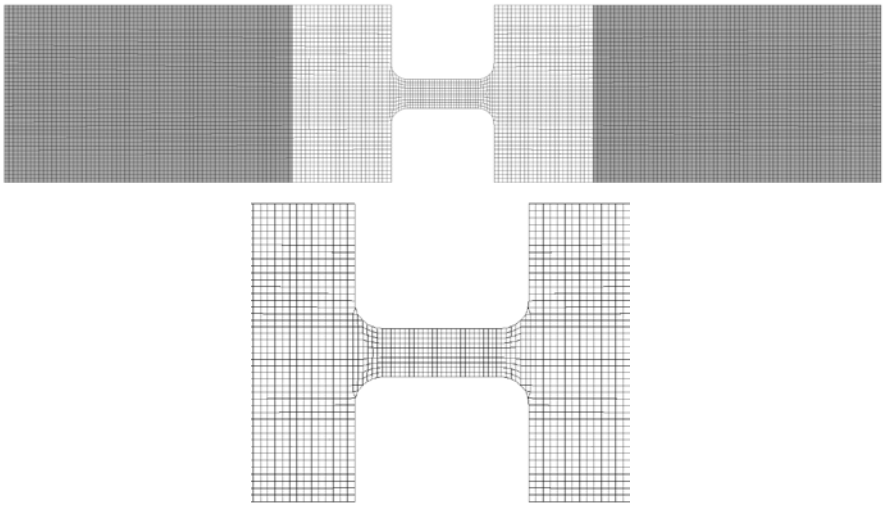

Figure 73. Meshed model of specimen SG1 showing rigid solid elements (gray) and titanium elements (white)

5.1.2 SG2—Plane-Stress Specimen

SG2 is a variation of the plane-stress specimen that has a specifically chosen center geometry, or notch, that will produce a unique triaxiality and Lode parameter. The dimensions of the specimen are shown in figure 74.

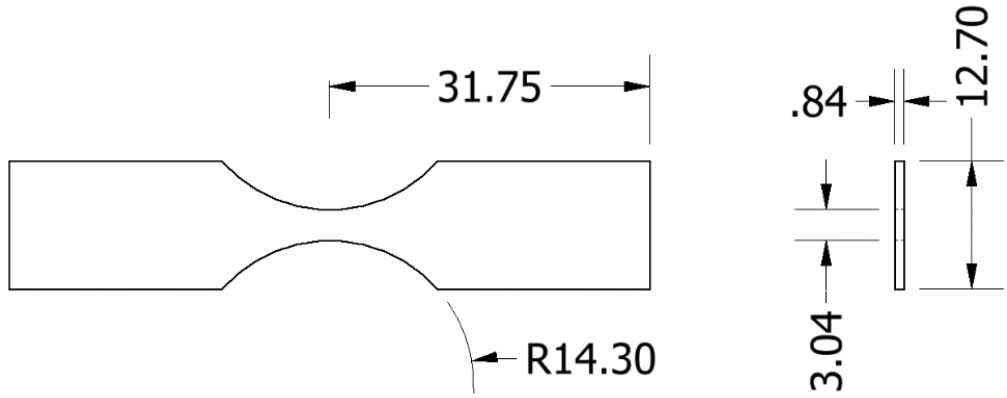

Figure 74. Geometry of specimen SG2

This specimen was then meshed with solid elements so that the average element size was 0.2 mm. The mesh of the SG2 specimen is shown in figure 75. An enlargement of the area containing the 4.00 mm virtual (DIC) extensometer gauge length is also shown in more detail. The mesh for this specimen contains approximately 22,000 solid elements. To model the mechanical grips of the material testing machine, some of the nodes on each end of the specimen were considered rigid elements. Of the 22,000 elements, approximately 12,000 were considered rigid solid elements (shown in gray). Figure 75 shows the proportion of rigid solid elements and elements modeled as titanium (shown in white).

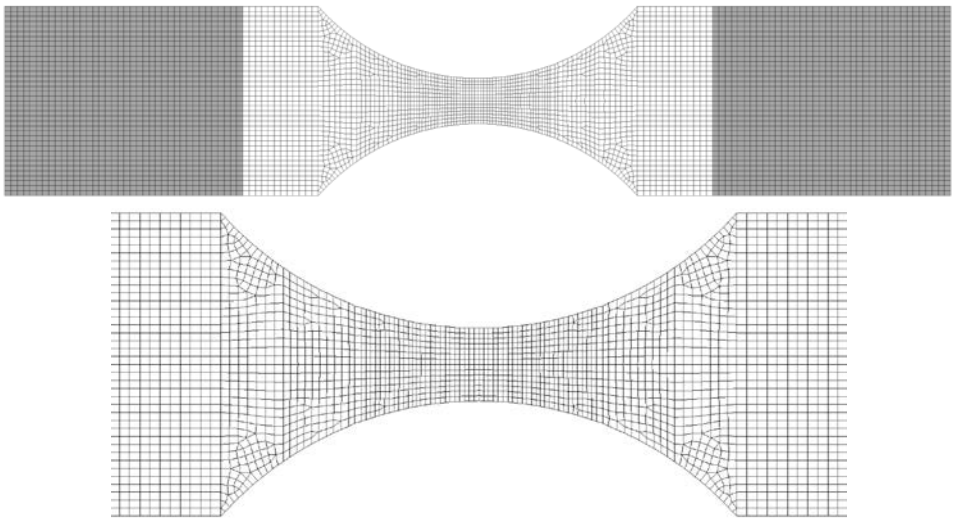

Figure 75. Meshed model of specimen SG2 showing rigid solid elements (gray) and titanium elements (white)

5.1.3 SG3—Plane-Stress Specimen

SG3 is a variation of the plane-stress specimen that has a specifically chosen center geometry, or notch, that will produce a unique triaxiality and Lode parameter. The dimensions of the specimen are shown in figure 76.

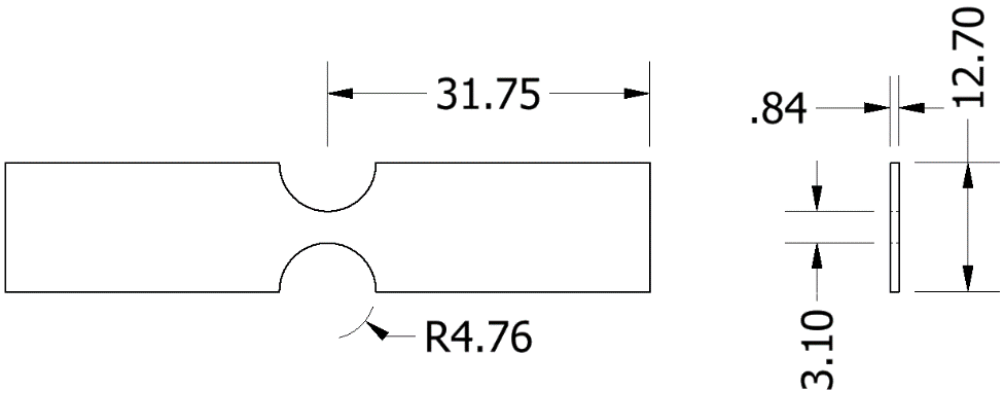

Figure 76. Geometry of specimen SG3

This specimen was then meshed with solid elements so that the average element size was 0.2 mm. The mesh of the SG3 specimen is shown in figure 77. An enlargement of the area containing the 4.00 mm virtual (DIC) extensometer gauge length is also shown in more detail. The mesh for this specimen contains approximately 20,000 solid elements. To model the mechanical grips of the material testing machine, some of the nodes on each end of the specimen were considered rigid elements. Of the 20,000 elements, approximately 14,000 were considered rigid solid elements (shown in gray). Figure 77 shows the proportion of rigid solid elements and elements modeled as titanium (shown in white).

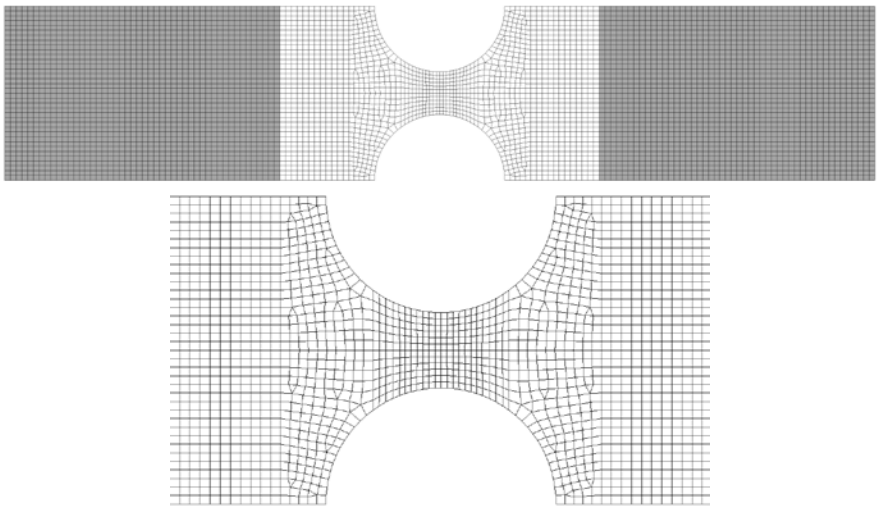

Figure 77. Meshed model of specimen SG3 showing rigid solid elements (gray) and titanium elements (white)

5.1.4 SG4—Plane-Stress Specimen

SG4 is a variation of the plane stress specimen that has a specifically chosen center geometry, or notch, that will produce a unique triaxiality and Lode parameter. The dimensions of the specimen are shown in figure 78.

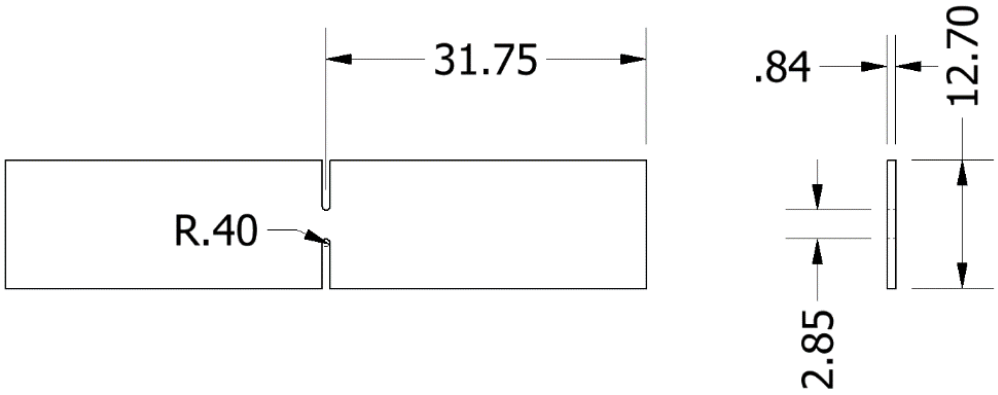

Figure 78. Geometry of specimen SG4

This specimen was then meshed with solid elements so that the average element size was 0.2 mm. The mesh of the SG4 specimen is shown in figure 79. An enlargement of the area containing the 4.00 mm virtual (DIC) extensometer gauge length is also shown in more detail. The mesh for this specimen contains approximately 41,000 solid elements. To model the mechanical grips of the material testing machine, some of the nodes on each end of the specimen were considered rigid elements. Of the 41,000 elements, approximately 30,000 were considered rigid solid elements (shown in gray). Figure 79 shows the proportion of rigid solid elements and elements modeled as titanium (shown in white).

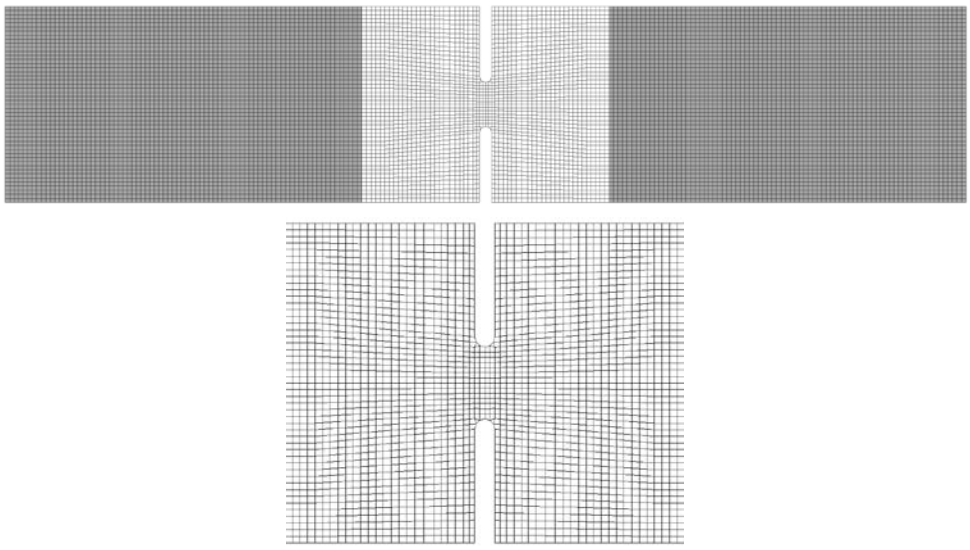

Figure 79. Meshed model of specimen SG4 showing rigid solid elements (gray) and titanium elements (white)

5.1.5 SG5—Axisymmetric Specimen (Pure Tension)

SG5 is an axisymmetric (cylindrical) specimen that has a center section that is under pure tension. The dimensions of the specimen are shown in figure 80.

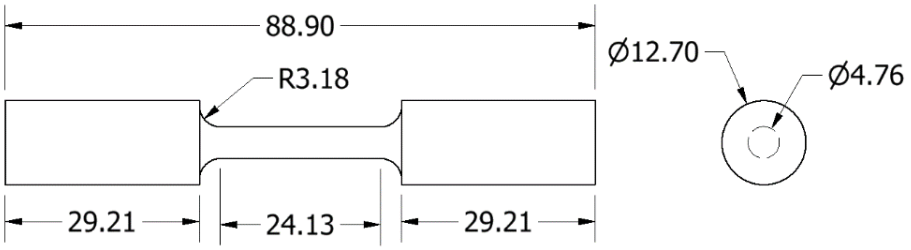

Figure 80. Geometry of specimen SG5

This specimen was then meshed with solid elements so that the average element size was 0.2 mm. The mesh of the SG5 specimen is shown in figure 81. An enlargement of the area containing the 4.00 mm virtual (DIC) extensometer gauge length and the center cross-section are also shown in more detail. The mesh for this specimen contains approximately 471,000 solid elements. To model the mechanical grips of the material testing machine, some of the nodes on each end of the specimen were considered rigid elements. Of the 471,000 elements, approximately 300,000 were considered rigid solid elements (shown in gray). Figure 81 shows the proportion of rigid solid elements and elements modeled as titanium (shown in white).

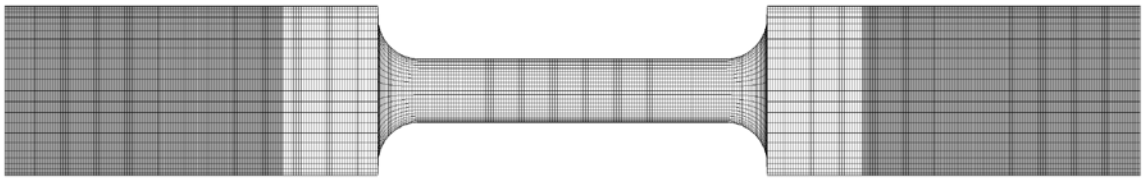

Figure 81. Meshed model of specimen SG5 showing rigid solid elements (gray) and titanium elements (white)

5.1.6 SG6—Axisymmetric Specimen

SG6 is a variation of the axisymmetric specimen that has a specifically chosen center geometry, or notch, that will produce a unique triaxiality and Lode parameter. The dimensions of the specimen are shown in figure 82.

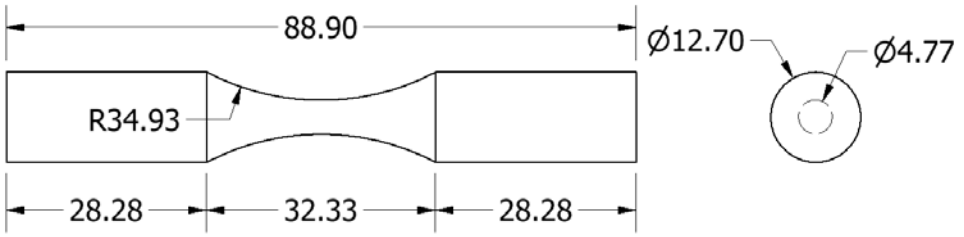

Figure 82. Geometry of specimen SG6

This specimen was then meshed with solid elements so that the average element size was 0.2 mm. The mesh of the SG6 specimen is shown in figure 83. An enlargement of the area containing the 4.00 mm virtual (DIC) extensometer gauge length and the center cross-section are also shown in more detail. The mesh for this specimen contains approximately 430,000 solid

elements. To model the mechanical grips of the material testing machine, some of the nodes on each end of the specimen were considered rigid elements. Of the 430,000 elements, approximately 250,000 were considered rigid solid elements (shown in gray). Figure 83 shows the proportion of rigid solid elements and elements modeled as titanium (shown in white).

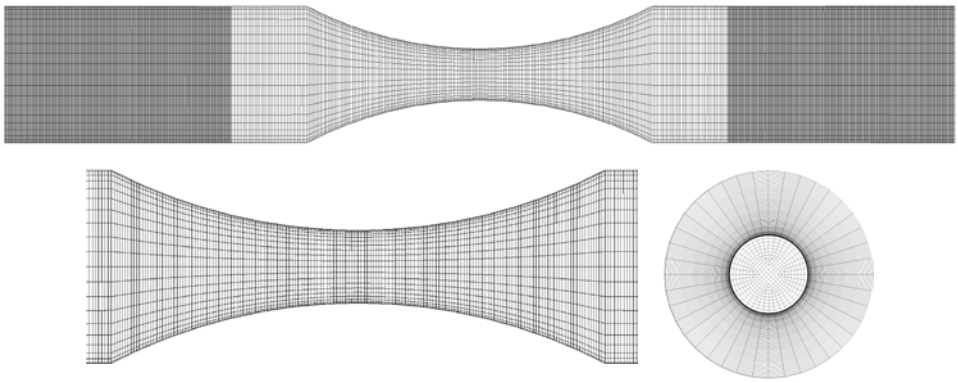

Figure 83. Meshed model of specimen SG6 showing rigid solid elements (gray) and titanium elements (white)

5.1.7 SG7—Axisymmetric Specimen

SG7 is a variation of the axisymmetric specimen that has a specifically chosen center geometry, or notch, that will produce a unique triaxiality and Lode parameter. The dimensions of the specimen are shown in figure 84.

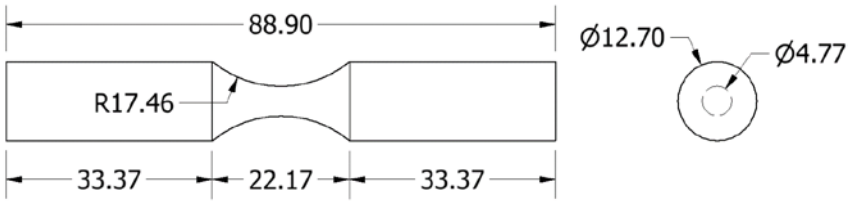

Figure 84. Geometry of specimen SG7

This specimen was then meshed with solid elements so that the average element size was 0.2 mm. The mesh of the SG7 specimen is shown in figure 85. An enlargement of the area containing the 4.00 mm virtual (DIC) extensometer gauge length and the center cross-section are also shown in more detail. The mesh for this specimen contains approximately 457,000 solid elements. To model the mechanical grips of the material testing machine, some of the nodes on each end of the specimen were considered rigid elements. Of the 457,000 elements, approximately 294,000 were considered rigid solid elements (shown in gray). Figure 85 shows the proportion of rigid solid elements and elements modeled as titanium (shown in white).

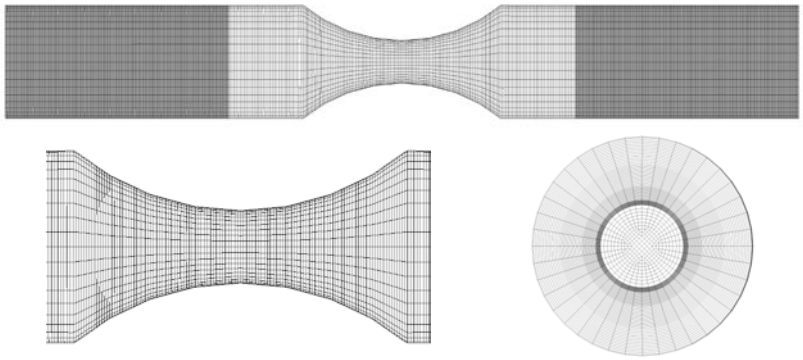

Figure 85. Meshed model of specimen SG7 showing rigid solid elements (gray) and titanium elements (white)

5.1.8 SG8—Axisymmetric Specimen

SG8 is a variation of the axisymmetric specimen that has a specifically chosen center geometry, or notch, that will produce a unique triaxiality and Lode parameter. The dimensions of the specimen are shown in figure 86.

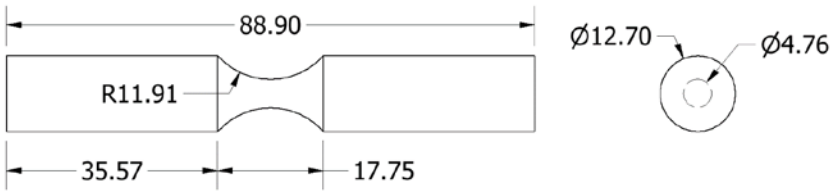

Figure 86. Geometry of specimen SG8

This specimen was then meshed with solid elements so that the average element size was 0.2 mm. The mesh of the SG8 specimen is shown in figure 87. An enlargement of the area containing the 4.00 mm virtual (DIC) extensometer gauge length and the center cross-section are also shown in more detail. The mesh for this specimen contains approximately 385,000 solid elements. To model the mechanical grips of the material testing machine, some of the nodes on each end of the specimen were considered rigid elements. Of the 385,000 elements, approximately 256,000 were considered rigid solid elements (shown in gray). Figure 87 shows the proportion of rigid solid elements and elements modeled as titanium (shown in white).

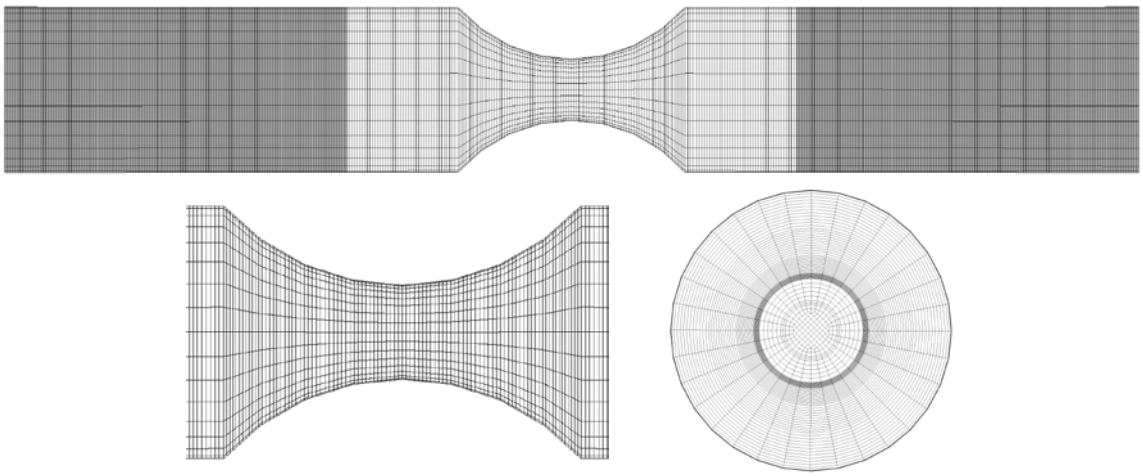

Figure 87. Meshed model of specimen SG8 showing rigid solid elements (gray) and titanium elements (white)

5.1.9 SG9—Axisymmetric Specimen

SG9 is a variation of the axisymmetric specimen that has a specifically chosen center geometry, or notch, that will produce a unique triaxiality and Lode parameter. The dimensions of the specimen are shown in figure 88.

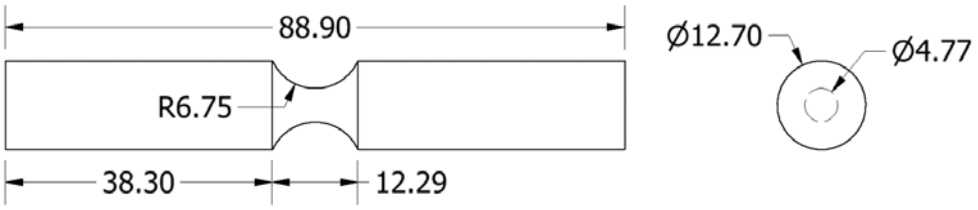

Figure 88. Geometry of specimen SG9

This specimen was then meshed with solid elements so that the average element size was 0.2 mm. The mesh of the SG9 specimen is shown in figure 89. An enlargement of the area containing the 4.00 mm virtual (DIC) extensometer gauge length and the center cross-section are also shown in more detail. The mesh for this specimen contains approximately 652,000 solid elements. To model the mechanical grips of the material testing machine, some of the nodes on each end of the specimen were considered rigid elements. Of the 652,000 elements, approximately 452,000 were considered rigid solid elements (shown in gray). Figure 89 shows the proportion of rigid solid elements and elements modeled as titanium (shown in white).

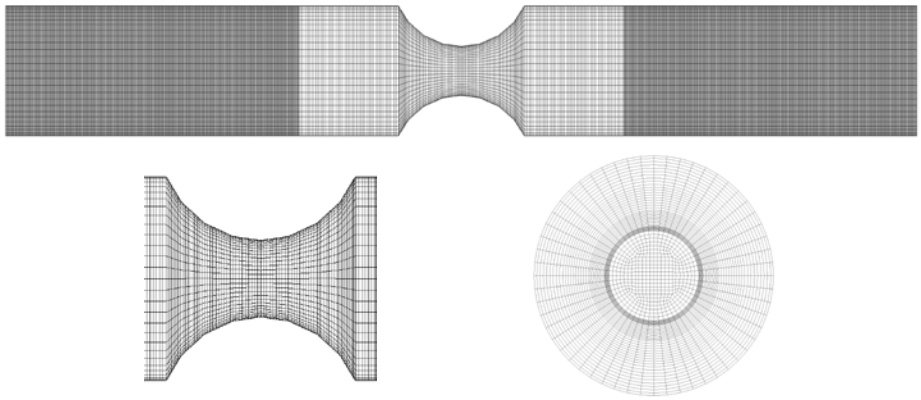

Figure 89. Meshed model of specimen SG9 showing rigid solid elements (gray) and titanium elements (white)

5.1.10 SG10—Axisymmetric Specimen

SG10 is a variation of the axisymmetric specimen that has a specifically chosen center geometry, or notch, that will produce a unique triaxiality and Lode parameter. The dimensions of the specimen are shown in figure 90.

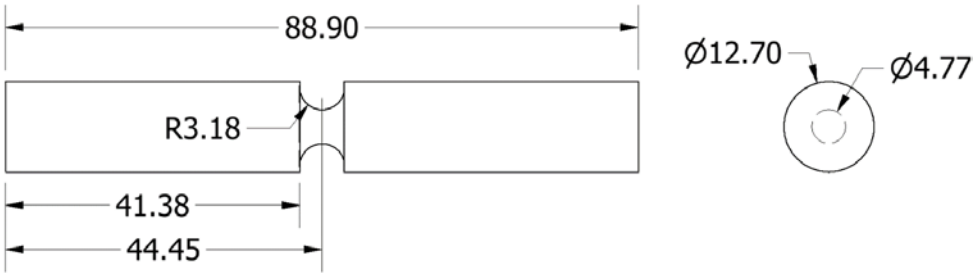

Figure 90. Geometry of specimen SG10

This specimen was then meshed with solid elements so that the average element size was 0.2 mm. The mesh of the SG10 specimen is shown in figure 91. An enlargement of the area containing the 4.00 mm virtual (DIC) extensometer gauge length and the center cross-section are also shown in more detail. The mesh for this specimen contains approximately 593,000 solid elements. To model the mechanical grips of the material testing machine, some of the nodes on each end of the specimen were considered rigid elements. Of the 593,000 elements, approximately 432,000 were considered rigid solid elements (shown in gray). Figure 91 shows the proportion of rigid solid elements and elements modeled as titanium (shown in white).

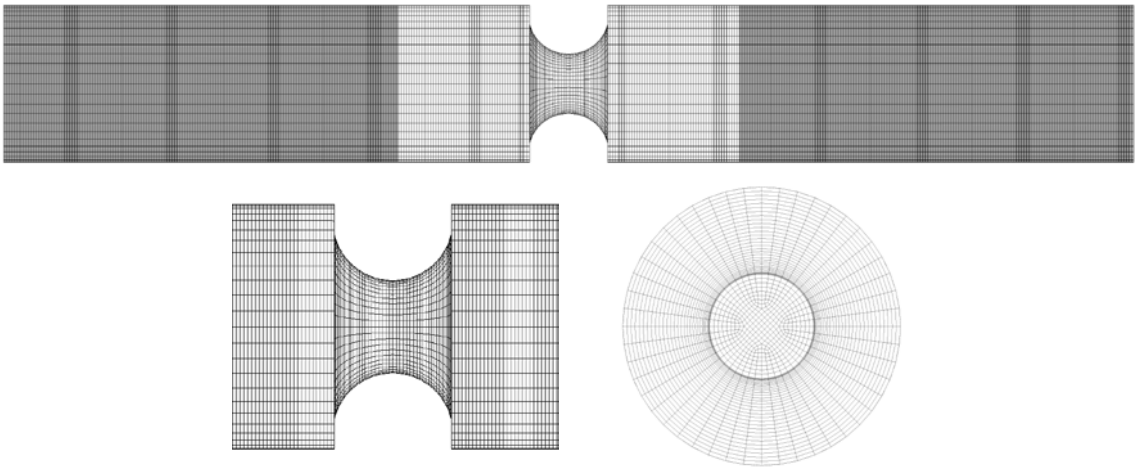

Figure 91. Meshed model of specimen SG10 showing rigid solid elements (gray) and titanium elements (white)

5.1.11 SG11—Plane Strain Specimen

SG11 is a plane strain specimen that has a specifically chosen center geometry that is under pure tension. The dimensions of the specimen are shown in figure 92.

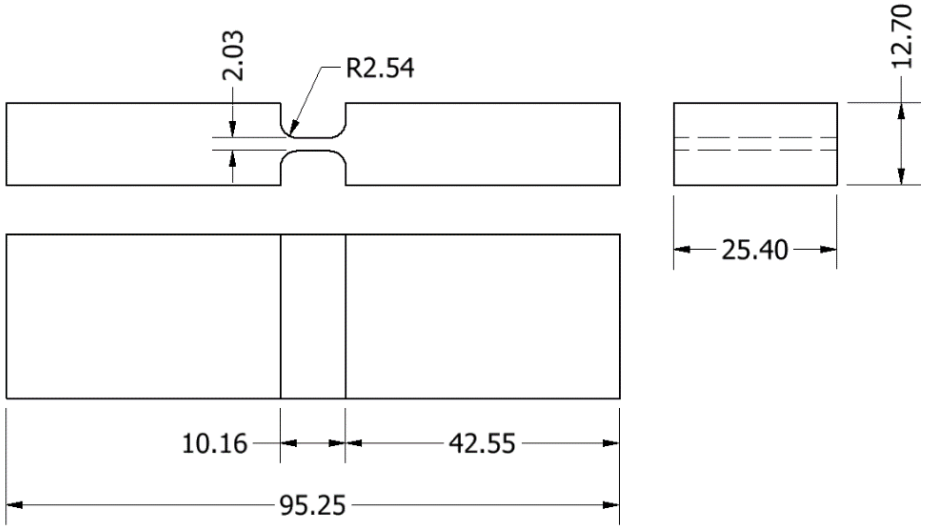

Figure 92. Geometry of specimen SG11

This specimen was then meshed with solid elements so that the average element size was 0.2 mm. The mesh of the SG11 specimen is shown in figure 93. An enlargement of the area containing the 4.00 mm virtual (DIC) extensometer gauge length and the center cross-section are also shown in more detail. The mesh for this specimen contains approximately 935,000 solid elements. To model the mechanical grips of the material testing machine, some of the nodes on each end of the specimen were considered rigid elements. Of the 935,000 elements, approximately 442,000 were considered rigid solid elements (shown in gray). Figure 93 shows the proportion of rigid solid elements and elements modeled as titanium (shown in white).

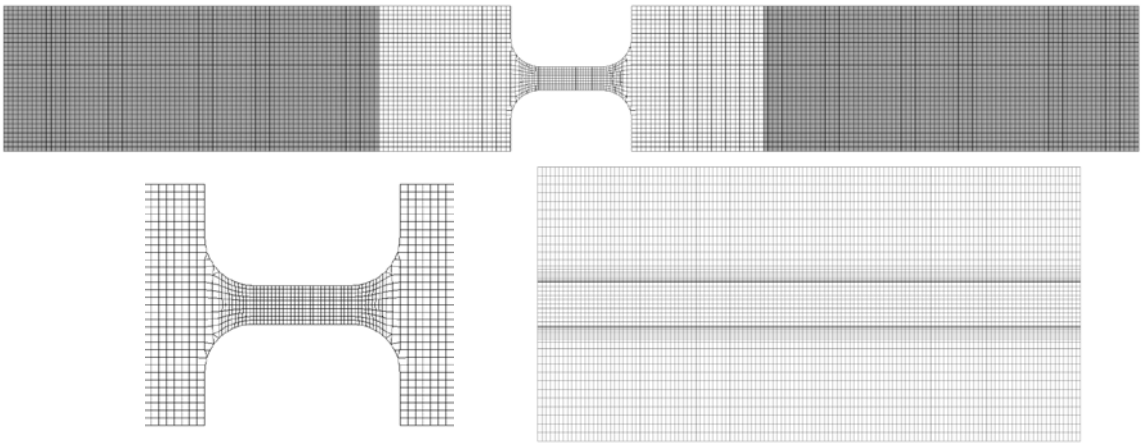

Figure 93. Meshed model of specimen SG11 showing rigid solid elements (gray) and titanium elements (white)

5.1.12 SG12—Plane Strain Specimen

SG12 is a variation of the plane strain specimen that has a specifically chosen center geometry, or notch, that will produce a unique triaxiality and Lode parameter. The dimensions of the specimen are shown in figure 94.

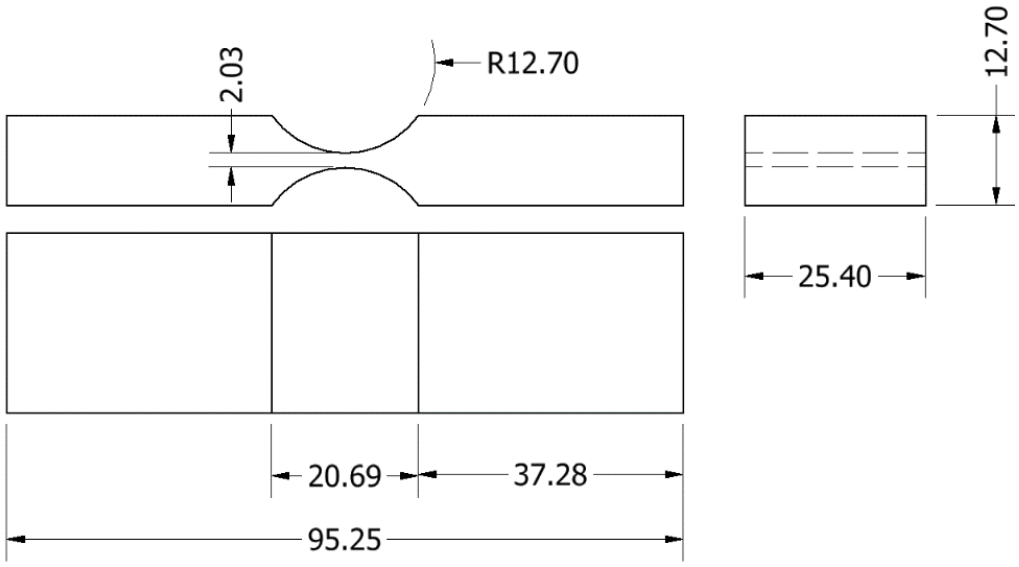

Figure 94. Geometry of specimen SG12

This specimen was then meshed with solid elements so that the average element size was 0.2 mm. The mesh of the SG12 specimen is shown in figure 95. An enlargement of the area containing the 4.00 mm virtual (DIC) extensometer gauge length and the center cross-section are also shown in more detail. The mesh for this specimen contains approximately 740,000 solid elements. To model the mechanical grips of the material testing machine, some of the nodes on each end of the specimen were considered rigid elements. Of the 740,000 elements,

approximately 452,000 were considered rigid solid elements (shown in gray). Figure 95 shows the proportion of rigid solid elements and elements modeled as titanium (shown in white).

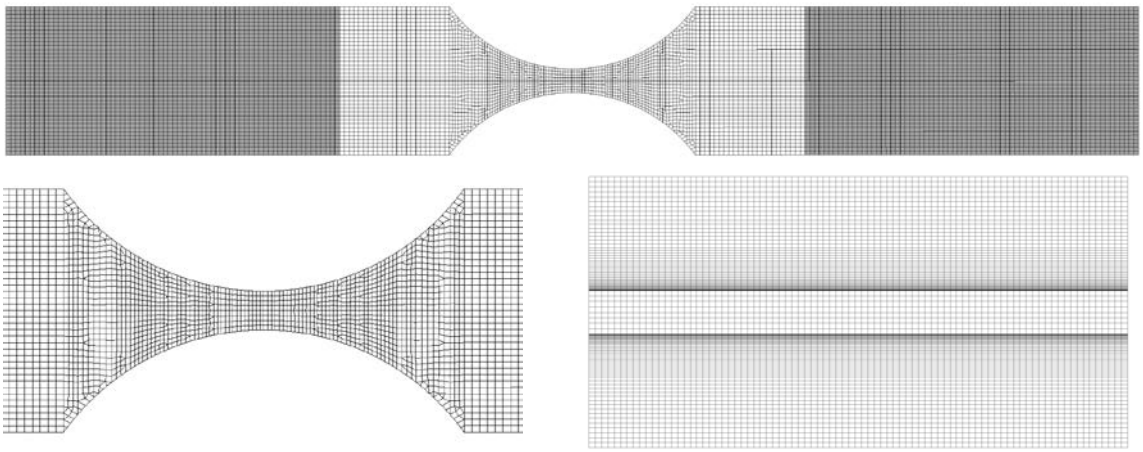

Figure 95. Meshed model of specimen SG12 showing rigid solid elements (gray) and titanium elements (white)

5.1.13 SG13—Plane Strain Specimen

SG13 is a variation of the plane strain specimen that has a specifically chosen center geometry, or notch, that will produce a unique triaxiality and Lode parameter. The dimensions of the specimen are shown in figure 96.

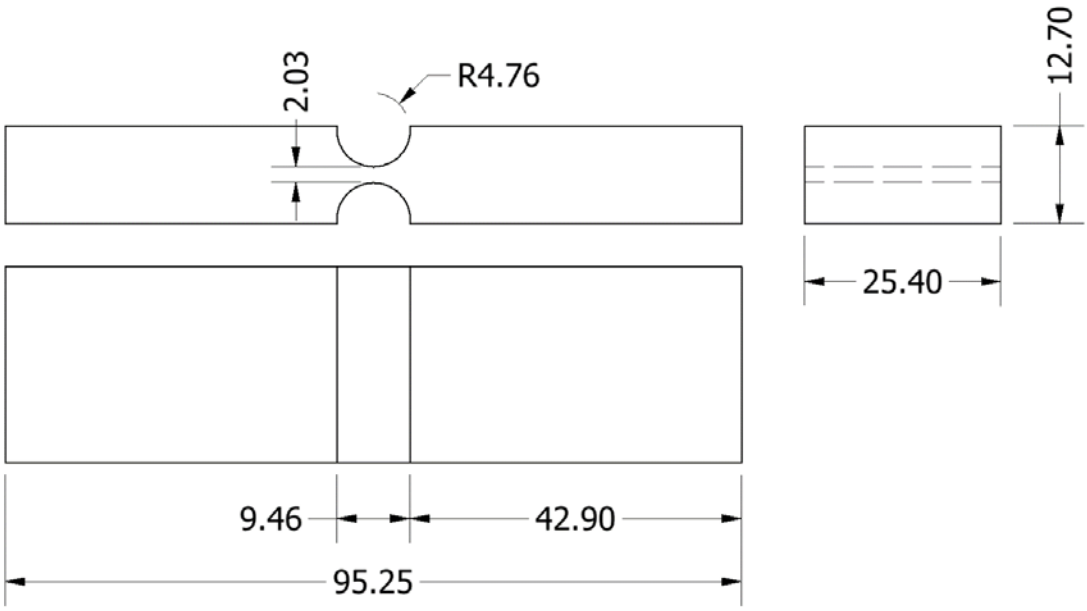

Figure 96. Geometry of specimen SG13

This specimen was then meshed with solid elements so that the average element size was 0.2 mm. The mesh of the SG13 specimen is shown in figure 97. An enlargement of the area containing the 4.00 mm virtual (DIC) extensometer gauge length and the center cross-section are

also shown in more detail. The mesh for this specimen contains approximately 2,639,000 solid elements. To model the mechanical grips of the material testing machine, some of the nodes on each end of the specimen were considered rigid elements. Of the 2,639,000 elements, approximately 1,924,000 were considered rigid solid elements (shown in gray). Figure 97 shows the proportion of rigid solid elements and elements modeled as titanium (shown in white).

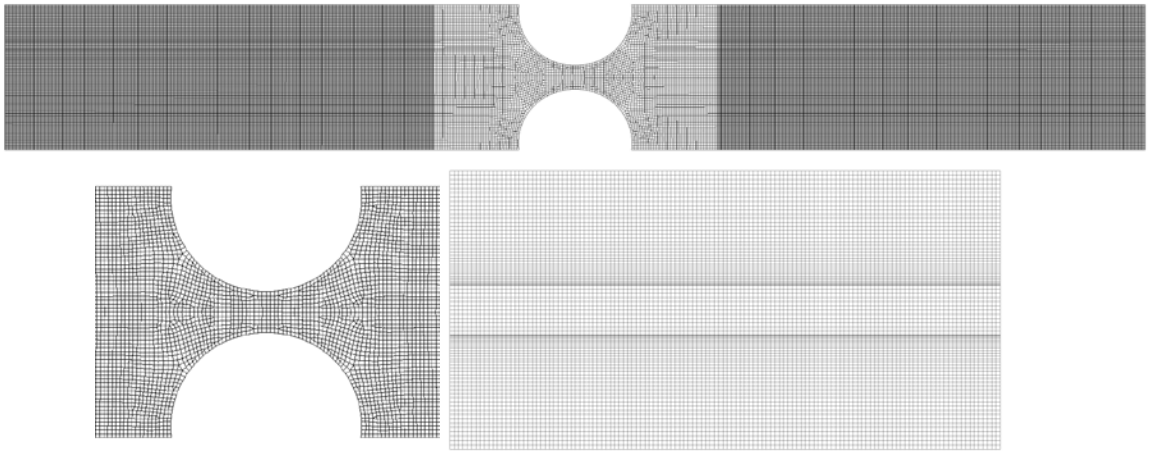

Figure 97. Meshed model of specimen SG13 showing rigid solid elements (gray) and titanium elements (white)

5.1.14 LR1–Combined (Tension/Torsion) Specimen

LR1 is a combined loading specimen in which the ratio of tensile and torsional stress is tuned so that the area of localization will result in a unique triaxiality and Lode parameter. The dimensions of the specimen are shown in figure 98.

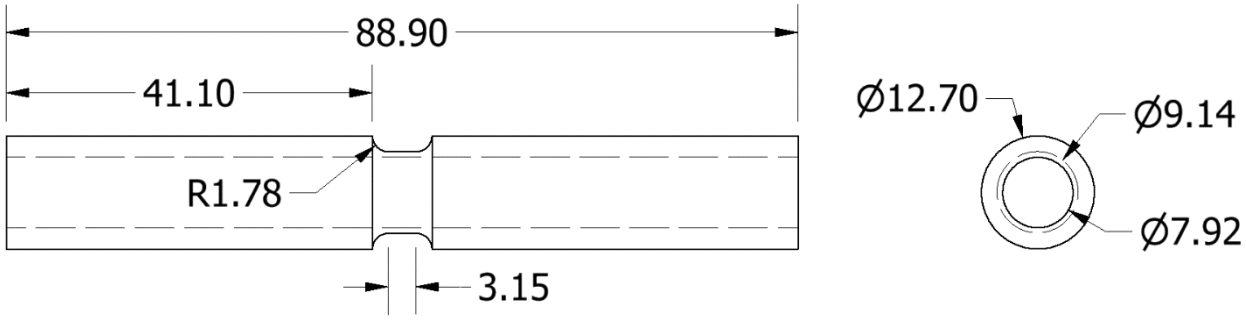

Figure 98. Geometry of specimen LR1

This specimen was then meshed with solid elements so that the average element size was 0.2 mm. The mesh of the LR1 specimen is shown in figure 99. An enlargement of the area containing the 4.00 mm virtual (DIC) extensometer gauge length and the center cross-section are also shown in more detail. The mesh for this specimen contains approximately 814,000 solid elements. To model the mechanical grips of the material testing machine, some of the nodes on each end of the specimen were considered rigid elements. Of the 814,000 elements,

approximately 442,000 were considered rigid solid elements (shown in gray). Figure 99 shows the proportion of rigid solid elements and elements modeled as titanium (shown in white).

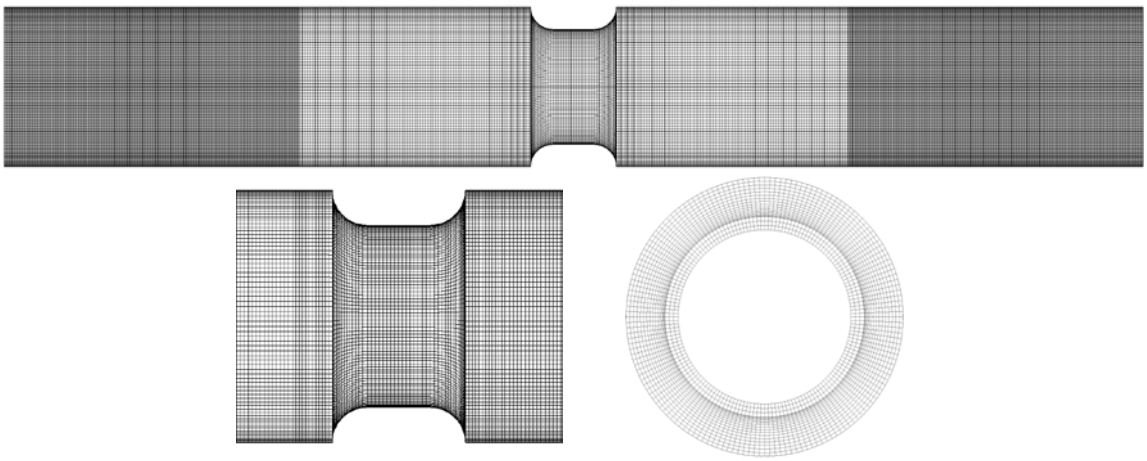

Figure 99. Meshed model of specimen LR1 showing rigid solid elements (gray) and titanium elements (white)

Because these specimens are highly sensitive to the ratio of the applied force and torque, this simulation was designed differently than the other tensile specimen tests. For these combined loading tests, the motion of the grips was controlled by a specific force and torque as described by two input curves. Instead of using a *BOUNDARY_PRESCRIBED_MOTION_RIGID keyword applied to the clamped elements, a *LOAD_RIGID_BODY keyword was used. Using a reference curve, both the applied tensile force and torque were controlled using this keyword. These curves were generated using the results from the physical tests. Each of the three tests in the data set was averaged and smoothed to approximately 100 data points. The input force and torque curves for this specimen are shown in figure 100. When using force and torque controls, extra care must be taken to verify that there is no significant oscillation or unstable conditions during the simulations. For reference, figure 100 also shows the cross-sectional output from the initial simulation. Because there is very little oscillation or instabilities, it was confirmed that this method can be used for the combined loading specimen simulations.

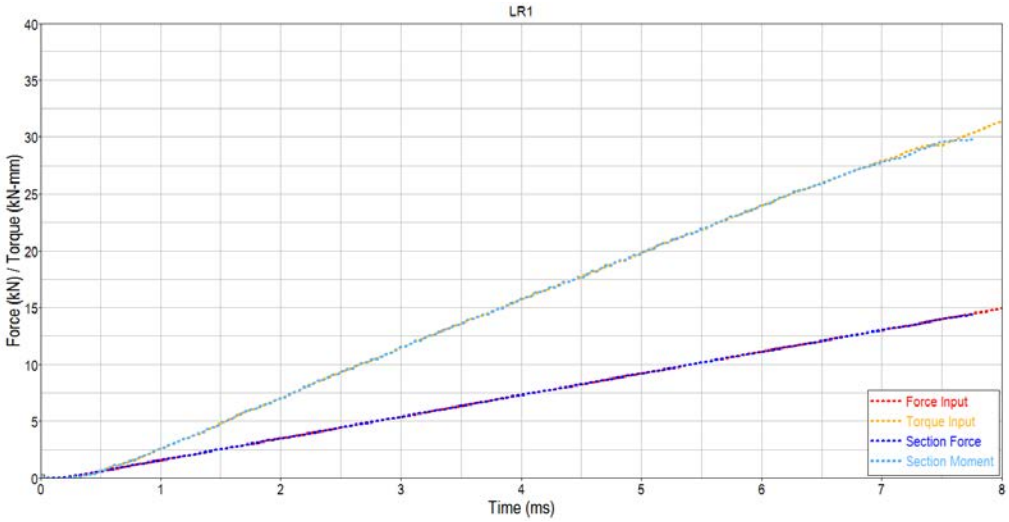

Figure 100. Cross-sectional simulation output for LR1

5.1.15 LR2—Combined (Tension/Torsion) Specimen

LR2 is a combined loading specimen in which the ratio of tensile and torsional stress is tuned so that the area of localization will result in a unique triaxiality and Lode parameter. Because the force and torque ratio changes the triaxiality and Lode parameter, the geometry is approximately the same as the LR1 specimen described in section 5.1.14. The mesh used was adjusted slightly to precisely match the actual test specimen dimensions. In addition, the mesh and mechanical grip positions are the same as LR1.

Like LR1, this specimen used a *LOAD_RIGID_BODY keyword to produce a specific force and toque that matches the measured values in the physical test. The input force and torque curves for this specimen are shown in figure 101. For reference, figure 101 also shows the cross-sectional output from the initial simulation.

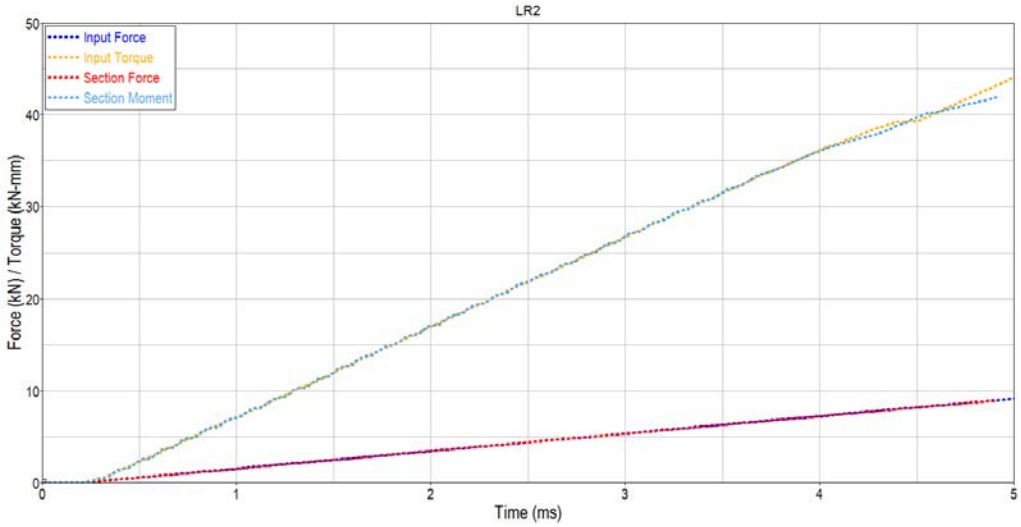

Figure 101. Cross-sectional simulation output for LR2

5.1.16 LR3—Torsion Specimen

LR3 is a pure torsion test specimen that has the same geometry as the LR1 and LR2 specimens. Unlike the LR1 and LR2 specimens, this test does not include a tensile component. The mesh and mechanical grip positions for the LR3 specimen are the same as LR1 and LR2. The mesh used was adjusted slightly to precisely match the actual test specimen dimensions.

Like LR1, this specimen used a *LOAD_RIGID_BODY keyword to produce a specific force and torque that matches the measured values in the physical test. The input force and torque curves for this specimen are shown in figure 102. For reference, figure 102 also shows the cross-sectional output from the initial simulation.

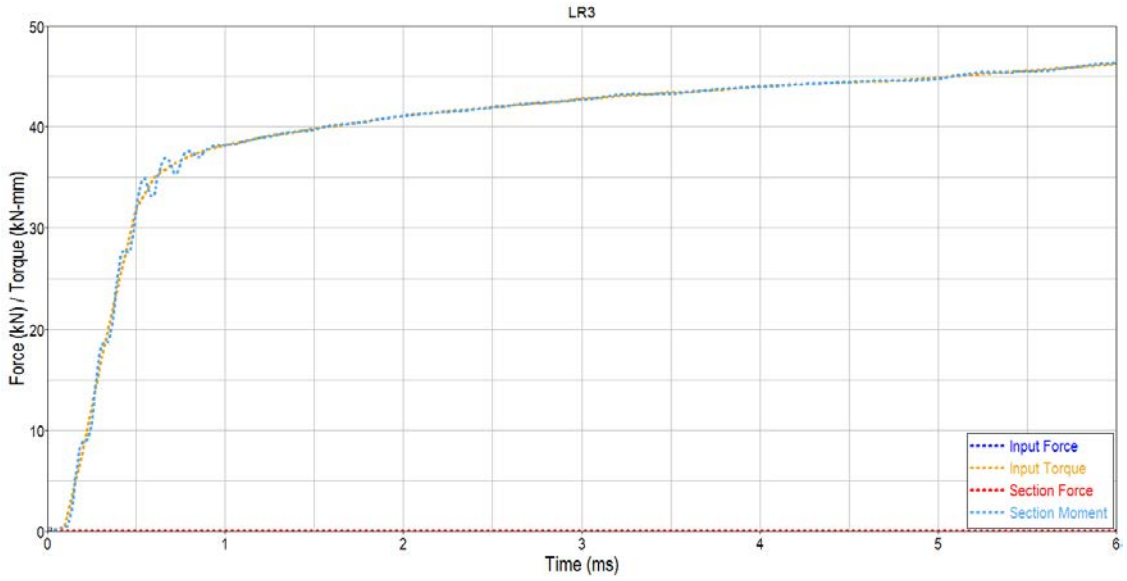

Figure 102. Cross-sectional simulation output for LR3

5.1.17 LR4—Combined (Compression/Torsion) Specimen

LR4 is a combined loading specimen in which the ratio of compressive and torsional stress is tuned so that the area of localization will result in a unique triaxiality and Lode parameter. The dimensions of the specimen are shown in figure 103.

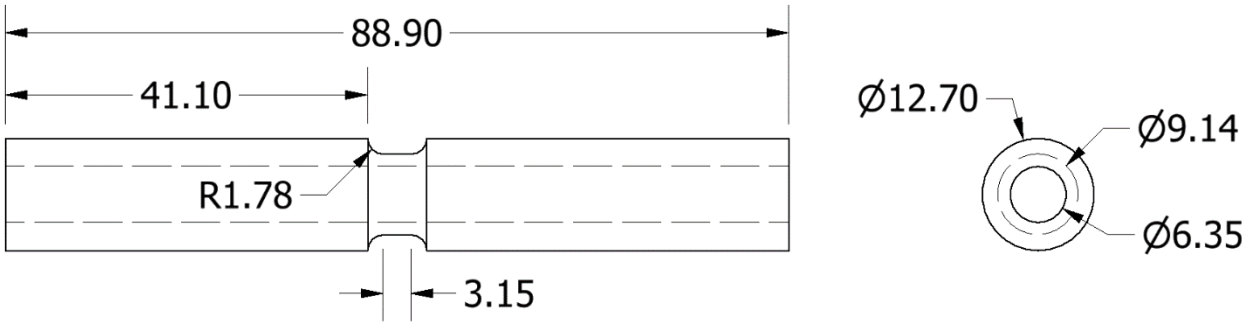

Figure 103. Geometry of specimen LR4

This specimen was then meshed with solid elements so that the average element size was 0.2 mm. The mesh of the LR4 specimen is shown in figure 104. An enlargement of the area containing the 4.00 mm virtual (DIC) extensometer gauge length and the center cross-section are also shown in more detail. The mesh for this specimen contains approximately 1,093,000 solid elements. To model the mechanical grips of the material testing machine, some of the nodes on each end of the specimen were considered rigid elements. Of the 1,093,000 elements, approximately 742,000 were considered rigid solid elements (shown in gray). Figure 104 shows the proportion of rigid solid elements and elements modeled as titanium (shown in white).

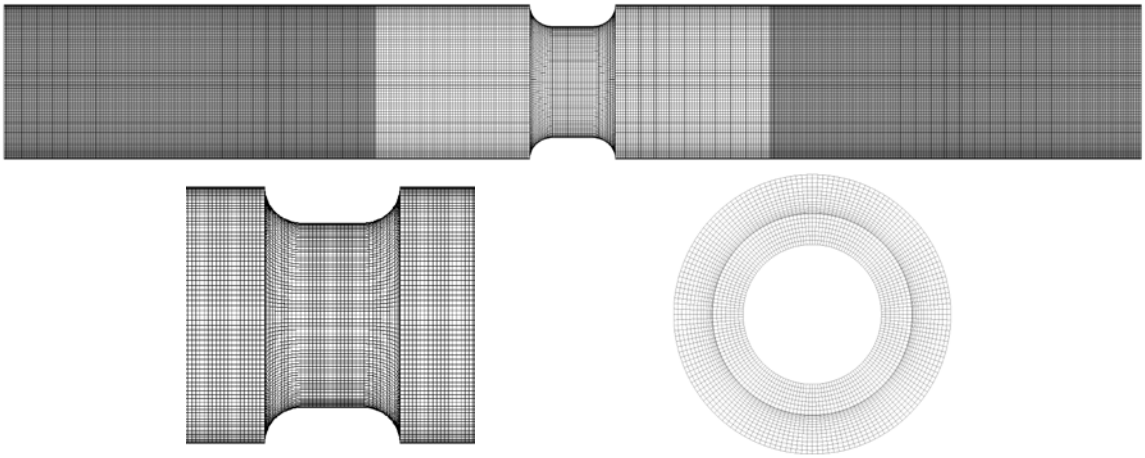

Figure 104. Meshed model of specimen LR4 showing rigid solid elements (gray) and titanium elements (white)

Like LR1, this specimen used a *LOAD_RIGID_BODY keyword to produce a specific force and torque that matches the measured values in the physical test. The input force and torque curves for this specimen are shown in figure 105. For reference, figure 105 also shows the cross-sectional output from the initial simulation.

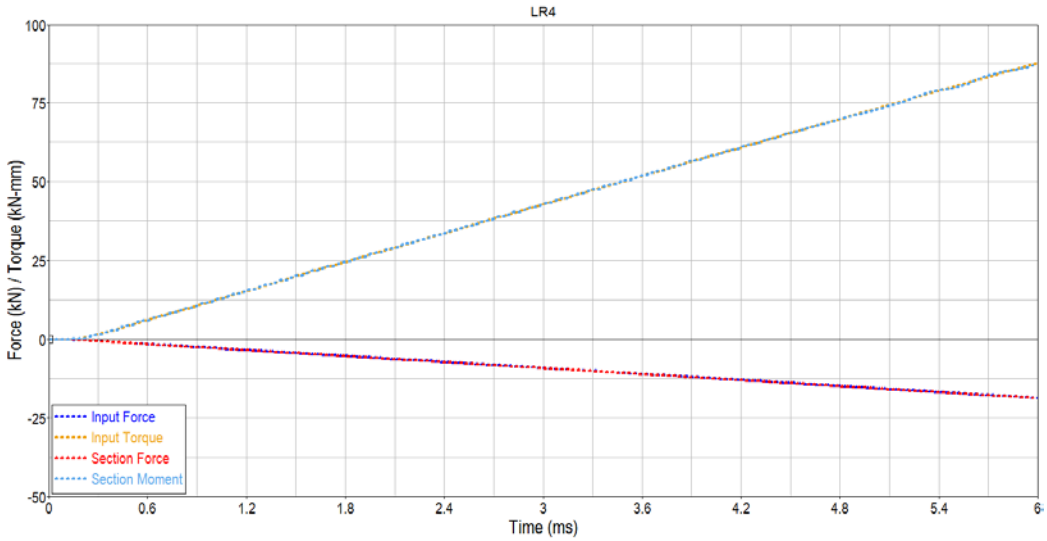

Figure 105. Cross-sectional simulation output for LR4

5.1.18 Punch1—Large Diameter Punch Specimen

Punch1 is a quasistatic, large diameter test in which a specifically designed punch is pushed through the center of a cylindrical plate of titanium. Each punch is designed to produce a unique triaxiality and Lode parameter on the far side of the titanium plate. The geometry and dimensions for Punch1 are shown in figure 106.

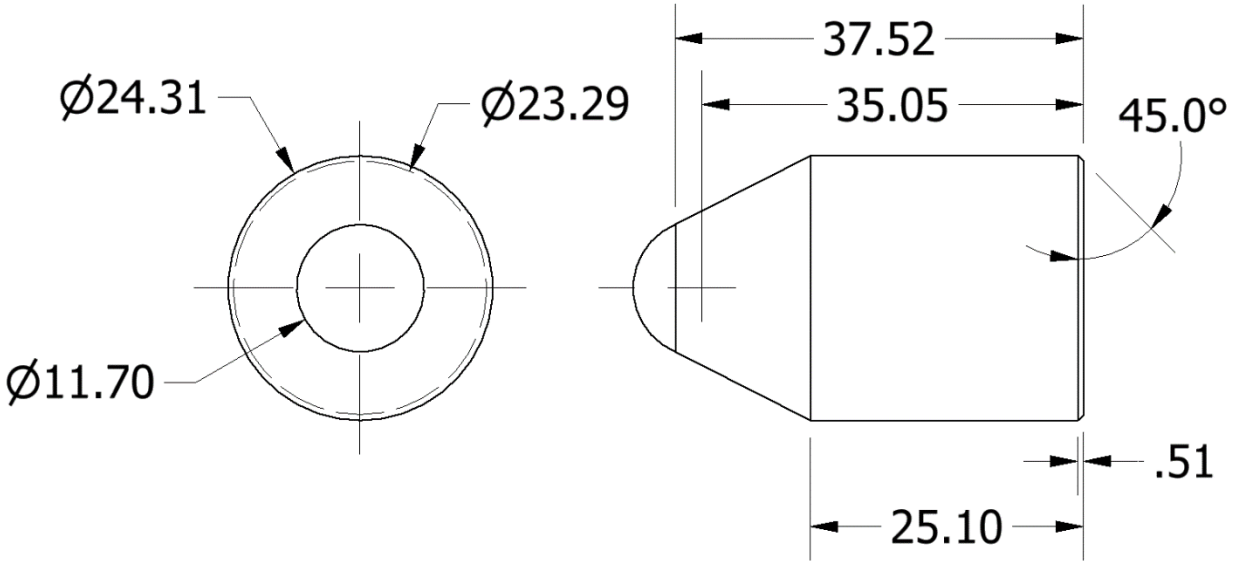

Figure 106. Geometry of specimen Punch1

For the simulation of this test, the punch was modeled as rigid shell elements. The nominal size for each element was set to 0.2 mm. The mesh (see figure 107) has approximately 50,000 rigid shell elements.

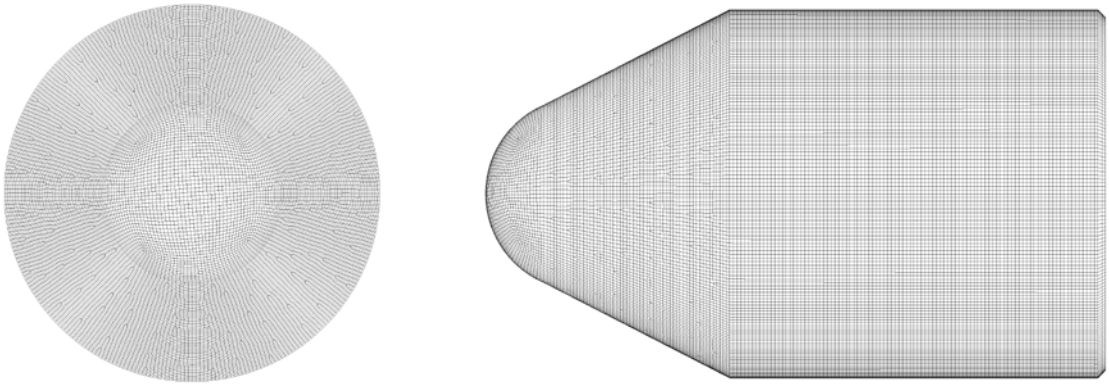

Figure 107. Meshed model of the specimen Punch1

The titanium plate is a cylinder with a 50.0 mm diameter and depth of 5.08 mm. To model the boundary conditions of the punch, some of the outer elements of the cylindrical plate are modeled as stationary rigid elements (shown in gray), whereas the inner elements are regular solid elements modeled as titanium (shown in white). The elements along the boundary are

connected by shared nodes. The mesh of the titanium plate (see figure 108) consists of approximately 420,000 elements. Of those 420,000 elements, 164,000 are modeled as rigid.

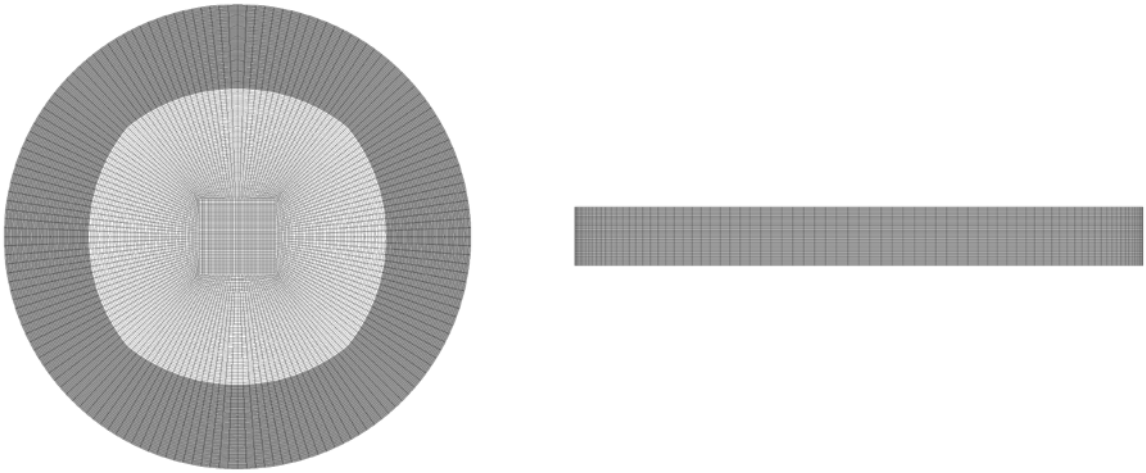

Figure 108. Meshed model of titanium plate

5.1.19 Punch2—Large Diameter Punch Specimen

Punch2 is a quasistatic, large diameter test in which a specifically designed punch is pushed through the center of a cylindrical plate of titanium. Each punch is designed to produce a unique triaxiality and Lode parameter on the far side of the titanium plate. The geometry and dimensions for Punch2 are shown in figure 109.

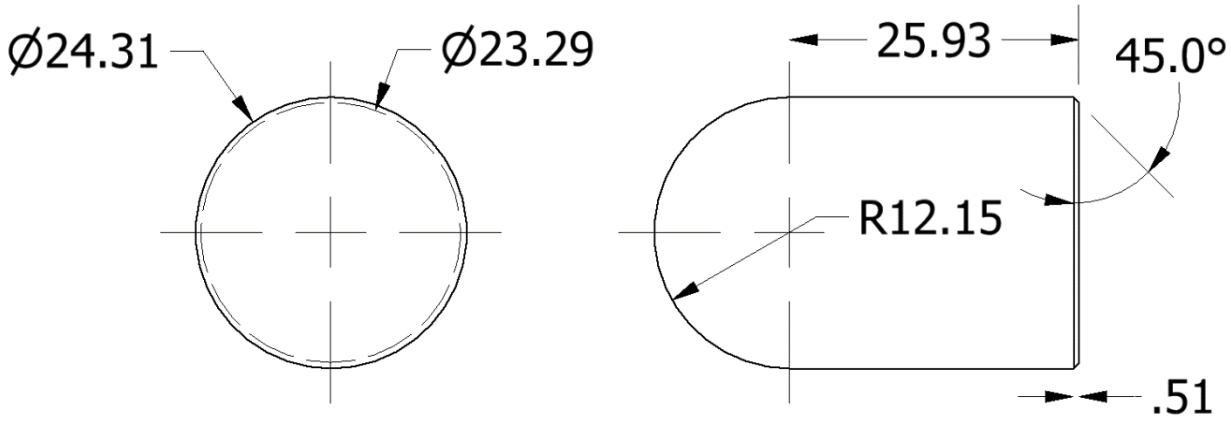

Figure 109. Geometry of the specimen Punch2

For the simulation of this test, the punch was modeled as rigid shell elements. The nominal size for each element was set to 0.2 mm. The mesh (see figure 110) has approximately 58,000 rigid shell elements.

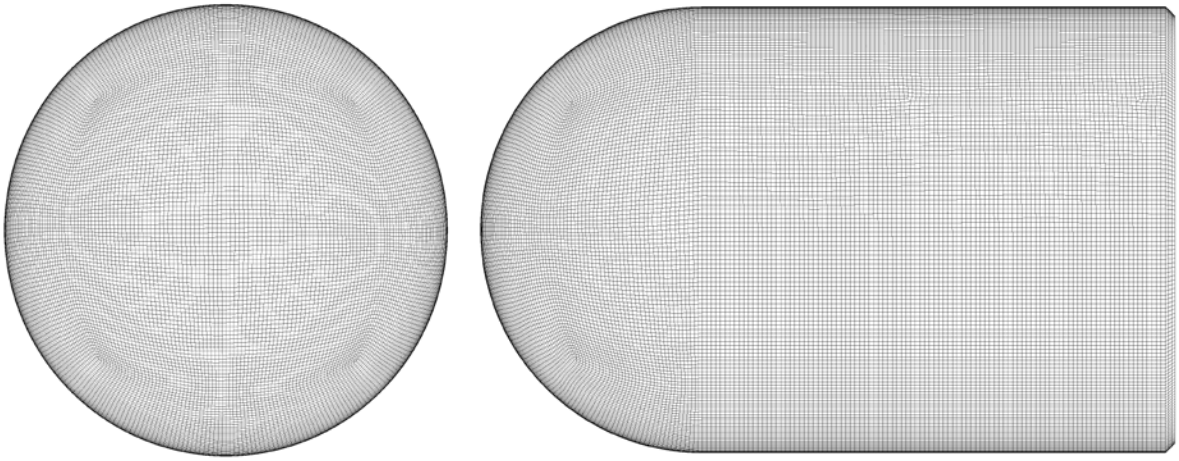

Figure 110. Meshed model of the specimen Punch2

The titanium plate that is used for this test is identical in geometry to the Punch1 plate specimen. Therefore, the exact same dimensions and mesh described in section 5.1.19 were used for this simulation.

5.1.20 Compression—Uniaxial (Cylindrical) Compression Specimen

The compression specimen is a quasistatic uniaxial compression test on a small cylinder of titanium. The cylinder has a diameter of 3.82 mm and a height of 3.73 mm. The mesh (see figure 111) has a nominal mesh size of 0.2 mm and is modeled as solid elements. In addition, rigid walls are modeled at the ends of the cylinder to simulate the compressive plates of the material testing machine. This specimen contains approximately 2000 solid elements.

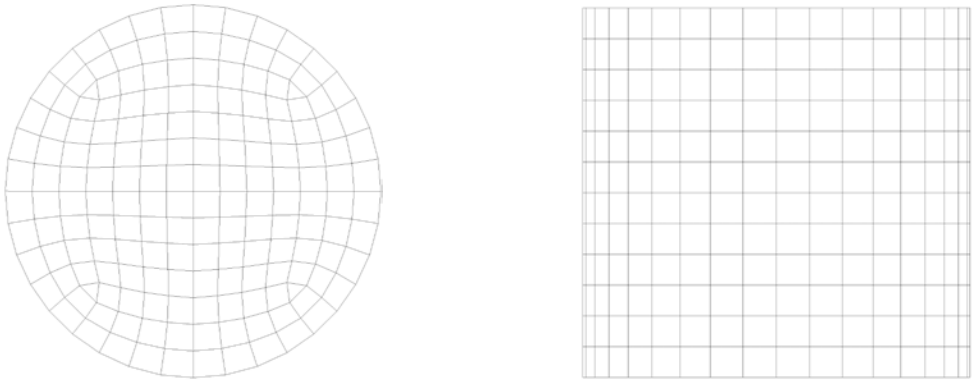

Figure 111. Meshed model of cylindrical compression specimen

After a preliminary analysis of the physical test of the compression specimens, it was noted that no failure occurred at any location. This is likely due to the lack of any shear which typically translates to very high failure strains in compression. Because no failure occurred in the tests, this specimen will only be used for validation in the final failure surface. The failure strain for high triaxialities (above one third) was initially set at an arbitrary value that was high enough for

this specimen not to fail in the simulation. Adjustments to these arbitrary values will be discussed in section 6.

5.2 SIMULATION RESULTS OF MECHANICAL PROPERTY TESTS

Each specimen is initially simulated without a failure surface, or failure criteria, to verify that the model works properly and determine the unique triaxiality and Lode parameter. Three response characteristics are used to verify that each specimen responds similar to the tests performed by OSU: displacement, force, and DIC strain field.

For each test, a virtual extensometer was defined using the DIC analysis software. This extensometer was duplicated in the finite element mesh. For each specimen, nodes were spaced so that there was 2.0 mm on each side of the geometric center. Two nodes were selected to represent the ends of the virtual extensometer used in the DIC analysis. These nodes were saved using the *DATABASE_HISTORY_NODE function in LS-DYNA.

For the combined loading simulations that may include tensile and shear stresses, the angle of twist was measured. This angle, which was compared directly to a rotary variable differential transformer during the test, can be calculated using the nodes at the end of the 4.0 mm virtual extensometer. Figure 112 shows how the angle of twist is measured.

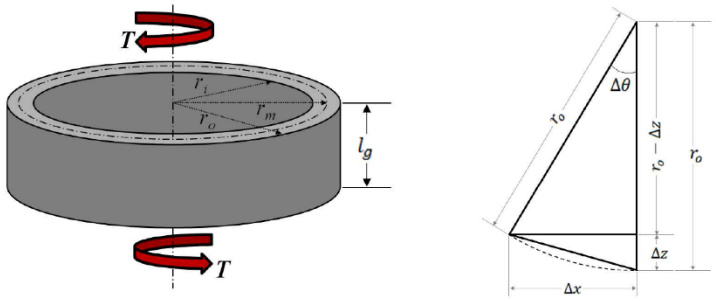

Figure 112. Measurement of twist angle

Using the dimensions in figure 112, the following equation shows how the angle of twist can be calculated from the displacements of the virtual extensometer nodes:

$$\Delta\theta = \arccos\left\{\frac{(r_0 - \Delta z)^2 + r_0^2 - \Delta x^2}{2r_0 - (r_0 - \Delta z)}\right\} \tag{35}$$

where r_0 is the outer radius of the cylinder, Δz is the displacement in the radial direction of the cylinder, and Δx is the displacement in the transverse lateral direction of the cylinder.

In addition to the extensometer displacement/twist measurement, the time history of the cross-sectional force was also stored in the simulation. To accomplish this, a *DATABASE_CROSS_SECTION_PLANE was used in the center of the specimen to measure

the tensile/compressive force. This cross-section was oriented so that the normal vector was in the direction of the tensile/compressive force.

Lastly, the fringe plot function of LS-PrePost can be used to compare the strain fields to the DIC images captured during the physical test. Using this comparison, the strains at multiple locations on the specimens can be verified. In addition, the general location of the failure seen in the DIC image can be compared to the localization point in the simulation. Note that this comparison requires that the virtual strain gauge length in the experiment be approximately the same (in the mesh) as the simulation.

The force versus displacement time history plots and DIC-fringe plot comparison for each specimen are shown in figures 113 (a–q) and figures 114 (a–t). For reference, the DIC-fringe plot comparisons are shown at a time close to the failure of the material. The force-displacement plots for the punch tests are not shown without failure because these tests are not a fail/not-fail type test. That is, the results are dependent on the failure of the elements over time, not instantaneously.

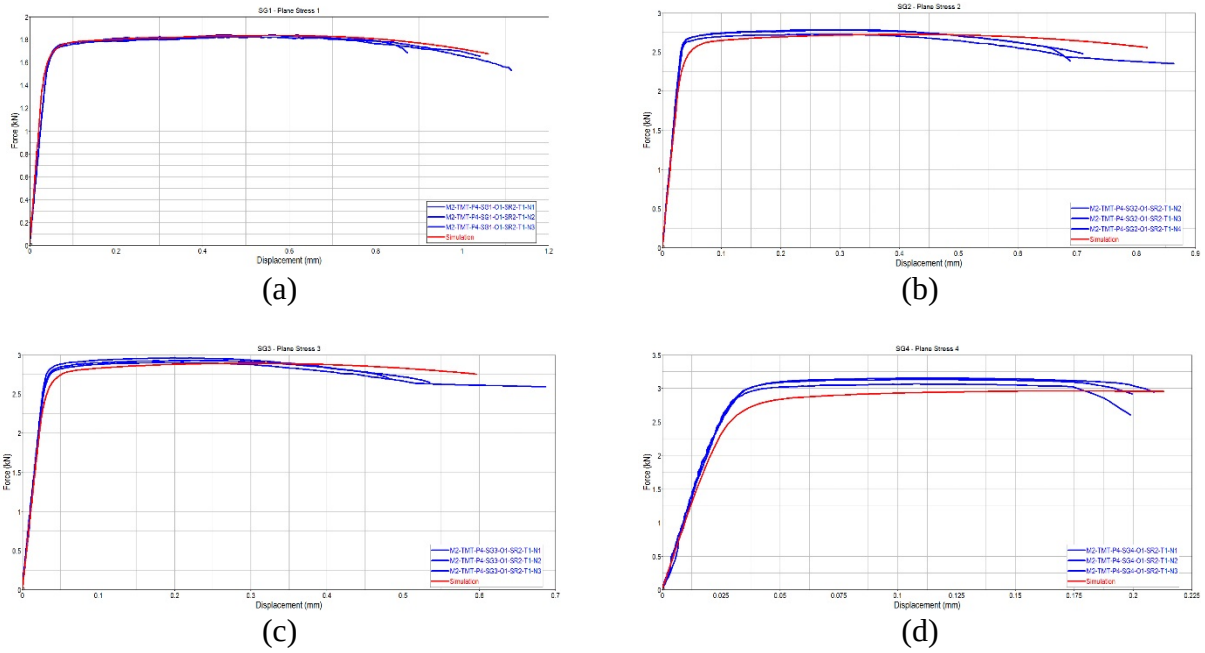

(a) (b)

(c) (d)

Figure 113. Force versus time history comparison plot for each specimen ((a) SG1, (b) SG2, (c) SG3, (d) SG4, (e) SG5, (f) SG6, (g) SG7, (h) SG8, (i) SG9, (j) SG10, (k) SG11, (l) SG12, (m) SG13, (n) LR1, (o) LR2, (p) LR3, and (q) LR4)

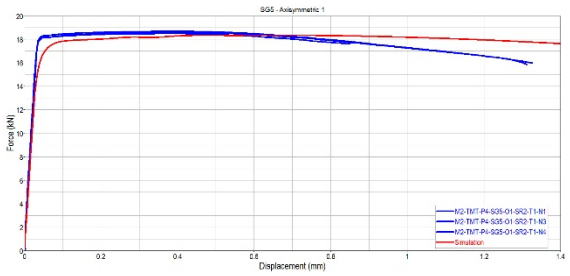

(e)

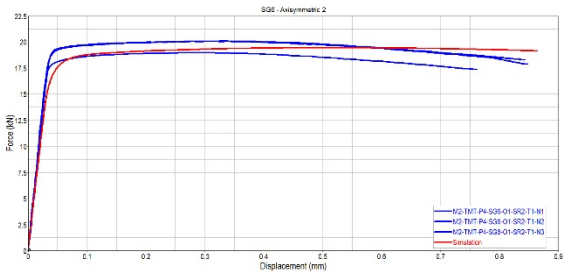

(f)

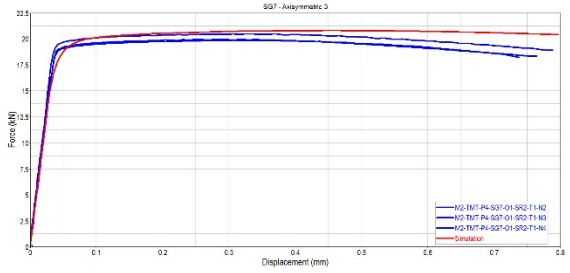

(g)

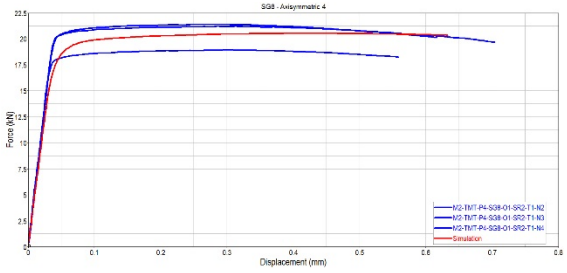

(h)

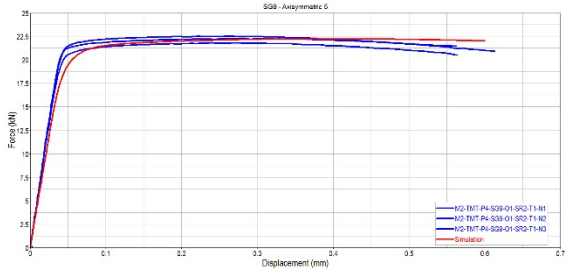

(i)

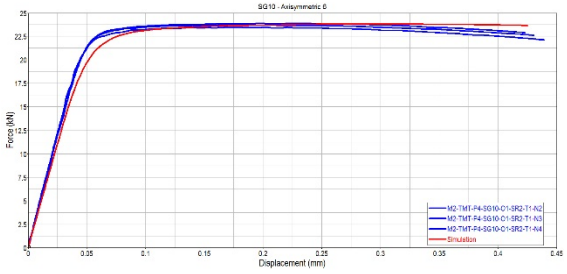

(j)

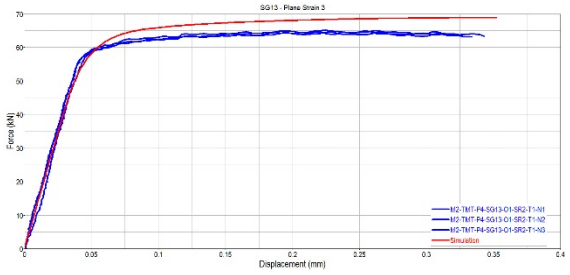

(k)

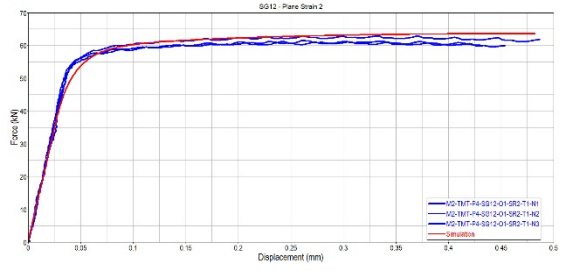

(l)

Figure 113. Force versus time history comparison plot for each specimen (continued) ((a) SG1, (b) SG2, (c) SG3, (d) SG4, (e) SG5, (f) SG6, (g) SG7, (h) SG8, (i) SG9, (j) SG10, (k) SG11, (l) SG12, (m) SG13, (n) LR1, (o) LR2, (p) LR3, and (q) LR4)

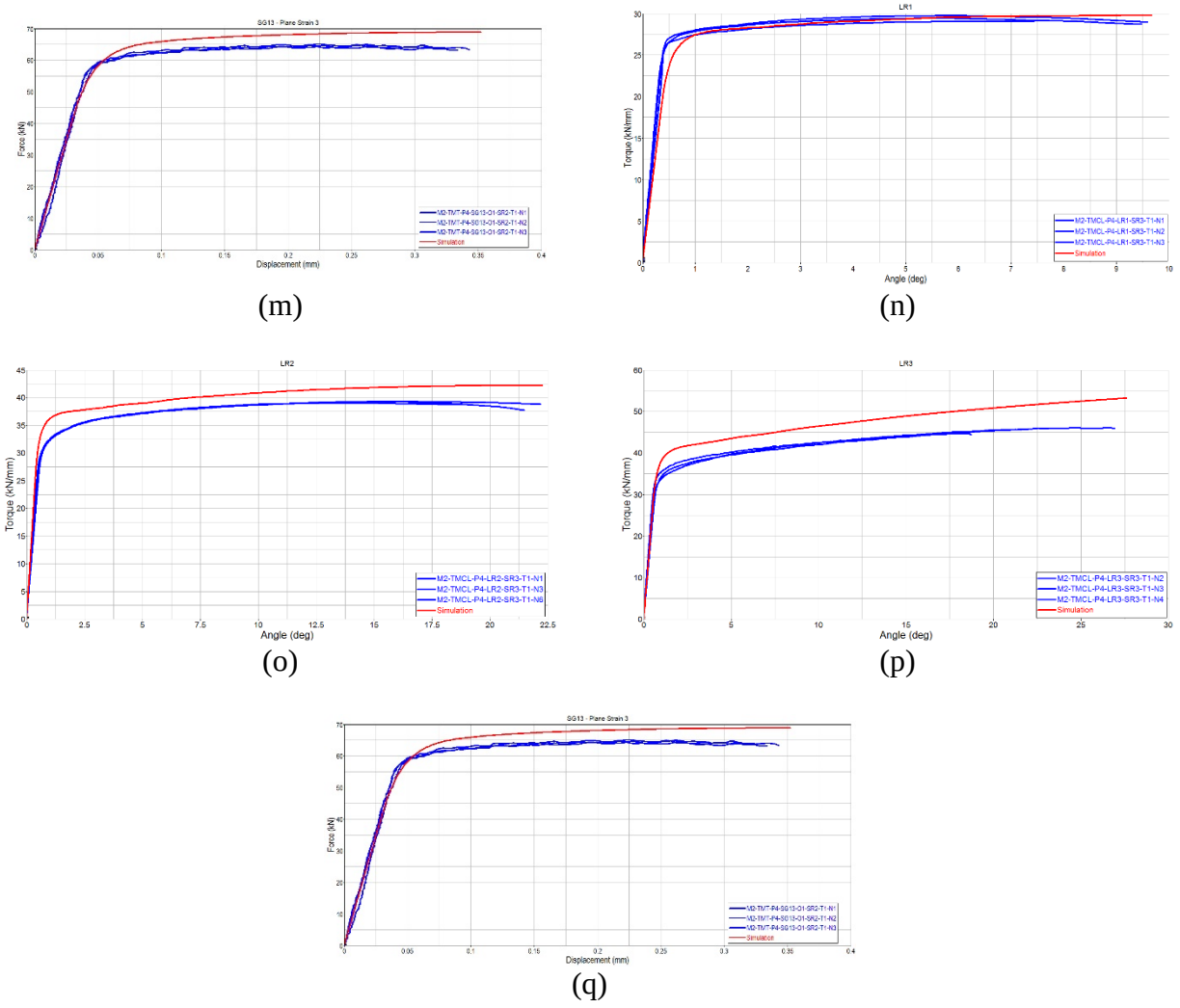

Figure 113. Force versus time history comparison plot for each specimen (continued) ((a) SG1, (b) SG2, (c) SG3, (d) SG4, (e) SG5, (f) SG6, (g) SG7, (h) SG8, (i) SG9, (j) SG10, (k) SG11, (l) SG12, (m) SG13, (n) LR1, (o) LR2, (p) LR3, and (q) LR4)

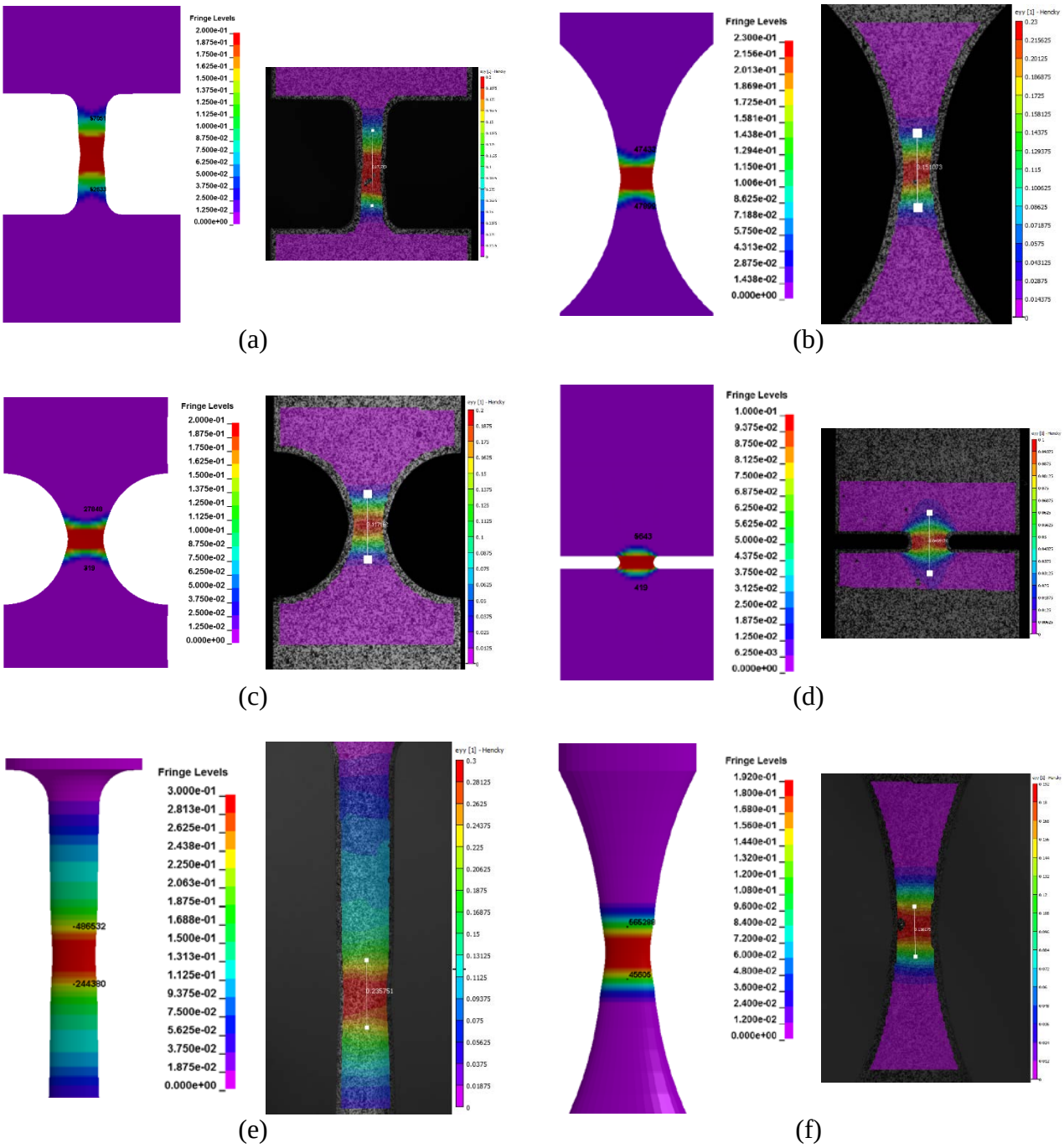

Figure 114. DIC versus Fringe Plot Plot Comparison for Each Specimen ((a) SG1, (b) SG2, (c) SG3, (d) SG4, (e) SG5, (f) SG6, (g) SG7, (h) SG8, (i) SG9, (j) SG10, (k) SG11, (l) SG12, (m) SG13, (n) LR1, (o) LR2, (p) LR3, (q) LR4, (r) compression, (s) Punch1, and (t) Punch2)

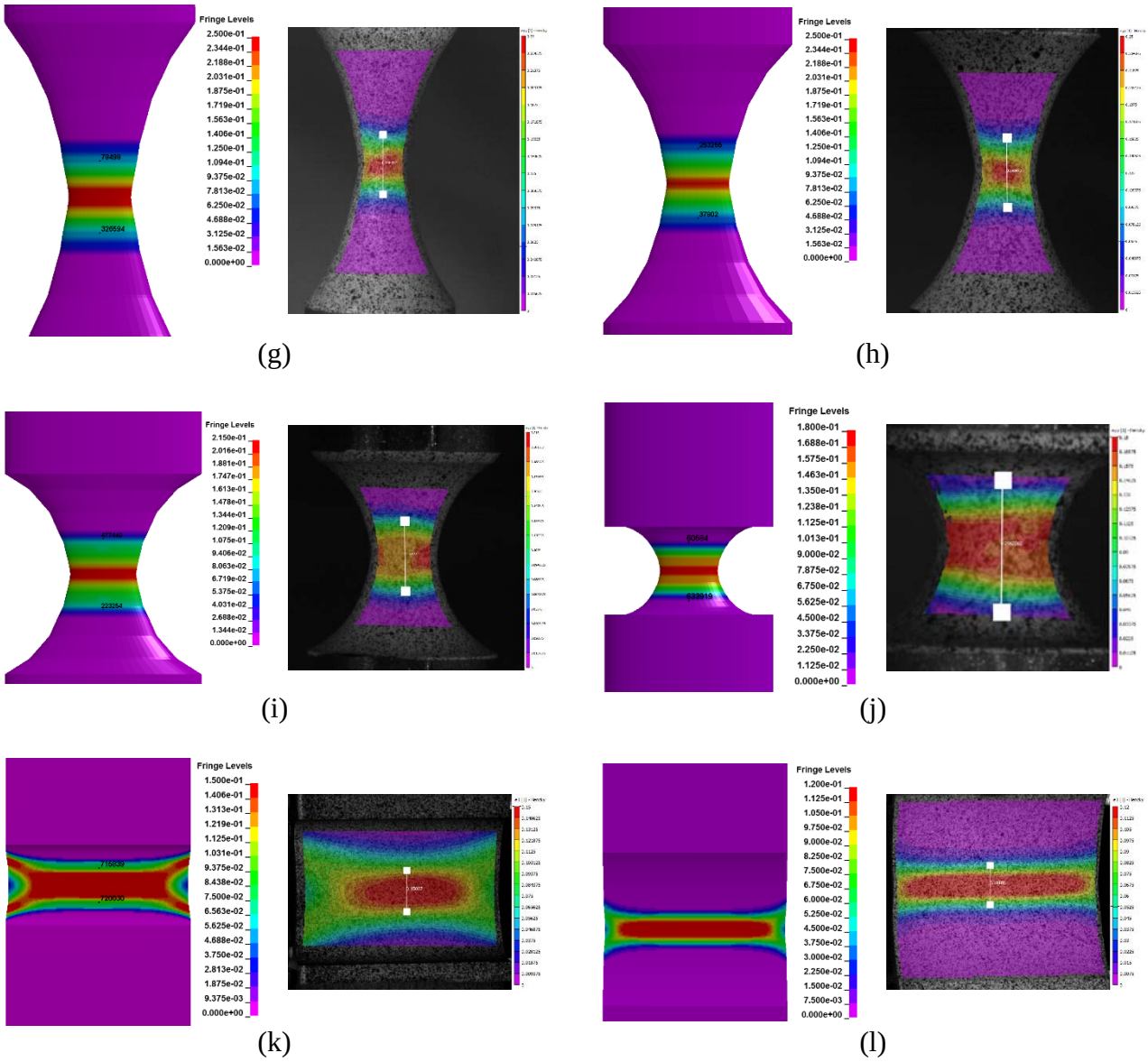

Figure 114. DIC versus Fringe Plot Plot Comparison for Each Specimen (continued) ((a) SG1, (b) SG2, (c) SG3, (d) SG4, (e) SG5, (f) SG6, (g) SG7, (h) SG8, (i) SG9, (j) SG10, (k) SG11, (l) SG12, (m) SG13, (n) LR1, (o) LR2, (p) LR3, (q) LR4, (r) compression, (s) Punch1, and (t) Punch2)

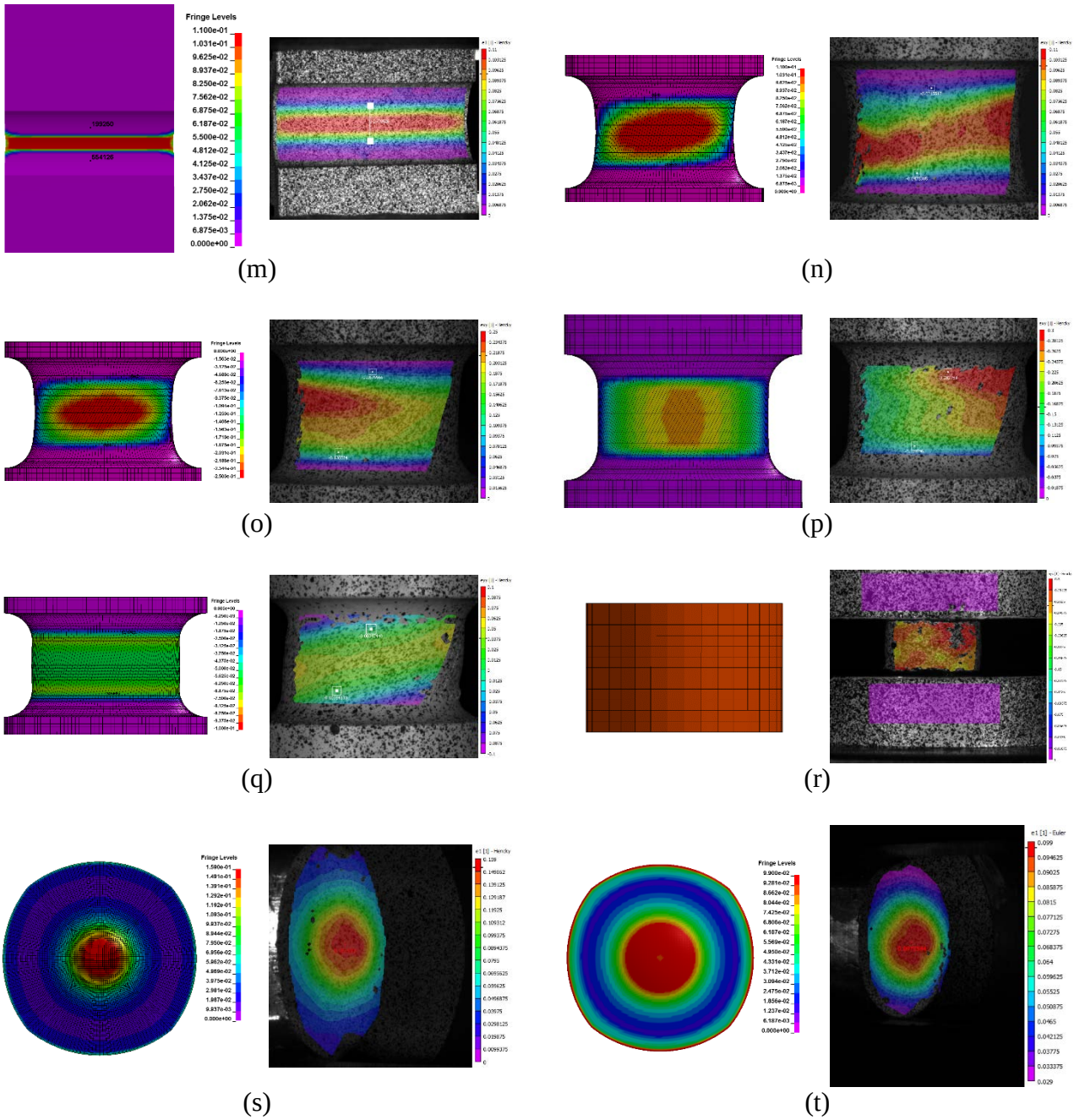

Figure 114. DIC versus Fringe Plot Plot Comparison for Each Specimen (continued) ((a) SG1, (b) SG2, (c) SG3, (d) SG4, (e) SG5, (f) SG6, (g) SG7, (h) SG8, (i) SG9, (j) SG10, (k) SG11, (l) SG12, (m) SG13, (n) LR1, (o) LR2, (p) LR3, (q) LR4, (r) compression, (s) Punch1, and (t) Punch2)

After comparing the force-displacement plots, it is also important to compare the stress-strain behavior in tension, shear, and compression. The mechanical properties of Ti-6Al-4V are sensitive to the specific processing each plate undergoes during manufacturing. As a result, the degree of asymmetry in yield and anisotropy will vary between manufacturing batches. The

specific Ti-6AL-4V material of this plate demonstrates asymmetry, yielding at different stresses in tension and compression. Moreover, the ratio of yield stresses in torsion and tension deviates from J2 flow theory. Figure 115 shows the comparison of these three types of stress.

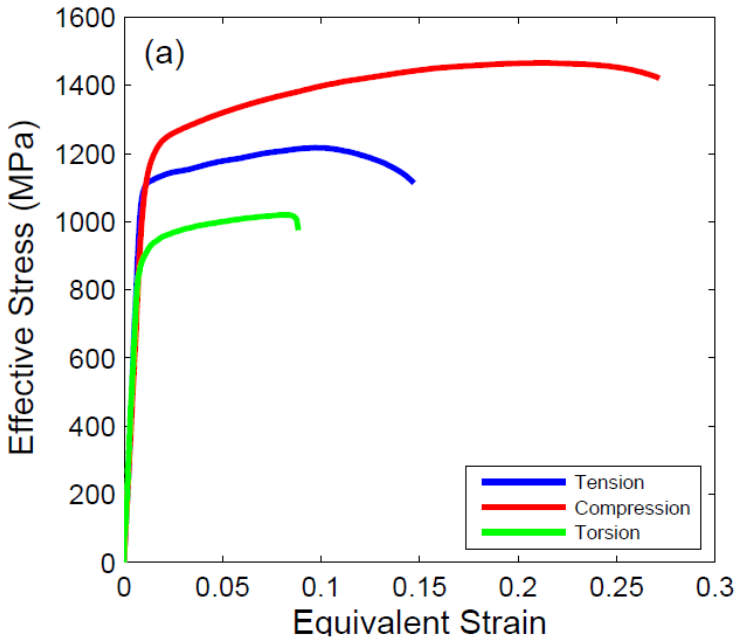

Figure 115. Comparison of plate response to different types of stress

Because the current constitutive model is based on J2 plasticity theory and the material model inputs are based only on tension data, any elements in shear or compression will either have a lower or higher effective stress. This will cause the force-displacement curves to diverge slightly from the test results. To correct this issue, the *MAT_224_GYS (general yield surface) option can be used to introduce additional load curves for shear and compressive stresses.

Because each specimen test simulation has been shown in figures 114 (s and t) to have results comparable to the physical tests provided by OSU, the unique triaxiality and Lode parameters can now be determined. The first step in determining these parameters is to select an element in the center of the specimen where the failure is likely to occur. After the likely failure element is selected, LS-PrePost can be used to obtain the time history data of history variables #9 (triaxiality) and #10 (Lode parameter) stored by the material algorithm. Figures 116 (a–s) show the area of the selected element (in red) for analysis of the triaxiality and Lode parameter for each specimen.

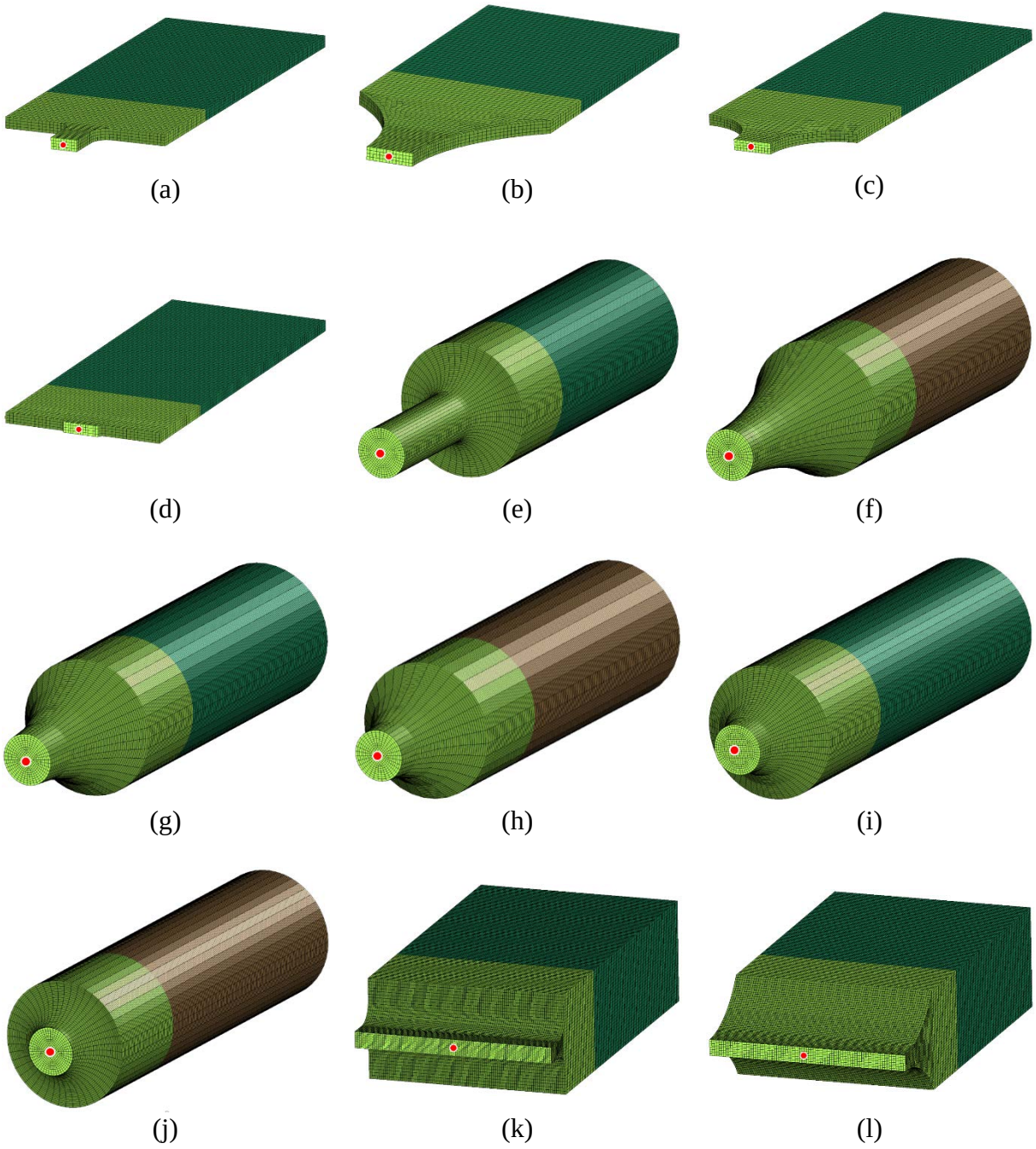

Figure 116. Elements (shown in red) analyzed for triaxiality and Lode parameter for each specimen ((a) SG1, (b) SG2, (c) SG3, (d) SG4, (e) SG5, (f) SG6, (g) SG7, (h) SG8, (i) SG9, (j) SG10, (k) SG11, (l) SG12, (m) SG13, (n) LR1, (o) LR2, (p) LR3, (q) LR4, (r) Punch1, and (s) Punch2)

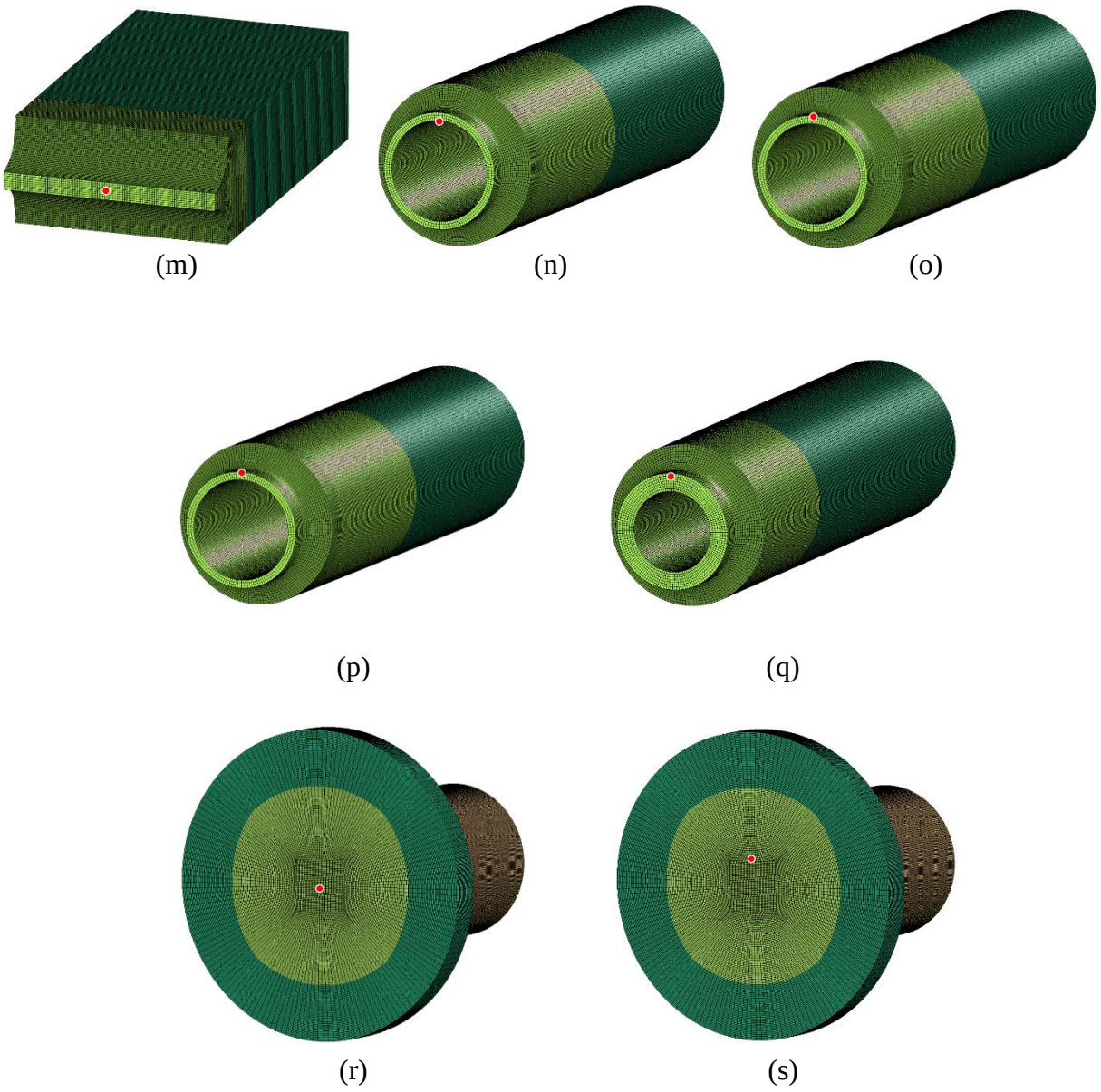

Figure 116. Elements (shown in red) analyzed for triaxiality and Lode parameter for each specimen (continued) ((a) SG1, (b) SG2, (c) SG3, (d) SG4, (e) SG5, (f) SG6, (g) SG7, (h) SG8, (i) SG9, (j) SG10, (k) SG11, (l) SG12, (m) SG13, (n) LR1, (o) LR2, (p) LR3, (q) LR4, (r) Punch1, and (s) Punch2)

The time history data obtained from the triaxiality and Lode parameter history variables can be individually plotted as a function of the effective plastic strain for the same element. Each specimen's triaxiality and Lode parameter is shown in figures 117 (a–t).

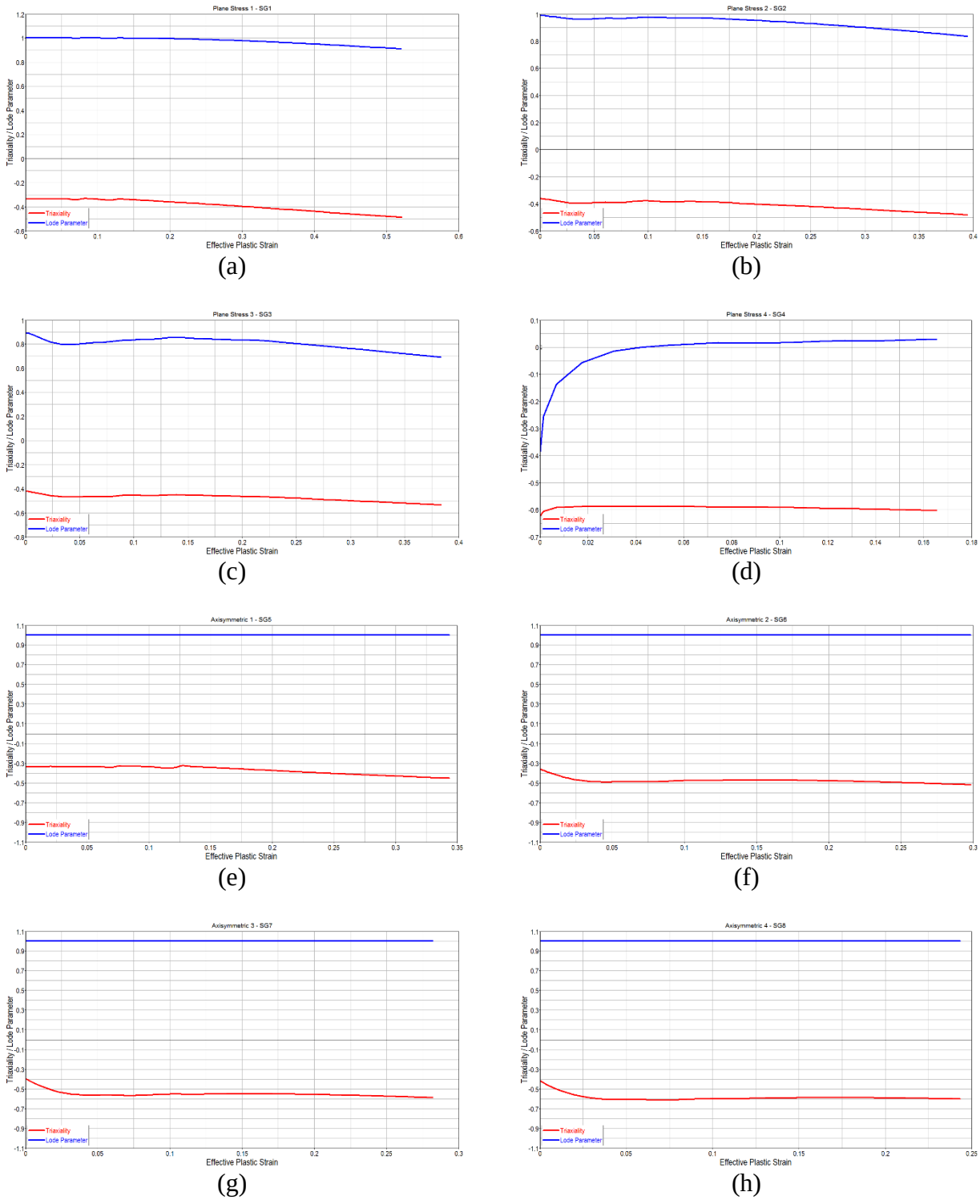

Figure 117. Triaxiality and lode parameter for each specimen ((a) SG1, (b) SG2, (c) SG3, (d) SG4, (e) SG5, (f) SG6, (g) SG7, (h) SG8, (i) SG9, (j) SG10, (k) SG11, (l) SG12, (m) SG13, (n) LR1, (o) LR2, (p) LR3, (q) LR4, (r) compression, (s) Punch1, and (t) Punch2)

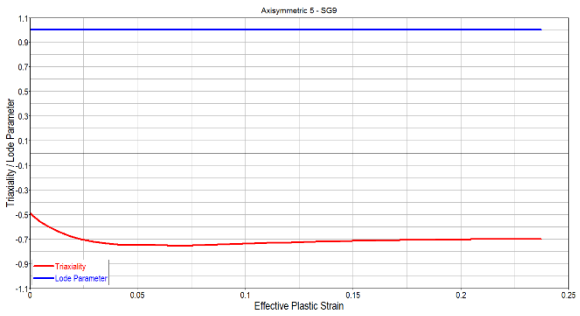

(i)

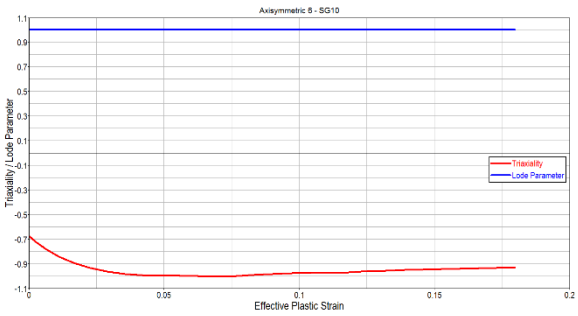

(j)

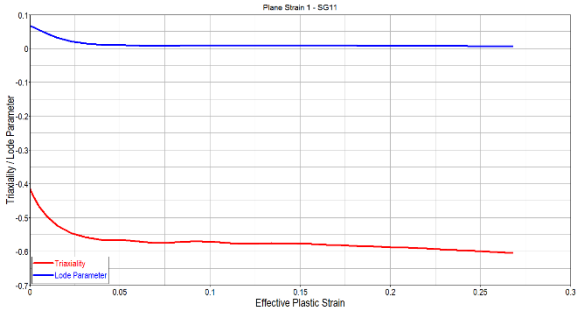

(k)

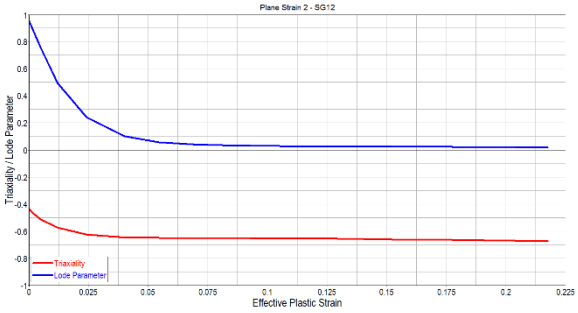

(l)

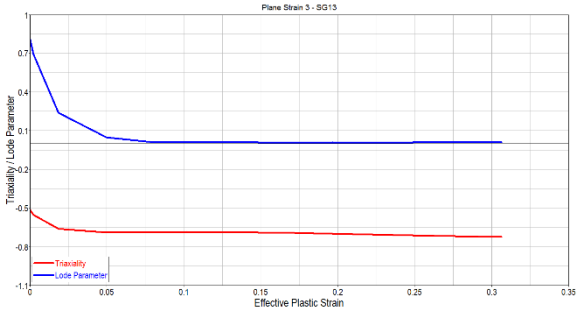

(m)

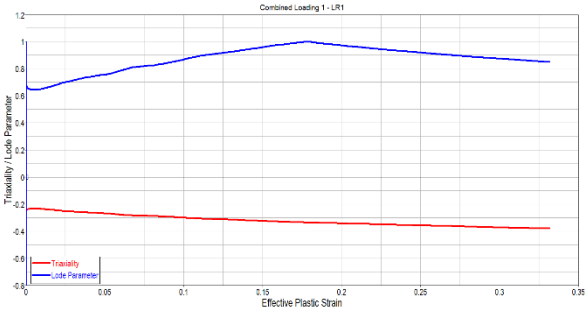

(n)

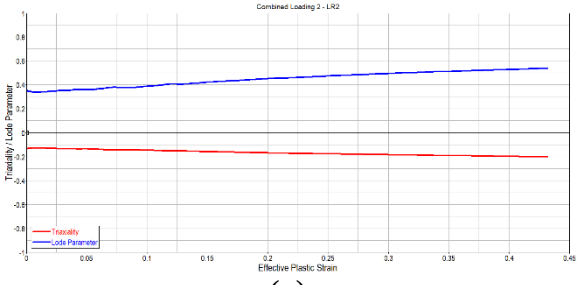

(o)

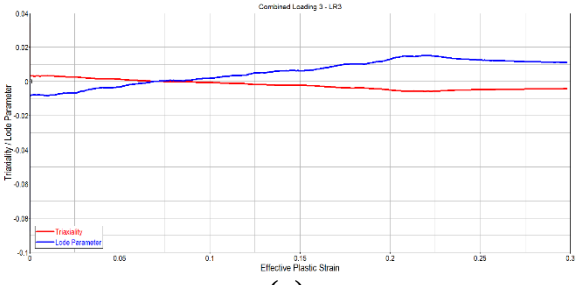

(p)

Figure 117. Triaxiality and lode parameter for each specimen (continued) ((a) SG1, (b) SG2, (c) SG3, (d) SG4, (e) SG5, (f) SG6, (g) SG7, (h) SG8, (i) SG9, (j) SG10, (k) SG11, (l) SG12, (m) SG13, (n) LR1, (o) LR2, (p) LR3, (q) LR4, (r) compression, (s) Punch1, and (t) Punch2)

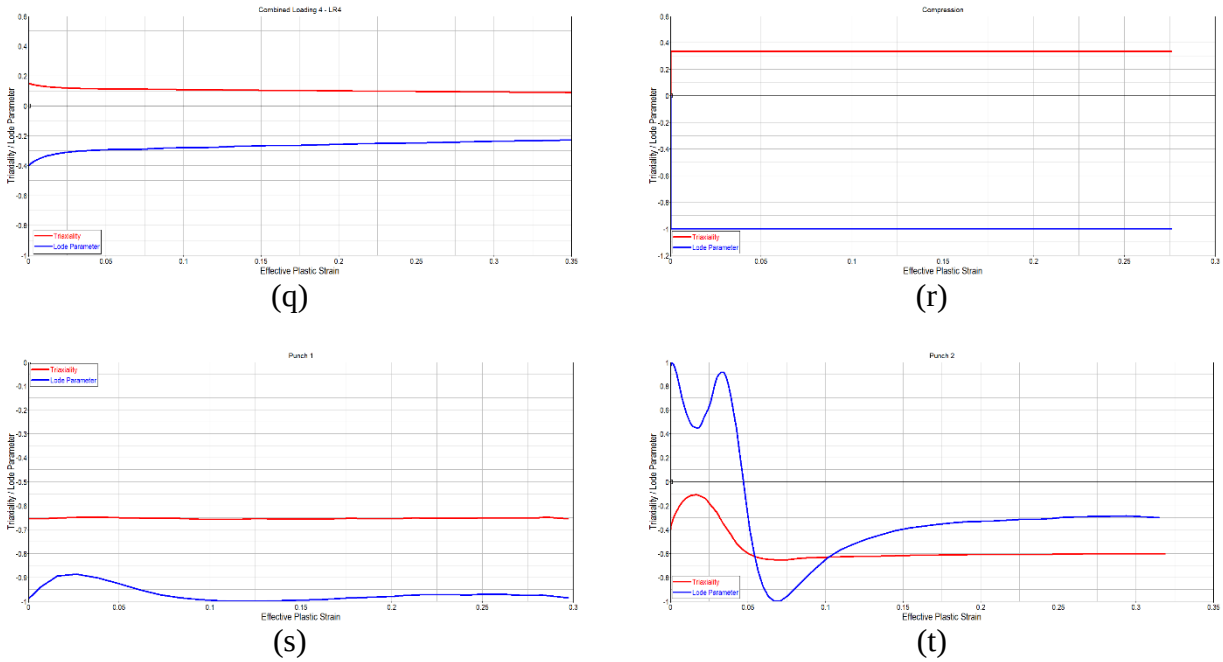

(q) (r)

(s) (t)

Figure 117. Triaxiality and lode parameter for each specimen (continued) ((a) SG1, (b) SG2, (c) SG3, (d) SG4, (e) SG5, (f) SG6, (g) SG7, (h) SG8, (i) SG9, (j) SG10, (k) SG11, (l) SG12, (m) SG13, (n) LR1, (o) LR2, (p) LR3, (q) LR4, (r) compression, (s) Punch1, and (t) Punch2)

To determine an average triaxiality and Lode parameter for each specimen, the following equations can be used:

$$\tau_{avg} = \frac{\int_0^{\varepsilon_{pf}} \tau d\varepsilon_p}{\varepsilon_{pf}}$$
$$\theta_{L_{avg}} = \frac{\int_0^{\varepsilon_{pf}} \theta_L d\varepsilon_p}{\varepsilon_{pf}} \quad (36)$$

where τ is the triaxiality as a function of effective plastic strain ε_p, θ_L is the Lode parameter as a function of effective plastic strain, and ε_{pf} is the final effective plastic strain.

Using equation 36, the average triaxiality and Lode parameter from the simulation can be compared to the values reported by OSU [5]. These OSU analytical results were calculated using a preliminary, conventional Johnson-Cook Ti-6Al-4V material model and produced to add in the specimen designs. Table 5 shows this comparison of how closely the design target matched the final result. The simulation failure strain was determined by evaluating the effective plastic strain for the center element (shown in figure 116) at the instant the simulated extensometer matched the displacement of the measured virtual extensometer from the physical test.

Table 5. Reported results versus simulation results for triaxiality, Lode parameter, and failure strain for all specimens

Test Number	Reported by OSU			Simulation		
	Tri-axiality	Lode Parameter	Failure Strain	Tri-axiality	Lode Parameter	Failure Strain
SG1	-0.400	0.850	0.590	-0.390	0.975	0.460
SG2	-0.431	0.719	0.440	-0.412	0.935	0.420
SG3	-0.489	0.528	0.430	-0.475	0.803	0.380
SG4	-0.583	0.014	0.140	-0.592	0.005	0.135
SG5	-0.369	1.000	0.310	-0.370	1.000	0.340
SG6	-0.492	1.000	0.310	-0.480	1.000	0.300
SG7	-0.564	1.000	0.320	-0.553	1.000	0.280
SG8	-0.618	1.000	0.270	-0.588	1.000	0.240
SG9	-0.751	1.000	0.270	-0.712	1.000	0.240
SG10	-0.956	1.000	0.220	-1.000	1.000	0.180
SG11	-0.470	0.506	0.210	-0.573	0.146	0.260
SG12	-0.660	0.040	0.220	-0.643	0.099	0.220
SG13	-0.768	0.025	0.210	-0.691	0.054	0.290
LR1	-0.252	0.706	0.290	-0.289	0.949	0.191
LR2	-0.150	0.400	0.510	-0.145	0.917	0.325
LR3	-0.000	0.000	0.430	-0.014	0.059	0.259
LR4	0.148	-0.394	0.420	0.147	-0.450	0.321
Punch1	N/A	N/A	N/A	-0.653	-0.969	0.297
Punch2	N/A	N/A	N/A	-0.565	-0.475	0.276

5.2.1 Failure Surface Generation

Using the specimen models and the results shown in table 5, a failure surface can be constructed using the failure surface generation tool. The triaxiality, Lode parameter, and failure strain were entered into the MATLAB script and an initial failure surface was generated. Figure 118 shows the first failure surface using the initial data set.

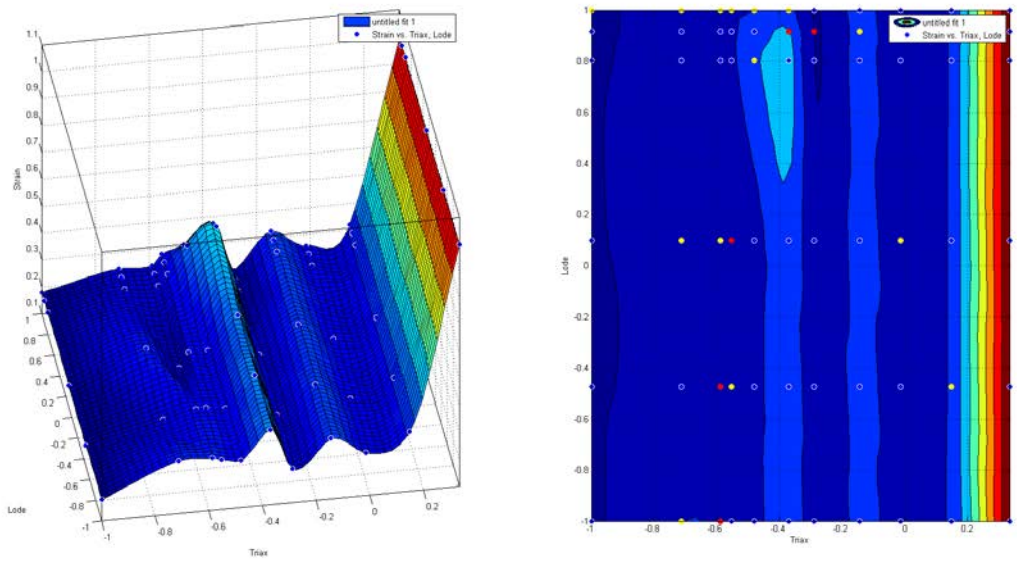

Figure 118. First failure surface generated using initial data set

As expected, some of the control points had to be manually updated because some of the specimens did not fail at the correct displacement in the initial set of analyses. To correct this, an adjustment was made to several of the failure strains of the specimens. Because the control points are determined by the specimen failure strains, they were also consequently adjusted. Table 6 shows the number of iterations and adjustments made to each specimen.

Table 6. Control point iterations and adjustments for each specimen

Test #	Triaxiality	Lode Parameter	Failure Strain	Adjustment #1	Adjustment #2	Adjustment #3
SG1	-0.390	0.975	0.460	+0.08	+0.00	+0.03
SG2	-0.412	0.935	0.420	+0.00	+0.00	+0.00
SG3	-0.475	0.803	0.380	+0.00	+0.00	+0.00
SG4	-0.592	0.005	0.135	+0.01	+0.00	+0.00
SG5	-0.370	1.000	0.340	+0.00	+0.00	-0.02
SG6	-0.480	1.000	0.300	+0.03	+0.00	-0.02
SG7	-0.553	1.000	0.280	+0.02	+0.00	+0.00
SG8	-0.588	1.000	0.240	+0.00	+0.00	+0.00
SG9	-0.712	1.000	0.240	+0.01	+0.00	+0.00
SG10	-1.000	1.000	0.180	+0.01	+0.00	+0.00
SG11	-0.573	0.146	0.260	+0.02	+0.04	+0.03
SG12	-0.643	0.099	0.220	-0.02	-0.06	+0.03
SG13	-0.691	0.054	0.290	-0.02	-0.06	+0.00
LR1	-0.289	0.949	0.191	+0.02	-0.06	+0.00
LR2	-0.145	0.917	0.325	+0.02	+0.08	+0.08
LR3	-0.014	0.059	0.259	+0.02	+0.02	+0.00
LR4	0.147	-0.450	0.321	+0.02	+0.08	+0.00
Punch1	-0.653	-0.969	0.297	+0.00	-0.02	+0.00
Punch2	-0.565	-0.475	0.276	-0.02	-0.02	+0.00

Graphically, the adjustments to the control points are shown in figure 119. The red circles are the original (and adjusted) points, whereas the blue dots are the final points.

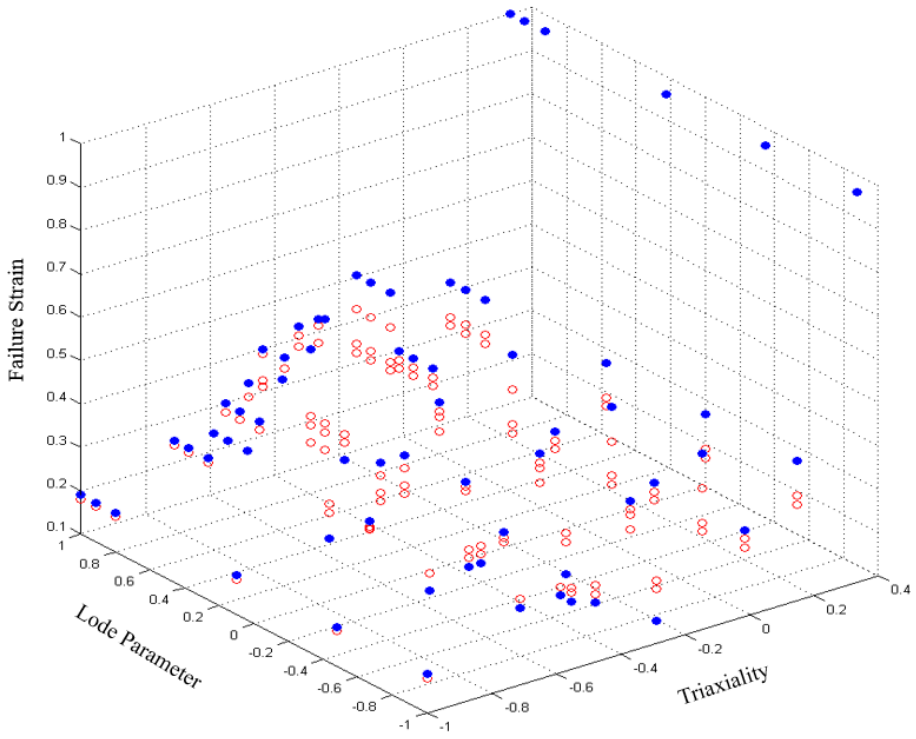

Figure 119. Adjustments to data points: original and intermediate adjustments (red) and final points (blue)

After the fourth iteration (three adjustments), the failure surface generation tool produced the failure surface shown in figure 120.

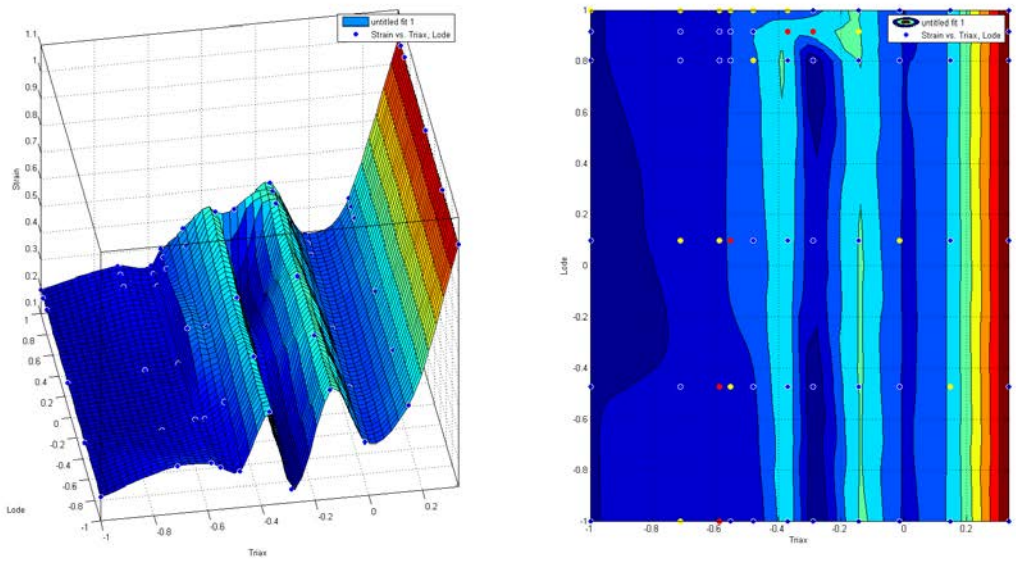

Figure 120. Failure surface generated after four iterations

This failure surface provided reasonable results for all of the specimens except for the first combined loading (LR1) specimen. After the first two iterations, it was noted that a correctional adjustment to the LR1 had a negative reaction to the results from the other specimens. For example, if the surface was adjusted in an attempt to match the LR1 specimen, the pure tension SG1 specimen would have the reverse effect (it would get worse). After some additional comparisons, it was discovered that the LR1 and SG1 specimens had similar triaxialities and Lode parameters but different failure strain. Figure 121 shows the comparison of triaxiality and Lode parameter for SG1, LR1, and SG5.

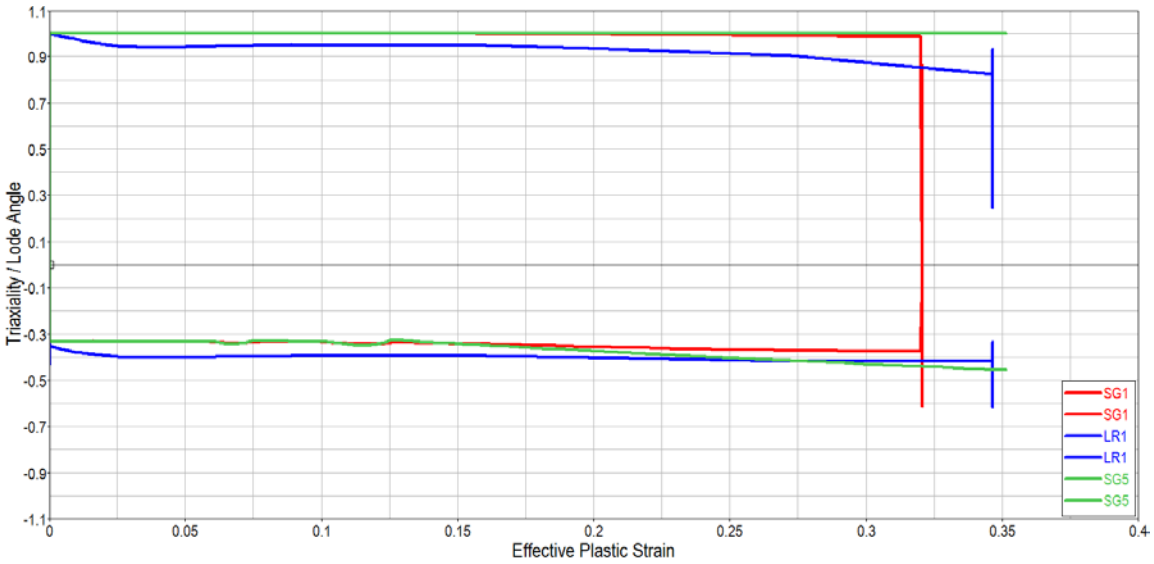

Figure 121. Comparison of triaxiality and Lode parameter for specimens SG1, LR1, and SG5

Because the purpose of the LR1 combined loading specimen was to produce a unique triaxiality and Lode parameter, this was not expected. It was determined that the Lode parameter equation used for the design of the specimen was actually an approximation rather than the actual definition. It is common to approximate the Lode parameter with the following equation:

$$\theta_L \cong \frac{2\sigma_2 - \sigma_1 - \sigma_3}{\sigma_1 - \sigma_3} \tag{37}$$

In some instances, the difference between the two equations can be significant. Figure 122 shows the difference between the two functions in which the abscissa is the ratio of the circumferential stress and the longitudinal stress and the ordinate is the Lode parameter. For LR1, the ratio of the circumferential stress and the longitudinal stress a is approximately 0.33:

$$\sigma \begin{pmatrix} 1 & 1 & 0 \\ 1 & a & 0 \\ 0 & 0 & 0 \end{pmatrix} \text{where } a = \frac{\textit{Circumferential stress}}{\textit{Longitudinal stress}} \tag{38}$$

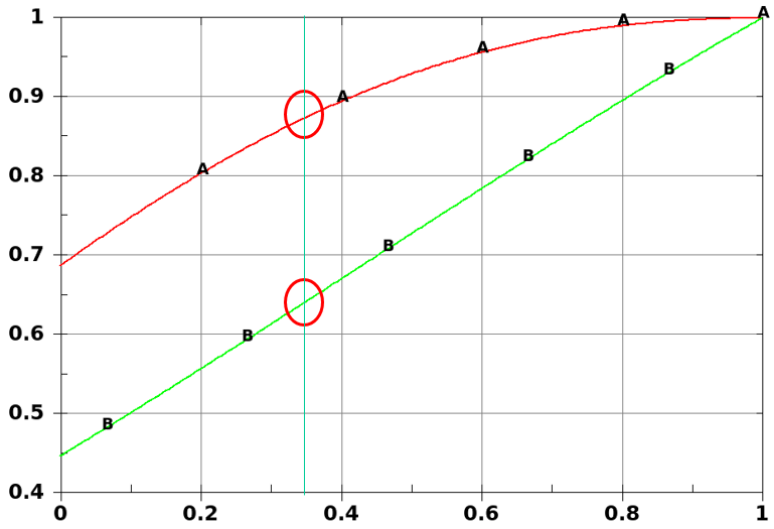

Figure 122. Lode parameter relationships for LR1

In figure 122, the red line (A) is the actual definition of the Lode parameter, and the green line (B) is the approximation. This analysis shows that when the definition of Lode parameter is used, this stress state should result in a Lode parameter of approximately 0.88, whereas the approximation results in a value of approximately 0.65. This difference resulted in an LR1 specimen design that has a similar Lode parameter to the plane stress (SG1) specimen. This explains why the changes to the control point of one have a large effect on the other; however, it does not explain why the two specimens have a significantly different failure strain. A possible source for the difference of failure strain for LR1 and SG1 is strain-rate dependency. The failure surface development was based on experiments that were performed at a strain rate of 0.01 sec^{-1}.

This strain rate was kept approximately constant in most of the tension experiments which were displacement controlled. The same was not achieved in the force-controlled combined loading tests, in which the strain rate increased substantially after the material transitioned from elastic to plastic. Because the strain rate for the combined loading specimens was approximately 0.1 sec^{-1}, it is conceivable, but not conclusive, that this difference may be the reason for the different failure strain.

For reference, the engineering failure strain for the pure tension specimen at a strain rate of 0.01 sec^{-1} is approximately 25%. In comparison, the engineering failure strain (using the virtual extensometer) for the pure tension specimen at a strain rate of 1.00 sec^{-1} is approximately 22%. In addition, figures 123 (a and b) show the DIC-fringe plot comparisons for the strain rates 0.01 sec^{-1} and 1.00 sec^{-1}. The virtual extensometer displacement at failure for the 0.01 sec^{-1} strain rate is approximately 1.01 mm and the displacement at failure for the 1.00 sec^{-1} strain rate is approximately 0.899 mm.

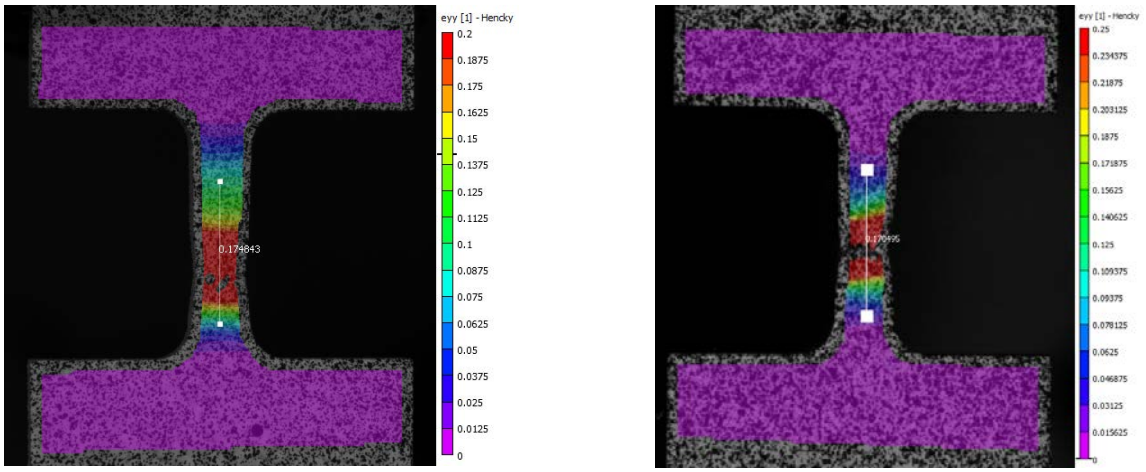

(a) (b)

Figure 123. DIC plots for strain rate 0.01 sec^{-1} with (a) an engineering failure strain of 28% and a displacement at failure of 1.12 mm, and (b) an engineering failure strain of 21% and a displacement at failure of 0.848 mm

These test results show that there is a significant difference in failure strain between those two strain rates. However, because no pure tension tests were completed for a strain rate of 0.10 sec^{-1}, it is not possible to conclusively state that the failure strain at a strain rate of 0.10 sec^{-1} (combined loading specimens) is different from the failure strain at 0.01 sec^{-1} (tension).

Because the possibility of strain rate dependency exists in the combined loading specimens, LR1 will be excluded from the failure surface generation. The triaxiality and Lode parameter for LR1 was a duplicate (with SG1), so that area of the surface is well-defined for the 0.01 sec^{-1} (quasistatic) strain rate. Because the other combined loading specimens are not duplicate points on the triaxiality-Lode plane, they will remain in the surface as a best approximation. Therefore, the final surface (with the exclusion of LR1, and previous to the modifications that are discussed in section 6.2) is shown in figure 124.

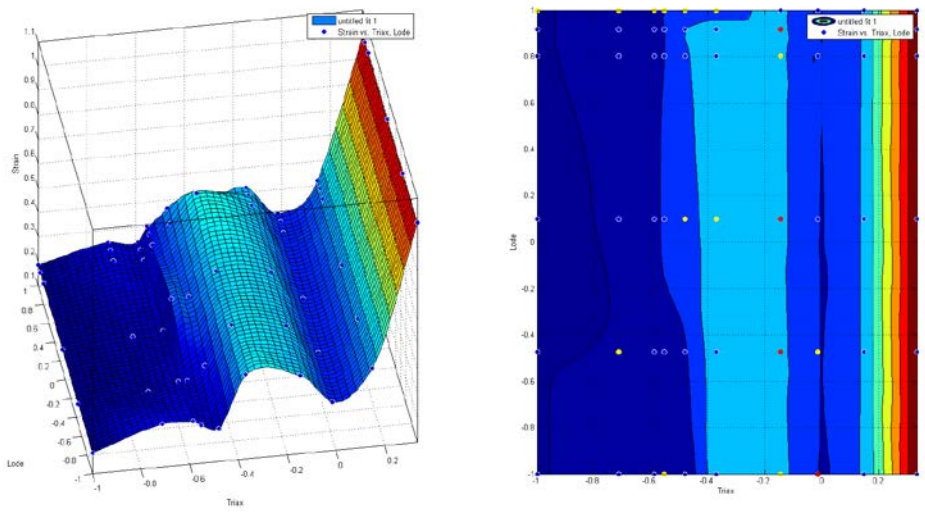

Figure 124. Final failure surface based on mechanical property tests (excluding LR1)

5.2.2 Simulation Results With Failure Surface

The failure surface described in section 5.2.1 was used to repeat each test specimen simulation. This was the primary verification step for the failure surface. For each specimen simulation, the force-displacement time history responses were compared to the physical test data provided by OSU. If the failure displacement occurred within the spread of the experimental test data, it was deemed to have passed this verification step. The force-displacement plots are shown in figures 125 (a–s). For reference, the simulation times for each test specimen simulation have been tabulated (see table 7).

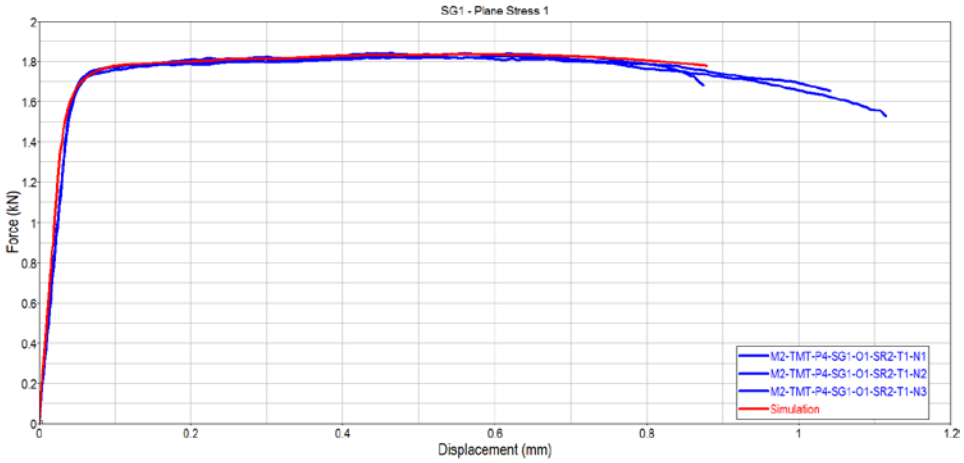

(a)

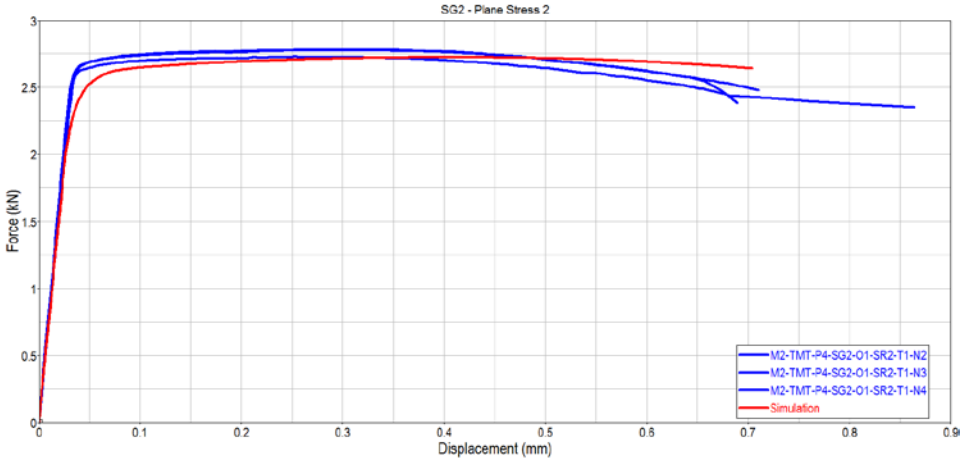

(b)

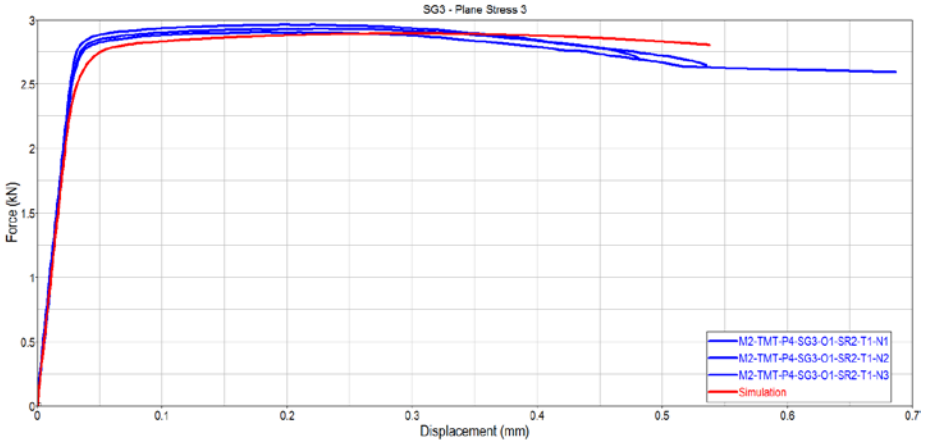

(c)

Figure 125. Force-displacement time history plots for each specimen ((a) SG1, (b) SG2, (c) SG3, (d) SG4, (e) SG5, (f) SG6, (g) SG7, (h) SG8, (i) SG9, (j) SG10, (k) SG11, (l) SG12, (m) SG13, (n) LR1, (o) LR2, (p) LR3, (q) LR4, (r) Punch1, and (s) Punch2)

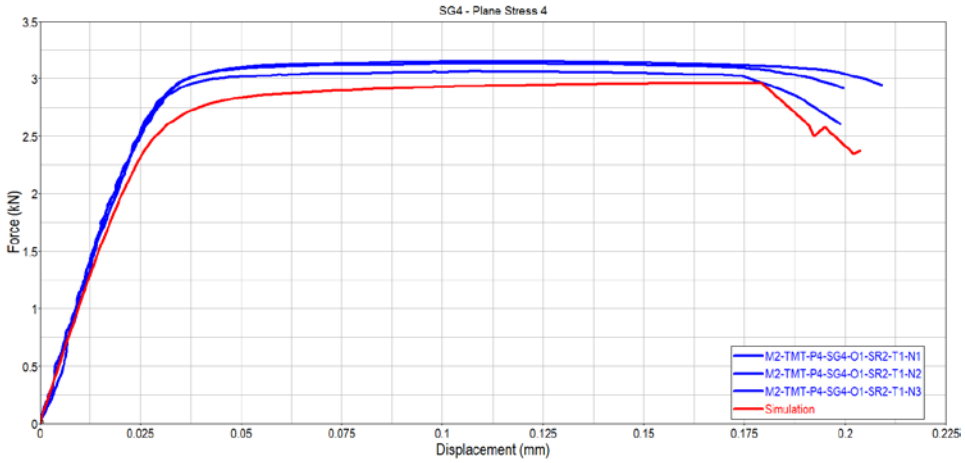

(d)

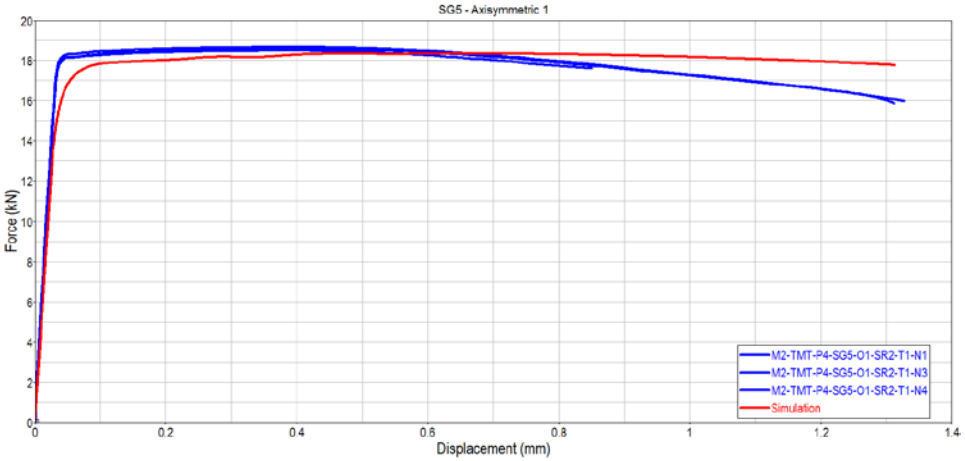

(e)

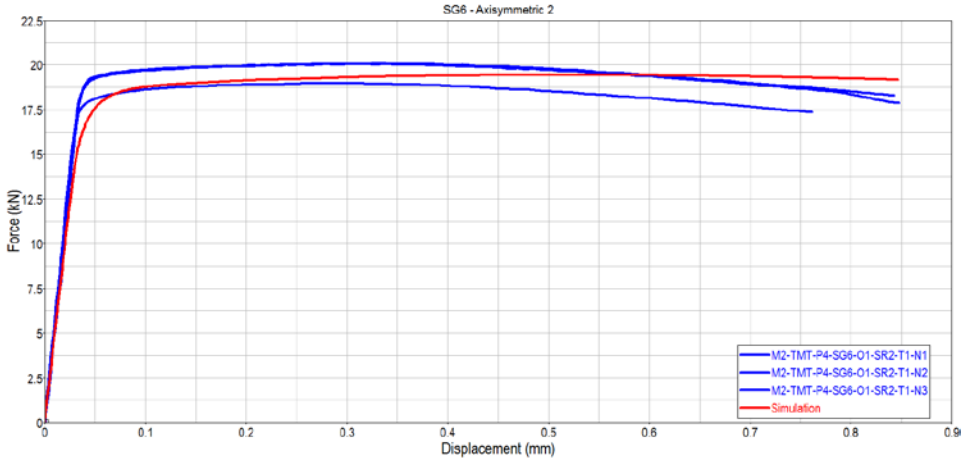

(f)

Figure 125. Force-displacement time history plots for each specimen (continued) ((a) SG1, (b) SG2, (c) SG3, (d) SG4, (e) SG5, (f) SG6, (g) SG7, (h) SG8, (i) SG9, (j) SG10, (k) SG11, (l) SG12, (m) SG13, (n) LR1, (o) LR2, (p) LR3, (q) LR4, (r) Punch1, and (s) Punch2)

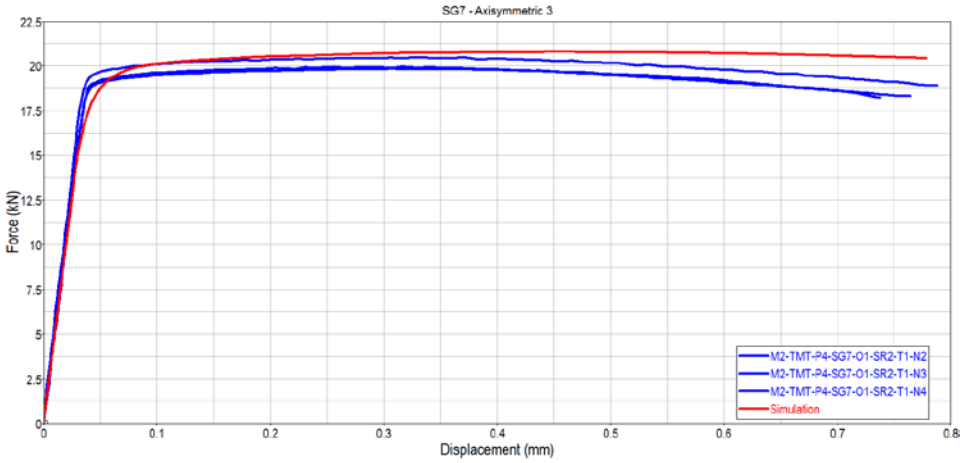

(g)

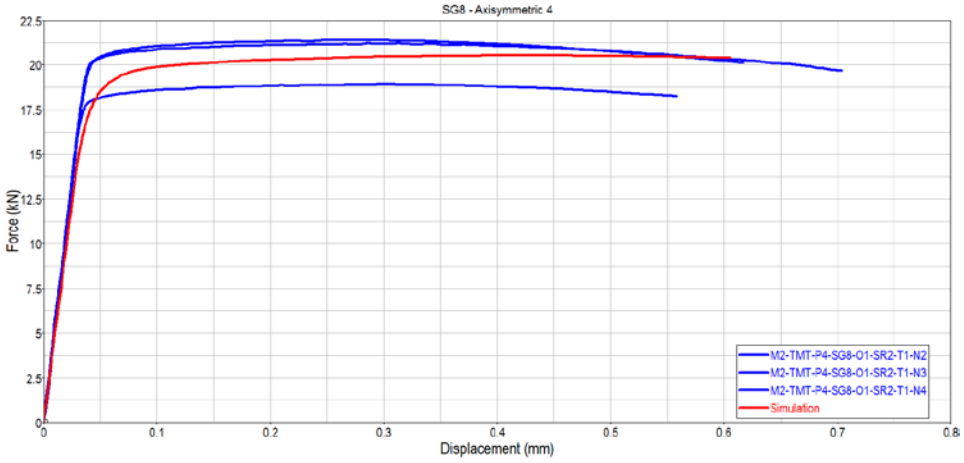

(h)

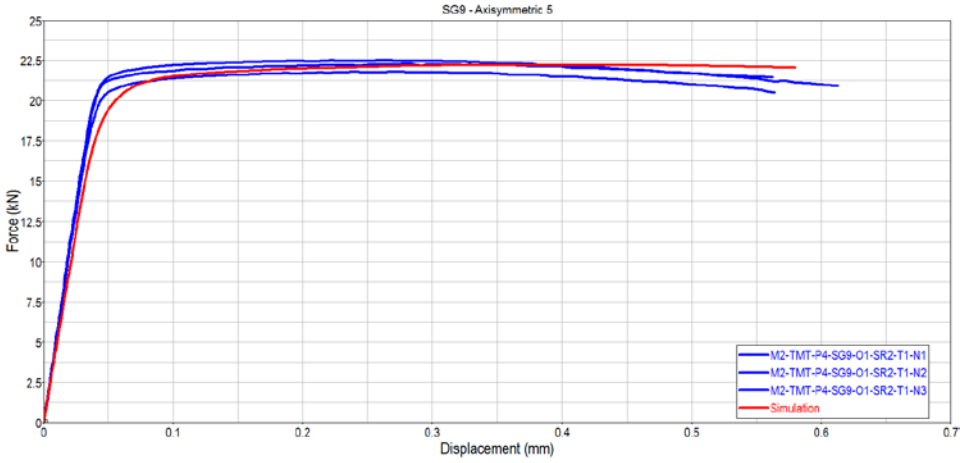

(i)

Figure 125. Force-displacement time history plots for each specimen (continued) ((a) SG1, (b) SG2, (c) SG3, (d) SG4, (e) SG5, (f) SG6, (g) SG7, (h) SG8, (i) SG9, (j) SG10, (k) SG11, (l) SG12, (m) SG13, (n) LR1, (o) LR2, (p) LR3, (q) LR4, (r) Punch1, and (s) Punch2)

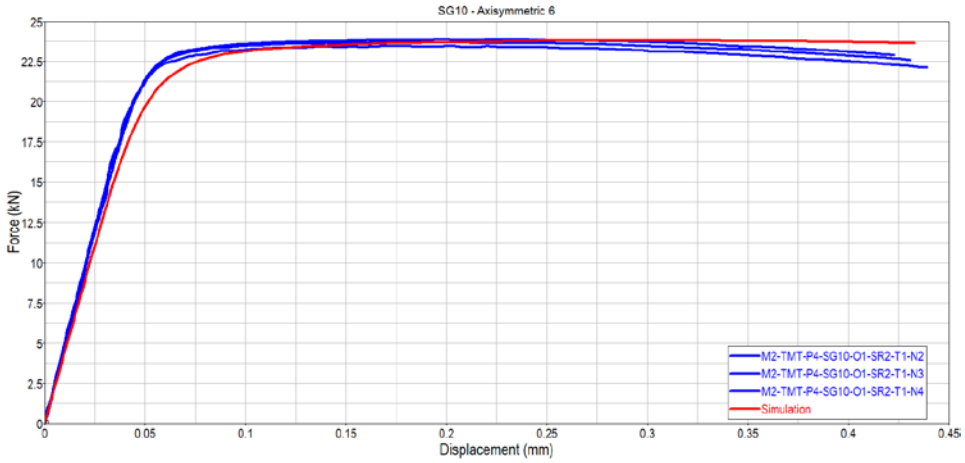

(j)

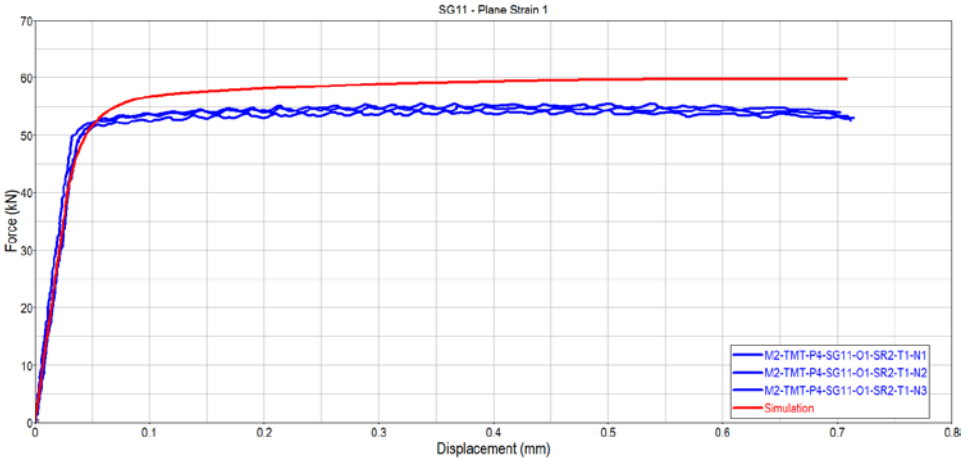

(k)

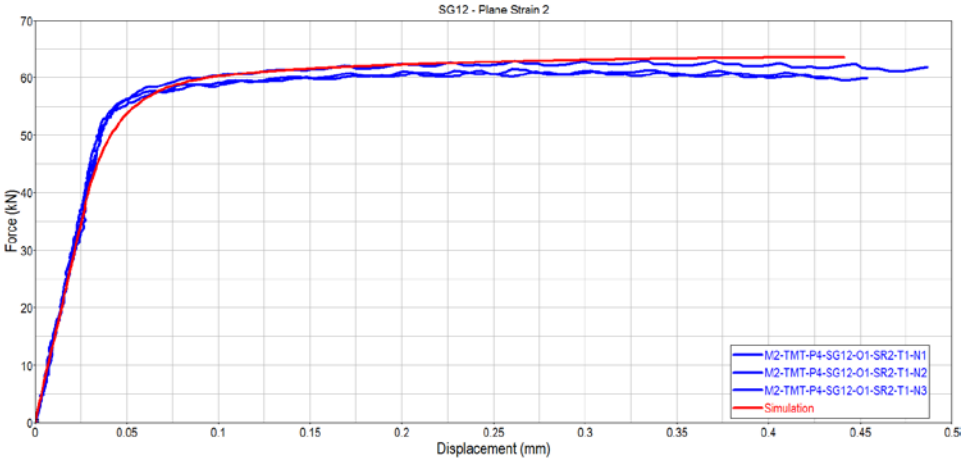

(l)

Figure 125. Force-displacement time history plots for each specimen (continued) ((a) SG1, (b) SG2, (c) SG3, (d) SG4, (e) SG5, (f) SG6, (g) SG7, (h) SG8, (i) SG9, (j) SG10, (k) SG11, (l) SG12, (m) SG13, (n) LR1, (o) LR2, (p) LR3, (q) LR4, (r) Punch1, and (s) Punch2)

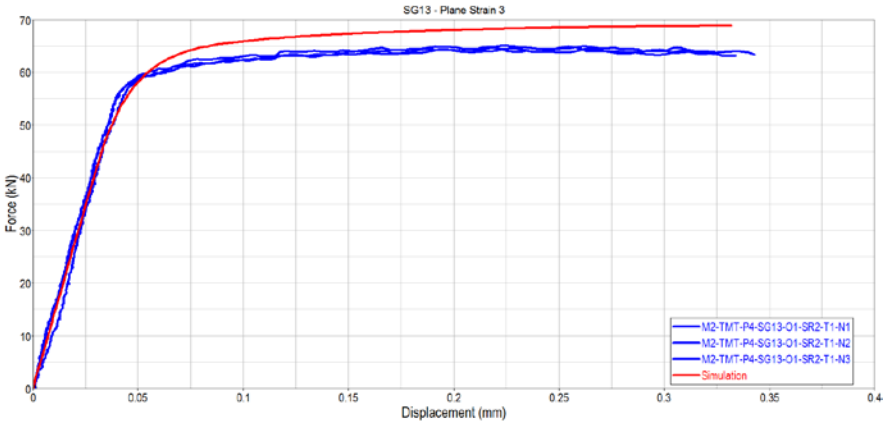

(m)

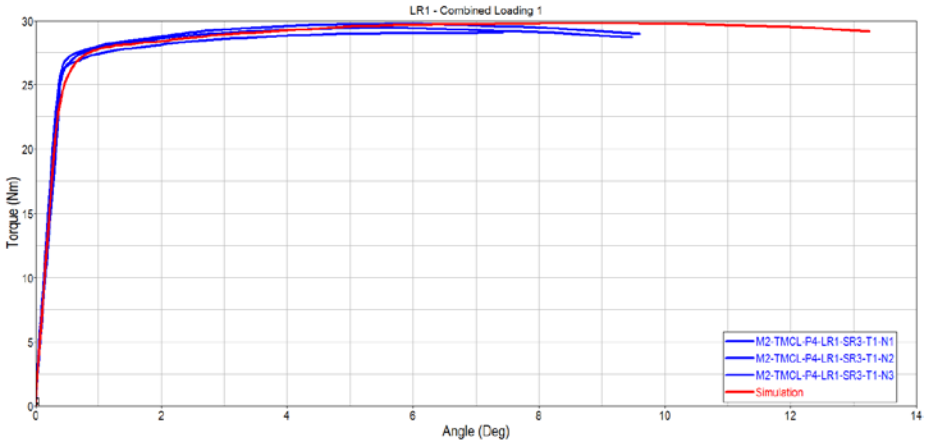

(n)

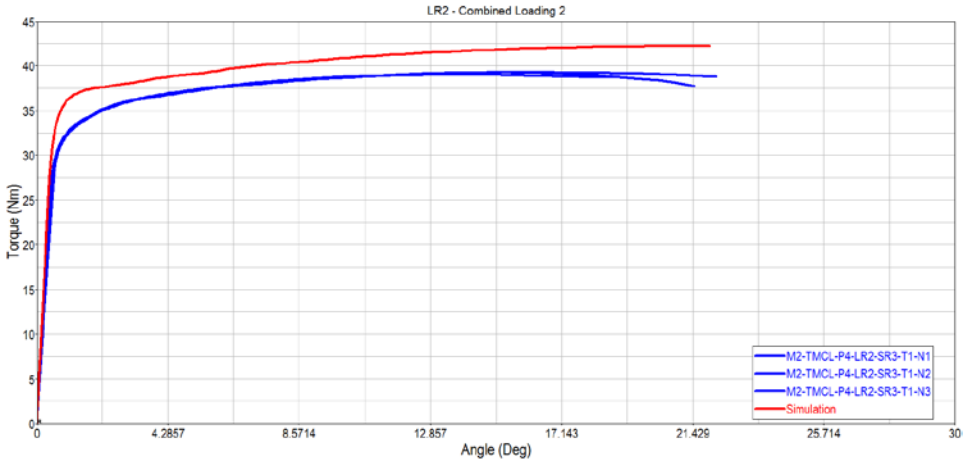

(o)

Figure 125. Force-displacement time history plots for each specimen (continued) ((a) SG1, (b) SG2, (c) SG3, (d) SG4, (e) SG5, (f) SG6, (g) SG7, (h) SG8, (i) SG9, (j) SG10, (k) SG11, (l) SG12, (m) SG13, (n) LR1, (o) LR2, (p) LR3, (q) LR4, (r) Punch1, and (s) Punch2)

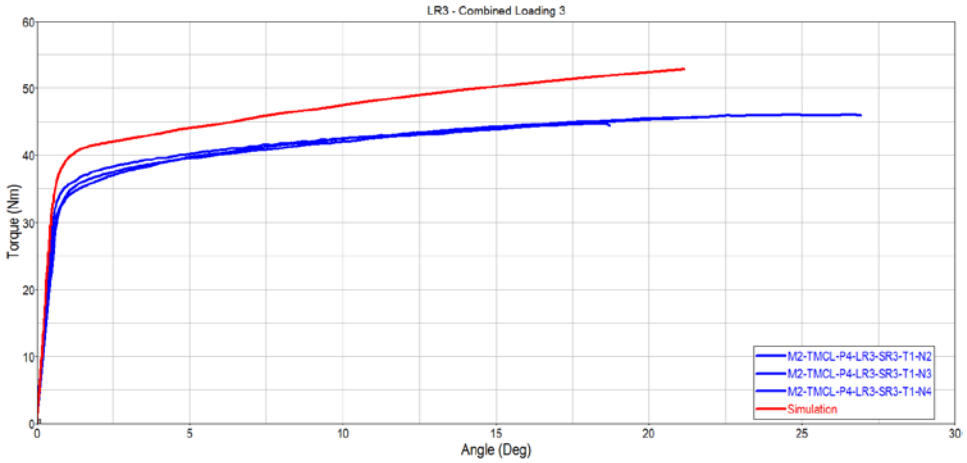

(p)

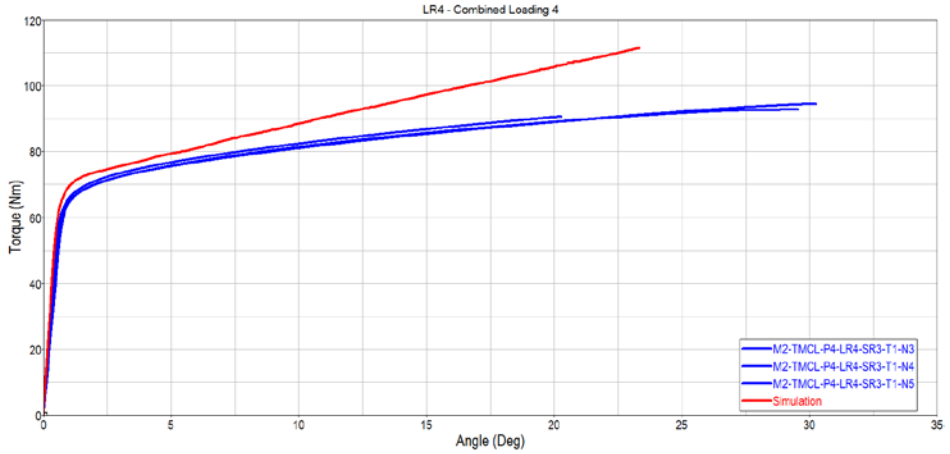

(q)

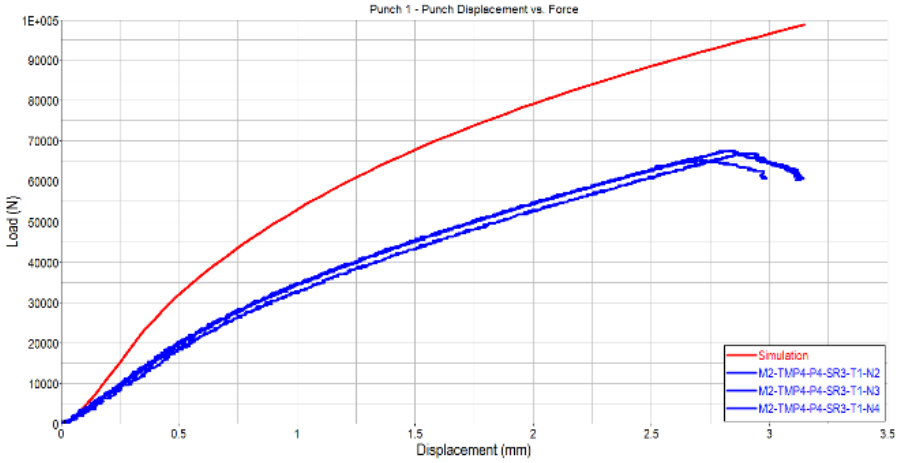

(r)

Figure 125. Force-displacement time history plots for each specimen (continued) ((a) SG1, (b) SG2, (c) SG3, (d) SG4, (e) SG5, (f) SG6, (g) SG7, (h) SG8, (i) SG9, (j) SG10, (k) SG11, (l) SG12, (m) SG13, (n) LR1, (o) LR2, (p) LR3, (q) LR4, (r) Punch1, and (s) Punch2)

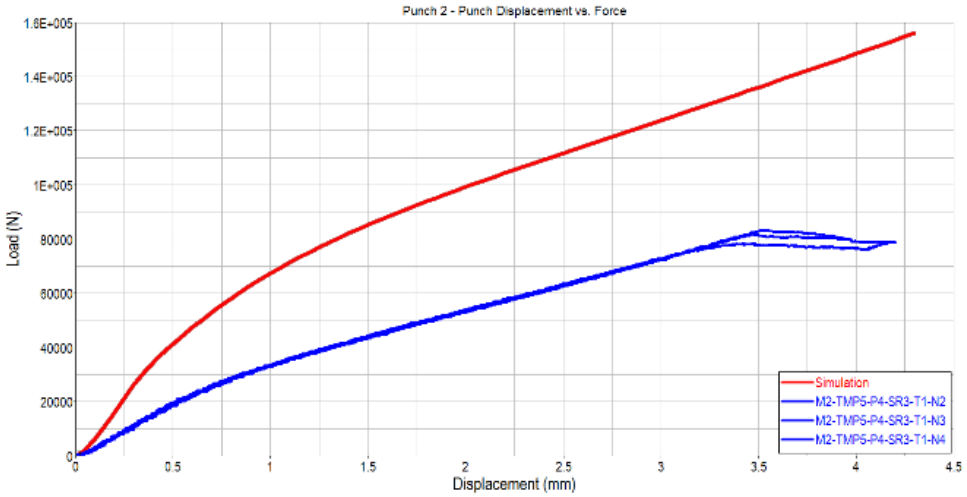

(s)

Figure 125. Force-displacement time history plots for each specimen (continued) ((a) SG1, (b) SG2, (c) SG3, (d) SG4, (e) SG5, (f) SG6, (g) SG7, (h) SG8, (i) SG9, (j) SG10, (k) SG11, (l) SG12, (m) SG13, (n) LR1, (o) LR2, (p) LR3, (q) LR4, (r) Punch1, and (s) Punch2)

Table 7. Simulation statistics for each specimen

Specimen number	Number of elements	Problem time (ms)	Problem cycles	Total CPU time(s)	Elapsed time (hh:mm:ss)
SG1	33,000	4.65	203,908	2,172	00:06:10
SG2	22,000	3.73	165,698	1,520	00:04:20
SG3	20,000	2.69	102,201	704	00:02:00
SG4	41,000	1.07	437,76	568	00:01:37
SG5	471,000	16.8	960,035	185,933	08:04:57
SG6	430,000	5.00	296,788	51,751	02:22:31
SG7	457,000	4.25	269,445	45,514	02:07:13
SG8	385,000	3.29	193,335	25,889	01:12:14
SG9	652,000	2.77	183,472	42,382	01:58:22
SG10	593,000	2.00	131,610	26,012	01:12:45
SG11	935,000	3.94	200,252	67,826	03:09:18
SG12	740,000	2.47	107,859	30,671	01:25:39
SG13	2,639,000	1.70	913,13	74,834	03:29:35
LR1	814,000	8.14	413,622	139,630	06:29:22
LR2	814,000	5.27	267,492	92,708	04:18:43
LR3	814,000	5.75	296,614	98,758	04:35:37
LR4	1,093,000	7.75	493,005	192,151	08:58:03
Punch1	471,000	6.40	346,273	128,598	05:58:44
Punch2	478,000	8.14	470,076	182,483	08:28:59

All of the simulations were computed with six Intel Core i-7-3770 3.4 GHz processors using SMP configuration. The time needed to run all of the simulations was approximately 55 hours,

37 minutes. To improve efficiency, each iteration was initiated via a Linux script. Each simulation was run, in series, one after another.

It is important to note that the simulations of the punch tests did not provide comparable force/displacement results when compared to the physical tests. This is likely due to the difficulty of accurately modeling the boundary conditions in this specific type of test. Because the punch diameter and clamp diameter were similar in size, the effects of the boundaries seemed to have a large influence on the total reactive force. It was difficult to determine the precise distribution of the boundary forces in the test. As a result, the analytical strains were compared to the test strains measured by the DIC. Figures 126 and 127 show a good comparison.

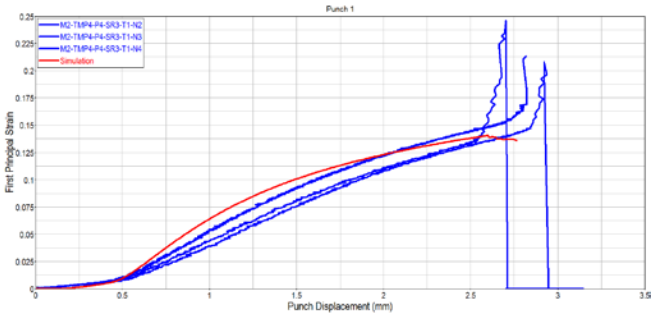

Figure 126. Point strain comparison for punch tests–Punch1

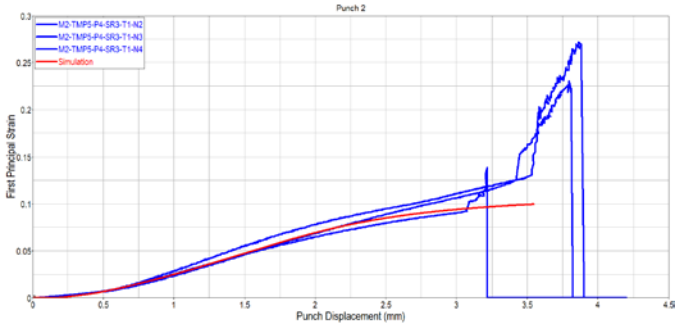

Figure 127. Point strain comparison for punch tests–Punch2

Likewise, the combined loading simulations resulted in force/displacement values that were not very similar to the physical tests. The primary driver of this disparity is based on the limitation of this current constitutive model. Because the hardening curves are J2 plasticity and based solely on uniaxial tension data, the shear component of this test is not accurately represented in the simulation. Because of this, the torque/angle metric was used to validate the failure surface.

In addition to the force-displacement plots, the path of the state of stress for each specimen was also overlaid onto the failure surface. Figures 128–132 show which areas of the failure surface affect each specimen. As the strain path of the specimen increases, the damage parameter is increased. The damage added at each time step is dependent on the value of the failure strain for that specific stress state. As the damage parameter reaches unity, the element will erode. The strain path plots are shown in four views: isometric, triaxiality-Lode plane, triaxiality-strain

plane, and Lode-strain plane. The specimens are grouped by type of stress (i.e., plane stress, plane strain, etc.).

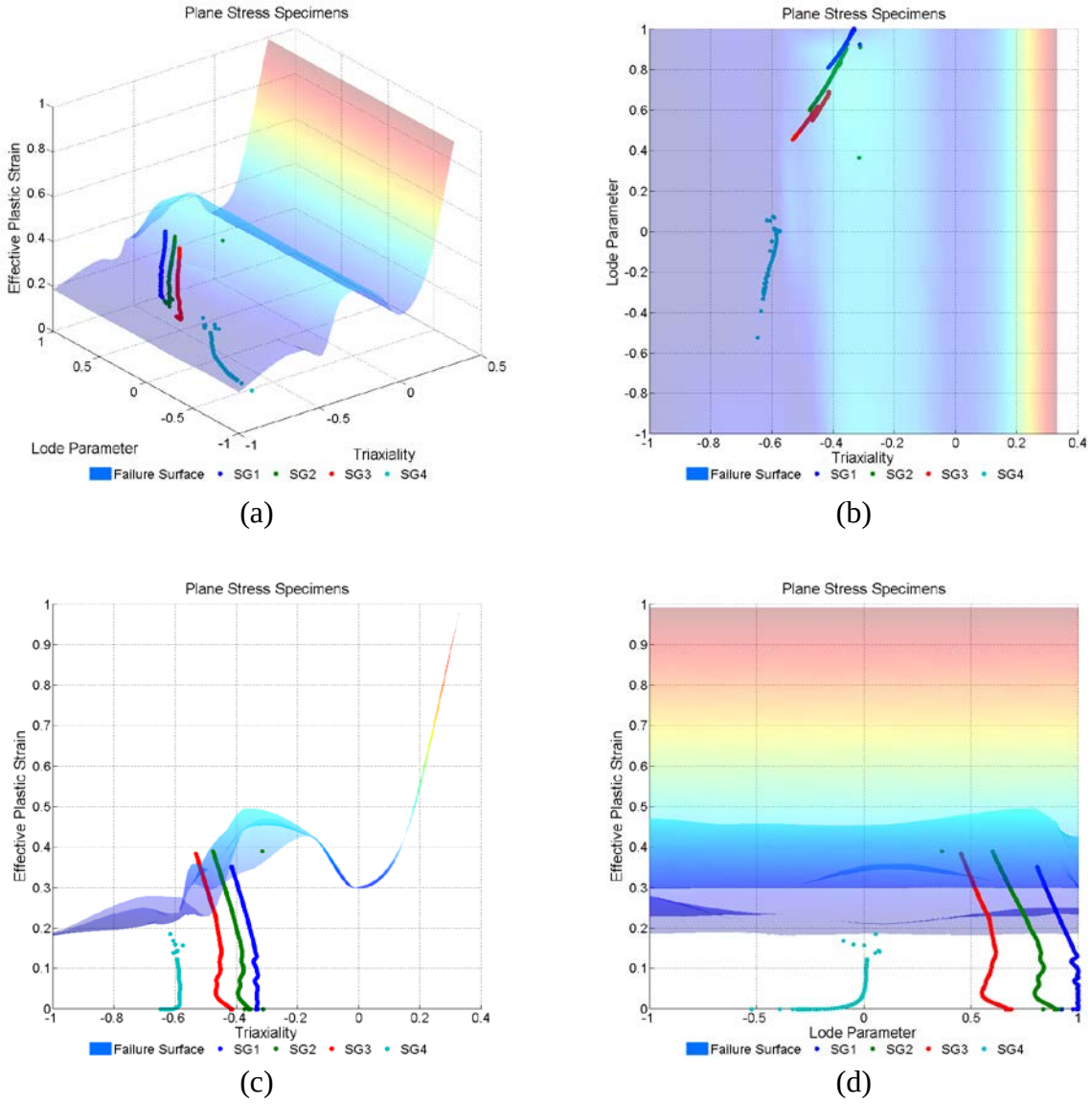

Figure 128. Strain path plots, plane-stress specimens: (a) isometric, (b) triaxiality-Lode plane, (c) Lode-strain plane, and (d) triaxiality-strain plane

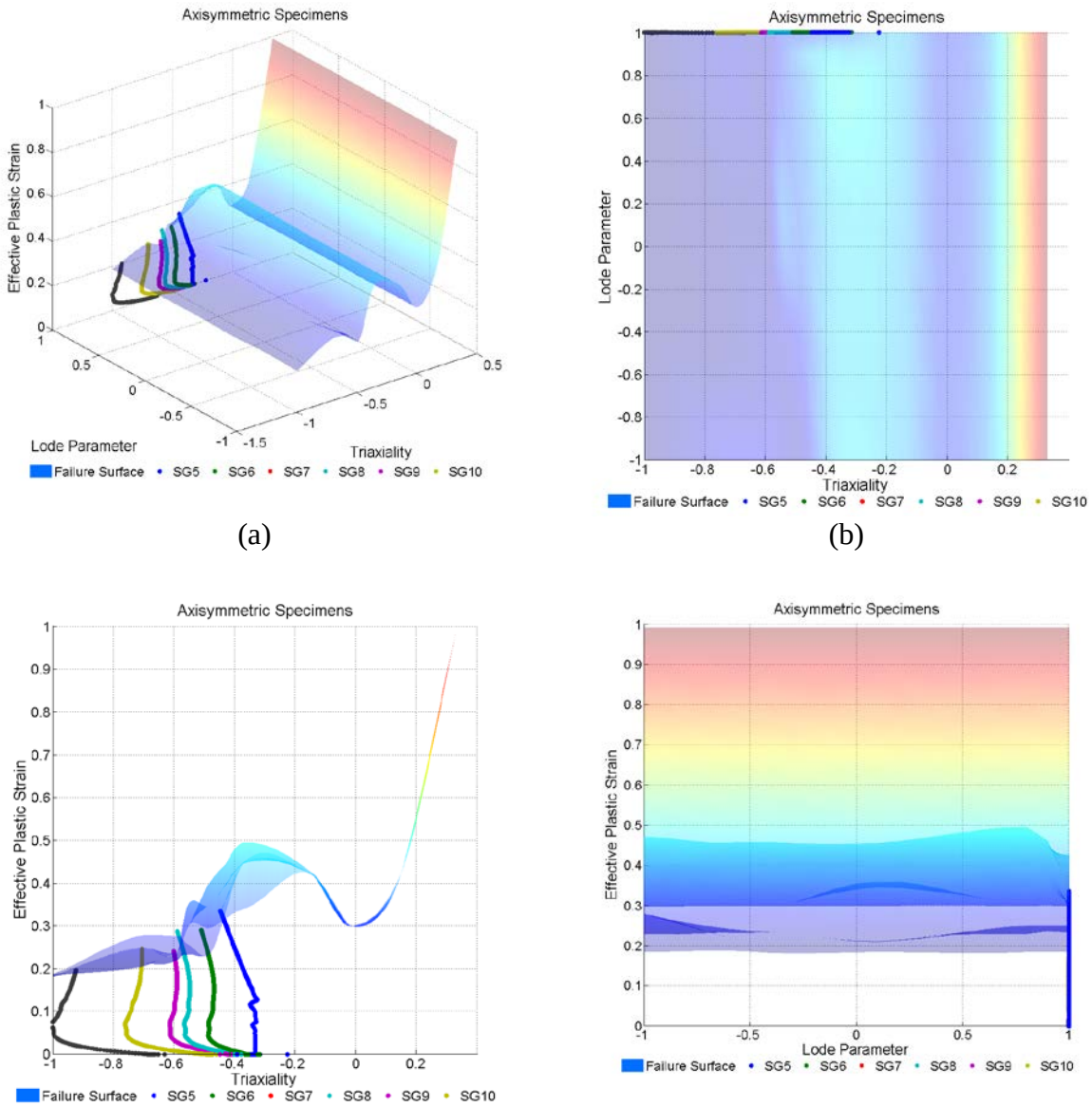

Figure 129. Strain path plots, axisymmetric specimens: (a) isometric, (b) triaxiality-Lode plane, (c) Lode-strain plane, and (d) triaxiality-strain plane

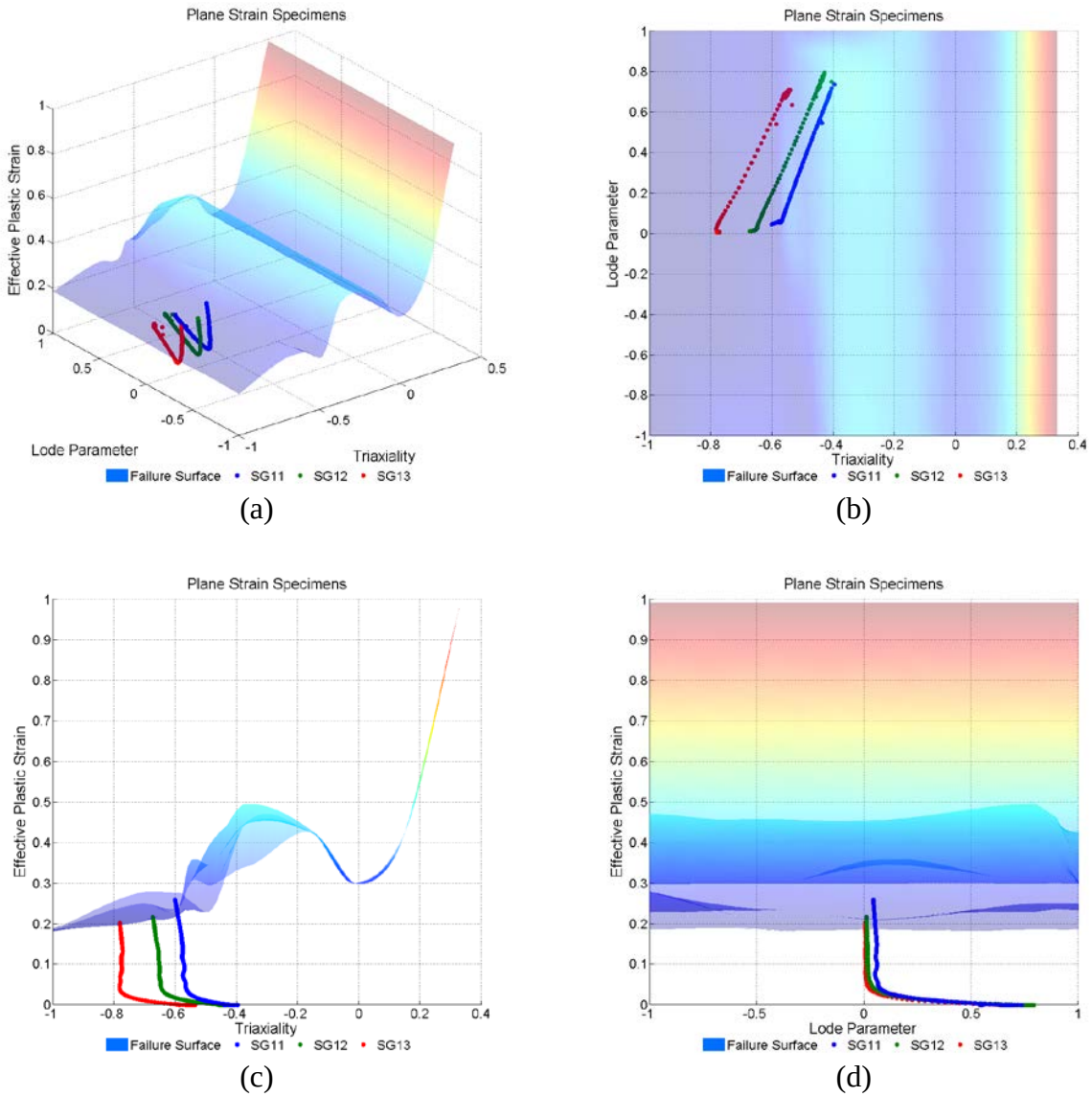

Figure 130. Strain path plots, plain-strain specimens: (a) isometric, (b) triaxiality-Lode plane, (c) Lode-strain plane, and (d) triaxiality-strain plane

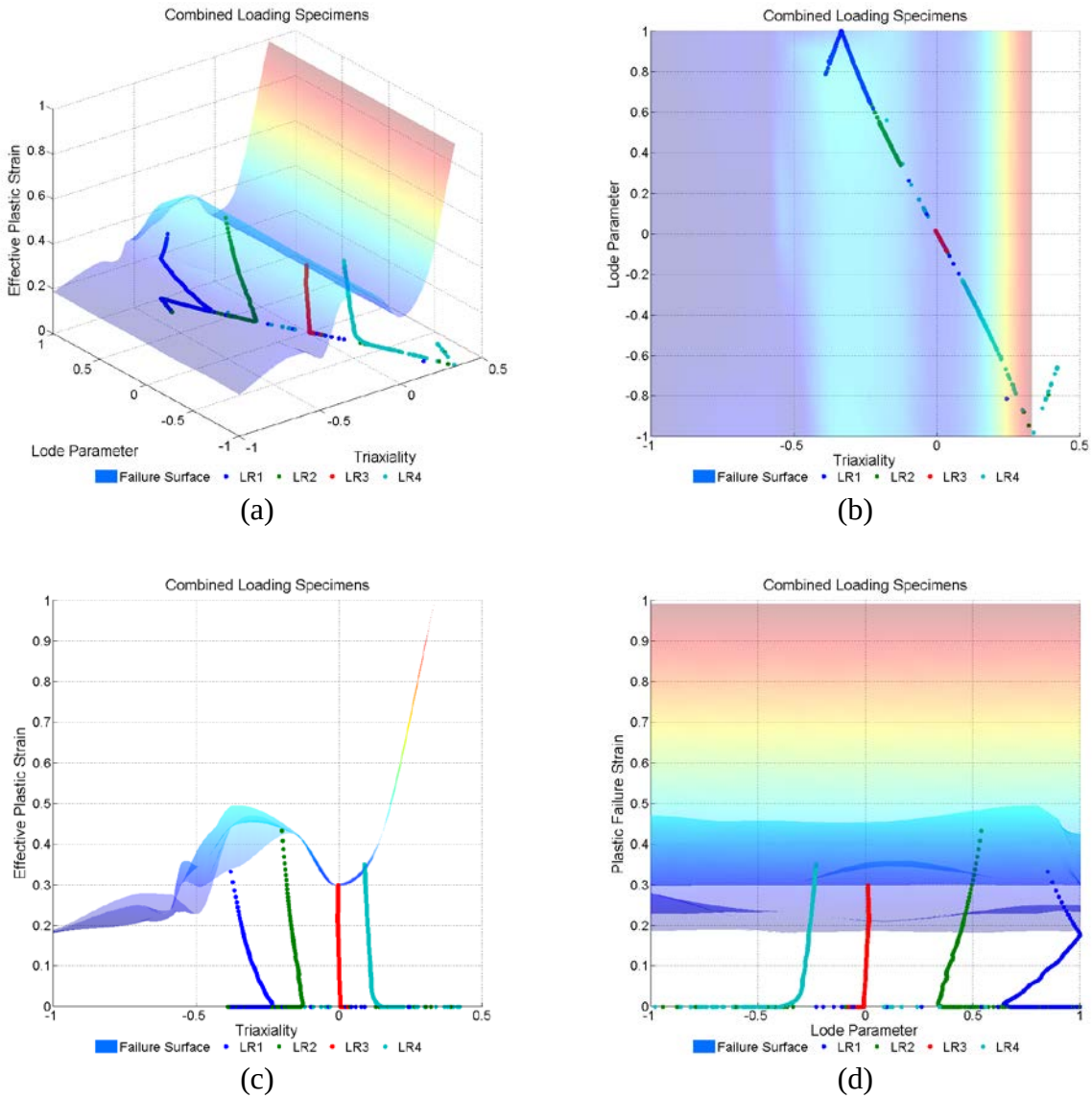

Figure 131. Strain path plots, combined loading specimens: (a) isometric, (b) triaxiality-Lode plane, (c) Lode-strain plane, and (d) triaxiality-strain plane

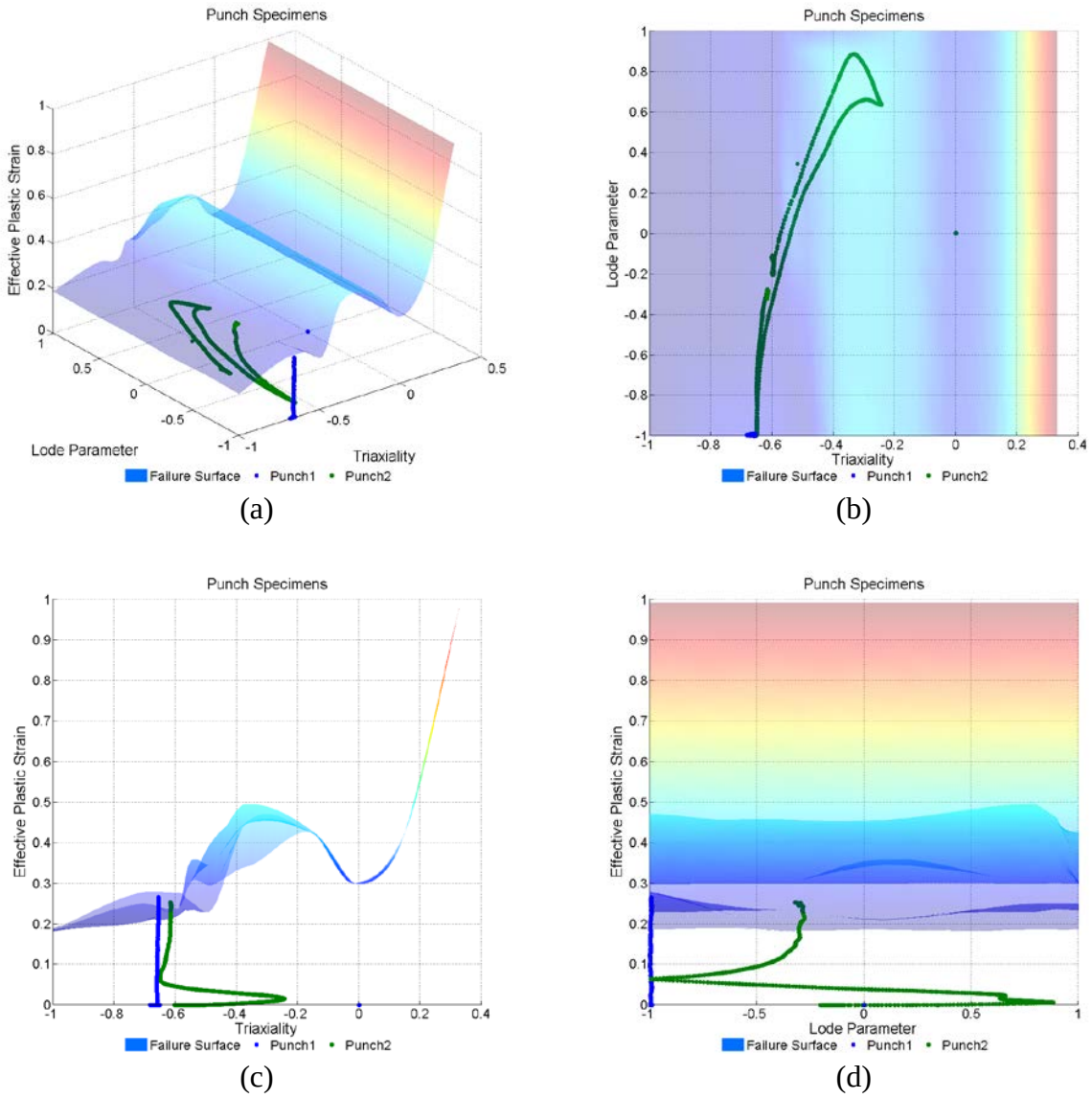

Figure 132. Strain path plots, punch specimens: (a) isometric, (b) triaxiality-Lode plane, (c) Lode-strain plane, and (d) triaxiality-strain plane

All of the specimens, except for LR1, fail at the appropriate displacement within the experimental spread. This verifies that the failure surface is acceptable and that it can accurately simulate fracture for this Ti-6Al-4V test series using the *MAT_224 material model.

5.3 CREATION OF A TEMPERATURE SCALING FUNCTION

The second component of the implementation of the *MAT_224 failure model is a failure-temperature scaling function. This function is a scaling factor for the failure surface that is dependent on the temperature of the element at a given time step. To create this function, a temperature-testing series is required. For this study, four different temperatures were tested: 293 K, 273 K, 673 K, and 873 K. For each temperature, the pure tension plane stress (SG1) specimen was used, the same tests that were described in section 3.2. Here, the failure strain is

used instead of the stress-strain relationship that was used in section 3.2. The temperature-testing series was considered quasistatic (no strain rate effects) and isothermal (no adiabatic effects). For each simulation, a single yield curve was used in the material keyword. A different yield curve was used for each temperature because the stress-strain response at each of these temperatures varies. It is assumed that the temperature scaling is independent of strain rate because the Johnson-Cook model applies the temperature scaling in the same manner for all strain rates. Though the failure surface was developed using tests at a strain rate of 0.01 sec^{-1} and the temperature tests were performed at a strain rate of 1.0 sec^{-1}, this is allowable because the strain rate and temperature scaling are multiplicative and independent in the Johnson-Cook law. Consequentially, the effect of a change in temperature is the same at every strain rate. The input yield curves for each temperature are shown in figure 133. Note that these are the same curves shown in figure 25, but with a Kelvin scale rather than a Celsius scale.

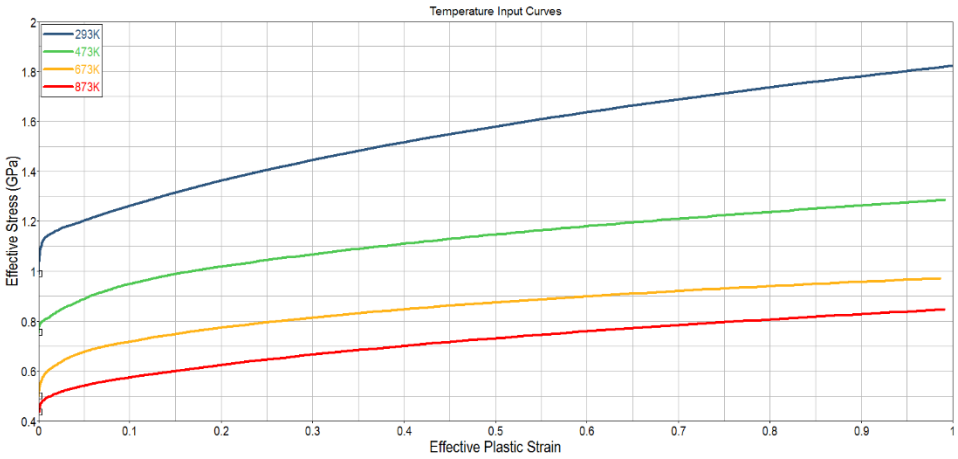

Figure 133. Input yield curves for each temperature

The first set of verification simulations was completed without using the full failure surface. These simulations were performed using the same method as previously described (arbitrary speed, single load curve) but with a unique yield curve. The force-displacement plots for these simulations are shown in figures 134 (a–d).

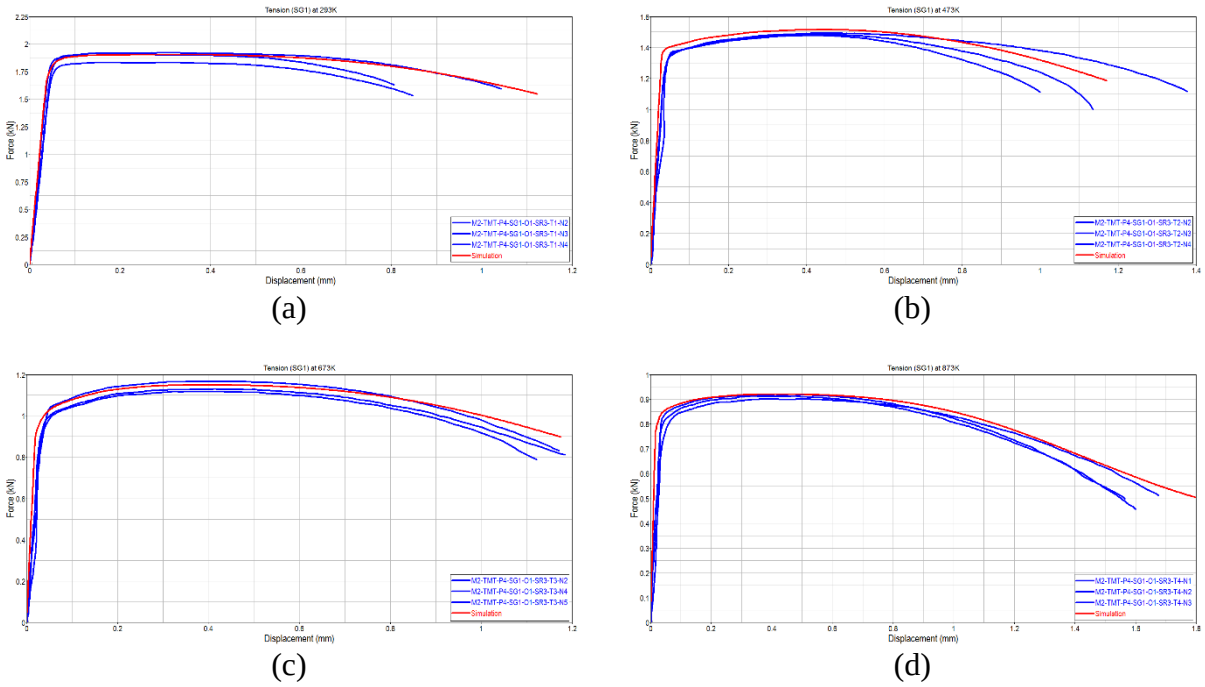

Figure 134. Force-displacement plots for each temperature ((a) 293K, (b) 473K, (c) 673K, and (d) 873K)

By initializing each of these simulations without the failure surface, a scaling function can be developed so that each of the temperature simulations can fail at the correct displacement. Table 8 shows the temperature, average failure displacement (from the physical test), simulation time to that average failure displacement, failure strain at the simulation time, and an initial scaling factor that is calculated using the following equation:

$$Scaling\ Factor = \frac{\varepsilon_{pf}}{\varepsilon_{pf_{RT}}} \tag{39}$$

Table 8. Normalizing factors for temperature simulations

Temp (K)	Average Failure Displacement	Simulation Time to Displacement	Failure Strain	Failure Strain Normalized to Room Temp
293	0.8989 mm	3.89 ms	0.541	1.000
473	1.1707 mm	5.00 ms	0.809	1.495
673	1.1592 mm	4.90 ms	0.789	1.458
873	1.6139 mm	6.61 ms	1.150	2.126

Using the failure strain normalized to room temperature as the scaling factor, the same simulations were run again. In this set of simulations, the failure surface table and the temperature scaling function were both present in the material keyword in addition to the single temperature yield curve. After some simulation-adjustment iterations, the temperature scaling

function was adjusted so that each simulation failure displacement occurred within the experimental spread. In addition, a value for the melting point of Ti-Al6-4V (1877K) was added to the end of the curve so that very high temperatures would not have extremely high scaling factors due to extrapolation. Table 9 shows the final temperature scaling function, and figures 135 (a–d) show the force-displacement plots when the scaling function is used.

Table 9. Scaling factors by temperature

Temp (K)	Scaling Factor
293	1.000
473	1.950
673	1.950
873	2.950
1877	2.950

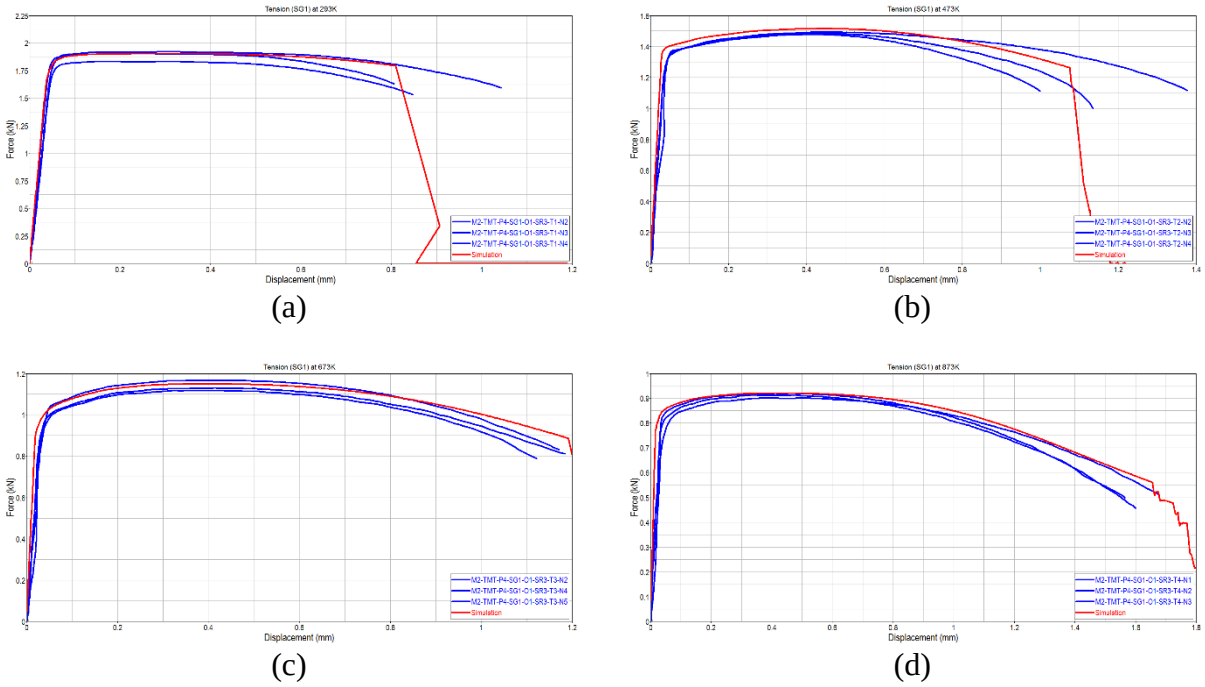

Figure 135. Force-displacement plots created using scaling function for each temperature ((a) 293K, (b) 473K, (c) 673K, and (d) 873K)

5.4 CREATION OF A STRAIN-RATE SCALING FUNCTION

Similar to the temperature scaling function described in section 5.3, a failure scaling function can also be created for different strain rates. Because the failure surface was based on a global strain rate of 0.01 sec^{-1}, other strain rates are not represented in the failure surface. A scaling function will allow the material model to scale the failure surface as a function of the elemental strain rate. To generate this scaling curve, the same strain-rate testing series described in section 3 was

used. This test series included tension tests at global strain rates of 0.01 sec^{-1} (SR2), 1.00 sec^{-1} (SR3), 650 sec^{-1} (SR4), and 1550 sec^{-1} (SR5).

Each of these strain rate tests was simulated using the same procedure as the original SG1 simulation; however, the full material model (strain rate curves, temperature curves, failure surface, temperature scaling curve) was used. This means that these rate-dependent tests are assumed to have rate and heat effects. The strain rate curves (table) are shown in figure 136. Note that these are the same curves described in section 3.4.

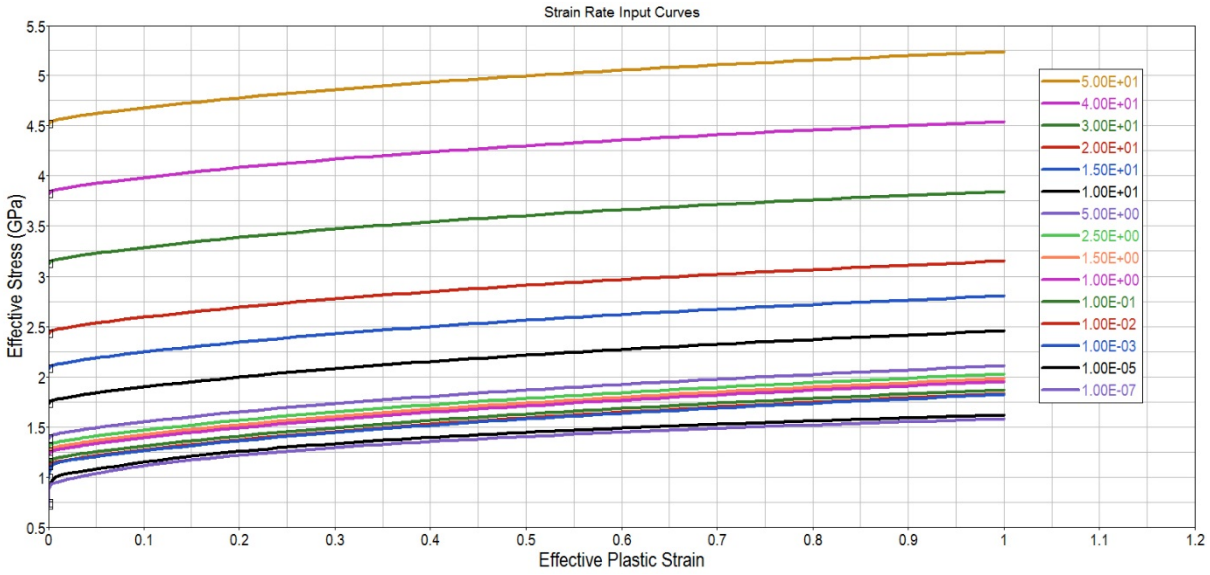

Figure 136. Strain rate input curves

In addition, the displacement imposed on the specimen in the simulation was generated from the physical test data (similar to the process described in section 3.4). To create the displacement input for the simulations, the average of the displacement time data for each physical test was averaged. Finally, the average curve was smoothed to minimize instabilities during the simulation. The input displacements (red) and the displacement time data from the physical tests (gray) are shown in figures 137 (a–c).

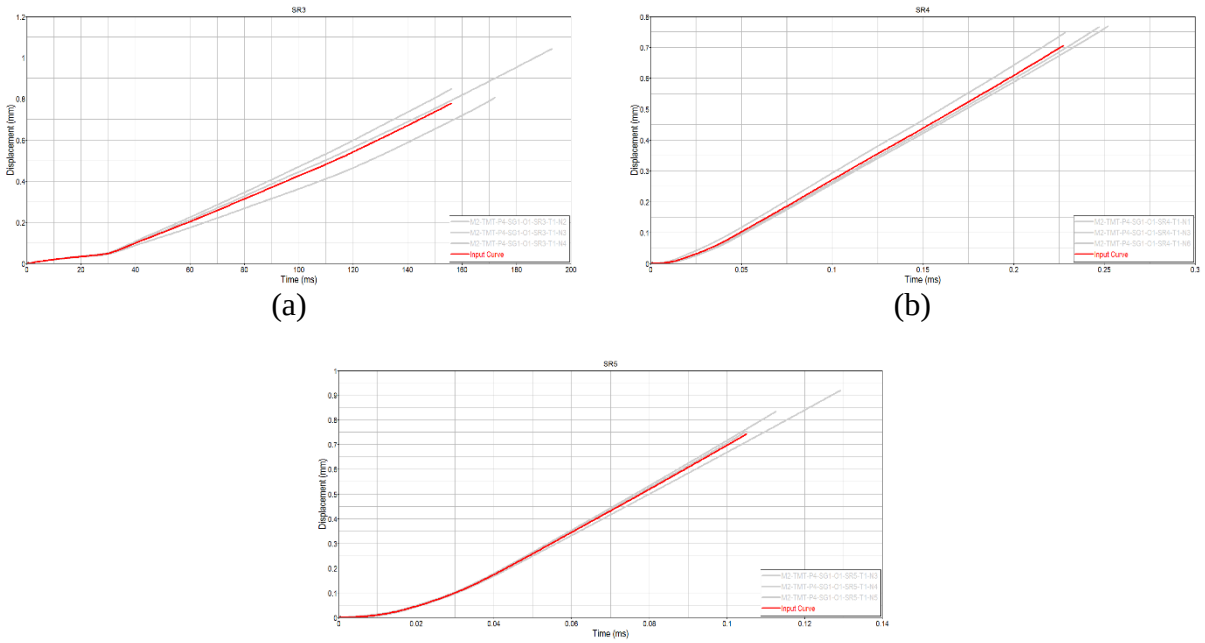

Figure 137. Input displacement curves (red) and physical test displacement measurements (gray) ((a) SR3, (b) SR4, and (c) SR5)

The purpose of these simulations was to generate the strain-rate scaling curve. A preliminary scaling curve was developed and adjusted until all of the specimens failed within the experimental spread of data. The strain rates for the table were chosen by analyzing the strain rates for the elements around the area of failure. This is different from the average global strain rates provided by OSU. Table 10 shows the final strain rate scaling data.

Table 10. Scaling factors by strain rate

Strain Rate	Scaling Factor
0.00001 $msec^{-1}$ (SR2)	1.000
0.00100 $msec^{-1}$ (SR3)	0.900
2.35000 $msec^{-1}$ (SR4)	0.370
6.61000 $msec^{-1}$ (SR5)	0.370

The final force-displacement curves, using the scaling function in figure table 10, were plotted with the original physical test data. These plots are shown in figures 138 (a–c) for SR3, SR4, and SR5 analyses, respectively. SR2 was previously shown in figure 44.

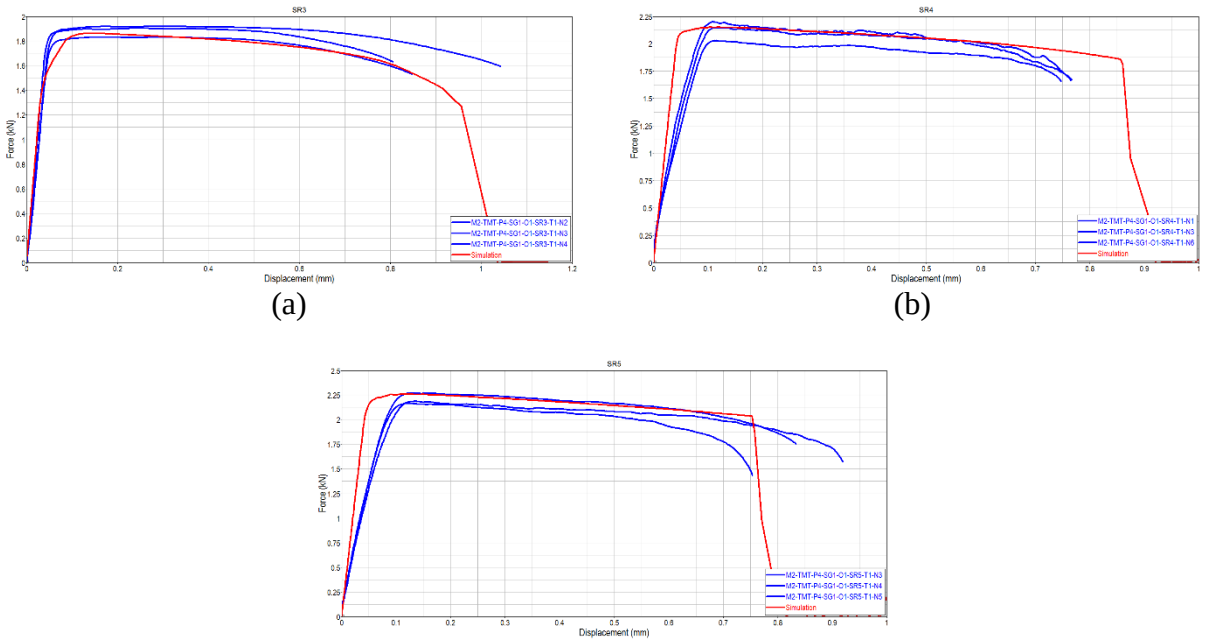

Figure 138. Final force-displacement curves plotted against physical test data for (a) SR3, (b) SR4, and (c) SR5

It is important to note that the SR4 prediction did not fail within the spread of the data. The analytical failure occurs at a larger displacement than is seen in the physical testing. Though a strain-rate scaling curve can be developed so that each simulation fails at the appropriate displacement, this curve would not be monotonically decreasing. It is physically more probable that, in the considered data range, both the temperature and strain-rate scaling curves are monotonically increasing or decreasing. To enforce this guideline, scaling values for SR4 and SR5 were chosen so that the error was minimized. In this case, the results using a scaling factor of 0.370 for SR5 fail inside of the experimental data spread; however, the SR4 prediction fails at a larger displacement when compared to the data set.

The lowest strain rate of 0.0001 sec^{-1} (SR1) was not used in the development of the failure scaling function. The strain rate of 0.01 sec^{-1} (SR2) was used for developing the scaling because the failure surface was developed with tests that had an average strain rate more similar to SR2 than to SR1. In addition, the failure strains occurring in the SR1 and SR2 tests were similar.

The temperature curves had to be adjusted before using them and the strain-rate curves together in a dynamic simulation. Originally, the temperature curves were created using a baseline quasistatic strain rate at 1.00 sec^{-1}. Because the failure surface was developed using the SR2 strain rate as quasistatic, each of the curves had to be scaled using the following function:

$$\sigma(\varepsilon_p, T) = \frac{\sigma(\varepsilon_p, RT, SR2)}{\sigma(\varepsilon_p, RT, SR3)} \sigma(\varepsilon_p, T) \tag{40}$$

where σ is the stress, ε_p is the plastic strain, T is the temperature, and RT is room temperature.

This scale factor was applied to each curve to transform the original (SR3-based temperature curves) to SR2 quasistatic-based curves. This transformation allowed for simultaneous use of the failure surface and scaling functions in dynamic simulations. The original (SR3) and the scaled (SR2) temperature curves are shown in figure 139.

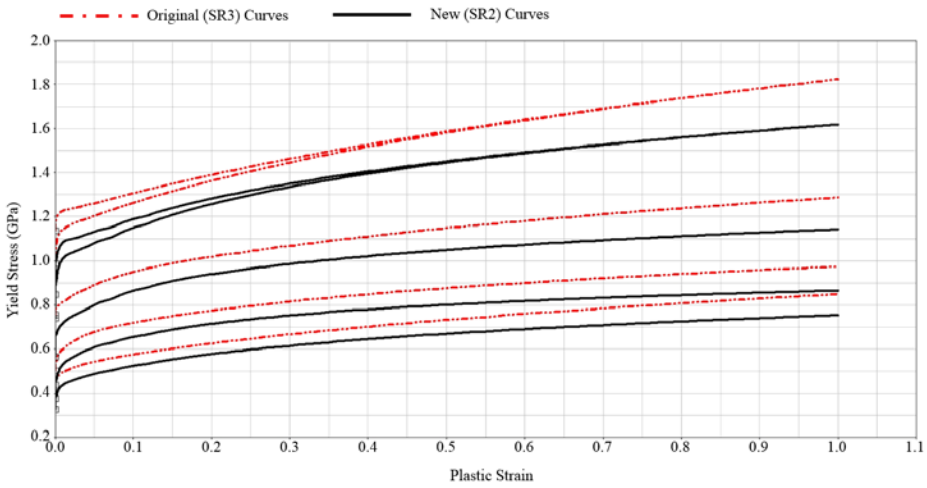

Figure 139. Original and scaled temperature function curves

5.5 CREATION OF A REGULARIZATION CURVE

The final component of the Ti-6Al-4V *MAT_224 material model is a mesh-size regularization scaling function for element erosion. The mesh-size regularization scaling function is critical because element erosion simulations do not converge as the mesh size is reduced [11]. This load curve defines the plastic failure strain as a function of the element size. The mesh size used in regularization is calculated by dividing the volume of the element by the area of the largest side of the element. Note that this will correspond exactly to the element side length for a perfectly cubical element (aspect ratio=1) and only in this case will regularization function perfectly. So for this type of applications elements should be used with an aspect ratio that is as close to unity as possible. The regularization curve is developed by simulating the tension (SG1) specimen with varying mesh sizes. Originally, the mesh size for all the specimens was 0.2 mm. Each specimen was re-meshed with 0.1 mm and 0.4 mm elements. The element configuration for each element size is shown in figures 140–142.

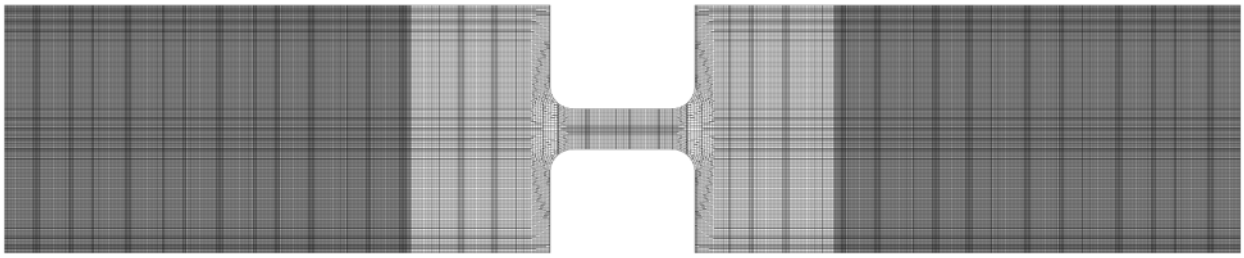

Figure 140. Element configuration using different element sizes–0.10 mm mesh (554,000 elements)

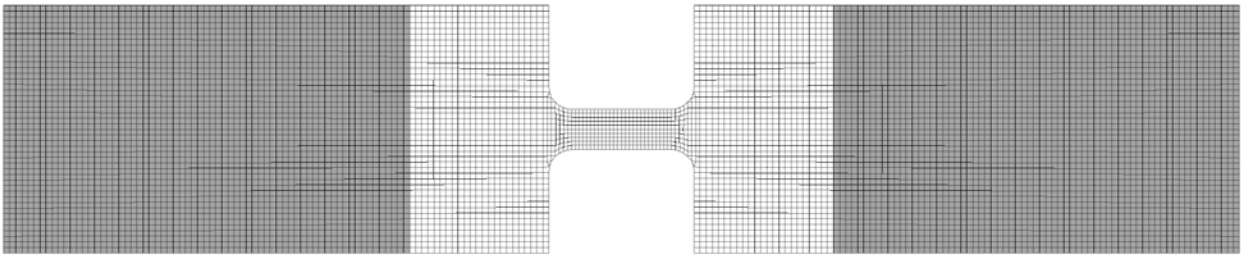

Figure 141. Element configuration using different element sizes–0.20 mm mesh (33,000 elements)

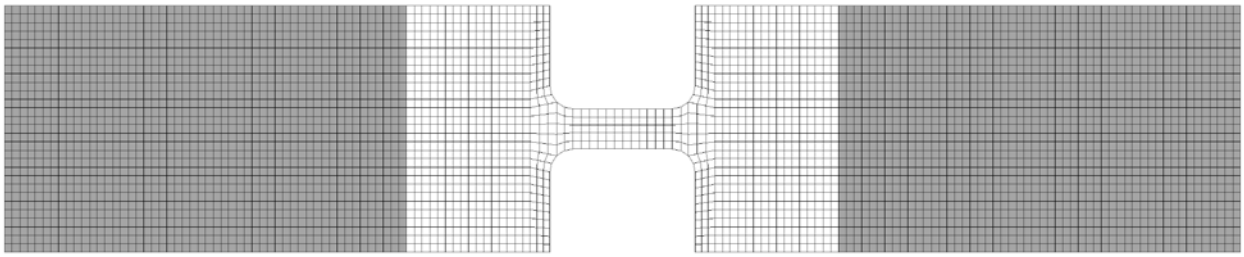

Figure 142. Element configuration using different element sizes–0.40 mm mesh (8400 elements)

Each of the three simulations was performed the same as it was for the original failure surface, with a single load curve and the failure surface; no other scaling factors were used. To generate the regularization scaling curve, each mesh was initially simulated with a scale factor of 1.0. If the specimen failed before the appropriate displacement was reached, the scale factor was increased. In contrast, if the specimen failed at a higher displacement than seen in the physical test, the scale factor was reduced. After some simulation iterations, the final regularization scaling factor was developed. Additional data points were created so that there was no extrapolation at very small and very large mesh sizes. The final regularization scaling curve is shown in table 11. Note that users of this material model with mesh sizes smaller than 0.1 mm or greater than 0.4 mm should perform additional analyses to extend this scaling curve.

Table 11. Scaling factors by mesh size

Mesh Size	Scaling Factor
0.00 mm	1.038
0.10 mm	1.038
0.20 mm	1.000
0.40 mm	0.912
0.50 mm	0.912

The force-displacement plots for the 0.10 mm, 0.20 mm, and 0.40 mm mesh sizes are shown in figure 143. With the scaling factors, all three of the specimens fail at virtually the same displacement (i.e., 0.879 mm).

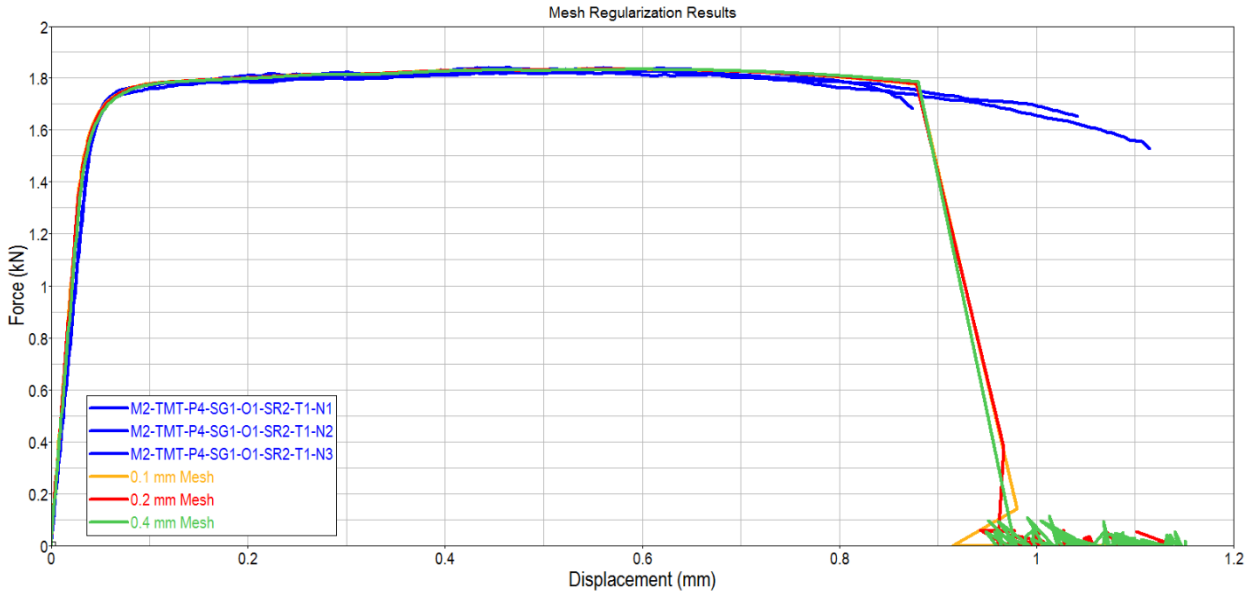

Figure 143. Comparison force-displacement plots for mesh sizes 0.10mm, 0.20mm, and 0.40mm

6. VALIDATION OF THE FAILURE MODEL

To analyze the effectiveness of the Ti-6Al-4V material model, dynamic impact simulations were completed and compared to the test results. First, two dynamic punch tests were simulated to verify failure predictions. Second, a series of ballistic tests were simulated to verify the ballistic limit of the Ti-6Al-4V material model. The complete material model was used for all the simulations. The input keyword is shown in figure 144.

```
*KEYWORD
*MAT_TABULATED_JOHNSON_COOK_TITLE
MAT_224_Ti64
$      mid        ro         e         pr        cp        tr      beta     numint
         1 4.4300E-6 110.00000  0.342000     526.3       293  0.800000  1.000000
$     lck1      lckt       lcf       lcg       lch       lci
      1000      2000      3000      4000      5000      6000
```

Figure 144. Input deck for *MAT_TABULATED_JOHNSON_COOK_TITLE

Referenced by this material keyword file are a strain rate table (1000), a temperature table (2000), the failure surface (3000), the strain-rate-failure scaling function (4000), the temperature-failure scaling function (5000), and the mesh-regularization scaling function (6000). Each of these curves or tables is referenced by the material keyword and all are used in the validation simulations discussed in this section.

6.1 DYNAMIC PUNCH TEST SERIES

Two dynamic punch tests were simulated based on physical testing performed by OSU [5]. These tests were similar to the punch tests used to create the failure surface, but the punches were smaller and impacted at a much faster velocity. The diameter of the titanium specimen is 14.7 mm.

Another difference is the modeling strategy for the dynamic punch tests. Initial simulations showed that the boundary conditions had a large influence on the results. Though the quasistatic punch tests were modeled with rigid boundary conditions where the specimen was clamped, these dynamic punch tests were modeled with the clamp. The inner diameter of the clamp is 11.0 mm. The clamp (red) and specimen (blue) assembly are shown in figure 145.

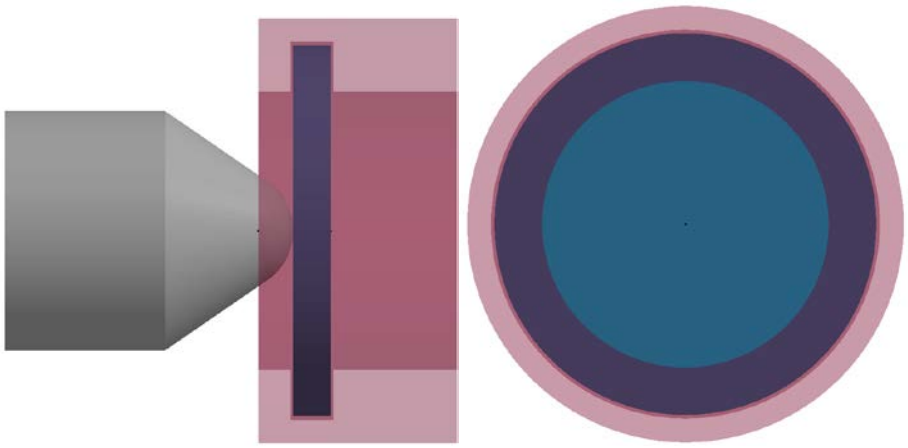

Figure 145. Diagram of clamp (red) and specimen (blue) assembly

The clamp was modeled with constrained, rigid shell elements. This model of the boundary conditions, though an improvement over the ring method used in the quasistatic punch tests, is still not an ideal representation of the test setup. Because it is difficult to model the deformation/displacement of the adapter assembly, an accurate boundary condition is nearly impossible to model correctly. This imperfection in the geometrical model has a significant

effect on the measured force-displacement results. Each punch test is discussed in sections 6.1.1 and 6.1.2.

6.1.1 Dynamic Punch1

Punch1 is 9.5 mm in diameter with a 2.39-mm radius nose. The punch consists of approximately 10,000 rigid shell elements with an average mesh size of 0.2 mm (see figure 146).

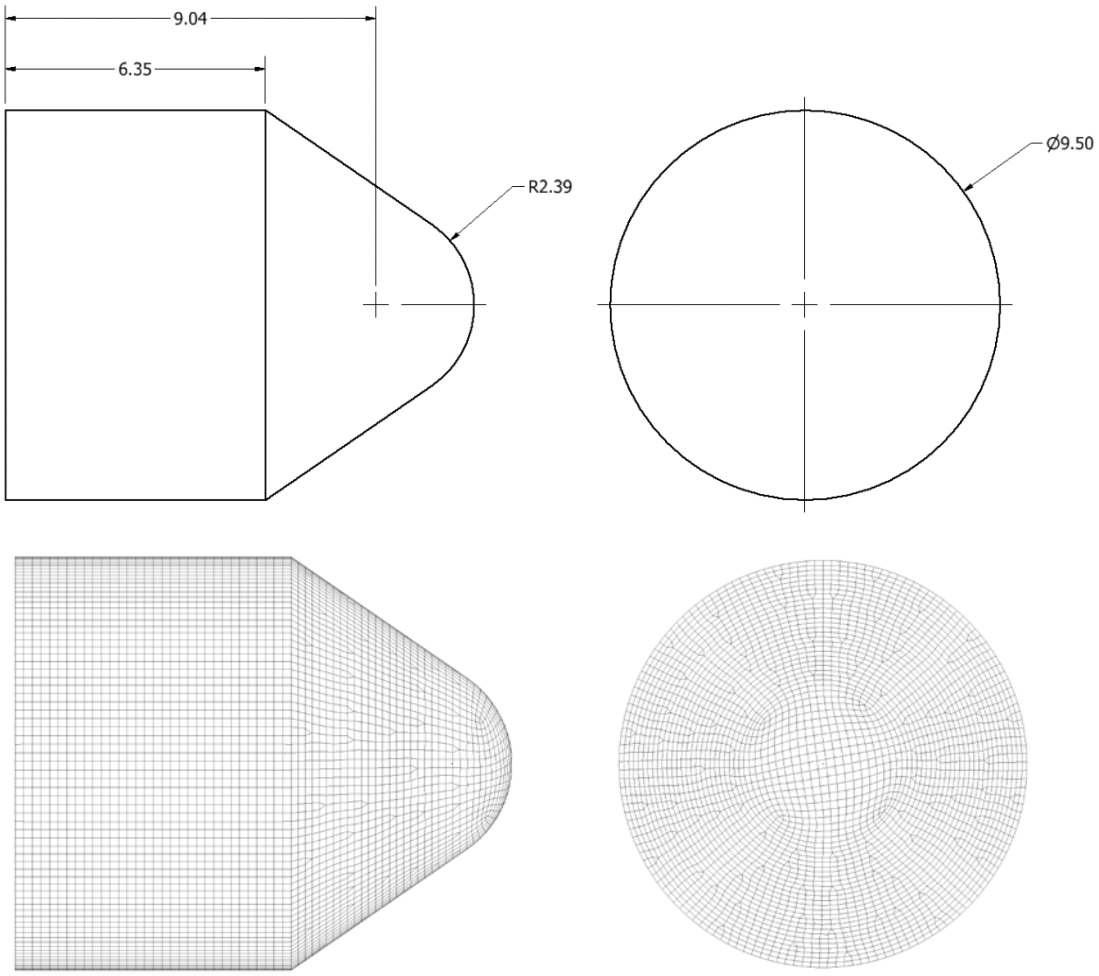

Figure 146. Geometry and mesh of the dynamic Punch1 specimen

To accurately simulate this dynamic punch test, the displacement of the punch was defined by the data provided by OSU. The punch displacement-time data were extracted from the data and used as the input displacement for the simulation. The three physical test displacements were averaged to create a single input curve. That input curve was then smoothed to minimize the possibility of instabilities in the simulation. Figure 147 shows the input curve (in red) along with the physical test displacement-time data (gray).

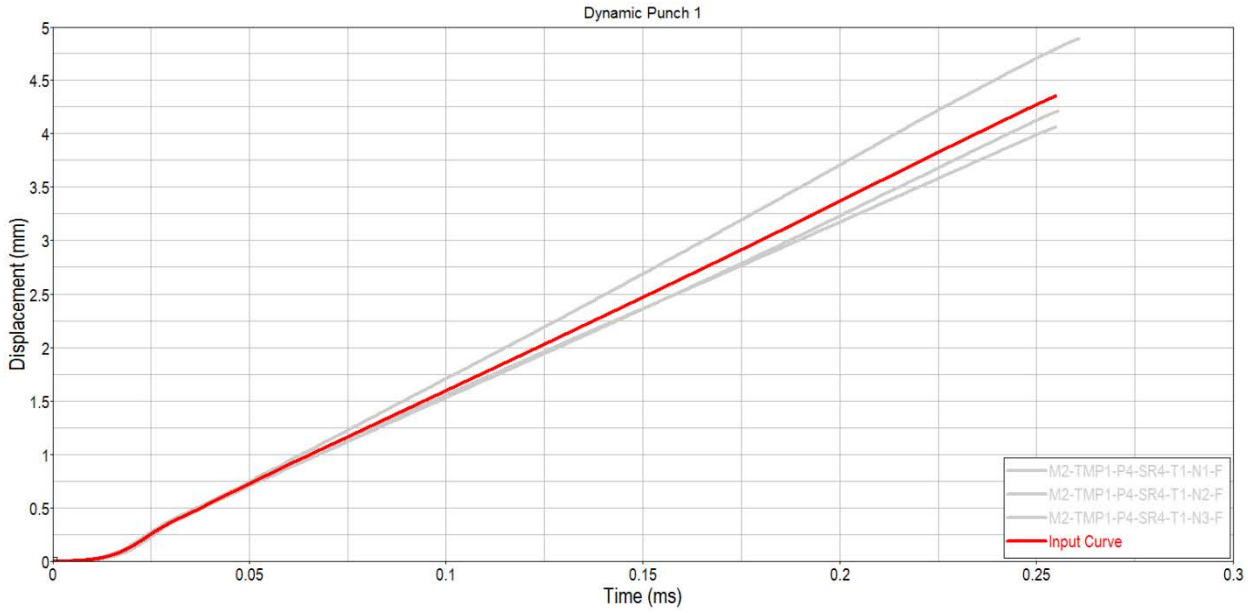

Figure 147. Displacement-time data input curve (red) and physical test data (gray)

The contact force-displacement time history data from the simulation were compared to the physical tests (see figure 148).

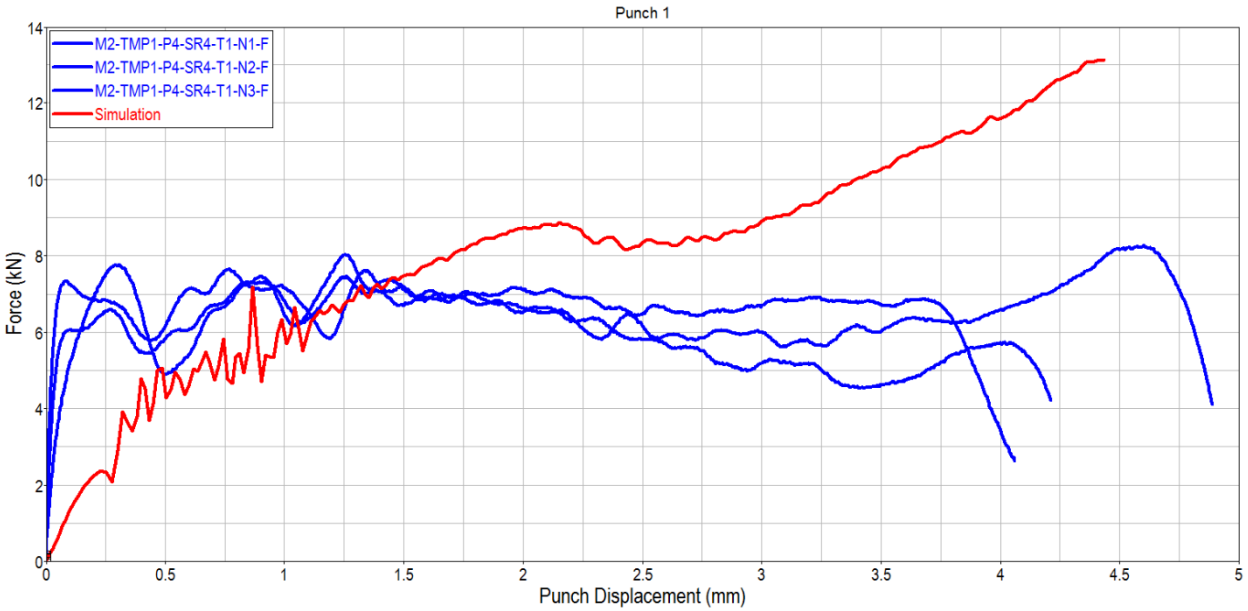

Figure 148. Contact force-displacement time history, simulation (red) versus test data (blue)

In addition to the force-displacement data, fringe plots of the effective plastic strain are shown at multiple time steps (see figure 149).

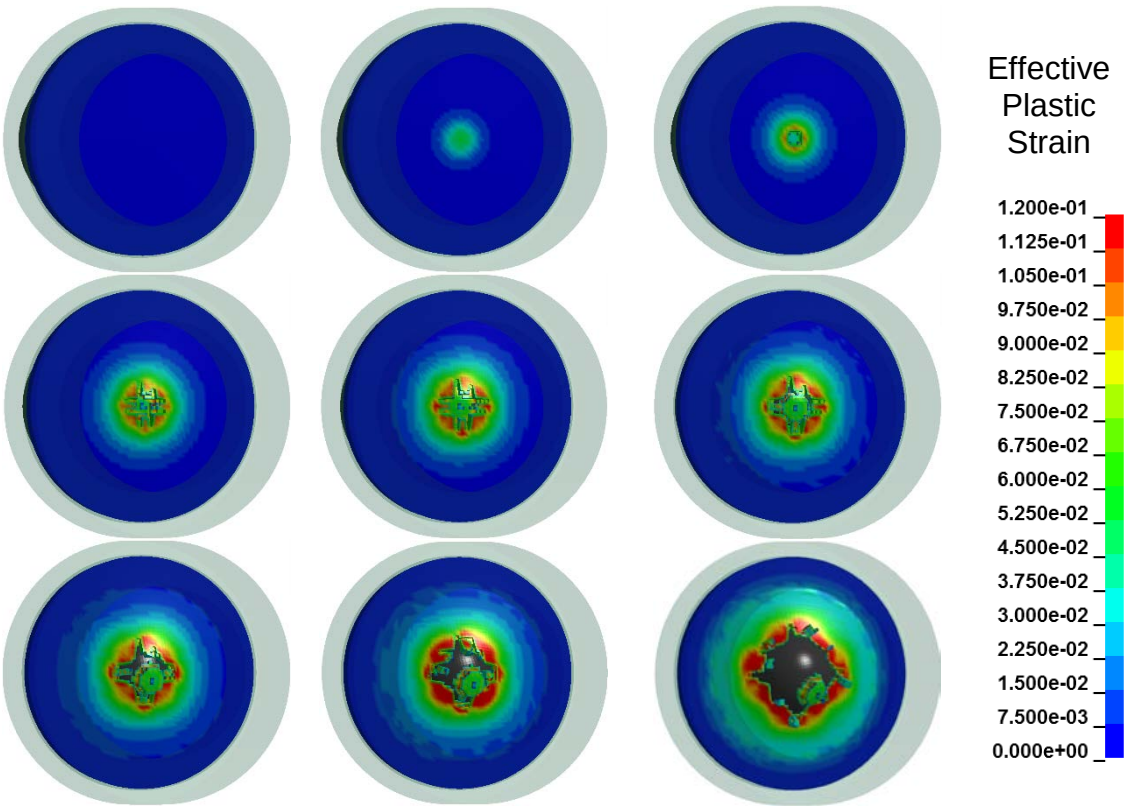

Figure 149. Effective plastic strain fringe plots for dynamic Punch1 specimen

6.1.2 Dynamic Punch2

Punch2 is 9.5 mm in diameter with a 4.75-mm radius nose. The punch consists of approximately 11,000 rigid shell elements with an average mesh size of 0.2 mm (see figure 150).

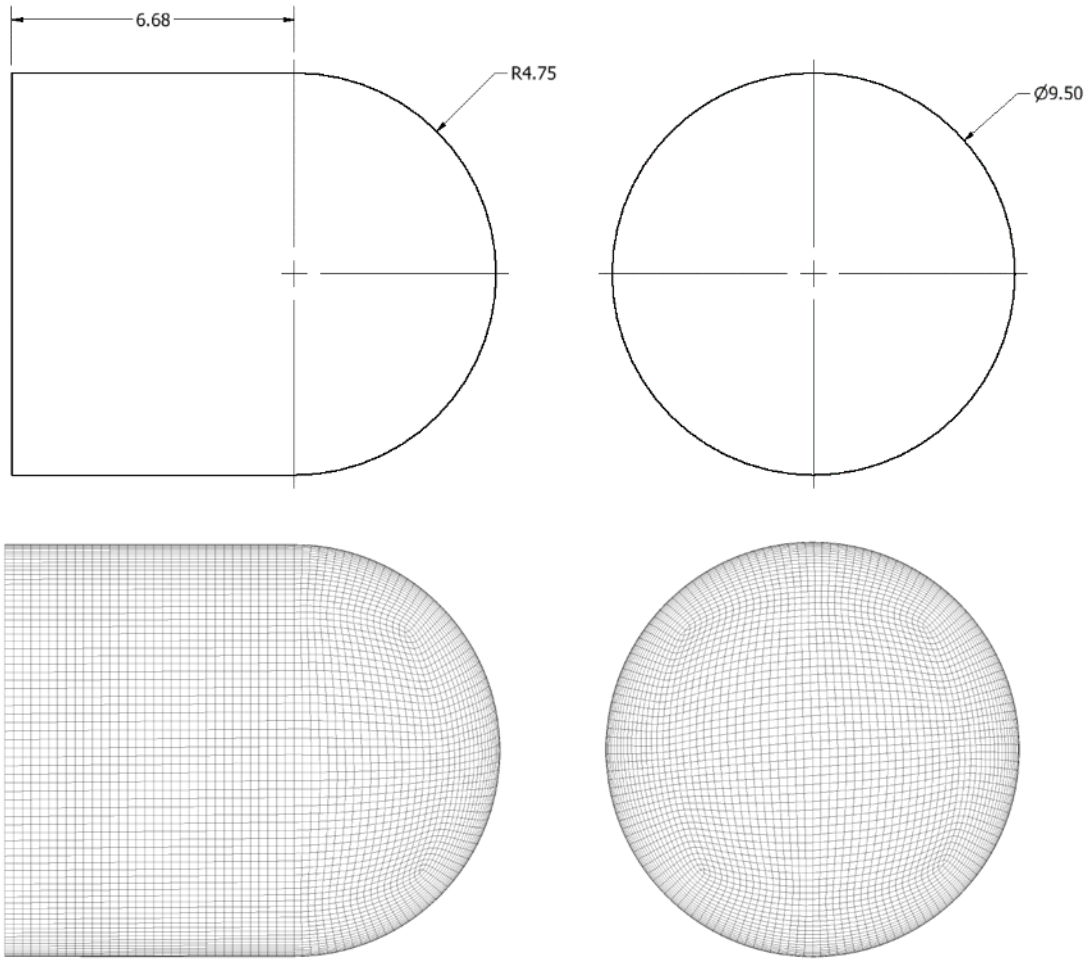

Figure 150. Geometry and mesh of the dynamic Punch2 specimen

To accurately simulate this dynamic punch test, the displacement of the punch was defined by the data provided by OSU. The punch displacement-time data were extracted from the data and used as the input displacement for the simulation. The three physical test displacements were averaged to create a single input curve. That input curve was then smoothed to minimize the possibility of instabilities in the simulation. Figure 151 shows the input curve (in red) along with the physical test displacement-time data (gray).

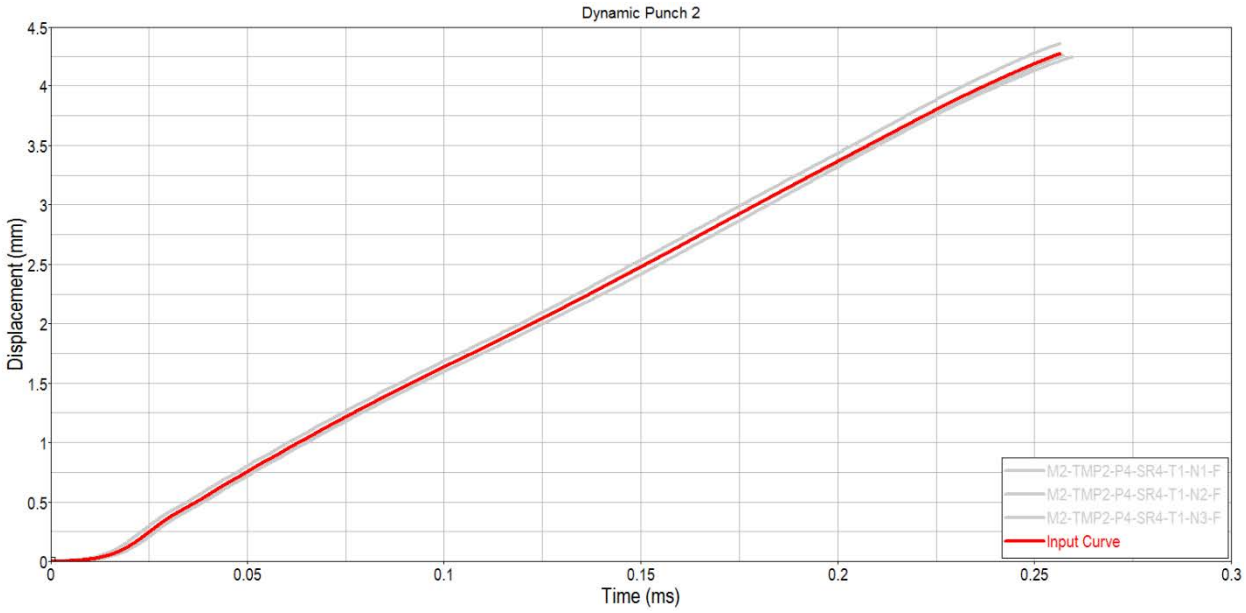

Figure 151. Displacement-time data input curve (red) and physical test data (gray)

The contact force-displacement time history data from the simulation were compared to the physical tests (see figure 152).

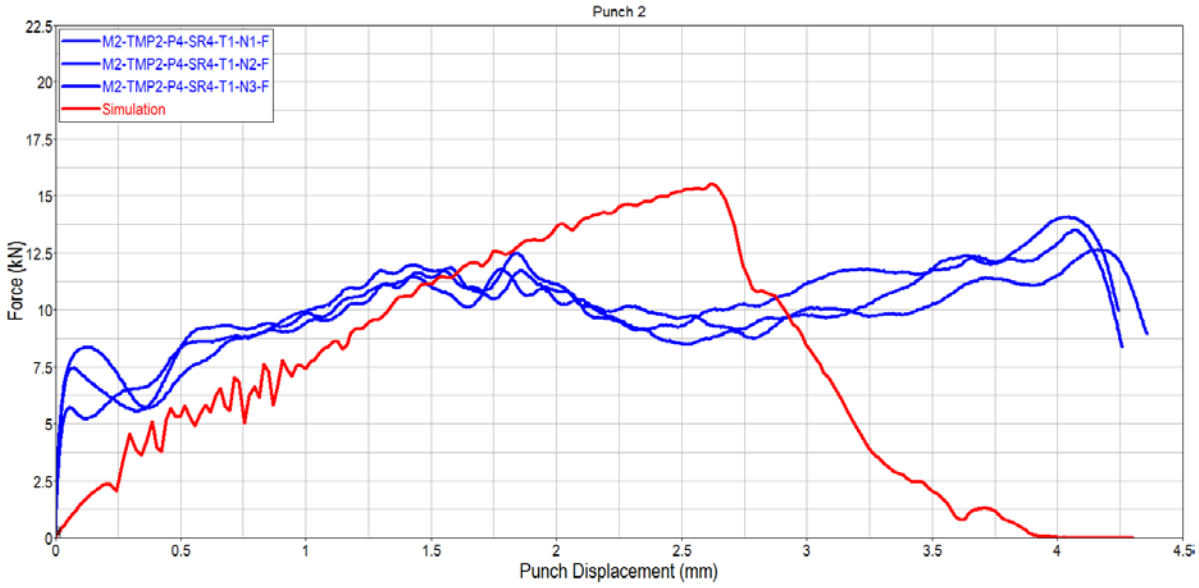

Figure 152. Contact force-displacement time history, simulation (red) versus test data (blue)

In addition to the force-displacement data, fringe plots of the effective plastic strain are shown at multiple time steps (see figure 153).

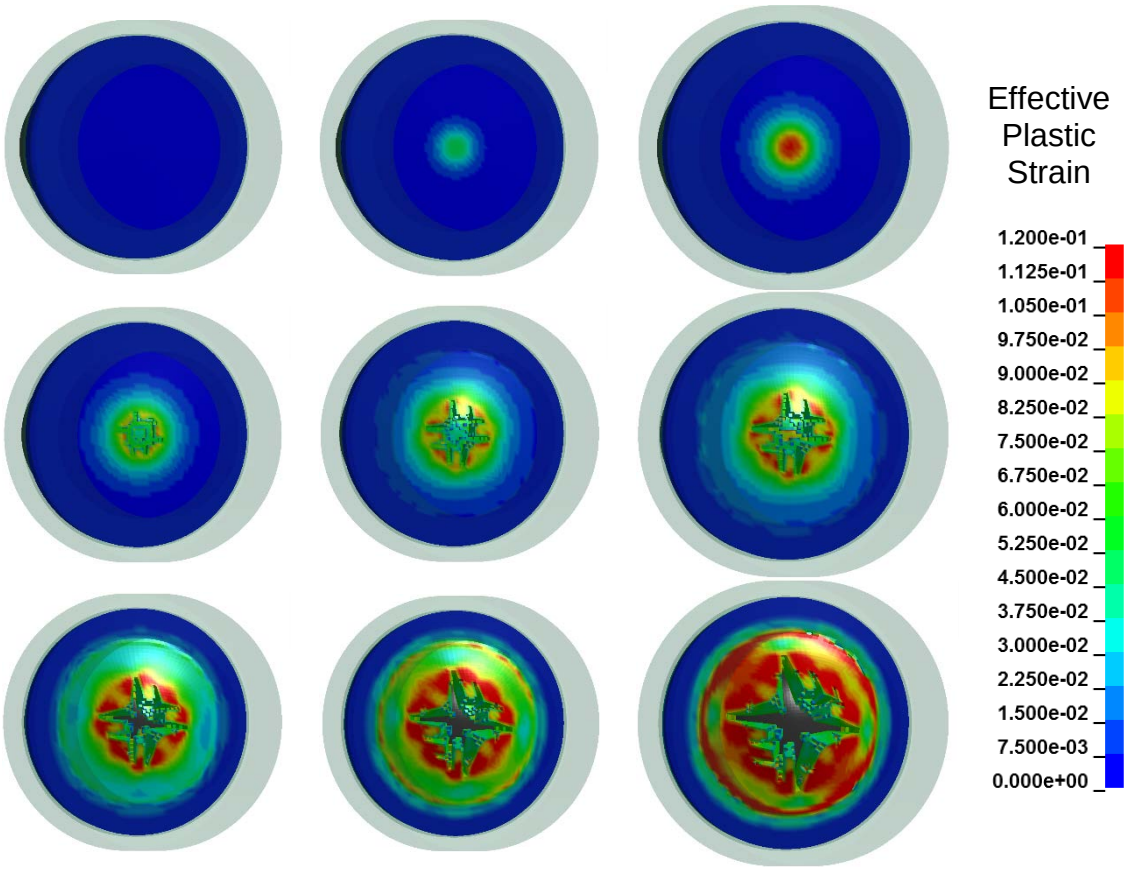

Figure 153. Effective plastic strain fringe plots for dynamic Punch1 specimen

6.2 NASA BALLISTIC TEST SERIES

In 2013, NASA performed a series of ballistic tests, the results of which are summarized in the report "Impact Testing of Aluminum 2024 and Titanium 6Al-4V for Material Model Development" [2]. This test series includes ballistic tests in which a 19.0-mm diameter cylindrical A2 tool steel projectile impacts a 381-mm square plate. The plate, made of Ti-6Al-4V, is 12.7-mm (0.5 inch) thick and constrained so that a circular impact area of 254 mm is free. The cylindrical projectile is aligned so that it strikes the center of the plate. The dimensions for the plate and projectile are shown in figure 154. Also shown are the orientation of the finite element model (see figure 155) and mesh configuration of the projectile (see figure 156).

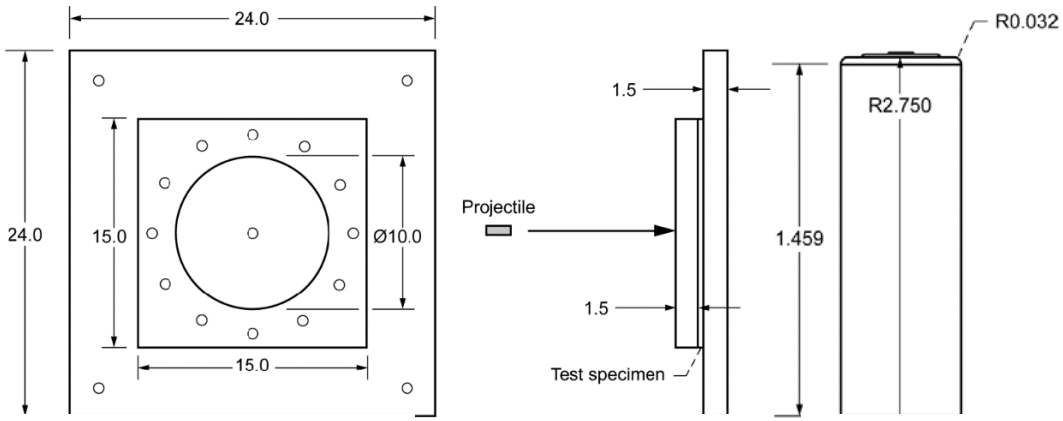

Figure 154. Design geometry for (a, b) NASA ballistic plate test setup and (c) projectile

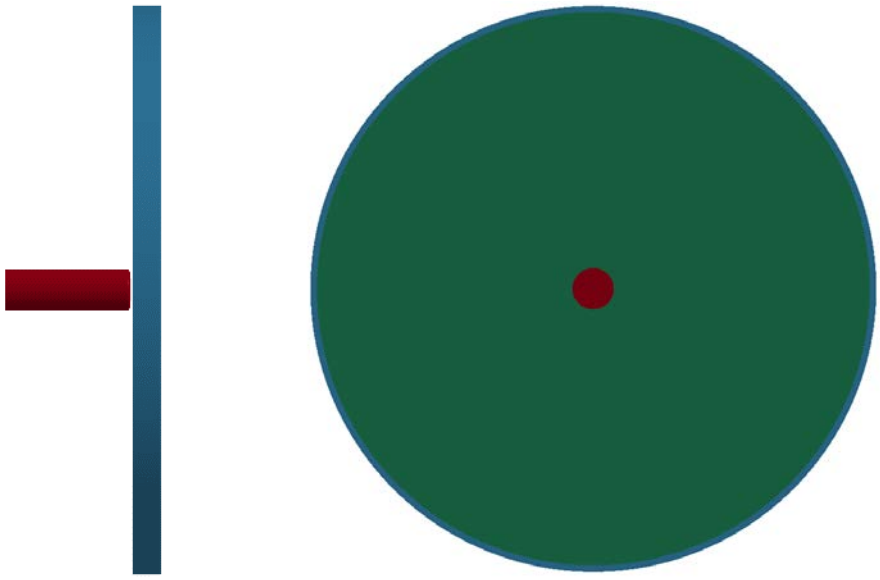

Figure 155. Orientation of projectile (red) to plate surface (green)

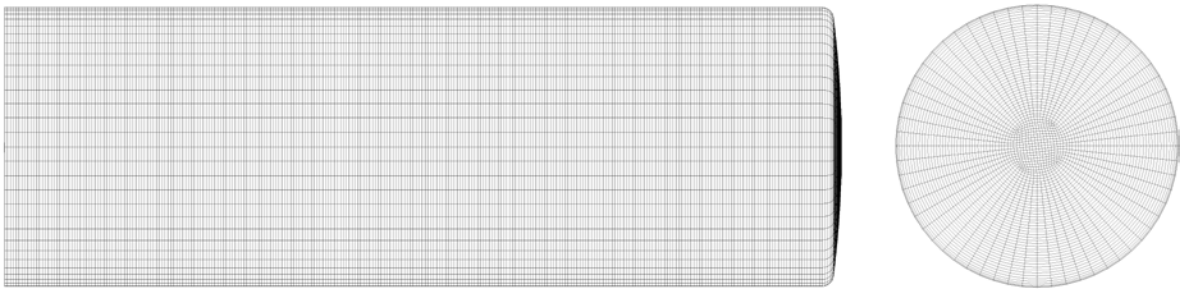

Figure 156. Meshed finite element model of projectile

The projectile was modeled with *MAT_ELASTIC, with the following material card (see figure 157).

```
*KEYWORD
*MAT_ELASTIC
$#     mid        ro          e          pr
         3 7.8600E-6  190.0000   0.32000
```

Figure 157. *MAT_ELASTIC input card

The justification for modeling the projectile as elastic was based on the test report stating that there was “no evidence of plasticity or macro deformation seen in the hardened A2 projectiles” [2]. For this simulation, it was assumed there was some elastic deformation but no plastic deformation. Additionally, the boundary condition, or outer ring, was modeled as rigid, stationary, solid elements. This assumption was also based on the report stating that “the boundary conditions do not play a role in panels of this thickness (0.14″)” [2]. Because the ratio of the plate diameter to the projectile diameter was so large, the boundary effects were assumed to be negligible.

A simulation matrix was defined based on the available test data. The primary independent variable was the projectile impact velocity, whereas the dependent variable was the exit velocity of the projectile. The impact and exit velocities from the physical tests are shown in table 12. The shaded rows are the tests that were to be simulated for this validation.

Table 12. Impact and exit velocities from physical tests (all) and for simulated tests (shaded)

Impact Velocity (m/s)	Exit Velocity (m/s)
273.1	144.8
263.7	129.2
217.3	73.5
196.9	46.3
160.6	0.0
177.1	0.0
182.0	0.0
176.2	0.0
192.0	0.0
191.7	31.7
187.8	0.0

After the initial simulations of each impact velocity, it was determined that the triaxiality in and around the adiabatic shear band (near the boundary of the impact) was between 0.2 and 5. In addition, these elements resulted in very high hydrostatic pressure contents. The stress tensor and triaxiality for these elements are shown in the following equation:

$$\sigma = \begin{pmatrix} -p & 0 & 0 \\ 0 & -p & 0 \\ 0 & 0 & -p \end{pmatrix} + \begin{pmatrix} \tau & 0 & 0 \\ 0 & 0 & 0 \\ 0 & 0 & -\tau \end{pmatrix}$$

$$p > 0 \; and \; \tau > 0 \tag{41}$$

$$Triaxiality = \frac{p}{\tau\sqrt{3}} > 0$$

where p is the pressure and τ is the shear stress.

Figure 158 shows the cross-sectional fringe plot of the triaxiality and pressure for one of the ballistic simulations.

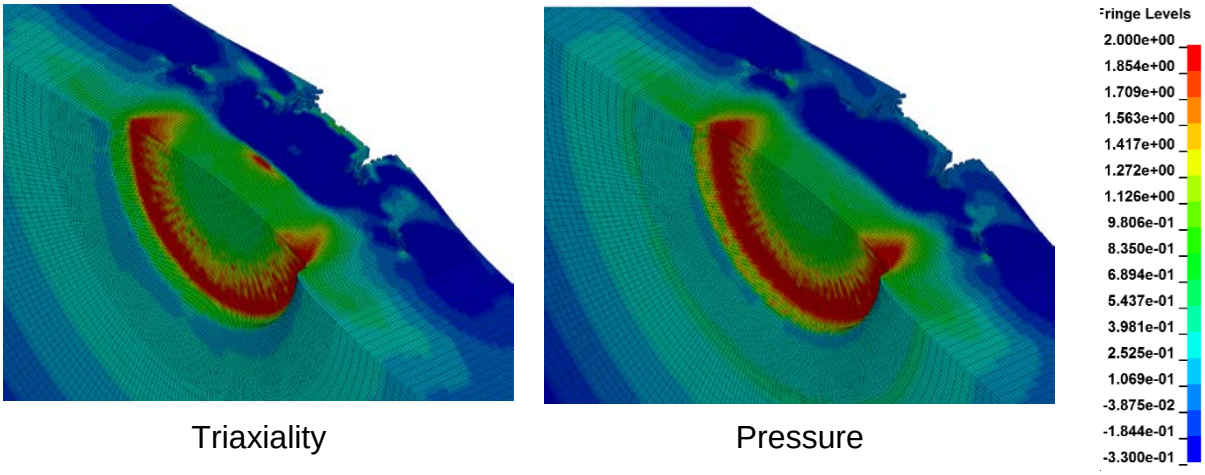

Figure 158. Cross-sectional fringe plots of plate

As described in the failure surface generation portion of this report, the maximum triaxiality test specimen was the combined compression torsion specimen. This test specimen only had triaxiality up to 0.147. Therefore, this adiabatic shear band in these ballistic tests represents an area of the failure surface that was previously assumed to have very high failure strains. The initial and often made assumption that no failure occurs when all three principal stress components are negative (triaxiality > 0.333) is false. Therefore, an update to the failure surface is necessary in that region.

To update the failure surface to account for this under-represented area, the failure strain between triaxialities of 0.20 and 4.00 were set to approximately 0.500 for all Lode parameters. This created a plateau in the compressive region between these two triaxialities. The actual failure surface in this region is more complicated than this. However, additional tests using new specimen designs will be required to fully define the surface in this region. The original failure surface (as seen from the triaxiality-failure strain plane) and the adjusted failure surface are shown in figure 159.

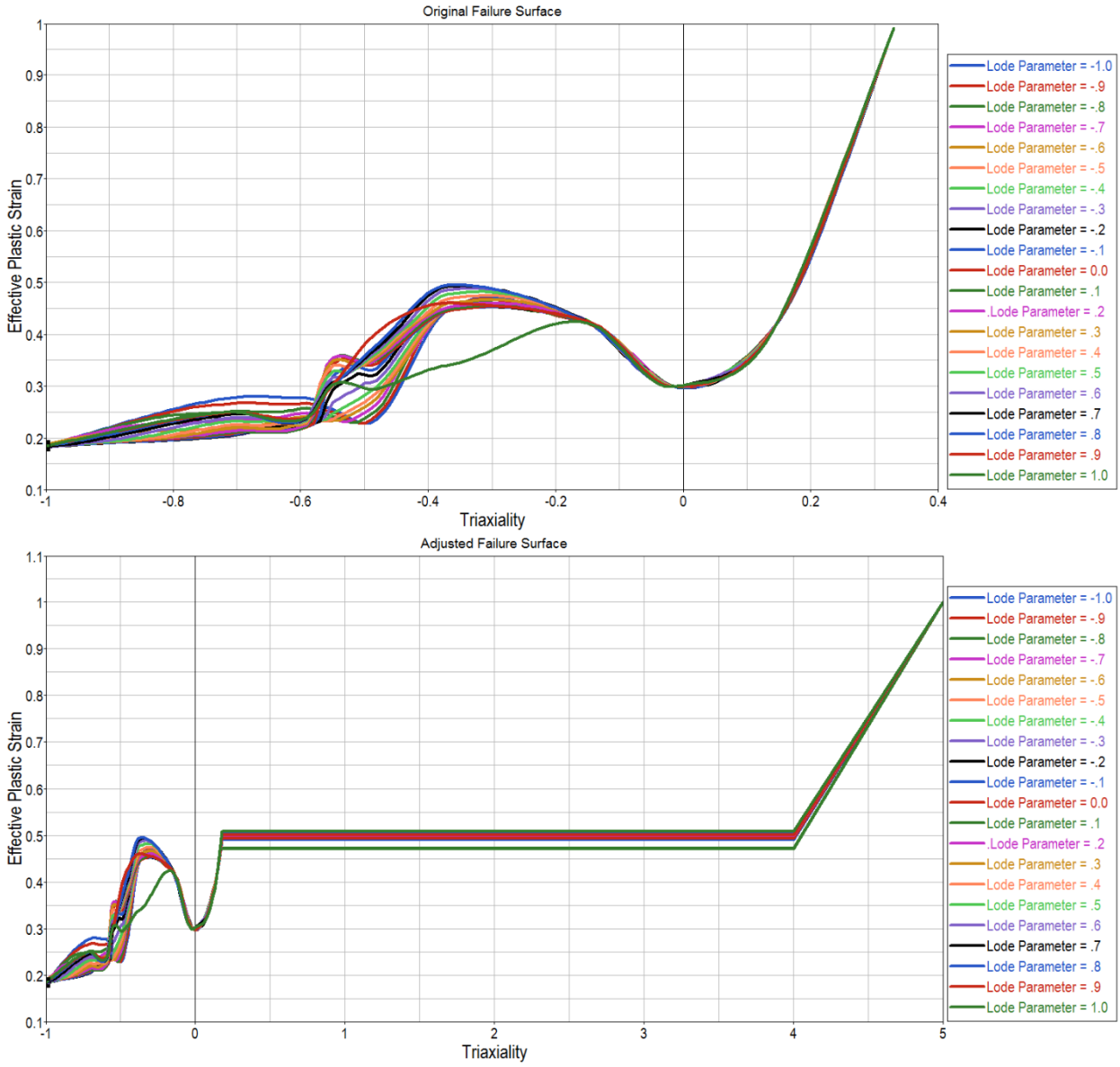

Figure 159. Original and adjusted failure surface triaxiality

After implementing the new failure surface adjustment, the elements in the adiabatic shear band resulted in a more realistic failure pattern. Figures 160 (a–f) show some cross-sectional fringe plots from the 273.1 m/s ballistic test.

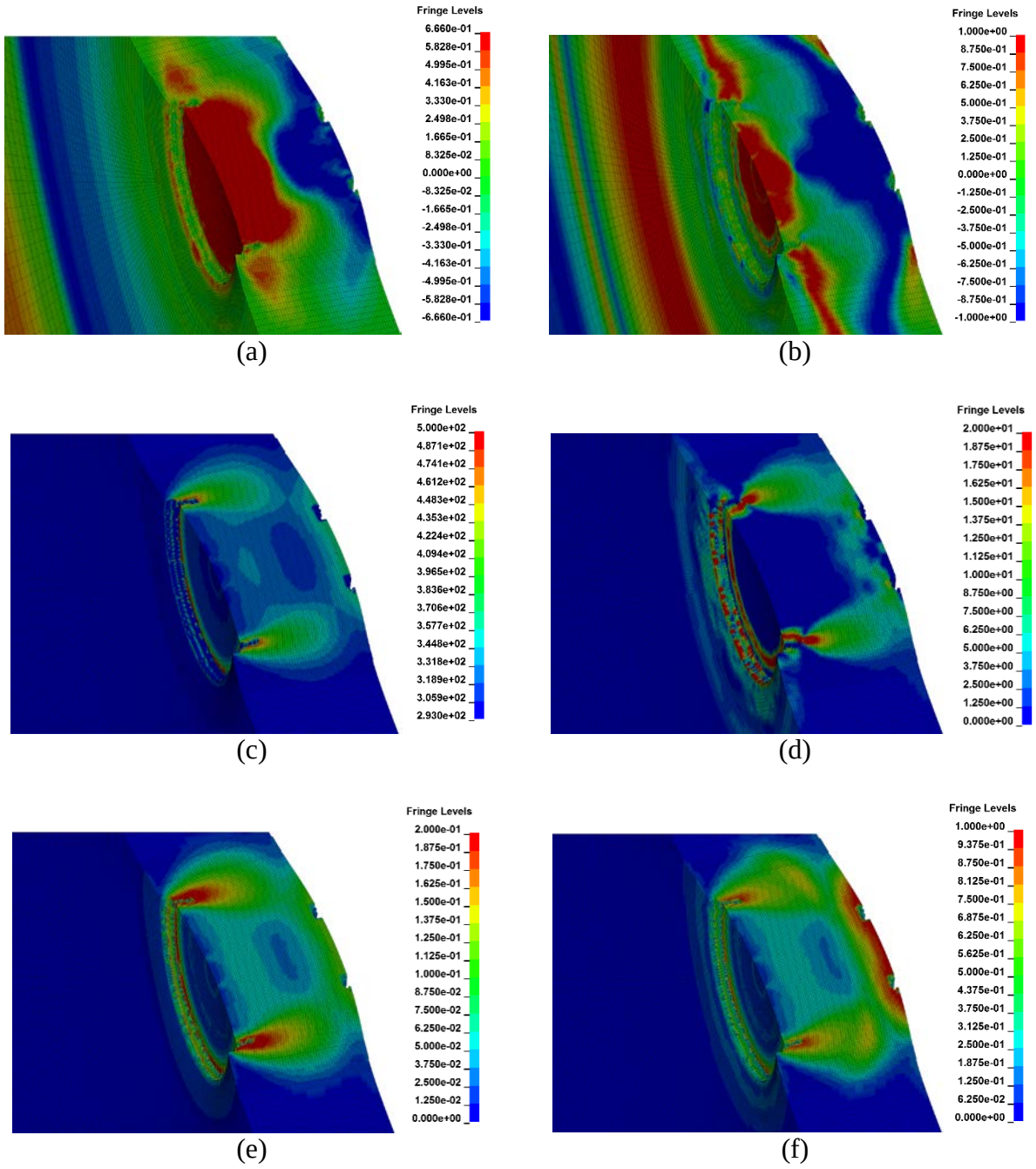

Figure 160. Cross-sectional results of ballistic test simulations ((a) triaxiality, (b) parameter, (c) temperature, (d) strain rate, (e) plastic strain, and (f) damage parameter)

The results of the NASA ballistic test simulations can be compared to the physical test results. The primary metric for comparison is the exit velocity for each impact velocity. Table 13 shows the physical test results and the simulation results. The analysis at an impact speed of 202 m/s was added to further refine the ballistic limit prediction.

Table 13. Comparison of measured and simulated exit velocities per impact velocity

Impact Velocity (m/s)	Physical Test Exit Velocity (m/s)	Simulation Exit Velocity (m/s)
273	144	143
264	129	132
217	73.5	80.5
202	(no test)	46.5
197	46.3	78.7
192	0	10.1
192	31.7	(no simulation)
188	0	0
182	0	(no simulation)
178	0	(no simulation)
176	0	(no simulation)
161	0	(no simulation)

Based on these results, it is clear that the ballistic limit for both the simulation and test data is close to 192 m/s. In addition, the overall trend of simulation exit velocity results closely resembles the results reported by NASA (see figure 161). These results provide reasonable validation of the Ti-6Al-4V material model, including the final failure surface model.

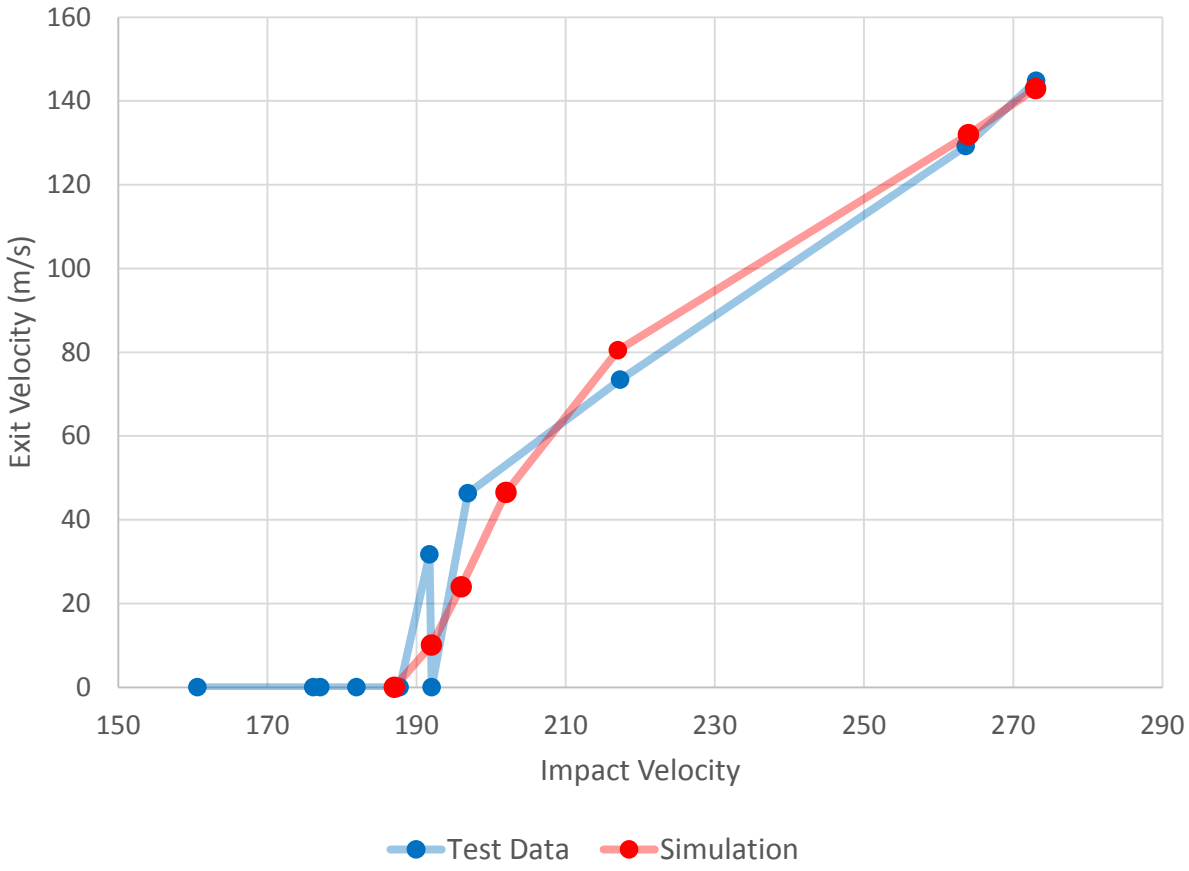

Figure 161. Test data (blue) and simulation (red) results for ballistic impact tests

The data provided by NASA also included some tests in which the projectile did not completely penetrate the plate. In one of these cases, the displacement of the plate at the area of impact was compared to the displacement in the simulation. This displacement was measured through the DIC. A similar fringe plot of the simulation results shows the displacement at the same time after impact (see figure 162). These plots show that the center displacement is nearly identical (approximately 0.13 inch).

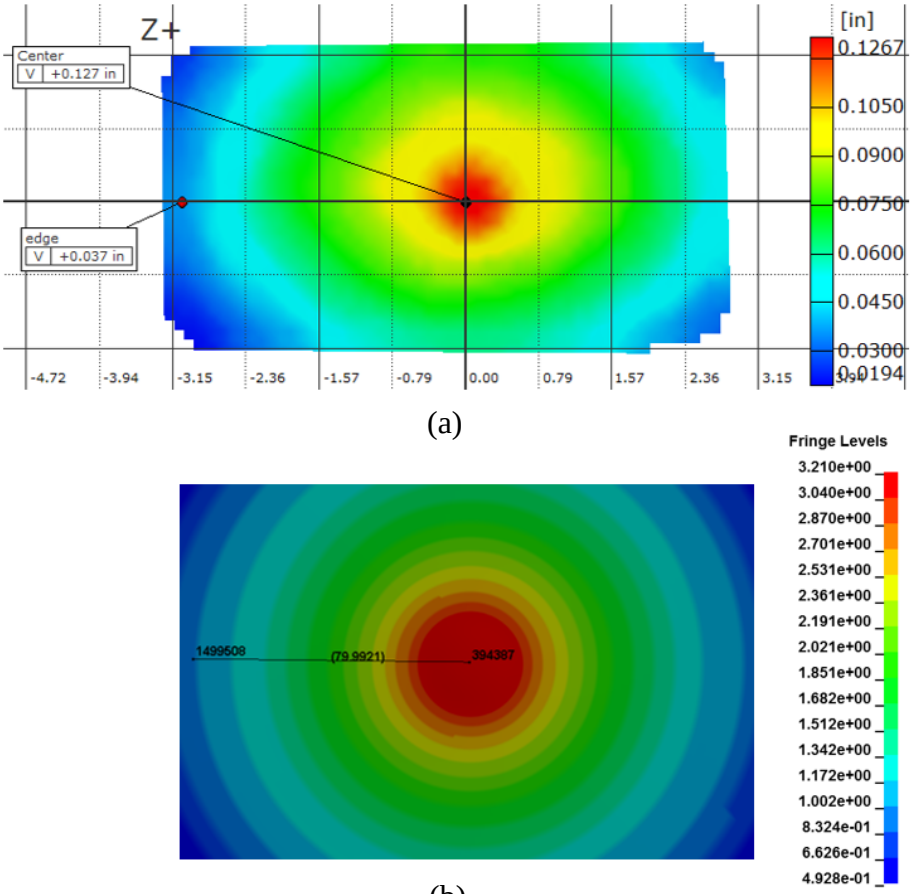

Figure 162. Plots showing center displacement measured (a) and simulated (b) after impact

7. CONCLUSIONS

In this report, a complete set of material input parameters was developed for Ti-6Al-4V to be used with LS-DYNA *MAT_224. The resulting elastic-plastic material model includes strain hardening, strain-rate effects, and temperature effects. The accompanying failure surface includes the effects of varying states of stress, strain rate, and temperature on the erosion failure strain. Mesh regularization to account for the effect of varying mesh densities on the failure strain is also included.

The complete set of material input parameters has been released and is available. In addition to the Ti-6Al-4V input parameters being available in the units presented in this report (mm, ms, kg, kN), the parameters are also available in SI units (mm, s, t, N) and English units (inch, s, lbf·s^2, psi).

The test samples used in the experiments were all taken from the same 1/2-inch Ti-6Al-4V plate stock. This includes samples for both the mechanical property tests and the ballistic impact tests. The mechanical property tests furnished the data that were used to create the material input parameters. The ballistic impact tests were used to validate the model, with the exception of the

modifications to the failure surface, which were required in the region of compression combined with shear.

The asymmetry of yield stress in compression and tension in the 1/2-inch Ti-6Al-4V plate stock was not included, and so the final model is consistent with J2 flow theory. In addition, as the chosen constitutive material model in LS-DYNA (*MAT_224) is isotropic, the anisotropy of the original material is not reflected in the numerical model.

8. REFERENCES

1. *LS_DYNA Manual*, Version 971, Livermore, California, 2007.

2. Pereira, J.M., Revilock, D.M., Lerch, B.A., and Ruggeri, C.R., "Impact Testing of Aluminum 2024 and Titanium 6Al-4V for Material Model Development," *Technical Memorandum NASA/TM 2013-217869*, NASA Glenn Research Center, Cleveland, 2013.

3. Yatnalkar, R.S., "Experimental Investigation of Plastic Deformation of Ti-6Al-4V Under Various Loading Conditions," B.E. Thesis, The Ohio State University, 2010.

4. Seidt, J.D., "Plastic Deformation and Ductile Fracture of 2024-T351 Aluminum under Various Loading Conditions," Dissertation, The Ohio State University, 2010.

5. Hammer, J.T., "Plastic Deformation and Ductile Fracture of Ti-6Al-4V Under Various Loading Conditions," M.S. Thesis, The Ohio State University, 2012.

6. "Tensile Strength or Tension Test," available at www.aboutcivil.org/tension-test-tensile-strength-test.html (accessed on 7/30/15).

7. "Tensile Modulus – Modulus of Elasticity or Young's Modulus – for Some Common Materials," available at http://www.engineeringtoolbox.com/young-modulus-d_417.html (accessed on 7/30/15).

8. Carney, K., Pereira, M., Revilock D., and Matheny P., "Jet Engine Fan Blade Containment Using an Alternate Geometry and the Effect of Very High Strain Rate Material Behavior," *International Journal of Impact Engineering,* Vol. 36, No. 5, 2009, pp. 720–728.

9. Ravichandran, G., Rosakis, A.J., Hodowany, J., and Rosakis, P., "On the Conversion of Plastic Work into Heat During High-Strain-Rate Deformation," *Shock Compression of Condensed Matter*, 2001.

10. Rosakis, P., Rosakis, A.J., Ravichandran, G., and Hodowany, J., "A Thermodynamic Internal Variable Model for the Partition of Plastic Work into Heat and Stored Energy in Metals," *Journal of the Mechanics and Physics of Solids*, 48(3) (2000), pp. 581-607.

11. "AWG Modeling Guidelines Document," LS-DYNA Aerospace Working Group, available at http://awg.lstc.com/tiki/tiki-index.php?page=MGD (accessed on 7/30/15).

APPENDIX A—MATHEMATICAL PROOFS

A.1 TRUE STRESS CALCULATION

In a simple tension test, engineering stress σ_e and true stress σ are defined as:

$$\sigma_e \equiv \frac{f}{A_0} \tag{A-1}$$

$$\sigma \equiv \frac{f}{A} \tag{A-2}$$

where f is the applied force, A_0 is the cross section area before deformation, and A is the cross section area after deformation.

The engineering strain ε_e and true strain ε are defined as:

$$\varepsilon_e \equiv \frac{l}{l_0} - 1 \tag{A-3}$$

$$\varepsilon \equiv \ln\left(\varepsilon_e + 1\right) \tag{A-4}$$

where l_0 and l are the length of the specimen before and after deformation respectively.

If constant volume is assumed:

$$Al = A_0 l_0 \tag{A-5}$$

The true stress σ can be rewritten as:

$$\sigma = \frac{f}{A} = \frac{f}{A_0}\frac{l}{l_0} = \sigma_e \frac{l}{l_0} \tag{A-6}$$

since

$$\varepsilon_e = \frac{l}{l_0} - 1 \tag{A-7}$$

And

$$\sigma = \sigma_e \frac{l}{l_0} \tag{A-8}$$

Therefore

$$\sigma = \sigma_e \left(1 + \varepsilon_e\right) \tag{A-9}$$

which is the formula converting engineering stress σ_e to true stress σ.

A.2 PROOF OF THE FORMULA THAT DETERMINES THE NECKING POINT

This section will prove that the necking occurs when true stress equals to the tangent modulus:

$$\sigma = \frac{d\sigma}{d\varepsilon} \tag{A-10}$$

The applied force F:

$$F = \sigma A \tag{A-11}$$

The infinitesimal increment of applied force is dF:

$$dF = \sigma dA + A d\sigma \tag{A-12}$$

Because necking happens at maximum applied force:

$$dF = 0 \tag{A-13}$$

Therefore:

$$\frac{d\sigma}{\sigma} = -\frac{dA}{A} \tag{A-14}$$

If constant volume is assumed:

$$dV = d\left(Al\right) = dA \cdot l + dl \cdot A = 0 \tag{A-15}$$

$$-\frac{dA}{A} = \frac{dl}{l} = \frac{d\sigma}{\sigma} \tag{A-16}$$

Because:

$$\varepsilon = \ln \frac{l}{l_0} \tag{A-17}$$

Therefore:

$$d\varepsilon = \frac{l_0}{l} \cdot \frac{1}{l_0} dl = \frac{dl}{l} \tag{A-18}$$

which leads to the equation:

$$\sigma = \frac{d\sigma}{d\varepsilon} \tag{A-19}$$

A.3 STRAIN RATE OF TENSILE TEST WITH CONSTANT GRIP SPEED

True strain ε can be written as:

$$\varepsilon = \ln(\varepsilon_e + 1) \tag{A-20}$$

Engineering strain ε_e:

$$\varepsilon_e = \frac{l - l_0}{l_0} = \frac{l}{l_0} - 1 \tag{A-21}$$

Therefore true strain ε:

$$\varepsilon = \ln\left(\frac{l}{l_0} - 1 + 1\right) = \ln\left(\frac{l}{l_0}\right) \tag{A-22}$$

true strain rate $\dot{\varepsilon}$ can be written as:

$$\dot{\varepsilon} = \frac{d}{dt}\left[\ln\left(\frac{l}{l_0}\right)\right] = \frac{l_0}{l} \cdot \frac{1}{l_0} \cdot \frac{dl}{dt} \tag{A-23}$$

$$\dot{\varepsilon}(t) = \frac{1}{l(t)} \frac{dl}{dt} \tag{A-24}$$

The instantaneous gauge length $l(t)$ changes with applied force. Though the grip speed $\frac{dl}{dt}$ is a constant, strain rate $\dot{\varepsilon}(t)$ is still a function of time. The constant loading speed does not imply a constant strain rate $\dot{\varepsilon}$ in the tensile test:

$$\begin{aligned} &\because dP = 0 \\ &\therefore \frac{d\sigma}{\sigma} = -\frac{dA}{A} \end{aligned} \tag{A-25}$$

Assume no volume change:

$$\begin{aligned} &dV = d(AL) = dA \cdot L + dL \cdot A = 0 \\ &Adl + ldA = 0 \\ &-\frac{dA}{A} = \frac{dl}{l} \\ &\because \varepsilon = \ln\frac{l}{l_0} \\ &d\varepsilon = \frac{l_0}{l} \cdot \frac{1}{l_0} dl = \frac{dl}{l} \\ &\therefore \sigma = \frac{d\sigma}{d\varepsilon} \end{aligned} \tag{A-26}$$

This formula holds when necking at maximum load [2].

A.4 PROOF THAT STRAIN RATE IS NOT CONSTANT UNDER CONSTANT LOADING SPEED

Given that grip speed is a constant value as the tensile test going on, gauge length is not a constant; therefore, $\frac{d\varepsilon}{dt}$ is also a function of time.

$$\begin{aligned} &\varepsilon = \ln(\varepsilon_{eng} + 1) \\ &\because \varepsilon_{eng} = \frac{l - l_0}{l_0} = \frac{l}{l_0} - 1 \\ &\therefore \varepsilon = \ln\left(\frac{l}{l_0} - 1 + 1\right) = \ln\left(\frac{l}{l_0}\right) \\ &\frac{d\varepsilon}{dt} = \frac{d}{dt}\left[\ln\left(\frac{l}{l_0}\right)\right] = \frac{l_0}{l} \cdot \frac{1}{l_0} \cdot \frac{dl}{dt} = \frac{1}{l}\frac{dl}{dt} \\ &\frac{d\varepsilon}{dt}(t) = \frac{1}{l(t)}\frac{dl}{dt} \end{aligned} \tag{A-27}$$

APPENDIX B—MATERIAL PROPERTY SUMMARY

The following is the Ti-6Al-4V 1/2-inch plate material property summary, as reported by Michael Periera of the NASA John H. Glenn Research Center.

rev 12-16-11		draft summary 10-31-11		6Al-4V, Condition A, AMS-4911L		
Material number	**Sheet/Plate Thickness**	**Material Supply Source**	**Ingot Source**	**Heat #**	**Rolling Source from Cert sheets**	
4	0.50"	Titanium Industries	TIMET (Henderson, NV)	H13980	TIMET (Toronto, OH)	

Tensile Test Source	**UTS- Long.**	**UTS- Trans.**	**0.2% Yield Long**	**0.2% Yield Transverse**	**% Elong. Long.**	**% Elong. Transverse**
	ksi (mPa)	**ksi (mPa)**	**ksi (mPa)**	**ksi (mPa)**		
TIMET (Toronto, Ohio)	144-145	150-150	133-133	139-139	18-18	18-18
	(993-1000)	(1034-1034)	(917-917)	(958-958)		
	(~1050-1100)	(~1000-1050)				

[NASA-GRC chemical analysis in ( )]

Chemistry Analysis	**Al**	**V**	**Fe**	**O**	**C**	**N**
TIMET Henderson Process Lab	6.27 (6.64)	4.08 (4.04)	0.16 (0.13)	0.170 (0.190)	0.016 (0.011)	0.006 (0.006)

APPENDIX C—VENDOR-SUPPLIED MATERIAL CERTIFICATIONS FOR 1/2-INCH TITANIUM PLATE

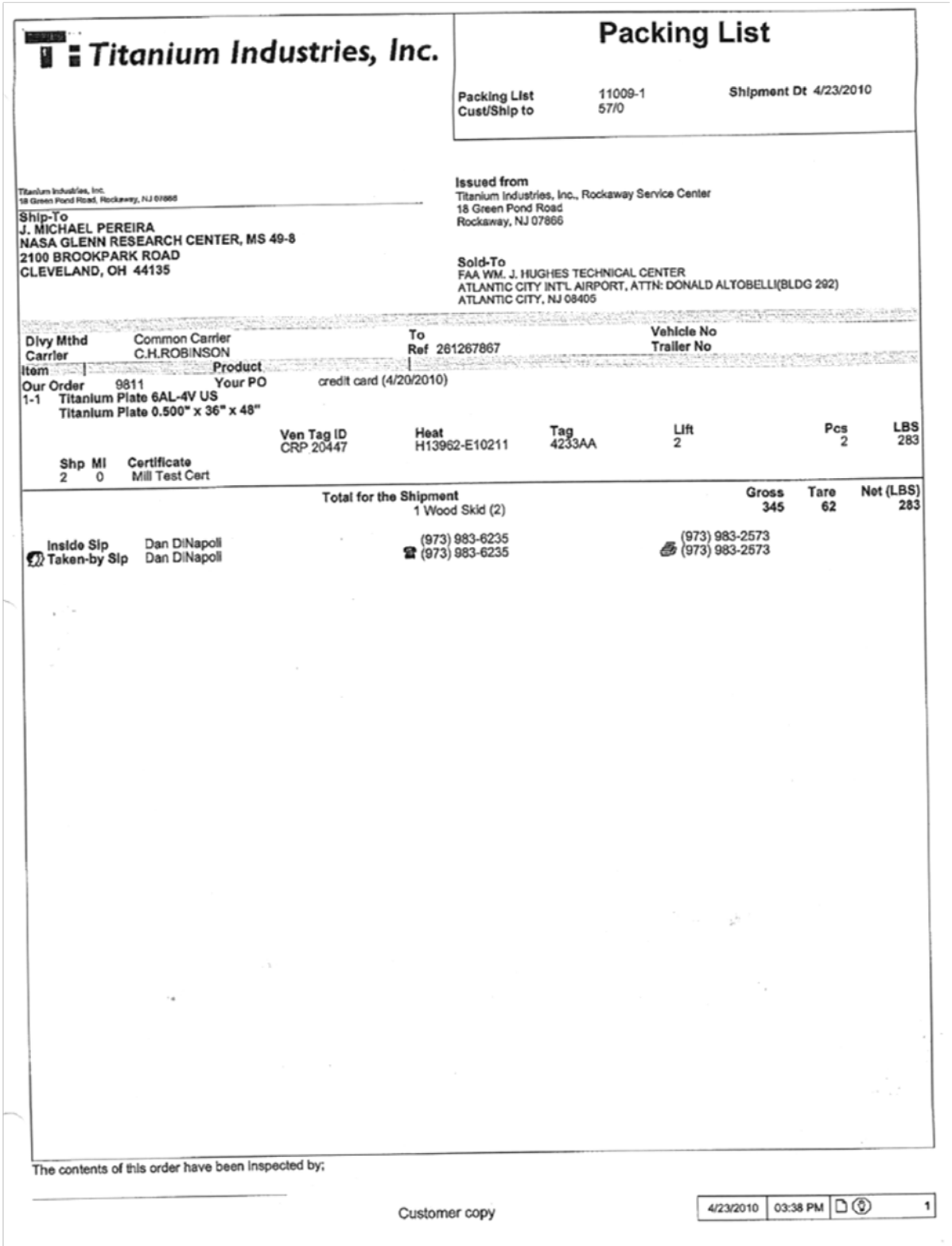

Titanium Industries, Inc.

Packing List

Packing List 11009-1 Shipment Dt 4/23/2010
Cust/Ship to 57/0

Titanium Industries, Inc.
18 Green Pond Road, Rockaway, NJ 07866

Ship-To
J. MICHAEL PEREIRA
NASA GLENN RESEARCH CENTER, MS 49-8
2100 BROOKPARK ROAD
CLEVELAND, OH 44135

Issued from
Titanium Industries, Inc., Rockaway Service Center
18 Green Pond Road
Rockaway, NJ 07866

Sold-To
FAA WM. J. HUGHES TECHNICAL CENTER
ATLANTIC CITY INT'L AIRPORT, ATTN: DONALD ALTOBELLI(BLDG 292)
ATLANTIC CITY, NJ 08405

Divy Mthd Common Carrier
Carrier C.H.ROBINSON
To
Ref 261267867
Vehicle No
Trailer No

Item	Product	Your PO
Our Order 9811		credit card (4/20/2010)
1-1	Titanium Plate 6AL-4V US Titanium Plate 0.500" x 36" x 48"	

Ven Tag ID	Heat	Tag	Lift	Pcs	LBS
CRP 20447	H13962-E10211	4233AA	2	2	283

Shp	MI	Certificate
2	0	Mill Test Cert

Total for the Shipment
1 Wood Skid (2)

	Gross	Tare	Net (LBS)
	345	62	283

Inside Slp Dan DiNapoli (973) 983-6235 (973) 983-2573
Taken-by Slp Dan DiNapoli (973) 983-6235 (973) 983-2573

The contents of this order have been inspected by:

Customer copy

4/23/2010 | 03:38 PM | 1

Titanium Industries, Inc.

Certificate of Analysis

Cert Number 1058
Test Reference 8740

4/23/2010

FAA WM. J. HUGHES TECHNICAL CENTER
ATLANTIC CITY INT'L AIRPORT
ATTN: DONALD ALTOBELLI(BLDG 292)
ATLANTIC CITY, NJ 08405

Issued from
Titanium Industries, Inc.
Rockaway Service Center
18 Green Pond Road
Rockaway, NJ 07866

Sold To: FAA WM. J. HUGHES TECHNICAL CENTER, ATLANTIC CITY INT'L AIRPORT, ATTN: DONALD ALTOBELLI(BLDG 292), ATLANTIC CITY, NJ 08405
Ship To: J. MICHAEL PEREIRA, NASA GLENN RESEARCH CENTER, MS 49-8, 2100 BROOKPARK ROAD, CLEVELAND, OH 44135

Reference

Customer 57/0 **Your Order** credit card (4/20/2010)
Our Order 9811-1-1 **Packing List** 11009-1 (4/23/2010)

Product Information

	Heat	Tag	Pcs	LBS
Titanium Plate 6AL-4V US Titanium Plate 0.500" x 36" x 48"	H13962-E10211	4233AA	2	283

Shipped Heats H13962-E10211
Conform To AMS-4911 8/28/2008

Chemical Composition

N	C	Fe	O	H	Al	V	Y
0.006	0.016	0.16	0.17	0.0085	6.27	4.08	0.0004

Ti
BAL

Physical Tests

Tensile L	Tensile T	Yield L	Yield T
148 KSI	145 KSI	137 KSI	136 KSI
Elongation L	**Elongation T**		
16 %	16 %		

CERTIFICATE OF COMPLIANCE

ALL ITEMS FURNISHED ARE IN FULL COMPLIANCE WITH PURCHASE ORDER AND SPECIFICATION REQUIREMENTS LISTED. THE MATERIAL APPLIED DID NOT COME IN CONTACT WITH MERCURY NOR WAS ANY WELD REPAIR PERFORMED DURING PROCESSING BY TITANIUM INDUSTRIES, INC.

THE MATERIAL SUPPLIED MEETS THE VISUAL AND DIMENSIONAL REQUIREMENTS OF THE PURCHASE ORDER AND TEST REPORTS/CERTIFICATIONS REPRESENT THE ACTUAL ATTRIBUTES OF THE ITEMS FURNISHED.

AUTHORIZED SIGNATURE: Denise Johnson 4/23/10

The contents of this order have been inspected by:

4/23/2010 | 03:58 PM | 1

TIMET

Titanium Metals Corporation
100 Titanium Way, Toronto, OH 43964
Telephone (740) 537-5694, Fax (740) 537-5653

Approved Certificate

CERT ID
H13980-A1X
26-FEB-2010 18:28:05 GMT

PURCHASE ORDER
20060408

SOLD TO CUSTOMER
TIMET Service Center St. Louis
109 Interstate Drive, Wentzville, MO 63385

HEAT NUMBER
H13980

GRADE
TIMETAL®6-4

SHIP TO CUSTOMER
TIMET Service Center St. Louis
109 Interstate Drive, Wentzville, MO 63385

TEST NUMBER
E10225

PRODUCT DESCRIPTION
.500" SQ Plate

DELIVERY CONDITION
Annealed

Specifications
This material complies with the following specifications:
AMS 4911 L DMS 1592 G

Release Statements
1. TIMET-Toronto has a Quality Management System that is in compliance with ISO 9001:2000, ANSI/ISO/ASQ Q9001-2000 and AS 9100:2001 Revision B, Certificate No. UQA 0113328, through Lloyd's Register Quality Assurance, effective 24-Jul-03.

Melt Method
3-VAR

Melt/Process Location
TIMET - Henderson, NV, USA / TIMET - Toronto, OH, USA

Compliance Statements
1. In accordance with AMS-T-9046 B cancellation notice, material is tested and certified to Table I superceding specification AMS 4911 Rev L.
2. Surface free from alpha case and product conforms to the other technical requirements of the referenced specification(s).
3. Microstructure examined and acceptable to the order specifications.
4. Immersion ultrasonic tested to a #3 FBH per AMS 2631 C Class A1 and acceptable.
5. Material meets the special flatness requirements of the purchase order.
6. TIMET-Toronto is an approved supplier of this product per DMS QPL 1592 Issue 18. Ingot melted in accordance with DMS 2442; TIMET-Henderson, NV, is an approved ingot source per DMS QPL-2442 Issue 18.

Accredited Nadcap Materials Testing Laboratory ISO/IEC 17025 Nondestructive Testing Heat Treating
REGISTERED ISO 9001/AS9100 FACILITY

First in Titanium Worldwide

TIMET

Titanium Metals Corporation
100 Titanium Way, Toronto, OH 43964
Telephone (740) 537-5694, Fax (740) 537-5653

Approved Certificate

CERT ID
H13980-A1X
26-FEB-2010 18:28:05 GMT

PURCHASE ORDER
20060408

SOLD TO CUSTOMER
TIMET Service Center St. Louis
109 Interstate Drive, Wentzville, MO 63385

Ingot Chemical Analysis
(Weight percent)

Unless otherwise noted, Ingot Chemical Analysis performed at Henderson Process Lab, 181 N. Water Street, Henderson, NV, 89015, US

Sample ID	Fe	V	Al	C	O	N	Y
TOP	0.16	4.05	6.28	0.015	0.18	0.008	<0.0004
BOTTOM	0.15	4.00	6.25	0.016	0.19	0.007	<0.0004

Product Analysis
(Weight percent)

Unless otherwise noted, Product Analysis performed at Toronto Laboratory, 100 Titanium Way, Toronto, OH, 43964, US

Sample ID	H
1	46
2	69

Chemistry Statements

1. Hydrogen values reported in PPM. Hydrogen determined by inert gas fusion per ASTM E1447. Carbon determined by combustion per ASTM E1941. Oxygen and Nitrogen determined by inert gas fusion per ASTM E1409. Henderson Melt: Metallics determined by Inductively Coupled Plasma-Atomic Emission Spectrometry (ICP-AES) per ASTM E2371. Morgantown Melt: Copper and Boron by atomic spectrometry (ingot only) and all other elements by x-ray fluorescence spectrometry.
2. Residual elements each less than 0.10% maximum, 0.40% maximum total.
3. Balance titanium.

Mechanical Properties

Unless otherwise noted, testing performed at Toronto Laboratory, 100 Titanium Way, Toronto, OH, 43964, US

RTT - Longitudinal (ASTM E 8)
Test Condition: Mill VCF 8 Hours Minimum @ 1400°F

Sample ID	0.2YS	U.T.S.	4DEL
	ksi	ksi	%
1	133	144	18
2	133	145	18

RTT - Transverse (ASTM E 8)
Test Condition: Mill VCF 8 Hours Minimum @ 1400°F

Sample ID	0.2YS	U.T.S.	4DEL
	ksi	ksi	%
1	139	150	18
2	139	150	18

Accredited Nadcap — Materials Testing Laboratory ISO/IEC 17025 — Nondestructive Testing — Heat Treating

REGISTERED ISO 9001/AS9100 FACILITY

First in Titanium Worldwide

Titanium Metals Corporation
100 Titanium Way, Toronto, OH 43964
Telephone (740) 537-5694, Fax (740) 537-5653

Approved Certificate

CERT ID
H13980-A1X
26-FEB-2010 18:28:05 GMT

PURCHASE ORDER
20060408

SOLD TO CUSTOMER
TIMET Service Center St. Louis
109 Interstate Drive, Wentzville, MO 63385

Tests on Other Material

Unless otherwise noted, testing performed at Toronto Laboratory, 100 Titanium Way, Toronto, OH, 43964, US

Batch: H13550-31 (J9833)
RTT - Longitudinal (ASTM E 8)
Test Condition: Periodic Test: Mill Annealed 60 Minutes 1400°F AC + Lab Annealed 20 Minutes @ 1325°F AC

Sample ID	0.2YS	U.T.S.	4DEL	R.A.
	ksi	ksi	%	%
1	126	137	15	31

Results are from TIMET Quality Control Records on file
Sales Order # 273575 Item # 10
v.1

Bill Williamson - Certification Specialist

Accredited Nadcap — Materials Testing Laboratory ISO/IEC 17025, Nondestructive Testing, Heat Treating

REGISTERED ISO 9001/AS9100 FACILITY

First in Titanium Worldwide

TIMET

St. Louis Mill Sales
108 Interstate Drive
WENTZVILLE MO 63385
USA
Tel:800-763-1550 Fax:636-887-9098
Shipping Plant: St. Louis Service Center

Attachment to Product Certification

Customer P.O. Number/Date
CRP-20447-KS/Feb 25, 2010
TIMET Sales Order Number/Date
281118/Feb 26, 2010
TIMET Packing List Number/Scheduled Ship Date
80417460/Apr 02, 2010

Sold-to Address
Titanium Industries Inc
18 Green Pond Road
ROCKAWAY NJ 07866
USA

Ship-to Address
Titanium Industries Inc
18 Green Pond Road
ROCKAWAY NJ 07866
USA

TIMET Item # / Customer Item #	Material # / Customer Material #	Material Description	Quantity	Weight
000010	110357	*TIMETAL®* 6-4 Titanium Aero Plate		
Heat Treatment Specifications		: Mill Annealed : 01 AMS 4911 * L : 02 AMS 2631 * C CL A1 : 03 AMS-STD-2154 TY1 CL A : 04 AMS-T-9046 * A AB-1 COND A : 05 ASTM B 265 * -09AE1 GR 5 : 08 DMS 1592 * G : 09 MIL-STD-2154 ORG TY1 CL A : 10 MIL-T-9046 J AMD2 AB-1 CD A		
Batch Number		: H13962-Y16 469.000LB	469.000LB	
Batch Dimensions		: 0.500" X 48.000" X 120.000"		
Batch Number of Pieces		: 1.000		
Country of Origin		: USA		
Heat Number		: H13962		
Test Number		: E10211		
Batch Number		: H13980-Y03 469.000LB	469.000LB	
Batch Dimensions		: 0.500" X 48.000" X 120.000"		
Batch Number of Pieces		: 1.000		
Country of Origin		: USA		
Heat Number		: H13980		
Test Number		: E10225		

TIMET

St. Louis Mill Sales
109 Interstate Drive
WENTZVILLE MO 63385
USA
Tel:800-753-1850 Fax:636-887-9088
Shipping Plant: St. Louis Service Center

Attachment to Product Certification

Customer P.O. Number/Date
CRP-20447-KS/Feb 25, 2010
TIMET Sales Order Number/Date
281118/Feb 26, 2010
TIMET Packing List Number/Scheduled Ship Date
80417460/Apr 02, 2010

Sold-to Address
Titanium Industries Inc
18 Green Pond Road
ROCKAWAY NJ 07866
USA

Ship-to Address
Titanium Industries Inc
18 Green Pond Road
ROCKAWAY NJ 07866
USA

TIMET Item # / Customer Item #	Material # / Customer Material #	Material Description	Quantity	Weight

B-Additional customer req
GEAE S-400 Approved Laboratory
GEAE S-1000 Supplier Quality Req'ts

Beta Transus Temperature Reading Required

PWA300

MCL F-17/F-14 Controlled

EN10204.3.1.

Inspection tolerances are to LN9297

Billing based on scale weight of gauge shown above

Fax Copy of Bill of Lading, packing slip and test reports at time of shipment to TI Inds Inc
Rockaway NJ Location
Attn: K Speer - Fax# 973.983.8015 email: kspeer@titanium.com

The following notes must appear on certificate of test:
1. During manufacturing, handling, testing and inspection this material did not come indirect contact with mercury or any device exploying a single boundary of containment.
2. The recording of false, flotitious or fraudulent statements or entries may be punishable as a felony under federal statutes including federal law, title 18, chapter 47.
3. No weld repair has been performed on this material
4. Material has not been exposed to radioctive contamination.

Melted and Manufactured in USA must appear on test report

Amount is required quantity, do not short ship.

TIMET

St. Louis Mill Sales
100 Interstate Drive
WENTZVILLE MO 63385
USA
Tel:800-753-1660 Fax:888-887-9098
Shipping Plant: St. Louis Service Center

Attachment to Product Certification

Customer P.O. Number/Date
CRP-20447-KS/Feb 25, 2010
TIMET Sales Order Number/Date
281118/Feb 26, 2010
TIMET Packing List Number/Scheduled Ship Date
80417460/Apr 02, 2010

Sold-to Address
Titanium Industries Inc
18 Green Pond Road
ROCKAWAY NJ 07866
USA

Ship-to Address
Titanium Industries Inc
18 Green Pond Road
ROCKAWAY NJ 07866
USA

TIMET Item # / Customer Item #	Material # / Customer Material #	Material Description	Quantity	Weight

Results are from TIMET Quality Control Records on file. The undersigned has verified that the information on the attached mill product certification meets the requirements of the above referenced order. This Attachment to Product Certification is specific to your referenced order, is an integral part of and amends the physical and chemical test reports attached. All specification(s) and revision(s) that differ from the attached have been approved for inclusion by the producing facility.

Authorized TIMET Signature _____ Date MAR 3 1 2010

Kenneth Renshaw
NASC Quality Supervisor

APPENDIX D—REPORT FOR 1/4-INCH TI-6AL-4V PLATE

D.1. INTRODUCTION

In the initial research effort, the team attempted to characterize a 1/4-inch plate. That effort found that the shear tests could not be performed on 1/4-inch plate with sufficient visualization to be useful in material characterization. The effort transitioned to 1/2-inch plate to get a complete material set. This incomplete data set is provided from the original work. This section closely follows the main body of the report but is characterizing a thinner plate with different material properties. The main body of this report is a more complete process and should be used for reference. This appendix provides the data for the thinner plate.

Titanium alloy Ti-6Al-4V is an important engineering material widely used in aerospace applications. Current constitutive models fall short in predicting the plastic and failure behavior of this material under medium and low strain rate. One reason for this may be the high dependency of the properties of titanium sheet on the manufacturing process and, therefore, on the thickness of the sheet. This research effort, therefore, involves the development and validation of a set of material constants using the tabulated input method of material model *MAT_224 in LS-DYNA, with consideration of strain rate and temperature, specifically for a rolled 1/4-inch Ti-6Al-4V plate. *MAT_224 is an elastic plastic material with arbitrary stress versus strain curve(s) and arbitrary strain-rate dependency can be defined. A thermodynamic and comprehensive plastic failure criterion can also be defined The chemical composition and microstructure of this material is summarized by the NASA John H. Glenn Research Center in appendix B. The material model is based on the results of uniaxial tensile testing conducted by Ohio State University (OSU) under plane-stress conditions at different strain rates and temperatures. Material model development procedures are included as a reference for similar study. Material directional anisotropy, tension compression anisotropy, plane stress, and plane strain comparison and temperature effects are evaluated by comparing the simulation results with the tests from OSU. Temperature effect and failure criteria are not included in this appendix.

D.2 RESULTS

D.2.1 TEST DATA

The following test series (see table D.1) are provided by Yatnalkar, Hammer, and Seidt of OSU. The supplied test data include time, force, and displacement information. Every test is accompanied by a computer-aided design plot of the exact specimen dimensions from measurement. A digital image correlation (DIC) image is taken at the failure time (the last data point of the test data).

Table D.1. Test series

Test Series	Test Name	Plate Stock	Specimen Geometry	Specimen Orientation	Strain Rate (1/s)	Temperature (°C)
Tension Strain Rate Dependence	M2-TMT-P3-SG1-O1-SR1-T1-N1	0.25"	Flat Dogbone	Rolled	1.0E-04	RT
	M2-TMT-P3-SG1-O1-SR1-T1-N2	0.25"	Flat Dogbone	Rolled	1.1E-04	RT
	M2-TMT-P3-SG1-O1-SR1-T1-N3	0.25"	Flat Dogbone	Rolled	1.0E-04	RT
	M2-TMT-P3-SG1-O1-SR2-T1-N3	0.25"	Flat Dogbone	Rolled	1.1E-02	RT
	M2-TMT-P3-SG1-O1-SR2-T1-N4	0.25"	Flat Dogbone	Rolled	1.1E-02	RT
	M2-TMT-P3-SG1-O1-SR2-T1-N5	0.25"	Flat Dogbone	Rolled	1.1E-02	RT
	M2-TMT-P3-SG1-O1-SR3-T1-N3	0.25"	Flat Dogbone	Rolled	1.1E+00	RT
	M2-TMT-P3-SG1-O1-SR3-T1-N4	0.25"	Flat Dogbone	Rolled	1.1E+00	RT
	M2-TMT-P3-SG1-O1-SR3-T1-N5	0.25"	Flat Dogbone	Rolled	1.1E+00	RT
	M2-TMT-P3-SG1-O1-SR4-T1-N1	0.25"	Flat Dogbone	Rolled	5.4E+02	RT
	M2-TMT-P3-SG1-O1-SR4-T1-N6	0.25"	Flat Dogbone	Rolled	6.4E+02	RT
	M2-TMT-P3-SG1-O1-SR4-T1-N7	0.25"	Flat Dogbone	Rolled	6.3E+02	RT
	M2-TMT-P3-SG1-O1-SR5-T1-N1	0.25"	Flat Dogbone	Rolled	1.3E+04	RT
	M2-TMT-P3-SG1-O1-SR5-T1-N3	0.25"	Flat Dogbone	Rolled	1.8E+03	RT
	M2-TMT-P3-SG1-O1-SR5-T1-N4	0.25"	Flat Dogbone	Rolled	1.4E+03	RT
Tension Anisotropy	M2-TMT-P3-SG1-02-SR3-T1-N2	0.25"	Flat Dogbone	45°	1.2E+00	RT
	M2-TMT-P3-SG1-02-SR3-T1-N3	0.25"	Flat Dogbone	45°	1.0E+00	RT
	M2-TMT-P3-SG1-03-SR3-T1-N2	0.25"	Flat Dogbone	90°	9.6E-01	RT
	M2-TMT-P3-SG1-03-SR3-T1-N3	0.25"	Flat Dogbone	90°	1.0E+00	RT
	M2-TMT-P3-SG1-04-SR3-T1-N1	0.25"	Flat Dogbone	135°	9.8E-01	RT
	M2-TMT-P3-SG1-04-SR3-T1-N2	0.25"	Flat Dogbone	135°	1.1E+00	RT
Tension Axisymmetric	M2-TMT-P4-SG5-01-SR2-T1-N1	0.25"	Axisymmetri	Rolled	2.0E-02	RT
	M2-TMT-P4-SG5-01-SR2-T1-N2	0.25"	Axisymmetri	Rolled	1.9E-02	RT
	M2-TMT-P4-SG5-01-SR2-T1-N3	0.25"	Axisymmetri	Rolled	2.1E-02	RT
	M2-TMT-P4-SG5-01-SR2-T1-N4	0.25"	Axisymmetri	Rolled	1.2E-02	RT
Tension Temperature	M2-TMT-P3-SG1-01-SR3-T2-N1	0.25"	Flat Dogbone	Rolled	1.0E+00	201.9
	M2-TMT-P3-SG1-01-SR3-T2-N2	0.25"	Flat Dogbone	Rolled	1.0E+00	201.3
	M2-TMT-P3-SG1-01-SR3-T2-N3	0.25"	Flat Dogbone	Rolled	1.0E+00	200.6
	M2-TMT-P3-SG1-01-SR3-T3-N2	0.25"	Flat Dogbone	Rolled	1.0E+00	404.2
	M2-TMT-P3-SG1-01-SR3-T3-N3	0.25"	Flat Dogbone	Rolled	1.0E+00	402.2
	M2-TMT-P3-SG1-01-SR3-T3-N4	0.25"	Flat Dogbone	Rolled	1.0E+00	401.2
	M2-TMT-P3-SG1-01-SR3-T4-N2	0.25"	Flat Dogbone	Rolled	1.0E+00	600.7
	M2-TMT-P3-SG1-01-SR3-T4-N4	0.25"	Flat Dogbone	Rolled	1.0E+00	602.1
	M2-TMT-P3-SG1-01-SR3-T4-N7	0.25"	Flat Dogbone	Rolled	1.0E+00	607.4

Note: Test results provided by OSU
RT = room temperature

Table D.1. Test series (continued)

Test Series	Test Name	Plate Stock	Specimen Geometry	Specimen Orientation	Strain Rate (1/s)	Temperature (°C)
Compression Strain Rate Dependence	M2-TMC-P3-SG1-01-SR1-T1-N1	0.25"	Cylinder	Rolled	6.9E-05	RT
	M2-TMC-P3-SG1-01-SR1-T1-N2	0.25"	Cylinder	Rolled	6.3E-05	RT
	M2-TMC-P3-SG1-01-SR1-T1-N3	0.25"	Cylinder	Rolled	8.1E-05	RT
	M2-TMC-P3-SG1-01-SR2-T1-N1	0.25"	Cylinder	Rolled	6.5E-03	RT
	M2-TMC-P3-SG1-01-SR2-T1-N3	0.25"	Cylinder	Rolled	6.5E-03	RT
	M2-TMC-P3-SG1-01-SR2-T1-N4	0.25"	Cylinder	Rolled	6.0E-03	RT
	M2-TMC-P3-SG1-01-SR3-T1-N2	0.25"	Cylinder	Rolled	7.8E-01	RT
	M2-TMC-P3-SG1-01-SR3-T1-N4	0.25"	Cylinder	Rolled	6.5E-01	RT
	M2-TMC-P3-SG1-01-SR3-T1-N5	0.25"	Cylinder	Rolled	7.4E-01	RT
	M2-TMC-P3-SG1-01-SR4-T1-N5	0.25"	Cylinder	Rolled	1.5E+03	RT
	M2-TMC-P3-SG1-01-SR4-T1-N6	0.25"	Cylinder	Rolled	1.7E+03	RT
	M2-TMC-P3-SG1-01-SR4-T1-N12	0.25"	Cylinder	Rolled	1.5E+03	RT
	M2-TMC-P3-SG1-01-SR5-T1-N4	0.25"	Cylinder	Rolled	2.1E+03	RT
	M2-TMC-P3-SG1-01-SR5-T1-N5	0.25"	Cylinder	Rolled	3.0E+03	RT
	M2-TMC-P3-SG1-01-SR5-T1-N7	0.25"	Cylinder	Rolled	2.7E+03	RT
	M2-TMC-P3-SG1-01-SR5-T1-N8	0.25"	Cylinder	Rolled	2.6E+03	RT
Compression Anisotropy	M2-TMC-P3-SG1-02-SR3-T1-N1	0.25"	Cylinder	45°	8.2E-01	RT
	M2-TMC-P3-SG1-02-SR3-T1-N2	0.25"	Cylinder	45°	8.1E-01	RT
	M2-TMC-P3-SG1-02-SR3-T1-N3	0.25"	Cylinder	45°	8.0E-01	RT
	M2-TMC-P3-SG1-03-SR3-T1-N1	0.25"	Cylinder	90°	7.1E-01	RT
	M2-TMC-P3-SG1-03-SR3-T1-N2	0.25"	Cylinder	90°	6.8E-01	RT
	M2-TMC-P3-SG1-03-SR3-T1-N3	0.25"	Cylinder	90°	7.0E-01	RT
	M2-TMC-P3-SG1-04-SR3-T1-N1	0.25"	Cylinder	135°	8.1E-01	RT
	M2-TMC-P3-SG1-04-SR3-T1-N2	0.25"	Cylinder	135°	8.1E-01	RT
	M2-TMC-P3-SG1-05-SR3-T1-N1	0.25"	Cylinder	Through	7.2E-01	RT
	M2-TMC-P3-SG1-05-SR3-T1-N2	0.25"	Cylinder	Through	7.1E-01	RT
Compression Temperature	M2-TMC-P3-SG1-01-SR3-T2-N1	0.25"	Cylinder	Rolled	1.0E+00	200
	M2-TMC-P3-SG1-01-SR3-T2-N2	0.25"	Cylinder	Rolled	1.0E+00	200
	M2-TMC-P3-SG1-01-SR3-T2-N3	0.25"	Cylinder	Rolled	1.0E+00	200
	M2-TMC-P3-SG1-01-SR3-T3-N1	0.25"	Cylinder	Rolled	1.0E+00	400
	M2-TMC-P3-SG1-01-SR3-T3-N2	0.25"	Cylinder	Rolled	1.0E+00	400
	M2-TMC-P3-SG1-01-SR3-T3-N4	0.25"	Cylinder	Rolled	1.0E+00	400
	M2-TMC-P3-SG1-01-SR3-T4-N3	0.25"	Cylinder	Rolled	1.0E+00	600
	M2-TMC-P3-SG1-01-SR3-T4-N4	0.25"	Cylinder	Rolled	1.0E+00	600
	M2-TMC-P3-SG1-01-SR3-T4-N5	0.25"	Cylinder	Rolled	1.0E+00	600

Note: Test results provided by OSU
RT = room temperature

D.2.2 STRESS-STRAIN RELATION OF A SINGLE STRAIN

A hardening curve is derived for each strain rate from the "Tension Strain Rate Dependence" series. Flat dogbone specimens were pulled on the Instron machine at room temperature.

Displacement and force were measured at a fixed-time interval. All simulations discussed in section D.2.2 were performed with a loading speed of 1 m/s for the reason given in section 2.2.1 of the main document. The simulation units were kg, mm, ms, kN, and GPa.

D.2.2.1 Stress-Strain Relation of Strain Rate 1E-4 Sec^{-1}

The three quasistatic tests at strain rate 1E-4 sec^{-1} are listed in table D.2. The force displacement relation of these tests is shown in figure D.1. The engineering strain versus stress relationship is derived and gives the engineering stress-strain curves in figure D.2. Test 1: M2-TMT-P3-SG1-O1-SR1-T1-N1 was selected to represent this group of data and undergo further processing. The selection criterion is based on engineering judgment considering smoothness, representative, and the monotonically increasing function requirement of the input curve. Choosing a single test instead of an average of multiple tests has its advantages; each test specimen has a different geometry (because the exact geometry from measurement is used for modeling). Though the input curve can take an average of all test results, only a single geometry may be used in the simulation. The force displacement result of that simulation will bear a larger error if the input curve contains the information from other tests of different geometry.

Table D.2. Strain rate dependence series data of strain rate = 1E-4 sec^{-1}

Test Series	Test Name	Plate Stock	Specimen Geometry	Specimen Orientation	Strain Rate (1/s)	Temp (˚C)
Tension Strain Rate Dependence	M2-TMT-P3-SG1-O1-SR1-T1-N1	0.25”	Flat Dogbone	Rolled	1.0E-04	RT
	M2-TMT-P3-SG1-O1-SR1-T1-N2	0.25”	Flat Dogbone	Rolled	1.1E-04	RT
	M2-TMT-P3-SG1-O1-SR1-T1-N3	0.25”	Flat Dogbone	Rolled	1.0E-04	RT

RT = room temperature

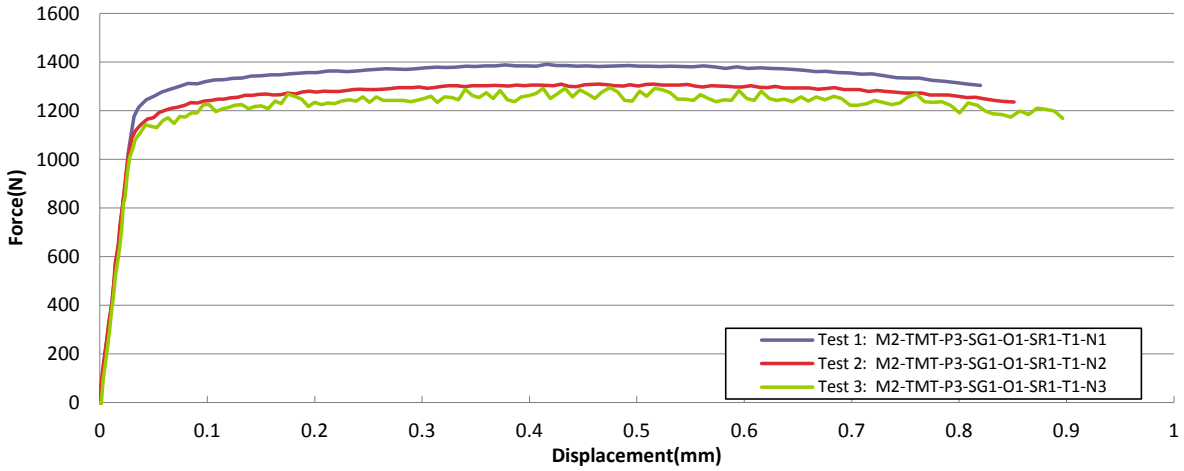

Figure D.1. Force displacement relation of all strain rate = 1E-4 sec^{-1} tests

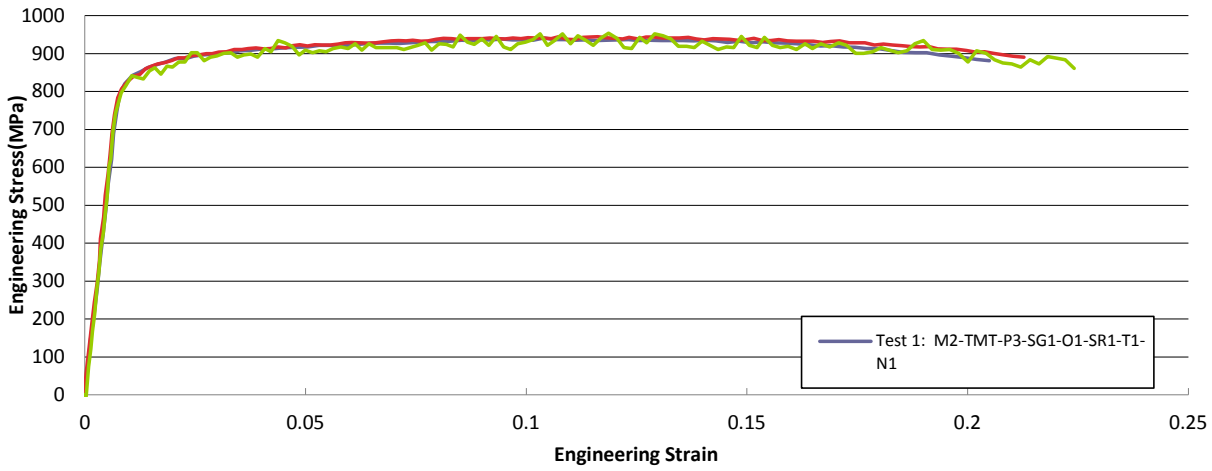

Figure D.2. Engineering stress-strain relation of all strain rate = 1E-4 sec^{-1} tests

The engineering stress-strain relationship was converted to the true stress-strain relationship shown in figure D.3. By adopting a Young's modulus of 110 GPa, the plastic strain versus stress relation is calculated, as shown in figure D.4.

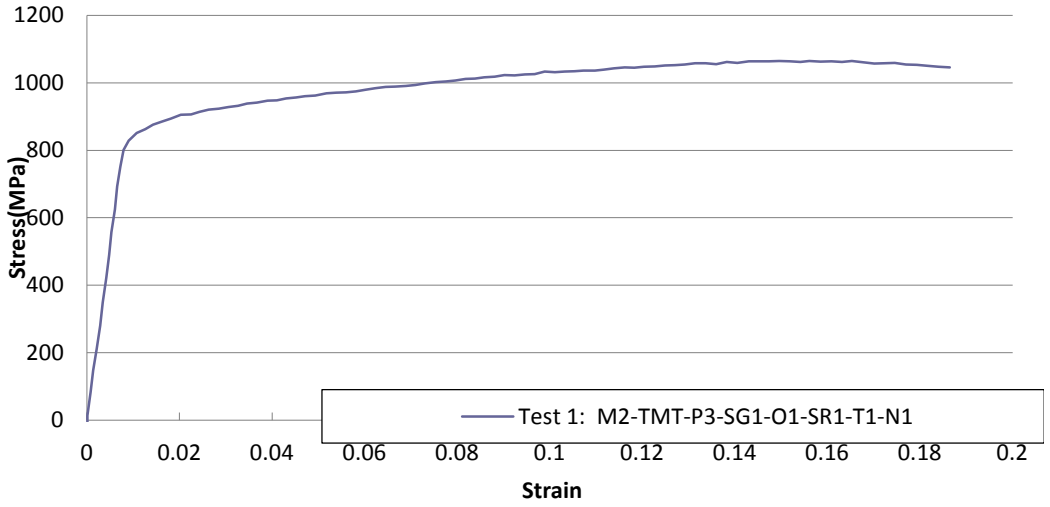

Figure D.3. True stress true strain relation (Test: M2-TMT-P3-SG1-O1-SR1-T1-N1)

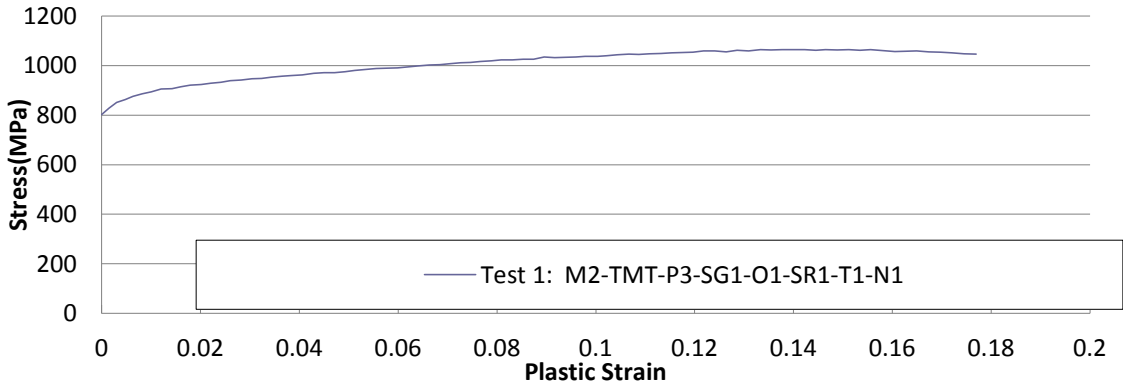

Figure D.4. Hardening curve (Test: M2-TMT-P3-SG1-O1-SR1-T1-N1)

To determine the necking point, the true strain versus stress curve was smoothed by a 9-point moving average and subsequently were used to obtain the tangent modulus curve. Another 9-point moving average was performed on the tangent modulus curve. The intersection between these two lines defines the necking point (see figure D.5).

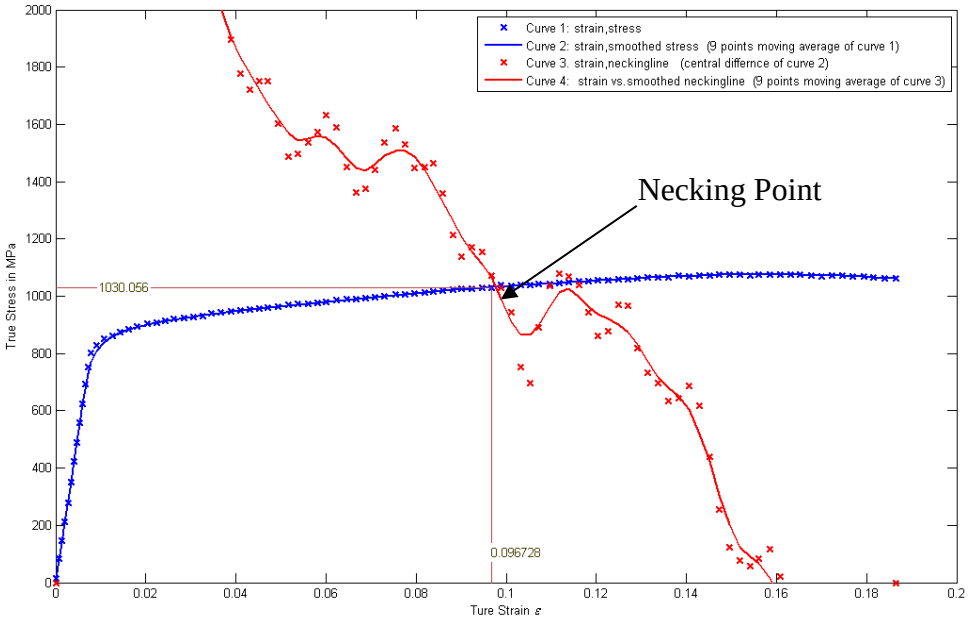

Figure D.5. Necking point judgment (Test: M2-TMT-P3-SG1-O1-SR1-T1-N1)

The true stress and true strain at necking were recorded. The corresponding plastic strain at necking was computed and only the part of the hardening curve before necking was kept. The hardening curve was extrapolated beyond necking. Eleven curves were generated by varying the exponent *n* between ~0.0871 and 0.2, as shown in figure D.6.

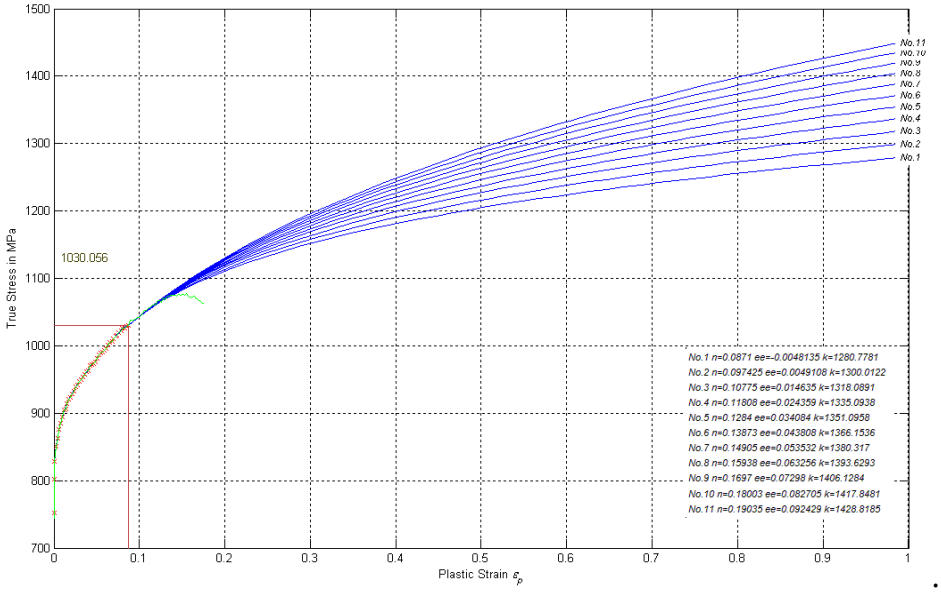

Figure D.6. Plastic strain versus stress extrapolated inputs (Test: M2-TMT-P3-SG1-O1-SR1-T1-N1)

The 11 values of n were obtained by non-uniform incremental steps. The remaining two parameters, ε_e and k, were calculated. Extrapolation was performed using MATLAB. Each of the generated hardening curves was then entered into an LS-DYNA *MAT_224 input deck and used to perform a simulation of the tensile test. In this model, the sample dimensions match the sample of test M2-TMT-P3-SG1-O1-SR1-T1-N1 exactly, giving: width = 2.06502 mm and thickness = 0.71628 mm. A DATABASE_CROSS_SECTION was defined to measure the cross-sectional force. Two nodal points corresponding to the base points of the extensometer are stored in the NODOUT file (see figure D.7). The difference in z displacement of these two nodal points gives the elongation of the extensometer, as predicted in the simulation. Node 91116 and Node 63281 correspond to the base points of the extensometer and have an initial distance of 4 mm. The cross-section for force measurement is located at the center of the specimen. A cross-plot of this elongation with the cross-sectional force can be directly compared to the force displacement curve from the test. Results in figure D.8 show that curve #8 gives the best match between test and simulation in terms of force displacement. The extrapolation parameters of curve #8 are n = 0.15938, ε_e = 0.0632567, and k = 1393.6293.

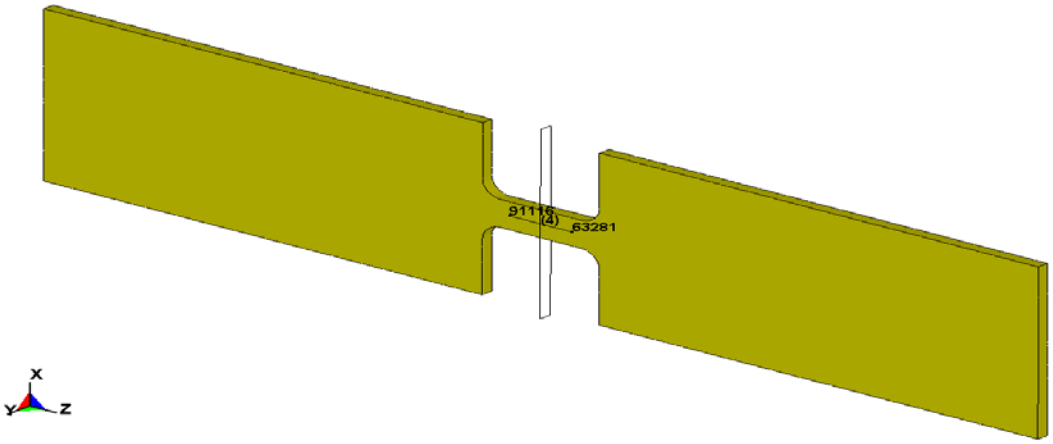

Figure D.7. FE model of tensile specimen (Test: M2-TMT-P3-SG1-O1-SR1-T1-N1)

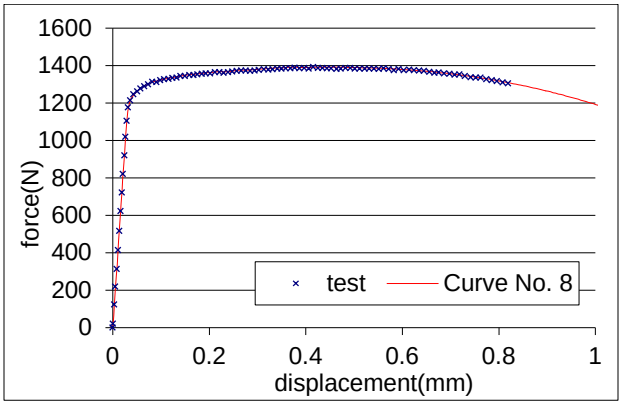

Figure D.8. Force displacement result of curve #8 (Test: M2-TMT-P3-SG1-O1-SR1-T1-N1)

In summary, the final hardening curve for strain rate 1E-4 sec^{-1} and corresponding force displacement curve from test and simulation are shown in figure D.9. In figure D.10, a contour of

1st principal strain generated by LS_PREPOST is compared to the DIC image from the test at the corresponding time. Both the curve and images show good agreement.

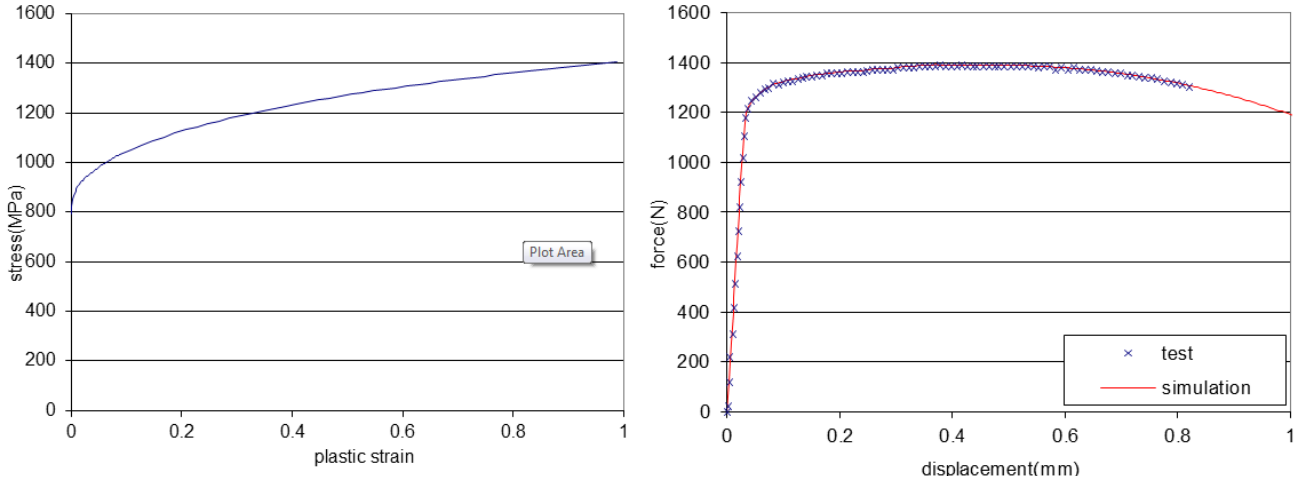

(a) (b)

Figure D.9. The (a) simulation plastic strain versus stress input and (b) force versus displacement comparison of simulation and test (Test 1: M2-TMT-P3-SG1-O1-SR1-T1-N1; strain rate = 1E-4 sec^{-1})

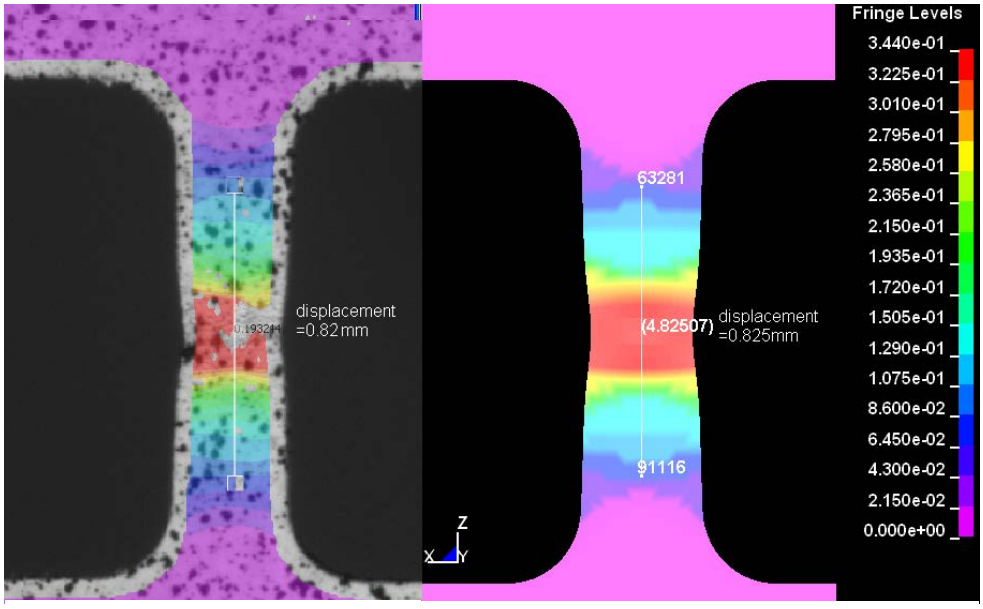

(a) (b)

Figure D.10. The (a) plastic strain DIC image immediately before failure and (b) 1st principal strain simulation contour immediately before failure (Test 1: M2-TMT-P3-SG1-O1-SR1-T1-N1; strain rate = 1E-4 sec^{-1}])

D.2.2.2 Stress-Strain Relation of Strain Rate 1E-2 Sec^{-1}

The three tests at strain rate 1E-2 sec^{-1} are listed in table D.3 and the results are shown in figures D.11–D.13. Using the same process as in section D.2.2.1, the true stress-strain relationship is found, as shown in figure D.13. The smoothed average of Test 5: M2-TMT-P3-SG1-O1-SR2-T1-N4 and Test 6: M2-TMT-P3-SG1-O1-SR2-T1-N5 was chosen to represent this group of data and will go through further processing. The smoothing method involved performing a 10-point moving average five times on the data. The input of two test averages instead of one increases the accuracy of the result. Tests 5 and 6 must be simulated individually with the same input curve until a candidate curve matches the simulation force displacement with the test result of Tests 5 and 6 simultaneously.

Table D.3. Strain rate dependence series data of strain rate = 1E-2 sec-1

M2-TMT-P3-SG1-O1-SR2-T1-N3	0.25"	Flat Dogbone	Rolled	1.1E-02	RT
M2-TMT-P3-SG1-O1-SR2-T1-N4	0.25"	Flat Dogbone	Rolled	1.1E-02	RT
M2-TMT-P3-SG1-O1-SR2-T1-N5	0.25"	Flat Dogbone	Rolled	1.1E-02	RT

RT = room temperature

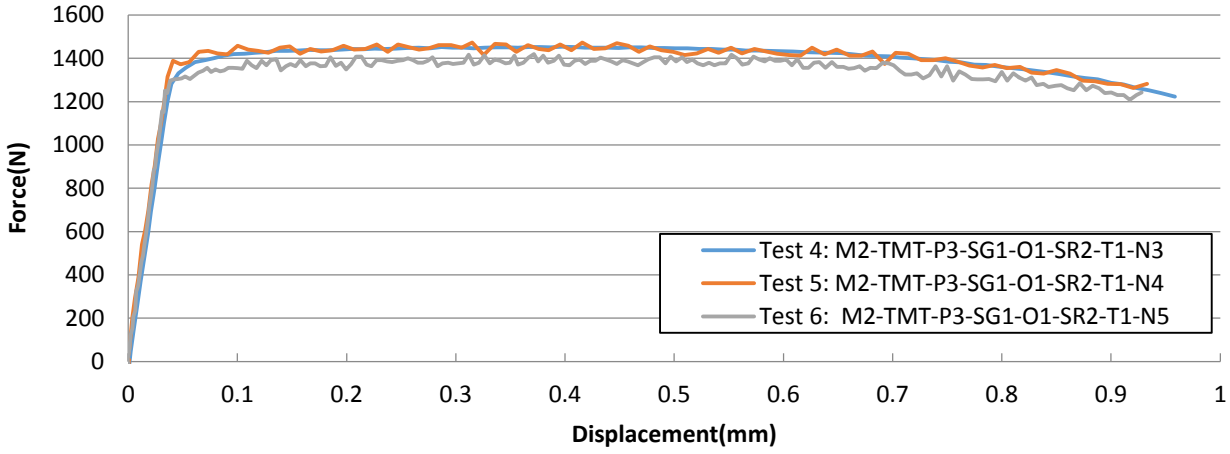

Figure D.11. Force displacement relation of all strain rate = 1E-2 sec^{-1} tests

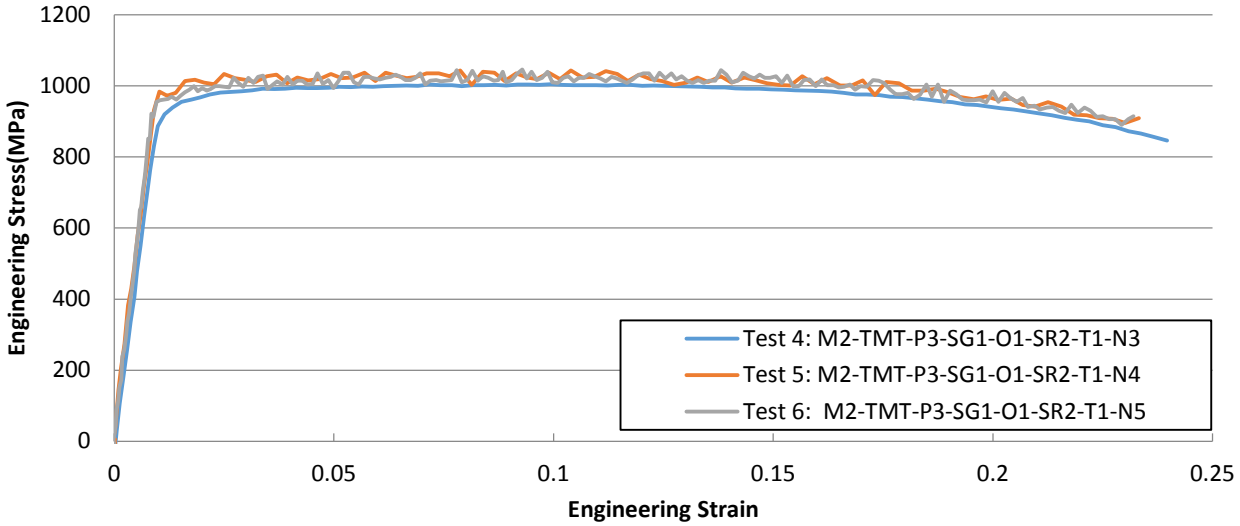

Figure D.12. Engineering stress-strain relation of strain rate = 1E-2 sec^{-1} tests

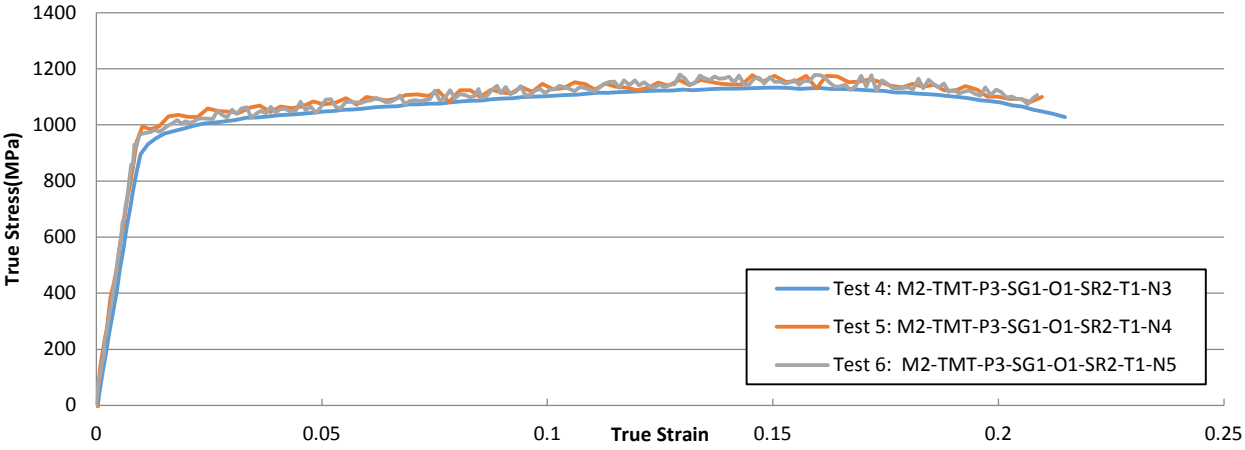

Figure D.13. True stress-strain relation of strain rate = 1E-2 sec^{-1} tests

To determine the necking point, the true stress is differentiated with respect to strain to obtain the tangent modulus curve. The intersection between the tangent modulus curve and stress-strain curve defines the necking point (see figure D.14). The true stress and true strain at necking were recorded and the corresponding plastic strain at necking was computed. Figure D.14 was generated using MATLAB, but other tools such as LS-PrePost would be equally suitable.

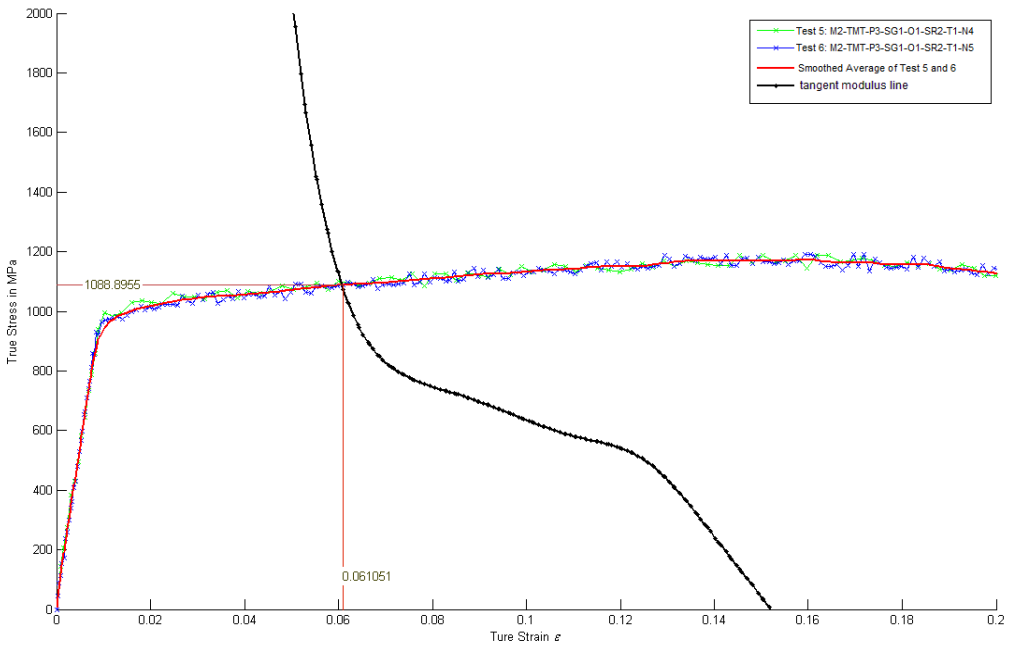

Figure D.14. Smoothed average of Tests 5 and 6, including necking point judgment

The plastic strain versus stress relation is calculated by adopting a Young's modulus of 110 GPa. The resulting curve is shown in figure D.15. Only the part of the hardening curve before necking was kept. Beyond necking, the hardening curve was extrapolated. Twenty-eight curves were generated by varying the exponent *n* between ~0.017 and 0.029, as shown in figure D.16.

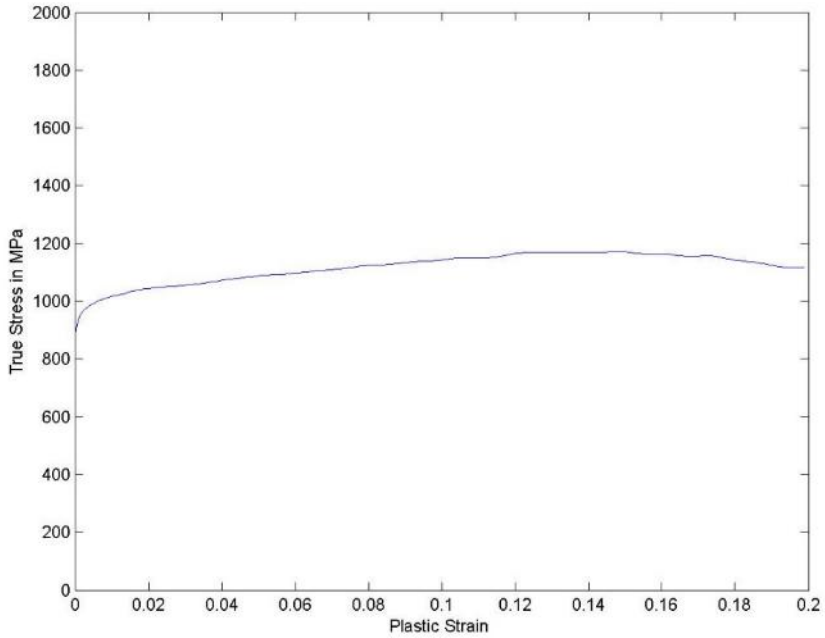

Figure D.15. Plastic strain versus true stress of Tests 5 and 6, smoothed average curve

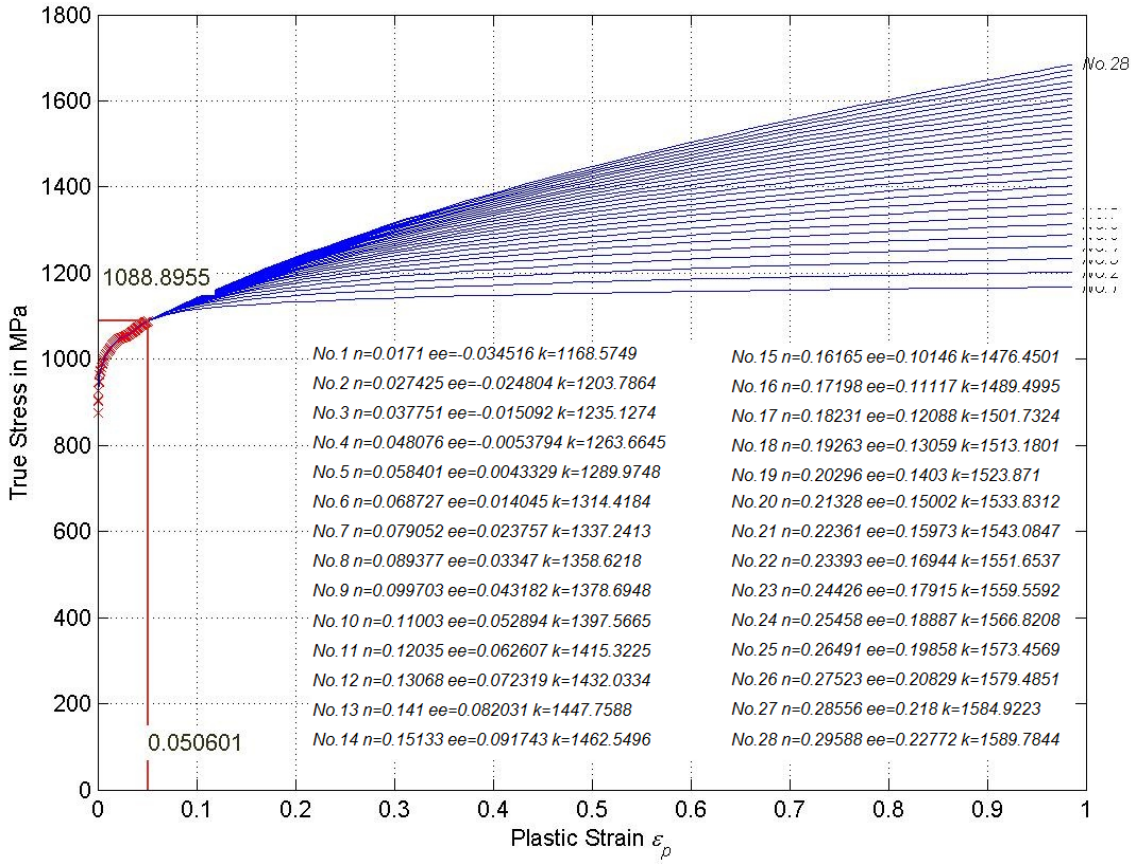

Figure D.16. Plastic strain versus stress extrapolated inputs of smoothed curve of strain rate = 1E-2 sec^{-1}

Each of the generated hardening curves were put into an LS-DYNA *MAT_224 input deck, and a simulation of the tensile Test 5: M2-TMT-P3-SG1-O1-SR2-T1-N4 was performed. In this model, the sample dimensions match the sample of Test 5: width = 2.04978 mm and thickness = 0.68834 mm. DATABASE_CROSS_SECTION was defined to measure the cross-sectional force. Two nodal points corresponding to the base points of extensometer are stored in the NODOUT file, as shown in figure D.17. Node 27012 and Node 9134 correspond to the base points of the extensometer and have an initial distance of 4 mm. The cross-section for force measurement is located at the center of the specimen. The difference in *z* displacement of the two nodal points gives the elongation of the extensometer, as predicted in the simulation. A cross-plot of this elongation with the cross-sectional force can be directly compared to the force displacement curve from the test. The results presented in figure D.18 show that Curve #22 gives a close match between Test 5 and the simulation in terms of force displacement. The extrapolation parameters of Curve #22 are n = 0.23393, ε_e = 0.16944, and k = 1551.6537.

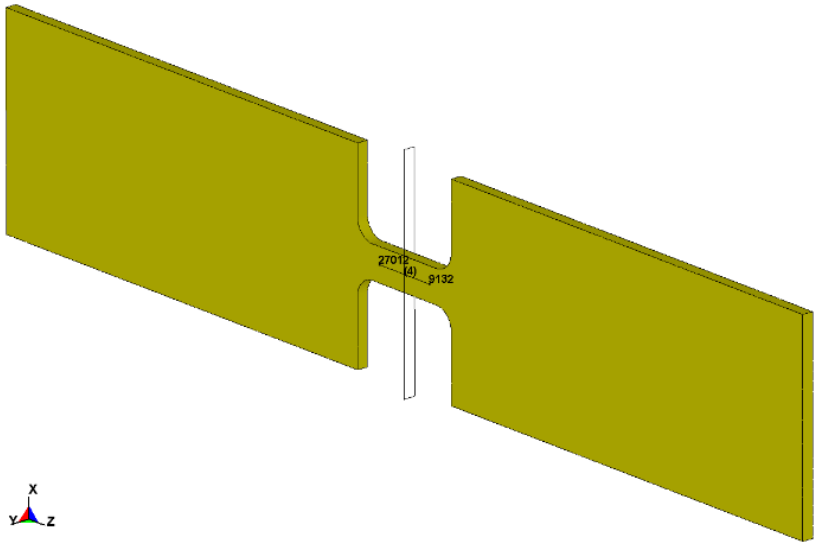

Figure D.17. FE model of tensile specimen (Test: M2-TMT-P3-SG1-O1-SR2-T1-N4)

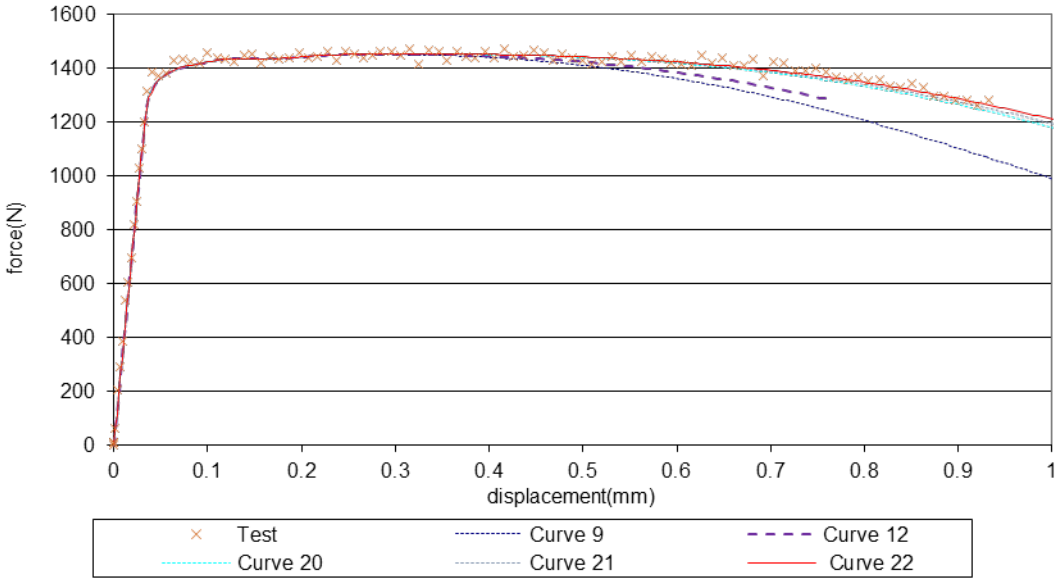

Figure D.18. Force displacement result of curve #22
(Test 5: M2-TMT-P3-SG1-O1-SR2-T1-N4)

In summary, the final hardening curve for strain rate 1E-2 sec^{-1} and corresponding force displacement curve from test and simulation are shown in figure D.19. In figure D.20, a contour of 1st principal strain generated by LS_PrePost is compared to the DIC image from the test at the corresponding time.

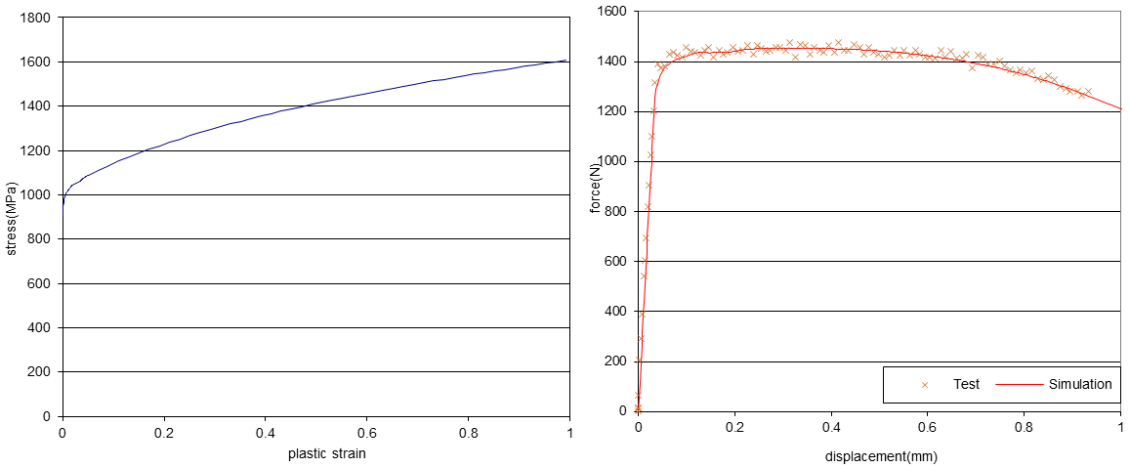

(a) (b)

Figure D.19. The (a) simulation plastic strain versus stress input and (b) force versus displacement comparison of simulation and test (Test 5: M2-TMT-P3-SG1-O1-SR2-T1-N4; strain rate = 1E-2 sec^{-1})

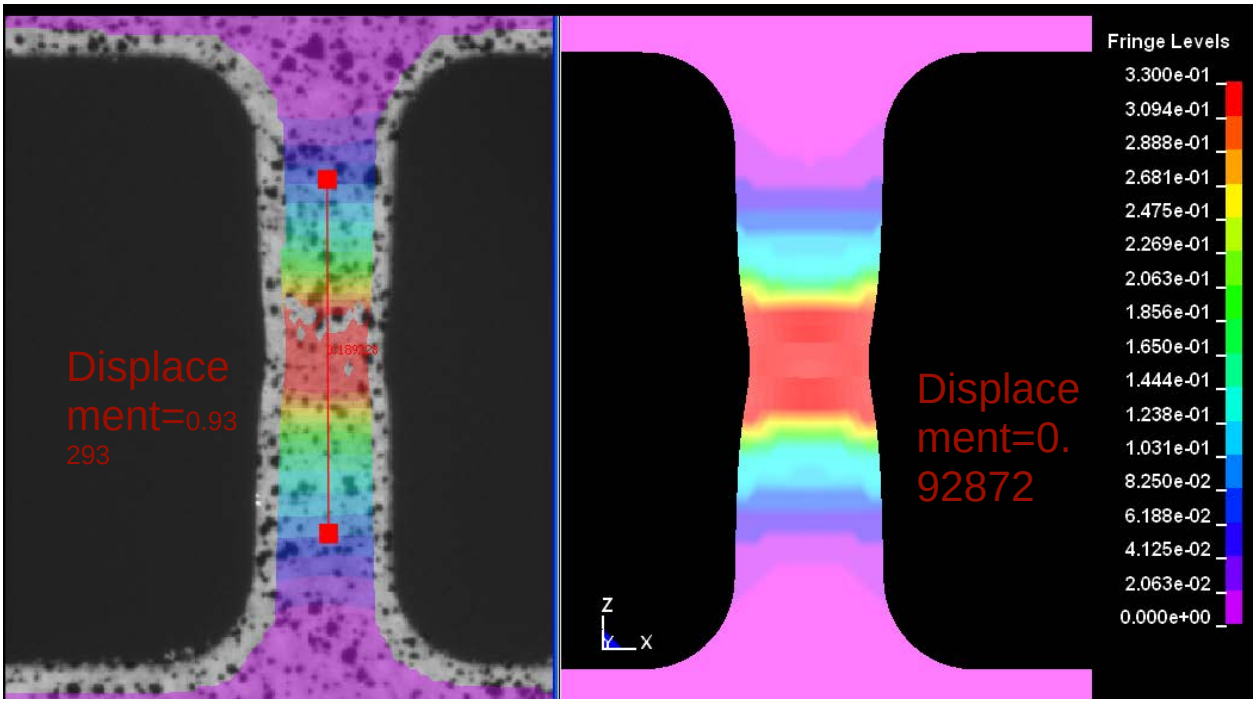

(a) (b)

Figure D.20. The (a) plastic strain DIC image immediately before failure and (b) 1st principal strain simulation contour immediately before failure (Test 5: M2-TMT-P3-SG1-O1-SR2-T1-N4; strain rate = 1E-2 sec^{-1})

To verify this result, Test 6: M2-TMT-P3-SG1-O1-SR2-T1-N4 was simulated with the same hardening curve derived from Test 5. In this model, the sample dimensions match the sample of Test 6: M2-TMT-P3-SG1-O1-SR2-T1-N5 exactly; therefore, the actual dimensions of Test 6

were used in the simulation (width = 2.02438 mm and thickness = 0.67056 mm). The results show a close match in force displacement and 1st principal strain contour, as shown in figures D.21 and D.22.

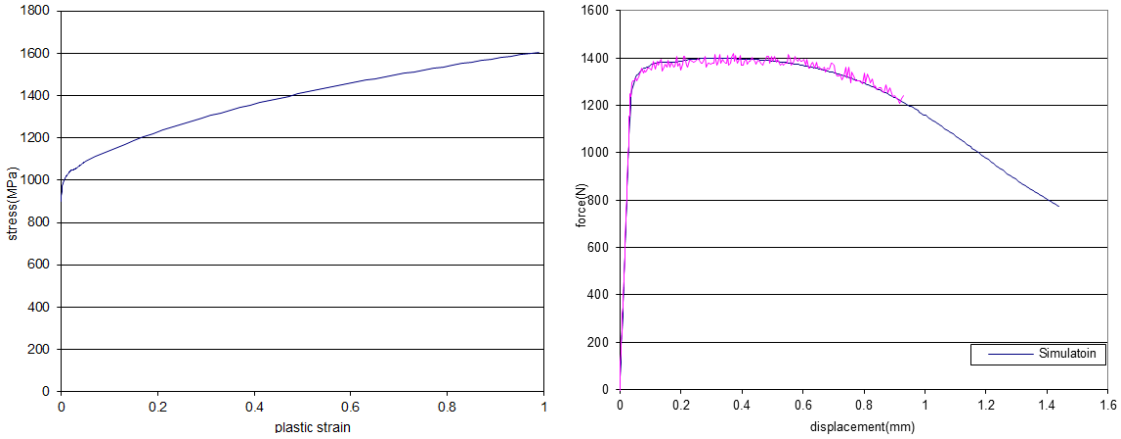

(a) (b)

Figure D.21. The (a) simulation plastic strain versus stress input same as Test 5 and (b) force versus displacement comparison of simulation and test (Test 6: M2-TMT-P3-SG1-O1-SR2-T1-N5; strain rate = 1E-2 sec^{-1})

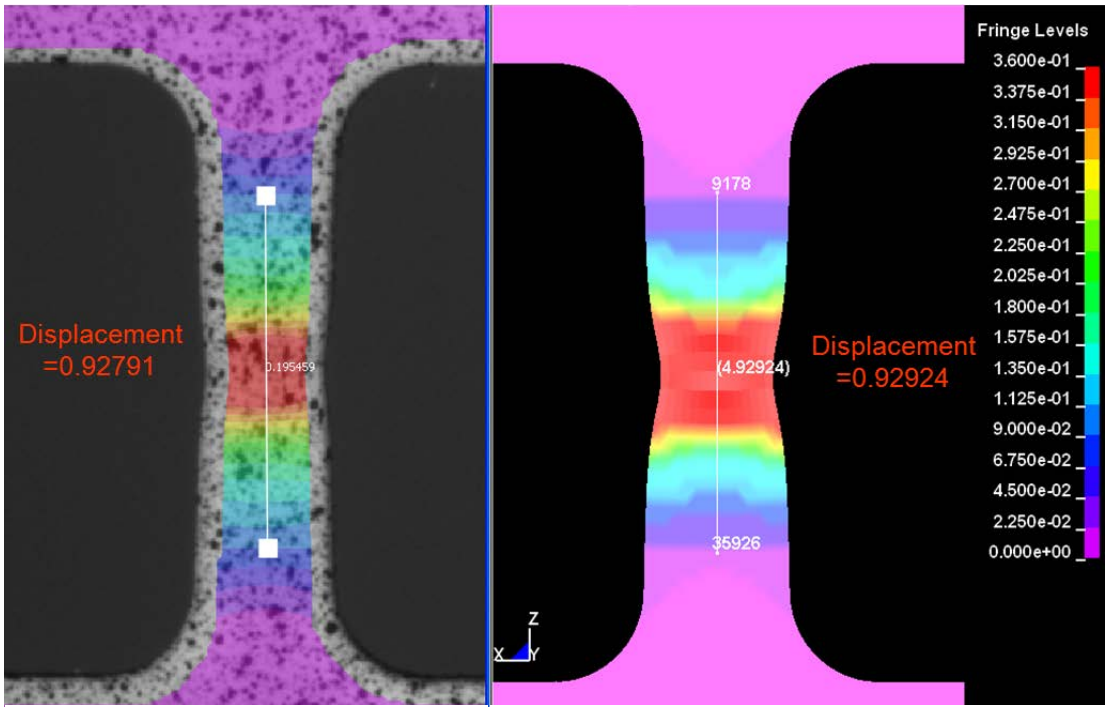

(a) (b)

Figure D.22. The (a) plastic strain DIC image at failure moment and (b) simulation contour of plastic strain at failure moment (Test 6: M2-TMT-P3-SG1-O1-SR2-T1-N5; strain rate = 1E-2 sec^{-1})

D.2.2.3 Stress-Strain Relation of Strain Rate 1 Sec^{-1}

The three quasistatic tests at strain rate = 1 sec^{-1} are listed in table D.4. The force-displacement relationship of these tests is shown in figure D.23. The engineering stress-strain relationship is derived using equation 8 from the main document and gives the engineering stress-strain curves in figure D.24. Test 9: M2-TMT-P3-SG1-O1-SR3-T1-N5 is selected to represent this group of data and will go through further processing. By applying [9, 10], engineering stress-strain is converted to true stress-strain, as shown in figure D.25. By applying equation 11 and adopting a Young's modulus of 110, the plastic strain versus stress relation is calculated, as shown in figure D.26.

Table D.4. Strain rate dependence series data of strain rate = 1 sec^{-1}

Test Series	Test Name	Plate Stock	Specimen Geometry	Specimen Orientation	Strain Rate (1/s)	Temp (°C)
Tension Strain Rate Dependence	M2-TMT-P3-SG1-O1-SR3-T1-N3	0.25"	Flat Dogbone	Rolled	1.1	RT
	M2-TMT-P3-SG1-O1-SR3-T1-N4	0.25"	Flat Dogbone	Rolled	1.1	RT
	M2-TMT-P3-SG1-O1-SR3-T1-N5	0.25"	Flat Dogbone	Rolled	1.1	RT

RT = room temperature

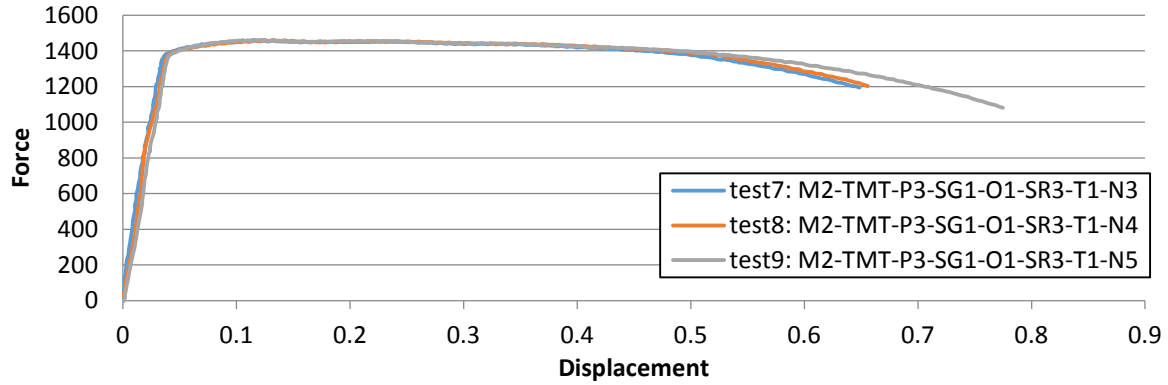

Figure D.23. Force displacement relation of strain rate = 1 sec^{-1} tests

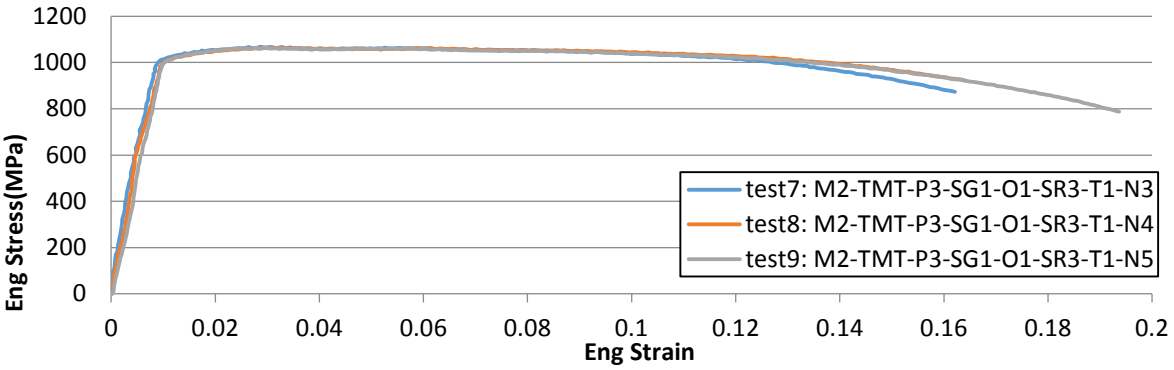

Figure D.24. Engineering stress-strain relation of strain rate = 1 sec^{-1} tests

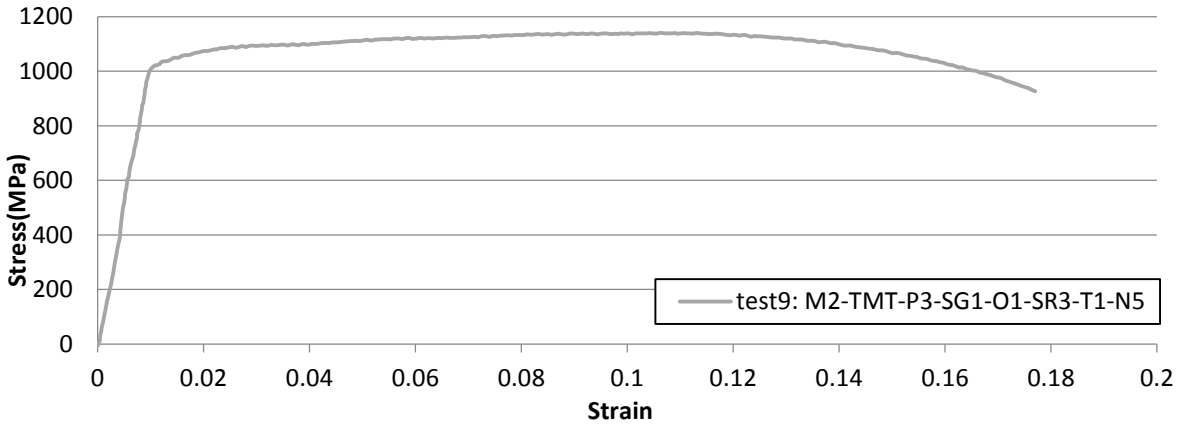

Figure D.25. Stress-strain relation of Test 9: M2-TMT-P3-SG1-O1-SR3-T1-N5

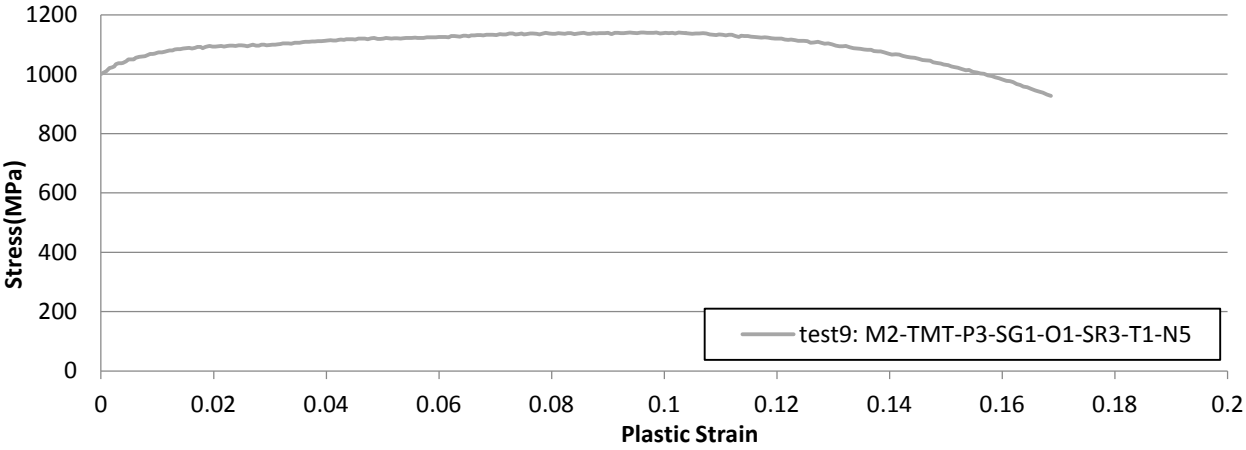

Figure D.26. Plastic strain versus stress relation of Test 9: M2-TMT-P3-SG1-O1-SR3-T1-N5

The true strain versus stress curve in figure D.25 was smoothed by a 9-point moving average followed by another 4-point moving average. This smoothed curve was then used for further

processing instead of the original data. The resulting smoothed hardening curve is shown in figure D.26.

The tangent modulus curve was obtained to determine the necking point. Another 9-point moving average was applied on the tangent modulus curve, and the intersection between the two curves defined the necking point (see figure D.27).

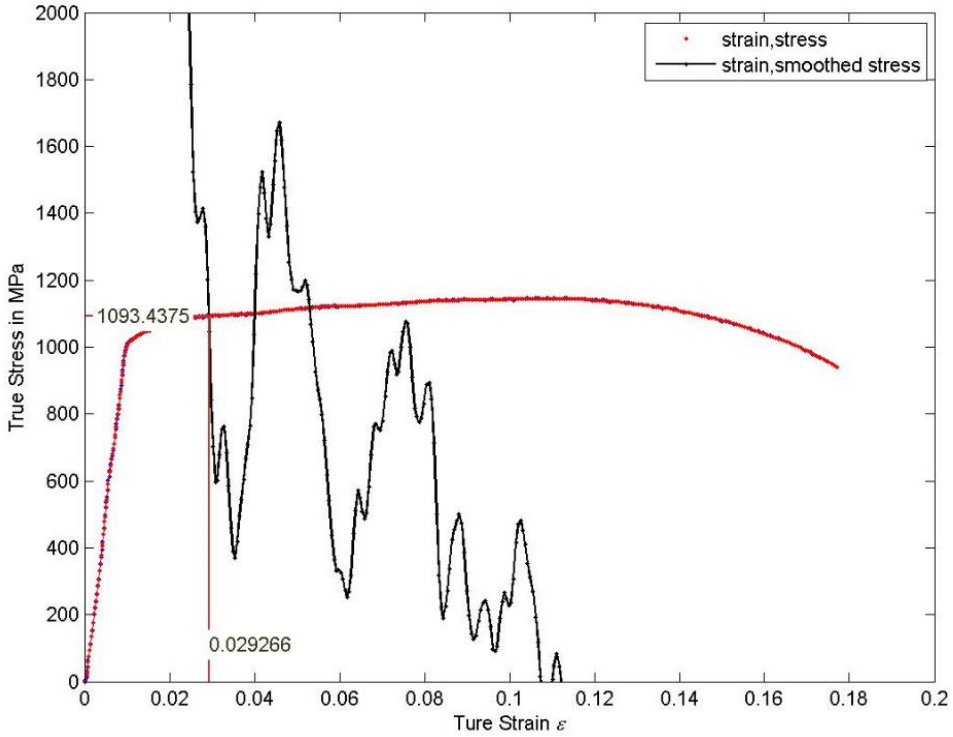

Figure D.27. Necking point judgment (Test 9: M2-TMT-P3-SG1-O1-SR3-T1-N5)

Twenty-nine curves were generated by varying the exponent *n* between ~0.871 and 0.29782 (see figure D.28). The 29 values of *n* were obtained by non-uniform incremental steps. The other two parameters, ε_e and *k*, were calculated.

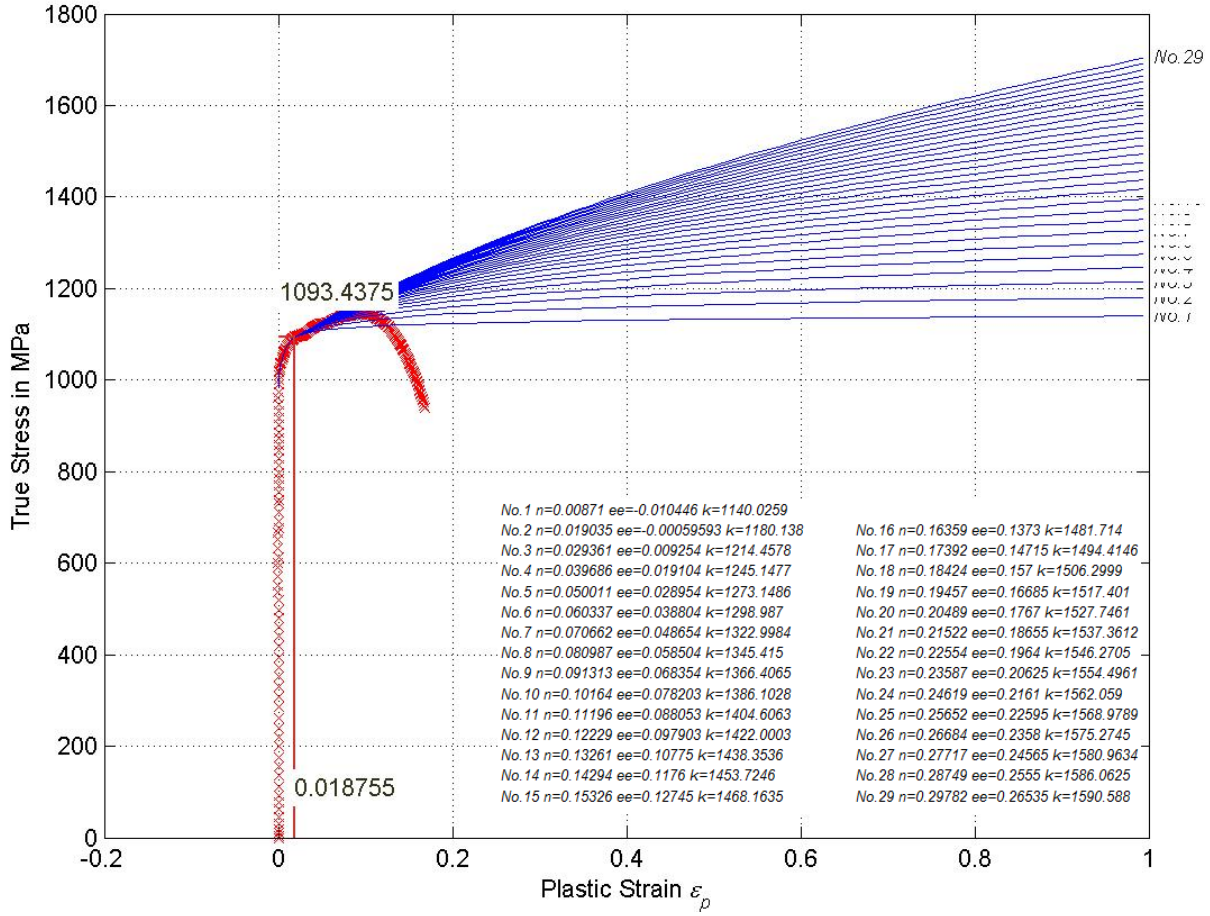

Figure D.28. Plastic strain versus stress extrapolated input (Test 9: M2-TMT-P3-SG1-O1-SR3-T1-N5)

Each of the generated hardening curves were entered into an LS-DYNA *MAT_224 input deck and a simulation of the tensile test was performed. In this model, the sample dimensions match the sample of Test M2-TMT-P3-SG1-O1-SR3-T1-N5 exactly: width = 2.032 mm and thickness = 0.67564 mm. Two nodal points—185 and 18065, corresponding to the base points of the extensometer—were stored in the NODOUT file (see figure D.29), and a cross-plot of elongation with the cross-sectional force is directly compared to the force-displacement curve from the test. Results in figure D.30 show that Curve #14 gives a close match between test and simulation in terms of force displacement. The extrapolation parameters of Curve #14 are n = 0.14294, ε_e = 0.1176, and k = 1453.726.

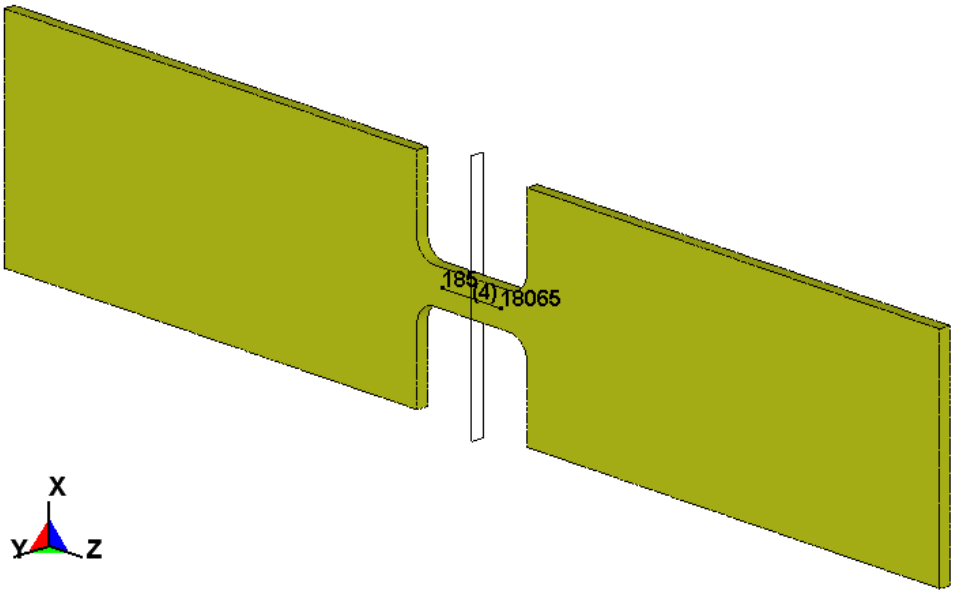

Figure D.29. FE model of tensile specimen (Test 9: M2-TMT-P3-SG1-O1-SR3-T1-N5)

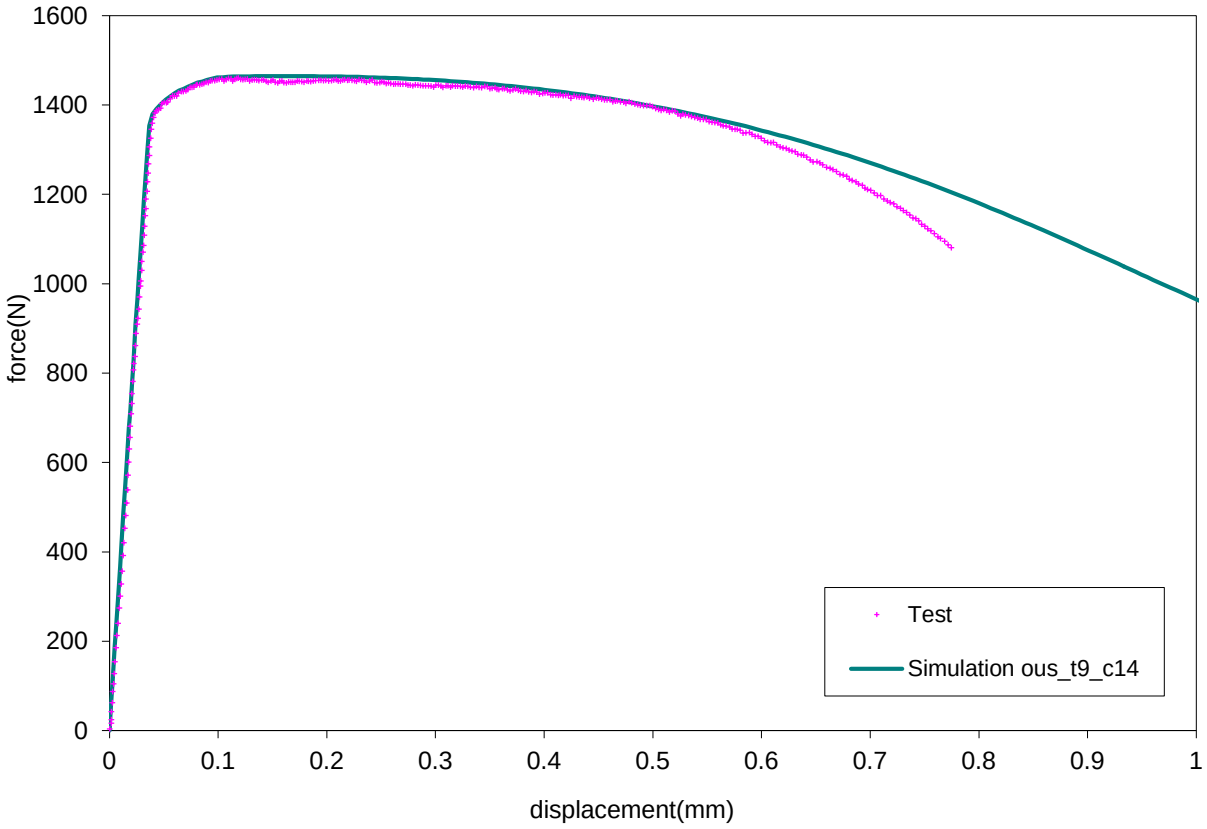

Figure D.30. Force displacement result of curve #14
(Test 9: M2-TMT-P3-SG1-O1-SR3-T1-N5)

To further improve the result, a second extrapolation was performed on Curve #14. The hardening curve was cut off at plastic strain ("necking" strain) B = 0.1989. A value of 0.035 was chosen for *n* and the remaining two parameters were computed. The curve was then extrapolated. The extrapolation parameters are listed in table D.5. The resulting hardening curve is shown in figure D.31. The force-displacement comparison between the simulation based on this second extrapolation and the test result is shown in figure D.32.

Table D.5. Extrapolation parameters of curve c14r5 from curve c14

Original Curve	C	B	A	*n* (guess)	*k*	ε_e	Result Curve
t9_c14	575	0.1989	1233.3	0.035	1350.290832	-0.12383	t9c14r5

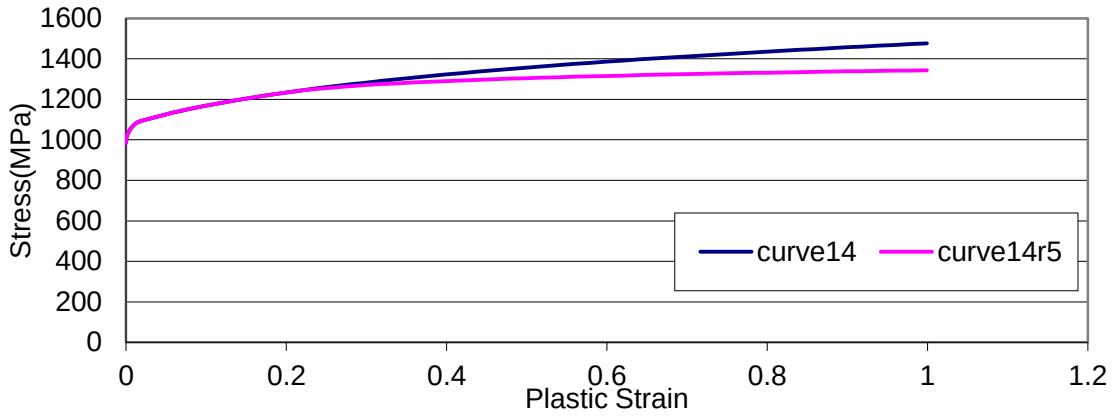

Figure D.31. Extrapolated hardening curve 14r5
(Test 9: M2-TMT-P3-SG1-O1-SR3-T1-N5)

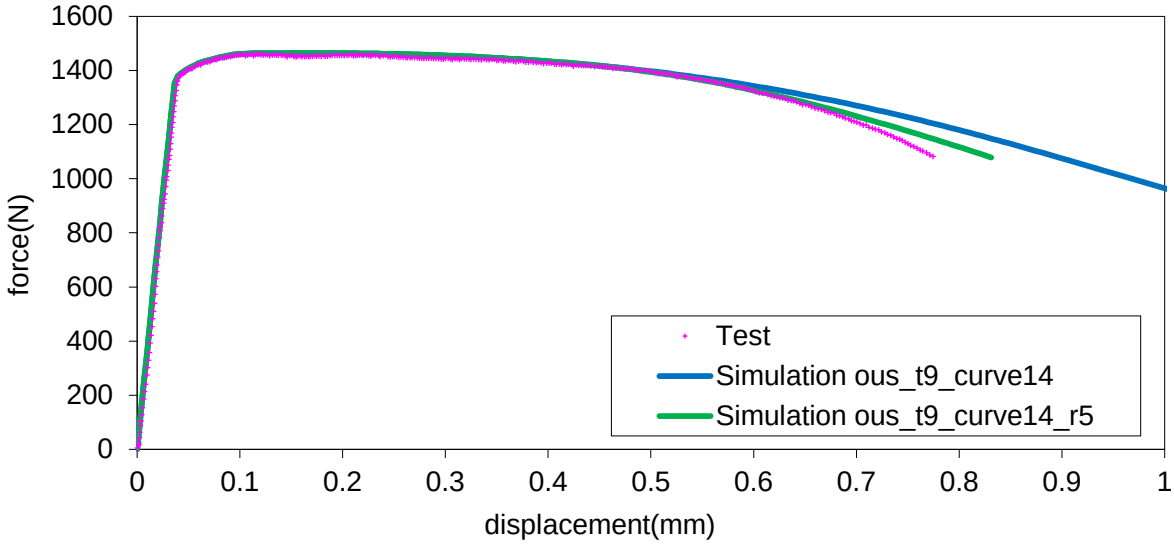

Figure D.32. Force versus displacement comparison of simulation c14r5 and Test 9: M2-TMT-P3-SG1-O1-SR3-T1-N5

A third extrapolation on the result curve t9c14r5 was necessary to further improve the accuracy.

The hardening curve was cut off at plastic strain ("necking" strain) B = 0.3589. A value of 0.002 was chosen for *n* and the remaining two parameters were then computed using [25]. The curve was then extrapolated. The extrapolation parameters are listed in table D.6 and the resulting hardening curve is shown in figure D.33. The force-displacement comparison between the simulation based on this second extrapolation and the test result is shown figure D.34.

Table D.6. Extrapolation parameter of curve c14r9 from curve c14r5

Original Curve	C	B	A	*n* (guess)	*k*	ε_e	Result Curve
t9c14r5	199.4248	0.3589	1283.569	0.002	1294.79170	-0.34603	t9c14r9

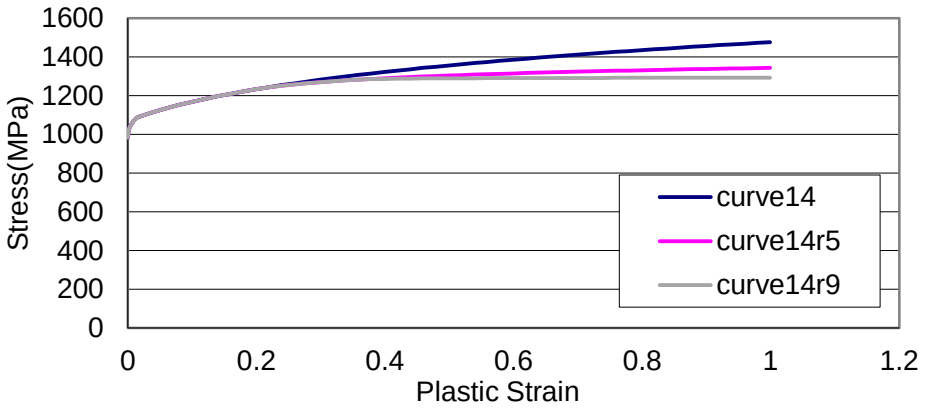

Figure D.33. Extrapolated hardening curve 14r9
(Test 9: M2-TMT-P3-SG1-O1-SR3-T1-N5)

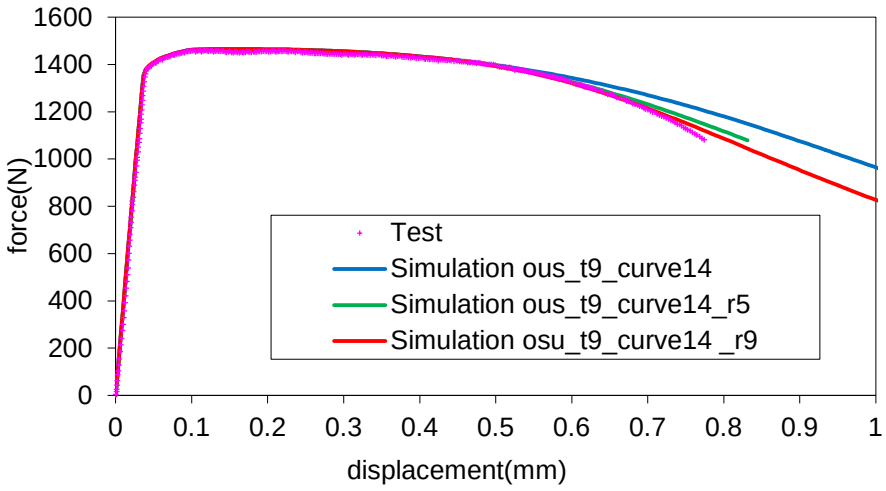

Figure D.34. Force versus displacement comparison of simulation c14r5 and Test 9: M2-TMT-P3-SG1-O1-SR3-T1-N5

In summary, the final hardening curve for strain rate 1 sec^{-1} and the corresponding force displacement curve from test and simulation are shown in figure D.35. In figure D.36, a contour of 1st principal strain generated by LS_PrePost is compared to the DIC image from the test at the corresponding time.

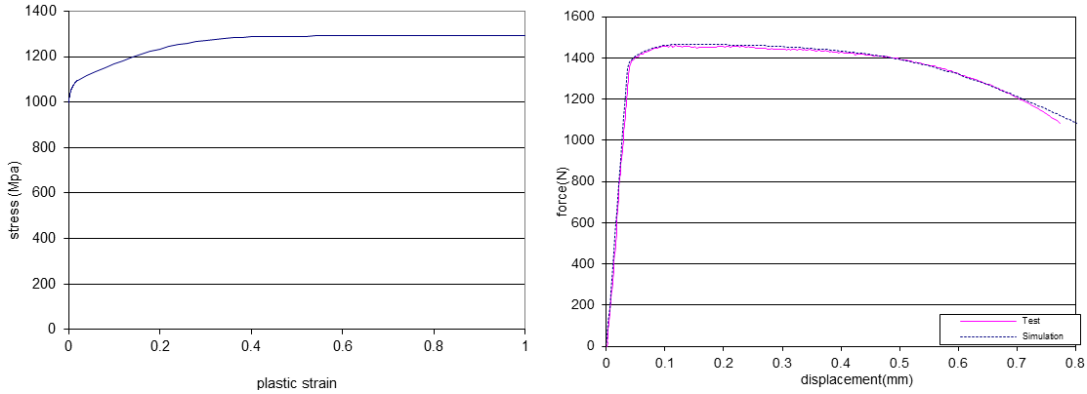

(a) (b)

Figure D.35. The (a) simulation plastic strain versus stress input and (b) force versus displacement comparison of simulation and test (Test ID: M2-TMT-P3-SG1-O1-SR3-T1-N5; strain rate = 1 sec^{-1})

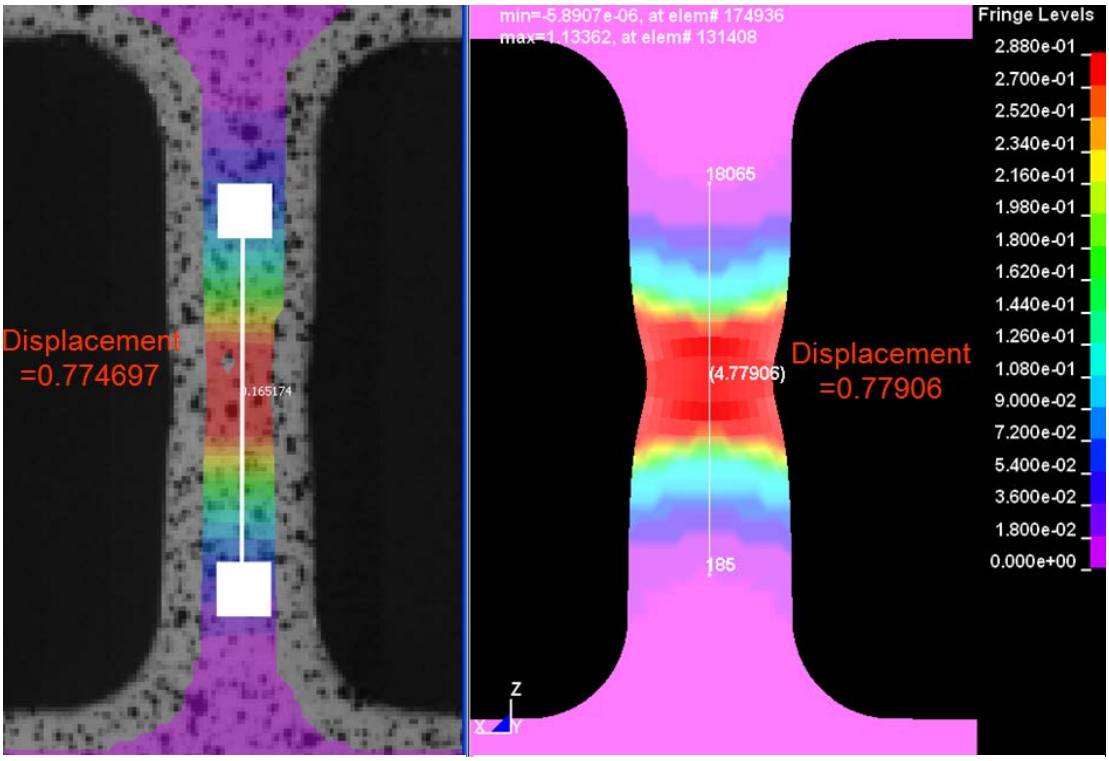

(a) (b)

Figure D.36. The (a) plastic strain DIC image at failure moment and (b) simulation contour of plastic strain at failure moment (Test ID: M2-TMT-P3-SG1-O1-SR3-T1-N5; strain rate = 1 sec^{-1})

D.2.2.4 Stress-Strain Relation of Strain Rate 500 Sec^{-1}

The three quasistatic tests of strain rate 500 sec^{-1} are listed in table D.7. The force-displacement relation of these tests is shown in figure D.37. The engineering strain versus stress relationship was derived and yields the engineering stress-strain curves in figure D.38. Test 12: M2-TMT-P3-SG1-O1-SR4-T1-N7 was selected to represent this group of data and undergo further processing. The engineering stress-strain relationship was converted to the true stress-strain relationship as shown in figure D.39.

Table D.7. Strain rate dependence series data of strain rate = 500 sec^{-1}

Test Series	Test Name	Plate Stock	Specimen Geometry	Specimen Orientation	Strain Rate (1/s)	Temp (˚C)
Tension Strain Rate Dependence	M2-TMT-P3-SG1-O1-SR5-T1-N1	0.25"	Flat Dog-bone	Rolled	1.3E+04	RT
	M2-TMT-P3-SG1-O1-SR5-T1-N3	0.25"	Flat Dog-bone	Rolled	1.8E+03	RT
	M2-TMT-P3-SG1-O1-SR5-T1-N4	0.25"	Flat Dog-bone	Rolled	1.4E+03	RT

RT = room temperature

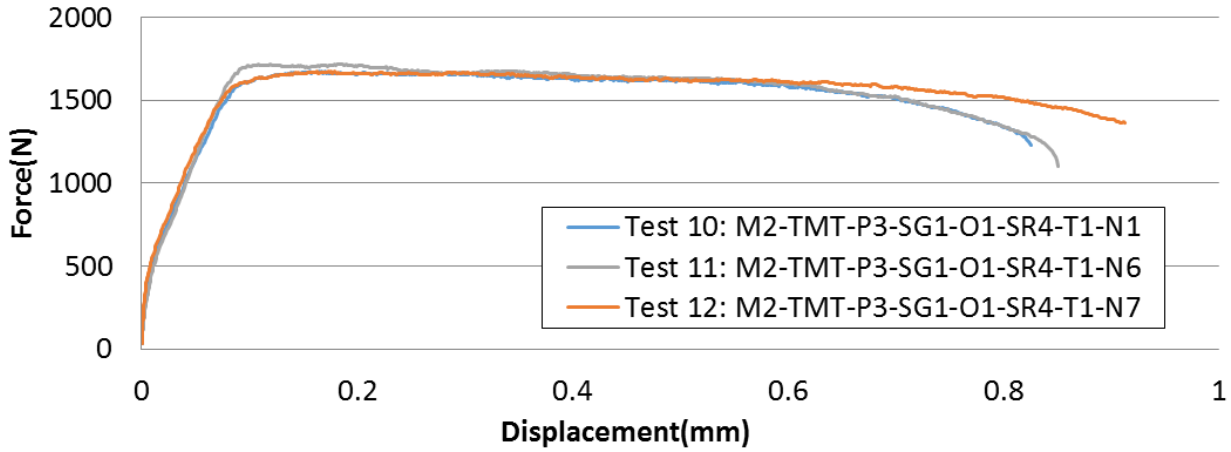

Figure D.37. Force displacement relation of all strain rate = 500 sec^{-1} tests

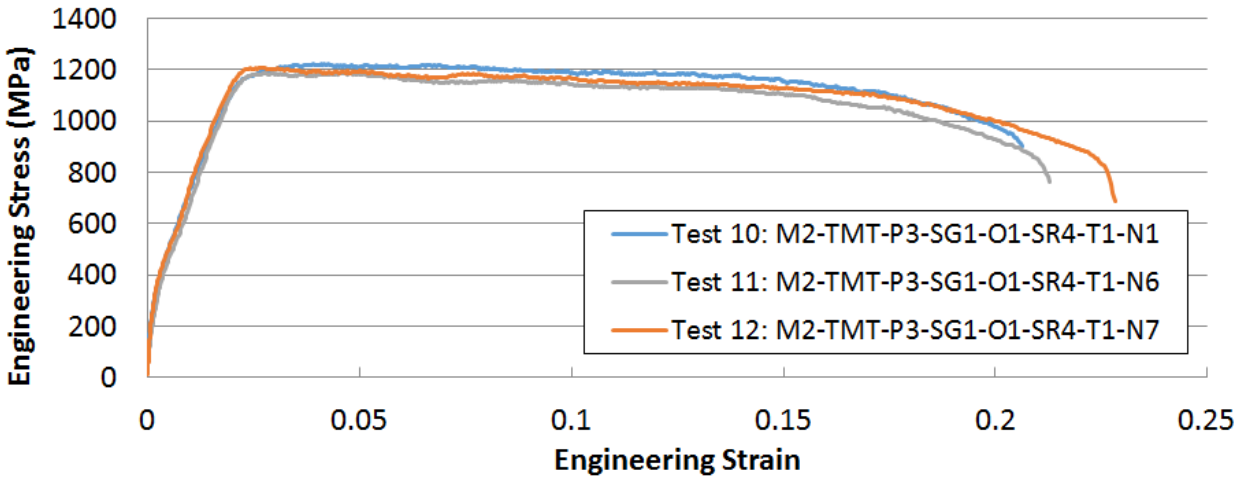

Figure D.38. Engineering stress-strain relation of strain rate = 500 sec^{-1} tests

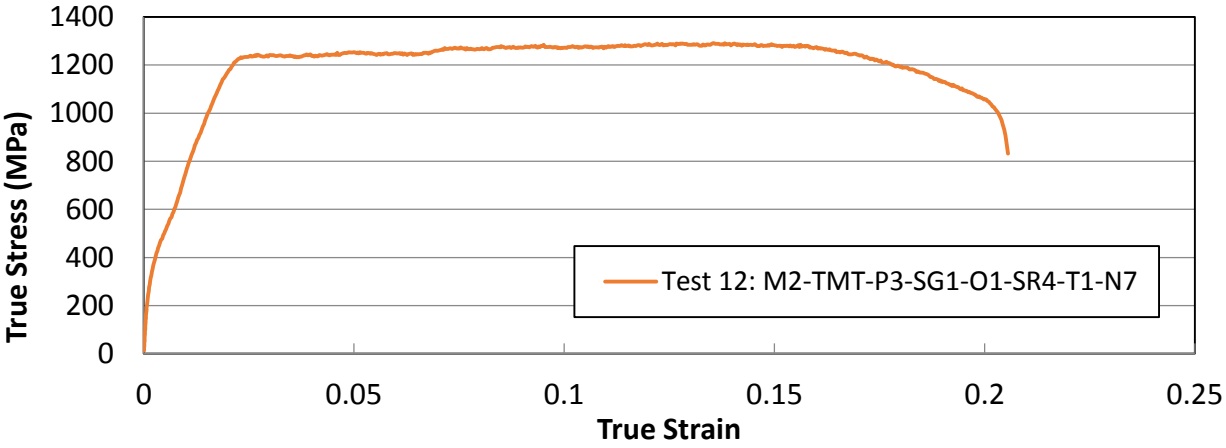

Figure D.39. Stress-strain relation (Test 12: M2-TMT-P3-SG1-O1-SR4-T1-N7)

The tests at strain rate 500 sec^{-1} and strain rate 1000 sec^{-1} showed a smaller Young's modulus than the other strain rate groups (see figure D.40). This was caused by the difference in testing method used at higher versus lower strain rate. The Young's modulus used in the simulation was fixed to the literature value because the high strain-rate experiments were considered to be not accurate enough to measure the Young's modulus.

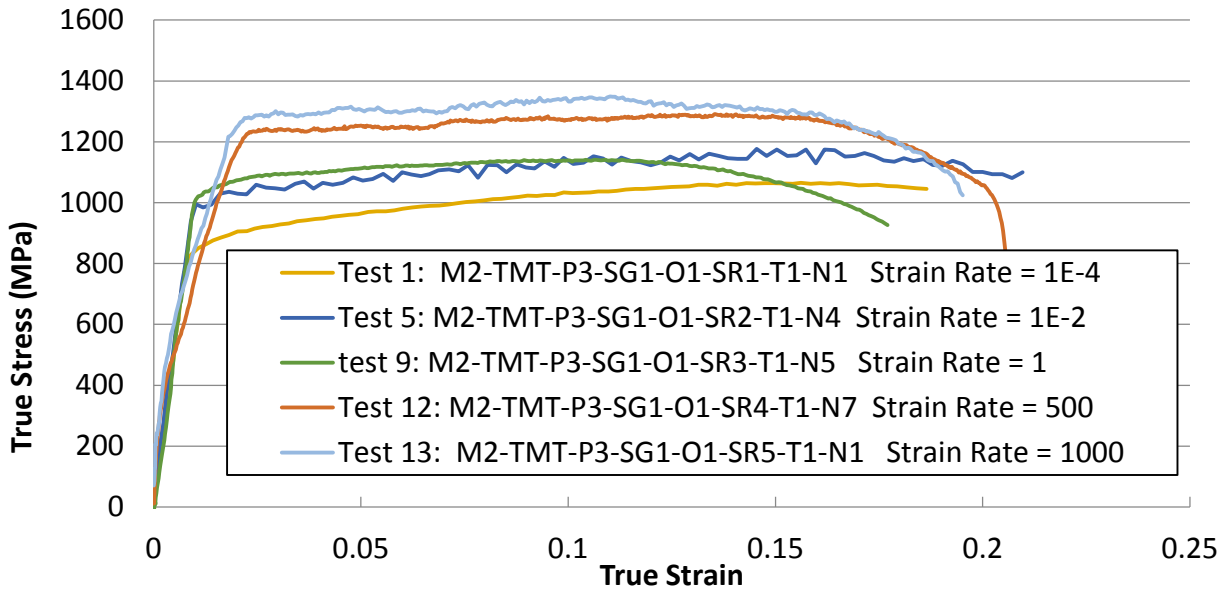

Figure D.40. Observed Young's modulus difference among tests of different strain rates

However, a smaller Young's modulus had to be adopted for the conversion to avoid the hardening curve from going negative. By adopting a Young's modulus of 55 GPa, the plastic strain versus stress relation was calculated (see figure D.41). The Young's modulus of 55 GPa comes from calculating the slope of the elastic region of the test curve.

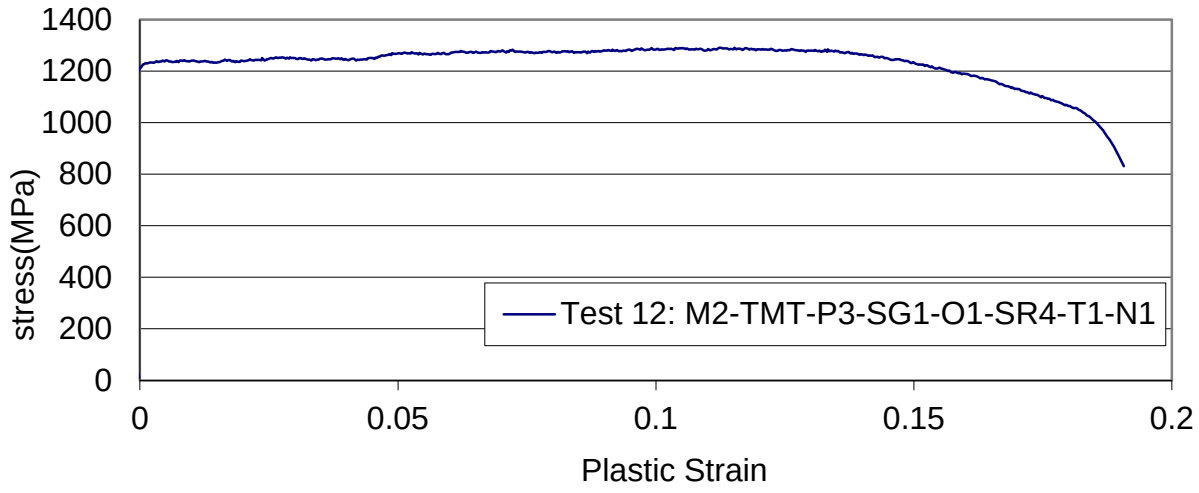

Figure D.41. Plastic strains versus stress (Test 12: M2-TMT-P3-SG1-O1-SR4-T1-N1)

The hardening curve was extrapolated in a slightly different manner due to the almost flat shape of the plastic strain versus stress curve, making it difficult to determine the necking point (see figure D.41). In this case, the transition between the extrapolated curve and the original curve is continuous but not smooth. First, the hardening curve was smoothed and the yield stress value was kept constant after reaching the maximum. The resulting hardening curve is named t12e3 (see figure D.42).

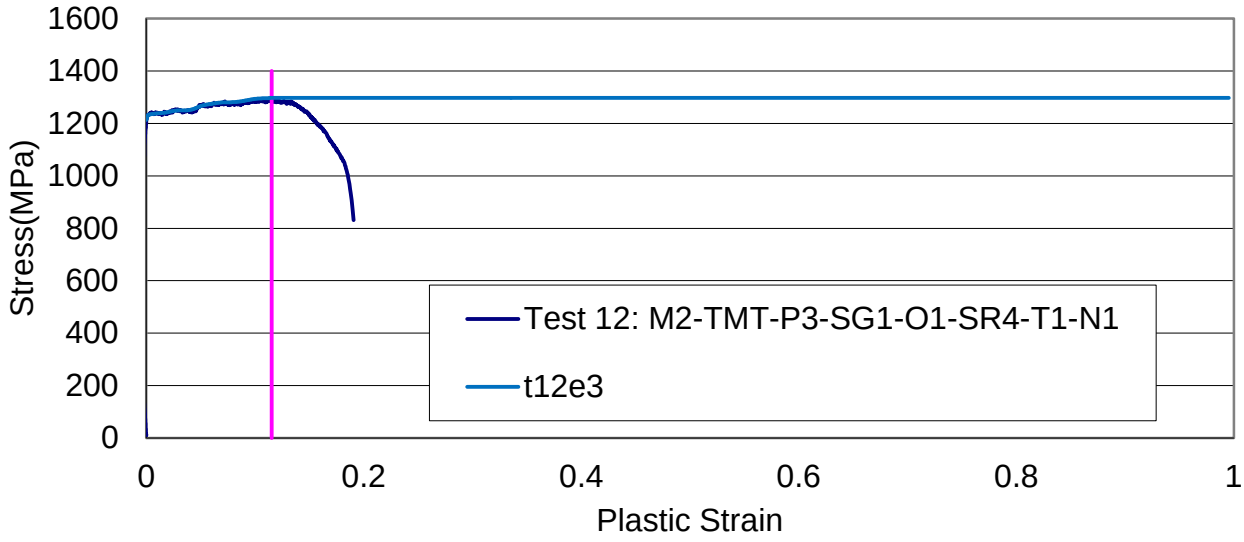

Figure D.42. Eyeball smoothed hardening curve cut at maximum stress (Test 12: M2-TMT-P3-SG1-O1-SR4-T1-N1)

Next, the hardening curve was cut at the maximum (corresponding to a plastic strain of 0.1152) and extrapolated using a value of n = 0.15. To achieve a hardening curve that is convex downward in the extrapolated region, the initial hardening modulus was chosen equal to the maximum stress (1300 MPa). The parameters ε_e and k were then calculated and the hardening curve was extrapolated (for the complete set of parameters, see table D.8). This extrapolation gives the curve t12e9 (see figure D.43).

Table D.8. First extrapolation parameters (Test 12: M2-TMT-P3-SG1-O1-SR4-T1-N1)

Processed Curve	A (neck stress)	B (neck plastic strain)	C (neck slope)	n (guess)	k	ε_e	Result Curve
t12e3	1296.8	0.11521	1300	0.15	1724.328	0.034421	t12e3_9

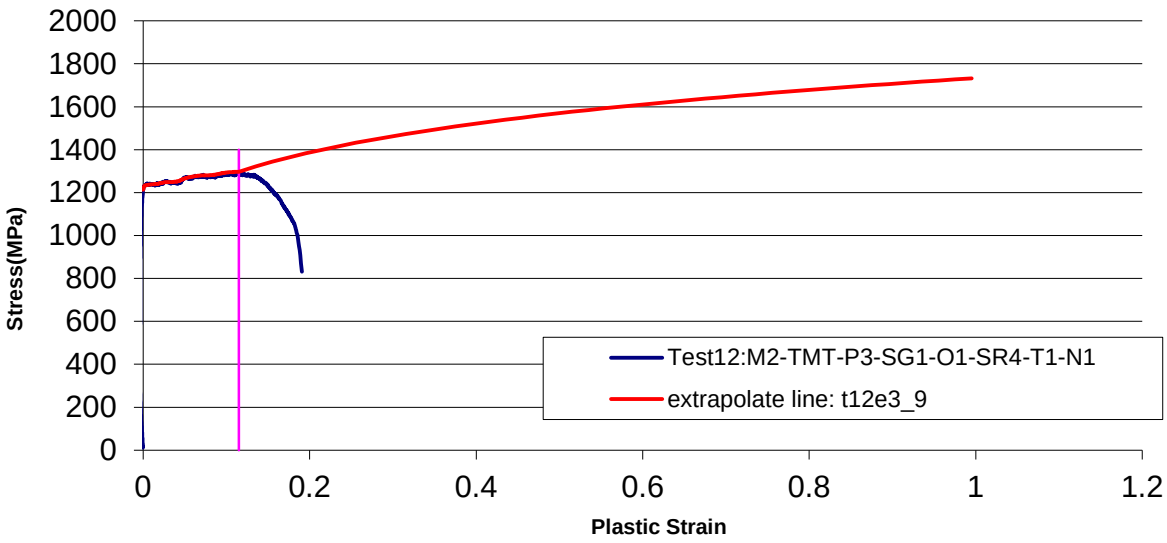

Figure D.43. Extrapolated hardening curve t12e39
(Test 12: M2-TMT-P3-SG1-O1-SR4-T1-N1)

The generated hardening curve was then entered into an LS-DYNA *MAT_224 input deck and a simulation of the tensile test was performed. In this model, the sample dimensions match the sample of Test 12: M2-TMT-P3-SG1-O1-SR4-T1-N7 exactly: width = 2.1082 mm and thickness = 0.6858 mm. As before, two nodal points—188 and 18120, corresponding to the base points of the extensometer—were stored in the NODOUT file (see figure D.44). An across-plot of this elongation with the cross-sectional force is directly compared to the force displacement curve from the test. Results shown in figure D.45 show that curve t12e3_9 gives a close match between test and simulation in terms of force displacement.

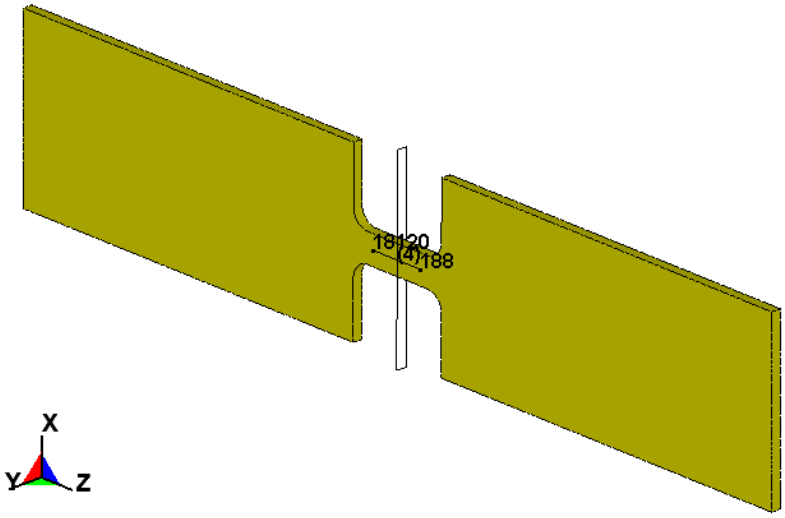

Figure D.44. FE model of tensile specimen (Test 12: M2-TMT-P3-SG1-O1-SR4-T1-N1)

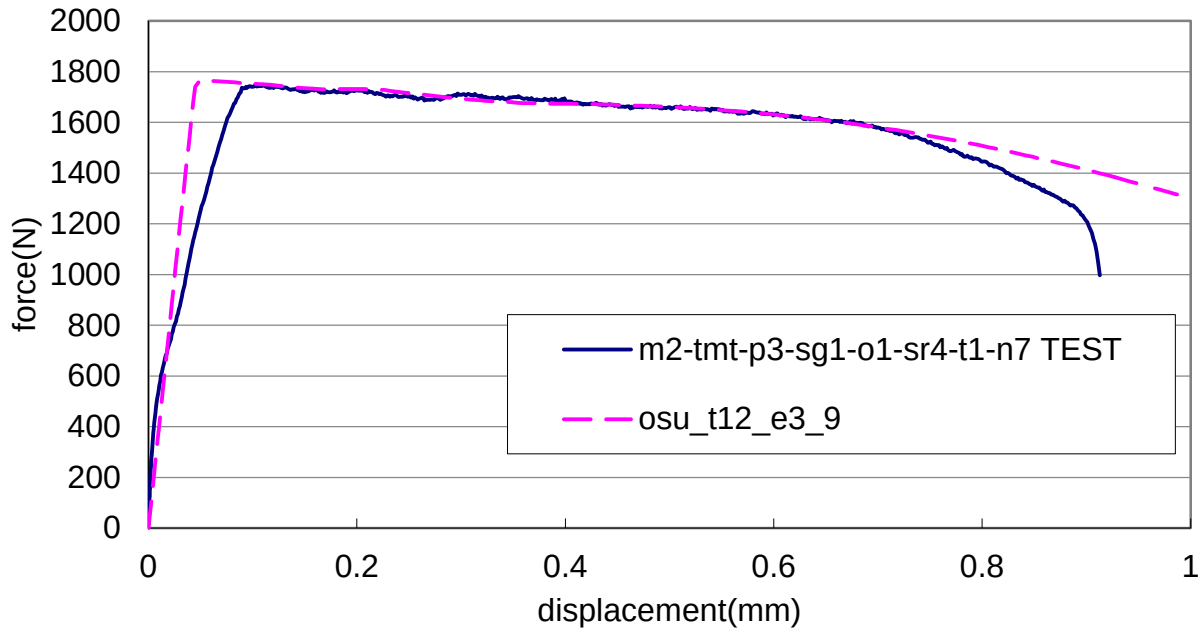

Figure D.45. Force displacement result of curve t12e3_9 and Test 12: M2-TMT-P3-SG1-O1-SR4-T1-N1

To further improve the result, a second extrapolation was performed on curve t12e3_9. The hardening curve was cut off at plastic strain ("necking" strain) B = 0.37521. A value of 0.000015 was chosen for *n*, and the remaining two parameters then used the method described in this section (the extrapolation parameters are listed in table D.9). The resulting hardening curve is called t12e3_10 (see figure D.46). The force displacement comparison between the simulation based on this second extrapolation and the test result is shown in figure D.47.

Table D.9. Second extrapolation parameters (Test 12: M2-TMT-P3-SG1-O1-SR4-T1-N1)

Processed Curve	A (neck stress)	B (neck plastic strain)	C (neck slope)	*n* (guess)	*k*	ε_e	Result Curve
t12e39	1508.26881	0.37521	1300	0.000015	1508.517	-0.375193	t12e310

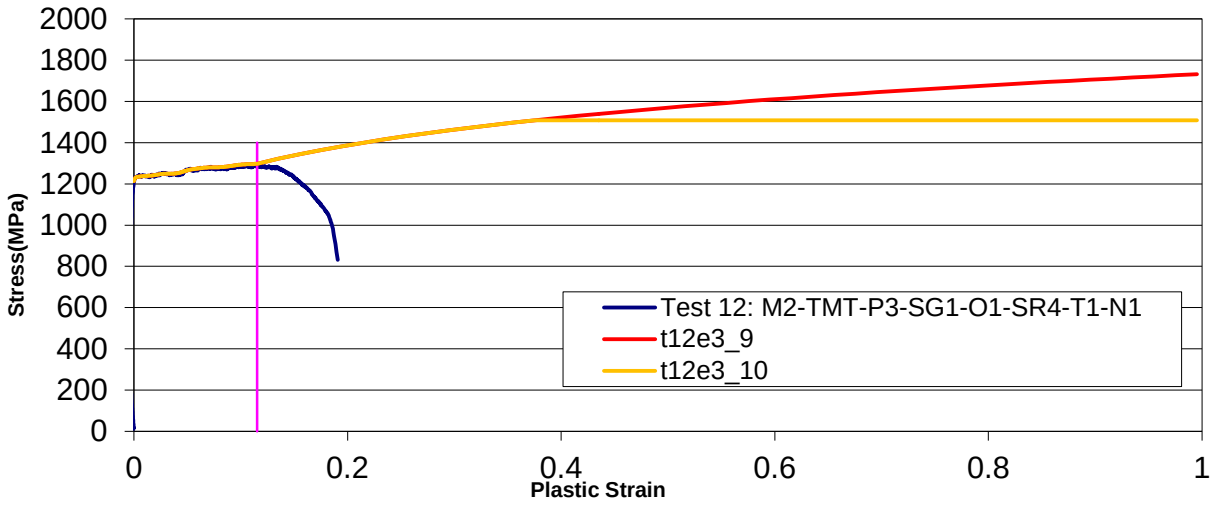

Figure D.46. Extrapolated hardening curve t12e3_10
(Test 12: M2-TMT-P3-SG1-O1-SR4-T1-N1)

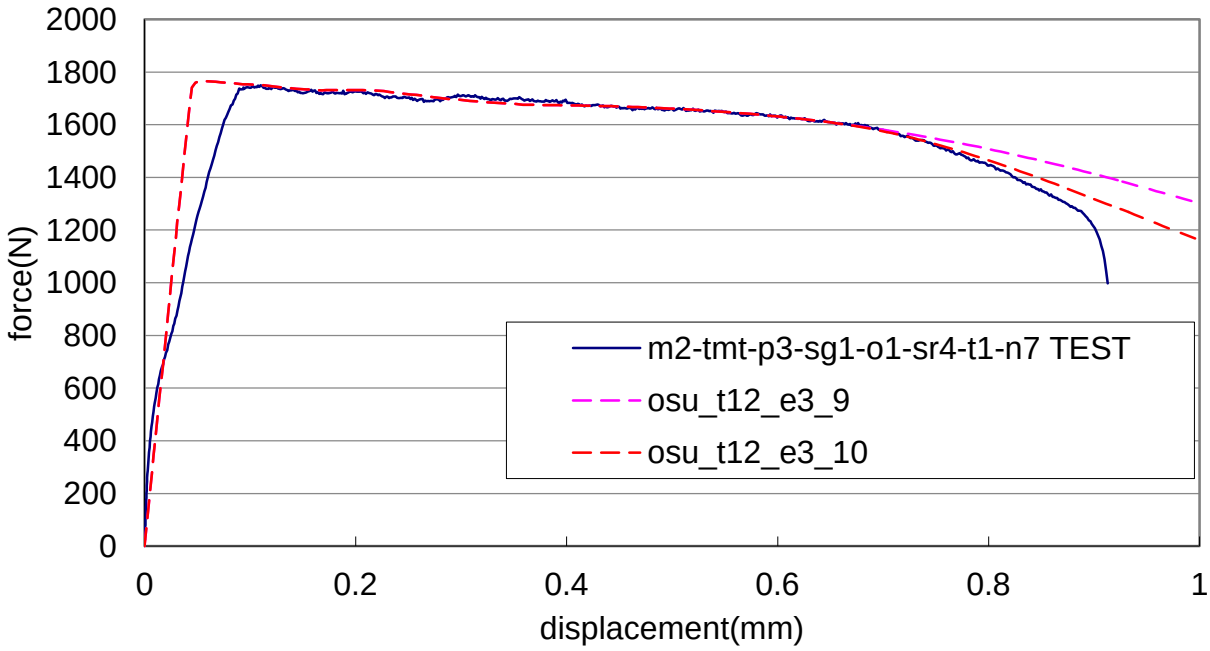

Figure D.47. Force displacement result of curve t12e3_10 and
Test 12: M2-TMT-P3-SG1-O1-SR4-T1-N1

It is noted that, at the beginning of the force displacement curve, the simulation deviates away from the test. This is caused by the Young's modulus mismatch.

The Young's modulus from the split-Hopkinson bar test is inaccurate because the specimen is not in dynamic equilibrium. Essentially, the force on one side of the sample is not equal to the force on the other. This happens because it takes a finite time for the loading wave to propagate through the sample. Once dynamic equilibrium is achieved, the force (engineering stress) data

are accurate. However, they are not accurate beforehand. Therefore, the Young's modulus is determined from static tests on tension samples instrumented with strain gages. It is commonly accepted that most metals do not have rate-sensitive moduli.

This gap is minimized by setting the Young's modulus equal to 55 GPa (see figure D.48), which comes from calculating the slope of the elastic region of the test curve. However, as of this writing, the Young's modulus in *MAT_224 is not dependent on strain rate or temperature, and only one scalar value can be set for all the strain rate input curves. Therefore, a Young's modulus value of 110 Gpa was used for all simulations.

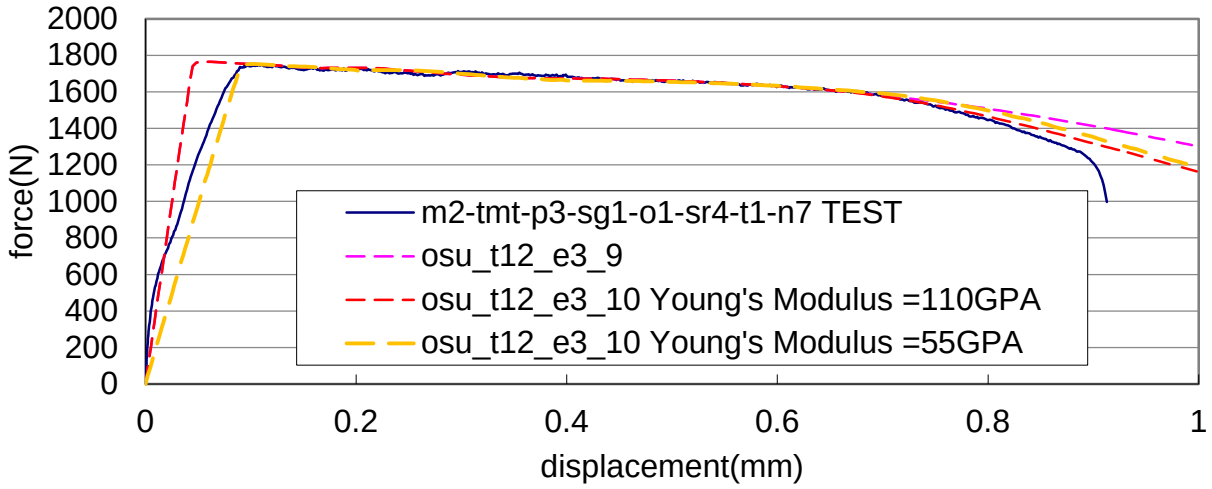

Figure D.48. Force displacement result of curve t12e3_10 with different Young's modulus input (Test 12: M2-TMT-P3-SG1-O1-SR4-T1-N1)

In summary, the final hardening curve for strain rate 500 sec^{-1} and the corresponding force displacement curve from test and simulation are shown in figure D.49. In figure D.50, a contour of 1st principal strain generated by LS_PREPOST is compared to the DIC image from the test at the corresponding time.

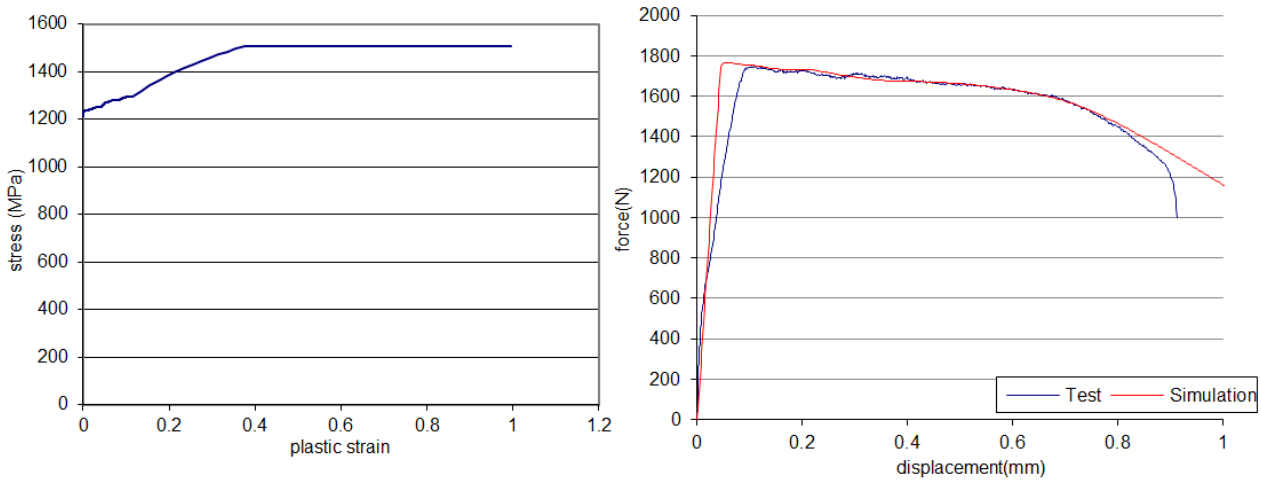

(a) (b)

Figure D.49. The (a) simulation plastic strain versus stress input and (b) force versus displacement comparison of simulation and test (Test 12: M2-TMT-P3-SG1-O1-SR3-T1-N5; strain rate = 1 sec^{-1})

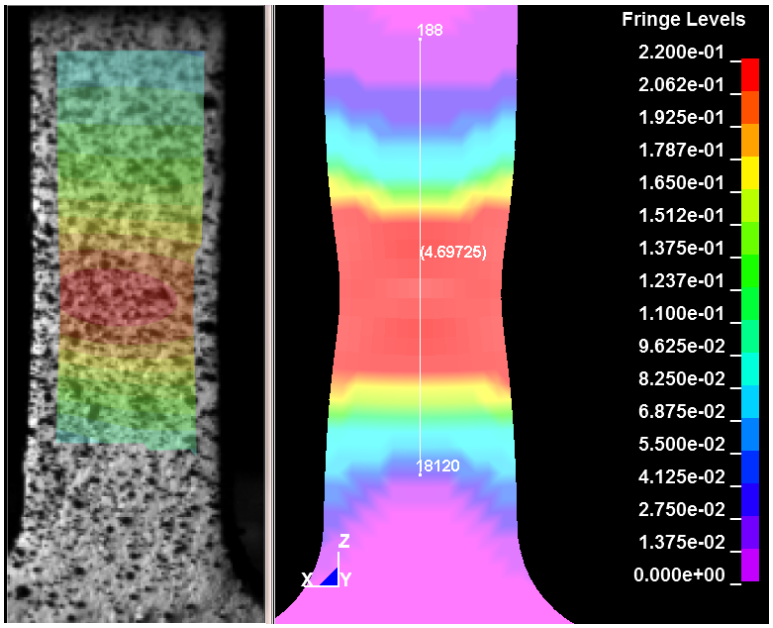

(a) (b)

Figure D.50. The (a) plastic strain DIC image at displacement = 0.69 and (b) simulation contour at displacement = 0.69 (Test 12: M2-TMT-P3-SG1-O1-SR4-T1-N1; strain rate = 500 sec^{-1})

In these simulations, some difference between the test and analysis is evident and is related to the difference in the Young's modulus not being strain rate dependent in the *MAT_224 model. Therefore, we fixed the Young's modulus to the literature value of 110 GPa for all simulations.

D.2.2.5 Stress-strain relation of strain rate 1000 sec^{-1}

The three tests at strain rate 1000 sec^{-1} are listed in table D.10. The force displacement relationship of these tests is shown in figure D.51. The engineering strain versus stress relation was derived and gives the engineering stress-strain curves in figure D.52. The engineering stress-strain relationship was converted to the true stress-strain relationship. The smoothed average of Test 13: M2-TMT-P3-SG1-O1-SR5-T1-N1 and Test 15: M2-TMT-P3-SG1-O1-SR5-T1-N4 was chosen to represent this group of data and undergo further processing. The smoothing method was to apply a 9-point moving average to the combined data followed by a 5-point moving average, a 160-point moving average, and another 5-point moving average. The details were stored in the file: ti_b32_combine.m. The smoothing procedure, an engineering judgment, terminated upon visual inspection of the smoothed and unsmoothed curves shown in figure D.53. As mentioned in section D.2.2.2, the candidate input curve should match the force displacement of both tests simultaneously.

Table D.10. Strain rate dependence series data of strain rate = 1000 sec^{-1}

Test Series	Test Name	Plate Stock	Specimen Geometry	Specimen Orientation	Strain Rate (1/s)	Temp (˚C)
Tension Strain Rate Dependence	M2-TMT-P3-SG1-O1-SR5-T1-N1	0.25"	Flat Dogbone	Rolled	1.3E4	RT
	M2-TMT-P3-SG1-O1-SR5-T1-N3	0.25"	Flat Dogbone	Rolled	1.8E3	RT
	M2-TMT-P3-SG1-O1-SR5-T1-N4	0.25"	Flat Dogbone	Rolled	1.4E3	RT

RT = room temperature

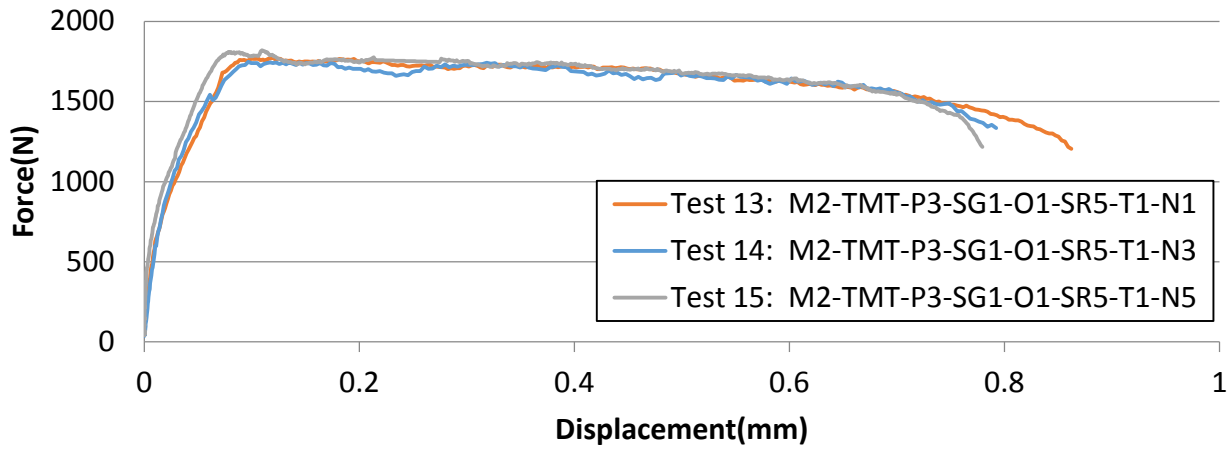

Figure D.51. Force displacement relation of all strain rate = 1000 sec^{-1} tests

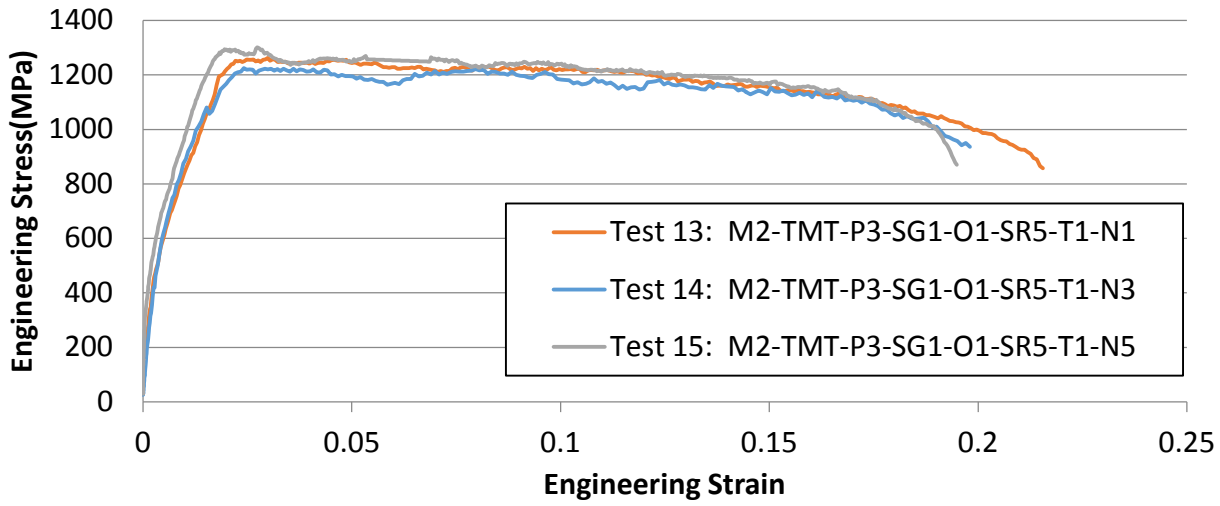

Figure D.52. Engineering stress-strain relation of strain rate = 1000 sec^{-1} tests

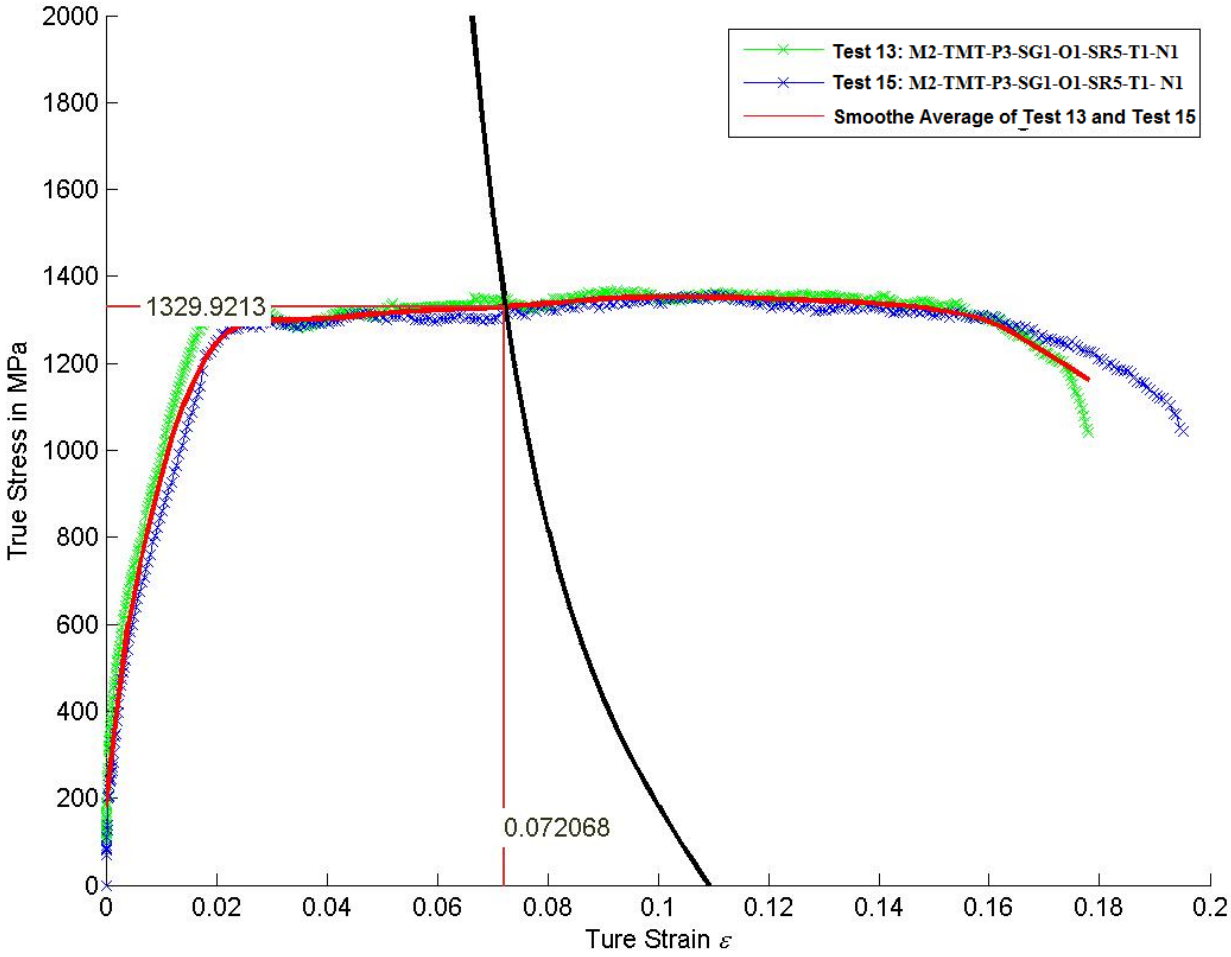

Figure D.53. Smoothed average of Test 13: M2-TMT-P3-SG1-O1-SR5-T1-N1 and Test 15: M2-TMT-P3-SG1-O1-SR5-T1-N1, including necking point judgment

To determine the necking point, the true stress was differentiated with respect to strain to obtain the tangent modulus curve. The intersection between the tangent modulus curve and the true stress curve defines the necking point (see figure D.53). The true stress and true strain at necking were recorded. The corresponding plastic strain at necking was computed using [21]. Figure D.53 was generated using MATLAB. For the reason addressed in section D.2.2.4, a smaller Young's modulus must be adopted to avoid having the hardening curve go negative. The plastic strain versus stress relation was calculated by adopting the Young's modulus of 66 GPa, as shown in figure D.54. The Young's modulus of 66 GPa is calculated from the slope of the stress-strain elastic region of the test data.

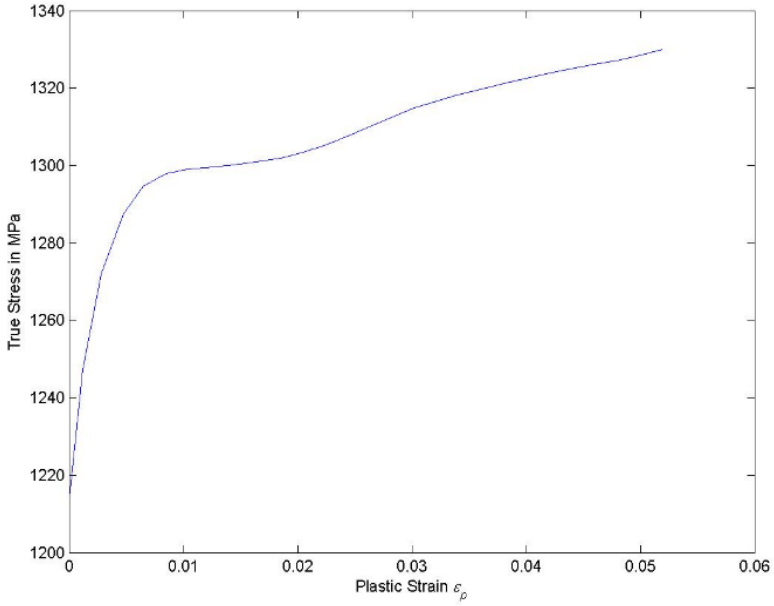

Figure D.54. Plastic strains versus stress of smoothed average of Test 13: M2-TMT-P3-SG1-O1-SR5-T1-N1 and Test 15: M2-TMT-P3-SG1-O1-SR5-T1-N1

Only the part of the hardening curve before necking was retained. Beyond necking, the hardening curve is extrapolated. Twenty-eight curves were generated by varying the exponent *n* between ~0.017 and 0.029 (see figure D.55).

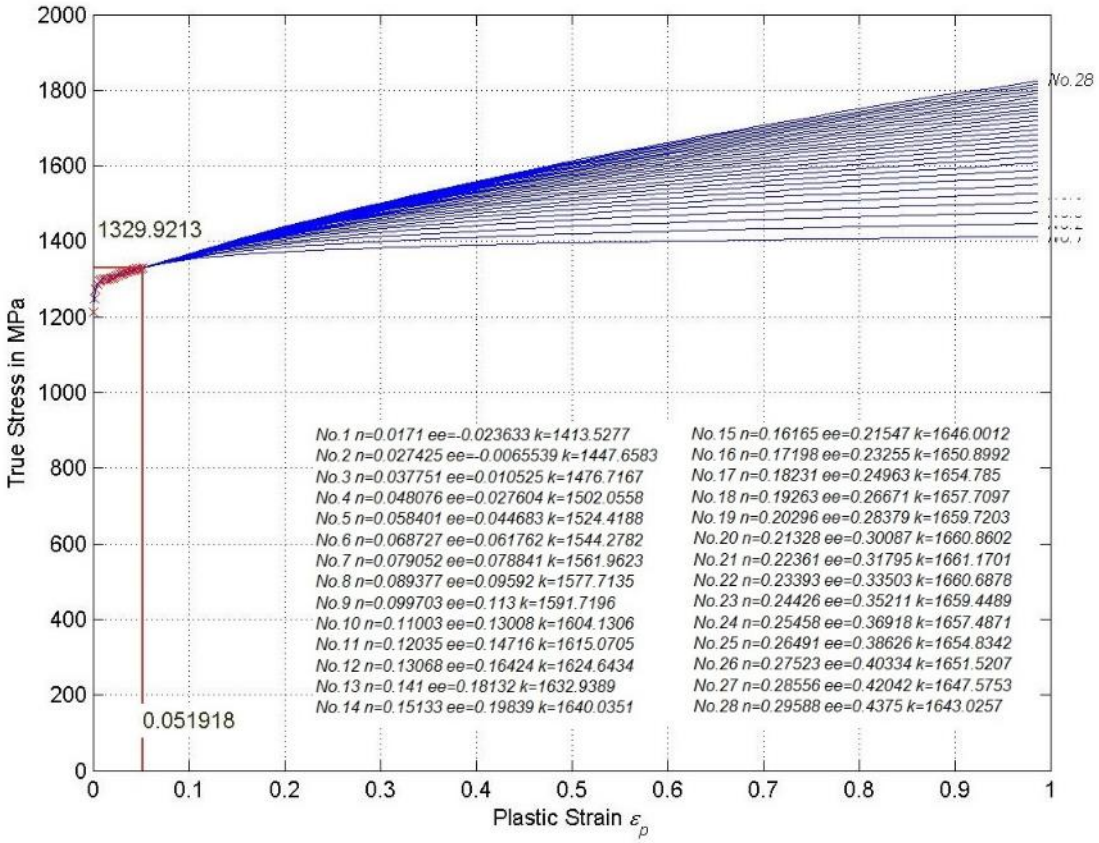

Figure D.55. Step 1: plastic strain versus stress extrapolated input of strain rate = 1000 sec-1

The 28 values of n were obtained by non-uniform incremental steps. The other two parameters, ε_e and k, were calculated. Extrapolation was performed using MATLAB. Each of the generated hardening curves was entered into an LS-DYNA *MAT_224 input deck and a simulation of the tensile Test 13: M2-TMT-P3-SG1-O1-SR5-T1-N1 was performed. In this model, the sample dimensions match the sample of Test 13: M2-TMT-P3-SG1-O1-SR5-T1-N1 exactly: width = 2.06502mm and thickness = 0.68072mm. Two nodal points, Node 515384 and Node 488602, were stored in the NODOUT file (see figure D.56) and a cross-plot of elongation with the cross-sectional force was directly compared to the force-displacement curve from the test. The results in figure D.57 show that curve #28 gives a close match between Test 13 and simulation in terms of force displacement. The extrapolation parameters of curve #28 are $n = 0.29588$, $\varepsilon_e = 0.4375$, and $k = 1643.0257$.

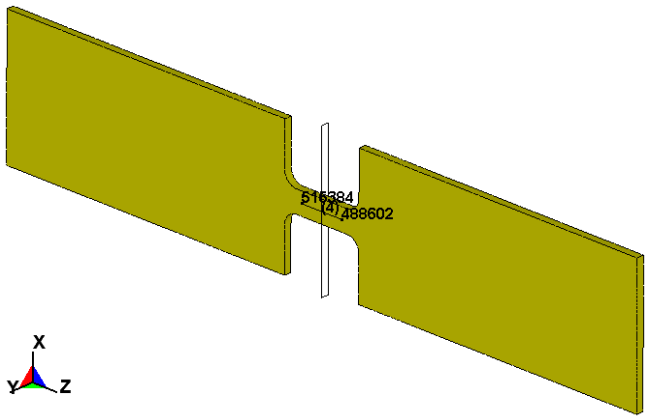

Figure D.56. FE model of tensile specimen (Test 13: M2-TMT-P3-SG1-O1-SR5-T1-N1)

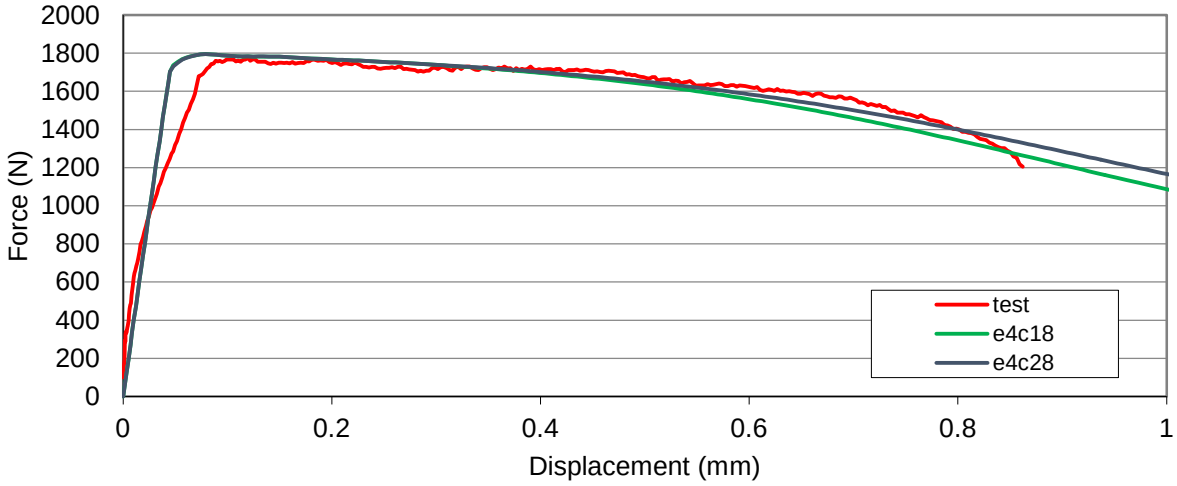

Figure D.57. Force displacement result of curve #28
(Test 13: M2-TMT-P3-SG1-O1-SR5-T1-N1)

To further improve the result, a second extrapolation was performed on Curve #28. The hardening curve was cut off at a plastic strain ("necking" strain) of B = 0.092068. A value of 0.11 was chosen for *n* and the remaining two parameters were then computed using [25]. The curve was then extrapolated. The extrapolation parameters are listed in table D.11. The resulting hardening curve is shown in figure D.58. The force-displacement comparison between the simulation based on this second extrapolation and the test result is shown in figure D.59.

Table D.11. Extrapolation parameters of curve t13_e4_c28_iter8 of Test 13

Original Curve	A (neck stress)	B (neck plastic strain)	C (neck slope)	*n* (guess)	*k*	ε_e	Result Curve
t13_e4_c28	1361.3	0.092068	1300	0.11	1726.631	0.023119	t13_e4_c28_iter8

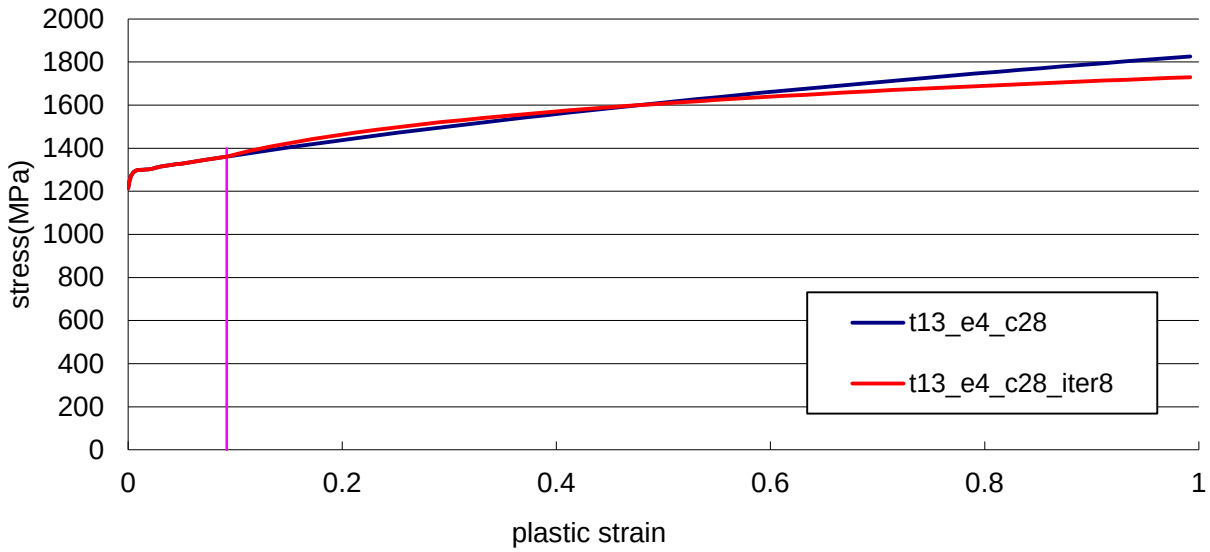

Figure D.58. Extrapolated hardening curve t13_e4_c28_iter8
(Test 12: M2-TMT-P3-SG1-O1-SR5-T1-N1)

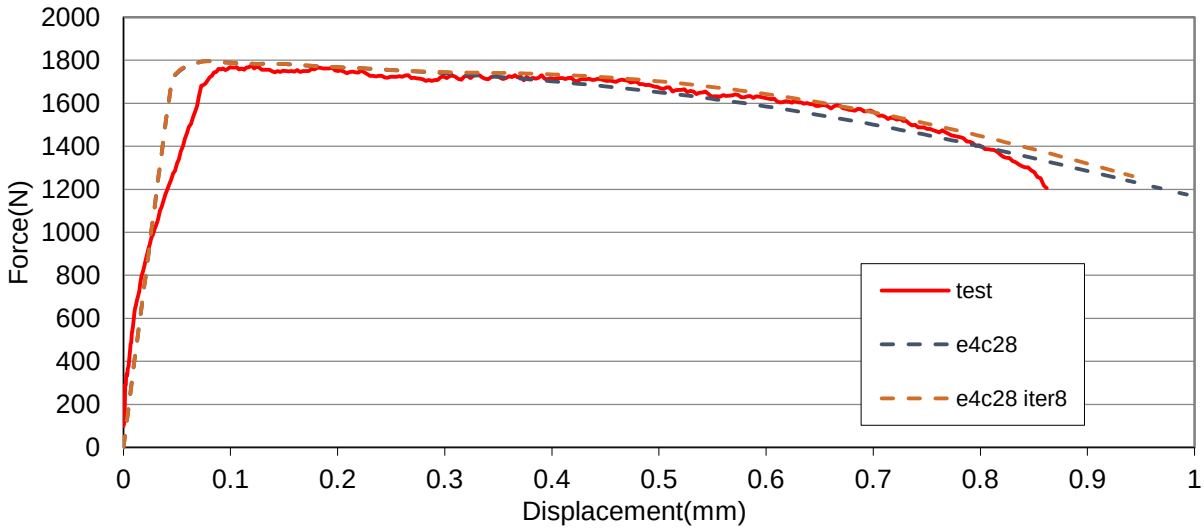

Figure D.59. Force displacement result of curve e4c28_iter8
(Test 12: M2-TMT-P3-SG1-O1-SR5-T1-N1)

A third extrapolation on the hardening curve was performed to further increase the accuracy. The hardening curve was cut off at a plastic strain ("necking" strain) of B = 0.49207. A value of 0.001 was chosen for *n*, and the remaining two parameters were then computed. The extrapolation parameters are listed in table D.12. The resulting hardening curve is called curve t13_e4_c28_iter12 (see figure D.60). The force displacement comparison between the simulation based on this third extrapolation and the test result is shown in figure D.61.

Table D.12. Extrapolation parameter of curve t13_e4_c28_iter12 of Test 13

Original Curve	A (neck stress)	B (neck plastic strain)	C (neck slope)	*n* (guess)	*k*	ε_e	Result Curve
t13_e4_c28_iter8	1605.1507	0.49207	1300	0.001	1615.936	-0.4908	t13_e4_c28_iter12

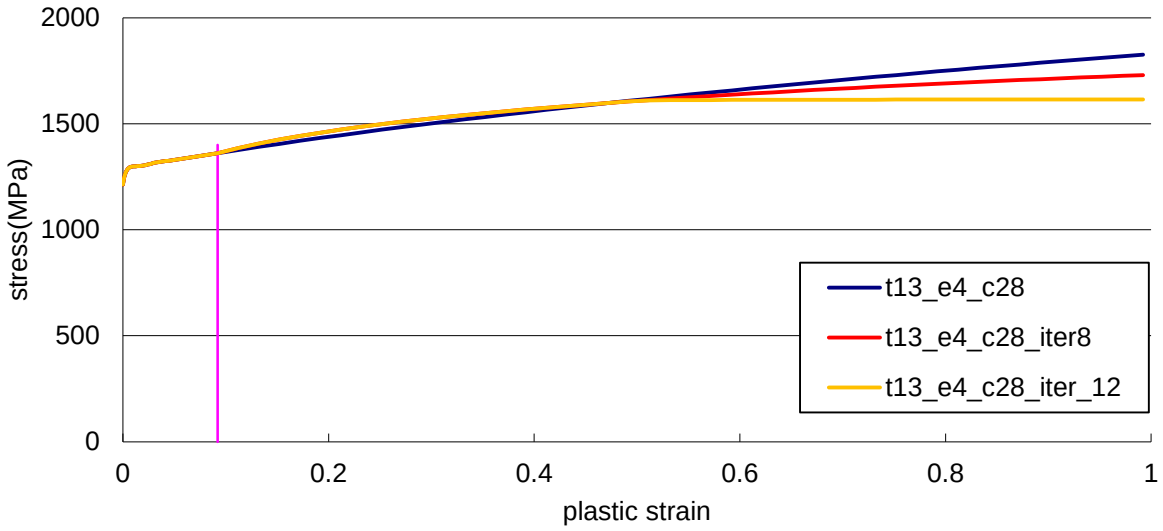

Figure D.60. Extrapolated hardening of curve t13_e4_c28_iter12 (Test 13: M2-TMT-P3-SG1-O1-SR5-T1-N1)

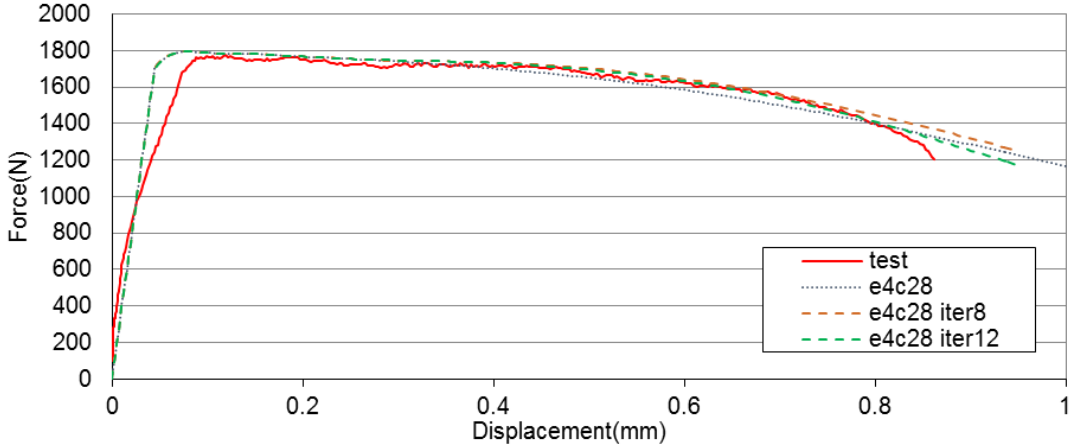

Figure D.61. Force displacement result of curve t13_e4_c28_iter12 (Test13: M2-T MT-P3-SG1-O1-SR5-T1-N1)

In summary, the final hardening curve for strain rate 1000 sec^{-1} and corresponding force displacement curve from test and simulation are shown in figure D.62. In figure D.63, a contour of 1st principal strain generated by LS_PrePost is presented.

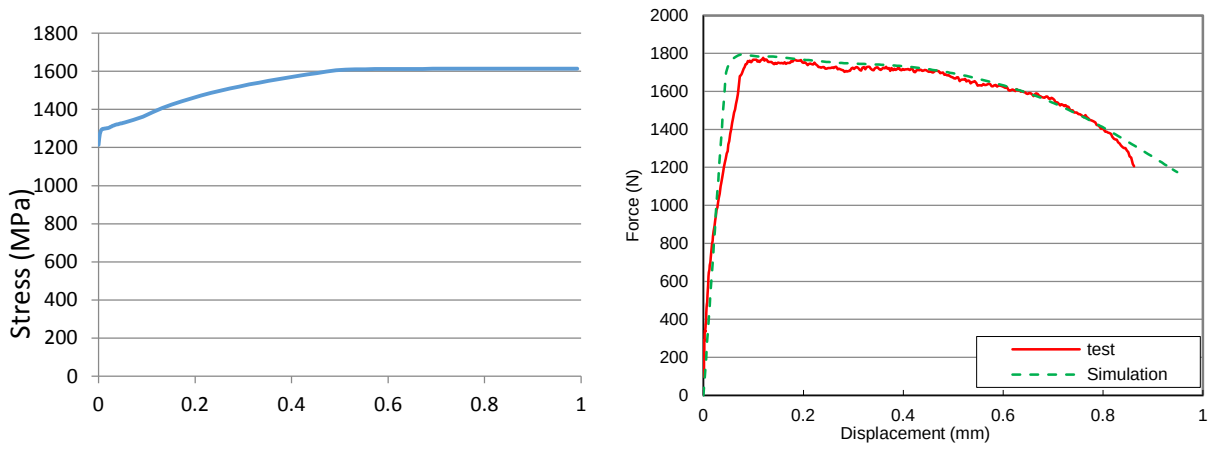

(a) (b)

Figure D.62. The (a) simulation plastic strain versus stress input and (b) force versus displacement comparison of simulation and test (Test ID: M2-TMT-P3-SG1-O1-SR5-T1-N; strain rate = 1000 sec-1)

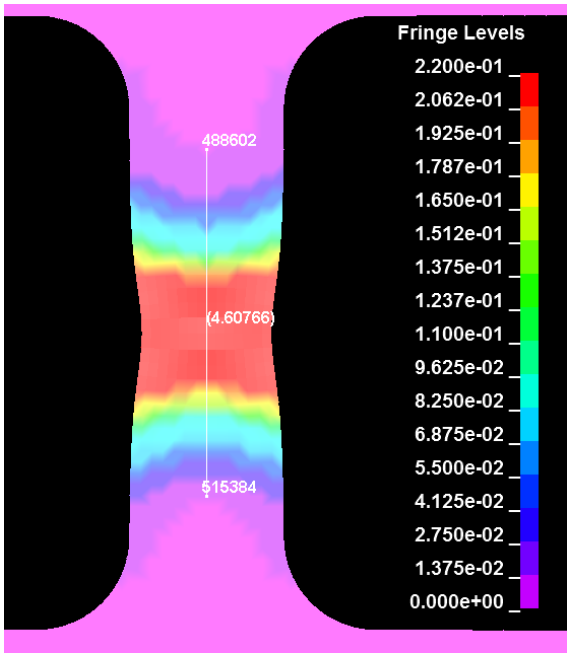

Figure D.63. Simulation contour at displacement = 0.60 (Test 15: M2-TMT-P3-SG1-O1-SR5-T1-N1; strain rate = 1000 sec-1)

To verify this result, Test 15: M2-TMT-P3-SG1-O1-SR2-T1-N4 was simulated with the same hardening curve derived from Test 13. In this model, the sample dimensions match the sample of Test 15, M2-TMT-P3-SG1-O1-SR5-T1-N4, exactly: width = 2.03962mm and thickness = 0.6858mm. The result is a close match in terms of force displacement and 1st principal strain contour, as shown in figures D.64 and D.65.

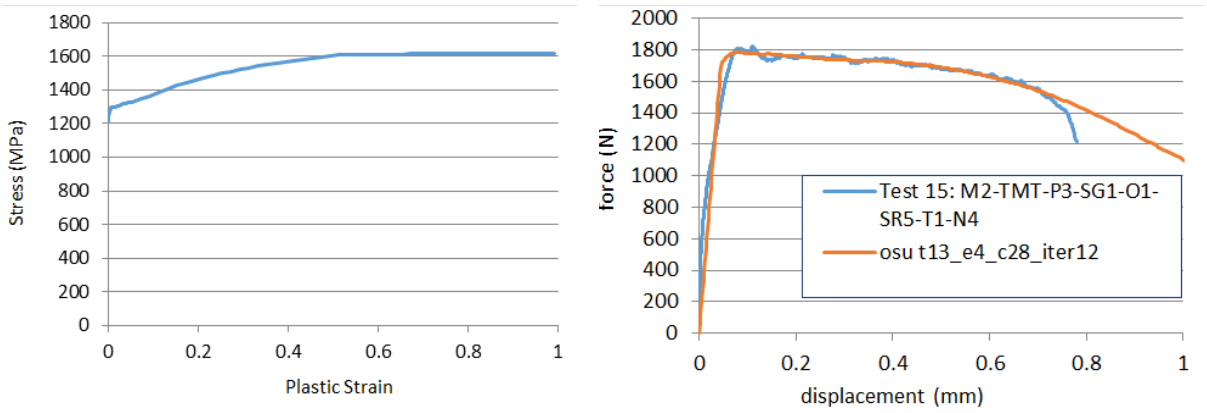

(a) (b)

Figure D.64. The (a) simulation plastic strain versus stress input and (b) force versus displacement comparison of simulation and test (Test 15: M2-TMT-P3-SG1-O1-SR5-T1-N4; strain rate = 1000 sec^{-1})

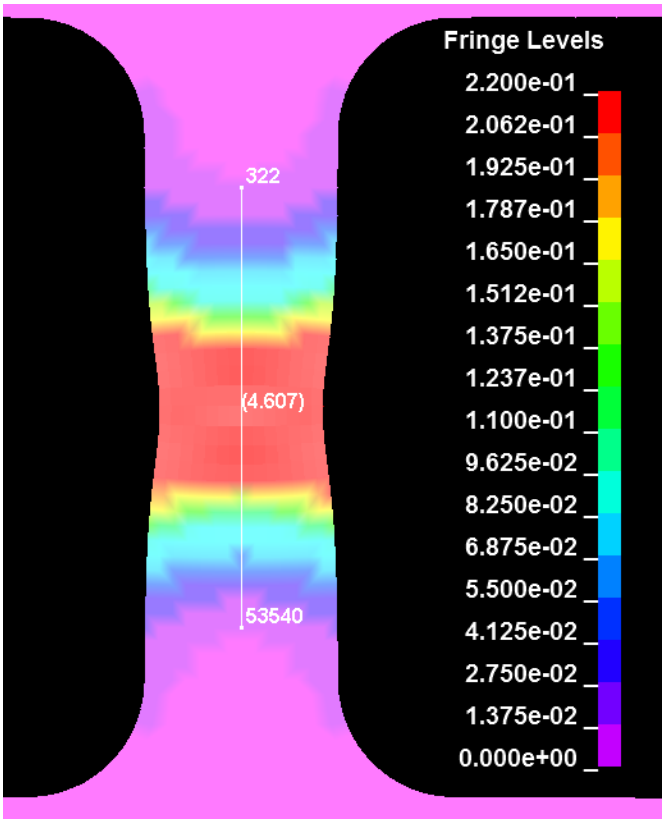

Figure D.65. Plastic strain DIC image at failure moment (Test 15: M2-TMT-P3-SG1-O1-SR5-T1-N4; Strain Rate = 1000 sec^{-1})

D.2.3 STRESS-STRAIN TABULATED INPUT OF MULTIPLE STRAIN RATES

After the hardening curves of all strain rates were summarized, the next step was to modify the nominal strain rate value in the *MAT_224 for these curves until a set of values gave a good match between the simulations and tests for all strain rates. As discussed in sections 2.3.2, 2.3.3, and appendix A, the strain rate is not a constant during the test. Therefore, the nominal strain rate is not the "real" strain rate of that test. A reverse-engineering method is used to determine the real strain rate of a particular test. The displacement time history in the test data is given as a boundary condition so the specimen is pulled at exactly the same speed in the simulation as in the real test. The local strain rate is, therefore, determined by the computer program. The nominal strain-rate value of each input curve is modified until a set of strain-rate values matches all simulations with test results simultaneously. As indicated by figure D.66, the nominal strain rate 500 sec^{-1} was modified to 650 sec^{-1}, and the nominal strain rate 1000 sec^{-1} was changed to 800 sec^{-1}.

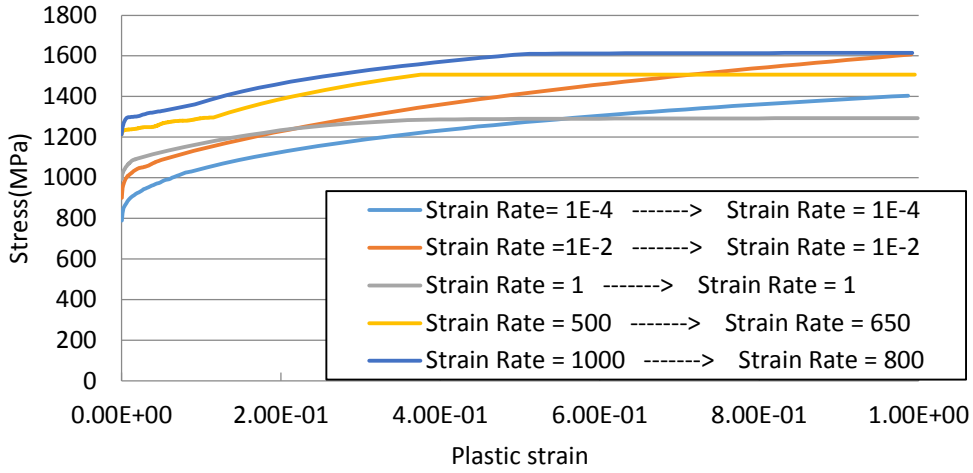

Figure D.66. Plastic strains versus stress curves of multiple strain rate input and their modified strain rates

A new tabulated input deck for *MAT_224 was then created based on the five hardening curves labeled with the new strain-rate values. LS-DYNA simulations were then performed for the tensile tests at nominal strain rates 1 sec^{-1}, 650 sec^{-1}, and 850 sec^{-1}. Unlike previous simulations that applied an arbitrary high loading speed, in these simulations the load speed was applied exactly as it was recorded in the actual experiment. Consequently, the load curve referenced in the "*Boundary_Prescribed_Motion" cards was set to use the displacement versus time curve measured in the test. The results of these simulations are shown in figures D.67–D.69. Because the loading speed of the experiments at nominal strain rates 1E-4 sec^{-1} and 1E-2 sec^{-1} are low, the time span of these tests is fairly long, making it impossible to simulate realistically with the current computing power. Consequently, these experiments were simulated only with a single hardening curve input. Future work may include implicit simulations of the quasistatic experiments using full tabulated input; however, this is currently not possible with *MAT_224, which is implemented in the explicit LS-DYNA only.

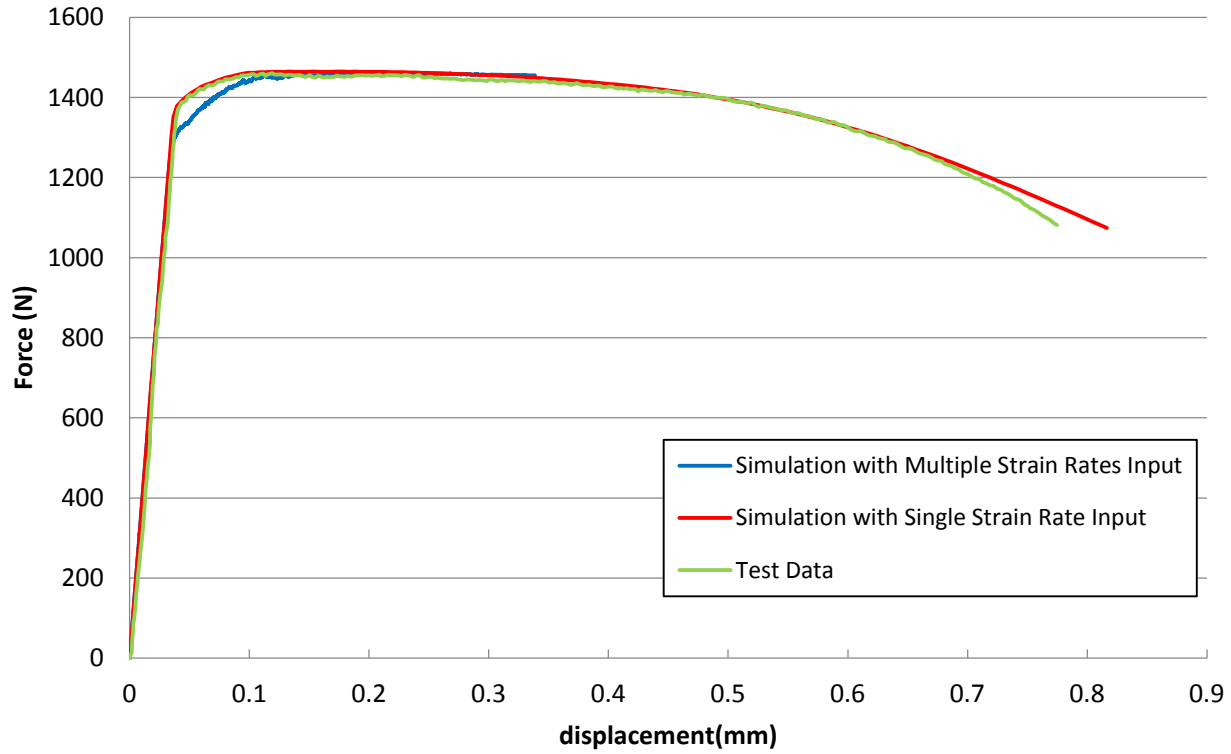

Figure D.67. Force displacement comparisons of tabulated strain rate input and single strain rate input of Test: M2-TMT-P3-SG1-O1-SR3-T1-N5 at nominal strain rate ≈ 1 sec^{-1}

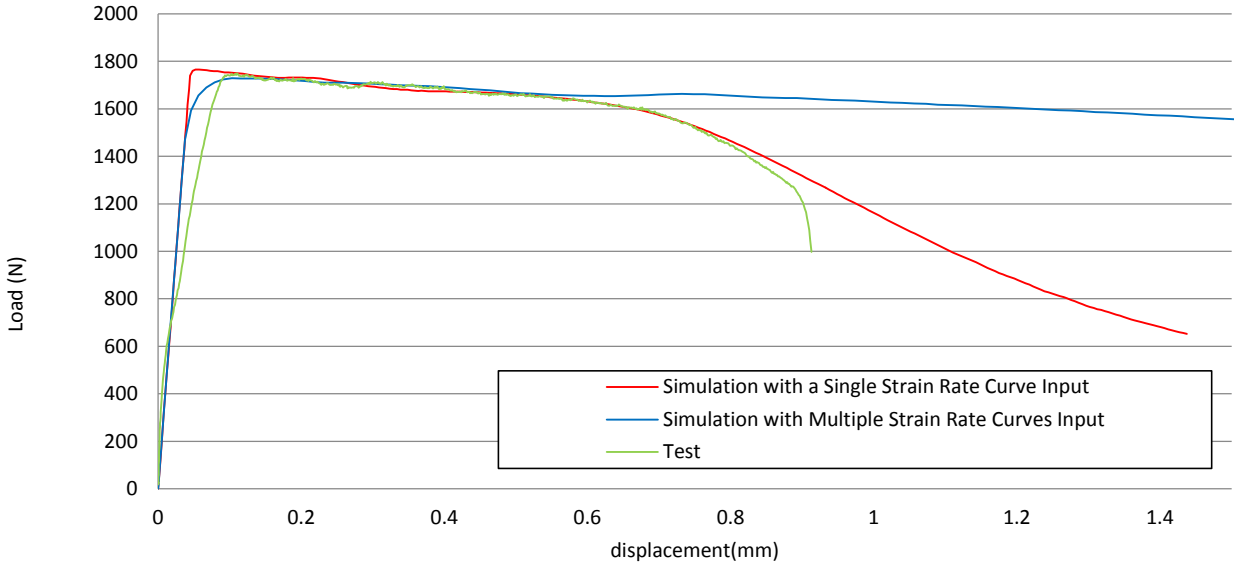

Figure D.68. Force displacement comparisons of tabulated strain rate input simulation and single strain rate input simulation (Test: M2-TMT-P3-SG1-O1-SR4-T1-N7; nominal strain rate ≈ 650 sec^{-1})

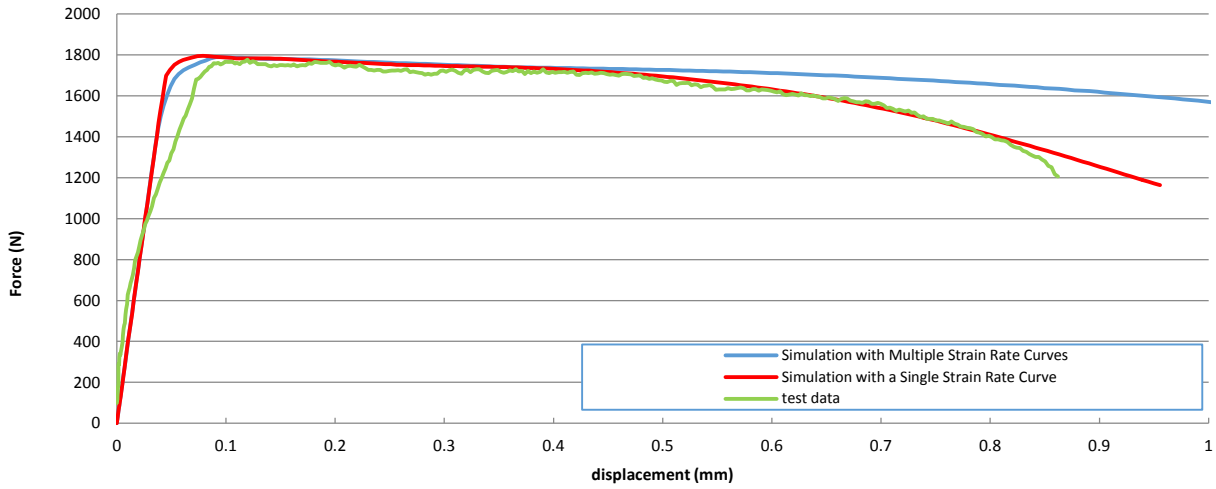

Figure D.69. Force displacement comparison with tabulated strain rate input simulation and single strain rate input simulation (Test: M2-TMT-P3-SG1-O1-SR5-T1-N1; strain rate ≈ 800 sec^{-1})

D.2.4 TENSION ANISOTROPIC EFFECT

Six tests measuring the anisotropy of the material are listed in table D.13. Three different orientations with respect to the rolling direction were selected to manufacture the specimen. The anisotropic effect was studied with an input deck for *MAT_224 based on a single hardening curve (as in section D.2.2) and the displacement was applied using a grip speed of 1 m/s. Because *MAT_224 is an isotropic material law, no directional effects can be taken into account and the simulations were performed only to help judge the importance of the anisotropy in future applications. In these models, the sample dimensions match the sample of the corresponding test exactly. The results show a high directional effect, and the rolled direction is the strongest, as shown in figure D.70. The 1st principal strain contour of DIC (when available) and simulation are shown in figures D.71–D.76.

Table D.13. Anisotropic effect tests

Test Series	Test Name	Plate Stock	Specimen Geometry	Specimen Orientation	Strain Rate (1/s)	Temp (˚C)
Tension Anisotropy	M2-TMT-P3-SG1-O2-SR3-T1-N2	0.25"	Flat	45°	1.2E+0	RT
	M2-TMT-P3-SG1-O2-SR3-T1-N3	0.25"	Flat	45°	1.0E+0	RT
	M2-TMT-P3-SG1-O3-SR3-T1-N2	0.25"	Flat	90°	9.6E-01	RT
	M2-TMT-P3-SG1-O3-SR3-T1-N3	0.25"	Flat	90°	1.0E+0	RT
	M2-TMT-P3-SG1-O4-SR3-T1-N1	0.25"	Flat	135°	9.8E-01	RT
	M2-TMT-P3-SG1-O4-SR3-T1-N2	0.25"	Flat	135°	1.1E+0	RT

RT = room temperature

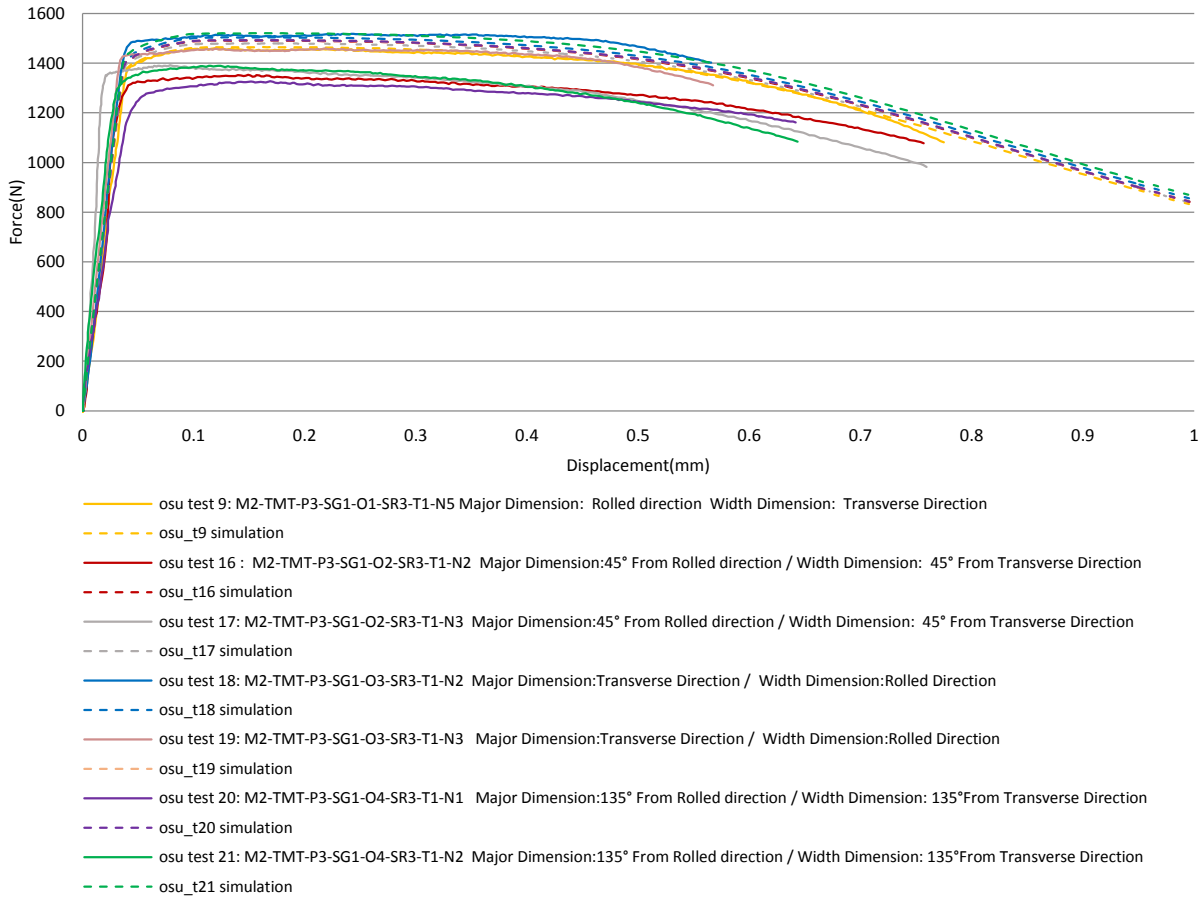

Figure D.70. Anisotropic effect

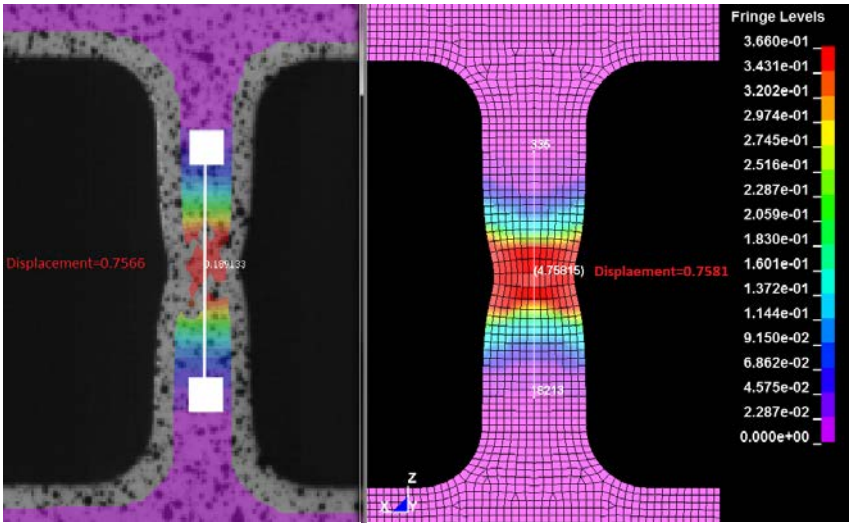

(a) (b)

Figure D.71. The (a) DIC image of 1st principal plastic strain and (b) LS-DYNA contour of 1st principal plastic strain (Test 16: M2-TMT-P3-SG1-O2-SR3-T1-N2; major dimension: 45° from rolled direction; width dimension: 45° from transverse direction)

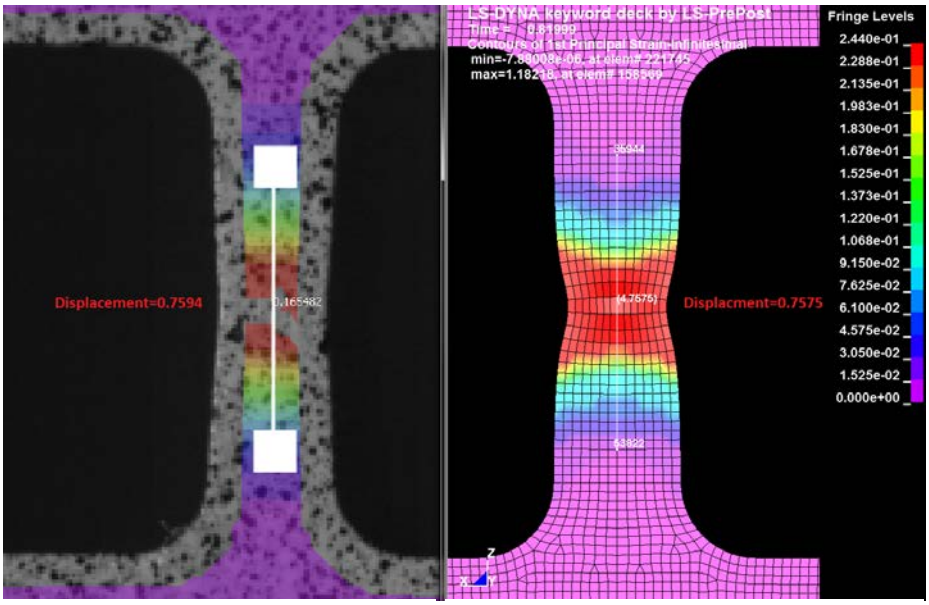

(a) (b)

Figure D.72. The (a) DIC image of 1st principal plastic strain and (b) LS-DYNA contour of 1st principal plastic strain (Test 17: M2-TMT-P3-SG1-O2-SR3-T1-N3; major dimension: 45° from rolled direction; width dimension: 45° from transverse direction)

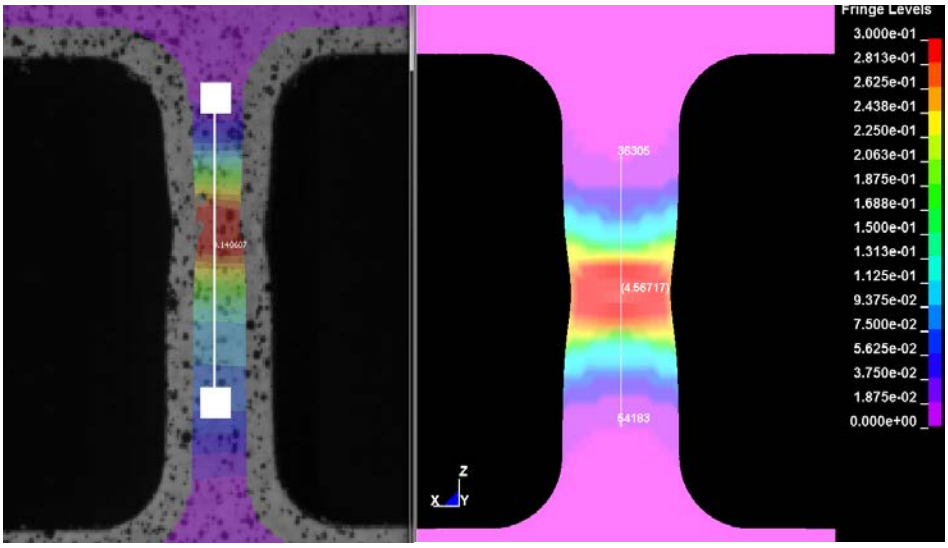

(a) (b)

Figure D.73. The (a) DIC image of 1st principal plastic strain and (b) LS-DYNA contour of 1st principal plastic strain (Test 18: M2-TMT-P3-SG1-O3-SR3-T1-N2; major dimension: transverse direction; width dimension: rolled direction)

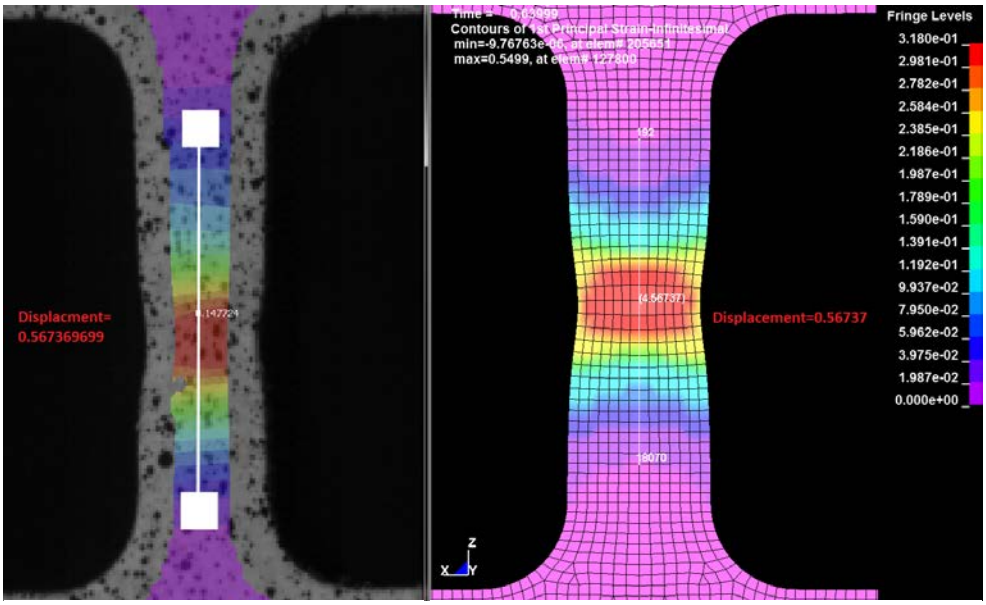

(a) (b)

Figure D.74. The (a) DIC image of 1st principal plastic strain and (b) LS-DYNA contour of 1st principal plastic strain (OSU Test 19: M2-TMT-P3-SG1-O3-SR3-T1-N3; major dimension: transverse direction; width dimension: rolled direction)

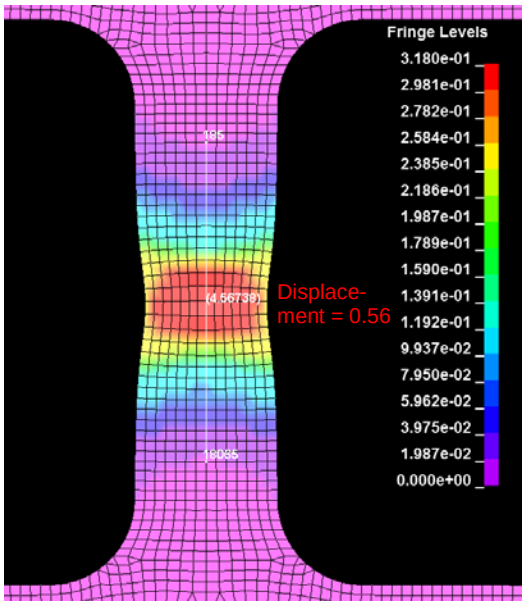

Figure D.75. LS-DYNA contour of 1st principal plastic strain; DIC image not available (OSU Test 20: M2-TMT-P3-SG1-O4-SR3-T1-N1; major dimension: 135° from rolled direction; width dimension: 135° from transverse direction)

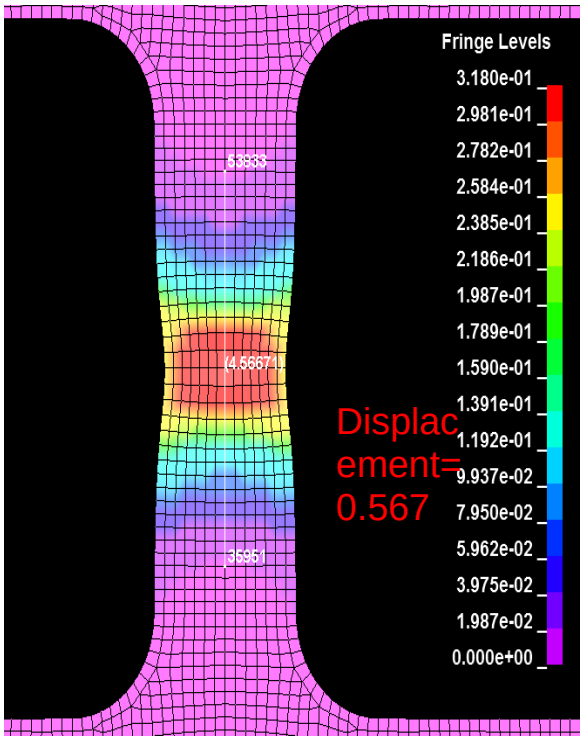

Figure D.76. LS-DYNA contour of 1st principal plastic strain; DIC image not available (OSU Test 21: M2-TMT-P3-SG1-O4-SR3-T1-N2; major dimension: 135° from rolled direction; width dimension: 135° from transverse direction)

D.2.5 TENSION AXISYMMETRIC SPECIMEN COMPARISON

The axisymmetric dogbone tensile tests (see table D.14) were conducted to study the difference in terms of the force displacement between the flat and cylindrical specimen, as shown in figure D.77. This group of experiments was studied with an input deck for *MAT_224 based on a single hardening curve (as in section D.2.2), and the displacement was applied using a grip speed of 1 m/s. In these models, the sample dimensions match the sample of the corresponding test exactly. The 1st principal strain contour of the DIC and simulation are shown in figures D.78–D.81.

Table D.14. Axisymmetric dogbone tests

Test Series	Test Name	Plate Stock	Specimen Geometry	Specimen Orientation	Strain Rate (1/s)	Temp (˚C)
Tension Axisymmetric	M2-TMT-P4-SG5-O1-SR2-T1-N1	0.25"	Axisymmetric	Rolled	2.0E-02	RT
	M2-TMT-P4-SG5-O1-SR2-T1-N2	0.25"	Axisymmetric	Rolled	1.9E-02	RT
	M2-TMT-P4-SG5-O1-SR2-T1-N3	0.25"	Axisymmetric	Rolled	2.1E-02	RT
	M2-TMT-P4-SG5-O1-SR2-T1-N4	0.25"	Axisymmetric	Rolled	1.2E-02	RT

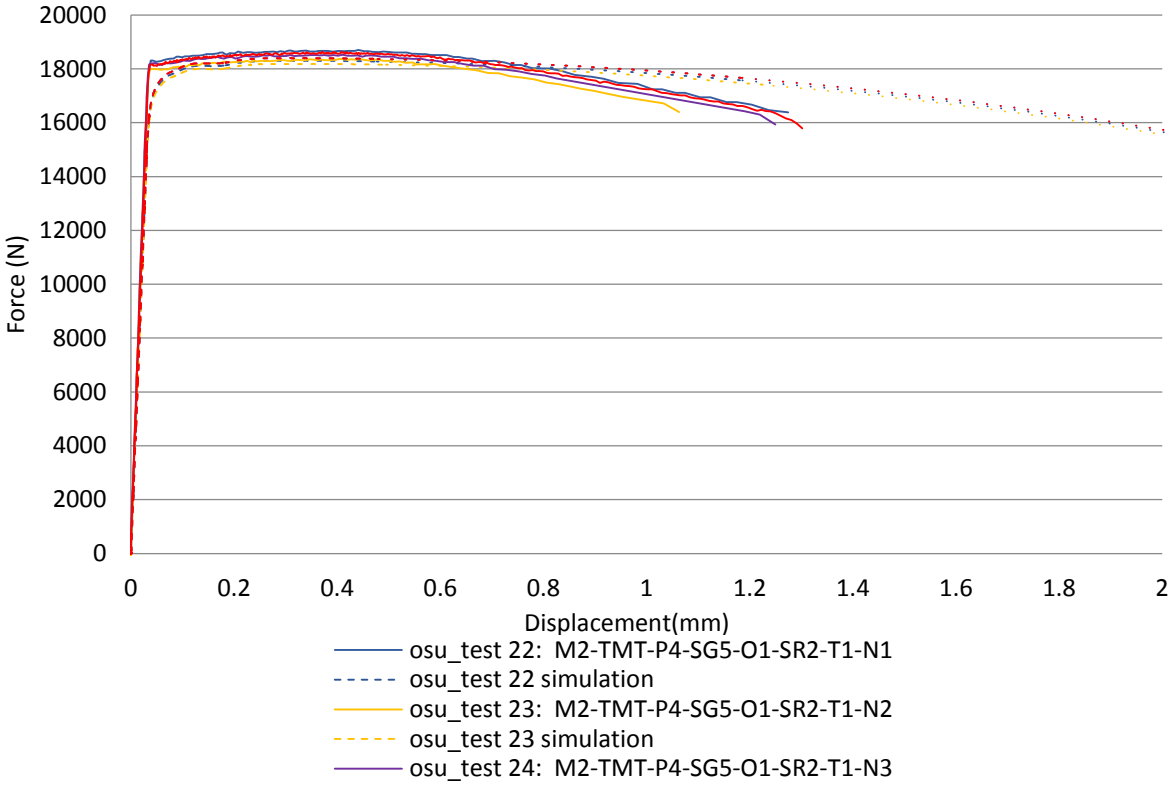

Figure D.77. Axisymmetric dogbone specimen

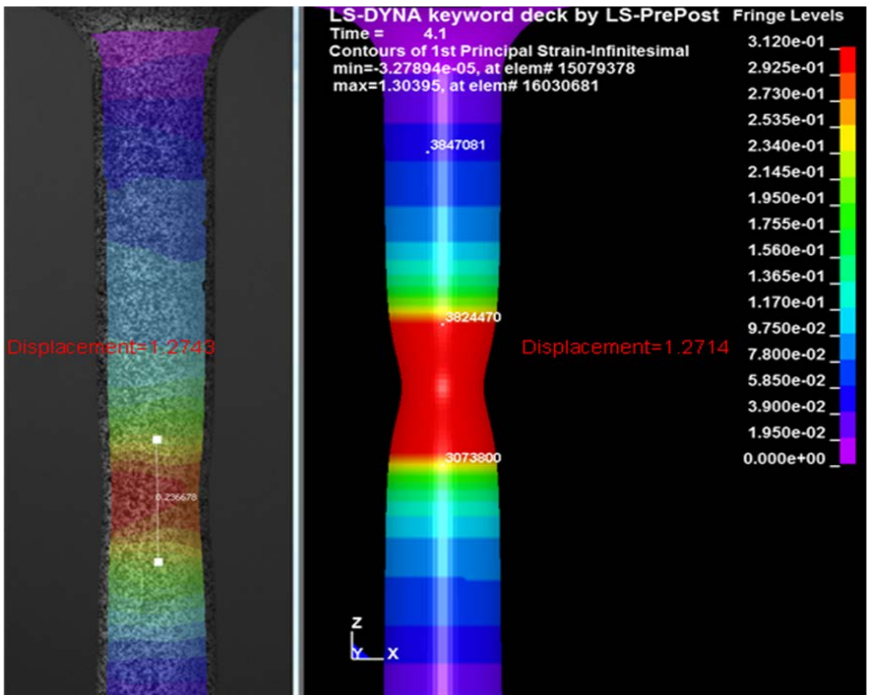

(a) (b)

Figure D.78. The (a) DIC image of 1st principal plastic strain and (b) LS-DYNA contour of 1st principal plastic strain (Test 22: M2-TMT-P4-SG5-O1-SR2-T1-N1; major dimension: rolled direction; strain rate = 0.019 sec^{-1})

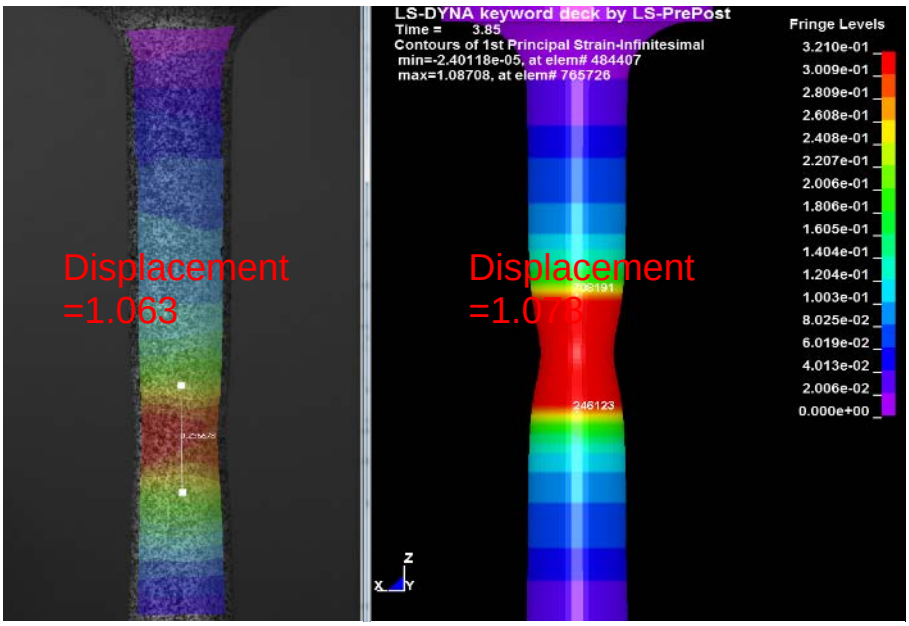

(a) (b)

Figure D.79. The (a) DIC image of 1st principal plastic strain and (b) LS-DYNA contour of 1st principal plastic strain (Test 23: M2-TMT-P4-SG5-O1-SR2-T1-N2; major dimension: rolled direction; strain rate = 0.0187 sec^{-1})

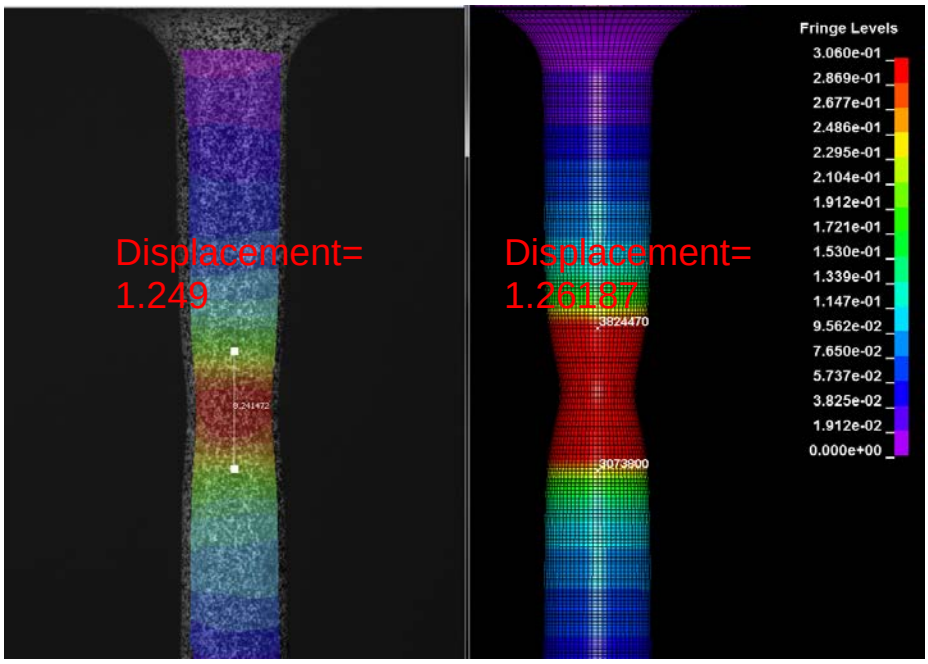

(a) (b)

Figure D.80. The (a) DIC image of 1st principal plastic strain (b) LS-DYNA contour of 1st principal plastic strain (Test 24: M2-TMT-P4-SG5-O1-SR2-T1-N3; major dimension: rolled direction; strain rate = 0.0187 sec^{-1})

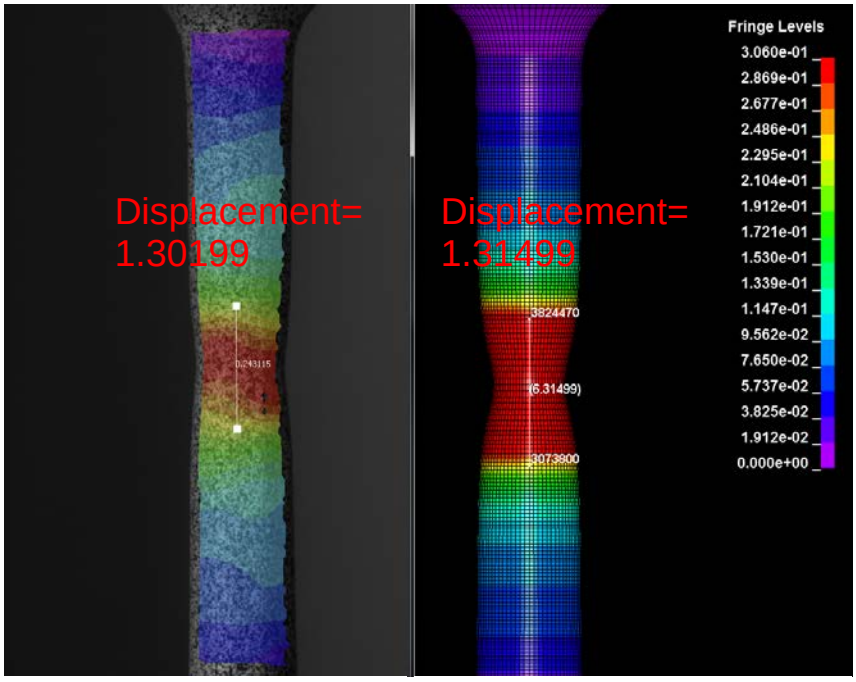

(a) (b)

Figure D.81. The (a) DIC image of 1st principal plastic strain (b) LS-DYNA contour of 1st principal plastic strain (Test 25: M2-TMT-P4-SG5-O1-SR2-T1-N4; major dimension: rolled direction; strain rate = 0.0122 sec^{-1})

D.2.6 COMPRESSION STRAIN RATE DEPENDENCY

The experiments in table D.15 were simulated to verify how well the new material model performs under compressive loading. This group of experiments was studied with an input deck for *MAT_224 based on a single hardening curve (as in section D.2.2) and the displacement speed of 1 m/s was applied at the grip. In these models, the sample dimensions match the sample of the corresponding test exactly. Figures D.82–D.85 show the force displacement relationship for the compression test under different strain rates. Figure D.86 gives a comparison among different strain-rate groups. The material model works better for higher strain rates in compression.

Table D.15. Compression strain rate dependence

Test Series	Test Name	Plate Stock	Specimen Geometry	Specimen Orientation	Strain Rate (1/s)	Temperature (˚C)
Compression Strain Rate Dependence	M2-TMC-P3-SG1-O1-SR1-T1-N1	0.25"	Cylinder	Rolled	6.9E-05	RT
	M2-TMC-P3-SG1-O1-SR1-T1-N2	0.25"	Cylinder	Rolled	6.3E-05	RT
	M2-TMC-P3-SG1-O1-SR1-T1-N3	0.25"	Cylinder	Rolled	8.1E-05	RT
	M2-TMC-P3-SG1-O1-SR2-T1-N1	0.25"	Cylinder	Rolled	6.5E-03	RT
	M2-TMC-P3-SG1-O1-SR2-T1-N3	0.25"	Cylinder	Rolled	6.5E-03	RT
	M2-TMC-P3-SG1-O1-SR2-T1-N4	0.25"	Cylinder	Rolled	6.0E-03	RT
	M2-TMC-P3-SG1-O1-SR3-T1-N2	0.25"	Cylinder	Rolled	7.8E-01	RT
	M2-TMC-P3-SG1-O1-SR3-T1-N4	0.25"	Cylinder	Rolled	6.5E-01	RT
	M2-TMC-P3-SG1-O1-SR3-T1-N5	0.25"	Cylinder	Rolled	7.4E-01	RT
	M2-TMC-P3-SG1-O1-SR4-T1-N5	0.25"	Cylinder	Rolled	1.5E+3	RT
	M2-TMC-P3-SG1-O1-SR4-T1-N6	0.25"	Cylinder	Rolled	1.7E+3	RT
	M2-TMC-P3-SG1-O1-SR4-T1-N1	0.25"	Cylinder	Rolled	1.5E+3	RT
	M2-TMC-P3-SG1-O1-SR5-T1-N4	0.25"	Cylinder	Rolled	2.1E+3	RT
	M2-TMC-P3-SG1-O1-SR5-T1-N5	0.25"	Cylinder	Rolled	3.0E+3	RT
	M2-TMC-P3-SG1-O1-SR5-T1-N7	0.25"	Cylinder	Rolled	2.7E+3	RT
	M2-TMC-P3-SG1-O1-SR5-T1-N8	0.25"	Cylinder	Rolled	2.6E+3	RT

RT = room temperature

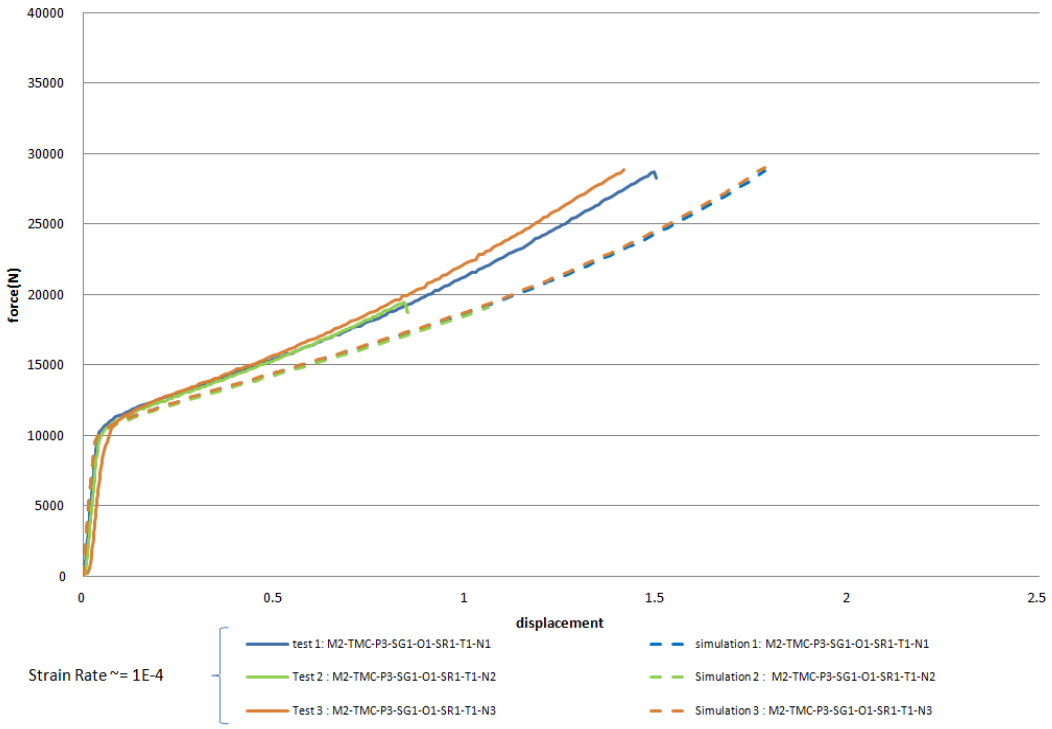

Figure D.82. Strain rate = 1e-4 sec^{-1} compression tests

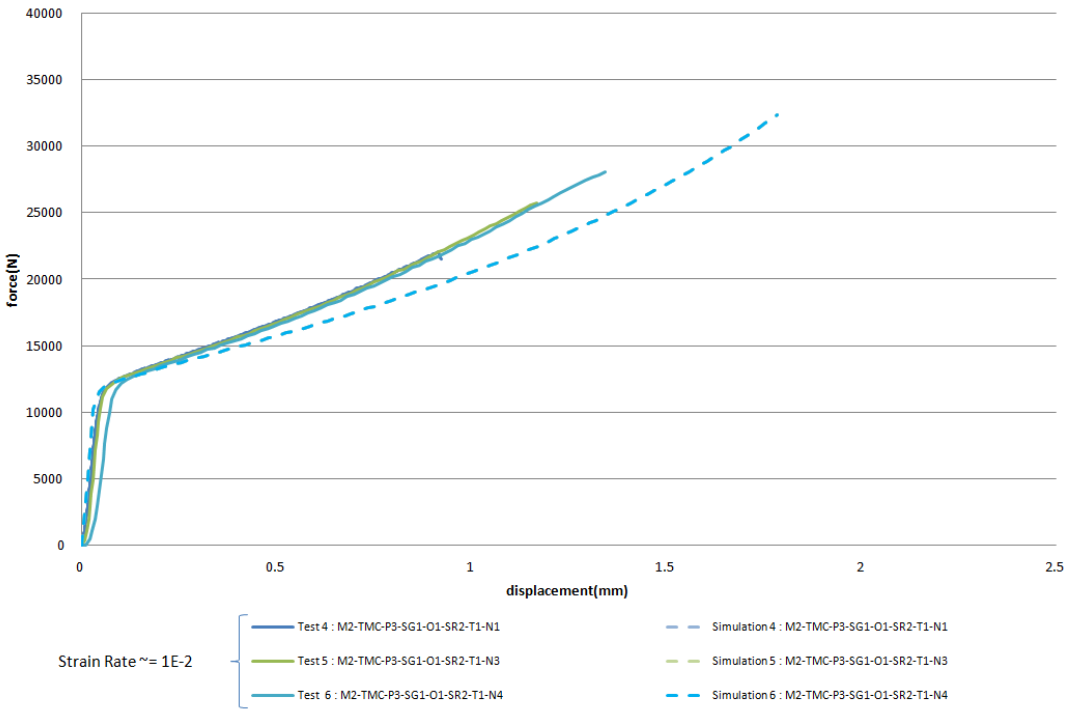

Figure D.83. Force displacement curve of strain rate = 1e-2 sec^{-1} compression tests

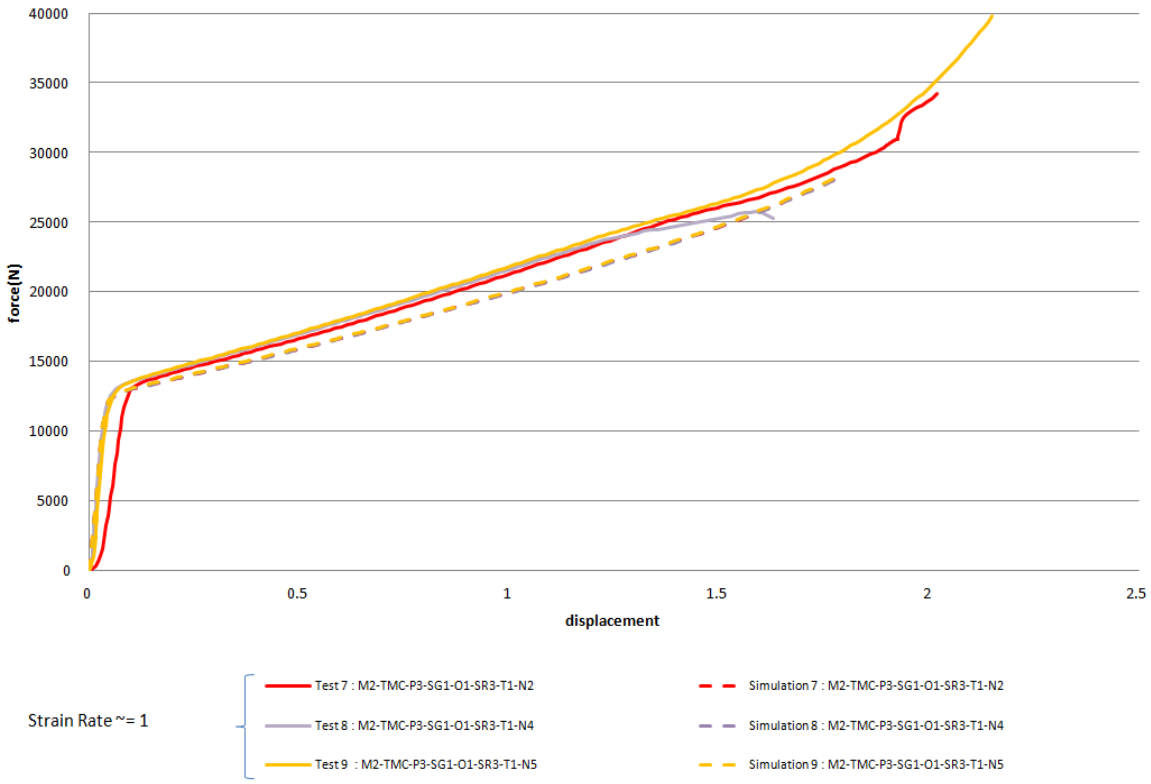

Figure D.84. Force displacement curve of strain rate = 1 sec^{-1} compression tests

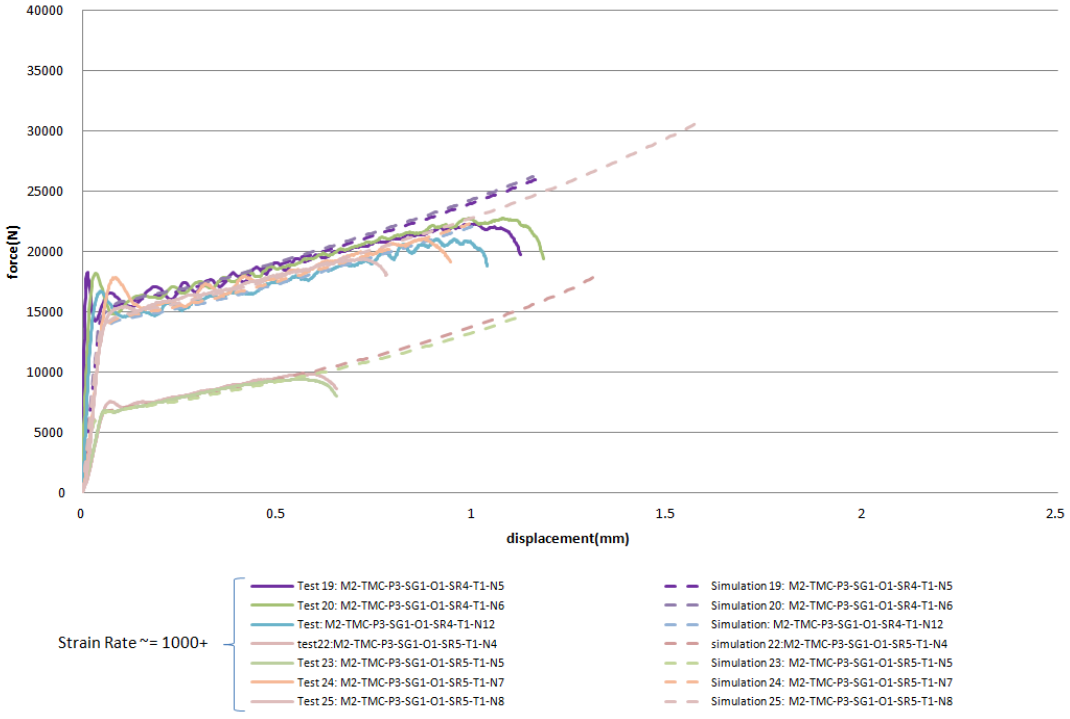

Figure D.85. Force displacement curve of strain rate = 1000+ sec^{-1} compression tests

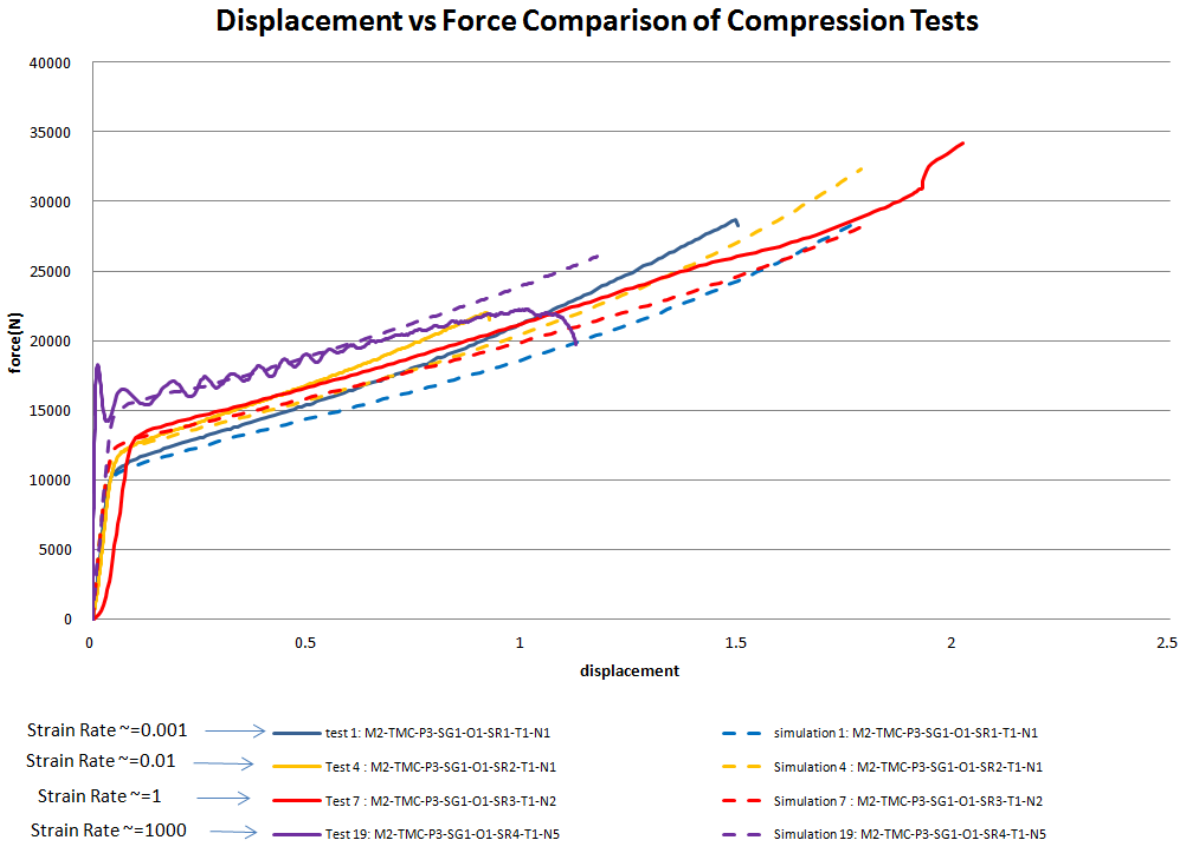

Figure D.86. Comparison between different strain rate groups

D.27 COMPRESSION ANISOTROPY

The experiments in table D.16 were simulated to determine the importance of the anisotropy of the material under compression. This group of experiments was studied with an input deck for *MAT_224 based on a single hardening curve (as in section D.2.2) and the displacement was applied using a grip speed of 1 m/s. Figure D.87 shows the force displacement relationship of compression tests at a strain rate of 1 sec^{-1}. It is observed the material has a significant anisotropy in compression.

Table D.16. Compression anisotropy tests

Test Series	Test Name	Plate Stock	Specimen Geometry	Specimen Orientation	Strain Rate (1/s)	Temperature (˚C)
Compression Anisotropy	M2-TMC-P3-SG1-O2-SR3-T1-N1	0.25"	Cylinder	45°	8.2E-1	RT
	M2-TMC-P3-SG1-O2-SR3-T1-N2	0.25"	Cylinder	45°	8.1E-1	RT
	M2-TMC-P3-SG1-O2-SR3-T1-N3	0.25"	Cylinder	45°	8.0E-1	RT
	M2-TMC-P3-SG1-O3-SR3-T1-N1	0.25"	Cylinder	90°	7.1E-1	RT
	M2-TMC-P3-SG1-O3-SR3-T1-N2	0.25"	Cylinder	90°	6.8E-1	RT
	M2-TMC-P3-SG1-O3-SR3-T1-N3	0.25"	Cylinder	90°	7.0E-1	RT
	M2-TMC-P3-SG1-O4-SR3-T1-N1	0.25"	Cylinder	135°	8.1E-1	RT
	M2-TMC-P3-SG1-O4-SR3-T1-N2	0.25"	Cylinder	135°	8.1E-1	RT
	M2-TMC-P3-SG1-O5-SR3-T1-N1	0.25"	Cylinder	Through	7.2E-1	RT
	M2-TMC-P3-SG1-O5-SR3-T1-N2	0.25"	Cylinder	Through	7.1E-1	RT

RT = room temperature

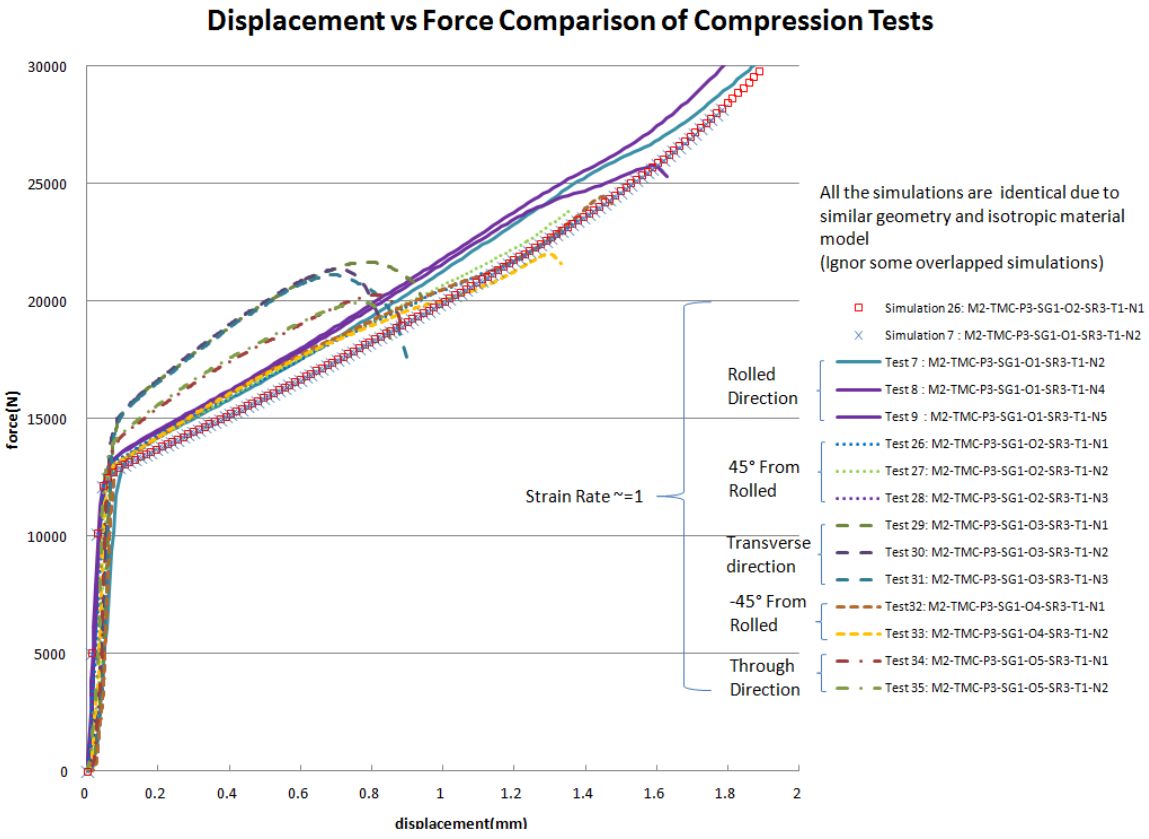

Figure D.87. Compression anisotropy effect

D.2.8 TEMPERATURE EFFECTS

Temperature effects had not yet been investigated at the time this appendix was written.

Temperature effect is a capability for *MAT_224, but for the 1/4-inch plate, it was not investigated.

D.3 CONCLUSIONS

In this report, material data were developed for Ti-6Al-4V. The resulting elastic-plastic material model includes strain hardening and strain-rate effects, but temperature effects were not accounted for. The samples used in the experiments that furnished the raw data for this model were taken from a 0.25″ plate stock, which demonstrated anisotropic behavior during testing. Because the chosen material model in LS-DYNA (*MAT_224) is isotropic, the measured anisotropy is not reflected in the numerical model.

All non-failure material input data were based on the results of tensile tests on plane dogbone specimens. Therefore, simulations of tensile tests on axisymmetric specimens show discrepancies when compared to testing in the post-necking area where the state of stress was no longer uniaxial. Simulation predictions of the material compressive response seem reasonable. The anisotropic effects that occur in compression cannot be modeled with the currently used material law.

This anisotropic material has highlighted a limitation to the current *MAT_224. Future work is planned to move from the von Mises-based theory to a generalized yield and fully anisotropic theory.

APPENDIX E—HIGH STRAIN-RATE LESSONS LEARNED

The following section describes the typical—though for this material, unsuccessful—process for generating higher-rate stress-strain curves. For Ti-6Al-4V, this typical process was not successful because, when loaded at a high strain rate, the material localized at relatively low strains. As a result, the test specimen did not remain at a constant strain rate or at a constant temperature. The required isothermal and isorate stress-strain curves must be generated indirectly, as described in section 2.4.

Sections E.1 and E.2 describe the approach taken for generating the individual stress-strain curves, which represent the higher strain-rate behavior. Sections E.3 and E.4 describe how these particular curves were combined and how the results were not able to recreate the behavior observed in the tests.

E.1 STRESS-STRAIN RELATIONSHIP OF STRAIN RATE = 500 SEC^{-1}

Three tests at strain rate 500 sec^{-1} are listed in table E.1. The engineering strain versus stress relationship was derived and gives the engineering stress-strain curves found in figure E.1.

Table E.1. Strain rate dependence series data of strain rate = 500 sec^{-1}

Series	Test Name	Plate Stock	Specimen Geometry	Specimen Orientation	Strain Rate (sec^{-1})	Temp (C)
Tension Strain Rate Dependence	M2-TMT-P4-SG1-O1-SR4-T1-N1	0.5″	Flat Dogbone	Rolled	500	RT
	M2-TMT-P4-SG1-O1-SR4-T1-N3	0.5″	Flat Dogbone	Rolled	500	RT
	M2-TMT-P4-SG1-O1-SR4-T1-N6	0.5″	Flat Dogbone	Rolled	500	RT

RT = room temperature

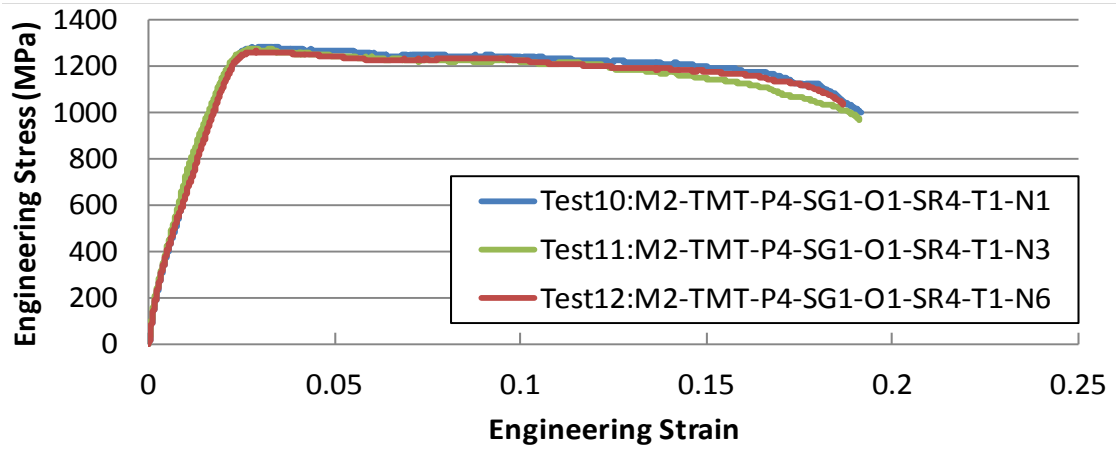

Figure E.1. Engineering stress-strain relationship of strain rate = 500 sec^{-1} tests

Test 12: M2-TMT-P4-SG1-O1-SR4-T1-N6 was selected to represent this group of data and undergo further processing. The selection criterion is based on engineering judgment considering the true stress-strain relationship (shown in figure E.2). By applying equation 11 from the main document and adopting a Young's modulus of 58 GPa (taken directly from the test data), the plastic strain versus stress relationship is calculated. Because of the isolation of the sampling point, the stress-strain data went through a 9-point moving average followed by a 250-point average of "loess" method in MATLAB and another 9-point moving average. An additional 9-point moving average was performed on the tangent modulus curve, and the intersection between these two lines defines the necking point. The true stress and true strain at the necking point were recorded. The corresponding plastic strain at necking was evaluated and only the part of the hardening curve before necking was kept.

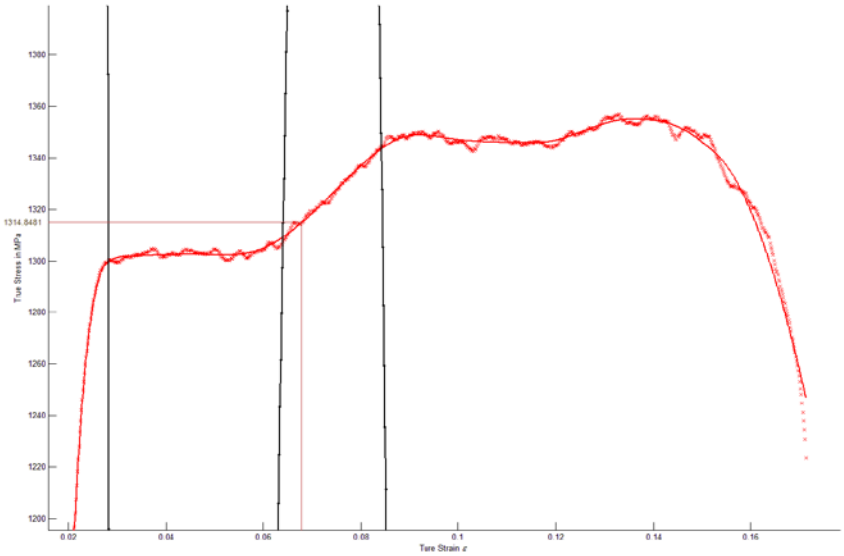

Figure E.2. True stress-strain relationship and necking point judgment of strain rate = 500 sec^{-1} (Test: M2-TMT-P4-SG1-O1-SR4-T1-N6)

The hardening curve was extrapolated beyond necking three times (see figure E.3). The first cut point is set to plastic strain = 0.036, and the extrapolation parameters are n = 0.089377, ε_e = 0.13881, and k = 1523.800. By applying the second cut on the resulting curve at 0.0639, the second extrapolation parameters are n = 0.25458, ε_e = 0.21637, and k = 1826.4. The third cut point is set to 0.30407, and the extrapolation parameters are n = 0.0171, ε_e = 0.21637, and k = 1826.4. These extrapolations were performed using MATLAB; the final input deck is shown in figure E.4. In this model, the sample dimensions match the sample of the test exactly.

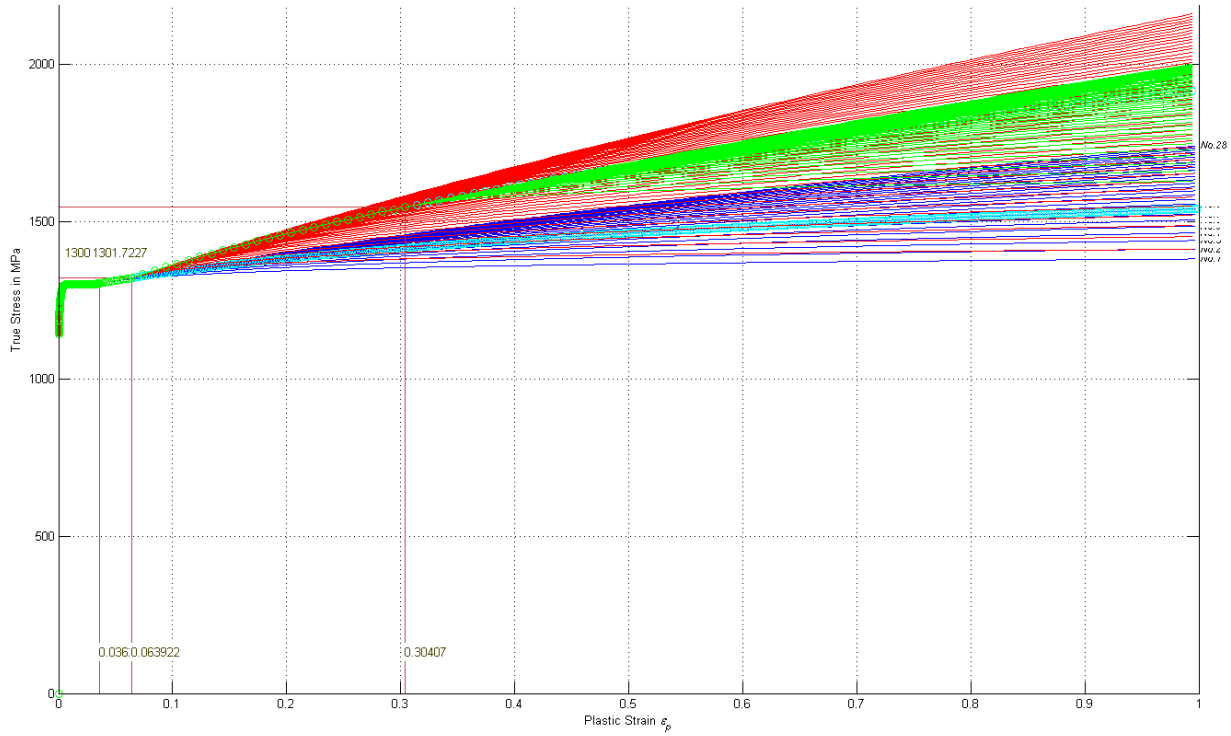

Figure E.3. Plastic strain versus stress relationship of strain rate = 500 sec^{-1} (Test 12: M2-TMT-P4-SG1-O1-SR4-T1-N6)

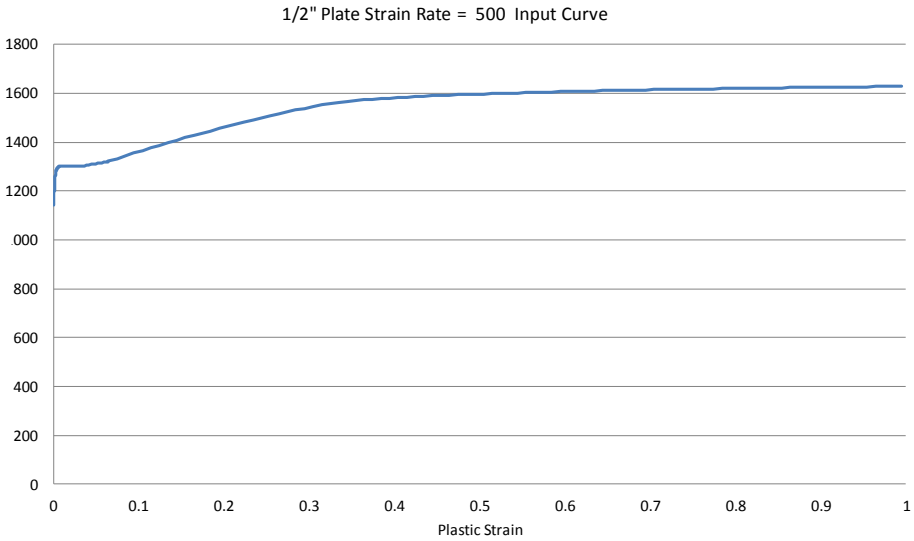

Figure E.4. Strain rate = 500 sec^{-1} group hardening curve input result

DATABASE_CROSS_SECTION is defined to measure the cross-sectional force. Two nodal points corresponding to the base points of the extensometer are stored in the NODOUT file (see figure E.5). The difference in *z* displacement of these two nodal points gives the elongation of the extensometer as predicted in the simulation. The measuring nodes have an initial distance of 4 mm. The cross-section for force measurement is located at the center of the specimen.

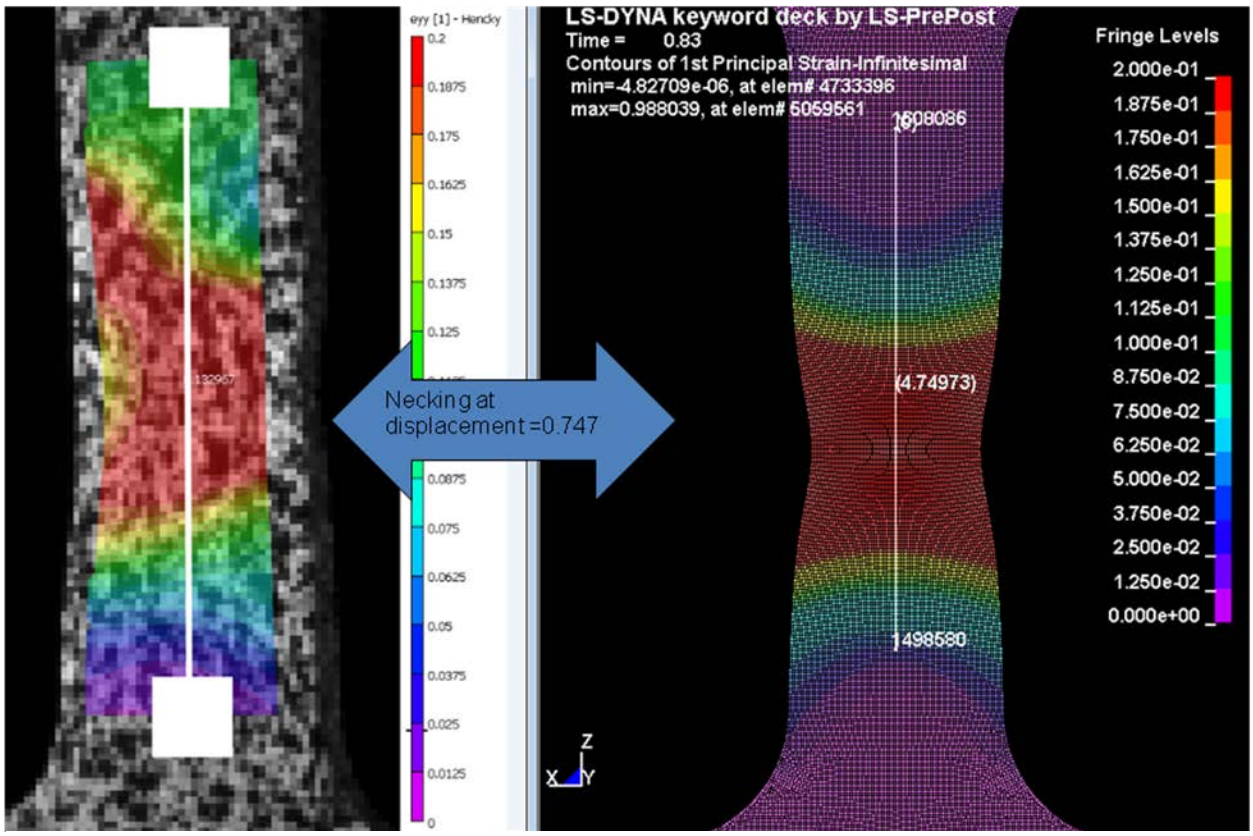

(a) (b)

Figure E.5. The (a) plastic strain digital image correlation image immediately before failure and (b) 1st principal strain simulation contour immediately before failure (Test: M2-TMT-P4-SG1-O1-SR4-T1-N6; strain rate = 500 sec^{-1})

A cross-plot of this elongation with the cross-sectional force can be directly compared to the force displacement curve from the test (see figure E.6). In figure E.5, a simulation contour of 1st principal strain is compared to the digital image correlation (DIC) image from the test at the time right before failure and the results yielded good agreement.

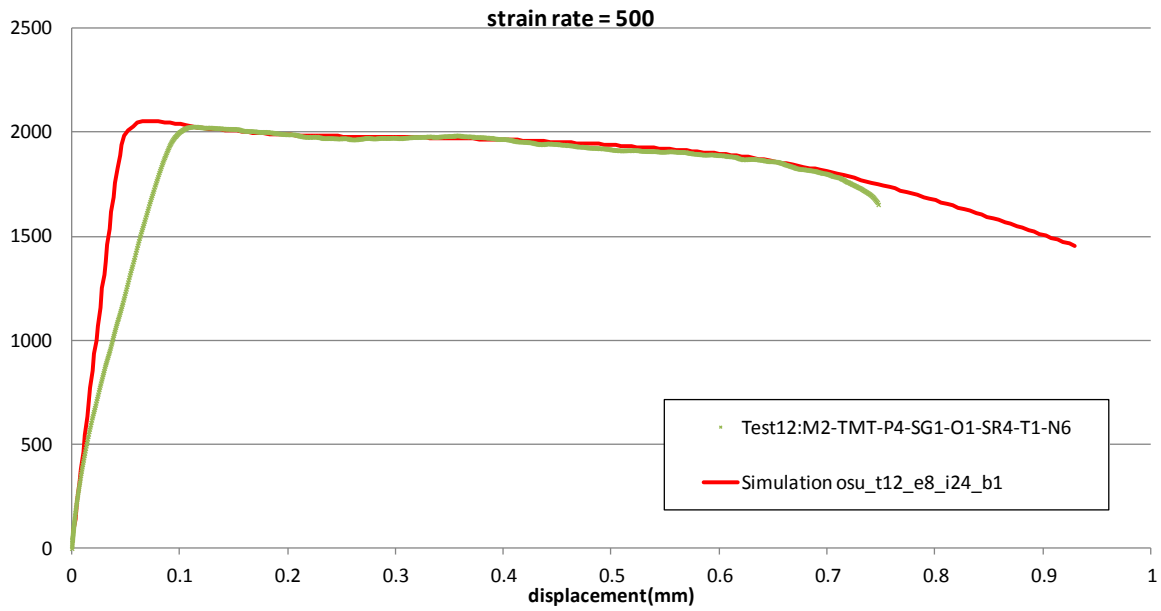

Figure E.6. Force displacement result (Test M2-TMT-P4-SG1-O1-SR4-T1-N6)

E.2 STRESS-STRAIN RELATIONSHIP OF STRAIN RATE = 1000 SEC^{-1}

Three tests at strain rate 1000 sec^{-1} are listed in table E.2. The engineering strain versus stress relationship was derived using equation 8 from the main document and gives the engineering stress-strain curves found in figure E.7. Test 15: M2-TMT-P4-SG1-O1-SR5-T1-N5 is selected to represent this group of data and undergo further processing. The selection criterion is based on engineering judgment.

Table E.2. Strain rate dependence series data of strain rate = 1000 sec^{-1}

Series	Test Name	Plate Stock	Specimen Geometry	Specimen Orientation	Strain Rate (sec^{-1})	Temp (C)
Tension Strain Rate Dependence	M2-TMT-P4-SG1-O1-SR5-T1-N3	0.5″	Flat Dogbone	Rolled	1.0E3	RT
	M2-TMT-P4-SG1-O1-SR5-T1-N4	0.5″	Flat Dogbone	Rolled	1.0E3	RT
	M2-TMT-P4-SG1-O1-SR5-T1-N5	0.5″	Flat Dogbone	Rolled	1.0E3	RT

RT = room temperature

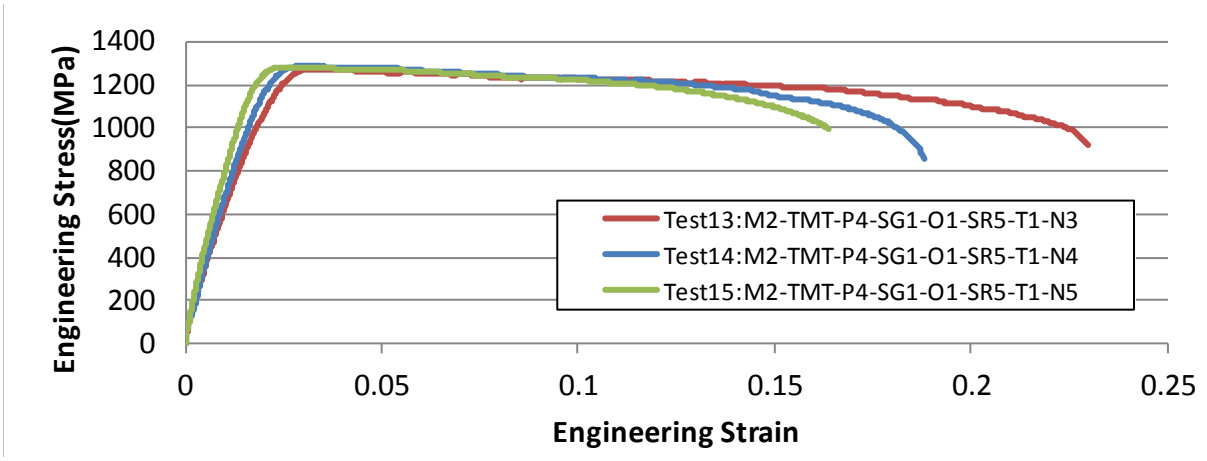

Figure E.7. Engineering stress-strain relationship of strain rate = 1000 sec^{-1} tests

The hardening curve was extrapolated beyond necking two times (see figure E.8). The first cut point is set to plastic strain = 0.036, and the extrapolation parameters are n = 0.33719, ε_e = 0.43493, and k = 1738.0052. By applying the second cut on the resulting curve at 0.33942, the second extrapolation parameters are n = 0.0171, ε_e = 0.21637, and k = 1826.4. These extrapolations were performed using MATLAB, and the final input deck is shown in figure E.9.

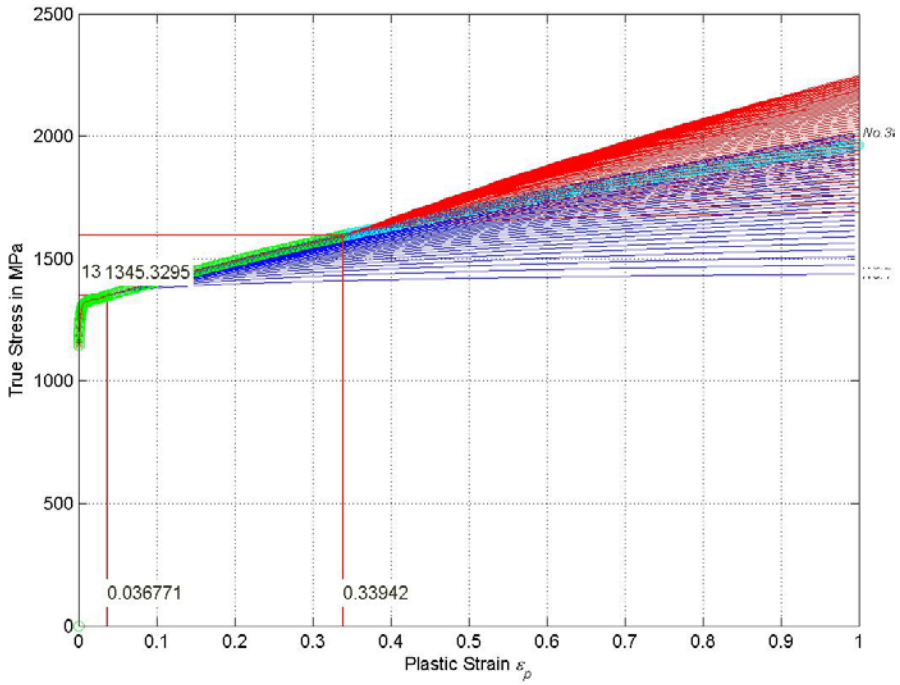

Figure E.8. Plastic strain versus stress relationship of strain rate = 1000 sec^{-1} (Test 15: M2-TMT-P4-SG1-O1-SR5-T1-N5)

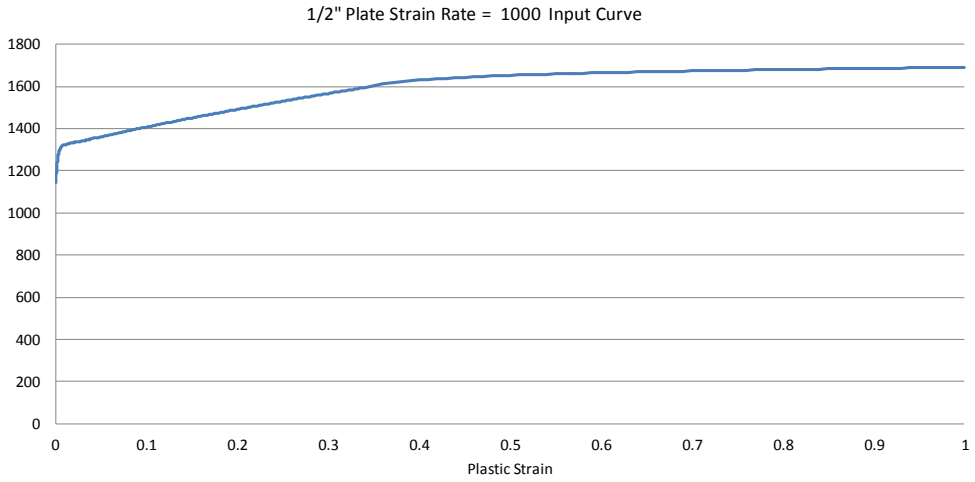

Figure E.9. Strain rate = 1000 sec^{-1} group hardening curve input result

The LS-DYNA input deck can be found in appendix F. In this model, the sample dimensions match the sample of the test exactly. DATABASE_CROSS_SECTION is defined to measure the cross-sectional force. Two nodal points corresponding to the base points of the extensometer are stored in the NODOUT file (see figure E.10). The difference in *z* displacement of these two nodal points gives the elongation of the extensometer as predicted in the simulation. The measuring nodes have an initial distance of 4 mm. The cross-section for force measurement is located at the center of the specimen.

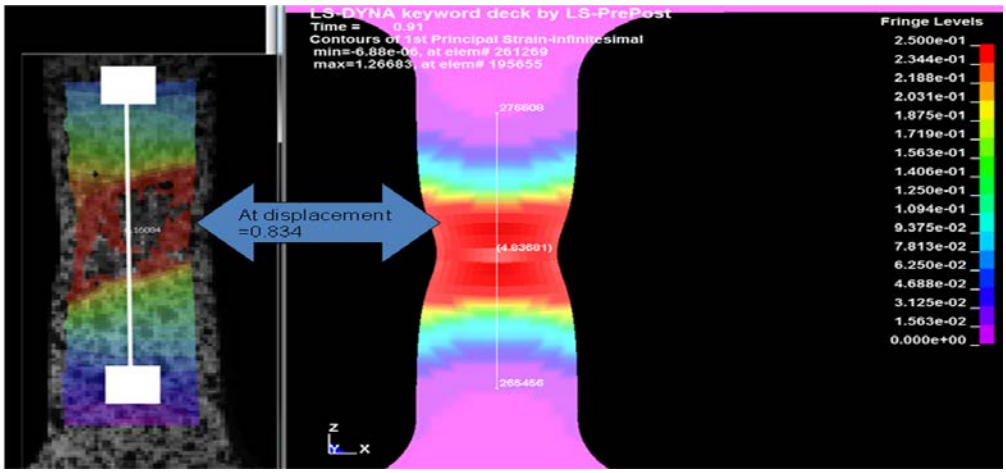

(a) (b)

Figure E.10. The (a) plastic strain DIC image immediately before failure and (b)1st principal strain simulation contour immediately before failure (Test: M2-TMT-P4-SG1-O1-SR5-T1-N5; strain rate = 1000 sec^{-1})

A cross-plot of this elongation with the cross-sectional force can be directly compared to the force displacement curve from the test, as shown in figure E.11. In figure E.10, a simulation contour of 1st principal strain is compared to the DIC image from the test at the time right before failure, and the results yield good agreement.

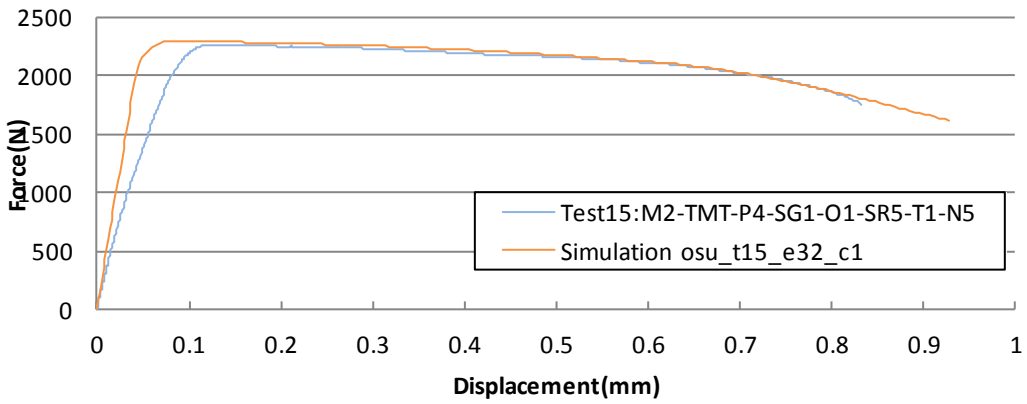

Figure E.11. Force displacement result (Test M2-TMT-P4-SG1-O1-SR5-T1-N5)

E.3 STRESS-STRAIN TABULATED INPUT OF MULTIPLE STRAIN RATES

After summarizing the hardening curves of all strain rates, the next step was to modify the nominal strain-rate value in the *MAT_224 for these curves until a set of values yielded a close match between the simulations and tests across all strain rates. At this time, the real loading speed was used in simulation rather than the artificial speed. As discussed in sections 2.3.2, 2.3.3, and appendix A, the strain rate is not a constant during the test. Therefore, the nominal strain rate is not the "real" strain rate of that test. A reverse-engineering method is used to determine the real strain rate of a particular test. The displacement time history of the test data is used as a boundary condition to ensure that the specimen in the simulation is pulled at exactly the same speed as in the real test. The local strain rate is therefore determined by the computer program. The nominal strain rate value of each of the input curves is modified until a set of strain rate values matches all simulations with test results simultaneously. As indicated by figure E.12, the nominal strain rate of 500 sec^{-1} was modified to a strain rate of 800 sec^{-1}, and the nominal strain rate of 1000 sec^{-1} was changed to a strain rate of 2800 sec^{-1}.

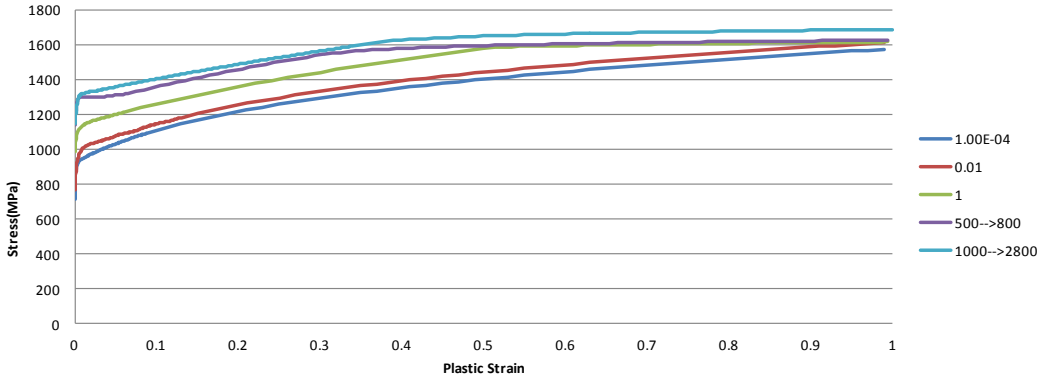

Figure E.12. Plastic strains versus stress curves of multiple strain rate inputs and associated modified strain rates

A new tabulated input deck for *MAT_224 was then created based on the five hardening curves labeled with the new strain-rate values. LS-DYNA simulations were then performed for the

tensile tests at nominal strain rates of 1 sec^{-1}, 650 sec^{-1}, and 850 sec^{-1}. Unlike previous simulations that applied an artificially high loading speed, the loading speed was applied exactly as it was recorded in the actual experiment in these simulations. The load curve referenced in the "*Boundary_Prescribed_Motion" cards was set to use the displacement versus time curve measured in the test. The results of these simulations are presented in figure E.13.

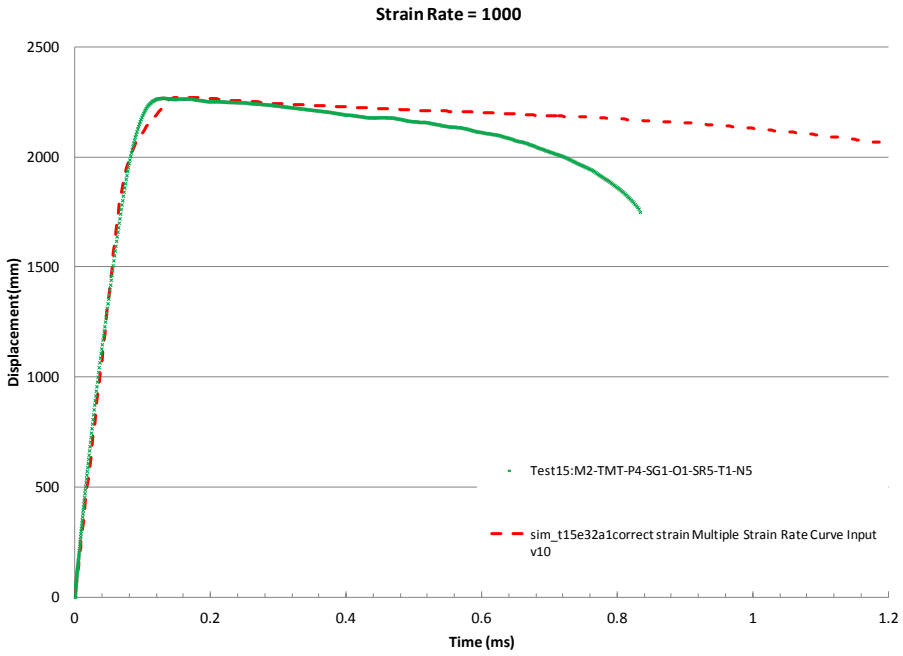

Figure E.13. Time displacement comparisons of tabulated strain rate input simulation and single strain-rate input simulation (Test: M2-TMT-P3-SG1-O1-SR4-T1-N7; nominal strain rate ≈ 1000 sec^{-1})

Because the loading speed of the experiments at the nominal strain rates of 1 sec^{-1}, 1E-2 sec^{-1}, and 1E-4 sec^{-1} is low, the time span of these tests is fairly long, making it impossible to realistically simulate with the current computing power. Consequently, these experiments were simulated with a single hardening curve input only.

Note these real tests were conducted in a room-temperature environment. There is also a local temperature rise due to the strain-hardening process, the effect of which is not negligible, especially in the higher strain-rate tests. In these tests, heat is generated near a small region of the necking point and does not have time to dissipate because of the short time span of the test. A temperature-softening effect is automatically included; this simulation input deck predicts the tensile behavior of Ti-6Al-4V 1/2-inch plate in a room-temperature environment. It does not represent the material behavior at 293 K, especially at higher strain rates.

The strain rate of the 1 sec^{-1} curve is modified to avoid intersection with higher strain-rate curves; this is required by *MAT_224 so that the material yield surface can maintain convexity.

E.4 STRESS-STRAIN TABULATED INPUT OF MULTIPLE STRAIN RATES AND TEMPERATURES

At this stage, strain rate and temperature effect are integrated into a single input deck. The temperature curves in figure E.14 are input as is, as are the strain rate curves of 1E-4 sec^{-1}, 1E-2 sec^{-1}, and 1 sec^{-1}. The higher strain-rate curve, however, changes in both the benchmark value and the curve shape. This is due to the localized high temperature increase in the high strain-rate test. Therefore, the curve derived from a single strain-rate test does not represent an isothermal case, which is required for *MAT_224. The initial guess of the benchmark value is referenced by back-calculating the strain rate out of the test data. The changing criterion is based on trial and error and engineering judgment. The strain-rate input result is shown in figure E.15.

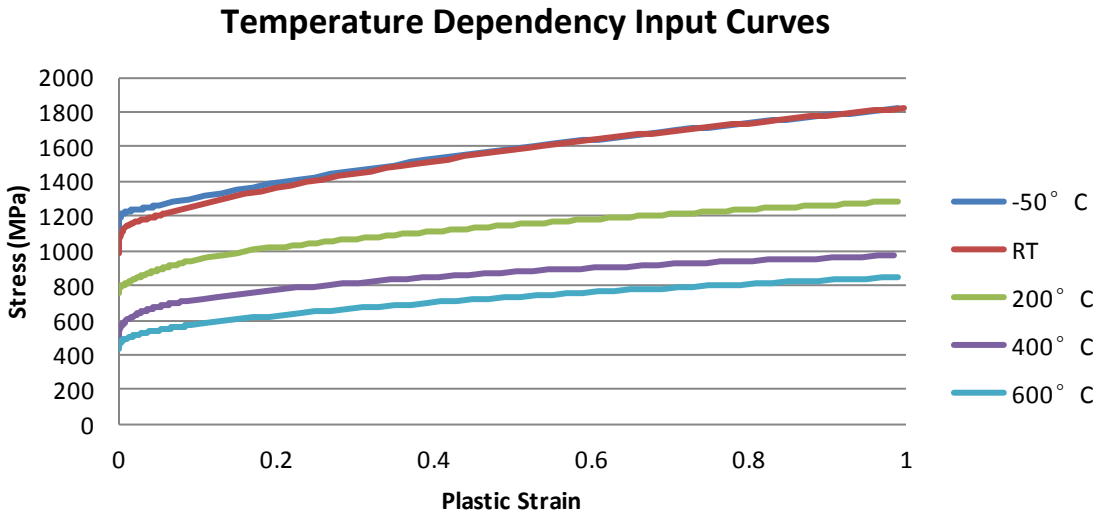

Figure E.14. Temperature dependency input curves

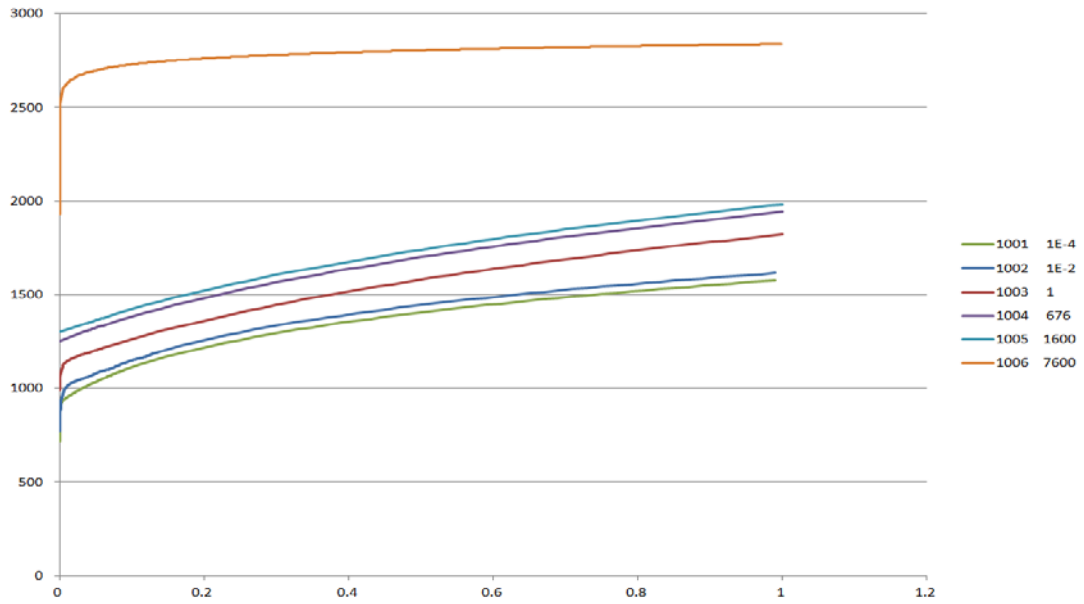

Figure E.15. Strain rates and temperature combined input curves, including benchmark value (the temperature input is given in figure E.15)

Resulting force displacement curves are found in figures E.16 and E.17. The DIC and LS-DYNA simulation comparisons are found in figures E.18 and E.19. Though the force-displacement result of the input deck matches, the time history shown in figure E.17 does not. The DIC contour does not match the LS-DYNA 1st principal strain contour.

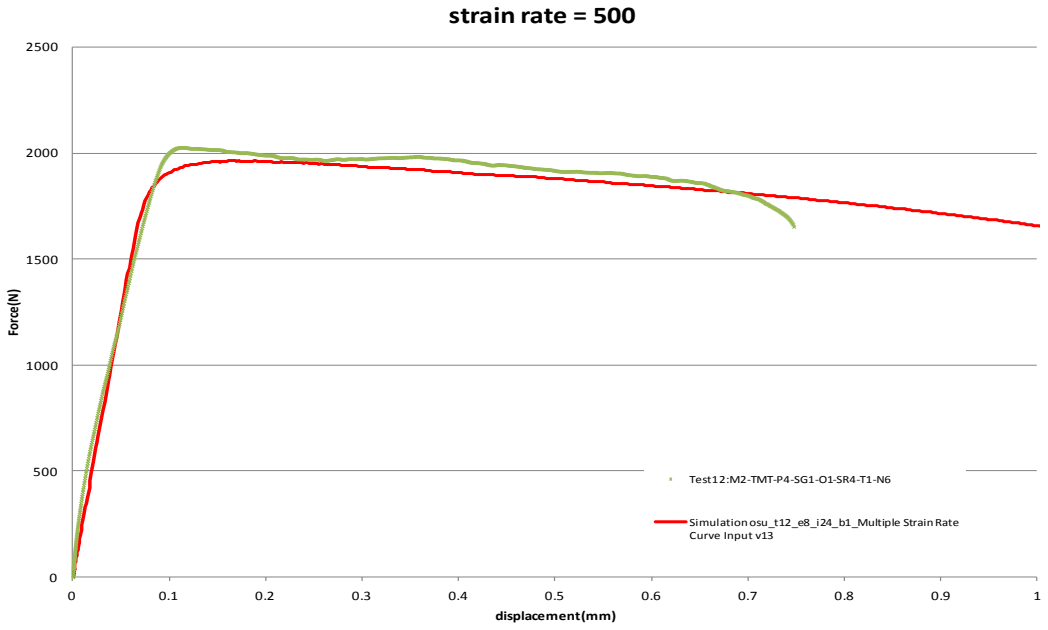

Figure E.16. Force displacement comparison of strain rate = 500 sec^{-1} test when using strain rate and temperature combined input

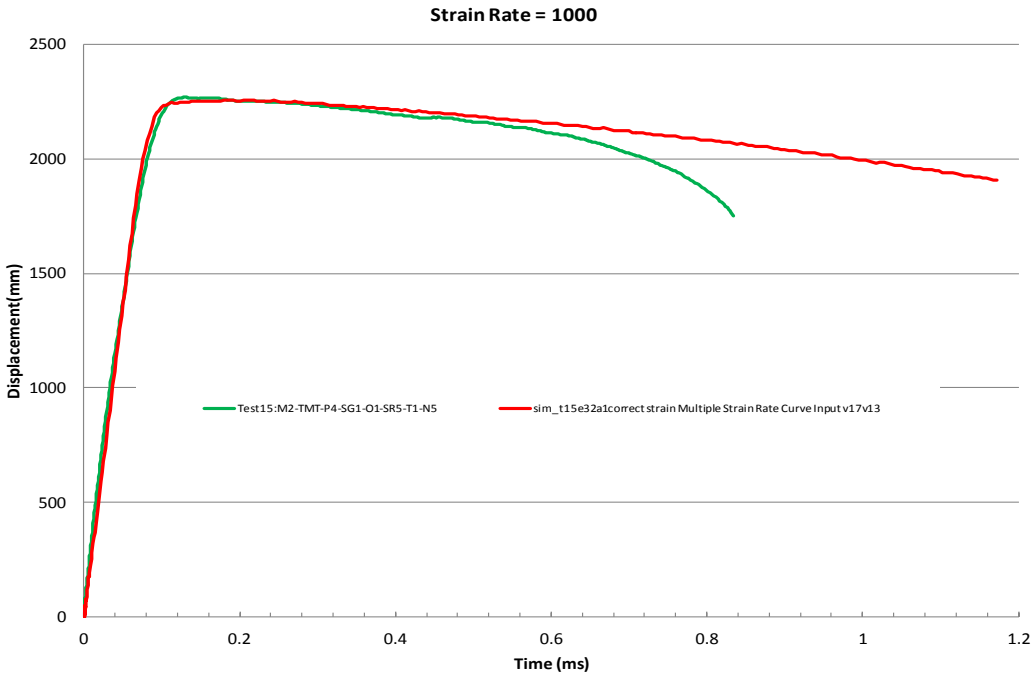

Figure E.17. Time displacement comparison of strain rate = 1000 sec^{-1} test when using strain rate and temperature combined input

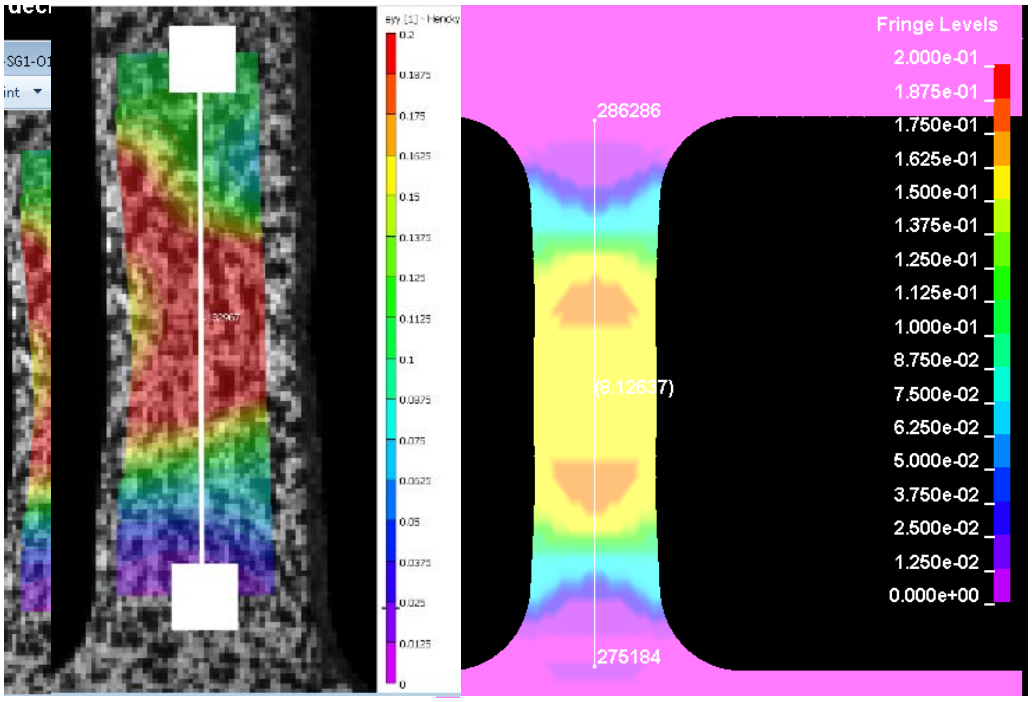

(a) (b)

Figure E.18. The (a) DIC image and (b) temperature and strain rate combined input deck (mat224_0_5_v16v13), failure at displacement = 0.747 mm, 1st principal strain contour (Test12: M2-TMT-P4-SG1-O1-SR4-T1-N6; strain rate =500 sec^{-1})

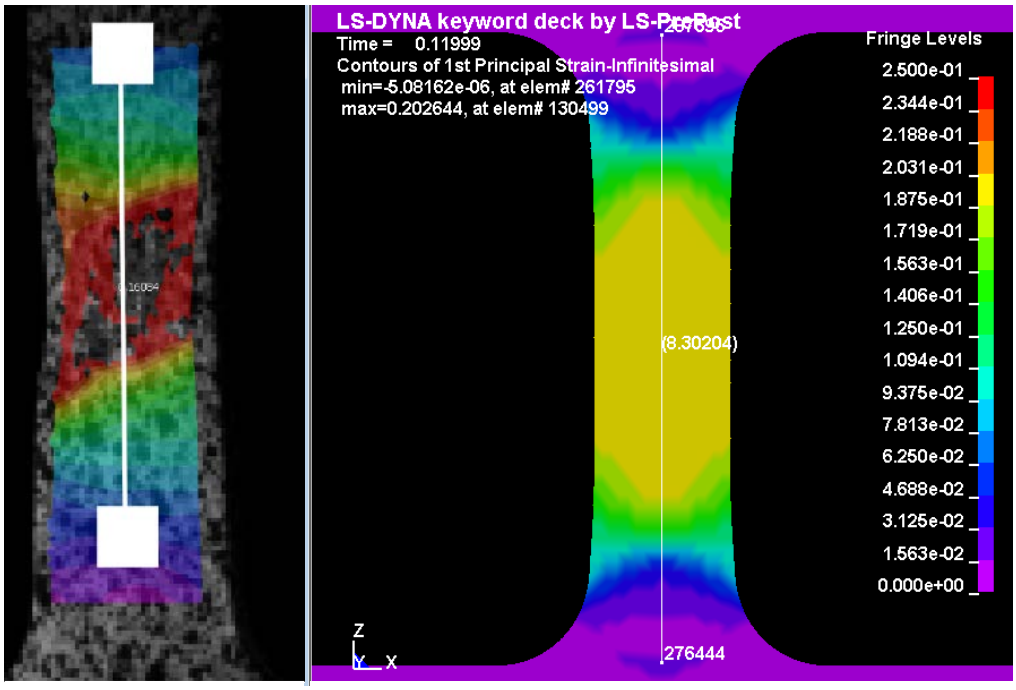

(a) (b)

Figure E.19. The (a) DIC image and (b) temperature and strain rate combined input deck (mat224_0_5_v16v13), failure at displacement = 0.834 mm, 1st principal strain contour (Test15:M2-TMT-P4-SG1-O1-SR5-T1-N5; strain rate =1000 sec^{-1})

Because the Ti-6Al-4V, when loaded at a high strain rate, localizes at relatively low strains, the preceding procedure was unsuccessful. In addition, the test specimens did not remain at a constant strain rate or at a constant temperature during the test; therefore, the resulting stress-strain curves cannot be used directly. The required isothermal and isorate stress-strain curves must be generated indirectly, as described in section 3.4 of the main document.

```
$$$$$$$$$$$$$$$$$$$$$$$$$$$$$$$$$$$$$$$$$$$$$$$$$$$$$$$$$$$$$$$$$$$$$$$
$                                                                       $
$    Center for Collision Safety and Analysis (CCSA)                    $
$             George Mason University (GMU)                            $
$         Federal Aviation Administration (FAA)                         $
$               Ti-6Al-4V Material Model                                $
$       Sean Haight - Paul DuBois - Dr. Steve Kan                       $
$                  Units: mm, ms, kg, kN                                $
$                                                                       $
$$$$$$$$$$$$$$$$$$$$$$$$$$$$$$$$$$$$$$$$$$$$$$$$$$$$$$$$$$$$$$$$$$$$$$$
*KEYWORD
$$$$$$$$$$$$$$$$$$$$$$$$$$$$$$$$$$$$$$$$$$$$$$$$$$$$$$$$$$$$$$$$$$$$$$$
$                          Material                                     $
$$$$$$$$$$$$$$$$$$$$$$$$$$$$$$$$$$$$$$$$$$$$$$$$$$$$$$$$$$$$$$$$$$$$$$$
*MAT_TABULATED_JOHNSON_COOK_TITLE
MAT_224_Ti64
$      mid        ro         e        pr        cp        tr      beta
numint
         1 4.4300E-6 110.00000  0.342000     526.3       293  0.800000
1.000000
$     lck1      lckt       lcf       lcg       lch       lci
      1000      2000      3000      4000      5000      6000
$$$$$$$$$$$$$$$$$$$$$$$$$$$$$$$$$$$$$$$$$$$$$$$$$$$$$$$$$$$$$$$$$$$$$$$
$                     Strain Rate Table                                 $
$$$$$$$$$$$$$$$$$$$$$$$$$$$$$$$$$$$$$$$$$$$$$$$$$$$$$$$$$$$$$$$$$$$$$$$
*DEFINE_TABLE
$     tbid       sfa      offa
      1000
$              value             curveid
            0.0000001                1001
              0.00001                1002
                0.001                1003
                0.010                1004
                0.100                1005
                1.000                1006
                1.500                1007
                2.500                1008
                5.000                1009
                10.00                1010
                15.00                1011
                20.00                1012
                30.00                1013
                40.00                1014
                50.00                1015
$$$$$$$$$$$$$$$$$$$$$$$$$$$$$$$$$$$$$$$$$$$$$$$$$$$$$$$$$$$$$$$$$$$$$$$
$                     Strain Rate Curves                                $
$$$$$$$$$$$$$$$$$$$$$$$$$$$$$$$$$$$$$$$$$$$$$$$$$$$$$$$$$$$$$$$$$$$$$$$
*DEFINE_CURVE
```

```
$ 1E-4 /s strain rate
$     LCID      SIDR      SCLA      SCLO      OFFA      OFFO    DATTYP
      1001         0       1.0       1.0       0.0       0.0         0
$           ABSCISSA          ORDINATE
            0.000000        0.7181500000
            0.000040        0.7461900000
            0.000066        0.7737700000
            0.000112        0.8003800000
            0.000219        0.8255600000
            0.000423        0.8484200000
            0.000738        0.8687600000
            0.001185        0.8863400000
            0.001732        0.9013400000
            0.002408        0.9137500000
            0.003209        0.9232900000
            0.004135        0.9307100000
            0.005164        0.9358900000
            0.006261        0.9399900000
            0.007400        0.9433300000
            0.008561        0.9460200000
            0.009691        0.9490100000
            0.010844        0.9520600000
            0.012005        0.9550900000
            0.013153        0.9581200000
            0.014293        0.9611200000
            0.015442        0.9639100000
            0.016583        0.9666200000
            0.017723        0.9694800000
            0.018864        0.9728800000
            0.020033        0.9756700000
            0.021204        0.9781600000
            0.022373        0.9806100000
            0.023552        0.9831900000
            0.024721        0.9851300000
            0.025873        0.9878100000
            0.027035        0.9905300000
            0.028186        0.9932000000
            0.029333        0.9952200000
            0.030487        0.9975900000
            0.031637        0.9998400000
            0.032770        1.0020000000
            0.033884        1.0041000000
            0.035017        1.0066000000
            0.036157        1.0088000000
            0.037309        1.0109000000
            0.038459        1.0125000000
            0.039610        1.0149000000
            0.040762        1.0171000000
            0.041910        1.0192000000
            0.043089        1.0211000000
            0.044276        1.0233000000
            0.045456        1.0258000000
```

0.046648	1.0277000000
0.047832	1.0296000000
0.049013	1.0319000000
0.050204	1.0337000000
0.051388	1.0357000000
0.052580	1.0378000000
0.053756	1.0402000000
0.054936	1.0423000000
0.056122	1.0441000000
0.057302	1.0460000000
0.058472	1.0478000000
0.059638	1.0497000000
0.060792	1.0521000000
0.061935	1.0542000000
0.063085	1.0563000000
0.064237	1.0579000000
0.065386	1.0597000000
0.066526	1.0615000000
0.067656	1.0639000000
0.068786	1.0660000000
0.069918	1.0678000000
0.071049	1.0691000000
0.072189	1.0712000000
0.073315	1.0732000000
0.074451	1.0749000000
0.075572	1.0766000000
0.076691	1.0785000000
0.077819	1.0797000000
0.078947	1.0816000000
0.080080	1.0838000000
0.081240	1.0853000000
0.082376	1.0869000000
0.083523	1.0883000000
0.084669	1.0901000000
0.085834	1.0922000000
0.086997	1.0941000000
0.088169	1.0963000000
0.089339	1.0981000000
0.089489	1.0983000000
0.109490	1.1247000000
0.129490	1.1486000000
0.149490	1.1705000000
0.169490	1.1907000000
0.189490	1.2094000000
0.209490	1.2270000000
0.229490	1.2434000000
0.249490	1.2590000000
0.269490	1.2737000000
0.289490	1.2877000000
0.309490	1.3011000000
0.329490	1.3138000000
0.349490	1.3260000000

```
            0.369490        1.3378000000
            0.389490        1.3491000000
            0.409490        1.3600000000
            0.429490        1.3705000000
            0.449490        1.3807000000
            0.469490        1.3905000000
            0.489490        1.4000000000
            0.509490        1.4093000000
            0.529490        1.4183000000
            0.549490        1.4270000000
            0.569490        1.4355000000
            0.589490        1.4438000000
            0.609490        1.4519000000
            0.629490        1.4598000000
            0.649490        1.4675000000
            0.669490        1.4750000000
            0.689490        1.4823000000
            0.709490        1.4895000000
            0.729490        1.4966000000
            0.749490        1.5035000000
            0.769490        1.5102000000
            0.789490        1.5168000000
            0.809490        1.5233000000
            0.829490        1.5297000000
            0.849490        1.5359000000
            0.869490        1.5421000000
            0.889490        1.5481000000
            0.909490        1.5541000000
            0.929490        1.5599000000
            0.949490        1.5656000000
            0.969490        1.5713000000
            0.989490        1.5768000000
            1.000000        1.5796902500
*DEFINE_CURVE
$ 1E-2 /s strain rate (quasistatic)
$     LCID      SIDR      SCLA      SCLO      OFFA      OFFO    DATTYP
      1002         0       1.0       1.0       0.0       0.0         0
$           ABSCISSA           ORDINATE
            0.000000        0.7400000000
            0.001000        0.8879110000
            0.002000        0.9176410000
            0.003000        0.9415790000
            0.004000        0.9591330000
            0.005000        0.9720840000
            0.006000        0.9827890000
            0.007000        0.9911060000
            0.008000        0.9977440000
            0.009000        1.0034200000
            0.010000        1.0084800000
            0.011000        1.0128300000
            0.012000        1.0164800000
            0.013000        1.0195900000
```

0.014000	1.0223500000
0.015000	1.0247800000
0.016000	1.0269700000
0.017000	1.0289400000
0.018000	1.0307000000
0.019000	1.0323400000
0.020000	1.0338800000
0.021000	1.0354200000
0.022000	1.0367800000
0.023000	1.0382200000
0.024000	1.0395800000
0.025000	1.0410200000
0.026000	1.0424700000
0.027000	1.0439100000
0.028000	1.0453800000
0.029000	1.0468900000
0.030000	1.0483500000
0.031000	1.0498500000
0.032000	1.0512700000
0.033000	1.0526900000
0.034000	1.0541100000
0.035000	1.0555200000
0.036000	1.0569200000
0.037000	1.0583200000
0.038000	1.0597200000
0.039000	1.0611500000
0.040000	1.0626300000
0.041000	1.0641100000
0.042000	1.0656200000
0.043000	1.0671900000
0.044000	1.0688100000
0.045000	1.0705200000
0.046000	1.0722800000
0.047000	1.0740000000
0.048000	1.0757900000
0.049000	1.0775800000
0.050000	1.0793700000
0.051000	1.0811400000
0.052000	1.0828200000
0.053000	1.0844300000
0.054000	1.0860100000
0.055000	1.0875100000
0.056000	1.0889300000
0.057000	1.0903000000
0.058000	1.0915000000
0.059000	1.0926400000
0.060000	1.0936900000
0.061000	1.0946600000
0.062000	1.0956400000
0.063000	1.0965200000
0.064000	1.0974100000
0.065000	1.0982900000

0.066000	1.0991900000
0.067000	1.1002100000
0.068000	1.1012500000
0.069000	1.1023000000
0.070000	1.1035300000
0.071000	1.1048000000
0.072000	1.1061900000
0.073000	1.1076700000
0.074000	1.1091900000
0.075000	1.1108700000
0.076000	1.1125400000
0.077000	1.1142400000
0.078000	1.1160500000
0.079000	1.1179000000
0.080000	1.1196800000
0.081000	1.1214500000
0.082000	1.1232100000
0.083000	1.1249200000
0.084000	1.1266200000
0.085000	1.1282500000
0.086000	1.1297900000
0.087000	1.1313300000
0.088000	1.1328600000
0.089000	1.1343200000
0.090000	1.1357300000
0.091000	1.1370800000
0.092000	1.1384600000
0.093000	1.1398100000
0.094000	1.1412000000
0.095000	1.1425600000
0.096000	1.1439000000
0.097000	1.1452400000
0.098000	1.1465800000
0.099000	1.1479300000
0.100000	1.1491900000
0.101000	1.1504400000
0.102000	1.1516800000
0.103000	1.1527100000
0.104000	1.1537400000
0.105000	1.1547900000
0.106000	1.1557300000
0.107000	1.1566700000
0.108000	1.1575000000
0.109000	1.1583400000
0.110000	1.1591900000
0.111000	1.1600300000
0.112000	1.1609200000
0.113000	1.1618700000
0.114000	1.1628300000
0.115000	1.1638500000
0.116000	1.1649800000
0.117000	1.1662200000

0.118000	1.1674900000
0.119000	1.1688400000
0.120000	1.1702000000
0.121000	1.1716900000
0.122000	1.1732600000
0.123000	1.1747400000
0.124000	1.1763000000
0.125000	1.1778500000
0.126000	1.1793000000
0.127000	1.1807400000
0.128000	1.1821400000
0.129000	1.1834400000
0.130000	1.1846700000
0.131000	1.1858100000
0.132000	1.1869500000
0.133000	1.1880900000
0.134000	1.1892300000
0.135000	1.1903700000
0.136000	1.1915100000
0.137000	1.1926500000
0.138000	1.1937900000
0.139000	1.1949300000
0.140000	1.1960700000
0.141000	1.1972100000
0.142000	1.1983500000
0.143000	1.1994900000
0.144000	1.2006300000
0.145000	1.2017700000
0.146000	1.2029100000
0.147000	1.2040500000
0.148000	1.2051900000
0.149000	1.2063300000
0.150000	1.2074600000
0.151000	1.2085100000
0.152000	1.2095600000
0.153000	1.2106100000
0.154000	1.2116600000
0.155000	1.2127100000
0.156000	1.2137600000
0.157000	1.2148100000
0.158000	1.2158600000
0.159000	1.2169100000
0.160000	1.2179600000
0.161000	1.2190100000
0.162000	1.2200600000
0.163000	1.2211100000
0.164000	1.2221600000
0.165000	1.2232100000
0.166000	1.2242600000
0.167000	1.2253100000
0.168000	1.2263600000
0.169000	1.2274100000

0.170000	1.2284400000
0.171000	1.2294100000
0.172000	1.2303700000
0.173000	1.2313400000
0.174000	1.2323000000
0.175000	1.2332700000
0.176000	1.2342300000
0.177000	1.2352000000
0.178000	1.2361600000
0.179000	1.2371300000
0.180000	1.2380900000
0.181000	1.2390600000
0.182000	1.2400200000
0.183000	1.2409900000
0.184000	1.2419500000
0.185000	1.2429200000
0.186000	1.2438800000
0.187000	1.2448500000
0.188000	1.2458100000
0.189000	1.2467800000
0.190000	1.2477300000
0.191000	1.2486400000
0.192000	1.2495300000
0.193000	1.2504300000
0.194000	1.2513300000
0.195000	1.2522300000
0.196000	1.2531400000
0.197000	1.2540300000
0.198000	1.2549300000
0.199000	1.2558300000
0.200000	1.2567300000
0.210000	1.2657300000
0.220000	1.2741800000
0.230000	1.2826200000
0.240000	1.2905200000
0.250000	1.2984100000
0.260000	1.3059100000
0.270000	1.3134100000
0.280000	1.3205100000
0.290000	1.3276000000
0.300000	1.3343500000
0.310000	1.3411000000
0.320000	1.3475500000
0.330000	1.3539900000
0.340000	1.3601400000
0.350000	1.3662900000
0.360000	1.3721900000
0.370000	1.3780800000
0.380000	1.3837300000
0.390000	1.3893800000
0.400000	1.3948300000
0.410000	1.4002800000

0.420000	1.4055300000
0.430000	1.4107800000
0.440000	1.4158300000
0.450000	1.4208700000
0.460000	1.4257700000
0.470000	1.4306700000
0.480000	1.4354200000
0.490000	1.4401700000
0.500000	1.4447700000
0.510000	1.4493700000
0.520000	1.4538700000
0.530000	1.4583600000
0.540000	1.4626600000
0.550000	1.4669600000
0.560000	1.4712100000
0.570000	1.4754600000
0.580000	1.4795600000
0.590000	1.4836600000
0.600000	1.4876600000
0.610000	1.4916600000
0.620000	1.4955600000
0.630000	1.4994600000
0.640000	1.5032600000
0.650000	1.5070600000
0.660000	1.5107600000
0.670000	1.5144500000
0.680000	1.5180500000
0.690000	1.5216500000
0.700000	1.5252000000
0.710000	1.5287500000
0.720000	1.5322500000
0.730000	1.5357500000
0.740000	1.5391000000
0.750000	1.5424500000
0.760000	1.5458000000
0.770000	1.5491500000
0.780000	1.5524000000
0.790000	1.5556500000
0.800000	1.5588500000
0.810000	1.5620500000
0.820000	1.5651500000
0.830000	1.5682500000
0.840000	1.5713500000
0.850000	1.5744500000
0.860000	1.5774500000
0.870000	1.5804400000
0.880000	1.5833900000
0.890000	1.5863400000
0.900000	1.5892400000
0.910000	1.5921400000
0.920000	1.5950400000
0.930000	1.5979400000

```
            0.940000        1.6007400000
            0.950000        1.6035400000
            0.960000        1.6062900000
            0.970000        1.6090400000
            0.980000        1.6117400000
            0.990000        1.6144400000
            1.000000        1.6171400000
*DEFINE_CURVE
$ 1 /s strain rate
$     LCID      SIDR      SCLA      SCLO      OFFA      OFFO    DATTYP
      1003         0       1.0       1.0       0.0       0.0         0
$           ABSCISSA           ORDINATE
            0.000000        0.9897900000
            0.000351        1.0145000000
            0.000721        1.0397000000
            0.001308        1.0635000000
            0.002086        1.0840000000
            0.003087        1.1019000000
            0.004274        1.1147000000
            0.005569        1.1245000000
            0.006898        1.1319000000
            0.008267        1.1373000000
            0.009619        1.1413000000
            0.010961        1.1447000000
            0.012297        1.1477000000
            0.013645        1.1506000000
            0.014972        1.1534000000
            0.016309        1.1561000000
            0.017651        1.1588000000
            0.018970        1.1613000000
            0.020255        1.1636000000
            0.021546        1.1658000000
            0.022833        1.1679000000
            0.024105        1.1699000000
            0.025406        1.1718000000
            0.026724        1.1736000000
            0.028034        1.1754000000
            0.029340        1.1770000000
            0.030650        1.1786000000
            0.031959        1.1801000000
            0.033285        1.1816000000
            0.034610        1.1830000000
            0.035941        1.1845000000
            0.037269        1.1859000000
            0.038585        1.1874000000
            0.039884        1.1890000000
            0.041229        1.1906000000
            0.042566        1.1923000000
            0.043911        1.1941000000
            0.045247        1.1959000000
            0.046571        1.1976000000
            0.047874        1.1994000000
```

0.049185	1.2012000000
0.050515	1.2030000000
0.051864	1.2049000000
0.053200	1.2067000000
0.054515	1.2084000000
0.055824	1.2101000000
0.057115	1.2118000000
0.058432	1.2135000000
0.059759	1.2152000000
0.059909	1.2154000000
0.079909	1.2394000000
0.099909	1.2623000000
0.119910	1.2841000000
0.139910	1.3048000000
0.159910	1.3247000000
0.179910	1.3438000000
0.199910	1.3622000000
0.219910	1.3799000000
0.239910	1.3970000000
0.259910	1.4136000000
0.279910	1.4296000000
0.299910	1.4451000000
0.319910	1.4602000000
0.339910	1.4749000000
0.359910	1.4892000000
0.379910	1.5031000000
0.399910	1.5166000000
0.419910	1.5299000000
0.439910	1.5428000000
0.459910	1.5554000000
0.479910	1.5678000000
0.499910	1.5798000000
0.519910	1.5917000000
0.539910	1.6033000000
0.559910	1.6146000000
0.579910	1.6258000000
0.599910	1.6367000000
0.619910	1.6475000000
0.639910	1.6580000000
0.659910	1.6684000000
0.679910	1.6786000000
0.699910	1.6886000000
0.719910	1.6984000000
0.739910	1.7081000000
0.759910	1.7177000000
0.779910	1.7271000000
0.799910	1.7364000000
0.819910	1.7455000000
0.839910	1.7545000000
0.859910	1.7634000000
0.879910	1.7721000000
0.899910	1.7808000000

```
            0.919910        1.7893000000
            0.939910        1.7977000000
            0.959910        1.8060000000
            0.979910        1.8142000000
            0.999910        1.8223000000
            1.000000        1.8223364500
*DEFINE_CURVE
$ 10 /s strain rate
$     LCID      SIDR      SCLA      SCLO      OFFA      OFFO    DATTYP
      1004         0       1.0       1.0       0.0       0.0         0
$           ABSCISSA            ORDINATE
            0.000000        1.1104800000
            0.001325        1.1224800000
            0.002650        1.1324800000
            0.003975        1.1384800000
            0.005300        1.1424800000
            0.006625        1.1454800000
            0.007950        1.1484800000
            0.009275        1.1514800000
            0.010600        1.1544800000
            0.011925        1.1574800000
            0.033285        1.1920800000
            0.034610        1.1934800000
            0.035941        1.1949800000
            0.037269        1.1963800000
            0.038585        1.1978800000
            0.039884        1.1994800000
            0.041229        1.2010800000
            0.042566        1.2027800000
            0.043911        1.2045800000
            0.045247        1.2063800000
            0.046571        1.2080800000
            0.047874        1.2098800000
            0.049185        1.2116800000
            0.050515        1.2134800000
            0.051864        1.2153800000
            0.053200        1.2171800000
            0.054515        1.2188800000
            0.055824        1.2205800000
            0.057115        1.2222800000
            0.058432        1.2239800000
            0.059759        1.2256800000
            0.059909        1.2258800000
            0.079909        1.2498800000
            0.099909        1.2727800000
            0.119910        1.2945800000
            0.139910        1.3152800000
            0.159910        1.3351800000
            0.179910        1.3542800000
            0.199910        1.3726800000
            0.219910        1.3903800000
            0.239910        1.4074800000
```

```
            0.259910        1.4240800000
            0.279910        1.4400800000
            0.299910        1.4555800000
            0.319910        1.4706800000
            0.339910        1.4853800000
            0.359910        1.4996800000
            0.379910        1.5135800000
            0.399910        1.5270800000
            0.419910        1.5403800000
            0.439910        1.5532800000
            0.459910        1.5658800000
            0.479910        1.5782800000
            0.499910        1.5902800000
            0.519910        1.6021800000
            0.539910        1.6137800000
            0.559910        1.6250800000
            0.579910        1.6362800000
            0.599910        1.6471800000
            0.619910        1.6579800000
            0.639910        1.6684800000
            0.659910        1.6788800000
            0.679910        1.6890800000
            0.699910        1.6990800000
            0.719910        1.7088800000
            0.739910        1.7185800000
            0.759910        1.7281800000
            0.779910        1.7375800000
            0.799910        1.7468800000
            0.819910        1.7559800000
            0.839910        1.7649800000
            0.859910        1.7738800000
            0.879910        1.7825800000
            0.899910        1.7912800000
            0.919910        1.7997800000
            0.939910        1.8081800000
            0.959910        1.8164800000
            0.979910        1.8246800000
            0.999910        1.8327800000
            1.000000        1.8328164500
*DEFINE_CURVE
$ 100 /s strain rate
$     LCID      SIDR      SCLA      SCLO      OFFA      OFFO    DATTYP
      1005         0       1.0       1.0       0.0       0.0         0
$           ABSCISSA           ORDINATE
            0.000000        1.1483800000
            0.001325        1.1603800000
            0.002650        1.1703800000
            0.003975        1.1763800000
            0.005300        1.1803800000
            0.006625        1.1833800000
            0.007950        1.1863800000
            0.009275        1.1893800000
```

0.010600	1.1923800000
0.011925	1.1953800000
0.033285	1.2299800000
0.034610	1.2313800000
0.035941	1.2328800000
0.037269	1.2342800000
0.038585	1.2357800000
0.039884	1.2373800000
0.041229	1.2389800000
0.042566	1.2406800000
0.043911	1.2424800000
0.045247	1.2442800000
0.046571	1.2459800000
0.047874	1.2477800000
0.049185	1.2495800000
0.050515	1.2513800000
0.051864	1.2532800000
0.053200	1.2550800000
0.054515	1.2567800000
0.055824	1.2584800000
0.057115	1.2601800000
0.058432	1.2618800000
0.059759	1.2635800000
0.059909	1.2637800000
0.079909	1.2877800000
0.099909	1.3106800000
0.119910	1.3324800000
0.139910	1.3531800000
0.159910	1.3730800000
0.179910	1.3921800000
0.199910	1.4105800000
0.219910	1.4282800000
0.239910	1.4453800000
0.259910	1.4619800000
0.279910	1.4779800000
0.299910	1.4934800000
0.319910	1.5085800000
0.339910	1.5232800000
0.359910	1.5375800000
0.379910	1.5514800000
0.399910	1.5649800000
0.419910	1.5782800000
0.439910	1.5911800000
0.459910	1.6037800000
0.479910	1.6161800000
0.499910	1.6281800000
0.519910	1.6400800000
0.539910	1.6516800000
0.559910	1.6629800000
0.579910	1.6741800000
0.599910	1.6850800000
0.619910	1.6958800000

```
            0.639910        1.7063800000
            0.659910        1.7167800000
            0.679910        1.7269800000
            0.699910        1.7369800000
            0.719910        1.7467800000
            0.739910        1.7564800000
            0.759910        1.7660800000
            0.779910        1.7754800000
            0.799910        1.7847800000
            0.819910        1.7938800000
            0.839910        1.8028800000
            0.859910        1.8117800000
            0.879910        1.8204800000
            0.899910        1.8291800000
            0.919910        1.8376800000
            0.939910        1.8460800000
            0.959910        1.8543800000
            0.979910        1.8625800000
            0.999910        1.8706800000
            1.000000        1.8707164500
*DEFINE_CURVE
$ 1000 /s strain rate
$     LCID      SIDR      SCLA      SCLO      OFFA      OFFO    DATTYP
      1006         0       1.0       1.0       0.0       0.0         0
$           ABSCISSA          ORDINATE
            0.000000        1.2298800000
            0.001325        1.2418800000
            0.002650        1.2518800000
            0.003975        1.2578800000
            0.005300        1.2618800000
            0.006625        1.2648800000
            0.007950        1.2678800000
            0.009275        1.2708800000
            0.010600        1.2738800000
            0.011925        1.2768800000
            0.033285        1.3114800000
            0.034610        1.3128800000
            0.035941        1.3143800000
            0.037269        1.3157800000
            0.038585        1.3172800000
            0.039884        1.3188800000
            0.041229        1.3204800000
            0.042566        1.3221800000
            0.043911        1.3239800000
            0.045247        1.3257800000
            0.046571        1.3274800000
            0.047874        1.3292800000
            0.049185        1.3310800000
            0.050515        1.3328800000
            0.051864        1.3347800000
            0.053200        1.3365800000
            0.054515        1.3382800000
```

0.055824	1.3399800000
0.057115	1.3416800000
0.058432	1.3433800000
0.059759	1.3450800000
0.059909	1.3452800000
0.079909	1.3692800000
0.099909	1.3921800000
0.119910	1.4139800000
0.139910	1.4346800000
0.159910	1.4545800000
0.179910	1.4736800000
0.199910	1.4920800000
0.219910	1.5097800000
0.239910	1.5268800000
0.259910	1.5434800000
0.279910	1.5594800000
0.299910	1.5749800000
0.319910	1.5900800000
0.339910	1.6047800000
0.359910	1.6190800000
0.379910	1.6329800000
0.399910	1.6464800000
0.419910	1.6597800000
0.439910	1.6726800000
0.459910	1.6852800000
0.479910	1.6976800000
0.499910	1.7096800000
0.519910	1.7215800000
0.539910	1.7331800000
0.559910	1.7444800000
0.579910	1.7556800000
0.599910	1.7665800000
0.619910	1.7773800000
0.639910	1.7878800000
0.659910	1.7982800000
0.679910	1.8084800000
0.699910	1.8184800000
0.719910	1.8282800000
0.739910	1.8379800000
0.759910	1.8475800000
0.779910	1.8569800000
0.799910	1.8662800000
0.819910	1.8753800000
0.839910	1.8843800000
0.859910	1.8932800000
0.879910	1.9019800000
0.899910	1.9106800000
0.919910	1.9191800000
0.939910	1.9275800000
0.959910	1.9358800000
0.979910	1.9440800000
0.999910	1.9521800000

```
          1.000000       1.9522164500
*DEFINE_CURVE
$ 1500 /s strain rate
$     LCID      SIDR      SCLA      SCLO      OFFA      OFFO    DATTYP
      1007         0       1.0       1.0       0.0       0.0         0
$           ABSCISSA          ORDINATE
          0.000000       1.2598800000
          0.001325       1.2718800000
          0.002650       1.2818800000
          0.003975       1.2878800000
          0.005300       1.2918800000
          0.006625       1.2948800000
          0.007950       1.2978800000
          0.009275       1.3008800000
          0.010600       1.3038800000
          0.011925       1.3068800000
          0.033285       1.3414800000
          0.034610       1.3428800000
          0.035941       1.3443800000
          0.037269       1.3457800000
          0.038585       1.3472800000
          0.039884       1.3488800000
          0.041229       1.3504800000
          0.042566       1.3521800000
          0.043911       1.3539800000
          0.045247       1.3557800000
          0.046571       1.3574800000
          0.047874       1.3592800000
          0.049185       1.3610800000
          0.050515       1.3628800000
          0.051864       1.3647800000
          0.053200       1.3665800000
          0.054515       1.3682800000
          0.055824       1.3699800000
          0.057115       1.3716800000
          0.058432       1.3733800000
          0.059759       1.3750800000
          0.059909       1.3752800000
          0.079909       1.3992800000
          0.099909       1.4221800000
          0.119910       1.4439800000
          0.139910       1.4646800000
          0.159910       1.4845800000
          0.179910       1.5036800000
          0.199910       1.5220800000
          0.219910       1.5397800000
          0.239910       1.5568800000
          0.259910       1.5734800000
          0.279910       1.5894800000
          0.299910       1.6049800000
          0.319910       1.6200800000
          0.339910       1.6347800000
```

```
            0.359910        1.6490800000
            0.379910        1.6629800000
            0.399910        1.6764800000
            0.419910        1.6897800000
            0.439910        1.7026800000
            0.459910        1.7152800000
            0.479910        1.7276800000
            0.499910        1.7396800000
            0.519910        1.7515800000
            0.539910        1.7631800000
            0.559910        1.7744800000
            0.579910        1.7856800000
            0.599910        1.7965800000
            0.619910        1.8073800000
            0.639910        1.8178800000
            0.659910        1.8282800000
            0.679910        1.8384800000
            0.699910        1.8484800000
            0.719910        1.8582800000
            0.739910        1.8679800000
            0.759910        1.8775800000
            0.779910        1.8869800000
            0.799910        1.8962800000
            0.819910        1.9053800000
            0.839910        1.9143800000
            0.859910        1.9232800000
            0.879910        1.9319800000
            0.899910        1.9406800000
            0.919910        1.9491800000
            0.939910        1.9575800000
            0.959910        1.9658800000
            0.979910        1.9740800000
            0.999910        1.9821800000
            1.000000        1.9822164500
*DEFINE_CURVE
$ 2500 /s strain rate
$     LCID      SIDR      SCLA      SCLO      OFFA      OFFO    DATTYP
      1008         0       1.0       1.0       0.0       0.0         0
$           ABSCISSA           ORDINATE
            0.000000        1.3048800000
            0.001325        1.3168800000
            0.002650        1.3268800000
            0.003975        1.3328800000
            0.005300        1.3368800000
            0.006625        1.3398800000
            0.007950        1.3428800000
            0.009275        1.3458800000
            0.010600        1.3488800000
            0.011925        1.3518800000
            0.033285        1.3864800000
            0.034610        1.3878800000
            0.035941        1.3893800000
```

0.037269	1.3907800000
0.038585	1.3922800000
0.039884	1.3938800000
0.041229	1.3954800000
0.042566	1.3971800000
0.043911	1.3989800000
0.045247	1.4007800000
0.046571	1.4024800000
0.047874	1.4042800000
0.049185	1.4060800000
0.050515	1.4078800000
0.051864	1.4097800000
0.053200	1.4115800000
0.054515	1.4132800000
0.055824	1.4149800000
0.057115	1.4166800000
0.058432	1.4183800000
0.059759	1.4200800000
0.059909	1.4202800000
0.079909	1.4442800000
0.099909	1.4671800000
0.119910	1.4889800000
0.139910	1.5096800000
0.159910	1.5295800000
0.179910	1.5486800000
0.199910	1.5670800000
0.219910	1.5847800000
0.239910	1.6018800000
0.259910	1.6184800000
0.279910	1.6344800000
0.299910	1.6499800000
0.319910	1.6650800000
0.339910	1.6797800000
0.359910	1.6940800000
0.379910	1.7079800000
0.399910	1.7214800000
0.419910	1.7347800000
0.439910	1.7476800000
0.459910	1.7602800000
0.479910	1.7726800000
0.499910	1.7846800000
0.519910	1.7965800000
0.539910	1.8081800000
0.559910	1.8194800000
0.579910	1.8306800000
0.599910	1.8415800000
0.619910	1.8523800000
0.639910	1.8628800000
0.659910	1.8732800000
0.679910	1.8834800000
0.699910	1.8934800000
0.719910	1.9032800000

```
            0.739910        1.9129800000
            0.759910        1.9225800000
            0.779910        1.9319800000
            0.799910        1.9412800000
            0.819910        1.9503800000
            0.839910        1.9593800000
            0.859910        1.9682800000
            0.879910        1.9769800000
            0.899910        1.9856800000
            0.919910        1.9941800000
            0.939910        2.0025800000
            0.959910        2.0108800000
            0.979910        2.0190800000
            0.999910        2.0271800000
            1.000000        2.0272164500
*DEFINE_CURVE
$ 5000 /s strain rate
$     LCID      SIDR      SCLA      SCLO      OFFA      OFFO    DATTYP
      1009         0       1.0       1.0       0.0       0.0         0
$           ABSCISSA           ORDINATE
            0.000000        1.3873800000
            0.001325        1.3993800000
            0.002650        1.4093800000
            0.003975        1.4153800000
            0.005300        1.4193800000
            0.006625        1.4223800000
            0.007950        1.4253800000
            0.009275        1.4283800000
            0.010600        1.4313800000
            0.011925        1.4343800000
            0.033285        1.4689800000
            0.034610        1.4703800000
            0.035941        1.4718800000
            0.037269        1.4732800000
            0.038585        1.4747800000
            0.039884        1.4763800000
            0.041229        1.4779800000
            0.042566        1.4796800000
            0.043911        1.4814800000
            0.045247        1.4832800000
            0.046571        1.4849800000
            0.047874        1.4867800000
            0.049185        1.4885800000
            0.050515        1.4903800000
            0.051864        1.4922800000
            0.053200        1.4940800000
            0.054515        1.4957800000
            0.055824        1.4974800000
            0.057115        1.4991800000
            0.058432        1.5008800000
            0.059759        1.5025800000
            0.059909        1.5027800000
```

```
            0.079909        1.5267800000
            0.099909        1.5496800000
            0.119910        1.5714800000
            0.139910        1.5921800000
            0.159910        1.6120800000
            0.179910        1.6311800000
            0.199910        1.6495800000
            0.219910        1.6672800000
            0.239910        1.6843800000
            0.259910        1.7009800000
            0.279910        1.7169800000
            0.299910        1.7324800000
            0.319910        1.7475800000
            0.339910        1.7622800000
            0.359910        1.7765800000
            0.379910        1.7904800000
            0.399910        1.8039800000
            0.419910        1.8172800000
            0.439910        1.8301800000
            0.459910        1.8427800000
            0.479910        1.8551800000
            0.499910        1.8671800000
            0.519910        1.8790800000
            0.539910        1.8906800000
            0.559910        1.9019800000
            0.579910        1.9131800000
            0.599910        1.9240800000
            0.619910        1.9348800000
            0.639910        1.9453800000
            0.659910        1.9557800000
            0.679910        1.9659800000
            0.699910        1.9759800000
            0.719910        1.9857800000
            0.739910        1.9954800000
            0.759910        2.0050800000
            0.779910        2.0144800000
            0.799910        2.0237800000
            0.819910        2.0328800000
            0.839910        2.0418800000
            0.859910        2.0507800000
            0.879910        2.0594800000
            0.899910        2.0681800000
            0.919910        2.0766800000
            0.939910        2.0850800000
            0.959910        2.0933800000
            0.979910        2.1015800000
            0.999910        2.1096800000
            1.000000        2.1097164500
*DEFINE_CURVE
$ 10000 /s strain rate
$     LCID      SIDR      SCLA      SCLO      OFFA      OFFO    DATTYP
      1010         0       1.0       1.0       0.0       0.0         0
```

$	ABSCISSA	ORDINATE
	0.000000	1.7348800000
	0.001325	1.7468800000
	0.002650	1.7568800000
	0.003975	1.7628800000
	0.005300	1.7668800000
	0.006625	1.7698800000
	0.007950	1.7728800000
	0.009275	1.7758800000
	0.010600	1.7788800000
	0.011925	1.7818800000
	0.033285	1.8164800000
	0.034610	1.8178800000
	0.035941	1.8193800000
	0.037269	1.8207800000
	0.038585	1.8222800000
	0.039884	1.8238800000
	0.041229	1.8254800000
	0.042566	1.8271800000
	0.043911	1.8289800000
	0.045247	1.8307800000
	0.046571	1.8324800000
	0.047874	1.8342800000
	0.049185	1.8360800000
	0.050515	1.8378800000
	0.051864	1.8397800000
	0.053200	1.8415800000
	0.054515	1.8432800000
	0.055824	1.8449800000
	0.057115	1.8466800000
	0.058432	1.8483800000
	0.059759	1.8500800000
	0.059909	1.8502800000
	0.079909	1.8742800000
	0.099909	1.8971800000
	0.119910	1.9189800000
	0.139910	1.9396800000
	0.159910	1.9595800000
	0.179910	1.9786800000
	0.199910	1.9970800000
	0.219910	2.0147800000
	0.239910	2.0318800000
	0.259910	2.0484800000
	0.279910	2.0644800000
	0.299910	2.0799800000
	0.319910	2.0950800000
	0.339910	2.1097800000
	0.359910	2.1240800000
	0.379910	2.1379800000
	0.399910	2.1514800000
	0.419910	2.1647800000
	0.439910	2.1776800000

```
            0.459910        2.1902800000
            0.479910        2.2026800000
            0.499910        2.2146800000
            0.519910        2.2265800000
            0.539910        2.2381800000
            0.559910        2.2494800000
            0.579910        2.2606800000
            0.599910        2.2715800000
            0.619910        2.2823800000
            0.639910        2.2928800000
            0.659910        2.3032800000
            0.679910        2.3134800000
            0.699910        2.3234800000
            0.719910        2.3332800000
            0.739910        2.3429800000
            0.759910        2.3525800000
            0.779910        2.3619800000
            0.799910        2.3712800000
            0.819910        2.3803800000
            0.839910        2.3893800000
            0.859910        2.3982800000
            0.879910        2.4069800000
            0.899910        2.4156800000
            0.919910        2.4241800000
            0.939910        2.4325800000
            0.959910        2.4408800000
            0.979910        2.4490800000
            0.999910        2.4571800000
            1.000000        2.4572164500
*DEFINE_CURVE
$ 15000 /s strain rate
$     LCID      SIDR      SCLA      SCLO      OFFA      OFFO    DATTYP
      1011         0       1.0       1.0       0.0       0.0         0
$           ABSCISSA           ORDINATE
            0.000000        2.0823800000
            0.001325        2.0943800000
            0.002650        2.1043800000
            0.003975        2.1103800000
            0.005300        2.1143800000
            0.006625        2.1173800000
            0.007950        2.1203800000
            0.009275        2.1233800000
            0.010600        2.1263800000
            0.011925        2.1293800000
            0.033285        2.1639800000
            0.034610        2.1653800000
            0.035941        2.1668800000
            0.037269        2.1682800000
            0.038585        2.1697800000
            0.039884        2.1713800000
            0.041229        2.1729800000
            0.042566        2.1746800000
```

0.043911	2.1764800000
0.045247	2.1782800000
0.046571	2.1799800000
0.047874	2.1817800000
0.049185	2.1835800000
0.050515	2.1853800000
0.051864	2.1872800000
0.053200	2.1890800000
0.054515	2.1907800000
0.055824	2.1924800000
0.057115	2.1941800000
0.058432	2.1958800000
0.059759	2.1975800000
0.059909	2.1977800000
0.079909	2.2217800000
0.099909	2.2446800000
0.119910	2.2664800000
0.139910	2.2871800000
0.159910	2.3070800000
0.179910	2.3261800000
0.199910	2.3445800000
0.219910	2.3622800000
0.239910	2.3793800000
0.259910	2.3959800000
0.279910	2.4119800000
0.299910	2.4274800000
0.319910	2.4425800000
0.339910	2.4572800000
0.359910	2.4715800000
0.379910	2.4854800000
0.399910	2.4989800000
0.419910	2.5122800000
0.439910	2.5251800000
0.459910	2.5377800000
0.479910	2.5501800000
0.499910	2.5621800000
0.519910	2.5740800000
0.539910	2.5856800000
0.559910	2.5969800000
0.579910	2.6081800000
0.599910	2.6190800000
0.619910	2.6298800000
0.639910	2.6403800000
0.659910	2.6507800000
0.679910	2.6609800000
0.699910	2.6709800000
0.719910	2.6807800000
0.739910	2.6904800000
0.759910	2.7000800000
0.779910	2.7094800000
0.799910	2.7187800000
0.819910	2.7278800000

```
            0.839910        2.7368800000
            0.859910        2.7457800000
            0.879910        2.7544800000
            0.899910        2.7631800000
            0.919910        2.7716800000
            0.939910        2.7800800000
            0.959910        2.7883800000
            0.979910        2.7965800000
            0.999910        2.8046800000
            1.000000        2.8047164500
*DEFINE_CURVE
$ 20000 /s strain rate
$     LCID      SIDR      SCLA      SCLO      OFFA      OFFO    DATTYP
      1012         0       1.0       1.0       0.0       0.0         0
$           ABSCISSA            ORDINATE
            0.000000        2.4298800000
            0.001325        2.4418800000
            0.002650        2.4518800000
            0.003975        2.4578800000
            0.005300        2.4618800000
            0.006625        2.4648800000
            0.007950        2.4678800000
            0.009275        2.4708800000
            0.010600        2.4738800000
            0.011925        2.4768800000
            0.033285        2.5114800000
            0.034610        2.5128800000
            0.035941        2.5143800000
            0.037269        2.5157800000
            0.038585        2.5172800000
            0.039884        2.5188800000
            0.041229        2.5204800000
            0.042566        2.5221800000
            0.043911        2.5239800000
            0.045247        2.5257800000
            0.046571        2.5274800000
            0.047874        2.5292800000
            0.049185        2.5310800000
            0.050515        2.5328800000
            0.051864        2.5347800000
            0.053200        2.5365800000
            0.054515        2.5382800000
            0.055824        2.5399800000
            0.057115        2.5416800000
            0.058432        2.5433800000
            0.059759        2.5450800000
            0.059909        2.5452800000
            0.079909        2.5692800000
            0.099909        2.5921800000
            0.119910        2.6139800000
            0.139910        2.6346800000
            0.159910        2.6545800000
```

```
            0.179910        2.6736800000
            0.199910        2.6920800000
            0.219910        2.7097800000
            0.239910        2.7268800000
            0.259910        2.7434800000
            0.279910        2.7594800000
            0.299910        2.7749800000
            0.319910        2.7900800000
            0.339910        2.8047800000
            0.359910        2.8190800000
            0.379910        2.8329800000
            0.399910        2.8464800000
            0.419910        2.8597800000
            0.439910        2.8726800000
            0.459910        2.8852800000
            0.479910        2.8976800000
            0.499910        2.9096800000
            0.519910        2.9215800000
            0.539910        2.9331800000
            0.559910        2.9444800000
            0.579910        2.9556800000
            0.599910        2.9665800000
            0.619910        2.9773800000
            0.639910        2.9878800000
            0.659910        2.9982800000
            0.679910        3.0084800000
            0.699910        3.0184800000
            0.719910        3.0282800000
            0.739910        3.0379800000
            0.759910        3.0475800000
            0.779910        3.0569800000
            0.799910        3.0662800000
            0.819910        3.0753800000
            0.839910        3.0843800000
            0.859910        3.0932800000
            0.879910        3.1019800000
            0.899910        3.1106800000
            0.919910        3.1191800000
            0.939910        3.1275800000
            0.959910        3.1358800000
            0.979910        3.1440800000
            0.999910        3.1521800000
*DEFINE_CURVE
$ 30000 /s strain rate
$     LCID      SIDR      SCLA      SCLO      OFFA      OFFO    DATTYP
      1013         0       1.0       1.0       0.0       0.0         0
$          ABSCISSA           ORDINATE
            0.000000        3.1248800000
            0.001325        3.1368800000
            0.002650        3.1468800000
            0.003975        3.1528800000
            0.005300        3.1568800000
```

0.006625	3.1598800000
0.007950	3.1628800000
0.009275	3.1658800000
0.010600	3.1688800000
0.011925	3.1718800000
0.033285	3.2064800000
0.034610	3.2078800000
0.035941	3.2093800000
0.037269	3.2107800000
0.038585	3.2122800000
0.039884	3.2138800000
0.041229	3.2154800000
0.042566	3.2171800000
0.043911	3.2189800000
0.045247	3.2207800000
0.046571	3.2224800000
0.047874	3.2242800000
0.049185	3.2260800000
0.050515	3.2278800000
0.051864	3.2297800000
0.053200	3.2315800000
0.054515	3.2332800000
0.055824	3.2349800000
0.057115	3.2366800000
0.058432	3.2383800000
0.059759	3.2400800000
0.059909	3.2402800000
0.079909	3.2642800000
0.099909	3.2871800000
0.119910	3.3089800000
0.139910	3.3296800000
0.159910	3.3495800000
0.179910	3.3686800000
0.199910	3.3870800000
0.219910	3.4047800000
0.239910	3.4218800000
0.259910	3.4384800000
0.279910	3.4544800000
0.299910	3.4699800000
0.319910	3.4850800000
0.339910	3.4997800000
0.359910	3.5140800000
0.379910	3.5279800000
0.399910	3.5414800000
0.419910	3.5547800000
0.439910	3.5676800000
0.459910	3.5802800000
0.479910	3.5926800000
0.499910	3.6046800000
0.519910	3.6165800000
0.539910	3.6281800000
0.559910	3.6394800000

```
            0.579910        3.6506800000
            0.599910        3.6615800000
            0.619910        3.6723800000
            0.639910        3.6828800000
            0.659910        3.6932800000
            0.679910        3.7034800000
            0.699910        3.7134800000
            0.719910        3.7232800000
            0.739910        3.7329800000
            0.759910        3.7425800000
            0.779910        3.7519800000
            0.799910        3.7612800000
            0.819910        3.7703800000
            0.839910        3.7793800000
            0.859910        3.7882800000
            0.879910        3.7969800000
            0.899910        3.8056800000
            0.919910        3.8141800000
            0.939910        3.8225800000
            0.959910        3.8308800000
            0.979910        3.8390800000
            0.999910        3.8471800000
*DEFINE_CURVE
$ 30000 /s strain rate
$     LCID      SIDR      SCLA      SCLO      OFFA      OFFO    DATTYP
      1014         0       1.0       1.0       0.0       0.0         0
$           ABSCISSA           ORDINATE
            0.000000        3.8198800000
            0.001325        3.8318800000
            0.002650        3.8418800000
            0.003975        3.8478800000
            0.005300        3.8518800000
            0.006625        3.8548800000
            0.007950        3.8578800000
            0.009275        3.8608800000
            0.010600        3.8638800000
            0.011925        3.8668800000
            0.033285        3.9014800000
            0.034610        3.9028800000
            0.035941        3.9043800000
            0.037269        3.9057800000
            0.038585        3.9072800000
            0.039884        3.9088800000
            0.041229        3.9104800000
            0.042566        3.9121800000
            0.043911        3.9139800000
            0.045247        3.9157800000
            0.046571        3.9174800000
            0.047874        3.9192800000
            0.049185        3.9210800000
            0.050515        3.9228800000
            0.051864        3.9247800000
```

0.053200	3.9265800000
0.054515	3.9282800000
0.055824	3.9299800000
0.057115	3.9316800000
0.058432	3.9333800000
0.059759	3.9350800000
0.059909	3.9352800000
0.079909	3.9592800000
0.099909	3.9821800000
0.119910	4.0039800000
0.139910	4.0246800000
0.159910	4.0445800000
0.179910	4.0636800000
0.199910	4.0820800000
0.219910	4.0997800000
0.239910	4.1168800000
0.259910	4.1334800000
0.279910	4.1494800000
0.299910	4.1649800000
0.319910	4.1800800000
0.339910	4.1947800000
0.359910	4.2090800000
0.379910	4.2229800000
0.399910	4.2364800000
0.419910	4.2497800000
0.439910	4.2626800000
0.459910	4.2752800000
0.479910	4.2876800000
0.499910	4.2996800000
0.519910	4.3115800000
0.539910	4.3231800000
0.559910	4.3344800000
0.579910	4.3456800000
0.599910	4.3565800000
0.619910	4.3673800000
0.639910	4.3778800000
0.659910	4.3882800000
0.679910	4.3984800000
0.699910	4.4084800000
0.719910	4.4182800000
0.739910	4.4279800000
0.759910	4.4375800000
0.779910	4.4469800000
0.799910	4.4562800000
0.819910	4.4653800000
0.839910	4.4743800000
0.859910	4.4832800000
0.879910	4.4919800000
0.899910	4.5006800000
0.919910	4.5091800000
0.939910	4.5175800000
0.959910	4.5258800000

```
            0.979910        4.5340800000
            0.999910        4.5421800000
*DEFINE_CURVE
$ 50000 /s strain rate
$     LCID      SIDR      SCLA      SCLO      OFFA      OFFO    DATTYP
      1015         0       1.0       1.0       0.0       0.0         0
$           ABSCISSA           ORDINATE
            0.000000        4.5148800000
            0.001325        4.5268800000
            0.002650        4.5368800000
            0.003975        4.5428800000
            0.005300        4.5468800000
            0.006625        4.5498800000
            0.007950        4.5528800000
            0.009275        4.5558800000
            0.010600        4.5588800000
            0.011925        4.5618800000
            0.033285        4.5964800000
            0.034610        4.5978800000
            0.035941        4.5993800000
            0.037269        4.6007800000
            0.038585        4.6022800000
            0.039884        4.6038800000
            0.041229        4.6054800000
            0.042566        4.6071800000
            0.043911        4.6089800000
            0.045247        4.6107800000
            0.046571        4.6124800000
            0.047874        4.6142800000
            0.049185        4.6160800000
            0.050515        4.6178800000
            0.051864        4.6197800000
            0.053200        4.6215800000
            0.054515        4.6232800000
            0.055824        4.6249800000
            0.057115        4.6266800000
            0.058432        4.6283800000
            0.059759        4.6300800000
            0.059909        4.6302800000
            0.079909        4.6542800000
            0.099909        4.6771800000
            0.119910        4.6989800000
            0.139910        4.7196800000
            0.159910        4.7395800000
            0.179910        4.7586800000
            0.199910        4.7770800000
            0.219910        4.7947800000
            0.239910        4.8118800000
            0.259910        4.8284800000
            0.279910        4.8444800000
            0.299910        4.8599800000
            0.319910        4.8750800000
```

```
            0.339910        4.8897800000
            0.359910        4.9040800000
            0.379910        4.9179800000
            0.399910        4.9314800000
            0.419910        4.9447800000
            0.439910        4.9576800000
            0.459910        4.9702800000
            0.479910        4.9826800000
            0.499910        4.9946800000
            0.519910        5.0065800000
            0.539910        5.0181800000
            0.559910        5.0294800000
            0.579910        5.0406800000
            0.599910        5.0515800000
            0.619910        5.0623800000
            0.639910        5.0728800000
            0.659910        5.0832800000
            0.679910        5.0934800000
            0.699910        5.1034800000
            0.719910        5.1132800000
            0.739910        5.1229800000
            0.759910        5.1325800000
            0.779910        5.1419800000
            0.799910        5.1512800000
            0.819910        5.1603800000
            0.839910        5.1693800000
            0.859910        5.1782800000
            0.879910        5.1869800000
            0.899910        5.1956800000
            0.919910        5.2041800000
            0.939910        5.2125800000
            0.959910        5.2208800000
            0.979910        5.2290800000
            0.999910        5.2371800000
$$$$$$$$$$$$$$$$$$$$$$$$$$$$$$$$$$$$$$$$$$$$$$$$$$$$$$$$$$$
$                   Temperature Table                     $
$$$$$$$$$$$$$$$$$$$$$$$$$$$$$$$$$$$$$$$$$$$$$$$$$$$$$$$$$$$
*DEFINE_TABLE
$     tbid       sfa      offa
      2000
$                value              curveid
              223.15                 2001
              293.00                 2002
              473.15                 2003
              673.15                 2004
              873.15                 2005
             1877.00                 2006
             2500.00                 2007
$$$$$$$$$$$$$$$$$$$$$$$$$$$$$$$$$$$$$$$$$$$$$$$$$$$$$$$$$$$
$                   Temperature Curves                    $
$$$$$$$$$$$$$$$$$$$$$$$$$$$$$$$$$$$$$$$$$$$$$$$$$$$$$$$$$$$
*DEFINE_CURVE
```

```
$ 223.15 K
$     LCID      SIDR      SCLA      SCLO      OFFA      OFFO    DATTYP
      2001         0       1.0       1.0       0.0       0.0         0
$           ABSCISSA           ORDINATE
            0.000000        0.8484143101
            0.001000        0.9935384558
            0.002000        1.0129069508
            0.003000        1.0302732003
            0.004000        1.0438265791
            0.005000        1.0535248886
            0.006000        1.0615499145
            0.007000        1.0677125505
            0.008000        1.0730149489
            0.009000        1.0775667208
            0.010000        1.0818032924
            0.011000        1.0855636492
            0.012000        1.0888192260
            0.013000        1.0911523162
            0.014000        1.0928271959
            0.015000        1.0937762502
            0.016000        1.0945796582
            0.017000        1.0953260934
            0.018000        1.0958599106
            0.019000        1.0964217933
            0.020000        1.0972119721
            0.021000        1.0982987854
            0.022000        1.0990557682
            0.023000        1.0998914198
            0.024000        1.1006894191
            0.025000        1.1015589915
            0.026000        1.1023630624
            0.027000        1.1029977353
            0.028000        1.1036725981
            0.029000        1.1047875780
            0.030000        1.1059740472
            0.031000        1.1070797366
            0.032000        1.1080848122
            0.033000        1.1092687012
            0.034000        1.1108380856
            0.035000        1.1124683472
            0.036000        1.1139702674
            0.037000        1.1153947632
            0.038000        1.1167543013
            0.039000        1.1177936190
            0.040000        1.1188203345
            0.041000        1.1198932399
            0.042000        1.1211197375
            0.043000        1.1223530804
            0.044000        1.1234399362
            0.045000        1.1245219080
            0.046000        1.1257206427
            0.047000        1.1266427528
```

0.048000	1.1276437291
0.049000	1.1288770970
0.050000	1.1303534669
0.051000	1.1317982281
0.052000	1.1331026428
0.053000	1.1343804945
0.054000	1.1356736933
0.055000	1.1368829882
0.056000	1.1380084592
0.057000	1.1390627260
0.058000	1.1399675169
0.059000	1.1408096377
0.060000	1.1415672243
0.061000	1.1423165001
0.062000	1.1430762615
0.063000	1.1437317650
0.064000	1.1443977920
0.065000	1.1450534836
0.066000	1.1457301169
0.067000	1.1465318875
0.068000	1.1473545233
0.069000	1.1481875937
0.070000	1.1492081283
0.071000	1.1502432633
0.072000	1.1513942096
0.073000	1.1526476407
0.074000	1.1539334776
0.075000	1.1553944974
0.076000	1.1568357993
0.077000	1.1583169907
0.078000	1.1599031663
0.079000	1.1615395458
0.080000	1.1631031687
0.081000	1.1647026357
0.082000	1.1662917548
0.083000	1.1678283119
0.084000	1.1693545491
0.085000	1.1708075215
0.086000	1.1721672094
0.087000	1.1735263455
0.088000	1.1748752376
0.089000	1.1761510054
0.090000	1.1773750978
0.091000	1.1785092705
0.092000	1.1796747156
0.093000	1.1808085947
0.094000	1.1819840864
0.095000	1.1831280262
0.096000	1.1842514358
0.097000	1.1853743867
0.098000	1.1864975188
0.099000	1.1876305428

0.100000	1.1886706482
0.101000	1.1897564957
0.102000	1.1908228035
0.103000	1.1916810279
0.104000	1.1925301312
0.105000	1.1934089975
0.106000	1.1941650765
0.107000	1.1949302826
0.108000	1.1955727823
0.109000	1.1962256693
0.110000	1.1968980419
0.111000	1.1975328335
0.112000	1.1982192925
0.113000	1.1989677081
0.114000	1.1997264577
0.115000	1.2005471120
0.116000	1.2014812017
0.117000	1.2025286614
0.118000	1.2036069509
0.119000	1.2047675897
0.120000	1.2059477834
0.121000	1.2072993551
0.122000	1.2087425727
0.123000	1.2100834943
0.124000	1.2115160479
0.125000	1.2129287129
0.126000	1.2142476379
0.127000	1.2155467055
0.128000	1.2168138628
0.129000	1.2179685507
0.130000	1.2190605160
0.131000	1.2200229222
0.132000	1.2209946784
0.133000	1.2219569511
0.134000	1.2229285739
0.135000	1.2238907137
0.136000	1.2248622038
0.137000	1.2258242113
0.138000	1.2267955693
0.139000	1.2277574451
0.140000	1.2287286717
0.141000	1.2297374993
0.142000	1.2307368465
0.143000	1.2317455478
0.144000	1.2327447679
0.145000	1.2337533434
0.146000	1.2347524370
0.147000	1.2357608873
0.148000	1.2367598550
0.149000	1.2377681806
0.150000	1.2387567637
0.151000	1.2396542771

0.152000	1.2405423279
0.153000	1.2414305715
0.154000	1.2423185388
0.155000	1.2432066964
0.156000	1.2440945807
0.157000	1.2449826527
0.158000	1.2458704543
0.159000	1.2467584410
0.160000	1.2476461604
0.161000	1.2485717327
0.162000	1.2494970397
0.163000	1.2504225264
0.164000	1.2513477502
0.165000	1.2522731516
0.166000	1.2531982925
0.167000	1.2541236091
0.168000	1.2550486675
0.169000	1.2559738995
0.170000	1.2568784127
0.171000	1.2577033065
0.172000	1.2585177350
0.173000	1.2593425796
0.174000	1.2601569640
0.175000	1.2609817595
0.176000	1.2617961002
0.177000	1.2626208468
0.178000	1.2634351439
0.179000	1.2642598418
0.180000	1.2650835091
0.181000	1.2659363981
0.182000	1.2667882586
0.183000	1.2676410952
0.184000	1.2684929072
0.185000	1.2693456914
0.186000	1.2701974552
0.187000	1.2710501874
0.188000	1.2719019030
0.189000	1.2727545833
0.190000	1.2735960438
0.191000	1.2743782145
0.192000	1.2751307386
0.193000	1.2759026786
0.194000	1.2766653836
0.195000	1.2774372991
0.196000	1.2782101790
0.197000	1.2789718701
0.198000	1.2797345248
0.199000	1.2805063916
0.200000	1.2812690213
0.210000	1.2892697920
0.220000	1.2965246398
0.230000	1.3040504221

0.240000	1.3108513687
0.250000	1.3178671640
0.260000	1.3243115557
0.270000	1.3310278218
0.280000	1.3372002962
0.290000	1.3435967386
0.300000	1.3495108648
0.310000	1.3556121510
0.320000	1.3612721668
0.330000	1.3671090211
0.340000	1.3725245258
0.350000	1.3781173952
0.360000	1.3833664666
0.370000	1.3887917787
0.380000	1.3938376102
0.390000	1.3990694327
0.400000	1.4040083283
0.410000	1.4090403104
0.420000	1.4137429194
0.430000	1.4186216967
0.440000	1.4232080338
0.450000	1.4279231709
0.460000	1.4324063486
0.470000	1.4369820758
0.480000	1.4412794177
0.490000	1.4457518769
0.500000	1.4500283647
0.510000	1.4543511240
0.520000	1.4584825607
0.530000	1.4627417896
0.540000	1.4667195235
0.550000	1.4708348167
0.560000	1.4748546536
0.570000	1.4789204215
0.580000	1.4827450786
0.590000	1.4867068099
0.600000	1.4904776239
0.610000	1.4942942380
0.620000	1.4979655319
0.630000	1.5017734215
0.640000	1.5053906119
0.650000	1.5090534057
0.660000	1.5125347548
0.670000	1.5160879281
0.680000	1.5195511843
0.690000	1.5231050866
0.700000	1.5265277217
0.710000	1.5300318268
0.720000	1.5333957323
0.730000	1.5368049158
0.740000	1.5400641113
0.750000	1.5433684788

```
            0.760000        1.5465829159
            0.770000        1.5498875020
            0.780000        1.5530471554
            0.790000        1.5562518544
            0.800000        1.5593617047
            0.810000        1.5625614151
            0.820000        1.5656162614
            0.830000        1.5687159836
            0.840000        1.5717261482
            0.850000        1.5747811824
            0.860000        1.5777362496
            0.870000        1.5807707875
            0.880000        1.5836759169
            0.890000        1.5865811000
            0.900000        1.5894363303
            0.910000        1.5923808158
            0.920000        1.5952806814
            0.930000        1.5982251014
            0.940000        1.6009804129
            0.950000        1.6037802787
            0.960000        1.6065301377
            0.970000        1.6093244492
            0.980000        1.6120242826
            0.990000        1.6147685190
            1.000000        1.6175127070
*DEFINE_CURVE
$ 293.00 K
$     LCID      SIDR      SCLA      SCLO      OFFA      OFFO    DATTYP
      2002         0       1.0       1.0       0.0       0.0         0
$           ABSCISSA           ORDINATE
            0.000000        0.7400000000
            0.001000        0.8879110000
            0.002000        0.9176410000
            0.003000        0.9415790000
            0.004000        0.9591330000
            0.005000        0.9720840000
            0.006000        0.9827890000
            0.007000        0.9911060000
            0.008000        0.9977440000
            0.009000        1.0034200000
            0.010000        1.0084800000
            0.011000        1.0128300000
            0.012000        1.0164800000
            0.013000        1.0195900000
            0.014000        1.0223500000
            0.015000        1.0247800000
            0.016000        1.0269700000
            0.017000        1.0289400000
            0.018000        1.0307000000
            0.019000        1.0323400000
            0.020000        1.0338800000
            0.021000        1.0354200000
```

0.022000	1.0367800000
0.023000	1.0382200000
0.024000	1.0395800000
0.025000	1.0410200000
0.026000	1.0424700000
0.027000	1.0439100000
0.028000	1.0453800000
0.029000	1.0468900000
0.030000	1.0483500000
0.031000	1.0498500000
0.032000	1.0512700000
0.033000	1.0526900000
0.034000	1.0541100000
0.035000	1.0555200000
0.036000	1.0569200000
0.037000	1.0583200000
0.038000	1.0597200000
0.039000	1.0611500000
0.040000	1.0626300000
0.041000	1.0641100000
0.042000	1.0656200000
0.043000	1.0671900000
0.044000	1.0688100000
0.045000	1.0705200000
0.046000	1.0722800000
0.047000	1.0740000000
0.048000	1.0757900000
0.049000	1.0775800000
0.050000	1.0793700000
0.051000	1.0811400000
0.052000	1.0828200000
0.053000	1.0844300000
0.054000	1.0860100000
0.055000	1.0875100000
0.056000	1.0889300000
0.057000	1.0903000000
0.058000	1.0915000000
0.059000	1.0926400000
0.060000	1.0936900000
0.061000	1.0946600000
0.062000	1.0956400000
0.063000	1.0965200000
0.064000	1.0974100000
0.065000	1.0982900000
0.066000	1.0991900000
0.067000	1.1002100000
0.068000	1.1012500000
0.069000	1.1023000000
0.070000	1.1035300000
0.071000	1.1048000000
0.072000	1.1061900000
0.073000	1.1076700000

0.074000	1.1091900000
0.075000	1.1108700000
0.076000	1.1125400000
0.077000	1.1142400000
0.078000	1.1160500000
0.079000	1.1179000000
0.080000	1.1196800000
0.081000	1.1214500000
0.082000	1.1232100000
0.083000	1.1249200000
0.084000	1.1266200000
0.085000	1.1282500000
0.086000	1.1297900000
0.087000	1.1313300000
0.088000	1.1328600000
0.089000	1.1343200000
0.090000	1.1357300000
0.091000	1.1370800000
0.092000	1.1384600000
0.093000	1.1398100000
0.094000	1.1412000000
0.095000	1.1425600000
0.096000	1.1439000000
0.097000	1.1452400000
0.098000	1.1465800000
0.099000	1.1479300000
0.100000	1.1491900000
0.101000	1.1504400000
0.102000	1.1516800000
0.103000	1.1527100000
0.104000	1.1537400000
0.105000	1.1547900000
0.106000	1.1557300000
0.107000	1.1566700000
0.108000	1.1575000000
0.109000	1.1583400000
0.110000	1.1591900000
0.111000	1.1600300000
0.112000	1.1609200000
0.113000	1.1618700000
0.114000	1.1628300000
0.115000	1.1638500000
0.116000	1.1649800000
0.117000	1.1662200000
0.118000	1.1674900000
0.119000	1.1688400000
0.120000	1.1702000000
0.121000	1.1716900000
0.122000	1.1732600000
0.123000	1.1747400000
0.124000	1.1763000000
0.125000	1.1778500000

0.126000	1.1793000000
0.127000	1.1807400000
0.128000	1.1821400000
0.129000	1.1834400000
0.130000	1.1846700000
0.131000	1.1858100000
0.132000	1.1869500000
0.133000	1.1880900000
0.134000	1.1892300000
0.135000	1.1903700000
0.136000	1.1915100000
0.137000	1.1926500000
0.138000	1.1937900000
0.139000	1.1949300000
0.140000	1.1960700000
0.141000	1.1972100000
0.142000	1.1983500000
0.143000	1.1994900000
0.144000	1.2006300000
0.145000	1.2017700000
0.146000	1.2029100000
0.147000	1.2040500000
0.148000	1.2051900000
0.149000	1.2063300000
0.150000	1.2074600000
0.151000	1.2085100000
0.152000	1.2095600000
0.153000	1.2106100000
0.154000	1.2116600000
0.155000	1.2127100000
0.156000	1.2137600000
0.157000	1.2148100000
0.158000	1.2158600000
0.159000	1.2169100000
0.160000	1.2179600000
0.161000	1.2190100000
0.162000	1.2200600000
0.163000	1.2211100000
0.164000	1.2221600000
0.165000	1.2232100000
0.166000	1.2242600000
0.167000	1.2253100000
0.168000	1.2263600000
0.169000	1.2274100000
0.170000	1.2284400000
0.171000	1.2294100000
0.172000	1.2303700000
0.173000	1.2313400000
0.174000	1.2323000000
0.175000	1.2332700000
0.176000	1.2342300000
0.177000	1.2352000000

0.178000	1.2361600000
0.179000	1.2371300000
0.180000	1.2380900000
0.181000	1.2390600000
0.182000	1.2400200000
0.183000	1.2409900000
0.184000	1.2419500000
0.185000	1.2429200000
0.186000	1.2438800000
0.187000	1.2448500000
0.188000	1.2458100000
0.189000	1.2467800000
0.190000	1.2477300000
0.191000	1.2486400000
0.192000	1.2495300000
0.193000	1.2504300000
0.194000	1.2513300000
0.195000	1.2522300000
0.196000	1.2531400000
0.197000	1.2540300000
0.198000	1.2549300000
0.199000	1.2558300000
0.200000	1.2567300000
0.210000	1.2657300000
0.220000	1.2741800000
0.230000	1.2826200000
0.240000	1.2905200000
0.250000	1.2984100000
0.260000	1.3059100000
0.270000	1.3134100000
0.280000	1.3205100000
0.290000	1.3276000000
0.300000	1.3343500000
0.310000	1.3411000000
0.320000	1.3475500000
0.330000	1.3539900000
0.340000	1.3601400000
0.350000	1.3662900000
0.360000	1.3721900000
0.370000	1.3780800000
0.380000	1.3837300000
0.390000	1.3893800000
0.400000	1.3948300000
0.410000	1.4002800000
0.420000	1.4055300000
0.430000	1.4107800000
0.440000	1.4158300000
0.450000	1.4208700000
0.460000	1.4257700000
0.470000	1.4306700000
0.480000	1.4354200000
0.490000	1.4401700000

```
            0.500000        1.4447700000
            0.510000        1.4493700000
            0.520000        1.4538700000
            0.530000        1.4583600000
            0.540000        1.4626600000
            0.550000        1.4669600000
            0.560000        1.4712100000
            0.570000        1.4754600000
            0.580000        1.4795600000
            0.590000        1.4836600000
            0.600000        1.4876600000
            0.610000        1.4916600000
            0.620000        1.4955600000
            0.630000        1.4994600000
            0.640000        1.5032600000
            0.650000        1.5070600000
            0.660000        1.5107600000
            0.670000        1.5144500000
            0.680000        1.5180500000
            0.690000        1.5216500000
            0.700000        1.5252000000
            0.710000        1.5287500000
            0.720000        1.5322500000
            0.730000        1.5357500000
            0.740000        1.5391000000
            0.750000        1.5424500000
            0.760000        1.5458000000
            0.770000        1.5491500000
            0.780000        1.5524000000
            0.790000        1.5556500000
            0.800000        1.5588500000
            0.810000        1.5620500000
            0.820000        1.5651500000
            0.830000        1.5682500000
            0.840000        1.5713500000
            0.850000        1.5744500000
            0.860000        1.5774500000
            0.870000        1.5804400000
            0.880000        1.5833900000
            0.890000        1.5863400000
            0.900000        1.5892400000
            0.910000        1.5921400000
            0.920000        1.5950400000
            0.930000        1.5979400000
            0.940000        1.6007400000
            0.950000        1.6035400000
            0.960000        1.6062900000
            0.970000        1.6090400000
            0.980000        1.6117400000
            0.990000        1.6144400000
            1.000000        1.6171400000
*DEFINE_CURVE
```

```
$ 473.15 K
$     LCID      SIDR      SCLA      SCLO      OFFA      OFFO    DATTYP
      2003         0       1.0       1.0       0.0       0.0         0
$           ABSCISSA           ORDINATE
            0.000000        0.5650612756
            0.001000        0.6599236450
            0.002000        0.6694795605
            0.003000        0.6793342522
            0.004000        0.6879798246
            0.005000        0.6944057149
            0.006000        0.7000651374
            0.007000        0.7046988613
            0.008000        0.7089738362
            0.009000        0.7129938109
            0.010000        0.7168484129
            0.011000        0.7203904774
            0.012000        0.7236341883
            0.013000        0.7265731013
            0.014000        0.7293213232
            0.015000        0.7319048662
            0.016000        0.7344655726
            0.017000        0.7369194160
            0.018000        0.7392440755
            0.019000        0.7414980833
            0.020000        0.7437057926
            0.021000        0.7458407046
            0.022000        0.7478015939
            0.023000        0.7497623545
            0.024000        0.7515729786
            0.025000        0.7534691234
            0.026000        0.7553549095
            0.027000        0.7572059935
            0.028000        0.7590196129
            0.029000        0.7608873539
            0.030000        0.7626543533
            0.031000        0.7644199164
            0.032000        0.7660940275
            0.033000        0.7677432996
            0.034000        0.7694184575
            0.035000        0.7710948915
            0.036000        0.7727518505
            0.037000        0.7744734737
            0.038000        0.7762138914
            0.039000        0.7779587035
            0.040000        0.7797284656
            0.041000        0.7815312372
            0.042000        0.7833082351
            0.043000        0.7851103764
            0.044000        0.7869342070
            0.045000        0.7888558613
            0.046000        0.7908794041
            0.047000        0.7928887756
```

0.048000	0.7949207161
0.049000	0.7969345426
0.050000	0.7989510565
0.051000	0.8008652693
0.052000	0.8026676857
0.053000	0.8044070064
0.054000	0.8061056764
0.055000	0.8077057473
0.056000	0.8092259681
0.057000	0.8106751462
0.058000	0.8119955868
0.059000	0.8132444031
0.060000	0.8143950944
0.061000	0.8154893562
0.062000	0.8165217270
0.063000	0.8174183286
0.064000	0.8182890260
0.065000	0.8191234216
0.066000	0.8199789651
0.067000	0.8209329762
0.068000	0.8219162759
0.069000	0.8229232061
0.070000	0.8240933083
0.071000	0.8253014521
0.072000	0.8266092490
0.073000	0.8279889708
0.074000	0.8293888995
0.075000	0.8309069127
0.076000	0.8324258356
0.077000	0.8339765131
0.078000	0.8356116632
0.079000	0.8372997064
0.080000	0.8389316446
0.081000	0.8405754286
0.082000	0.8421800160
0.083000	0.8437090060
0.084000	0.8452185638
0.085000	0.8466101758
0.086000	0.8479339680
0.087000	0.8492438484
0.088000	0.8505558896
0.089000	0.8518014311
0.090000	0.8530317819
0.091000	0.8541949109
0.092000	0.8553320727
0.093000	0.8564053969
0.094000	0.8575156388
0.095000	0.8585956359
0.096000	0.8596683785
0.097000	0.8607334094
0.098000	0.8618062190
0.099000	0.8628797387

0.100000	0.8638915663
0.101000	0.8649310378
0.102000	0.8659621242
0.103000	0.8668362442
0.104000	0.8677103707
0.105000	0.8685986361
0.106000	0.8694050740
0.107000	0.8702105921
0.108000	0.8709342450
0.109000	0.8716653951
0.110000	0.8724031348
0.111000	0.8731342339
0.112000	0.8738365021
0.113000	0.8745347807
0.114000	0.8752405874
0.115000	0.8759915551
0.116000	0.8768253137
0.117000	0.8777418586
0.118000	0.8786809751
0.119000	0.8796802924
0.120000	0.8806939834
0.121000	0.8818329495
0.122000	0.8830390074
0.123000	0.8841704838
0.124000	0.8853690617
0.125000	0.8865532625
0.126000	0.8876690898
0.127000	0.8887705289
0.128000	0.8898487577
0.129000	0.8908448419
0.130000	0.8917951311
0.131000	0.8926707900
0.132000	0.8935048282
0.133000	0.8942944281
0.134000	0.8950908985
0.135000	0.8958804557
0.136000	0.8966768848
0.137000	0.8974663994
0.138000	0.8982627873
0.139000	0.8990522597
0.140000	0.8998486066
0.141000	0.9006725208
0.142000	0.9014895238
0.143000	0.9023134108
0.144000	0.9031303846
0.145000	0.9039542445
0.146000	0.9047711892
0.147000	0.9055950221
0.148000	0.9064119378
0.149000	0.9072357439
0.150000	0.9080451105
0.151000	0.9088012099

0.152000	0.9095118157
0.153000	0.9101999148
0.154000	0.9108820021
0.155000	0.9115700542
0.156000	0.9122520950
0.157000	0.9129401003
0.158000	0.9136220948
0.159000	0.9143100536
0.160000	0.9149920018
0.161000	0.9157075421
0.162000	0.9164170732
0.163000	0.9171325708
0.164000	0.9178420588
0.165000	0.9185575139
0.166000	0.9192669590
0.167000	0.9199823718
0.168000	0.9206880926
0.169000	0.9214089859
0.170000	0.9220987302
0.171000	0.9227595386
0.172000	0.9233690904
0.173000	0.9239654173
0.174000	0.9245565209
0.175000	0.9251528093
0.176000	0.9257438790
0.177000	0.9263401292
0.178000	0.9269311650
0.179000	0.9275273771
0.180000	0.9281252855
0.181000	0.9287421773
0.182000	0.9293607672
0.183000	0.9299776173
0.184000	0.9305961690
0.185000	0.9312129776
0.186000	0.9318314913
0.187000	0.9324482586
0.188000	0.9330667345
0.189000	0.9336834605
0.190000	0.9342944108
0.191000	0.9348661743
0.192000	0.9354321767
0.193000	0.9359687678
0.194000	0.9365053475
0.195000	0.9370419160
0.196000	0.9375859551
0.197000	0.9381150192
0.198000	0.9386515540
0.199000	0.9391880776
0.200000	0.9397245900
0.210000	0.9453303527
0.220000	0.9503673897
0.230000	0.9554919964

0.240000	0.9602114674
0.250000	0.9650143586
0.260000	0.9693518285
0.270000	0.9738673654
0.280000	0.9780125614
0.290000	0.9823031932
0.300000	0.9861856332
0.310000	0.9901773563
0.320000	0.9939481257
0.330000	0.9976914091
0.340000	1.0012008467
0.350000	1.0047662607
0.360000	1.0081301899
0.370000	1.0115400646
0.380000	1.0147654045
0.390000	1.0180529638
0.400000	1.0211763923
0.410000	1.0242852725
0.420000	1.0271661305
0.430000	1.0301638768
0.440000	1.0330164960
0.450000	1.0358897696
0.460000	1.0386435539
0.470000	1.0413825731
0.480000	1.0440108994
0.490000	1.0466934298
0.500000	1.0492495234
0.510000	1.0518397430
0.520000	1.0542761025
0.530000	1.0567963679
0.540000	1.0591068742
0.550000	1.0614991851
0.560000	1.0638561743
0.570000	1.0662469402
0.580000	1.0684482581
0.590000	1.0707399506
0.600000	1.0728875764
0.610000	1.0750507119
0.620000	1.0771426977
0.630000	1.0793335894
0.640000	1.0813807182
0.650000	1.0834431708
0.660000	1.0854345859
0.670000	1.0874032434
0.680000	1.0893804971
0.690000	1.0913510771
0.700000	1.0932117396
0.710000	1.0951856171
0.720000	1.0970702144
0.730000	1.0989697849
0.740000	1.1007627630
0.750000	1.1025076807

```
            0.760000        1.1042444177
            0.770000        1.1061271330
            0.780000        1.1077952430
            0.790000        1.1095411167
            0.800000        1.1111981649
            0.810000        1.1129737468
            0.820000        1.1146248803
            0.830000        1.1162906805
            0.840000        1.1178765203
            0.850000        1.1195665214
            0.860000        1.1211234062
            0.870000        1.1227195291
            0.880000        1.1242878502
            0.890000        1.1257764270
            0.900000        1.1272927203
            0.910000        1.1288194023
            0.920000        1.1303288480
            0.930000        1.1318704544
            0.940000        1.1333417996
            0.950000        1.1348452341
            0.960000        1.1362426782
            0.970000        1.1377255222
            0.980000        1.1391202364
            0.990000        1.1405291552
            1.000000        1.1419386270
*DEFINE_CURVE
$ 673.15 K
$     LCID      SIDR      SCLA      SCLO      OFFA      OFFO    DATTYP
      2004         0       1.0       1.0       0.0       0.0         0
$           ABSCISSA          ORDINATE
            0.000000        0.3751773609
            0.001000        0.4484482362
            0.002000        0.4639545119
            0.003000        0.4784061626
            0.004000        0.4902677240
            0.005000        0.4993571731
            0.006000        0.5078940874
            0.007000        0.5143002475
            0.008000        0.5198305512
            0.009000        0.5248583949
            0.010000        0.5293279552
            0.011000        0.5333355629
            0.012000        0.5368672983
            0.013000        0.5400044826
            0.014000        0.5428528879
            0.015000        0.5454621789
            0.016000        0.5478924234
            0.017000        0.5501396355
            0.018000        0.5522315762
            0.019000        0.5542777331
            0.020000        0.5563115982
            0.021000        0.5583376597
```

0.022000	0.5602828301
0.023000	0.5622791051
0.024000	0.5642223067
0.025000	0.5662471147
0.026000	0.5682986608
0.027000	0.5703438093
0.028000	0.5724068088
0.029000	0.5744699655
0.030000	0.5764692233
0.031000	0.5784700214
0.032000	0.5803938607
0.033000	0.5822660372
0.034000	0.5841147350
0.035000	0.5858794228
0.036000	0.5875668966
0.037000	0.5892125770
0.038000	0.5907421298
0.039000	0.5921978263
0.040000	0.5936230036
0.041000	0.5950426811
0.042000	0.5964236453
0.043000	0.5977786666
0.044000	0.5991330615
0.045000	0.6005279005
0.046000	0.6019709878
0.047000	0.6033712800
0.048000	0.6047802122
0.049000	0.6061859690
0.050000	0.6076019086
0.051000	0.6089882484
0.052000	0.6103060264
0.053000	0.6115964796
0.054000	0.6128785703
0.055000	0.6140869971
0.056000	0.6152180542
0.057000	0.6162856298
0.058000	0.6172553354
0.059000	0.6181677187
0.060000	0.6190027523
0.061000	0.6198233009
0.062000	0.6206350662
0.063000	0.6213703278
0.064000	0.6220859922
0.065000	0.6227698386
0.066000	0.6234478816
0.067000	0.6241813660
0.068000	0.6249153964
0.069000	0.6256568903
0.070000	0.6264888801
0.071000	0.6273436199
0.072000	0.6282593653
0.073000	0.6292209089

0.074000	0.6301962656
0.075000	0.6312671355
0.076000	0.6323252387
0.077000	0.6333942002
0.078000	0.6345204027
0.079000	0.6356541301
0.080000	0.6367505889
0.081000	0.6378538955
0.082000	0.6389477397
0.083000	0.6399981524
0.084000	0.6410399700
0.085000	0.6420278252
0.086000	0.6429651505
0.087000	0.6438638152
0.088000	0.6447610642
0.089000	0.6456133290
0.090000	0.6464423179
0.091000	0.6472320024
0.092000	0.6480439459
0.093000	0.6488327467
0.094000	0.6496504122
0.095000	0.6504458393
0.096000	0.6512350693
0.097000	0.6520191343
0.098000	0.6528083907
0.099000	0.6535981727
0.100000	0.6543409936
0.101000	0.6551049642
0.102000	0.6558632632
0.103000	0.6565019836
0.104000	0.6571407073
0.105000	0.6577908267
0.106000	0.6583782883
0.107000	0.6589156542
0.108000	0.6593894459
0.109000	0.6598689340
0.110000	0.6603541186
0.111000	0.6608336062
0.112000	0.6613415771
0.113000	0.6618837281
0.114000	0.6624315757
0.115000	0.6630136036
0.116000	0.6636582957
0.117000	0.6643656522
0.118000	0.6650900993
0.119000	0.6658601210
0.120000	0.6666410312
0.121000	0.6675167789
0.122000	0.6684433264
0.123000	0.6693134307
0.124000	0.6702343438
0.125000	0.6711443873

0.126000	0.6720026831
0.127000	0.6728089552
0.128000	0.6735958056
0.129000	0.6743204542
0.130000	0.6750104228
0.131000	0.6756438910
0.132000	0.6762825698
0.133000	0.6769160285
0.134000	0.6775546994
0.135000	0.6781881486
0.136000	0.6788268116
0.137000	0.6794602514
0.138000	0.6800989064
0.139000	0.6807323369
0.140000	0.6813709841
0.141000	0.6820305181
0.142000	0.6826848322
0.143000	0.6833443730
0.144000	0.6839986918
0.145000	0.6846582392
0.146000	0.6853125626
0.147000	0.6859363216
0.148000	0.6865539231
0.149000	0.6871767432
0.150000	0.6877886259
0.151000	0.6883601616
0.152000	0.6889264593
0.153000	0.6894979823
0.154000	0.6900642666
0.155000	0.6906357768
0.156000	0.6912020477
0.157000	0.6917735453
0.158000	0.6923398029
0.159000	0.6929112879
0.160000	0.6934775322
0.161000	0.6940699454
0.162000	0.6946571210
0.163000	0.6952495304
0.164000	0.6958367008
0.165000	0.6964291063
0.166000	0.6970162716
0.167000	0.6975783044
0.168000	0.6981341670
0.169000	0.6986952582
0.170000	0.6992397143
0.171000	0.6997552503
0.172000	0.7002598487
0.173000	0.7007753735
0.174000	0.7012799612
0.175000	0.7017954750
0.176000	0.7023000520
0.177000	0.7028155547

0.178000	0.7033201213
0.179000	0.7038356129
0.180000	0.7043454100
0.181000	0.7048766150
0.182000	0.7054021272
0.183000	0.7059333242
0.184000	0.7064588288
0.185000	0.7069900179
0.186000	0.7075155149
0.187000	0.7080199612
0.188000	0.7085187110
0.189000	0.7090222170
0.190000	0.7095152630
0.191000	0.7099846348
0.192000	0.7104435527
0.193000	0.7109072306
0.194000	0.7113718267
0.195000	0.7118354967
0.196000	0.7123057693
0.197000	0.7127637472
0.198000	0.7132283279
0.199000	0.7136919822
0.200000	0.7141565552
0.210000	0.7188858619
0.220000	0.7231574898
0.230000	0.7274953984
0.240000	0.7314045909
0.250000	0.7353588463
0.260000	0.7389776539
0.270000	0.7426840353
0.280000	0.7460580853
0.290000	0.7494980014
0.300000	0.7526575326
0.310000	0.7558642770
0.320000	0.7588164446
0.330000	0.7618165755
0.340000	0.7645807869
0.350000	0.7673960623
0.360000	0.7699995821
0.370000	0.7726618734
0.380000	0.7751285105
0.390000	0.7776565731
0.400000	0.7800098383
0.410000	0.7823802863
0.420000	0.7845873581
0.430000	0.7868637594
0.440000	0.7889760990
0.450000	0.7911291456
0.460000	0.7931582361
0.470000	0.7952079523
0.480000	0.7971334910
0.490000	0.7991307827

```
            0.500000        0.8010071548
            0.510000        0.8028822496
            0.520000        0.8046616714
            0.530000        0.8064875490
            0.540000        0.8081699379
            0.550000        0.8099068837
            0.560000        0.8115841833
            0.570000        0.8132655384
            0.580000        0.8148322815
            0.590000        0.8164550148
            0.600000        0.8179934980
            0.610000        0.8195377971
            0.620000        0.8209980353
            0.630000        0.8225147755
            0.640000        0.8239465932
            0.650000        0.8253877444
            0.660000        0.8267504955
            0.670000        0.8281418553
            0.680000        0.8294603858
            0.690000        0.8308128564
            0.700000        0.8321193285
            0.710000        0.8334564389
            0.720000        0.8347453409
            0.730000        0.8360432971
            0.740000        0.8372360164
            0.750000        0.8384414365
            0.760000        0.8396287342
            0.770000        0.8408530485
            0.780000        0.8420049196
            0.790000        0.8431684263
            0.800000        0.8442831212
            0.810000        0.8454363806
            0.820000        0.8465200670
            0.830000        0.8476179586
            0.840000        0.8487004161
            0.850000        0.8497951981
            0.860000        0.8508179061
            0.870000        0.8518734222
            0.880000        0.8528919415
            0.890000        0.8539004198
            0.900000        0.8548666209
            0.910000        0.8558725797
            0.920000        0.8568657856
            0.930000        0.8578728442
            0.940000        0.8588108026
            0.950000        0.8597661606
            0.960000        0.8606846622
            0.970000        0.8616169463
            0.980000        0.8625070823
            0.990000        0.8634216087
            1.000000        0.8643367225
*DEFINE_CURVE
```

```
$ 873.15 K
$     LCID      SIDR      SCLA      SCLO      OFFA      OFFO    DATTYP
      2005         0       1.0       1.0       0.0       0.0         0
$           ABSCISSA           ORDINATE
            0.000000        0.3253924570
            0.001000        0.3803737360
            0.002000        0.3915820804
            0.003000        0.4031979304
            0.004000        0.4118116367
            0.005000        0.4177227702
            0.006000        0.4226306662
            0.007000        0.4266561215
            0.008000        0.4303246822
            0.009000        0.4336508834
            0.010000        0.4366112920
            0.011000        0.4391826016
            0.012000        0.4414571497
            0.013000        0.4434468139
            0.014000        0.4452734497
            0.015000        0.4469386254
            0.016000        0.4485061369
            0.017000        0.4499426817
            0.018000        0.4512826068
            0.019000        0.4525975543
            0.020000        0.4538684668
            0.021000        0.4551289866
            0.022000        0.4563150927
            0.023000        0.4575452320
            0.024000        0.4587267951
            0.025000        0.4599363437
            0.026000        0.4611588001
            0.027000        0.4623701986
            0.028000        0.4635675729
            0.029000        0.4648080200
            0.030000        0.4659866395
            0.031000        0.4671832500
            0.032000        0.4683373777
            0.033000        0.4694633101
            0.034000        0.4705792175
            0.035000        0.4716750201
            0.036000        0.4727266890
            0.037000        0.4737848043
            0.038000        0.4747973871
            0.039000        0.4757787079
            0.040000        0.4767412099
            0.041000        0.4776949478
            0.042000        0.4786356027
            0.043000        0.4795654198
            0.044000        0.4804946324
            0.045000        0.4814577674
            0.046000        0.4824529839
            0.047000        0.4834151812
```

0.048000	0.4843902381
0.049000	0.4853663660
0.050000	0.4863512123
0.051000	0.4873123940
0.052000	0.4882259517
0.053000	0.4891292288
0.054000	0.4900393860
0.055000	0.4909090822
0.056000	0.4917391701
0.057000	0.4925404267
0.058000	0.4932780187
0.059000	0.4939875985
0.060000	0.4946542366
0.061000	0.4953100107
0.062000	0.4959630712
0.063000	0.4965636120
0.064000	0.4971650127
0.065000	0.4977438304
0.066000	0.4983199634
0.067000	0.4989405740
0.068000	0.4995612516
0.069000	0.5001774677
0.070000	0.5008600927
0.071000	0.5015465247
0.072000	0.5022811873
0.073000	0.5030369880
0.074000	0.5038092177
0.075000	0.5046451925
0.076000	0.5054694941
0.077000	0.5063002845
0.078000	0.5071675963
0.079000	0.5080576591
0.080000	0.5089119491
0.081000	0.5097754741
0.082000	0.5106431644
0.083000	0.5114868080
0.084000	0.5123255730
0.085000	0.5131266467
0.086000	0.5138900627
0.087000	0.5146475960
0.088000	0.5154047575
0.089000	0.5161287147
0.090000	0.5168268309
0.091000	0.5174817388
0.092000	0.5181526402
0.093000	0.5188057763
0.094000	0.5194812788
0.095000	0.5201390115
0.096000	0.5207918003
0.097000	0.5214404700
0.098000	0.5220933027
0.099000	0.5227465670

0.100000	0.5233630101
0.101000	0.5239956504
0.102000	0.5246237637
0.103000	0.5251562315
0.104000	0.5256887034
0.105000	0.5262302932
0.106000	0.5267217571
0.107000	0.5272132151
0.108000	0.5276536126
0.109000	0.5280994622
0.110000	0.5285498549
0.111000	0.5289856591
0.112000	0.5294269587
0.113000	0.5298965266
0.114000	0.5303697427
0.115000	0.5308712351
0.116000	0.5314219970
0.117000	0.5320238591
0.118000	0.5326385127
0.119000	0.5332905945
0.120000	0.5339505078
0.121000	0.5346873206
0.122000	0.5354639477
0.123000	0.5361963070
0.124000	0.5369684915
0.125000	0.5377329169
0.126000	0.5384550005
0.127000	0.5391693087
0.128000	0.5398686590
0.129000	0.5405191181
0.130000	0.5411409008
0.131000	0.5417082633
0.132000	0.5422660914
0.133000	0.5428197487
0.134000	0.5433776003
0.135000	0.5439312792
0.136000	0.5444891544
0.137000	0.5450428548
0.138000	0.5456007534
0.139000	0.5461544752
0.140000	0.5467123970
0.141000	0.5472870941
0.142000	0.5478576199
0.143000	0.5484323573
0.144000	0.5490029209
0.145000	0.5495776985
0.146000	0.5501482998
0.147000	0.5507231174
0.148000	0.5512937562
0.149000	0.5518686135
0.150000	0.5524347145
0.151000	0.5529601644

0.152000	0.5534685621
0.153000	0.5539811697
0.154000	0.5544895802
0.155000	0.5550022019
0.156000	0.5555106251
0.157000	0.5560232610
0.158000	0.5565316969
0.159000	0.5570443468
0.160000	0.5575527953
0.161000	0.5580822970
0.162000	0.5586076023
0.163000	0.5591371313
0.164000	0.5596624619
0.165000	0.5601920179
0.166000	0.5607173737
0.167000	0.5612469568
0.168000	0.5617723377
0.169000	0.5623019477
0.170000	0.5628181905
0.171000	0.5633038051
0.172000	0.5637686549
0.173000	0.5642423096
0.174000	0.5647071661
0.175000	0.5651808290
0.176000	0.5656456924
0.177000	0.5661193635
0.178000	0.5665842336
0.179000	0.5670579128
0.180000	0.5675270127
0.181000	0.5680133717
0.182000	0.5684951543
0.183000	0.5689815294
0.184000	0.5694633275
0.185000	0.5699497186
0.186000	0.5704315321
0.187000	0.5709179392
0.188000	0.5713997679
0.189000	0.5718861909
0.190000	0.5723634476
0.191000	0.5728149833
0.192000	0.5732481246
0.193000	0.5736849332
0.194000	0.5741226660
0.195000	0.5745594786
0.196000	0.5750018040
0.197000	0.5754340320
0.198000	0.5758717729
0.199000	0.5763085934
0.200000	0.5767463383
0.210000	0.5812676222
0.220000	0.5853889355
0.230000	0.5896238863

0.240000	0.5934801331
0.250000	0.5974254768
0.260000	0.6010657538
0.270000	0.6048252727
0.280000	0.6082832466
0.290000	0.6118355367
0.300000	0.6151266985
0.310000	0.6184964284
0.320000	0.6216326118
0.330000	0.6248427394
0.340000	0.6278281417
0.350000	0.6308878253
0.360000	0.6337489635
0.370000	0.6366858362
0.380000	0.6394297007
0.390000	0.6422529616
0.400000	0.6449053975
0.410000	0.6475956032
0.420000	0.6501242287
0.430000	0.6527330986
0.440000	0.6551850001
0.450000	0.6576912226
0.460000	0.6600673647
0.470000	0.6624821296
0.480000	0.6647756545
0.490000	0.6671459302
0.500000	0.6693861706
0.510000	0.6716437977
0.520000	0.6738037810
0.530000	0.6760188504
0.540000	0.6780982438
0.550000	0.6802381957
0.560000	0.6823037628
0.570000	0.6843866913
0.580000	0.6863525820
0.590000	0.6883789498
0.600000	0.6903160499
0.610000	0.6922713988
0.620000	0.6941375475
0.630000	0.6960640653
0.640000	0.6979059419
0.650000	0.6997660366
0.660000	0.7015415463
0.670000	0.7033507409
0.680000	0.7050809375
0.690000	0.7068503261
0.700000	0.7085671454
0.710000	0.7103189185
0.720000	0.7120175685
0.730000	0.7137352795
0.740000	0.7153444215
0.750000	0.7169726210

```
            0.760000        0.7185719342
            0.770000        0.7202103075
            0.780000        0.7217760274
            0.790000        0.7233616647
            0.800000        0.7248907455
            0.810000        0.7264588079
            0.820000        0.7279542652
            0.830000        0.7294696003
            0.840000        0.7309561892
            0.850000        0.7324608602
            0.860000        0.7338929940
            0.870000        0.7353611314
            0.880000        0.7367900176
            0.890000        0.7382170514
            0.900000        0.7395913022
            0.910000        0.7410052473
            0.920000        0.7424021838
            0.930000        0.7438189123
            0.940000        0.7451596338
            0.950000        0.7465192461
            0.960000        0.7478395078
            0.970000        0.7491777495
            0.980000        0.7504686585
            0.990000        0.7517784244
            1.000000        0.7530881321
*DEFINE_CURVE
$ melt
$     LCID      SIDR      SCLA      SCLO      OFFA      OFFO    DATTYP
      2006         0       1.0       1.0       0.0       0.0         0
$           ABSCISSA           ORDINATE
            0.000000        0.0000000000
            1.000000        0.0000000000
*DEFINE_CURVE
$ melt
$     LCID      SIDR      SCLA      SCLO      OFFA      OFFO    DATTYP
      2007         0       1.0       1.0       0.0       0.0         0
$           ABSCISSA           ORDINATE
            0.000000        0.0000000000
            1.000000        0.0000000000
$$$$$$$$$$$$$$$$$$$$$$$$$$$$$$$$$$$$$$$$$$$$$$$$$$$$$$$$$$$$$$$$$$$$$$
$                 Failure Surface Table                 $
$$$$$$$$$$$$$$$$$$$$$$$$$$$$$$$$$$$$$$$$$$$$$$$$$$$$$$$$$$$$$$$$$$$$$$
*DEFINE_TABLE
$     TBID       SFA      OFFA
      3000         1         0
$    VALUE
   -1.0000
   -0.9000
   -0.8000
   -0.7000
   -0.6000
   -0.5000
```

```
   -0.4000
   -0.3000
   -0.2000
   -0.1000
    0.0000
    0.1000
    0.2000
    0.3000
    0.4000
    0.5000
    0.6000
    0.7000
    0.8000
    0.9000
    1.0000
*DEFINE_CURVE
$     LCID      SIDR       SFA       SFO      OFFA      OFFO    DATYP
      3001
$                 A1                  O1
   -1.0000000000e+00    1.8500000000e-01
   -9.9000000000e-01    1.8824644836e-01
   -9.8000000000e-01    1.9158942197e-01
   -9.7000000000e-01    1.9501769697e-01
   -9.6000000000e-01    1.9852004948e-01
   -9.5000000000e-01    2.0208525565e-01
   -9.4000000000e-01    2.0570209160e-01
   -9.3000000000e-01    2.0935933347e-01
   -9.2000000000e-01    2.1304575740e-01
   -9.1000000000e-01    2.1675013951e-01
   -9.0000000000e-01    2.2046125594e-01
   -8.9000000000e-01    2.2416788282e-01
   -8.8000000000e-01    2.2785879630e-01
   -8.7000000000e-01    2.3152277249e-01
   -8.6000000000e-01    2.3514858753e-01
   -8.5000000000e-01    2.3872501757e-01
   -8.4000000000e-01    2.4224083872e-01
   -8.3000000000e-01    2.4568482713e-01
   -8.2000000000e-01    2.4904575893e-01
   -8.1000000000e-01    2.5231241025e-01
   -8.0000000000e-01    2.5547355722e-01
   -7.9000000000e-01    2.5851797598e-01
   -7.8000000000e-01    2.6143444267e-01
   -7.7000000000e-01    2.6421173341e-01
   -7.6000000000e-01    2.6683862434e-01
   -7.5000000000e-01    2.6930389159e-01
   -7.4000000000e-01    2.7159631130e-01
   -7.3000000000e-01    2.7370465960e-01
   -7.2000000000e-01    2.7561771262e-01
   -7.1000000000e-01    2.7731727279e-01
   -7.0000000000e-01    2.7858237996e-01
   -6.9000000000e-01    2.7936614932e-01
   -6.8000000000e-01    2.7974234027e-01
```

-6.7000000000e-01	2.7978471217e-01
-6.6000000000e-01	2.7956702440e-01
-6.5000000000e-01	2.7916303635e-01
-6.4000000000e-01	2.7864650738e-01
-6.3000000000e-01	2.7809119687e-01
-6.2000000000e-01	2.7757086421e-01
-6.1000000000e-01	2.7715926876e-01
-6.0000000000e-01	2.7693016991e-01
-5.9000000000e-01	2.7695732703e-01
-5.8000000000e-01	2.7473232243e-01
-5.7000000000e-01	2.6744431687e-01
-5.6000000000e-01	2.5949617870e-01
-5.5000000000e-01	2.5499694475e-01
-5.4000000000e-01	2.4997668372e-01
-5.3000000000e-01	2.4343179554e-01
-5.2000000000e-01	2.3673833886e-01
-5.1000000000e-01	2.3127237233e-01
-5.0000000000e-01	2.2840995457e-01
-4.9000000000e-01	2.2952714425e-01
-4.8000000000e-01	2.3600000000e-01
-4.7000000000e-01	2.4822454024e-01
-4.6000000000e-01	2.6498143371e-01
-4.5000000000e-01	2.8522371453e-01
-4.4000000000e-01	3.0790441682e-01
-4.3000000000e-01	3.3197657470e-01
-4.2000000000e-01	3.5639322229e-01
-4.1000000000e-01	3.8010739370e-01
-4.0000000000e-01	4.0207212306e-01
-3.9000000000e-01	4.2124044448e-01
-3.8000000000e-01	4.3656539209e-01
-3.7000000000e-01	4.4700000000e-01
-3.6000000000e-01	4.5394905045e-01
-3.5000000000e-01	4.5957083596e-01
-3.4000000000e-01	4.6394865611e-01
-3.3000000000e-01	4.6716581046e-01
-3.2000000000e-01	4.6930559859e-01
-3.1000000000e-01	4.7045132007e-01
-3.0000000000e-01	4.7068627446e-01
-2.9000000000e-01	4.7009376134e-01
-2.8000000000e-01	4.6875708028e-01
-2.7000000000e-01	4.6675953084e-01
-2.6000000000e-01	4.6418441260e-01
-2.5000000000e-01	4.6111502513e-01
-2.4000000000e-01	4.5763466800e-01
-2.3000000000e-01	4.5382664078e-01
-2.2000000000e-01	4.4977424304e-01
-2.1000000000e-01	4.4556077435e-01
-2.0000000000e-01	4.4126953427e-01
-1.9000000000e-01	4.3698382239e-01
-1.8000000000e-01	4.3278693827e-01
-1.7000000000e-01	4.2876218148e-01
-1.6000000000e-01	4.2499285159e-01

```
   -1.5000000000e-01    4.2156224817e-01
   -1.4000000000e-01    4.1814345869e-01
   -1.3000000000e-01    4.1249279223e-01
   -1.2000000000e-01    4.0462650174e-01
   -1.1000000000e-01    3.9498597250e-01
   -1.0000000000e-01    3.8401258980e-01
   -9.0000000000e-02    3.7214773893e-01
   -8.0000000000e-02    3.5983280517e-01
   -7.0000000000e-02    3.4750917381e-01
   -6.0000000000e-02    3.3561823012e-01
   -5.0000000000e-02    3.2460135941e-01
   -4.0000000000e-02    3.1489994695e-01
   -3.0000000000e-02    3.0695537803e-01
   -2.0000000000e-02    3.0120903794e-01
   -1.0000000000e-02    2.9798610671e-01
    0.0000000000e+00    2.9649533984e-01
    1.0000000000e-02    2.9646278122e-01
    2.0000000000e-02    2.9784696551e-01
    3.0000000000e-02    3.0060642739e-01
    4.0000000000e-02    3.0469970151e-01
    5.0000000000e-02    3.1008532254e-01
    6.0000000000e-02    3.1672182516e-01
    7.0000000000e-02    3.2456774402e-01
    8.0000000000e-02    3.3358161379e-01
    9.0000000000e-02    3.4372196914e-01
    1.0000000000e-01    3.5494734474e-01
    1.1000000000e-01    3.6721627524e-01
    1.2000000000e-01    3.8048729532e-01
    1.3000000000e-01    3.9471893964e-01
    1.4000000000e-01    4.0986974287e-01
    1.5000000000e-01    4.2600353805e-01
    1.6000000000e-01    4.4467898970e-01
    1.7000000000e-01    4.6622824499e-01
    1.8000000000e-01    4.9039240269e-01
    1.9000000000e-01    4.9039240269e-01
    4.00000000000000    4.9039240269e-01
    5.00000000000000    1.00000000000000
*DEFINE_CURVE
$     LCID      SIDR       SFA       SFO      OFFA      OFFO    DATYP
      3002
$                A1                  O1
   -1.0000000000e+00    1.8565473574e-01
   -9.9000000000e-01    1.8862282299e-01
   -9.8000000000e-01    1.9173054745e-01
   -9.7000000000e-01    1.9494915438e-01
   -9.6000000000e-01    1.9825716570e-01
   -9.5000000000e-01    2.0163688815e-01
   -9.4000000000e-01    2.0507274026e-01
   -9.3000000000e-01    2.0855037692e-01
   -9.2000000000e-01    2.1205619539e-01
   -9.1000000000e-01    2.1557703596e-01
   -9.0000000000e-01    2.1909998571e-01
```

-8.9000000000e-01	2.2261223683e-01
-8.8000000000e-01	2.2610097107e-01
-8.7000000000e-01	2.2955325096e-01
-8.6000000000e-01	2.3295590163e-01
-8.5000000000e-01	2.3629536572e-01
-8.4000000000e-01	2.3955750802e-01
-8.3000000000e-01	2.4272733414e-01
-8.2000000000e-01	2.4578856302e-01
-8.1000000000e-01	2.4872294575e-01
-8.0000000000e-01	2.5150912643e-01
-7.9000000000e-01	2.5412063217e-01
-7.8000000000e-01	2.5652209407e-01
-7.7000000000e-01	2.5866156310e-01
-7.6000000000e-01	2.6043121621e-01
-7.5000000000e-01	2.6178311712e-01
-7.4000000000e-01	2.6288101608e-01
-7.3000000000e-01	2.6389914192e-01
-7.2000000000e-01	2.6501723815e-01
-7.1000000000e-01	2.6639602010e-01
-7.0000000000e-01	2.6733123146e-01
-6.9000000000e-01	2.6767255298e-01
-6.8000000000e-01	2.6759282112e-01
-6.7000000000e-01	2.6720817823e-01
-6.6000000000e-01	2.6661778958e-01
-6.5000000000e-01	2.6591763391e-01
-6.4000000000e-01	2.6520964534e-01
-6.3000000000e-01	2.6461533030e-01
-6.2000000000e-01	2.6431047051e-01
-6.1000000000e-01	2.6464880426e-01
-6.0000000000e-01	2.6582469578e-01
-5.9000000000e-01	2.6687688890e-01
-5.8000000000e-01	2.6511397275e-01
-5.7000000000e-01	2.5876734955e-01
-5.6000000000e-01	2.5292549639e-01
-5.5000000000e-01	2.4923285775e-01
-5.4000000000e-01	2.4511872889e-01
-5.3000000000e-01	2.3922139450e-01
-5.2000000000e-01	2.3328905280e-01
-5.1000000000e-01	2.2901397283e-01
-5.0000000000e-01	2.2851159081e-01
-4.9000000000e-01	2.3507635526e-01
-4.8000000000e-01	2.4392707812e-01
-4.7000000000e-01	2.5681868327e-01
-4.6000000000e-01	2.7454901662e-01
-4.5000000000e-01	2.9583080382e-01
-4.4000000000e-01	3.1949097267e-01
-4.3000000000e-01	3.4435903399e-01
-4.2000000000e-01	3.6920543879e-01
-4.1000000000e-01	3.9264043233e-01
-4.0000000000e-01	4.1283226699e-01
-3.9000000000e-01	4.2649004950e-01
-3.8000000000e-01	4.3834436302e-01

-3.7000000000e-01	4.4851506116e-01
-3.6000000000e-01	4.5467738731e-01
-3.5000000000e-01	4.5956290162e-01
-3.4000000000e-01	4.6324200324e-01
-3.3000000000e-01	4.6579237680e-01
-3.2000000000e-01	4.6729533908e-01
-3.1000000000e-01	4.6783440535e-01
-3.0000000000e-01	4.6749473499e-01
-2.9000000000e-01	4.6636300740e-01
-2.8000000000e-01	4.6452757793e-01
-2.7000000000e-01	4.6207889328e-01
-2.6000000000e-01	4.5911023243e-01
-2.5000000000e-01	4.5571893892e-01
-2.4000000000e-01	4.5200847602e-01
-2.3000000000e-01	4.4809196345e-01
-2.2000000000e-01	4.4409856582e-01
-2.1000000000e-01	4.4018579475e-01
-2.0000000000e-01	4.3656524492e-01
-1.9000000000e-01	4.3356265602e-01
-1.8000000000e-01	4.3108695705e-01
-1.7000000000e-01	4.2816468445e-01
-1.6000000000e-01	4.2494754975e-01
-1.5000000000e-01	4.2163167168e-01
-1.4000000000e-01	4.1797849027e-01
-1.3000000000e-01	4.1177195729e-01
-1.2000000000e-01	4.0321144560e-01
-1.1000000000e-01	3.9283040209e-01
-1.0000000000e-01	3.8112561007e-01
-9.0000000000e-02	3.6858931522e-01
-8.0000000000e-02	3.5572735481e-01
-7.0000000000e-02	3.4308145299e-01
-6.0000000000e-02	3.3127384741e-01
-5.0000000000e-02	3.2112270219e-01
-4.0000000000e-02	3.1402156424e-01
-3.0000000000e-02	3.0821670323e-01
-2.0000000000e-02	3.0145648107e-01
-1.0000000000e-02	2.9817612716e-01
0.0000000000e+00	2.9704458926e-01
1.0000000000e-02	2.9727619464e-01
2.0000000000e-02	2.9887071933e-01
3.0000000000e-02	3.0180516187e-01
4.0000000000e-02	3.0604691277e-01
5.0000000000e-02	3.1155842117e-01
6.0000000000e-02	3.1829893188e-01
7.0000000000e-02	3.2622487010e-01
8.0000000000e-02	3.3528920682e-01
9.0000000000e-02	3.4543938681e-01
1.0000000000e-01	3.5661212935e-01
1.1000000000e-01	3.6871946308e-01
1.2000000000e-01	3.8158423071e-01
1.3000000000e-01	3.9504080627e-01
1.4000000000e-01	4.0968238932e-01

```
    1.5000000000e-01    4.2622969983e-01
    1.6000000000e-01    4.4573551490e-01
    1.7000000000e-01    4.6817406817e-01
    1.8000000000e-01    4.9324356832e-01
    1.9000000000e-01    4.9324356832e-01
    4.00000000000000    4.9324356832e-01
    5.00000000000000    1.00000000000000
*DEFINE_CURVE
$     LCID      SIDR       SFA       SFO      OFFA      OFFO    DATYP
      3003
$                A1                  O1
   -1.0000000000e+00    1.8700272109e-01
   -9.9000000000e-01    1.8968751673e-01
   -9.8000000000e-01    1.9255742104e-01
   -9.7000000000e-01    1.9557272354e-01
   -9.6000000000e-01    1.9870061055e-01
   -9.5000000000e-01    2.0191286547e-01
   -9.4000000000e-01    2.0518434726e-01
   -9.3000000000e-01    2.0849193339e-01
   -9.2000000000e-01    2.1181374219e-01
   -9.1000000000e-01    2.1512851801e-01
   -9.0000000000e-01    2.1841509988e-01
   -8.9000000000e-01    2.2165191233e-01
   -8.8000000000e-01    2.2481642267e-01
   -8.7000000000e-01    2.2788450369e-01
   -8.6000000000e-01    2.3082962387e-01
   -8.5000000000e-01    2.3362175260e-01
   -8.4000000000e-01    2.3622580592e-01
   -8.3000000000e-01    2.3859934552e-01
   -8.2000000000e-01    2.4068718880e-01
   -8.1000000000e-01    2.4237996829e-01
   -8.0000000000e-01    2.4370609922e-01
   -7.9000000000e-01    2.4474636411e-01
   -7.8000000000e-01    2.4557412357e-01
   -7.7000000000e-01    2.4625813264e-01
   -7.6000000000e-01    2.4686495863e-01
   -7.5000000000e-01    2.4746120718e-01
   -7.4000000000e-01    2.4811573473e-01
   -7.3000000000e-01    2.4890202274e-01
   -7.2000000000e-01    2.4990091008e-01
   -7.1000000000e-01    2.5116878549e-01
   -7.0000000000e-01    2.5178359373e-01
   -6.9000000000e-01    2.5165673806e-01
   -6.8000000000e-01    2.5112061061e-01
   -6.7000000000e-01    2.5041422591e-01
   -6.6000000000e-01    2.4974435098e-01
   -6.5000000000e-01    2.4932544003e-01
   -6.4000000000e-01    2.4942608575e-01
   -6.3000000000e-01    2.5042965305e-01
   -6.2000000000e-01    2.5226082715e-01
   -6.1000000000e-01    2.5433421154e-01
   -6.0000000000e-01    2.5617798159e-01
```

-5.9000000000e-01	2.5738682251e-01
-5.8000000000e-01	2.5561517052e-01
-5.7000000000e-01	2.5038430569e-01
-5.6000000000e-01	2.4565887815e-01
-5.5000000000e-01	2.4212133018e-01
-5.4000000000e-01	2.3871453034e-01
-5.3000000000e-01	2.3333426548e-01
-5.2000000000e-01	2.2916147478e-01
-5.1000000000e-01	2.3007996254e-01
-5.0000000000e-01	2.3752773132e-01
-4.9000000000e-01	2.4508227646e-01
-4.8000000000e-01	2.5419867602e-01
-4.7000000000e-01	2.6811137920e-01
-4.6000000000e-01	2.8762878606e-01
-4.5000000000e-01	3.1068999118e-01
-4.4000000000e-01	3.3538714516e-01
-4.3000000000e-01	3.5962810426e-01
-4.2000000000e-01	3.8072272894e-01
-4.1000000000e-01	3.9487160106e-01
-4.0000000000e-01	4.0904348944e-01
-3.9000000000e-01	4.2493289804e-01
-3.8000000000e-01	4.3905681686e-01
-3.7000000000e-01	4.4842810840e-01
-3.6000000000e-01	4.5368166158e-01
-3.5000000000e-01	4.5754397201e-01
-3.4000000000e-01	4.6015652800e-01
-3.3000000000e-01	4.6164906788e-01
-3.2000000000e-01	4.6214569921e-01
-3.1000000000e-01	4.6176910473e-01
-3.0000000000e-01	4.6064395134e-01
-2.9000000000e-01	4.5890021231e-01
-2.8000000000e-01	4.5667699864e-01
-2.7000000000e-01	4.5412757823e-01
-2.6000000000e-01	4.5142655932e-01
-2.5000000000e-01	4.4878085023e-01
-2.4000000000e-01	4.4644729576e-01
-2.3000000000e-01	4.4475818373e-01
-2.2000000000e-01	4.4311515116e-01
-2.1000000000e-01	4.4094122244e-01
-2.0000000000e-01	4.3833288424e-01
-1.9000000000e-01	4.3537713002e-01
-1.8000000000e-01	4.3215603433e-01
-1.7000000000e-01	4.2875067523e-01
-1.6000000000e-01	4.2524493322e-01
-1.5000000000e-01	4.2172966793e-01
-1.4000000000e-01	4.1778123488e-01
-1.3000000000e-01	4.1074881371e-01
-1.2000000000e-01	4.0106660492e-01
-1.1000000000e-01	3.8956895307e-01
-1.0000000000e-01	3.7705078005e-01
-9.0000000000e-02	3.6436148667e-01
-8.0000000000e-02	3.5251216231e-01

```
   -7.0000000000e-02    3.4286033179e-01
   -6.0000000000e-02    3.3659136727e-01
   -5.0000000000e-02    3.2797141494e-01
   -4.0000000000e-02    3.1768875189e-01
   -3.0000000000e-02    3.0804733680e-01
   -2.0000000000e-02    3.0107149054e-01
   -1.0000000000e-02    2.9838734041e-01
    0.0000000000e+00    2.9777385390e-01
    1.0000000000e-02    2.9847841918e-01
    2.0000000000e-02    3.0048862142e-01
    3.0000000000e-02    3.0377696080e-01
    4.0000000000e-02    3.0830566253e-01
    5.0000000000e-02    3.1402819950e-01
    6.0000000000e-02    3.2088849449e-01
    7.0000000000e-02    3.2881752636e-01
    8.0000000000e-02    3.3772565085e-01
    9.0000000000e-02    3.4743186177e-01
    1.0000000000e-01    3.5757002915e-01
    1.1000000000e-01    3.6846585352e-01
    1.2000000000e-01    3.8049006948e-01
    1.3000000000e-01    3.9396065860e-01
    1.4000000000e-01    4.0916853068e-01
    1.5000000000e-01    4.2647281006e-01
    1.6000000000e-01    4.4707760693e-01
    1.7000000000e-01    4.7089802372e-01
    4.00000000000000    4.7089802372e-01
    5.00000000000000    1.00000000000000
*DEFINE_CURVE
$     LCID      SIDR       SFA       SFO      OFFA      OFFO    DATYP
      3004
$                A1                  O1
   -1.0000000000e+00    1.8811962323e-01
   -9.9000000000e-01    1.9051666382e-01
   -9.8000000000e-01    1.9313072654e-01
   -9.7000000000e-01    1.9590563948e-01
   -9.6000000000e-01    1.9879166445e-01
   -9.5000000000e-01    2.0174352611e-01
   -9.4000000000e-01    2.0471884905e-01
   -9.3000000000e-01    2.0767684462e-01
   -9.2000000000e-01    2.1057712768e-01
   -9.1000000000e-01    2.1337856209e-01
   -9.0000000000e-01    2.1603803795e-01
   -8.9000000000e-01    2.1850907272e-01
   -8.8000000000e-01    2.2074010135e-01
   -8.7000000000e-01    2.2265530822e-01
   -8.6000000000e-01    2.2420269920e-01
   -8.5000000000e-01    2.2545033069e-01
   -8.4000000000e-01    2.2645818868e-01
   -8.3000000000e-01    2.2727520940e-01
   -8.2000000000e-01    2.2794262462e-01
   -8.1000000000e-01    2.2849632145e-01
   -8.0000000000e-01    2.2896858372e-01
```

```
-7.9000000000e-01    2.2938945084e-01
-7.8000000000e-01    2.2978785587e-01
-7.7000000000e-01    2.3019266540e-01
-7.6000000000e-01    2.3063372759e-01
-7.5000000000e-01    2.3114303760e-01
-7.4000000000e-01    2.3175615302e-01
-7.3000000000e-01    2.3251404158e-01
-7.2000000000e-01    2.3346563676e-01
-7.1000000000e-01    2.3463288144e-01
-7.0000000000e-01    2.3501129312e-01
-6.9000000000e-01    2.3466577125e-01
-6.8000000000e-01    2.3415545082e-01
-6.7000000000e-01    2.3393154487e-01
-6.6000000000e-01    2.3442216316e-01
-6.5000000000e-01    2.3597512780e-01
-6.4000000000e-01    2.3825069266e-01
-6.3000000000e-01    2.4081920008e-01
-6.2000000000e-01    2.4338702329e-01
-6.1000000000e-01    2.4572499063e-01
-6.0000000000e-01    2.4763044410e-01
-5.9000000000e-01    2.4889880088e-01
-5.8000000000e-01    2.4729940463e-01
-5.7000000000e-01    2.4439733294e-01
-5.6000000000e-01    2.3749027700e-01
-5.5000000000e-01    2.3596523199e-01
-5.4000000000e-01    2.3372063225e-01
-5.3000000000e-01    2.3108335823e-01
-5.2000000000e-01    2.3486727748e-01
-5.1000000000e-01    2.4161409261e-01
-5.0000000000e-01    2.4834684578e-01
-4.9000000000e-01    2.5617243964e-01
-4.8000000000e-01    2.6575792832e-01
-4.7000000000e-01    2.8062501863e-01
-4.6000000000e-01    3.0129388087e-01
-4.5000000000e-01    3.2399745412e-01
-4.4000000000e-01    3.4468495611e-01
-4.3000000000e-01    3.5894685503e-01
-4.2000000000e-01    3.7452664817e-01
-4.1000000000e-01    3.9246472779e-01
-4.0000000000e-01    4.1037205244e-01
-3.9000000000e-01    4.2651775004e-01
-3.8000000000e-01    4.3941883955e-01
-3.7000000000e-01    4.4755979768e-01
-3.6000000000e-01    4.5191866416e-01
-3.5000000000e-01    4.5480488167e-01
-3.4000000000e-01    4.5645878343e-01
-3.3000000000e-01    4.5710611346e-01
-3.2000000000e-01    4.5696822684e-01
-3.1000000000e-01    4.5627115015e-01
-3.0000000000e-01    4.5525480720e-01
-2.9000000000e-01    4.5418368851e-01
-2.8000000000e-01    4.5336053010e-01
```

```
   -2.7000000000e-01    4.5304422072e-01
   -2.6000000000e-01    4.5240034697e-01
   -2.5000000000e-01    4.5121696226e-01
   -2.4000000000e-01    4.4956595522e-01
   -2.3000000000e-01    4.4750603553e-01
   -2.2000000000e-01    4.4508762231e-01
   -2.1000000000e-01    4.4235607205e-01
   -2.0000000000e-01    4.3935400484e-01
   -1.9000000000e-01    4.3612319063e-01
   -1.8000000000e-01    4.3270632688e-01
   -1.7000000000e-01    4.2914901239e-01
   -1.6000000000e-01    4.2550228827e-01
   -1.5000000000e-01    4.2182631076e-01
   -1.4000000000e-01    4.1758367530e-01
   -1.3000000000e-01    4.0981501919e-01
   -1.2000000000e-01    3.9947191293e-01
   -1.1000000000e-01    3.8810339022e-01
   -1.0000000000e-01    3.7738750361e-01
   -9.0000000000e-02    3.6938445853e-01
   -8.0000000000e-02    3.6215636632e-01
   -7.0000000000e-02    3.5144033779e-01
   -6.0000000000e-02    3.3921435644e-01
   -5.0000000000e-02    3.2692312273e-01
   -4.0000000000e-02    3.1571465085e-01
   -3.0000000000e-02    3.0660942779e-01
   -2.0000000000e-02    3.0062405372e-01
   -1.0000000000e-02    2.9859728947e-01
    0.0000000000e+00    2.9849999293e-01
    1.0000000000e-02    2.9967955587e-01
    2.0000000000e-02    3.0209670790e-01
    3.0000000000e-02    3.0570007516e-01
    4.0000000000e-02    3.1042533789e-01
    5.0000000000e-02    3.1619182477e-01
    6.0000000000e-02    3.2278718850e-01
    7.0000000000e-02    3.2968074881e-01
    8.0000000000e-02    3.3717209079e-01
    9.0000000000e-02    3.4557568810e-01
    1.0000000000e-01    3.5513519379e-01
    1.1000000000e-01    3.6605231132e-01
    1.2000000000e-01    3.7850292003e-01
    1.3000000000e-01    3.9264678850e-01
    1.4000000000e-01    4.0863405473e-01
    1.5000000000e-01    4.2671454594e-01
    1.6000000000e-01    4.4837529518e-01
    1.7000000000e-01    4.7339974648e-01
    1.8000000000e-01    5.0099721651e-01
    1.9000000000e-01    5.0099721651e-01
    4.00000000000000    5.0099721651e-01
    5.00000000000000    1.00000000000000
*DEFINE_CURVE
$     LCID      SIDR       SFA       SFO      OFFA      OFFO    DATYP
      3005
```

```
$                 A1                  O1
   -1.0000000000e+00    1.8808110937e-01
   -9.9000000000e-01    1.9018259507e-01
   -9.8000000000e-01    1.9249854843e-01
   -9.7000000000e-01    1.9492914601e-01
   -9.6000000000e-01    1.9738095049e-01
   -9.5000000000e-01    1.9976425397e-01
   -9.4000000000e-01    2.0199061835e-01
   -9.3000000000e-01    2.0396948713e-01
   -9.2000000000e-01    2.0559966033e-01
   -9.1000000000e-01    2.0693269019e-01
   -9.0000000000e-01    2.0804340584e-01
   -8.9000000000e-01    2.0898222309e-01
   -8.8000000000e-01    2.0978534593e-01
   -8.7000000000e-01    2.1048026687e-01
   -8.6000000000e-01    2.1108891872e-01
   -8.5000000000e-01    2.1162957669e-01
   -8.4000000000e-01    2.1211806120e-01
   -8.3000000000e-01    2.1256853420e-01
   -8.2000000000e-01    2.1299405403e-01
   -8.1000000000e-01    2.1340698705e-01
   -8.0000000000e-01    2.1381934001e-01
   -7.9000000000e-01    2.1424305956e-01
   -7.8000000000e-01    2.1469033978e-01
   -7.7000000000e-01    2.1517398269e-01
   -7.6000000000e-01    2.1570787307e-01
   -7.5000000000e-01    2.1630766433e-01
   -7.4000000000e-01    2.1699184526e-01
   -7.3000000000e-01    2.1778350867e-01
   -7.2000000000e-01    2.1871347413e-01
   -7.1000000000e-01    2.1978631659e-01
   -7.0000000000e-01    2.2008816716e-01
   -6.9000000000e-01    2.2014903788e-01
   -6.8000000000e-01    2.2100308281e-01
   -6.7000000000e-01    2.2292304467e-01
   -6.6000000000e-01    2.2540468552e-01
   -6.5000000000e-01    2.2815561037e-01
   -6.4000000000e-01    2.3099157669e-01
   -6.3000000000e-01    2.3376990153e-01
   -6.2000000000e-01    2.3636573709e-01
   -6.1000000000e-01    2.3866110677e-01
   -6.0000000000e-01    2.4053689193e-01
   -5.9000000000e-01    2.4186011757e-01
   -5.8000000000e-01    2.4118787269e-01
   -5.7000000000e-01    2.3702200089e-01
   -5.6000000000e-01    2.3202980955e-01
   -5.5000000000e-01    2.3308065684e-01
   -5.4000000000e-01    2.3382938876e-01
   -5.3000000000e-01    2.3961185821e-01
   -5.2000000000e-01    2.4572953273e-01
   -5.1000000000e-01    2.5202779531e-01
   -5.0000000000e-01    2.5913765050e-01
```

-4.9000000000e-01	2.6751595457e-01
-4.8000000000e-01	2.7754796964e-01
-4.7000000000e-01	2.9292634205e-01
-4.6000000000e-01	3.1143278102e-01
-4.5000000000e-01	3.2551862096e-01
-4.4000000000e-01	3.4178836383e-01
-4.3000000000e-01	3.6029648130e-01
-4.2000000000e-01	3.7929796363e-01
-4.1000000000e-01	3.9764873458e-01
-4.0000000000e-01	4.1442241645e-01
-3.9000000000e-01	4.2877375040e-01
-3.8000000000e-01	4.3986063374e-01
-3.7000000000e-01	4.4673078498e-01
-3.6000000000e-01	4.5023341480e-01
-3.5000000000e-01	4.5234869321e-01
-3.4000000000e-01	4.5355706722e-01
-3.3000000000e-01	4.5433444482e-01
-3.2000000000e-01	4.5517247957e-01
-3.1000000000e-01	4.5627144484e-01
-3.0000000000e-01	4.5683535790e-01
-2.9000000000e-01	4.5686412881e-01
-2.8000000000e-01	4.5641795351e-01
-2.7000000000e-01	4.5554095953e-01
-2.6000000000e-01	4.5426857808e-01
-2.5000000000e-01	4.5263125367e-01
-2.4000000000e-01	4.5065647382e-01
-2.3000000000e-01	4.4836997375e-01
-2.2000000000e-01	4.4579652398e-01
-2.1000000000e-01	4.4296051908e-01
-2.0000000000e-01	4.3988650808e-01
-1.9000000000e-01	4.3659978938e-01
-1.8000000000e-01	4.3312722719e-01
-1.7000000000e-01	4.2949855838e-01
-1.6000000000e-01	4.2574874109e-01
-1.5000000000e-01	4.2192262832e-01
-1.4000000000e-01	4.1740452481e-01
-1.3000000000e-01	4.0948793069e-01
-1.2000000000e-01	4.0088445910e-01
-1.1000000000e-01	3.9452166086e-01
-1.0000000000e-01	3.8528245917e-01
-9.0000000000e-02	3.7345958137e-01
-8.0000000000e-02	3.6044964238e-01
-7.0000000000e-02	3.4717449876e-01
-6.0000000000e-02	3.3436270003e-01
-5.0000000000e-02	3.2265492436e-01
-4.0000000000e-02	3.1265267279e-01
-3.0000000000e-02	3.0494951067e-01
-2.0000000000e-02	3.0016840124e-01
-1.0000000000e-02	2.9880514206e-01
0.0000000000e+00	2.9919913299e-01
1.0000000000e-02	3.0079061392e-01
2.0000000000e-02	3.0349319848e-01

```
    3.0000000000e-02    3.0701927854e-01
    4.0000000000e-02    3.1071619000e-01
    5.0000000000e-02    3.1493323088e-01
    6.0000000000e-02    3.1995622611e-01
    7.0000000000e-02    3.2598680483e-01
    8.0000000000e-02    3.3318687117e-01
    9.0000000000e-02    3.4169724014e-01
    1.0000000000e-01    3.5164616827e-01
    1.1000000000e-01    3.6315323017e-01
    1.2000000000e-01    3.7633045018e-01
    1.3000000000e-01    3.9128083563e-01
    1.4000000000e-01    4.0809242191e-01
    1.5000000000e-01    4.2695285479e-01
    1.6000000000e-01    4.4946602981e-01
    1.7000000000e-01    4.7479442023e-01
    1.8000000000e-01    5.0126422909e-01
    1.9000000000e-01    5.0126422909e-01
    4.00000000000000    5.0126422909e-01
    5.00000000000000    1.00000000000000
*DEFINE_CURVE
$     LCID      SIDR       SFA       SFO      OFFA      OFFO    DATYP
      3006
$                A1                  O1
   -1.0000000000e+00    1.8596284668e-01
   -9.9000000000e-01    1.8770332779e-01
   -9.8000000000e-01    1.8930081955e-01
   -9.7000000000e-01    1.9065931884e-01
   -9.6000000000e-01    1.9187809289e-01
   -9.5000000000e-01    1.9298700021e-01
   -9.4000000000e-01    1.9400084544e-01
   -9.3000000000e-01    1.9493013227e-01
   -9.2000000000e-01    1.9578375167e-01
   -9.1000000000e-01    1.9656987803e-01
   -9.0000000000e-01    1.9729632766e-01
   -8.9000000000e-01    1.9797072179e-01
   -8.8000000000e-01    1.9860056818e-01
   -8.7000000000e-01    1.9919330510e-01
   -8.6000000000e-01    1.9975632666e-01
   -8.5000000000e-01    2.0029699813e-01
   -8.4000000000e-01    2.0082266580e-01
   -8.3000000000e-01    2.0134066367e-01
   -8.2000000000e-01    2.0185831852e-01
   -8.1000000000e-01    2.0238295408e-01
   -8.0000000000e-01    2.0292189536e-01
   -7.9000000000e-01    2.0348247391e-01
   -7.8000000000e-01    2.0407203549e-01
   -7.7000000000e-01    2.0469795318e-01
   -7.6000000000e-01    2.0536765221e-01
   -7.5000000000e-01    2.0608866287e-01
   -7.4000000000e-01    2.0686874878e-01
   -7.3000000000e-01    2.0771627724e-01
   -7.2000000000e-01    2.0864161201e-01
```

-7.1000000000e-01	2.0963263188e-01
-7.0000000000e-01	2.1080720782e-01
-6.9000000000e-01	2.1265899657e-01
-6.8000000000e-01	2.1491623756e-01
-6.7000000000e-01	2.1746653386e-01
-6.6000000000e-01	2.2021023161e-01
-6.5000000000e-01	2.2305014080e-01
-6.4000000000e-01	2.2588981972e-01
-6.3000000000e-01	2.2863310978e-01
-6.2000000000e-01	2.3118396111e-01
-6.1000000000e-01	2.3344632085e-01
-6.0000000000e-01	2.3532390326e-01
-5.9000000000e-01	2.3671846117e-01
-5.8000000000e-01	2.3609767565e-01
-5.7000000000e-01	2.3307454483e-01
-5.6000000000e-01	2.3189786739e-01
-5.5000000000e-01	2.3603921481e-01
-5.4000000000e-01	2.4252906558e-01
-5.3000000000e-01	2.4868259922e-01
-5.2000000000e-01	2.5494536181e-01
-5.1000000000e-01	2.6169161045e-01
-5.0000000000e-01	2.6929030777e-01
-4.9000000000e-01	2.7810911214e-01
-4.8000000000e-01	2.8851193460e-01
-4.7000000000e-01	3.0122763350e-01
-4.6000000000e-01	3.1637619390e-01
-4.5000000000e-01	3.3330645633e-01
-4.4000000000e-01	3.5122838179e-01
-4.3000000000e-01	3.6944300441e-01
-4.2000000000e-01	3.8726652563e-01
-4.1000000000e-01	4.0401945733e-01
-4.0000000000e-01	4.1902387326e-01
-3.9000000000e-01	4.3160237757e-01
-3.8000000000e-01	4.4107711191e-01
-3.7000000000e-01	4.4676172625e-01
-3.6000000000e-01	4.4973872143e-01
-3.5000000000e-01	4.5235471663e-01
-3.4000000000e-01	4.5441421449e-01
-3.3000000000e-01	4.5597046085e-01
-3.2000000000e-01	4.5705040181e-01
-3.1000000000e-01	4.5767594944e-01
-3.0000000000e-01	4.5786757795e-01
-2.9000000000e-01	4.5764522291e-01
-2.8000000000e-01	4.5702858119e-01
-2.7000000000e-01	4.5603723122e-01
-2.6000000000e-01	4.5469068804e-01
-2.5000000000e-01	4.5300843137e-01
-2.4000000000e-01	4.5100992166e-01
-2.3000000000e-01	4.4871461068e-01
-2.2000000000e-01	4.4614195019e-01
-2.1000000000e-01	4.4331140186e-01
-2.0000000000e-01	4.4024245199e-01

```
   -1.9000000000e-01    4.3695463938e-01
   -1.8000000000e-01    4.3346761762e-01
   -1.7000000000e-01    4.2980131991e-01
   -1.6000000000e-01    4.2597650720e-01
   -1.5000000000e-01    4.2201740683e-01
   -1.4000000000e-01    4.1753963456e-01
   -1.3000000000e-01    4.1137930606e-01
   -1.2000000000e-01    4.0244736265e-01
   -1.1000000000e-01    3.9170572832e-01
   -1.0000000000e-01    3.7971727820e-01
   -9.0000000000e-02    3.6699862619e-01
   -8.0000000000e-02    3.5405570198e-01
   -7.0000000000e-02    3.4139085948e-01
   -6.0000000000e-02    3.2950495283e-01
   -5.0000000000e-02    3.1889806650e-01
   -4.0000000000e-02    3.1006972844e-01
   -3.0000000000e-02    3.0351863411e-01
   -2.0000000000e-02    2.9974016698e-01
   -1.0000000000e-02    2.9900863358e-01
    0.0000000000e+00    2.9955073153e-01
    1.0000000000e-02    3.0040216871e-01
    2.0000000000e-02    3.0183120908e-01
    3.0000000000e-02    3.0398053657e-01
    4.0000000000e-02    3.0696903003e-01
    5.0000000000e-02    3.1091035429e-01
    6.0000000000e-02    3.1591647380e-01
    7.0000000000e-02    3.2209865066e-01
    8.0000000000e-02    3.2956779548e-01
    9.0000000000e-02    3.3843459679e-01
    1.0000000000e-01    3.4880954266e-01
    1.1000000000e-01    3.6080283833e-01
    1.2000000000e-01    3.7452409931e-01
    1.3000000000e-01    3.9008123876e-01
    1.4000000000e-01    4.0757474915e-01
    1.5000000000e-01    4.2715907767e-01
    1.6000000000e-01    4.4869507568e-01
    1.7000000000e-01    4.7246792702e-01
    1.8000000000e-01    4.9835850419e-01
    1.9000000000e-01    4.9835850419e-01
    4.00000000000000    4.9835850419e-01
    5.00000000000000    1.00000000000000
*DEFINE_CURVE
$     LCID      SIDR       SFA       SFO      OFFA      OFFO    DATYP
      3007
$                A1                  O1
   -1.0000000000e+00    1.8258279179e-01
   -9.9000000000e-01    1.8401596909e-01
   -9.8000000000e-01    1.8535338633e-01
   -9.7000000000e-01    1.8659307303e-01
   -9.6000000000e-01    1.8773783564e-01
   -9.5000000000e-01    1.8879253141e-01
   -9.4000000000e-01    1.8976301917e-01
```

-9.3000000000e-01	1.9065569572e-01
-9.2000000000e-01	1.9147726949e-01
-9.1000000000e-01	1.9223464117e-01
-9.0000000000e-01	1.9293483735e-01
-8.9000000000e-01	1.9358497221e-01
-8.8000000000e-01	1.9419222524e-01
-8.7000000000e-01	1.9476382894e-01
-8.6000000000e-01	1.9530706335e-01
-8.5000000000e-01	1.9582925636e-01
-8.4000000000e-01	1.9633778955e-01
-8.3000000000e-01	1.9684011112e-01
-8.2000000000e-01	1.9734375896e-01
-8.1000000000e-01	1.9785640007e-01
-8.0000000000e-01	1.9838589864e-01
-7.9000000000e-01	1.9894043799e-01
-7.8000000000e-01	1.9952875127e-01
-7.7000000000e-01	2.0016059176e-01
-7.6000000000e-01	2.0084779226e-01
-7.5000000000e-01	2.0160699771e-01
-7.4000000000e-01	2.0245272318e-01
-7.3000000000e-01	2.0337747282e-01
-7.2000000000e-01	2.0437349560e-01
-7.1000000000e-01	2.0544660125e-01
-7.0000000000e-01	2.0699428394e-01
-6.9000000000e-01	2.0906227847e-01
-6.8000000000e-01	2.1152376085e-01
-6.7000000000e-01	2.1427187240e-01
-6.6000000000e-01	2.1720427740e-01
-6.5000000000e-01	2.2021889836e-01
-6.4000000000e-01	2.2321115005e-01
-6.3000000000e-01	2.2606950276e-01
-6.2000000000e-01	2.2866378344e-01
-6.1000000000e-01	2.3080219712e-01
-6.0000000000e-01	2.3206017041e-01
-5.9000000000e-01	2.3290701386e-01
-5.8000000000e-01	2.3391920473e-01
-5.7000000000e-01	2.3383559018e-01
-5.6000000000e-01	2.3601790909e-01
-5.5000000000e-01	2.4744347846e-01
-5.4000000000e-01	2.5448834337e-01
-5.3000000000e-01	2.6110408651e-01
-5.2000000000e-01	2.6764321216e-01
-5.1000000000e-01	2.7449523660e-01
-5.0000000000e-01	2.8211110333e-01
-4.9000000000e-01	2.9128679777e-01
-4.8000000000e-01	2.9893901566e-01
-4.7000000000e-01	3.1143338568e-01
-4.6000000000e-01	3.2639526554e-01
-4.5000000000e-01	3.4302585646e-01
-4.4000000000e-01	3.6060659438e-01
-4.3000000000e-01	3.7842975731e-01
-4.2000000000e-01	3.9577775374e-01

-4.1000000000e-01	4.1189940027e-01
-4.0000000000e-01	4.2594840864e-01
-3.9000000000e-01	4.3674210042e-01
-3.8000000000e-01	4.4262173082e-01
-3.7000000000e-01	4.4740965254e-01
-3.6000000000e-01	4.5035597998e-01
-3.5000000000e-01	4.5277130735e-01
-3.4000000000e-01	4.5467743783e-01
-3.3000000000e-01	4.5609490045e-01
-3.2000000000e-01	4.5704378204e-01
-3.1000000000e-01	4.5754400989e-01
-3.0000000000e-01	4.5761547596e-01
-2.9000000000e-01	4.5727810945e-01
-2.8000000000e-01	4.5655193580e-01
-2.7000000000e-01	4.5545714148e-01
-2.6000000000e-01	4.5401416016e-01
-2.5000000000e-01	4.5224380108e-01
-2.4000000000e-01	4.5016745404e-01
-2.3000000000e-01	4.4780743617e-01
-2.2000000000e-01	4.4518761417e-01
-2.1000000000e-01	4.4233459942e-01
-2.0000000000e-01	4.3928024570e-01
-1.9000000000e-01	4.3606747641e-01
-1.8000000000e-01	4.3276610038e-01
-1.7000000000e-01	4.2946028115e-01
-1.6000000000e-01	4.2584803108e-01
-1.5000000000e-01	4.2192044248e-01
-1.4000000000e-01	4.1737547097e-01
-1.3000000000e-01	4.1025011536e-01
-1.2000000000e-01	4.0081910853e-01
-1.1000000000e-01	3.8963958291e-01
-1.0000000000e-01	3.7723777927e-01
-9.0000000000e-02	3.6413408650e-01
-8.0000000000e-02	3.5085266344e-01
-7.0000000000e-02	3.3793057697e-01
-6.0000000000e-02	3.2593472931e-01
-5.0000000000e-02	3.1550501603e-01
-4.0000000000e-02	3.0749590926e-01
-3.0000000000e-02	3.0355912621e-01
-2.0000000000e-02	3.0017145301e-01
-1.0000000000e-02	2.9897585975e-01
0.0000000000e+00	2.9916466668e-01
1.0000000000e-02	2.9983563923e-01
2.0000000000e-02	3.0111805963e-01
3.0000000000e-02	3.0313063407e-01
4.0000000000e-02	3.0598892398e-01
5.0000000000e-02	3.0980773930e-01
6.0000000000e-02	3.1470235570e-01
7.0000000000e-02	3.2078961537e-01
8.0000000000e-02	3.2818953499e-01
9.0000000000e-02	3.3702835866e-01
1.0000000000e-01	3.4744536349e-01

```
    1.1000000000e-01    3.5961060643e-01
    1.2000000000e-01    3.7378203693e-01
    1.3000000000e-01    3.9025493318e-01
    1.4000000000e-01    4.0769184984e-01
    1.5000000000e-01    4.2711895822e-01
    1.6000000000e-01    4.4912751788e-01
    1.7000000000e-01    4.7337158706e-01
    1.8000000000e-01    4.9960408980e-01
    1.9000000000e-01    4.9960408980e-01
    4.00000000000000    4.9960408980e-01
    5.00000000000000    1.00000000000000
*DEFINE_CURVE
$     LCID      SIDR       SFA       SFO      OFFA      OFFO    DATYP
      3008
$                A1                  O1
   -1.0000000000e+00    1.8136402305e-01
   -9.9000000000e-01    1.8267189639e-01
   -9.8000000000e-01    1.8389064693e-01
   -9.7000000000e-01    1.8502042543e-01
   -9.6000000000e-01    1.8606368745e-01
   -9.5000000000e-01    1.8702437014e-01
   -9.4000000000e-01    1.8790740707e-01
   -9.3000000000e-01    1.8871843189e-01
   -9.2000000000e-01    1.8946359340e-01
   -9.1000000000e-01    1.9014943993e-01
   -9.0000000000e-01    1.9078284956e-01
   -8.9000000000e-01    1.9137099322e-01
   -8.8000000000e-01    1.9192132427e-01
   -8.7000000000e-01    1.9244159282e-01
   -8.6000000000e-01    1.9293988681e-01
   -8.5000000000e-01    1.9342470711e-01
   -8.4000000000e-01    1.9390509014e-01
   -8.3000000000e-01    1.9439080255e-01
   -8.2000000000e-01    1.9489265207e-01
   -8.1000000000e-01    1.9542299502e-01
   -8.0000000000e-01    1.9599659550e-01
   -7.9000000000e-01    1.9662867304e-01
   -7.8000000000e-01    1.9732268554e-01
   -7.7000000000e-01    1.9807846928e-01
   -7.6000000000e-01    1.9889595378e-01
   -7.5000000000e-01    1.9977503787e-01
   -7.4000000000e-01    2.0071546743e-01
   -7.3000000000e-01    2.0171670653e-01
   -7.2000000000e-01    2.0277779243e-01
   -7.1000000000e-01    2.0391600327e-01
   -7.0000000000e-01    2.0565842474e-01
   -6.9000000000e-01    2.0803484630e-01
   -6.8000000000e-01    2.1083749256e-01
   -6.7000000000e-01    2.1389939680e-01
   -6.6000000000e-01    2.1706219205e-01
   -6.5000000000e-01    2.2015503116e-01
   -6.4000000000e-01    2.2296744677e-01
```

-6.3000000000e-01	2.2519283262e-01
-6.2000000000e-01	2.2637129065e-01
-6.1000000000e-01	2.2679435630e-01
-6.0000000000e-01	2.2728949532e-01
-5.9000000000e-01	2.2863942395e-01
-5.8000000000e-01	2.3071055588e-01
-5.7000000000e-01	2.3306809934e-01
-5.6000000000e-01	2.4463013780e-01
-5.5000000000e-01	2.6816216003e-01
-5.4000000000e-01	2.7609954460e-01
-5.3000000000e-01	2.8318579171e-01
-5.2000000000e-01	2.8971616632e-01
-5.1000000000e-01	2.9654322166e-01
-5.0000000000e-01	3.0515367455e-01
-4.9000000000e-01	3.0685272995e-01
-4.8000000000e-01	3.1093521938e-01
-4.7000000000e-01	3.2326110551e-01
-4.6000000000e-01	3.3860967520e-01
-4.5000000000e-01	3.5575207219e-01
-4.4000000000e-01	3.7364200317e-01
-4.3000000000e-01	3.9121961397e-01
-4.2000000000e-01	4.0724825818e-01
-4.1000000000e-01	4.2001489829e-01
-4.0000000000e-01	4.2733384740e-01
-3.9000000000e-01	4.3468895681e-01
-3.8000000000e-01	4.4195067229e-01
-3.7000000000e-01	4.4686846668e-01
-3.6000000000e-01	4.4962760012e-01
-3.5000000000e-01	4.5181241668e-01
-3.4000000000e-01	4.5346549057e-01
-3.3000000000e-01	4.5462194649e-01
-3.2000000000e-01	4.5531289080e-01
-3.1000000000e-01	4.5556733671e-01
-3.0000000000e-01	4.5541342512e-01
-2.9000000000e-01	4.5487933151e-01
-2.8000000000e-01	4.5399408492e-01
-2.7000000000e-01	4.5278846987e-01
-2.6000000000e-01	4.5129619408e-01
-2.5000000000e-01	4.4955558243e-01
-2.4000000000e-01	4.4761223993e-01
-2.3000000000e-01	4.4552351942e-01
-2.2000000000e-01	4.4336650593e-01
-2.1000000000e-01	4.4121798083e-01
-2.0000000000e-01	4.3877167522e-01
-1.9000000000e-01	4.3594767577e-01
-1.8000000000e-01	4.3277786255e-01
-1.7000000000e-01	4.2929326895e-01
-1.6000000000e-01	4.2552561151e-01
-1.5000000000e-01	4.2150887346e-01
-1.4000000000e-01	4.1678925834e-01
-1.3000000000e-01	4.0891345626e-01
-1.2000000000e-01	3.9837808854e-01

```
   -1.1000000000e-01    3.8599612548e-01
   -1.0000000000e-01    3.7250875712e-01
   -9.0000000000e-02    3.5866799092e-01
   -8.0000000000e-02    3.4530880817e-01
   -7.0000000000e-02    3.3345925602e-01
   -6.0000000000e-02    3.2457307433e-01
   -5.0000000000e-02    3.2006677024e-01
   -4.0000000000e-02    3.1346648094e-01
   -3.0000000000e-02    3.0581077682e-01
   -2.0000000000e-02    3.0018780624e-01
   -1.0000000000e-02    2.9894832507e-01
    0.0000000000e+00    2.9894470216e-01
    1.0000000000e-02    2.9930678751e-01
    2.0000000000e-02    3.0022474599e-01
    3.0000000000e-02    3.0186515405e-01
    4.0000000000e-02    3.0438694230e-01
    5.0000000000e-02    3.0795140558e-01
    6.0000000000e-02    3.1273152889e-01
    7.0000000000e-02    3.1892451915e-01
    8.0000000000e-02    3.2677317715e-01
    9.0000000000e-02    3.3660824687e-01
    1.0000000000e-01    3.4887304907e-01
    1.1000000000e-01    3.6204255439e-01
    1.2000000000e-01    3.7579498854e-01
    1.3000000000e-01    3.9081213102e-01
    1.4000000000e-01    4.0771555729e-01
    1.5000000000e-01    4.2712696648e-01
    1.6000000000e-01    4.4940905494e-01
    1.7000000000e-01    4.7420618203e-01
    1.8000000000e-01    5.0115367102e-01
    1.9000000000e-01    5.0115367102e-01
    4.00000000000000    5.0115367102e-01
    5.00000000000000    1.00000000000000
*DEFINE_CURVE
$     LCID      SIDR       SFA       SFO      OFFA      OFFO    DATYP
      3009
$                A1                  O1
   -1.0000000000e+00    1.8174734096e-01
   -9.9000000000e-01    1.8292904005e-01
   -9.8000000000e-01    1.8402386414e-01
   -9.7000000000e-01    1.8503383741e-01
   -9.6000000000e-01    1.8596240457e-01
   -9.5000000000e-01    1.8681410002e-01
   -9.4000000000e-01    1.8759432919e-01
   -9.3000000000e-01    1.8830922793e-01
   -9.2000000000e-01    1.8896557972e-01
   -9.1000000000e-01    1.8957077918e-01
   -9.0000000000e-01    1.9013283726e-01
   -8.9000000000e-01    1.9066042826e-01
   -8.8000000000e-01    1.9116298488e-01
   -8.7000000000e-01    1.9165085369e-01
   -8.6000000000e-01    1.9213553315e-01
```

-8.5000000000e-01	1.9263003089e-01
-8.4000000000e-01	1.9315413026e-01
-8.3000000000e-01	1.9371914838e-01
-8.2000000000e-01	1.9432604007e-01
-8.1000000000e-01	1.9497617023e-01
-8.0000000000e-01	1.9567118940e-01
-7.9000000000e-01	1.9641293458e-01
-7.8000000000e-01	1.9720334892e-01
-7.7000000000e-01	1.9804441194e-01
-7.6000000000e-01	1.9893807359e-01
-7.5000000000e-01	1.9988618635e-01
-7.4000000000e-01	2.0089042902e-01
-7.3000000000e-01	2.0195221499e-01
-7.2000000000e-01	2.0307257466e-01
-7.1000000000e-01	2.0427493485e-01
-7.0000000000e-01	2.0619734863e-01
-6.9000000000e-01	2.0882862208e-01
-6.8000000000e-01	2.1183437063e-01
-6.7000000000e-01	2.1491303110e-01
-6.6000000000e-01	2.1774232634e-01
-6.5000000000e-01	2.1991776443e-01
-6.4000000000e-01	2.2096509822e-01
-6.3000000000e-01	2.2118622222e-01
-6.2000000000e-01	2.2120283433e-01
-6.1000000000e-01	2.2150111231e-01
-6.0000000000e-01	2.2250731791e-01
-5.9000000000e-01	2.2464440445e-01
-5.8000000000e-01	2.2777841472e-01
-5.7000000000e-01	2.3257992092e-01
-5.6000000000e-01	2.6830415798e-01
-5.5000000000e-01	2.9384675687e-01
-5.4000000000e-01	3.0232118820e-01
-5.3000000000e-01	3.0950670482e-01
-5.2000000000e-01	3.1654767470e-01
-5.1000000000e-01	3.2398150465e-01
-5.0000000000e-01	3.2224433511e-01
-4.9000000000e-01	3.1943791359e-01
-4.8000000000e-01	3.2334606463e-01
-4.7000000000e-01	3.3549331263e-01
-4.6000000000e-01	3.5108937217e-01
-4.5000000000e-01	3.6814577848e-01
-4.4000000000e-01	3.8475240263e-01
-4.3000000000e-01	3.9867188955e-01
-4.2000000000e-01	4.0720494632e-01
-4.1000000000e-01	4.1558631159e-01
-4.0000000000e-01	4.2499425798e-01
-3.9000000000e-01	4.3391323870e-01
-3.8000000000e-01	4.4118923974e-01
-3.7000000000e-01	4.4578872157e-01
-3.6000000000e-01	4.4836363281e-01
-3.5000000000e-01	4.5032464478e-01
-3.4000000000e-01	4.5173789376e-01

-3.3000000000e-01	4.5266070962e-01
-3.2000000000e-01	4.5314544263e-01
-3.1000000000e-01	4.5324227358e-01
-3.0000000000e-01	4.5300155848e-01
-2.9000000000e-01	4.5247610266e-01
-2.8000000000e-01	4.5172372363e-01
-2.7000000000e-01	4.5081052731e-01
-2.6000000000e-01	4.4981551262e-01
-2.5000000000e-01	4.4881939336e-01
-2.4000000000e-01	4.4754949850e-01
-2.3000000000e-01	4.4589614159e-01
-2.2000000000e-01	4.4388095492e-01
-2.1000000000e-01	4.4152228904e-01
-2.0000000000e-01	4.3883650412e-01
-1.9000000000e-01	4.3583894473e-01
-1.8000000000e-01	4.3254476404e-01
-1.7000000000e-01	4.2896972381e-01
-1.6000000000e-01	4.2513109043e-01
-1.5000000000e-01	4.2104877363e-01
-1.4000000000e-01	4.1615148191e-01
-1.3000000000e-01	4.0752511286e-01
-1.2000000000e-01	3.9602375268e-01
-1.1000000000e-01	3.8297850752e-01
-1.0000000000e-01	3.6972977591e-01
-9.0000000000e-02	3.5781495050e-01
-8.0000000000e-02	3.4922847410e-01
-7.0000000000e-02	3.4380238484e-01
-6.0000000000e-02	3.3495035307e-01
-5.0000000000e-02	3.2442782760e-01
-4.0000000000e-02	3.1409519989e-01
-3.0000000000e-02	3.0549485772e-01
-2.0000000000e-02	3.0007887826e-01
-1.0000000000e-02	2.9892025252e-01
0.0000000000e+00	2.9872324271e-01
1.0000000000e-02	2.9879456751e-01
2.0000000000e-02	2.9942693975e-01
3.0000000000e-02	3.0089606037e-01
4.0000000000e-02	3.0348575777e-01
5.0000000000e-02	3.0751314544e-01
6.0000000000e-02	3.1336184013e-01
7.0000000000e-02	3.2153513206e-01
8.0000000000e-02	3.3100321257e-01
9.0000000000e-02	3.4072161404e-01
1.0000000000e-01	3.5118841314e-01
1.1000000000e-01	3.6279520609e-01
1.2000000000e-01	3.7587570232e-01
1.3000000000e-01	3.9073896995e-01
1.4000000000e-01	4.0769783313e-01
1.5000000000e-01	4.2713524617e-01
1.6000000000e-01	4.4968537422e-01
1.7000000000e-01	4.7499678783e-01
1.8000000000e-01	5.0253442162e-01

```
    1.9000000000e-01    5.0253442162e-01
    4.00000000000000    5.0253442162e-01
    5.00000000000000    1.00000000000000
*DEFINE_CURVE
$     LCID      SIDR       SFA       SFO      OFFA      OFFO    DATYP
      3010
$                A1                  O1
   -1.0000000000e+00    1.8298176406e-01
   -9.9000000000e-01    1.8403765099e-01
   -9.8000000000e-01    1.8500885734e-01
   -9.7000000000e-01    1.8589900659e-01
   -9.6000000000e-01    1.8671298625e-01
   -9.5000000000e-01    1.8745680741e-01
   -9.4000000000e-01    1.8813752996e-01
   -9.3000000000e-01    1.8876324540e-01
   -9.2000000000e-01    1.8934311515e-01
   -9.1000000000e-01    1.8988746815e-01
   -9.0000000000e-01    1.9040796736e-01
   -8.9000000000e-01    1.9093039081e-01
   -8.8000000000e-01    1.9147295773e-01
   -8.7000000000e-01    1.9203636711e-01
   -8.6000000000e-01    1.9262210206e-01
   -8.5000000000e-01    1.9323216682e-01
   -8.4000000000e-01    1.9386891831e-01
   -8.3000000000e-01    1.9453495566e-01
   -8.2000000000e-01    1.9523304470e-01
   -8.1000000000e-01    1.9596606398e-01
   -8.0000000000e-01    1.9673696391e-01
   -7.9000000000e-01    1.9754873350e-01
   -7.8000000000e-01    1.9840437066e-01
   -7.7000000000e-01    1.9930685266e-01
   -7.6000000000e-01    2.0025910332e-01
   -7.5000000000e-01    2.0126395247e-01
   -7.4000000000e-01    2.0232408187e-01
   -7.3000000000e-01    2.0344194776e-01
   -7.2000000000e-01    2.0461966392e-01
   -7.1000000000e-01    2.0588550279e-01
   -7.0000000000e-01    2.0794467125e-01
   -6.9000000000e-01    2.1062384331e-01
   -6.8000000000e-01    2.1331524210e-01
   -6.7000000000e-01    2.1538885784e-01
   -6.6000000000e-01    2.1623324317e-01
   -6.5000000000e-01    2.1621303899e-01
   -6.4000000000e-01    2.1590985755e-01
   -6.3000000000e-01    2.1571643865e-01
   -6.2000000000e-01    2.1593965081e-01
   -6.1000000000e-01    2.1684475987e-01
   -6.0000000000e-01    2.1867813766e-01
   -5.9000000000e-01    2.2168385079e-01
   -5.8000000000e-01    2.2602858540e-01
   -5.7000000000e-01    2.4566384646e-01
   -5.6000000000e-01    2.9533542578e-01
```

-5.5000000000e-01	3.1975168884e-01
-5.4000000000e-01	3.2848872136e-01
-5.3000000000e-01	3.3660736395e-01
-5.2000000000e-01	3.4210666119e-01
-5.1000000000e-01	3.3855282993e-01
-5.0000000000e-01	3.3321356894e-01
-4.9000000000e-01	3.3068273414e-01
-4.8000000000e-01	3.3486490647e-01
-4.7000000000e-01	3.4670834224e-01
-4.6000000000e-01	3.6162762877e-01
-4.5000000000e-01	3.7587868274e-01
-4.4000000000e-01	3.8547098915e-01
-4.3000000000e-01	3.9444799776e-01
-4.2000000000e-01	4.0485489594e-01
-4.1000000000e-01	4.1543519212e-01
-4.0000000000e-01	4.2536022977e-01
-3.9000000000e-01	4.3397956589e-01
-3.8000000000e-01	4.4070776769e-01
-3.7000000000e-01	4.4493860415e-01
-3.6000000000e-01	4.4733673718e-01
-3.5000000000e-01	4.4910794694e-01
-3.4000000000e-01	4.5036015060e-01
-3.3000000000e-01	4.5119295912e-01
-3.2000000000e-01	4.5170267801e-01
-3.1000000000e-01	4.5198685686e-01
-3.0000000000e-01	4.5214896401e-01
-2.9000000000e-01	4.5229587461e-01
-2.8000000000e-01	4.5219744874e-01
-2.7000000000e-01	4.5171609494e-01
-2.6000000000e-01	4.5087267567e-01
-2.5000000000e-01	4.4968257338e-01
-2.4000000000e-01	4.4815785995e-01
-2.3000000000e-01	4.4630855762e-01
-2.2000000000e-01	4.4414342410e-01
-2.1000000000e-01	4.4167048338e-01
-2.0000000000e-01	4.3889742662e-01
-1.9000000000e-01	4.3583196452e-01
-1.8000000000e-01	4.3248219887e-01
-1.7000000000e-01	4.2885709055e-01
-1.6000000000e-01	4.2496714048e-01
-1.5000000000e-01	4.2082549396e-01
-1.4000000000e-01	4.1575608916e-01
-1.3000000000e-01	4.0662975581e-01
-1.2000000000e-01	3.9524382155e-01
-1.1000000000e-01	3.8421140509e-01
-1.0000000000e-01	3.7652226201e-01
-9.0000000000e-02	3.6965594153e-01
-8.0000000000e-02	3.5919574828e-01
-7.0000000000e-02	3.4710889818e-01
-6.0000000000e-02	3.3469641034e-01
-5.0000000000e-02	3.2294531456e-01
-4.0000000000e-02	3.1269843055e-01

```
   -3.0000000000e-02    3.0475359497e-01
   -2.0000000000e-02    2.9995436127e-01
   -1.0000000000e-02    2.9889259343e-01
    0.0000000000e+00    2.9854342360e-01
    1.0000000000e-02    2.9851598762e-01
    2.0000000000e-02    2.9934004358e-01
    3.0000000000e-02    3.0156892242e-01
    4.0000000000e-02    3.0583171637e-01
    5.0000000000e-02    3.1178285501e-01
    6.0000000000e-02    3.1787872445e-01
    7.0000000000e-02    3.2453554195e-01
    8.0000000000e-02    3.3207949059e-01
    9.0000000000e-02    3.4075560246e-01
    1.0000000000e-01    3.5076558446e-01
    1.1000000000e-01    3.6228866590e-01
    1.2000000000e-01    3.7549537089e-01
    1.3000000000e-01    3.9055967111e-01
    1.4000000000e-01    4.0767453436e-01
    1.5000000000e-01    4.2714322964e-01
    1.6000000000e-01    4.4990267853e-01
    1.7000000000e-01    4.7543594705e-01
    1.8000000000e-01    5.0283245177e-01
    1.9000000000e-01    5.0283245177e-01
    4.00000000000000    5.0283245177e-01
    5.00000000000000    1.00000000000000
*DEFINE_CURVE
$     LCID      SIDR       SFA       SFO      OFFA      OFFO    DATYP
      3011
$                  A1                  O1
   -1.0000000000e+00    1.8431631090e-01
   -9.9000000000e-01    1.8524704183e-01
   -9.8000000000e-01    1.8609675443e-01
   -9.7000000000e-01    1.8687159829e-01
   -9.6000000000e-01    1.8757967635e-01
   -9.5000000000e-01    1.8823106886e-01
   -9.4000000000e-01    1.8885795433e-01
   -9.3000000000e-01    1.8948394609e-01
   -9.2000000000e-01    1.9010884468e-01
   -9.1000000000e-01    1.9073411007e-01
   -9.0000000000e-01    1.9136203255e-01
   -8.9000000000e-01    1.9199535498e-01
   -8.8000000000e-01    1.9263708382e-01
   -8.7000000000e-01    1.9329038727e-01
   -8.6000000000e-01    1.9395853696e-01
   -8.5000000000e-01    1.9464487277e-01
   -8.4000000000e-01    1.9535278063e-01
   -8.3000000000e-01    1.9608567786e-01
   -8.2000000000e-01    1.9684700303e-01
   -8.1000000000e-01    1.9764020837e-01
   -8.0000000000e-01    1.9846875383e-01
   -7.9000000000e-01    1.9933610147e-01
   -7.8000000000e-01    2.0024570975e-01
```

```
-7.7000000000e-01    2.0120102642e-01
-7.6000000000e-01    2.0220547858e-01
-7.5000000000e-01    2.0326245723e-01
-7.4000000000e-01    2.0437529084e-01
-7.3000000000e-01    2.0554719647e-01
-7.2000000000e-01    2.0678118124e-01
-7.1000000000e-01    2.0810935599e-01
-7.0000000000e-01    2.1014164423e-01
-6.9000000000e-01    2.1202551596e-01
-6.8000000000e-01    2.1261189582e-01
-6.7000000000e-01    2.1239835895e-01
-6.6000000000e-01    2.1189199287e-01
-6.5000000000e-01    2.1139335527e-01
-6.4000000000e-01    2.1113950261e-01
-6.3000000000e-01    2.1134203634e-01
-6.2000000000e-01    2.1219966343e-01
-6.1000000000e-01    2.1390178613e-01
-6.0000000000e-01    2.1662572260e-01
-5.9000000000e-01    2.2051908828e-01
-5.8000000000e-01    2.2775660161e-01
-5.7000000000e-01    2.7037030864e-01
-5.6000000000e-01    3.1882694587e-01
-5.5000000000e-01    3.4114172470e-01
-5.4000000000e-01    3.5096034250e-01
-5.3000000000e-01    3.5435487333e-01
-5.2000000000e-01    3.5105267882e-01
-5.1000000000e-01    3.4570822674e-01
-5.0000000000e-01    3.4112437437e-01
-4.9000000000e-01    3.3976337284e-01
-4.8000000000e-01    3.4418509991e-01
-4.7000000000e-01    3.5515873906e-01
-4.6000000000e-01    3.6533485492e-01
-4.5000000000e-01    3.7454976266e-01
-4.4000000000e-01    3.8523362551e-01
-4.3000000000e-01    3.9636662240e-01
-4.2000000000e-01    4.0736167322e-01
-4.1000000000e-01    4.1775476826e-01
-4.0000000000e-01    4.2712694150e-01
-3.9000000000e-01    4.3507675203e-01
-3.8000000000e-01    4.4120465283e-01
-3.7000000000e-01    4.4508630132e-01
-3.6000000000e-01    4.4732613720e-01
-3.5000000000e-01    4.4901801429e-01
-3.4000000000e-01    4.5039399080e-01
-3.3000000000e-01    4.5167898580e-01
-3.2000000000e-01    4.5274819487e-01
-3.1000000000e-01    4.5343909099e-01
-3.0000000000e-01    4.5377448895e-01
-2.9000000000e-01    4.5376767734e-01
-2.8000000000e-01    4.5342771555e-01
-2.7000000000e-01    4.5276155405e-01
-2.6000000000e-01    4.5177500018e-01
```

```
   -2.5000000000e-01    4.5047320382e-01
   -2.4000000000e-01    4.4886092273e-01
   -2.3000000000e-01    4.4694267978e-01
   -2.2000000000e-01    4.4472286574e-01
   -2.1000000000e-01    4.4220581675e-01
   -2.0000000000e-01    4.3939588614e-01
   -1.9000000000e-01    4.3629752984e-01
   -1.8000000000e-01    4.3291543409e-01
   -1.7000000000e-01    4.2925474218e-01
   -1.6000000000e-01    4.2532151664e-01
   -1.5000000000e-01    4.2112381648e-01
   -1.4000000000e-01    4.1592568975e-01
   -1.3000000000e-01    4.0756581827e-01
   -1.2000000000e-01    4.0101984520e-01
   -1.1000000000e-01    3.9270922641e-01
   -1.0000000000e-01    3.8163815127e-01
   -9.0000000000e-02    3.6919722233e-01
   -8.0000000000e-02    3.5621769445e-01
   -7.0000000000e-02    3.4334521603e-01
   -6.0000000000e-02    3.3115040165e-01
   -5.0000000000e-02    3.2017084092e-01
   -4.0000000000e-02    3.1093190365e-01
   -3.0000000000e-02    3.0396386449e-01
   -2.0000000000e-02    2.9983346046e-01
   -1.0000000000e-02    2.9886926343e-01
    0.0000000000e+00    2.9857657077e-01
    1.0000000000e-02    2.9935527704e-01
    2.0000000000e-02    3.0189447028e-01
    3.0000000000e-02    3.0467534115e-01
    4.0000000000e-02    3.0796814863e-01
    5.0000000000e-02    3.1204856518e-01
    6.0000000000e-02    3.1709877446e-01
    7.0000000000e-02    3.2326326433e-01
    8.0000000000e-02    3.3066908914e-01
    9.0000000000e-02    3.3943457695e-01
    1.0000000000e-01    3.4967369189e-01
    1.1000000000e-01    3.6149873956e-01
    1.2000000000e-01    3.7502281599e-01
    1.3000000000e-01    3.9036350672e-01
    1.4000000000e-01    4.0765151424e-01
    1.5000000000e-01    4.2714818896e-01
    1.6000000000e-01    4.4983535836e-01
    1.7000000000e-01    4.7425233282e-01
    1.8000000000e-01    4.9822728386e-01
    1.9000000000e-01    4.9822728386e-01
    4.00000000000000    4.9822728386e-01
    5.00000000000000    1.00000000000000
*DEFINE_CURVE
$     LCID      SIDR       SFA        SFO      OFFA      OFFO    DATYP
      3012
$                 A1                  O1
   -1.0000000000e+00    1.8500000000e-01
```

-9.9000000000e-01	1.8583085278e-01
-9.8000000000e-01	1.8663275827e-01
-9.7000000000e-01	1.8740925645e-01
-9.6000000000e-01	1.8816388728e-01
-9.5000000000e-01	1.8890019073e-01
-9.4000000000e-01	1.8962170679e-01
-9.3000000000e-01	1.9033197541e-01
-9.2000000000e-01	1.9103453658e-01
-9.1000000000e-01	1.9173293026e-01
-9.0000000000e-01	1.9243069642e-01
-8.9000000000e-01	1.9313137504e-01
-8.8000000000e-01	1.9383850609e-01
-8.7000000000e-01	1.9455562954e-01
-8.6000000000e-01	1.9528628536e-01
-8.5000000000e-01	1.9603401353e-01
-8.4000000000e-01	1.9680235401e-01
-8.3000000000e-01	1.9759484677e-01
-8.2000000000e-01	1.9841503180e-01
-8.1000000000e-01	1.9926644906e-01
-8.0000000000e-01	2.0015263851e-01
-7.9000000000e-01	2.0107714015e-01
-7.8000000000e-01	2.0204349392e-01
-7.7000000000e-01	2.0305523982e-01
-7.6000000000e-01	2.0411591781e-01
-7.5000000000e-01	2.0522906785e-01
-7.4000000000e-01	2.0639822993e-01
-7.3000000000e-01	2.0762694401e-01
-7.2000000000e-01	2.0891875007e-01
-7.1000000000e-01	2.1025943603e-01
-7.0000000000e-01	2.1111099758e-01
-6.9000000000e-01	2.1135773703e-01
-6.8000000000e-01	2.1118766651e-01
-6.7000000000e-01	2.1078879812e-01
-6.6000000000e-01	2.1034914399e-01
-6.5000000000e-01	2.1005671624e-01
-6.4000000000e-01	2.1009952697e-01
-6.3000000000e-01	2.1066558831e-01
-6.2000000000e-01	2.1194291237e-01
-6.1000000000e-01	2.1411951127e-01
-6.0000000000e-01	2.1738339713e-01
-5.9000000000e-01	2.2192258206e-01
-5.8000000000e-01	2.4087983746e-01
-5.7000000000e-01	2.8638282016e-01
-5.6000000000e-01	3.3224214804e-01
-5.5000000000e-01	3.5309169703e-01
-5.4000000000e-01	3.5866058081e-01
-5.3000000000e-01	3.5860688828e-01
-5.2000000000e-01	3.5510205427e-01
-5.1000000000e-01	3.5031751360e-01
-5.0000000000e-01	3.4642470111e-01
-4.9000000000e-01	3.4559505164e-01
-4.8000000000e-01	3.5000000000e-01

-4.7000000000e-01	3.5845940816e-01
-4.6000000000e-01	3.6809916144e-01
-4.5000000000e-01	3.7854972970e-01
-4.4000000000e-01	3.8944158282e-01
-4.3000000000e-01	4.0040519067e-01
-4.2000000000e-01	4.1107102312e-01
-4.1000000000e-01	4.2106955005e-01
-4.0000000000e-01	4.3003124133e-01
-3.9000000000e-01	4.3758656684e-01
-3.8000000000e-01	4.4336599643e-01
-3.7000000000e-01	4.4700000000e-01
-3.6000000000e-01	4.4926306808e-01
-3.5000000000e-01	4.5117852868e-01
-3.4000000000e-01	4.5275010790e-01
-3.3000000000e-01	4.5398153183e-01
-3.2000000000e-01	4.5487652655e-01
-3.1000000000e-01	4.5543881816e-01
-3.0000000000e-01	4.5567213273e-01
-2.9000000000e-01	4.5558019637e-01
-2.8000000000e-01	4.5516673515e-01
-2.7000000000e-01	4.5443547516e-01
-2.6000000000e-01	4.5339014250e-01
-2.5000000000e-01	4.5203446326e-01
-2.4000000000e-01	4.5037216351e-01
-2.3000000000e-01	4.4840696935e-01
-2.2000000000e-01	4.4614260687e-01
-2.1000000000e-01	4.4358280215e-01
-2.0000000000e-01	4.4073128129e-01
-1.9000000000e-01	4.3759177037e-01
-1.8000000000e-01	4.3416799548e-01
-1.7000000000e-01	4.3046368271e-01
-1.6000000000e-01	4.2648255814e-01
-1.5000000000e-01	4.2222834787e-01
-1.4000000000e-01	4.1739663068e-01
-1.3000000000e-01	4.1032054129e-01
-1.2000000000e-01	4.0115129469e-01
-1.1000000000e-01	3.9036806345e-01
-1.0000000000e-01	3.7845002014e-01
-9.0000000000e-02	3.6587633734e-01
-8.0000000000e-02	3.5312618761e-01
-7.0000000000e-02	3.4067874353e-01
-6.0000000000e-02	3.2901317766e-01
-5.0000000000e-02	3.1860866257e-01
-4.0000000000e-02	3.0994437084e-01
-3.0000000000e-02	3.0349947503e-01
-2.0000000000e-02	2.9975314772e-01
-1.0000000000e-02	2.9893722841e-01
0.0000000000e+00	2.9911987493e-01
1.0000000000e-02	2.9986929258e-01
2.0000000000e-02	3.0128756045e-01
3.0000000000e-02	3.0347675763e-01
4.0000000000e-02	3.0653896318e-01

```
    5.0000000000e-02    3.1057625621e-01
    6.0000000000e-02    3.1569071580e-01
    7.0000000000e-02    3.2198442102e-01
    8.0000000000e-02    3.2955945098e-01
    9.0000000000e-02    3.3851788474e-01
    1.0000000000e-01    3.4896180141e-01
    1.1000000000e-01    3.6099328005e-01
    1.2000000000e-01    3.7471439976e-01
    1.3000000000e-01    3.9022723963e-01
    1.4000000000e-01    4.0763387873e-01
    1.5000000000e-01    4.2705156541e-01
    1.6000000000e-01    4.4873766908e-01
    1.7000000000e-01    4.7260283461e-01
    4.00000000000000    4.7260283461e-01
    5.00000000000000    1.00000000000000
*DEFINE_CURVE
$     LCID      SIDR       SFA       SFO      OFFA      OFFO    DATYP
      3013
$                A1                  O1
   -1.0000000000e+00    1.8475832336e-01
   -9.9000000000e-01    1.8568078293e-01
   -9.8000000000e-01    1.8655107927e-01
   -9.7000000000e-01    1.8738323647e-01
   -9.6000000000e-01    1.8818612641e-01
   -9.5000000000e-01    1.8896630578e-01
   -9.4000000000e-01    1.8972916837e-01
   -9.3000000000e-01    1.9047947575e-01
   -9.2000000000e-01    1.9122162657e-01
   -9.1000000000e-01    1.9195980468e-01
   -9.0000000000e-01    1.9269806703e-01
   -8.9000000000e-01    1.9344040032e-01
   -8.8000000000e-01    1.9419076147e-01
   -8.7000000000e-01    1.9495311056e-01
   -8.6000000000e-01    1.9573144202e-01
   -8.5000000000e-01    1.9652981940e-01
   -8.4000000000e-01    1.9735241910e-01
   -8.3000000000e-01    1.9820359126e-01
   -8.2000000000e-01    1.9908795061e-01
   -8.1000000000e-01    2.0001051988e-01
   -8.0000000000e-01    2.0097696873e-01
   -7.9000000000e-01    2.0199403451e-01
   -7.8000000000e-01    2.0307031275e-01
   -7.7000000000e-01    2.0421786387e-01
   -7.6000000000e-01    2.0545582717e-01
   -7.5000000000e-01    2.0682768911e-01
   -7.4000000000e-01    2.0845404259e-01
   -7.3000000000e-01    2.1021781046e-01
   -7.2000000000e-01    2.1193382261e-01
   -7.1000000000e-01    2.1340227862e-01
   -7.0000000000e-01    2.1424361777e-01
   -6.9000000000e-01    2.1446431038e-01
   -6.8000000000e-01    2.1425117389e-01
```

```
-6.7000000000e-01    2.1379491086e-01
-6.6000000000e-01    2.1328915353e-01
-6.5000000000e-01    2.1293178024e-01
-6.4000000000e-01    2.1292858570e-01
-6.3000000000e-01    2.1350250213e-01
-6.2000000000e-01    2.1492025585e-01
-6.1000000000e-01    2.1759181188e-01
-6.0000000000e-01    2.2148767894e-01
-5.9000000000e-01    2.2506930040e-01
-5.8000000000e-01    2.4577443027e-01
-5.7000000000e-01    2.9426288011e-01
-5.6000000000e-01    3.4001346153e-01
-5.5000000000e-01    3.5464903612e-01
-5.4000000000e-01    3.5901615466e-01
-5.3000000000e-01    3.5766609253e-01
-5.2000000000e-01    3.5302421657e-01
-5.1000000000e-01    3.4745199616e-01
-5.0000000000e-01    3.4356349135e-01
-4.9000000000e-01    3.4564654261e-01
-4.8000000000e-01    3.5356801088e-01
-4.7000000000e-01    3.6232571130e-01
-4.6000000000e-01    3.7222750106e-01
-4.5000000000e-01    3.8292770724e-01
-4.4000000000e-01    3.9405707621e-01
-4.3000000000e-01    4.0523619039e-01
-4.2000000000e-01    4.1607351213e-01
-4.1000000000e-01    4.2615330584e-01
-4.0000000000e-01    4.3499683489e-01
-3.9000000000e-01    4.4190584844e-01
-3.8000000000e-01    4.4685214892e-01
-3.7000000000e-01    4.5179547484e-01
-3.6000000000e-01    4.5385041193e-01
-3.5000000000e-01    4.5564901808e-01
-3.4000000000e-01    4.5714703926e-01
-3.3000000000e-01    4.5832680839e-01
-3.2000000000e-01    4.5918101825e-01
-3.1000000000e-01    4.5970707116e-01
-3.0000000000e-01    4.5990474514e-01
-2.9000000000e-01    4.5977510067e-01
-2.8000000000e-01    4.5931991180e-01
-2.7000000000e-01    4.5854133657e-01
-2.6000000000e-01    4.5744169794e-01
-2.5000000000e-01    4.5602330644e-01
-2.4000000000e-01    4.5428827546e-01
-2.3000000000e-01    4.5223827581e-01
-2.2000000000e-01    4.4987414206e-01
-2.1000000000e-01    4.4719515127e-01
-2.0000000000e-01    4.4419754210e-01
-1.9000000000e-01    4.4087108201e-01
-1.8000000000e-01    4.3718976927e-01
-1.7000000000e-01    4.3307808841e-01
-1.6000000000e-01    4.2856098851e-01
```

```
   -1.5000000000e-01    4.2383588202e-01
   -1.4000000000e-01    4.1869336194e-01
   -1.3000000000e-01    4.1113184425e-01
   -1.2000000000e-01    4.0137918832e-01
   -1.1000000000e-01    3.8997154050e-01
   -1.0000000000e-01    3.7741746600e-01
   -9.0000000000e-02    3.6422135766e-01
   -8.0000000000e-02    3.5089379712e-01
   -7.0000000000e-02    3.3796280527e-01
   -6.0000000000e-02    3.2599573221e-01
   -5.0000000000e-02    3.1565565079e-01
   -4.0000000000e-02    3.0788670008e-01
   -3.0000000000e-02    3.0425472428e-01
   -2.0000000000e-02    3.0019029063e-01
   -1.0000000000e-02    2.9903359348e-01
    0.0000000000e+00    2.9929055022e-01
    1.0000000000e-02    2.9999663725e-01
    2.0000000000e-02    3.0131549873e-01
    3.0000000000e-02    3.0337536116e-01
    4.0000000000e-02    3.0629262697e-01
    5.0000000000e-02    3.1017948784e-01
    6.0000000000e-02    3.1514732518e-01
    7.0000000000e-02    3.2130906927e-01
    8.0000000000e-02    3.2878196908e-01
    9.0000000000e-02    3.3769238080e-01
    1.0000000000e-01    3.4818613778e-01
    1.1000000000e-01    3.6045538295e-01
    1.2000000000e-01    3.7482476068e-01
    1.3000000000e-01    3.9118679044e-01
    1.4000000000e-01    4.0784056687e-01
    1.5000000000e-01    4.2718663843e-01
    1.6000000000e-01    4.4932496184e-01
    1.7000000000e-01    4.7364225762e-01
    1.8000000000e-01    4.9993913668e-01
    1.9000000000e-01    4.9993913668e-01
    4.00000000000000    4.9993913668e-01
    5.00000000000000    1.00000000000000
*DEFINE_CURVE
$     LCID      SIDR       SFA       SFO      OFFA      OFFO    DATYP
      3014
$                A1                  O1
   -1.0000000000e+00    1.8403915630e-01
   -9.9000000000e-01    1.8505978115e-01
   -9.8000000000e-01    1.8600705808e-01
   -9.7000000000e-01    1.8689901024e-01
   -9.6000000000e-01    1.8774907722e-01
   -9.5000000000e-01    1.8856788466e-01
   -9.4000000000e-01    1.8936427371e-01
   -9.3000000000e-01    1.9014593383e-01
   -9.2000000000e-01    1.9091981339e-01
   -9.1000000000e-01    1.9169240273e-01
   -9.0000000000e-01    1.9246994417e-01
```

-8.9000000000e-01	1.9325860335e-01
-8.8000000000e-01	1.9406462583e-01
-8.7000000000e-01	1.9489449912e-01
-8.6000000000e-01	1.9575514100e-01
-8.5000000000e-01	1.9665414011e-01
-8.4000000000e-01	1.9760008668e-01
-8.3000000000e-01	1.9860305369e-01
-8.2000000000e-01	1.9967533112e-01
-8.1000000000e-01	2.0083259815e-01
-8.0000000000e-01	2.0209588481e-01
-7.9000000000e-01	2.0350826472e-01
-7.8000000000e-01	2.0519220619e-01
-7.7000000000e-01	2.0709693491e-01
-7.6000000000e-01	2.0913729166e-01
-7.5000000000e-01	2.1123136072e-01
-7.4000000000e-01	2.1329808285e-01
-7.3000000000e-01	2.1525494400e-01
-7.2000000000e-01	2.1701557745e-01
-7.1000000000e-01	2.1847533459e-01
-7.0000000000e-01	2.1922713219e-01
-6.9000000000e-01	2.1927750540e-01
-6.8000000000e-01	2.1885079007e-01
-6.7000000000e-01	2.1817722995e-01
-6.6000000000e-01	2.1750478553e-01
-6.5000000000e-01	2.1711685104e-01
-6.4000000000e-01	2.1736812738e-01
-6.3000000000e-01	2.1877060053e-01
-6.2000000000e-01	2.2184952764e-01
-6.1000000000e-01	2.2344672316e-01
-6.0000000000e-01	2.2473654371e-01
-5.9000000000e-01	2.2814208025e-01
-5.8000000000e-01	2.5162406838e-01
-5.7000000000e-01	3.0343695711e-01
-5.6000000000e-01	3.3454538793e-01
-5.5000000000e-01	3.4962046313e-01
-5.4000000000e-01	3.5223860799e-01
-5.3000000000e-01	3.4889583007e-01
-5.2000000000e-01	3.4309247998e-01
-5.1000000000e-01	3.3846439697e-01
-5.0000000000e-01	3.4072934447e-01
-4.9000000000e-01	3.4881594824e-01
-4.8000000000e-01	3.5711802643e-01
-4.7000000000e-01	3.6634298325e-01
-4.6000000000e-01	3.7682614328e-01
-4.5000000000e-01	3.8810939341e-01
-4.4000000000e-01	3.9973539786e-01
-4.3000000000e-01	4.1121136633e-01
-4.2000000000e-01	4.2195842931e-01
-4.1000000000e-01	4.3119630848e-01
-4.0000000000e-01	4.3769879211e-01
-3.9000000000e-01	4.4544815557e-01
-3.8000000000e-01	4.5412276808e-01

-3.7000000000e-01	4.5927656703e-01
-3.6000000000e-01	4.6108148932e-01
-3.5000000000e-01	4.6269899293e-01
-3.4000000000e-01	4.6406880244e-01
-3.3000000000e-01	4.6515487689e-01
-3.2000000000e-01	4.6593468297e-01
-3.1000000000e-01	4.6639362508e-01
-3.0000000000e-01	4.6652192487e-01
-2.9000000000e-01	4.6631273967e-01
-2.8000000000e-01	4.6576092709e-01
-2.7000000000e-01	4.6486213428e-01
-2.6000000000e-01	4.6361200828e-01
-2.5000000000e-01	4.6200535972e-01
-2.4000000000e-01	4.6003508418e-01
-2.3000000000e-01	4.5769053200e-01
-2.2000000000e-01	4.5495473395e-01
-2.1000000000e-01	4.5179919307e-01
-2.0000000000e-01	4.4816390751e-01
-1.9000000000e-01	4.4407556707e-01
-1.8000000000e-01	4.3963584929e-01
-1.7000000000e-01	4.3493660398e-01
-1.6000000000e-01	4.3006395362e-01
-1.5000000000e-01	4.2510231749e-01
-1.4000000000e-01	4.1966391999e-01
-1.3000000000e-01	4.1136737512e-01
-1.2000000000e-01	4.0060334599e-01
-1.1000000000e-01	3.8809379992e-01
-1.0000000000e-01	3.7450574663e-01
-9.0000000000e-02	3.6051802865e-01
-8.0000000000e-02	3.4687928148e-01
-7.0000000000e-02	3.3449713301e-01
-6.0000000000e-02	3.2462768942e-01
-5.0000000000e-02	3.1925294135e-01
-4.0000000000e-02	3.1330611434e-01
-3.0000000000e-02	3.0564309834e-01
-2.0000000000e-02	2.9999439043e-01
-1.0000000000e-02	2.9914352786e-01
0.0000000000e+00	2.9952652571e-01
1.0000000000e-02	3.0018930552e-01
2.0000000000e-02	3.0135864024e-01
3.0000000000e-02	3.0321631552e-01
4.0000000000e-02	3.0592610495e-01
5.0000000000e-02	3.0964850001e-01
6.0000000000e-02	3.1455218927e-01
7.0000000000e-02	3.2082750206e-01
8.0000000000e-02	3.2870788584e-01
9.0000000000e-02	3.3851148311e-01
1.0000000000e-01	3.5073407585e-01
1.1000000000e-01	3.6421096163e-01
1.2000000000e-01	3.7722255584e-01
1.3000000000e-01	3.9122090072e-01
1.4000000000e-01	4.0752916307e-01

```
    1.5000000000e-01    4.2733608423e-01
    1.6000000000e-01    4.5013551208e-01
    1.7000000000e-01    4.7526868479e-01
    1.8000000000e-01    5.0245135243e-01
    1.9000000000e-01    5.0245135243e-01
    4.00000000000000    5.0245135243e-01
    5.00000000000000    1.00000000000000
*DEFINE_CURVE
$     LCID      SIDR       SFA       SFO      OFFA      OFFO    DATYP
      3015
$                A1                  O1
   -1.0000000000e+00    1.8317509237e-01
   -9.9000000000e-01    1.8429513376e-01
   -9.8000000000e-01    1.8532414346e-01
   -9.7000000000e-01    1.8628419482e-01
   -9.6000000000e-01    1.8719332033e-01
   -9.5000000000e-01    1.8806678105e-01
   -9.4000000000e-01    1.8891794476e-01
   -9.3000000000e-01    1.8975892245e-01
   -9.2000000000e-01    1.9060105651e-01
   -9.1000000000e-01    1.9145532291e-01
   -9.0000000000e-01    1.9233269269e-01
   -8.9000000000e-01    1.9324449045e-01
   -8.8000000000e-01    1.9420278664e-01
   -8.7000000000e-01    1.9522086645e-01
   -8.6000000000e-01    1.9631383205e-01
   -8.5000000000e-01    1.9749942138e-01
   -8.4000000000e-01    1.9879917415e-01
   -8.3000000000e-01    2.0025969030e-01
   -8.2000000000e-01    2.0199515341e-01
   -8.1000000000e-01    2.0396159849e-01
   -8.0000000000e-01    2.0609821155e-01
   -7.9000000000e-01    2.0835083665e-01
   -7.8000000000e-01    2.1066989222e-01
   -7.7000000000e-01    2.1300868426e-01
   -7.6000000000e-01    2.1532195435e-01
   -7.5000000000e-01    2.1756453502e-01
   -7.4000000000e-01    2.1968999942e-01
   -7.3000000000e-01    2.2164919049e-01
   -7.2000000000e-01    2.2338849576e-01
   -7.1000000000e-01    2.2483125987e-01
   -7.0000000000e-01    2.2546187953e-01
   -6.9000000000e-01    2.2529299091e-01
   -6.8000000000e-01    2.2464590282e-01
   -6.7000000000e-01    2.2387695886e-01
   -6.6000000000e-01    2.2341814340e-01
   -6.5000000000e-01    2.2384711496e-01
   -6.4000000000e-01    2.2600198987e-01
   -6.3000000000e-01    2.2719950315e-01
   -6.2000000000e-01    2.2668124108e-01
   -6.1000000000e-01    2.2623444884e-01
   -6.0000000000e-01    2.2727443941e-01
```

```
-5.9000000000e-01    2.3107146992e-01
-5.8000000000e-01    2.5726847325e-01
-5.7000000000e-01    3.0497717401e-01
-5.6000000000e-01    3.2567540395e-01
-5.5000000000e-01    3.4019452335e-01
-5.4000000000e-01    3.4123927034e-01
-5.3000000000e-01    3.3671880883e-01
-5.2000000000e-01    3.3233283919e-01
-5.1000000000e-01    3.3510538829e-01
-5.0000000000e-01    3.4346378820e-01
-4.9000000000e-01    3.5208981087e-01
-4.8000000000e-01    3.6079913626e-01
-4.7000000000e-01    3.7051433664e-01
-4.6000000000e-01    3.8162185891e-01
-4.5000000000e-01    3.9343990168e-01
-4.4000000000e-01    4.0525865674e-01
-4.3000000000e-01    4.1622644845e-01
-4.2000000000e-01    4.2516018548e-01
-4.1000000000e-01    4.3269587868e-01
-4.0000000000e-01    4.4326848078e-01
-3.9000000000e-01    4.5436270898e-01
-3.8000000000e-01    4.6351194432e-01
-3.7000000000e-01    4.6824356327e-01
-3.6000000000e-01    4.6979056840e-01
-3.5000000000e-01    4.7119877021e-01
-3.4000000000e-01    4.7239417690e-01
-3.3000000000e-01    4.7332463473e-01
-3.2000000000e-01    4.7395207932e-01
-3.1000000000e-01    4.7424767481e-01
-3.0000000000e-01    4.7418858403e-01
-2.9000000000e-01    4.7375566385e-01
-2.8000000000e-01    4.7293165134e-01
-2.7000000000e-01    4.7169953113e-01
-2.6000000000e-01    4.7004080594e-01
-2.5000000000e-01    4.6793333765e-01
-2.4000000000e-01    4.6534804325e-01
-2.3000000000e-01    4.6225022339e-01
-2.2000000000e-01    4.5869230105e-01
-2.1000000000e-01    4.5474625243e-01
-2.0000000000e-01    4.5047281381e-01
-1.9000000000e-01    4.4592537865e-01
-1.8000000000e-01    4.4115293275e-01
-1.7000000000e-01    4.3620248005e-01
-1.6000000000e-01    4.3112130068e-01
-1.5000000000e-01    4.2595935687e-01
-1.4000000000e-01    4.2022025192e-01
-1.3000000000e-01    4.1115513518e-01
-1.2000000000e-01    3.9938831104e-01
-1.1000000000e-01    3.8598390832e-01
-1.0000000000e-01    3.7199781396e-01
-9.0000000000e-02    3.5861525733e-01
-8.0000000000e-02    3.4733174922e-01
```

```
   -7.0000000000e-02    3.4028307296e-01
   -6.0000000000e-02    3.3374733012e-01
   -5.0000000000e-02    3.2399472526e-01
   -4.0000000000e-02    3.1369554276e-01
   -3.0000000000e-02    3.0496516999e-01
   -2.0000000000e-02    2.9969833915e-01
   -1.0000000000e-02    2.9925241698e-01
    0.0000000000e+00    2.9976467675e-01
    1.0000000000e-02    3.0040784611e-01
    2.0000000000e-02    3.0149247850e-01
    3.0000000000e-02    3.0329261174e-01
    4.0000000000e-02    3.0607673123e-01
    5.0000000000e-02    3.1013393293e-01
    6.0000000000e-02    3.1580452357e-01
    7.0000000000e-02    3.2352613908e-01
    8.0000000000e-02    3.3383640970e-01
    9.0000000000e-02    3.4424047179e-01
    1.0000000000e-01    3.5414160993e-01
    1.1000000000e-01    3.6457920961e-01
    1.2000000000e-01    3.7640224595e-01
    1.3000000000e-01    3.9035759839e-01
    1.4000000000e-01    4.0715650078e-01
    1.5000000000e-01    4.2748584526e-01
    1.6000000000e-01    4.5096192791e-01
    1.7000000000e-01    4.7694427500e-01
    1.8000000000e-01    5.0502581100e-01
    1.9000000000e-01    5.0502581100e-01
    4.00000000000000    5.0502581100e-01
    5.00000000000000    1.00000000000000
*DEFINE_CURVE
$     LCID      SIDR       SFA       SFO      OFFA      OFFO    DATYP
      3016
$                A1                  O1
   -1.0000000000e+00    1.8249872511e-01
   -9.9000000000e-01    1.8371938630e-01
   -9.8000000000e-01    1.8483592752e-01
   -9.7000000000e-01    1.8587715754e-01
   -9.6000000000e-01    1.8686816532e-01
   -9.5000000000e-01    1.8783143761e-01
   -9.4000000000e-01    1.8878773931e-01
   -9.3000000000e-01    1.8975684680e-01
   -9.2000000000e-01    1.9075820191e-01
   -9.1000000000e-01    1.9181154268e-01
   -9.0000000000e-01    1.9293756408e-01
   -8.9000000000e-01    1.9415866693e-01
   -8.8000000000e-01    1.9549986658e-01
   -8.7000000000e-01    1.9701740352e-01
   -8.6000000000e-01    1.9881559305e-01
   -8.5000000000e-01    2.0084307514e-01
   -8.4000000000e-01    2.0304501683e-01
   -8.3000000000e-01    2.0537604068e-01
   -8.2000000000e-01    2.0779743477e-01
```

-8.1000000000e-01	2.1027520197e-01
-8.0000000000e-01	2.1277864154e-01
-7.9000000000e-01	2.1527926828e-01
-7.8000000000e-01	2.1774993817e-01
-7.7000000000e-01	2.2016408528e-01
-7.6000000000e-01	2.2249499194e-01
-7.5000000000e-01	2.2471501755e-01
-7.4000000000e-01	2.2679470144e-01
-7.3000000000e-01	2.2870162816e-01
-7.2000000000e-01	2.3039889158e-01
-7.1000000000e-01	2.3182087486e-01
-7.0000000000e-01	2.3231989183e-01
-6.9000000000e-01	2.3198581683e-01
-6.8000000000e-01	2.3137480706e-01
-6.7000000000e-01	2.3117186250e-01
-6.6000000000e-01	2.3230387622e-01
-6.5000000000e-01	2.3348176826e-01
-6.4000000000e-01	2.3222536381e-01
-6.3000000000e-01	2.3014302863e-01
-6.2000000000e-01	2.2839397722e-01
-6.1000000000e-01	2.2788280100e-01
-6.0000000000e-01	2.2939932700e-01
-5.9000000000e-01	2.3371570949e-01
-5.8000000000e-01	2.6146476648e-01
-5.7000000000e-01	2.9148966097e-01
-5.6000000000e-01	3.1522353673e-01
-5.5000000000e-01	3.2853295171e-01
-5.4000000000e-01	3.2858431286e-01
-5.3000000000e-01	3.2533556920e-01
-5.2000000000e-01	3.2863199004e-01
-5.1000000000e-01	3.3732419237e-01
-5.0000000000e-01	3.4645804689e-01
-4.9000000000e-01	3.5565160754e-01
-4.8000000000e-01	3.6476042999e-01
-4.7000000000e-01	3.7495457796e-01
-4.6000000000e-01	3.8654764611e-01
-4.5000000000e-01	3.9841185818e-01
-4.4000000000e-01	4.0924923088e-01
-4.3000000000e-01	4.1766808055e-01
-4.2000000000e-01	4.2822162478e-01
-4.1000000000e-01	4.4083626814e-01
-4.0000000000e-01	4.5353644806e-01
-3.9000000000e-01	4.6483205652e-01
-3.8000000000e-01	4.7334616251e-01
-3.7000000000e-01	4.7749675028e-01
-3.6000000000e-01	4.7877962895e-01
-3.5000000000e-01	4.7995234180e-01
-3.4000000000e-01	4.8092007827e-01
-3.3000000000e-01	4.8160940736e-01
-3.2000000000e-01	4.8196171248e-01
-3.1000000000e-01	4.8192852832e-01
-3.0000000000e-01	4.8146802463e-01

```
   -2.9000000000e-01    4.8054212882e-01
   -2.8000000000e-01    4.7911389651e-01
   -2.7000000000e-01    4.7714577032e-01
   -2.6000000000e-01    4.7464838926e-01
   -2.5000000000e-01    4.7169366879e-01
   -2.4000000000e-01    4.6834055381e-01
   -2.3000000000e-01    4.6463558538e-01
   -2.2000000000e-01    4.6061730357e-01
   -2.1000000000e-01    4.5631909242e-01
   -2.0000000000e-01    4.5177114879e-01
   -1.9000000000e-01    4.4700197556e-01
   -1.8000000000e-01    4.4203966505e-01
   -1.7000000000e-01    4.3691318881e-01
   -1.6000000000e-01    4.3165392484e-01
   -1.5000000000e-01    4.2629774343e-01
   -1.4000000000e-01    4.2025622996e-01
   -1.3000000000e-01    4.1050075077e-01
   -1.2000000000e-01    3.9814679653e-01
   -1.1000000000e-01    3.8495821903e-01
   -1.0000000000e-01    3.7288266645e-01
   -9.0000000000e-02    3.6435320881e-01
   -8.0000000000e-02    3.5748025745e-01
   -7.0000000000e-02    3.4684014248e-01
   -6.0000000000e-02    3.3466736482e-01
   -5.0000000000e-02    3.2260917588e-01
   -4.0000000000e-02    3.1195397294e-01
   -3.0000000000e-02    3.0383597420e-01
   -2.0000000000e-02    2.9938464484e-01
   -1.0000000000e-02    2.9936005080e-01
    0.0000000000e+00    3.0001351637e-01
    1.0000000000e-02    3.0072862159e-01
    2.0000000000e-02    3.0197949488e-01
    3.0000000000e-02    3.0423408539e-01
    4.0000000000e-02    3.0800135557e-01
    5.0000000000e-02    3.1388636414e-01
    6.0000000000e-02    3.2207656778e-01
    7.0000000000e-02    3.2951906795e-01
    8.0000000000e-02    3.3655348181e-01
    9.0000000000e-02    3.4400830114e-01
    1.0000000000e-01    3.5251513304e-01
    1.1000000000e-01    3.6259423727e-01
    1.2000000000e-01    3.7470530469e-01
    1.3000000000e-01    3.8928304373e-01
    1.4000000000e-01    4.0676959191e-01
    1.5000000000e-01    4.2763533513e-01
    1.6000000000e-01    4.5176572591e-01
    1.7000000000e-01    4.7848674720e-01
    1.8000000000e-01    5.0718022374e-01
    1.9000000000e-01    5.0718022374e-01
    4.00000000000000    5.0718022374e-01
    5.00000000000000    1.00000000000000
*DEFINE_CURVE
```

```
$     LCID      SIDR       SFA        SFO       OFFA       OFFO     DATYP
      3017
$                  A1                  O1
   -1.0000000000e+00    1.8234264806e-01
   -9.9000000000e-01    1.8366584183e-01
   -9.8000000000e-01    1.8488091962e-01
   -9.7000000000e-01    1.8603094511e-01
   -9.6000000000e-01    1.8715541715e-01
   -9.5000000000e-01    1.8829155306e-01
   -9.4000000000e-01    1.8947542892e-01
   -9.3000000000e-01    1.9074305916e-01
   -9.2000000000e-01    1.9213149145e-01
   -9.1000000000e-01    1.9371704143e-01
   -9.0000000000e-01    1.9559040794e-01
   -8.9000000000e-01    1.9768543561e-01
   -8.8000000000e-01    1.9994709629e-01
   -8.7000000000e-01    2.0233368064e-01
   -8.6000000000e-01    2.0481200985e-01
   -8.5000000000e-01    2.0735455482e-01
   -8.4000000000e-01    2.0993762559e-01
   -8.3000000000e-01    2.1254018720e-01
   -8.2000000000e-01    2.1514305398e-01
   -8.1000000000e-01    2.1772831688e-01
   -8.0000000000e-01    2.2027891387e-01
   -7.9000000000e-01    2.2277828405e-01
   -7.8000000000e-01    2.2521006134e-01
   -7.7000000000e-01    2.2755776996e-01
   -7.6000000000e-01    2.2980448096e-01
   -7.5000000000e-01    2.3193237721e-01
   -7.4000000000e-01    2.3392214583e-01
   -7.3000000000e-01    2.3575206118e-01
   -7.2000000000e-01    2.3739650651e-01
   -7.1000000000e-01    2.3879508702e-01
   -7.0000000000e-01    2.3919845631e-01
   -6.9000000000e-01    2.3901287969e-01
   -6.8000000000e-01    2.3940894594e-01
   -6.7000000000e-01    2.4050199843e-01
   -6.6000000000e-01    2.3898641328e-01
   -6.5000000000e-01    2.3613492455e-01
   -6.4000000000e-01    2.3300976242e-01
   -6.3000000000e-01    2.3036057017e-01
   -6.2000000000e-01    2.2879668555e-01
   -6.1000000000e-01    2.2886032439e-01
   -6.0000000000e-01    2.3106559523e-01
   -5.9000000000e-01    2.3593151093e-01
   -5.8000000000e-01    2.6126146562e-01
   -5.7000000000e-01    2.8127447508e-01
   -5.6000000000e-01    3.0458699405e-01
   -5.5000000000e-01    3.1680218491e-01
   -5.4000000000e-01    3.1724616029e-01
   -5.3000000000e-01    3.2116659907e-01
   -5.2000000000e-01    3.3023183173e-01
```

-5.1000000000e-01	3.3995675837e-01
-5.0000000000e-01	3.4987106501e-01
-4.9000000000e-01	3.5964444831e-01
-4.8000000000e-01	3.6915099723e-01
-4.7000000000e-01	3.7976245374e-01
-4.6000000000e-01	3.9134279527e-01
-4.5000000000e-01	4.0172448482e-01
-4.4000000000e-01	4.1169871065e-01
-4.3000000000e-01	4.2462929557e-01
-4.2000000000e-01	4.3851939789e-01
-4.1000000000e-01	4.5211949215e-01
-4.0000000000e-01	4.6450492389e-01
-3.9000000000e-01	4.7485748655e-01
-3.8000000000e-01	4.8232899753e-01
-3.7000000000e-01	4.8583641478e-01
-3.6000000000e-01	4.8684721426e-01
-3.5000000000e-01	4.8774467254e-01
-3.4000000000e-01	4.8839307197e-01
-3.3000000000e-01	4.8868075859e-01
-3.2000000000e-01	4.8851337360e-01
-3.1000000000e-01	4.8780856982e-01
-3.0000000000e-01	4.8650499317e-01
-2.9000000000e-01	4.8467279392e-01
-2.8000000000e-01	4.8239330318e-01
-2.7000000000e-01	4.7971726114e-01
-2.6000000000e-01	4.7668160924e-01
-2.5000000000e-01	4.7331531051e-01
-2.4000000000e-01	4.6964250803e-01
-2.3000000000e-01	4.6568436316e-01
-2.2000000000e-01	4.6146020528e-01
-2.1000000000e-01	4.5698831771e-01
-2.0000000000e-01	4.5228654682e-01
-1.9000000000e-01	4.4737286337e-01
-1.8000000000e-01	4.4226599669e-01
-1.7000000000e-01	4.3698630128e-01
-1.6000000000e-01	4.3155713038e-01
-1.5000000000e-01	4.2600727596e-01
-1.4000000000e-01	4.1967051850e-01
-1.3000000000e-01	4.0954799412e-01
-1.2000000000e-01	3.9799297291e-01
-1.1000000000e-01	3.8844035260e-01
-1.0000000000e-01	3.8125915849e-01
-9.0000000000e-02	3.7029572335e-01
-8.0000000000e-02	3.5738839590e-01
-7.0000000000e-02	3.4394886173e-01
-6.0000000000e-02	3.3097479479e-01
-5.0000000000e-02	3.1927613120e-01
-4.0000000000e-02	3.0957916482e-01
-3.0000000000e-02	3.0259128948e-01
-2.0000000000e-02	2.9907040368e-01
-1.0000000000e-02	2.9946750303e-01
0.0000000000e+00	3.0032353139e-01

```
    1.0000000000e-02    3.0142188534e-01
    2.0000000000e-02    3.0362921677e-01
    3.0000000000e-02    3.0789093484e-01
    4.0000000000e-02    3.1367608252e-01
    5.0000000000e-02    3.1834626931e-01
    6.0000000000e-02    3.2277868931e-01
    7.0000000000e-02    3.2764149663e-01
    8.0000000000e-02    3.3341722948e-01
    9.0000000000e-02    3.4049300415e-01
    1.0000000000e-01    3.4920379801e-01
    1.1000000000e-01    3.5985573470e-01
    1.2000000000e-01    3.7274065171e-01
    1.3000000000e-01    3.8814794085e-01
    1.4000000000e-01    4.0637899170e-01
    1.5000000000e-01    4.2778387205e-01
    1.6000000000e-01    4.5249171625e-01
    1.7000000000e-01    4.7959021420e-01
    1.8000000000e-01    5.0800309430e-01
    1.9000000000e-01    5.0800309430e-01
    4.00000000000000    5.0800309430e-01
    5.00000000000000    1.00000000000000
*DEFINE_CURVE
$     LCID      SIDR       SFA       SFO      OFFA      OFFO    DATYP
      3018
$                A1                  O1
   -1.0000000000e+00    1.8303945476e-01
   -9.9000000000e-01    1.8447089340e-01
   -9.8000000000e-01    1.8582193660e-01
   -9.7000000000e-01    1.8717970899e-01
   -9.6000000000e-01    1.8862774606e-01
   -9.5000000000e-01    1.9029181697e-01
   -9.4000000000e-01    1.9223463084e-01
   -9.3000000000e-01    1.9437092483e-01
   -9.2000000000e-01    1.9664958412e-01
   -9.1000000000e-01    1.9903721045e-01
   -9.0000000000e-01    2.0150926200e-01
   -8.9000000000e-01    2.0404602578e-01
   -8.8000000000e-01    2.0663060316e-01
   -8.7000000000e-01    2.0924782457e-01
   -8.6000000000e-01    2.1188362849e-01
   -8.5000000000e-01    2.1452468768e-01
   -8.4000000000e-01    2.1715817420e-01
   -8.3000000000e-01    2.1977160539e-01
   -8.2000000000e-01    2.2235273847e-01
   -8.1000000000e-01    2.2488949461e-01
   -8.0000000000e-01    2.2736990012e-01
   -7.9000000000e-01    2.2978203602e-01
   -7.8000000000e-01    2.3211398818e-01
   -7.7000000000e-01    2.3435378892e-01
   -7.6000000000e-01    2.3648933683e-01
   -7.5000000000e-01    2.3850827001e-01
   -7.4000000000e-01    2.4039774266e-01
```

-7.3000000000e-01	2.4214398853e-01
-7.2000000000e-01	2.4373137171e-01
-7.1000000000e-01	2.4510554914e-01
-7.0000000000e-01	2.4566745777e-01
-6.9000000000e-01	2.4659564032e-01
-6.8000000000e-01	2.4527650266e-01
-6.7000000000e-01	2.4238596780e-01
-6.6000000000e-01	2.3883367400e-01
-6.5000000000e-01	2.3520912336e-01
-6.4000000000e-01	2.3200379168e-01
-6.3000000000e-01	2.2967053772e-01
-6.2000000000e-01	2.2864388047e-01
-6.1000000000e-01	2.2934739166e-01
-6.0000000000e-01	2.3219423447e-01
-5.9000000000e-01	2.3757556066e-01
-5.8000000000e-01	2.5268841935e-01
-5.7000000000e-01	2.7427620734e-01
-5.6000000000e-01	2.9571990633e-01
-5.5000000000e-01	3.0720501723e-01
-5.4000000000e-01	3.1256562292e-01
-5.3000000000e-01	3.2198893672e-01
-5.2000000000e-01	3.3228332980e-01
-5.1000000000e-01	3.4299380364e-01
-5.0000000000e-01	3.5373916167e-01
-4.9000000000e-01	3.6417783591e-01
-4.8000000000e-01	3.7411992759e-01
-4.7000000000e-01	3.8486625896e-01
-4.6000000000e-01	3.9511806650e-01
-4.5000000000e-01	4.0770569039e-01
-4.4000000000e-01	4.2169474249e-01
-4.3000000000e-01	4.3597026621e-01
-4.2000000000e-01	4.4981685976e-01
-4.1000000000e-01	4.6263113357e-01
-4.0000000000e-01	4.7384738129e-01
-3.9000000000e-01	4.8290642210e-01
-3.8000000000e-01	4.8922200104e-01
-3.7000000000e-01	4.9206284347e-01
-3.6000000000e-01	4.9278232181e-01
-3.5000000000e-01	4.9328849788e-01
-3.4000000000e-01	4.9332704091e-01
-3.3000000000e-01	4.9274014093e-01
-3.2000000000e-01	4.9165044060e-01
-3.1000000000e-01	4.9013614172e-01
-3.0000000000e-01	4.8823548767e-01
-2.9000000000e-01	4.8597366853e-01
-2.8000000000e-01	4.8337008156e-01
-2.7000000000e-01	4.8044123830e-01
-2.6000000000e-01	4.7720208996e-01
-2.5000000000e-01	4.7366669549e-01
-2.4000000000e-01	4.6984858924e-01
-2.3000000000e-01	4.6576100240e-01
-2.2000000000e-01	4.6141701372e-01

```
   -2.1000000000e-01    4.5682967214e-01
   -2.0000000000e-01    4.5201212429e-01
   -1.9000000000e-01    4.4697778583e-01
   -1.8000000000e-01    4.4174062457e-01
   -1.7000000000e-01    4.3631570684e-01
   -1.6000000000e-01    4.3072040294e-01
   -1.5000000000e-01    4.2497747693e-01
   -1.4000000000e-01    4.1839552208e-01
   -1.3000000000e-01    4.0938040218e-01
   -1.2000000000e-01    4.0195930476e-01
   -1.1000000000e-01    3.9129606621e-01
   -1.0000000000e-01    3.7866618679e-01
   -9.0000000000e-02    3.6516550360e-01
   -8.0000000000e-02    3.5152557664e-01
   -7.0000000000e-02    3.3835701480e-01
   -6.0000000000e-02    3.2622142772e-01
   -5.0000000000e-02    3.1565871650e-01
   -4.0000000000e-02    3.0720057351e-01
   -3.0000000000e-02    3.0138186141e-01
   -2.0000000000e-02    2.9876364237e-01
   -1.0000000000e-02    2.9958065373e-01
    0.0000000000e+00    3.0095337829e-01
    1.0000000000e-02    3.0382683141e-01
    2.0000000000e-02    3.0697606481e-01
    3.0000000000e-02    3.0931580117e-01
    4.0000000000e-02    3.1166650028e-01
    5.0000000000e-02    3.1447756234e-01
    6.0000000000e-02    3.1807803177e-01
    7.0000000000e-02    3.2274822052e-01
    8.0000000000e-02    3.2874560425e-01
    9.0000000000e-02    3.3631576133e-01
    1.0000000000e-01    3.4569752358e-01
    1.1000000000e-01    3.5712557323e-01
    1.2000000000e-01    3.7083174172e-01
    1.3000000000e-01    3.8704542395e-01
    1.4000000000e-01    4.0599277556e-01
    1.5000000000e-01    4.2792850711e-01
    1.6000000000e-01    4.5289715035e-01
    1.7000000000e-01    4.7888721790e-01
    1.8000000000e-01    5.0440494912e-01
    1.9000000000e-01    5.0440494912e-01
    4.00000000000000    5.0440494912e-01
    5.00000000000000    1.00000000000000
*DEFINE_CURVE
$     LCID      SIDR       SFA       SFO      OFFA      OFFO    DATYP
      3019
$                A1                  O1
   -1.0000000000e+00    1.8492173876e-01
   -9.9000000000e-01    1.8660541071e-01
   -9.8000000000e-01    1.8843396683e-01
   -9.7000000000e-01    1.9039259434e-01
   -9.6000000000e-01    1.9246998953e-01
```

```
-9.5000000000e-01    1.9465490574e-01
-9.4000000000e-01    1.9693610581e-01
-9.3000000000e-01    1.9930235530e-01
-9.2000000000e-01    2.0174242078e-01
-9.1000000000e-01    2.0424506929e-01
-9.0000000000e-01    2.0679906808e-01
-8.9000000000e-01    2.0939318454e-01
-8.8000000000e-01    2.1201618611e-01
-8.7000000000e-01    2.1465684030e-01
-8.6000000000e-01    2.1730391462e-01
-8.5000000000e-01    2.1994617663e-01
-8.4000000000e-01    2.2257239389e-01
-8.3000000000e-01    2.2517133396e-01
-8.2000000000e-01    2.2773176442e-01
-8.1000000000e-01    2.3024245286e-01
-8.0000000000e-01    2.3269216687e-01
-7.9000000000e-01    2.3506967406e-01
-7.8000000000e-01    2.3736374203e-01
-7.7000000000e-01    2.3956313842e-01
-7.6000000000e-01    2.4165663091e-01
-7.5000000000e-01    2.4363298726e-01
-7.4000000000e-01    2.4548097549e-01
-7.3000000000e-01    2.4718936445e-01
-7.2000000000e-01    2.4874692858e-01
-7.1000000000e-01    2.5011294961e-01
-7.0000000000e-01    2.5014657213e-01
-6.9000000000e-01    2.4861754740e-01
-6.8000000000e-01    2.4594090744e-01
-6.7000000000e-01    2.4253065368e-01
-6.6000000000e-01    2.3880074788e-01
-6.5000000000e-01    2.3516514412e-01
-6.4000000000e-01    2.3203779405e-01
-6.3000000000e-01    2.2983264827e-01
-6.2000000000e-01    2.2896365662e-01
-6.1000000000e-01    2.2984476760e-01
-6.0000000000e-01    2.3288992398e-01
-5.9000000000e-01    2.3851295185e-01
-5.8000000000e-01    2.5042487218e-01
-5.7000000000e-01    2.7076541351e-01
-5.6000000000e-01    2.9088694412e-01
-5.5000000000e-01    3.0265950633e-01
-5.4000000000e-01    3.1221231531e-01
-5.3000000000e-01    3.2287684307e-01
-5.2000000000e-01    3.3427993555e-01
-5.1000000000e-01    3.4604847323e-01
-5.0000000000e-01    3.5780933932e-01
-4.9000000000e-01    3.6918942176e-01
-4.8000000000e-01    3.7981631070e-01
-4.7000000000e-01    3.9086188071e-01
-4.6000000000e-01    4.0333287031e-01
-4.5000000000e-01    4.1671001807e-01
-4.4000000000e-01    4.3048184207e-01
```

```
-4.3000000000e-01    4.4413691879e-01
-4.2000000000e-01    4.5716383436e-01
-4.1000000000e-01    4.6905117768e-01
-4.0000000000e-01    4.7928753854e-01
-3.9000000000e-01    4.8736150671e-01
-3.8000000000e-01    4.9276166951e-01
-3.7000000000e-01    4.9497632308e-01
-3.6000000000e-01    4.9520840098e-01
-3.5000000000e-01    4.9502480263e-01
-3.4000000000e-01    4.9443968653e-01
-3.3000000000e-01    4.9346514482e-01
-3.2000000000e-01    4.9211325325e-01
-3.1000000000e-01    4.9039608485e-01
-3.0000000000e-01    4.8832571187e-01
-2.9000000000e-01    4.8591420627e-01
-2.8000000000e-01    4.8317363988e-01
-2.7000000000e-01    4.8011608445e-01
-2.6000000000e-01    4.7675361172e-01
-2.5000000000e-01    4.7309829340e-01
-2.4000000000e-01    4.6916220119e-01
-2.3000000000e-01    4.6495740678e-01
-2.2000000000e-01    4.6049598187e-01
-2.1000000000e-01    4.5578999817e-01
-2.0000000000e-01    4.5085152741e-01
-1.9000000000e-01    4.4569264135e-01
-1.8000000000e-01    4.4032541188e-01
-1.7000000000e-01    4.3476191124e-01
-1.6000000000e-01    4.2901421304e-01
-1.5000000000e-01    4.2309440403e-01
-1.4000000000e-01    4.1671301101e-01
-1.3000000000e-01    4.0821907697e-01
-1.2000000000e-01    3.9780276996e-01
-1.1000000000e-01    3.8596709758e-01
-1.0000000000e-01    3.7321465942e-01
-9.0000000000e-02    3.6004801799e-01
-8.0000000000e-02    3.4696972725e-01
-7.0000000000e-02    3.3448233828e-01
-6.0000000000e-02    3.2308840096e-01
-5.0000000000e-02    3.1329046457e-01
-4.0000000000e-02    3.0559107797e-01
-3.0000000000e-02    3.0049278923e-01
-2.0000000000e-02    2.9849814129e-01
-1.0000000000e-02    2.9976099599e-01
 0.0000000000e+00    3.0137747786e-01
 1.0000000000e-02    3.0278831059e-01
 2.0000000000e-02    3.0422091641e-01
 3.0000000000e-02    3.0590216468e-01
 4.0000000000e-02    3.0805888380e-01
 5.0000000000e-02    3.1091789321e-01
 6.0000000000e-02    3.1470600942e-01
 7.0000000000e-02    3.1965004777e-01
 8.0000000000e-02    3.2597682299e-01
```

```
    9.0000000000e-02    3.3391314950e-01
    1.0000000000e-01    3.4368584140e-01
    1.1000000000e-01    3.5552171247e-01
    1.2000000000e-01    3.6964757562e-01
    1.3000000000e-01    3.8629024082e-01
    1.4000000000e-01    4.0567649602e-01
    1.5000000000e-01    4.2796426326e-01
    1.6000000000e-01    4.5228498135e-01
    1.7000000000e-01    4.7817773871e-01
    1.8000000000e-01    5.0549995493e-01
    1.9000000000e-01    5.0549995493e-01
    4.00000000000000    5.0549995493e-01
    5.00000000000000    1.00000000000000
*DEFINE_CURVE
$     LCID      SIDR       SFA       SFO      OFFA      OFFO    DATYP
      3020
$                A1                  O1
   -1.0000000000e+00    1.8505676443e-01
   -9.9000000000e-01    1.8728872621e-01
   -9.8000000000e-01    1.8963411193e-01
   -9.7000000000e-01    1.9205861261e-01
   -9.6000000000e-01    1.9453801818e-01
   -9.5000000000e-01    1.9705149946e-01
   -9.4000000000e-01    1.9958018141e-01
   -9.3000000000e-01    2.0212512329e-01
   -9.2000000000e-01    2.0468397372e-01
   -9.1000000000e-01    2.0725223666e-01
   -9.0000000000e-01    2.0982434312e-01
   -8.9000000000e-01    2.1239413804e-01
   -8.8000000000e-01    2.1495512362e-01
   -8.7000000000e-01    2.1750059000e-01
   -8.6000000000e-01    2.2002368970e-01
   -8.5000000000e-01    2.2251748180e-01
   -8.4000000000e-01    2.2497495905e-01
   -8.3000000000e-01    2.2738906463e-01
   -8.2000000000e-01    2.2975270237e-01
   -8.1000000000e-01    2.3205874224e-01
   -8.0000000000e-01    2.3430002206e-01
   -7.9000000000e-01    2.3646934562e-01
   -7.8000000000e-01    2.3855947632e-01
   -7.7000000000e-01    2.4056312446e-01
   -7.6000000000e-01    2.4247292416e-01
   -7.5000000000e-01    2.4428139147e-01
   -7.4000000000e-01    2.4598084573e-01
   -7.3000000000e-01    2.4756325235e-01
   -7.2000000000e-01    2.4901987931e-01
   -7.1000000000e-01    2.5028068804e-01
   -7.0000000000e-01    2.4997527862e-01
   -6.9000000000e-01    2.4892676561e-01
   -6.8000000000e-01    2.4749253668e-01
   -6.7000000000e-01    2.4557434080e-01
   -6.6000000000e-01    2.4334044063e-01
```

-6.5000000000e-01	2.4101236471e-01
-6.4000000000e-01	2.3882901390e-01
-6.3000000000e-01	2.3703798636e-01
-6.2000000000e-01	2.3589459161e-01
-6.1000000000e-01	2.3566644421e-01
-6.0000000000e-01	2.3665060307e-01
-5.9000000000e-01	2.3924311973e-01
-5.8000000000e-01	2.4712716691e-01
-5.7000000000e-01	2.6559286279e-01
-5.6000000000e-01	2.8730195667e-01
-5.5000000000e-01	3.0340224919e-01
-5.4000000000e-01	3.1698865800e-01
-5.3000000000e-01	3.3266149634e-01
-5.2000000000e-01	3.4916245738e-01
-5.1000000000e-01	3.6530265848e-01
-5.0000000000e-01	3.8028989928e-01
-4.9000000000e-01	3.9336942698e-01
-4.8000000000e-01	4.0354873147e-01
-4.7000000000e-01	4.1336070919e-01
-4.6000000000e-01	4.2229201285e-01
-4.5000000000e-01	4.2958269499e-01
-4.4000000000e-01	4.3614904940e-01
-4.3000000000e-01	4.4204840786e-01
-4.2000000000e-01	4.4725108757e-01
-4.1000000000e-01	4.5170183198e-01
-4.0000000000e-01	4.5533436485e-01
-3.9000000000e-01	4.5807414744e-01
-3.8000000000e-01	4.5983259936e-01
-3.7000000000e-01	4.6047151767e-01
-3.6000000000e-01	4.6018884612e-01
-3.5000000000e-01	4.5949812164e-01
-3.4000000000e-01	4.5860400073e-01
-3.3000000000e-01	4.5771770936e-01
-3.2000000000e-01	4.5691280374e-01
-3.1000000000e-01	4.5610905485e-01
-3.0000000000e-01	4.5526069932e-01
-2.9000000000e-01	4.5433901073e-01
-2.8000000000e-01	4.5332282043e-01
-2.7000000000e-01	4.5219472098e-01
-2.6000000000e-01	4.5093933402e-01
-2.5000000000e-01	4.4954243517e-01
-2.4000000000e-01	4.4799047018e-01
-2.3000000000e-01	4.4627025954e-01
-2.2000000000e-01	4.4436879235e-01
-2.1000000000e-01	4.4227305121e-01
-2.0000000000e-01	4.3996982066e-01
-1.9000000000e-01	4.3744542018e-01
-1.8000000000e-01	4.3468525419e-01
-1.7000000000e-01	4.3167294014e-01
-1.6000000000e-01	4.2838839003e-01
-1.5000000000e-01	4.2480293330e-01
-1.4000000000e-01	4.2051360346e-01

```
   -1.3000000000e-01    4.1387017607e-01
   -1.2000000000e-01    4.0507015539e-01
   -1.1000000000e-01    3.9438314555e-01
   -1.0000000000e-01    3.8229228786e-01
   -9.0000000000e-02    3.6931769938e-01
   -8.0000000000e-02    3.5599254906e-01
   -7.0000000000e-02    3.4285557035e-01
   -6.0000000000e-02    3.3044983977e-01
   -5.0000000000e-02    3.1932431018e-01
   -4.0000000000e-02    3.1003902112e-01
   -3.0000000000e-02    3.0317993689e-01
   -2.0000000000e-02    2.9940915877e-01
   -1.0000000000e-02    2.9920816286e-01
    0.0000000000e+00    2.9949344260e-01
    1.0000000000e-02    3.0014564440e-01
    2.0000000000e-02    3.0156223729e-01
    3.0000000000e-02    3.0369083674e-01
    4.0000000000e-02    3.0659045433e-01
    5.0000000000e-02    3.1037230355e-01
    6.0000000000e-02    3.1516470233e-01
    7.0000000000e-02    3.2110313625e-01
    8.0000000000e-02    3.2832680847e-01
    9.0000000000e-02    3.3697742267e-01
    1.0000000000e-01    3.4719904621e-01
    1.1000000000e-01    3.5913890729e-01
    1.2000000000e-01    3.7294974034e-01
    1.3000000000e-01    3.8879595326e-01
    1.4000000000e-01    4.0687200915e-01
    1.5000000000e-01    4.2743915274e-01
    1.6000000000e-01    4.5016033218e-01
    1.7000000000e-01    4.7453464439e-01
    1.8000000000e-01    5.0051230457e-01
    1.9000000000e-01    5.0051230457e-01
    4.00000000000000    5.0051230457e-01
    5.00000000000000    1.00000000000000
*DEFINE_CURVE
$     LCID      SIDR       SFA       SFO      OFFA      OFFO    DATYP
      3021
$                A1                  O1
   -1.0000000000e+00    1.8500000000e-01
   -9.9000000000e-01    1.8730445060e-01
   -9.8000000000e-01    1.8969707808e-01
   -9.7000000000e-01    1.9216762933e-01
   -9.6000000000e-01    1.9470585121e-01
   -9.5000000000e-01    1.9730149060e-01
   -9.4000000000e-01    1.9994429437e-01
   -9.3000000000e-01    2.0262400940e-01
   -9.2000000000e-01    2.0533038255e-01
   -9.1000000000e-01    2.0805316071e-01
   -9.0000000000e-01    2.1078209074e-01
   -8.9000000000e-01    2.1350691953e-01
   -8.8000000000e-01    2.1621739393e-01
```

```
-8.7000000000e-01    2.1890326084e-01
-8.6000000000e-01    2.2155426711e-01
-8.5000000000e-01    2.2416015962e-01
-8.4000000000e-01    2.2671068526e-01
-8.3000000000e-01    2.2919559088e-01
-8.2000000000e-01    2.3160462337e-01
-8.1000000000e-01    2.3392752959e-01
-8.0000000000e-01    2.3615405643e-01
-7.9000000000e-01    2.3827395075e-01
-7.8000000000e-01    2.4027695943e-01
-7.7000000000e-01    2.4215282934e-01
-7.6000000000e-01    2.4389130735e-01
-7.5000000000e-01    2.4548214035e-01
-7.4000000000e-01    2.4691507519e-01
-7.3000000000e-01    2.4817985876e-01
-7.2000000000e-01    2.4926623793e-01
-7.1000000000e-01    2.5013682157e-01
-7.0000000000e-01    2.4996433268e-01
-6.9000000000e-01    2.4859661796e-01
-6.8000000000e-01    2.4635063466e-01
-6.7000000000e-01    2.4354334008e-01
-6.6000000000e-01    2.4049169149e-01
-6.5000000000e-01    2.3751264618e-01
-6.4000000000e-01    2.3492316141e-01
-6.3000000000e-01    2.3304019448e-01
-6.2000000000e-01    2.3218070267e-01
-6.1000000000e-01    2.3266164324e-01
-6.0000000000e-01    2.3479997349e-01
-5.9000000000e-01    2.3891265069e-01
-5.8000000000e-01    2.4946252779e-01
-5.7000000000e-01    2.6984274570e-01
-5.6000000000e-01    2.9055858746e-01
-5.5000000000e-01    3.0230129125e-01
-5.4000000000e-01    3.0651691334e-01
-5.3000000000e-01    3.0653921382e-01
-5.2000000000e-01    3.0383245291e-01
-5.1000000000e-01    2.9986089084e-01
-5.0000000000e-01    2.9608878785e-01
-4.9000000000e-01    2.9398040416e-01
-4.8000000000e-01    2.9500000000e-01
-4.7000000000e-01    2.9844645563e-01
-4.6000000000e-01    3.0252962767e-01
-4.5000000000e-01    3.0708024086e-01
-4.4000000000e-01    3.1192901998e-01
-4.3000000000e-01    3.1690668980e-01
-4.2000000000e-01    3.2184397507e-01
-4.1000000000e-01    3.2657160056e-01
-4.0000000000e-01    3.3092029103e-01
-3.9000000000e-01    3.3472077125e-01
-3.8000000000e-01    3.3780376599e-01
-3.7000000000e-01    3.4000000000e-01
-3.6000000000e-01    3.4215028643e-01
```

-3.5000000000e-01	3.4513922252e-01
-3.4000000000e-01	3.4886320921e-01
-3.3000000000e-01	3.5321864743e-01
-3.2000000000e-01	3.5810193811e-01
-3.1000000000e-01	3.6340948220e-01
-3.0000000000e-01	3.6903768062e-01
-2.9000000000e-01	3.7488293430e-01
-2.8000000000e-01	3.8084164418e-01
-2.7000000000e-01	3.8681021119e-01
-2.6000000000e-01	3.9268503627e-01
-2.5000000000e-01	3.9836252034e-01
-2.4000000000e-01	4.0373906435e-01
-2.3000000000e-01	4.0871106923e-01
-2.2000000000e-01	4.1317493590e-01
-2.1000000000e-01	4.1702706530e-01
-2.0000000000e-01	4.2016385838e-01
-1.9000000000e-01	4.2248171605e-01
-1.8000000000e-01	4.2387703925e-01
-1.7000000000e-01	4.2424622892e-01
-1.6000000000e-01	4.2348568598e-01
-1.5000000000e-01	4.2149181138e-01
-1.4000000000e-01	4.1789609875e-01
-1.3000000000e-01	4.1127854611e-01
-1.2000000000e-01	4.0196841824e-01
-1.1000000000e-01	3.9059022510e-01
-1.0000000000e-01	3.7776847664e-01
-9.0000000000e-02	3.6412768280e-01
-8.0000000000e-02	3.5029235356e-01
-7.0000000000e-02	3.3688699886e-01
-6.0000000000e-02	3.2453612864e-01
-5.0000000000e-02	3.1386425288e-01
-4.0000000000e-02	3.0549588152e-01
-3.0000000000e-02	3.0005552451e-01
-2.0000000000e-02	2.9816769181e-01
-1.0000000000e-02	3.0002224201e-01
0.0000000000e+00	3.0210667673e-01
1.0000000000e-02	3.0373235387e-01
2.0000000000e-02	3.0516720202e-01
3.0000000000e-02	3.0667914978e-01
4.0000000000e-02	3.0853612574e-01
5.0000000000e-02	3.1100605849e-01
6.0000000000e-02	3.1435687661e-01
7.0000000000e-02	3.1885650870e-01
8.0000000000e-02	3.2477288335e-01
9.0000000000e-02	3.3237392915e-01
1.0000000000e-01	3.4192757469e-01
1.1000000000e-01	3.5370174856e-01
1.2000000000e-01	3.6796437935e-01
1.3000000000e-01	3.8498339565e-01
1.4000000000e-01	4.0502672606e-01
1.5000000000e-01	4.2827279299e-01
1.6000000000e-01	4.5346709828e-01

```
    1.7000000000e-01    4.8003090849e-01
    1.8000000000e-01    5.0784084481e-01
    1.9000000000e-01    5.0784084481e-01
    4.00000000000000    5.0784084481e-01
    5.00000000000000    1.00000000000000
$$$$$$$$$$$$$$$$$$$$$$$$$$$$$$$$$$$$$$$$$$$$$$$$$$$$$$$$$$$
$              Failure - Strain Rate Curve                $
$$$$$$$$$$$$$$$$$$$$$$$$$$$$$$$$$$$$$$$$$$$$$$$$$$$$$$$$$$$
*DEFINE_CURVE
$     LCID      SIDR       SFA       SFO      OFFA      OFFO    DATYP
      4000
$                 A1                  O1
            0.000010               1.000
            0.001000               0.900
            2.350000               0.370
            6.610000               0.370
$$$$$$$$$$$$$$$$$$$$$$$$$$$$$$$$$$$$$$$$$$$$$$$$$$$$$$$$$$$
$              Failure - Temperature Curve                $
$$$$$$$$$$$$$$$$$$$$$$$$$$$$$$$$$$$$$$$$$$$$$$$$$$$$$$$$$$$
*DEFINE_CURVE
$     LCID      SIDR       SFA       SFO      OFFA      OFFO    DATYP
      5000
$                 A1                  O1
              293.00               1.000
              473.15               1.950
              673.15               1.950
              873.15               2.950
             1877.00               2.950
$$$$$$$$$$$$$$$$$$$$$$$$$$$$$$$$$$$$$$$$$$$$$$$$$$$$$$$$$$$
$             Failure - Regularization Curve              $
$$$$$$$$$$$$$$$$$$$$$$$$$$$$$$$$$$$$$$$$$$$$$$$$$$$$$$$$$$$
*DEFINE_CURVE
$#    lcid      sidr       sfa       sfo      offa      offo    dattyp
      6000         0       1.0       1.0       0.0       0.0         0
$           ABSCISSA            ORDINATE
                0.00               1.038
                0.10               1.038
                0.20               1.000
                0.40               0.912
                0.50               0.912
*END
```